The Institution of Engineering and Technology

# Condition Monitoring of Rotating Electrical Machines

3rd Edition

Peter Tavner, Li Ran and Christopher Crabtree

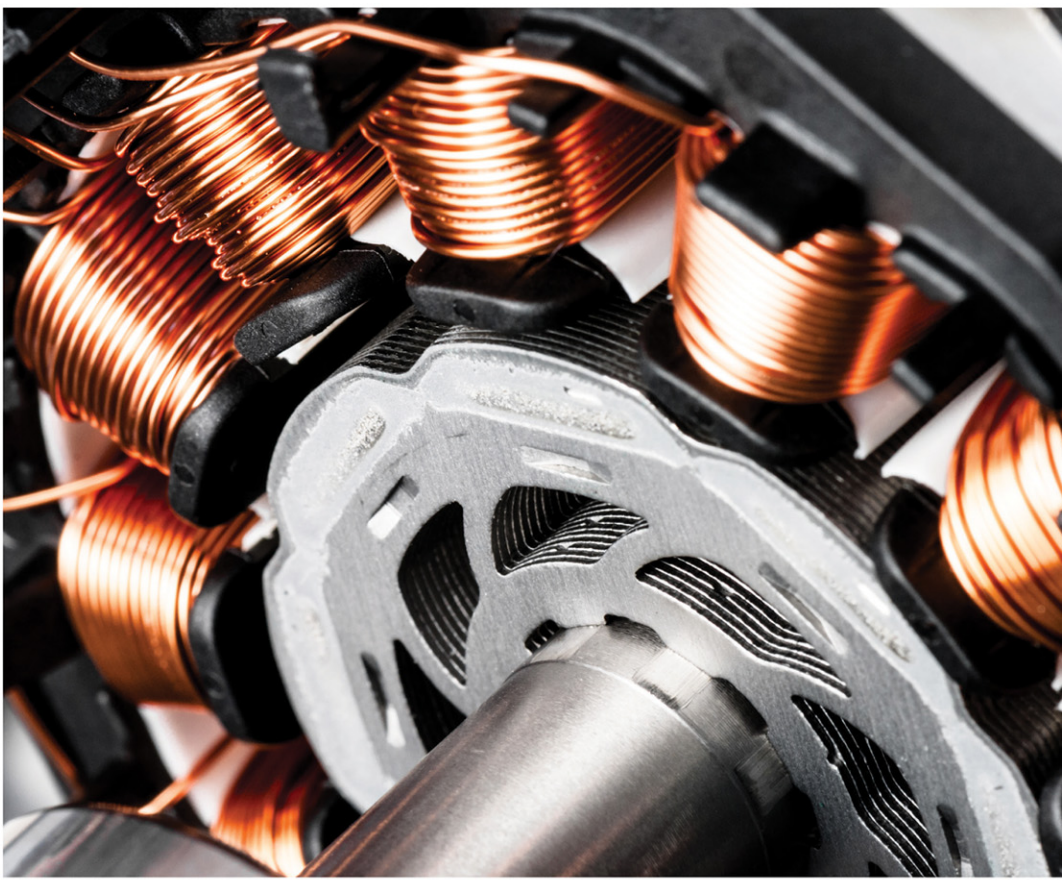

IET ENERGY ENGINEERING 145

# Condition Monitoring of Rotating Electrical Machines

## Other volumes in this series:

Volume 1 **Power Circuit Breaker Theory and Design** C.H. Flurscheim (Editor)
Volume 4 **Industrial Microwave Heating** A.C. Metaxas and R.J. Meredith
Volume 7 **Insulators for High Voltages** J.S.T. Looms
Volume 8 **Variable Frequency AC Motor Drive Systems** D. Finney
Volume 10 **$SF_6$ Switchgear** H.M. Ryan and G.R. Jones
Volume 11 **Conduction and Induction Heating** E.J. Davies
Volume 13 **Statistical Techniques for High Voltage Engineering** W. Hauschild and W. Mosch
Volume 14 **Uninterruptible Power Supplies** J. Platts and J.D. St Aubyn (Editors)
Volume 15 **Digital Protection for Power Systems** A.T. Johns and S.K. Salman
Volume 16 **Electricity Economics and Planning** T.W. Berrie
Volume 18 **Vacuum Switchgear** A. Greenwood
Volume 19 **Electrical Safety: A guide to causes and prevention of hazards** J. Maxwell Adams
Volume 21 **Electricity Distribution Network Design, 2nd Edition** E. Lakervi and E.J. Holmes
Volume 22 **Artificial Intelligence Techniques in Power Systems** K. Warwick, A.O. Ekwue and R. Aggarwal (Editors)
Volume 24 **Power System Commissioning and Maintenance Practice** K. Harker
Volume 25 **Engineers' Handbook of Industrial Microwave Heating** R.J. Meredith
Volume 26 **Small Electric Motors** H. Moczala *et al.*
Volume 27 **AC–DC Power System Analysis** J. Arrillaga and B.C. Smith
Volume 29 **High Voltage Direct Current Transmission, 2nd Edition** J. Arrillaga
Volume 30 **Flexible AC Transmission Systems (FACTS)** Y.-H. Song (Editor)
Volume 31 **Embedded Generation** N. Jenkins *et al.*
Volume 32 **High Voltage Engineering and Testing, 2nd Edition** H.M. Ryan (Editor)
Volume 33 **Overvoltage Protection of Low-Voltage Systems, Revised Edition** P. Hasse
Volume 36 **Voltage Quality in Electrical Power Systems** J. Schlabbach *et al.*
Volume 37 **Electrical Steels for Rotating Machines** P. Beckley
Volume 38 **The Electric Car: Development and future of battery, hybrid and fuel-cell cars** M. Westbrook
Volume 39 **Power Systems Electromagnetic Transients Simulation** J. Arrillaga and N. Watson
Volume 40 **Advances in High Voltage Engineering** M. Haddad and D. Warne
Volume 41 **Electrical Operation of Electrostatic Precipitators** K. Parker
Volume 43 **Thermal Power Plant Simulation and Control** D. Flynn
Volume 44 **Economic Evaluation of Projects in the Electricity Supply Industry** H. Khatib
Volume 45 **Propulsion Systems for Hybrid Vehicles** J. Miller
Volume 46 **Distribution Switchgear** S. Stewart
Volume 47 **Protection of Electricity Distribution Networks, 2nd Edition** J. Gers and E. Holmes
Volume 48 **Wood Pole Overhead Lines** B. Wareing
Volume 49 **Electric Fuses, 3rd Edition** A. Wright and G. Newbery
Volume 50 **Wind Power Integration: Connection and system operational aspects** B. Fox *et al.*
Volume 51 **Short Circuit Currents** J. Schlabbach
Volume 52 **Nuclear Power** J. Wood
Volume 53 **Condition Assessment of High Voltage Insulation in Power System Equipment** R.E. James and Q. Su
Volume 55 **Local Energy: Distributed generation of heat and power** J. Wood
Volume 56 **Condition Monitoring of Rotating Electrical Machines** P. Tavner, L. Ran, J. Penman and H. Sedding
Volume 57 **The Control Techniques Drives and Controls Handbook, 2nd Edition** B. Drury
Volume 58 **Lightning Protection** V. Cooray (Editor)
Volume 59 **Ultracapacitor Applications** J.M. Miller

Volume 62 **Lightning Electromagnetics** V. Cooray
Volume 63 **Energy Storage for Power Systems, 2nd Edition** A. Ter-Gazarian
Volume 65 **Protection of Electricity Distribution Networks, 3rd Edition** J. Gers
Volume 66 **High Voltage Engineering Testing, 3rd Edition** H. Ryan (Editor)
Volume 67 **Multicore Simulation of Power System Transients** F.M. Uriate
Volume 68 **Distribution System Analysis and Automation** J. Gers
Volume 69 **The Lightening Flash, 2nd Edition** V. Cooray (Editor)
Volume 70 **Economic Evaluation of Projects in the Electricity Supply Industry, 3rd Edition** H. Khatib
Volume 72 **Control Circuits in Power Electronics: Practical issues in design and implementation** M. Castilla (Editor)
Volume 73 **Wide Area Monitoring, Protection and Control Systems: The enabler for smarter grids** A. Vaccaro and A. Zobaa (Editors)
Volume 74 **Power Electronic Converters and Systems: Frontiers and applications** A.M. Trzynadlowski (Editor)
Volume 75 **Power Distribution Automation** B. Das (Editor)
Volume 76 **Power System Stability: Modelling, analysis and control** B. Om P. Malik
Volume 78 **Numerical Analysis of Power System Transients and Dynamics** A. Ametani (Editor)
Volume 79 **Vehicle-to-Grid: Linking electric vehicles to the smart grid** J. Lu and J. Hossain (Editors)
Volume 81 **Cyber-Physical-Social Systems and Constructs in Electric Power Engineering** S. Suryanarayanan, R. Roche and T.M. Hansen (Editors)
Volume 82 **Periodic Control of Power Electronic Converters** F. Blaabjerg, K. Zhou, D. Wang and Y. Yang
Volume 86 **Advances in Power System Modelling, Control and Stability Analysis** F. Milano (Editor)
Volume 87 **Cogeneration: Technologies, optimisation and implementation** C.A. Frangopoulos (Editor)
Volume 88 **Smarter Energy: From smart metering to the smart grid** H. Sun, N. Hatziargyriou, H.V. Poor, L. Carpanini and M.A. Sánchez Fornié (Editors)
Volume 89 **Hydrogen Production, Separation and Purification for Energy** A. Basile, F. Dalena, J. Tong and T.N. Veziroğlu (Editors)
Volume 90 **Clean Energy Microgrids** S. Obara and J. Morel (Editors)
Volume 91 **Fuzzy Logic Control in Energy Systems with Design Applications in MATLAB®/Simulink®** İ.H. Altaş
Volume 92 **Power Quality in Future Electrical Power Systems** A.F. Zobaa and S.H.E.A. Aleem (Editors)
Volume 93 **Cogeneration and District Energy Systems: Modelling, analysis and optimization** M.A. Rosen and S. Koohi-Fayegh
Volume 94 **Introduction to the Smart Grid: Concepts, technologies and evolution** S.K. Salman
Volume 95 **Communication, Control and Security Challenges for the Smart Grid** S.M. Muyeen and S. Rahman (Editors)
Volume 96 **Industrial Power Systems with Distributed and Embedded Generation** R Belu
Volume 97 **Synchronized Phasor Measurements for Smart Grids** M.J.B. Reddy and D.K. Mohanta (Editors)
Volume 98 **Large Scale Grid Integration of Renewable Energy Sources** A. Moreno-Munoz (Editor)
Volume 100 **Modeling and Dynamic Behaviour of Hydropower Plants** N. Kishor and J. Fraile-Ardanuy (Editors)
Volume 101 **Methane and Hydrogen for Energy Storage** R. Carriveau and D.S.-K. Ting
Volume 104 **Power Transformer Condition Monitoring and Diagnosis** A. Abu-Siada (Editor)
Volume 106 **Surface Passivation of Industrial Crystalline Silicon Solar Cells** J. John (Editor)
Volume 107 **Bifacial Photovoltaics: Technology, applications and economics** J. Libal and R. Kopecek (Editors)

Volume 108 **Fault Diagnosis of Induction Motors** J. Faiz, V. Ghorbanian and G. Joksimović
Volume 110 **High Voltage Power Network Construction** K. Harker
Volume 111 **Energy Storage at Different Voltage Levels: Technology, integration, and market aspects** A.F. Zobaa, P.F. Ribeiro, S.H.A. Aleem and S.N. Afifi (Editors)
Volume 112 **Wireless Power Transfer: Theory, technology and application** N.Shinohara
Volume 115 **DC Distribution Systems and Microgrids** T. Dragičević, F. Blaabjerg and P. Wheeler
Volume 117 **Structural Control and Fault Detection of Wind Turbine Systems** H.R. Karimi
Volume 119 **Thermal Power Plant Control and Instrumentation: The control of boilers and HRSGs, 2nd Edition** D. Lindsley, J. Grist and D. Parker
Volume 120 **Fault Diagnosis for Robust Inverter Power Drives** A. Ginart (Editor)
Volume 123 **Power Systems Electromagnetic Transients Simulation, 2nd Edition** N. Watson and J. Arrillaga
Volume 124 **Power Market Transformation** B. Murray
Volume 125 **Wind Energy Modeling and Simulation Volume 1: Atmosphere and plant** P. Veers (Editor)
Volume 126 **Diagnosis and Fault Tolerance of Electrical Machines, Power Electronics and Drives** A.J.M. Cardoso
Volume 128 **Characterization of Wide Bandgap Power Semiconductor Devices** F. Wang, Z. Zhang and E.A. Jones
Volume 129 **Renewable Energy from the Oceans: From wave, tidal and gradient systems to offshore wind and solar** D. Coiro and T. Sant (Editors)
Volume 130 **Wind and Solar Based Energy Systems for Communities** R. Carriveau and D.S.-K. Ting (Editors)
Volume 131 **Metaheuristic Optimization in Power Engineering** J. Radosavljević
Volume 132 **Power Line Communication Systems for Smart Grids** I.R.S Casella and A. Anpalagan
Volume 139 **Variability, Scalability and Stability of Microgrids** S.M. Muyeen, S.M. Islam and F. Blaabjerg (Editors)
Volume 146 **Energy Storage for Power Systems, 3rd Edition** A.G. Ter-Gazarian
Volume 155 **Energy Generation and Efficiency Technologies for Green Residential Buildings** D. Ting and R. Carriveau (Editors)
Volume 157 **Electrical Steels, 2 Volumes** A. Moses, K. Jenkins, Philip Anderson and H. Stanbury
Volume 172 **Lighting interaction with Power Systems, 2 volumes** A. Piantini (Editor)
Volume 905 **Power System Protection, 4 volumes**

# Condition Monitoring of Rotating Electrical Machines

3rd Edition

Peter Tavner, Li Ran and Christopher Crabtree

The Institution of Engineering and Technology

Published by The Institution of Engineering and Technology, London, United Kingdom

The Institution of Engineering and Technology is registered as a Charity in England & Wales (no. 211014) and Scotland (no. SC038698).

© The Institution of Engineering and Technology 2020

First published 2020

This publication is copyright under the Berne Convention and the Universal Copyright Convention. All rights reserved. Apart from any fair dealing for the purposes of research or private study, or criticism or review, as permitted under the Copyright, Designs and Patents Act 1988, this publication may be reproduced, stored or transmitted, in any form or by any means, only with the prior permission in writing of the publishers, or in the case of reprographic reproduction in accordance with the terms of licences issued by the Copyright Licensing Agency. Enquiries concerning reproduction outside those terms should be sent to the publisher at the undermentioned address:

The Institution of Engineering and Technology
Michael Faraday House
Six Hills Way, Stevenage
Herts, SG1 2AY, United Kingdom

www.theiet.org

While the author and publisher believe that the information and guidance given in this work are correct, all parties must rely upon their own skill and judgement when making use of them. Neither the authors nor publisher assumes any liability to anyone for any loss or damage caused by any error or omission in the work, whether such an error or omission is the result of negligence or any other cause. Any and all such liability is disclaimed.

The moral rights of the authors to be identified as authors of this work have been asserted by them in accordance with the Copyright, Designs and Patents Act 1988.

**British Library Cataloguing in Publication Data**
A catalogue record for this product is available from the British Library

**ISBN 978-1-78561-865-9 (hardback)**
**ISBN 978-1-78561-866-6 (PDF)**

Typeset in India by MPS Limited
Printed in the UK by CPI Group (UK) Ltd, Croydon

***This Book is Dedicated to our children:***
*Charles and Sarah,*
*Shaolu, Jason and Sam,*
*Alfred*

*As I walked down by the river*
*Down by the frozen fen*
*I saw the grey cathedral*
*With the eyes of a child of ten.*

*O the railway arch is smoky*
*As the Flying Scot goes by*
*And but for the Education Act*
*Go Jumper Cross and I.*

*Ballad for Katherine of Aragon, Charles Causley (1947)*

*Choral Symphony No.3, Gala and Gloria, Will Todd (2004)*
*First performed Durham Cathedral,*
*Riverside Band and banner marching its length,*
*closing with Cathedral bells*

*This page intentionally left blank*

# Contents


**About the authors** xv
**Preface** xvii
**Acknowledgements** xxi
**Nomenclature** xxiii
**Abbreviations** xxix

**1 Introduction to condition monitoring** 1
1.1 Introduction 1
1.2 Need for monitoring 4
1.3 What and when to monitor 8
1.4 Technological timelines 10
1.5 Structure of text and bibliographies 14

**2 Rotating electrical machines** 17
2.1 Introduction 17
2.2 Electrical machines structures and types 18
2.3 DC machines 25
2.4 AC machines, synchronous 26
2.5 AC machines, asynchronous or induction 28
2.6 Permanent magnet or reluctance machines 33
2.7 Other machine types 33
2.7.1 Multi-phase machines 33
2.7.2 Doubly fed and variable-speed drive machines 35
2.8 Conclusions 37

**3 Electrical machine construction, operation and failure modes** 39
3.1 Introduction 39
3.2 Materials, strength and temperature 39
3.3 Electrical machine construction 43
3.3.1 General 43
3.3.2 Stator core and frame 44
3.3.3 Stator windings 44
3.3.4 Rotors and windings 45
3.3.5 Enclosures 46
3.3.6 Connections and heat exchangers 47
3.3.7 Summary 47

3.4 Machine specification and failure modes 48
3.5 Insulation ageing mechanisms 50
3.5.1 General 50
3.5.2 Thermal ageing 51
3.5.3 Electrical ageing 52
3.5.4 Mechanical ageing 54
3.5.5 Environmental ageing 54
3.5.6 Synergism between ageing stresses 55
3.6 Insulation failure modes 55
3.6.1 General 55
3.6.2 Stator winding insulation 56
3.6.3 Stator winding faults 61
3.6.4 Rotor winding faults 67
3.7 Other failure modes 71
3.7.1 Stator core faults (Turbo- and hydro-generators) 71
3.7.2 Connection faults (HV motors and generators) 72
3.7.3 Water coolant faults (All machines) 73
3.7.4 Bearing faults (All machines) 73
3.7.5 Shaft voltages (Large machines) 75
3.8 Conclusions 76

**4 Reliability of machines and typical failure rates 77**
4.1 Introduction and business of failure 77
4.2 Definition of terms 78
4.3 Root cause and FMEA 81
4.3.1 General 81
4.3.2 Typical root causes and failure modes 82
4.3.3 Root causes 83
4.3.4 Failure modes 83
4.4 Reliability analysis 84
4.5 Machine structure 87
4.6 Typical failure rates and MTBFs 89
4.7 Conclusions 93

**5 Signal processing and instrumentation requirements 95**
5.1 Introduction 95
5.2 Spectral analysis 99
5.3 Higher-order spectral analysis 104
5.4 Correlation analysis 105
5.5 Vibration signal processing 107
5.5.1 General 107
5.5.2 Cepstrum analysis 108
5.5.3 Time averaging and trend analysis 110
5.6 Wavelet analysis 111
5.7 Model-based information extraction 113

5.7.1 Kalman filter 114
5.7.2 Observer 116
5.8 Temperature instrumentation 117
5.9 Vibration instrumentation 123
5.9.1 General 123
5.9.2 Displacement transducers 124
5.9.3 Velocity transducers 127
5.9.4 Accelerometers 128
5.10 Force and torque instrumentation 129
5.11 Electromagnetic instrumentation 132
5.12 Wear and debris instrumentation 136
5.13 Signal conditioning 137
5.14 Data acquisition 139
5.15 Conclusions 141

**6 Online temperature monitoring 143**
6.1 Introduction 143
6.2 Local temperature measurement 143
6.3 Hot-spot measurement and thermal images 149
6.4 Bulk measurement 149
6.5 Conclusions 151

**7 Online chemical monitoring 153**
7.1 Introduction 153
7.2 Insulation degradation 153
7.3 Factors that affect detection 154
7.4 Insulation degradation detection 158
7.4.1 Particulate detection – core monitors 158
7.4.2 Particulate detection – chemical analysis 162
7.4.3 Gas analysis offline 164
7.4.4 Gas analysis online 166
7.5 Lubrication oil and bearing degradation 169
7.6 Oil degradation detection 169
7.7 Wear debris detection 170
7.7.1 General 170
7.7.2 Ferromagnetic techniques 170
7.7.3 Other wear debris detection techniques 173
7.8 Conclusions 173

**8 Online vibration monitoring 175**
8.1 Introduction 175
8.2 Stator core response 175
8.2.1 General 175
8.2.2 Calculation of natural modes 177
8.2.3 Stator electromagnetic force wave 181

8.3 Stator end winding response 183
8.4 Rotor response 185
8.4.1 Transverse response 185
8.4.2 Torsional response 188
8.5 Bearing response 190
8.5.1 General 190
8.5.2 Rolling element bearings 190
8.5.3 Sleeve bearings 192
8.6 Monitoring techniques 193
8.6.1 Overall level monitoring 194
8.6.2 Frequency spectrum monitoring 196
8.6.3 Faults detectable from the stator force wave 199
8.6.4 Torsional oscillation monitoring (IAS) 200
8.6.5 Shock pulse monitoring 204
8.7 Conclusions 206

**9 Online current, flux and power monitoring 209**
9.1 Introduction 209
9.2 Generator and motor stator faults 209
9.2.1 Generator stator winding insulation detection 209
9.2.2 Stator current monitoring for stator faults 209
9.2.3 Brush-gear fault detection 210
9.2.4 Rotor-mounted search coils 210
9.3 Generator rotor faults 210
9.3.1 General 210
9.3.2 Earth leakage faults on-line 211
9.3.3 Turn-to-turn faults on-line 212
9.4 Motor rotor faults 220
9.4.1 General 220
9.4.2 Air-gap search coils 220
9.4.3 Stator current monitoring for rotor faults (MCSA) 220
9.4.4 Rotor current monitoring 223
9.5 Generator and motor comprehensive methods 225
9.5.1 General 225
9.5.2 Shaft flux 226
9.5.3 Stator and rotor currents 230
9.5.4 Power 231
9.5.5 Shaft voltage or current 235
9.5.6 Mechanical and electrical interaction 236
9.6 Conclusions 237

**10 Online partial discharge (PD) electrical monitoring 239**
10.1 Introduction 239
10.2 Background to discharge detection 239
10.3 Early discharge detection methods 241

10.3.1 RF coupling method 241
10.3.2 Earth loop transient method 244
10.3.3 Capacitive coupling method 245
10.3.4 Wide-band RF method 246
10.3.5 Insulation remanent life 248
10.4 Detection problems 248
10.5 Modern discharge detection methods 250
10.6 Conclusions 253

**11 Online variable speed drive machine monitoring 255**
11.1 Introduction 255
11.2 Operation and fault mechanisms 256
11.2.1 Insulation degradation mechanisms 256
11.2.2 Bearing current discharges 258
11.3 Bearing current discharge detection 261
11.4 Insulation degradation detection 263
11.4.1 PD measurement 263
11.4.2 Capacitance and dissipation factor measurement 266
11.4.3 Built-in winding insulation degradation detector 267
11.5 Control in-loop machine fault detection 269
11.6 Conclusions 272

**12 Offline monitoring 273**
12.1 Introduction 273
12.2 Stator core 273
12.2.1 General 273
12.2.2 Turbo-generators 277
12.2.3 Hydro-generators 277
12.3 Stator windings 278
12.3.1 Summary of offline tests 278
12.3.2 Frequency response analysis 278
12.4 Rotor windings 278
12.4.1 Summary of offline tests 278
12.4.2 Synchronous rotor surge tests 281
12.5 Conclusions 284

**13 Condition-based maintenance and asset management 285**
13.1 Introduction 285
13.2 Preventative maintenance 285
13.3 Condition-based maintenance 288
13.3.1 Signals and data for condition-based maintenance 288
13.3.2 Targeted monitoring 290
13.4 Economics of maintenance strategies 292
13.4.1 Basic economic justification 292
13.4.2 Life-cycle costing 294

13.4.3 Cost–benefit analysis of condition monitoring for CBM 296
13.4.4 Asset management 297
13.5 Conclusions 300

**14 Application of artificial intelligence techniques to CM 303**
14.1 Introduction 303
14.2 Multi-parameter monitoring 305
14.3 Expert systems 309
14.4 Fuzzy logic 312
14.5 Machine learning using ANNs 316
14.5.1 What can be learned for CM? 316
14.5.2 Supervised learning through ANN 317
14.5.3 Unsupervised learning 320
14.6 Deep learning with big data 322
14.7 An AI example 324
14.7.1 Systems incorporating AI 324
14.7.2 How an MBVI system works 326
14.7.3 An MBVI system and AI 327
14.8 Conclusions 329

**15 Safety, training and qualification 331**
15.1 Introduction 331
15.2 Safety 331
15.3 Training and qualification 332
15.3.1 Training and qualification categories 333
15.3.2 Category I – data collector 333
15.3.3 Category II – specialist 333
15.3.4 Category III – analyst 334
15.3.5 Category IV – expert 334
15.4 Conclusions 335

**16 Overall conclusions 337**
16.1 CM techniques 337
16.2 AI and ML 339
16.3 Standards, training, safety and qualification 340
16.4 The future importance 340

**References 341**
**Standards 361**
**Appendix A Failure modes and root causes in the rotating electrical machines 365**
**Appendix B Draft CM good practice guide, MCSA 371**
**Appendix C Electrical machines, drives and condition monitoring timeline 383**
**Index 391**

# About the authors

**Professor Peter Tavner**, Eur Ing, CEng, FIET, is an Emeritus Professor of the Department of Engineering, Durham University, UK. He received an MA in Mechanical Sciences from Cambridge University in 1971, a PhD from Southampton University in 1978 and DSc from Durham University in 2012.

He trained in the Royal Navy as a Weapons Electrical Officer and served on the Guided Missile Destroyers Bristol and London, subsequently teaching at the University of Benin, Benin City, Nigeria. He has held a number of research and technical positions in the health-care, electrical supply and manufacturing industries including Group Head in a former CEGB laboratory, Technical Director of Laurence, Scott & Electromotors Ltd. (LSE) and Brush Electrical Machines Ltd (BEM), two of the UK's large electrical machine manufacturers, then Group Technical Director of FKI Energy Technology, owner of LSE and BEM, an international business-manufacturing wind turbines, electrical machines, electrical drives, dynamometers, transformers and switchgear in the UK, Holland, Italy, Germany and Czech Republic. At Durham University, he led a number of UK and Europe research initiatives to improve the reliability of wind turbines, wave and tidal generation devices. He retains a particular interest in practical electromagnetic analysis, the application of condition monitoring, the reliability of electrical machines and the use of converters.

He was the winner in 1988 with Richard Jackson of the Institution Premium of the IEE and is an Honorary Member of the European Academy of Wind Energy.

**Professor Li Ran**, BSc, PhD, FIET, SMIEEE, joined the University of Warwick as a professor in Power Electronics Systems in 2012. He is also a professor at Chongqing University, China, and former deputy director for the State Key Laboratory there in Power Transmission Equipment and System Security. Li obtained a PhD in 1989 in Power Systems Engineering from Chongqing University for his work on reliability evaluation of the transmission networks planned for the Three-Gorges Hydro Power Plant. He then participated in commissioning the Gezhouba-Shanghai HVDC System (1989–1990). He was a postdoctoral research fellow with the Universities of Aberdeen, Nottingham and Heriot-Watt (1992–1999), working on marine electrical propulsion, offshore electrical systems and electro-magnetic compatibility (EMC) in power electronic motor drives. He became a lecturer with Northumbria University, Newcastle, in 1999 and moved to Durham University in 2003. He had a secondment to Alstom Power Conversion, Kidsgrove (2001–2004), took sabbatical leave to MIT (2007–2008), was promoted

to Reader and then a Chair in 2010. He has the Stanley Gray Award of the IMarEST for his published work on the monitoring of motors in the offshore environment and IEEE prize paper awards for work on wind turbine converter control and industrial power systems.

**Dr Christopher Crabtree** MEng, PhD, MIET, MIEEE, FHEA, is an Associate Professor in wind energy systems in the Department of Engineering at Durham University, UK. He joined Durham in 2012. After receiving an MEng in General Engineering in 2007, Christopher received a PhD degree from Durham in 2011 for research on condition monitoring techniques for wind turbines. Christopher's research focuses on operation and maintenance aspects of wind energy, onshore and offshore, with the aim of improving reliability, raising availability and reducing the cost of energy. His areas of focus include the development of condition monitoring techniques, power conversion system reliability, performance analysis of wind energy systems, and high-frequency thermal monitoring for power electronics. He also has interests in the movement of church bell towers during full-circle change ringing, with early work focused on Durham Cathedral.

# Preface

An electrical machine is one of the most fundamental, yet subtle human innovations. It uses the electromagnetic field to transfer energy from one system to another, associated with rotational mechanical torque, and quantum electronics within control transistors and power switches to make variable-speed operation possible.

Condition monitoring of plant increases in importance as engineering processes are automated whilst operational and supervisory plant workforce is reduced. But electrical machines have traditionally been thought reliable, requiring little attention except at infrequent intervals, when plant is shut-down for inspection. Indeed, the application to electrical machines of fast-acting, digital protective relays reduces the attention operators pay to this equipment.

However, electrical machines are at the heart of these processes, being designed to increasingly tighter margins and there is a need, for the reliability of these processes, to monitor the machine performance. The control of electrical machines by variable-speed drives, with sophisticated means to vary supply voltages and currents, facilitates the ability to monitor the machine and its drive. This book is a guide to the techniques available.

The subject of condition monitoring of electrical machines covers a wide field including rotating machines and transformers. To restrict that field, the authors concentrate here on rotating machines only but in this edition widen that from traditional induction and synchronous machines to DC, permanent magnet, multiphase and other machines, considering both online and offline techniques, as well as the effect of variable-speed drives connected to such machines.

The nature of electrical machine condition monitoring is dominated by their materials:

- Strong but brittle ferromagnetic steel laminations, steel pole pieces and permanent magnets – the electromagnetic core,
- Ductile and mechanically weak machine conductors – the windings,
- Separated by dielectrically strong but mechanically weak and thermally vulnerable tapes, boards and resins – the insulation,
- Supported on structures and lubricants which separate rotating from stationary parts – the bearings.

To condition monitor electrical machines, we must make electrical, mechanical, thermal or chemical measurements to detect the deterioration and progression

to failure. The authors have been inspired in this respect by an earlier book by Professor Miles Walker (1929) who said about rotating electrical machine troubles:

'First find out the facts; let your conclusions be drawn from ascertained data and not from supposition. After the facts have been clearly stated and the necessary conclusions drawn, a happening that was very elusive in the telling may be very simple in the seeing'. Wise condition monitoring words.

In Professor Miles Walker's day in the 1920s, plant measurements were costly and difficult, in fact he stressed

'the investigator's difficulty often arises from his neglecting to take a measurement, which is the key of the situation'.

In our modern international world, this has changed dramatically: there is no shortage of measurements, simply a lack of interpretation and, in these authors' view, a lack of comparison between key measurements.

The first edition, entitled 'Condition Monitoring of Electrical Machines' written by Peter Tavner and Jim Penman, was published in 1987 by the Research Studies Press. It had the intention of bringing together two strands of work active at that time. These were, respectively,

- From industry, an interest in large machine monitoring as rising maintenance costs competed with heavy financial impact from large machine failures,
- From universities growing confidence in complex electrical machine equivalent circuit modelling and the application of finite element variational methods to predict magnetic fields.

The book was aimed at larger machines in energy production, reflecting that such machines were costly enough to warrant condition monitoring. It also reflected that one author worked in the nationalised generating utility, colouring our approach to the subject. That edition showed that in respect of condition monitoring, electrical machines are unusual compared to other rotating plant in that the all-embracing nature of the electromagnetic field, their modus operandi, enables us to infer far more about operation from terminal conditions than could be the case with non-electrical rotating plant. The edition covered elemental aspects of electrical machine condition monitoring, eliciting some important facts leading to further work:

- Electromagnetic behaviour and the ability to model,
- Dynamic behaviour associated with control now available from modern power electronics and the ability to model that behaviour.

Each has now matured and is a rich source of fundamental knowledge covering the whole range of machine behaviours in their operating state, especially under fault conditions. Three relevant sources are the books by Miles Walker (1929), Vas (1993) on modelling and Jones (1967) exploiting a machine's field modus operandi by measuring terminal 'performance' conditions, rather than using 'design' parameters, such as reactance.

In the second edition, published by the IET, the first two authors were joined by Li Ran and Howard Sedding, Li an expert in variable-speed drives and the application of power electronics to those drives and Howard an expert on electrical

insulation diagnostics. The economics of industry had changed, as a result of privatisation and deregulation of energy, placing greater emphasis on the importance of reliable plant and machinery operation throughout the whole life-cycle, regardless of first capital cost. The availability of advanced electronics and software in computerised instrumentation has also simplified and extended our ability to monitor and analyse machinery, not least in the important area of visualising the results of complex condition monitoring analysis. As a result, condition monitoring was being applied to a wider range of systems, from fault-tolerant drives of a few hundred watts in the aerospace industry, to machinery of a few hundred megawatts in major capital plant. The value of the fundamental contribution to these advances by many analysts over the last 30 years cannot be underestimated and will play a major future role, particular contributions being:

- Behaviour of electrical machine insulation systems,
- Inspection of large machines.

Stone *et al.* (2014) is relevant on both these topics.

In this third edition, two earlier authors, who collaborated at Durham University, have been joined by another Durham colleague, Christopher Crabtree, an expert in the presentation and use of monitoring information for operation and maintenance, reflecting the important combination of rotating machines and variable-speed drives and their rapidly expanding use, particularly in traction, propulsion, distributed and renewable generation, most particularly in wind power. Together we have decided to build on earlier editions by extending the book to cover the whole range of rotating machines without exclusion of type, including both online and offline techniques and taking more cognisance of the interaction between the machine and the power electronics to which it may be connected. Earlier work on electrical machine condition monitoring concentrated on the electrical signals, current and voltage. Later work included mechanical signals, such as vibration, debris-in-oil and also thermal or chemical signals. Vibration and electrical signals lent themselves to the fast Fourier transform (FFT), leading to the application of motor current signal analysis (MCSA) to induction motors. As variable-speed drives have been applied to machines, more attention has been placed on transforms that deal with the effects of changing speed on signals, hence recent interest in Wigner-Ville, Hilbert-Huang and discrete and continuous wavelet (DWT and CWT) transforms. In this third edition, a particular difference from earlier editions, where single signal applications, such as the FFT dominated, more signal measurements are available, especially from drives and condition monitoring is moving from the analogue to digital age. Our revised Chapter 13 on condition-based maintenance and asset management draws on this increased availability of data and change of analysis methodology. This then leads into Chapter 14, which emphasises the importance of multi-parameter monitoring and the use of artificial intelligence (AI) to infer machine condition from multiple signals. However, machine learning (ML), a branch of AI, could learn appropriate condition monitoring transforms from rich data originating from multiple signals, bypassing the need to select a pre-existing mathematical transform and contributing to better

plant asset management. We have also given an example from Faraday Predictive of the impact AI is making in the condition monitoring of electrical machines. Finally we have added some material on the training and qualification issues appropriate to condition monitoring of machines and in the Appendices given a draft Good Practice Guide for one of the most popular techniques. Our method continues to emphasise the all-embracing effect of machine electromagnetic and thermal fields on their signals, by inferring deterioration from terminal 'performance' conditions, amplified by the increased information available from variable-speed drives. We have merged our own experience with that of the machine analysts to bring the reader a thoroughly up-to-date but practicable set of techniques that reflect the work of the last 30 years.

Relevant books are Drury (2009) on drives and machines, Krause *et al.* (2013) on machine modelling and Chung *et al.* (2016) on drive reliability, all in our references list.

Our book is aimed at professional engineers in the energy, process engineering and manufacturing industries, research workers and students. In this edition, we have maintained and expanded the 'Nomenclature' and 'Abbreviation' sections, taken the opportunity to correct previous errors, added important information about failure mechanisms, reliability, instrumentation, signal processing and the management of rotating machine assets, as these factors critically affect the way condition monitoring needs to be applied. We omitted case studies from this third and the second editions, simply because the range of condition monitoring techniques on electrical machines is so wide and complex that it is impossible to select appropriate applications from which general conclusions can be drawn. The diagrams and photographs representing the machines, monitoring systems and signal processing have, where appropriate, been updated and increased in number.

We have extensively updated the references to a single list, in Harvard format, at the end of the book based on well-known bibliographies of the subject and have added a list of standards appropriate to the condition monitoring of rotating electrical machines. We have also presented a draft guide for MCSA condition monitoring of electrical machines, as a prototype for future CM training documents.

Finally, at the end of the book, we have added a historical timeline, to compare the development of these electromagnetic and quantum technologies of electrical machines and drives, developing an uncertain reliability theory to apply to their condition monitoring.

Peter Tavner,
Durham and Cambridge, 2019

# Acknowledgements

The authors acknowledge the assistance they have had from Durham University in preparing this book, particularly from Chris Orton in preparing diagrams.

Our first author acknowledges Prof Percy Hammond, his PhD Supervisor whose inspiration taught him electromagnetism, see the listed papers, Prof Kurt Schwarz his former Technical Director, who taught him the consequent logic of electrical machines and drives and Geoff Walker of Faraday Predictive Ltd., who contributed to Chapter 14, for his advice on modern condition monitoring.

We also acknowledge our academic colleagues in the field, Mike Barnes, Mohamed Benbouzid, Jim Bumby, Sinisa Djurović, Alan Jack, Barrie Mecrow, Phil Mellor, Jim Penman, Phil Taylor, Phil Mawby and Steve Williamson as well as former research students and post-doctoral researchers, Xuan Guo, Borong Hu, Michael Wilkinson, Fabio Spinato, Wenjuan Wang, Wenxian Yang, Mahmoud Zaggout and Donatella Zappalà for their contributions through papers, discussions, diagrams and their understanding of the reliability and monitoring problems of machines.

Special thanks to an old friend, Doug Warne, who gave us sound research advice for many years and encouraged us to produce the second and third editions of this book.

The authors also acknowledge the assistance of companies who contributed photographs and diagrams, in particular, Brush Turbo-generators, UK and Czech Republic, Dong Fang Electrical Machinery Ltd., China, Equipmake, UK, Faraday Predictive Ltd, UK, Laurence, Scott & Electromotors Ltd. and Marelli Motori SpA, Italy.

*This page intentionally left blank*

# Nomenclature

| Symbol | Explanation |
|---|---|
| $A$ | effective cross-sectional area of a coil, $m^2$ |
| $A$ | availability, $A = \text{MTBF}/(\text{MTBF} + \text{MTTR})$ |
| $A(t)$ | availability function of a population of components as a function of time, % |
| $A_v$ | vibration acceleration, $m/s^2$ |
| $a$ | scaling factor of time in a mother wavelet transform |
| $a$ | scale parameter in a power law expression |
| $a_t$ | cross-sectional area of a tooth, $m^2$ |
| $\alpha_r$ | resistance temperature coefficient, °C/Ω |
| $\alpha_s$ | skew angle of a stator, ° |
| $B$ | radial flux density in an air-gap, T |
| $B(f_1, f_2)$ | bispectrum |
| $b$ | instantaneous radial flux density, T |
| $b$ | time-shifting parameter in a mother wavelet function |
| $\beta$ | shape function in a power law expression |
| $\beta$ | half angle subtended by a shorted turn, ° |
| $C$ | volumetric concentration of a degradation product in a machine, $\%/m^3$ |
| $C$ | Carter factor to account for air-gap slotting |
| $C(\psi, v)$ | inverse wavelet transform |
| $C(\tau)$ | cepstrum function |
| $c$ | damping constant of a support system, N/m/s |
| $D$ | damping factor for rotor vibrations |
| $d$ | rolling element diameter, m |
| $\delta$ | core fault current, largely in the quad axis, A |
| $E$ | Young's modulus of a material, $N/m^2$ |
| $E_e$ | stored energy in an electrical system, Joules |
| $E_1$ | transformer primary emf, V |
| $V_1$ | transformer primary voltage, V |

| | |
|---|---|
| $I_1$ | transformer primary current, A |
| $E_2$ | transformer secondary emf, V |
| $V_2$ | transformer secondary voltage, V |
| $I_2$ | transformer secondary current, A |
| $I_c$ | shorted stator winding circulating current, A |
| $e$ | specific unbalance $e = mr/M$, m |
| $e(t)$ | instantaneous induced EMF, V |
| $\varepsilon$ | strain in a material, % |
| $F$ | parameter from shock pulse measurement of a rolling element bearing |
| $F_{brg}$ | bearing frictional force, N |
| $F_m(\theta,t)$ | forcing function on a rotor or stator expressed in circumferential angle $\theta$ and time $t$, N |
| $f(t)$ | failure mode probability density, a Weibull function |
| $F_s$ , $F_r$ | stator and rotor magnetomotive forces (MMF), $NI$, ampere-turns |
| $F$ or $F^{-1}$ | forward or backward Fourier transform |
| $f_1$ | instantaneous MMF wave in an electrical machine air-gap, A/m |
| $f_0$ | first critical or natural frequency of a rotor system, Hz |
| $f_c$ | coolant flow rate, l/s |
| $f_n$ | the $n$th component of an unbalanced forcing function, Hz |
| $f_m$ | higher $m$th natural frequencies of the stator core, Hz |
| $f_{se}$ | electrical supply side frequency $= 1/T$, Hz |
| $f_{sw}$ | PWM switching frequency, Hz |
| $f_{sm}$ | mechanical vibration frequency on the stator side, Hz |
| $f_{rm}$ | mechanical rotational frequency $= N/60$, Hz |
| $G$ | strain gauge factor |
| $G$ | degree of residual unbalance as denoted by the quantity $G = e\omega$ |
| $G(f_k)$ | generalised power spectral function of frequency, $f_k$, the $k$th harmonic |
| $G^*(f_k)$ | complex conjugate of $G(f_k)$ |
| $G(m)$ | stiffness function of an $m$th natural frequencies of the stator core |
| $G(t_n)$ | generalised periodic function of time, $t_n$ |
| $g$ | acceleration due to gravity, m/s$^2$ |
| $g$ | air-gap length, mm |
| $g_n(z)$ | natural frequency function an $n$th solution of the balance equation |
| $h$ | heat transfer coefficient from an insulation surface, W/m$^2$K |
| $h_t$ | tooth depth, m |

| | |
|---|---|
| $I$ | rms current, A |
| $I_e$ | stator core magnetising current, A |
| $I_s$ | stator winding current, A |
| $I_w$ | stator core loss current, A |
| $I_o$ | stator core current $I_o = \sqrt{(I_e^2 + I_w^2)}$, A |
| $i(t)$ | instantaneous current, A |
| $J$ | polar moment of inertia of the core cylinder, Joule $s^2$ |
| $k$ | integer constant, indicates the $k$th space harmonic |
| $k$ | heat transfer coefficient through an insulating material, W/mK |
| $k$ | stiffness constant of a support system, N/m |
| $k_c$ | integer number of commutator segments in a DC machine |
| $k_c$ | integer constant, indicating vibrating stator core circumferential modes |
| $k_e$ | integer constant, indicating eccentricity order number, zero for static eccentricity, low integer value for dynamic eccentricity. |
| $k_l$ | integer constant, indicating vibrating stator core lengthwise modes |
| $k_r$ | reflection coefficient in the recurrent surge oscillography (RSO) test |
| $k_{wn}$ | stator winding factor for the $n$th harmonic |
| $k/nq$ | Hall-effect constant of an electronic material |
| $L$ | active length of a core, m |
| $L$ | inductance of a coil, H |
| $\Lambda$ | magnetic permeance, H |
| $\lambda$ | integer number of stator time harmonics or rotor winding fault harmonics |
| $\lambda$ | instantaneous failure rate or hazard function of a component, $\lambda = 1/\text{MTBF}$, failures/component/year |
| $\lambda(t)$ | failure rate of a component or machine varying with time, failures/component/year |
| $M$ | mass of a rotating system, kg |
| $M_s$ | mass of a support system, kg |
| $m$ | integer constant |
| $m$ | equivalent unbalance mass on a shaft, kg |
| $\mu$ | permeability in a magnetic field |
| $\mu$ | instantaneous repair rate, $\mu = 1/\text{MTTR}$, repairs/component/year |
| $N$ | integer number of turns of a coil |
| $N$ | speed of a machine rotor, rev/min |
| $N_r$ | integer number of rotor slots |

| | |
|---|---|
| $N_s$ | integer number of stator slots |
| $n$ | number of charge carriers per unit volume in a semiconductor |
| $\dot{v}n$ | integer constant |
| $n_b$ | integer number of rolling elements in a rolling element bearing |
| $P$ | active power, W |
| $P_{elcid}$ | phase axis in El CID testing |
| $Q$ | reactive power, Var |
| $Q$ | heat flow, W/m$^2$ |
| $Q_{elcid}$ | quad axis in El CID testing |
| $q$ | electronic charge, Coulomb |
| $q$ | integer number of stator MMF space harmonics, 1, 3, 5, 7 . . . |
| $\Delta R$ | change in resistance, Ω |
| $R$ | shock pulse meter reading |
| $R$ | resistance, Ω |
| $R_{\text{wind}}$ | winding resistance, Ω |
| $R_{\text{core}}$ | core resistance, Ω |
| $R_{\text{ins}}$ | insulation resistance, Ω |
| $R(t)$ | reliability or survivor function of a population of components as a function of time, failures/machine/yr |
| $R_{ff}(\tau)$ | auto-correlation function on a time function $f(t)$ with a delay of $\tau$ |
| $R_{fh}(\tau)$ | cross-correlation function between time functions $f(t)$ and $h(t)$ with a delay of $\tau$ |
| $R_0$ | resistance of a device made of the metal at 0 °C, Ω |
| $R_T$ | resistance, Ω |
| $r$ | effective radius of an equivalent unbalanced mass, m |
| $r_{\text{mean}}$ | mean radius of a core, m |
| $r_{\text{air-gap}}$ | radius of the air-gap, m |
| $\psi(t)$ | mother wavelet function of time |
| $S$ | total power, $S = \sqrt{(P^2 + Q^2)}$, VA |
| $S$ | constant related to the stiffness of a winding, insulation and tooth components |
| $S_d$ | smoke detection from a core monitor |
| $s$ | normalised slip of an induction machine, between 0 and 1, % |
| $\Delta T$ | change in temperature, K |
| $T$ | torque, Nm |
| $T$ | temperature, °C |
| $T$ | period of a wave, s |

| | |
|---|---|
| $T_e$ | volumetric vibration kinetic energy, J/m$^3$ |
| $T(f_1,f_2,f_3)$ | tri-spectrum |
| $t_0$ | radial thickness of a stator core annulus, m |
| $\tau$ | time delay in a correlation function, s |
| $\tau_0$ | time duration of an overheating incident, s |
| $\tau_r$ | residence time of an overheating product in a machine, or leakage factor, s |
| $\theta$ | MTBF of a component, $\theta = 1/\lambda$, h |
| $\theta_1$ | space position in the stator field, ° |
| $\theta_2$ | space position in the rotor field, ° |
| $u$ | lateral displacement of a machine rotor, μm |
| $u_r$ and $u_\theta$ | radial and peripheral displacements in a strained stator core, μm |
| VOC | Volumetric detection of total organic matter |
| $V$ | rms voltage, V |
| $V$ | machine volume, m$^3$ |
| $V_\iota$ | volumetric strain potential energy, J/m$^3$ |
| $v$ | velocity of the rotor, relative to the travelling flux wave produced by the stator, m/s |
| $v_v$ | volumetric rate of production of a detectable substance, m$^3$/s |
| $v_b$ | background rate of production of the substance, m$^3$/s |
| $\nu$ | Poisson's ratio of a material |
| $\Phi$ | flux, Wb |
| $\phi$ | contact angle with races of a rolling element bearing, ° |
| $\phi$ | electrical phase angle of a stator MMF wave $F_s$, ° |
| $\omega$ | angular frequency of an electrical supply, rad/s |
| $\omega_0$ | first critical or natural angular frequency of a rotor system, rad/s |
| $\omega_{se}$ | electrical supply side angular frequency, rad/s |
| $\omega_{sm}$ | mechanical angular vibration frequency on the stator side, rad/s |
| $\omega_{rm}$ | mechanical rotational angular frequency $=2\pi N/60$, rad/s |
| $\omega_{ecc}$ | angular velocity of an eccentricity, rad/s |
| $W$ | work function for strain energy in stator core |
| $W(a,b)$ | wavelet transform |
| $w_y$, $w_t$, $w_i$ and $w_w$ | weights of a core yoke, teeth, insulation and windings, respectively, kg |
| $w$ | weight per unit length per unit circumferential angle of a stator core cylinder, N/m |
| $X_{m_2}$ | second harmonic magnetising reactance, Ω |

| | |
|---|---|
| $X_{\lambda_2}$ | second harmonic leakage reactance, Ω |
| $Z_0$ | surge impedance of a winding, Ω |
| $z$ | longitudinal distance from the centre of a machine, m |
| $\rho$ | density of a material, kg/m$^3$ |
| $\sigma$ | electrical conductivity of a material, $\Omega^{-1}\text{m}^{-1}$ |
| $\sigma_r$ | radial Maxwell stress in the air-gap, N/m$^2$ |

# Abbreviations

| | |
|---|---|
| AI | Artificial intelligence |
| BDFIM | Brushless doubly fed induction machine, a specialised induction motor/generator |
| BJT | Band-gap junction transistor |
| BP | Back-propagation |
| CACA | Closed air-cooled internal open air-cooled external |
| CACW | Closed air-cooled internal open water-cooled external |
| CAPEX | Capital expenditure |
| CBM | Condition-based maintenance |
| COCW | Closed oil-cooled internal open water-cooled external |
| CM | Condition monitoring |
| CNN | Convolutional neural network |
| CSC | Current source converter |
| CWT | Continuous wavelet transform |
| BINDT | British Institute of Non-Destructive Testing |
| DBN | Deep belief network |
| DFIM | Doubly fed induction machine |
| DFT | Discrete Fourier transform |
| DL | Discharge locator |
| DSP | Digital signal processor |
| DWT | Discrete wavelet transform |
| EMI | Electromagnetic interference |
| ETD | Embedded temperature device |
| FBG | Fibre Bragg grating |
| FPGA | Field-programmable gate array |
| FFT | Fast Fourier transform |
| FMEA | Failure modes and effects analysis |
| FMECA | Failure modes effects and criticality analysis |
| FRA | Frequency response analysis |

| | |
|---|---|
| GTO | Gate turn off thyristor |
| HFPD | High-frequency PD detection device |
| HHT | Hilbert–Huang transform |
| HPP | Homogeneous Poisson process |
| HPSRA | Hybrid physics statistics reliability analysis |
| IAS | Instantaneous angular speed method |
| IC | Integrated circuit |
| IGBT | Insulated gate bipolar transistor |
| IR | Insulation resistance |
| JFET | Junction field effect transistor |
| LCC | Lifecycle costing |
| LCOE | Levelised cost of energy |
| LFPD | Low-frequency PD detection device |
| LVDT | Linear variable differential transformer |
| MAR | Mercury arc rectifier |
| MBVI | Model-base voltage and current systems |
| MCSA | Motor current signal analysis |
| ML | Machine learning |
| MLP | Multi-layered perceptron |
| MOSFET | Metal-oxide semiconductor field-effect transistor |
| MTBF | Mean Time Before Failure or Mean Time Between Failures |
| MTTR | Mean time to repair |
| OPEX | Operational expenditure |
| PD | Partial discharge |
| PHM | Prognostics and health management |
| PI | Polarisation index |
| PID | Proportional-integral-derivative |
| PLP | Power law process |
| PoF | Physics of failure reliability analysis, applicable to power electronics |
| PSD | Power spectral density |
| PWM | Pulse width modulation |
| RBM | Restricted Boltzmann machine |
| RCA | Root cause analysis |
| RF | Radio frequency |
| RFCT | Radio-frequency CT |
| RFI | Radio-frequency interference |

| | |
|---|---|
| RIFI | Radio-interference field intensity |
| RPDIV | Repetitive partial discharge inception voltage |
| RSO | Recurrent surge oscillograph |
| RTD | Resistance temperature device |
| SCADA | Supervisory control and data acquisition |
| RUL | Remaining useful lifetime |
| SSC | Stator slot coupler |
| SOM | Self-organising mapping |
| TVA | Tennessee Valley Authority probe |
| TBF | Time between failures |
| TEFC | Totally enclosed forced air-cooled |
| TTF | Time to failure |
| UMP | Unbalanced magnetic pull |
| VSC | Voltage source converter |
| VSD | Variable-speed drive |
| WVT | Wigner–Ville transform |

*This page intentionally left blank*

*Chapter 1*

# Introduction to condition monitoring

## 1.1 Introduction

This book is about the condition monitoring (CM) of rotating electrical machines. To develop this understanding, we need to acknowledge:

- Fundamental electrical machines principles,
- Principles of variable speed drives applied to electrical machines,
- Principles of reliability applied to machines and drives so that we can understand how CM can best be applied.

Rotating electrical machines permeate all areas of modern life at both the domestic and industrial level. The average modern home in the developed world contains 20 to 30 electric motors in the range 0–10 kW for clocks, toys, domestic appliances, air conditioning or heating systems. Modern cars use electric motors for windows, windscreen wipers, starting and now even for propulsion in hybrid and electric vehicles. A modern Jaguar E-Pace car has two permanent magnet synchronous drive motors and more than 40 other electrical machines.

The majority of smaller applications of electrical machines do not require monitoring; the components are sufficiently reliable that they can outlive the life of the parent product.

However, modern society depends, directly or indirectly, upon machines of greater rating and complexity in order to support an increased standard of living.

The electricity we use so freely is generated in power plants by machines, whose ratings can exceed 1 000 MW, have evolved to a state of great sophistication. These power plants are supported by fossil fuel and nuclear energy industries that are transporting raw materials using pumps, compressors and conveyors in sophisticated engineering processes incorporating rotating electrical machines of powers from 100 kW to 100 MW. These have been joined by a growing renewable energy industry using many of these and new techniques to extract energy from sources with machines of ratings from 200 kW to 10 MW, often in combination with traditional sources.

The steel used in cars will have been rolled using large electrical machines, and at an earlier stage still the furnaces will have been charged using more electrical machines.

Our water and waste systems are also driven by electrical machines as are the processes that produce the raw materials for the agricultural, chemical and pharmaceutical industries.

Without all these our society, as it is arranged at the moment, would cease to function.

The overall picture is that electrical machines come in many sizes and they fulfil their function either independently, or as part of a highly complex process in which all elements must function smoothly so that production can be maintained.

It is the usage of electrical machinery in the latter role that rose dramatically towards the end of the twentieth century, and there is no reason to suspect this trend will do other than accelerate through the twenty-first century. However, historically the function of an individual electrical machine was seen as separable from the rest of the electromechanical system. It must be remembered that the power-to-weight ratio of electrical machines has been much lower than steam, diesel and gas engines and consequently their reliability has been much higher.

It is against this background that the basic principles of protective relaying evolved. Protection is designed to intercept faults as they occur and to initiate action that ensures that the minimum of further damage occurs before failure. In its basic form, the protective relay has the function outlined in Figure 1.1.

The signal provided by the transducer will be in the form of a current or voltage, and will be interpreted by the relay as an acceptable, or unacceptable, level according to a pre-set value worked out by the relay designer or maintenance staff. If the pre-set value is exceeded, then the relay will initiate further electromechanical action that will often result in disconnection of the electrical machine, and it will flag the fact that a fault, or even failure, has been identified. This is a simplistic view of the protective relay, which were configured using electromechanical devices such as relays to carry out their function, as the name implies. However, nowadays most protective relays use digital processors to deploy a wide range of functions, and are programmable to allow more sophisticated criteria for initiating interrupt procedures to be applied. For example, to block the restart of a motor until it has cooled to an acceptable degree. Figure 1.2 shows a typical modern programmable relays for fulfilling such functions.

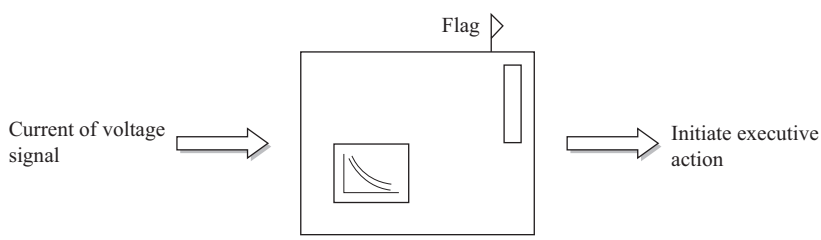


*Figure 1.1 The basic function of an electrical protective relay*

*Figure 1.2 Typical modern digital protection relays*

From what has been said above, it is apparent that protective relaying can be regarded as a form of monitoring, and indeed it is widely used with great success. Modern digital relays have also started to fulfil a monitoring function since they can record the voltages and currents they measure for a period before and after any fault. In fact, many failure investigations on electrical machines, involving root cause analysis, start with the download and analysis of the digital protective relay data, which can usually be displayed clearly in an Excel spreadsheet. Virtually all electrical machine protection systems embody some form of protection device, and on typical machines they are used in some or all of the following schemes:

- earth fault protection,
- overcurrent protection,
- differential current protection,
- under and overvoltage protection,
- negative phase sequence protection,
- field failure protection,
- reverse power protection,
- overspeed protection,
- excessive vibration protection,
- thermal overload protection.

This list is representative rather than exhaustive.

It is important to stress the fact that protection is basically designed to act only once a fault has occurred, and it will normally initiate some executive action, 'the function of protective equipment is not the preventive one its name would imply, in that it takes action only after a fault has occurred; it is the ambulance at the foot of the cliff rather than the fence at the top'.

CM needs to establish itself as 'the fence at the cliff-top'.

The executive action may very well be the disconnection of the piece of machinery from the supply. Such action is acceptable if the item of plant is readily dissociated from the process it is involved with, or if it exists

substantially in isolation. If, however, the piece of plant is vital to the operation of a process then an unscheduled shutdown of the complete process may occur. The losses involved may then be significantly greater than those resulting simply from the loss of output during a scheduled shutdown. It must also be borne in mind that the capital cost of an individual machine is more often than not small compared with the capital costs involved in a plant shutdown. Maintenance is most effective when it is planned to service many items in the course of a single outage.

In summary, CM of an electrical machine is not necessarily aimed solely at the machine itself, but at the wider health of the process of which it is part.

## 1.2 Need for monitoring

The notion of the scheduled shutdown or outage introduces us logically to the case to be made on behalf of monitoring.

By CM we mean the continuous evaluation of the health of plant and equipment throughout its serviceable life. CM and protection are closely related functions. The approach to the implementation of each is, however, quite different. Also, the advantages that accrue due to monitoring are entirely different to those to be expected from protection.

This is principally because monitoring should be designed to pre-empt faults, whereas protection is essentially retroactive. CM can, in many cases, be extended to provide primary protection, but its real function must always be to attempt to recognise the development of faults at an early stage. Such advanced warning is desirable since it allows maintenance staff greater freedom to schedule outages in the most convenient manner, resulting in lower down time and lower capitalised losses. Figure 1.3 shows this process.

We have said above that advanced warnings of malfunctions, as provided by monitoring, are desirable. Are they? We must justify this because the implementation of a monitoring system can involve the operator in considerable expense. There are other questions to be answered too, for example,

- Once one has chosen to embark upon a programme of monitoring what form should it take?
- Should the monitoring be intermittent, regular at fixed time intervals, or continuous?
- If one employs a fixed time interval maintenance programme then is it necessary to monitor at all?
- Monitoring can generate large quantities of data; how can this information be best stored and used to minimise future expenditure?

Finally, and perhaps most importantly, how much needs to be spent on monitoring in order to make it truly effective?

These questions do not have simple answers but we can get some indications by considering the magnitude of the maintenance and replacement burden that

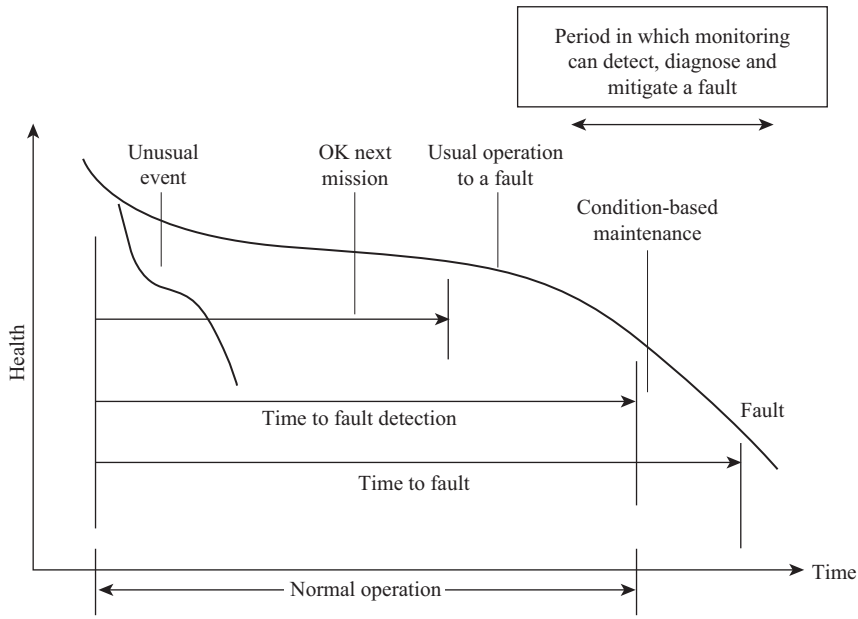


*Figure 1.3 Progression of an electrical machine to failure showing the benefit of CM*

industry is continually facing, and the implications for the costs of various maintenance strategies. We could consider three different courses of action:

- Breakdown maintenance,
- Fixed-time interval or planned maintenance,
- Condition-based maintenance.

Method (i) demands no more than a 'run it until it breaks then replace it' strategy, whilst method (ii) may or may not include a degree of monitoring to aid in the planning of machinery outages. The final scenario method (iii) requires a definite commitment to monitoring.

The scale of investment can be seen from figures provided by Neale (1979). This information is now 30 years old from before a long period of privatisation but is still invaluable. Table 1.1 shows the annual investment per employee in plant and machinery. We have modified these values in order to reflect more realistically today's costs and have selected those industries that would have a high proportion of expenditure in electrical machinery and ancillary plant.

The same report shows that the average annual expenditure on maintenance was 80% of the capital annually invested in plant and machinery. The figures for some selected industries and industrial groupings are shown in Table 1.2, which shows the annual maintenance expenditure as a percentage of the annual plant

*Table 1.1 Expenditure on plant per employee of selected industries, Neale (1979)*

| **Industry** | **Annual investment/employee in plant and machinery** |
|---|---|
| North Sea Oil and Gas | £160 000 |
| Oil refining | £14 000 |
| Electricity supply | £8 000 |
| Chemical industry | £2 400 |
| Iron and steel | £1 800 |
| Water supply | £800 |
| Textile manufacture | £600 |
| Instrumentation manufacture | £400 |
| Electrical engineering manufacture | £400 |

*Table 1.2 Annual maintenance expenditure as a percentage of annual capital investment in plant, for selected industries, Neale (1979)*

| **Industry** | **Maintenance expenditure/ Plant expenditure** |
|---|---|
| Printing | 160% |
| Instrumentation manufacture | 150% |
| Mechanical engineering | 100% |
| Textile manufacture | 82% |
| Water supply | 80% |
| Gas supply | 80% |
| Electricity supply | 80% |
| Electrical machinery manufacture | 80% |
| Chemical manufacture | 78% |
| Marine engineering | 50% |
| Iron and steel manufacture | 42% |
| Coal production | 26% |

investment expenditure. This is a high figure in real terms and anything that helps to reduce it must be welcome. The Hewlett–Packard Journal has quoted the staggering figure of $200 billion as the annual maintenance bill for U.S. business, and a growth rate of 12%. Now only a fraction of this sum will be spent on maintaining electrical machinery, but even if it amounts to only points of per cent of the total it is still an enormous amount of money.

There are great incentives to maintain plant more efficiently, particularly when it is estimated that approximately 70% of the maintenance work carried out by

companies that use no planning at all may be classified as emergency work and must be done at premium costs.

It is apparent that careful thought should be given to the most appropriate form of maintenance planning. Breakdown maintenance can only be effective when there is a substantial amount of redundant capacity or spares are available, and a single breakdown does not cause the failure of a complete system. The question to be answered in such circumstances is, 'why is there a significant redundancy'? And should it be allowed to continue?

Many sectors of industry, and particularly the electricity, water and gas utilities and the railways, have adopted maintenance planning based on replacement and overhaul at fixed time periods, so that outage work can be scheduled, diversions and loads can be planned. Such scheduling is usually planned on the basis of plant monitoring, and the monitoring is typically done on a discontinuous basis. There are many estimates of the savings that accrue by adopting such an approach, and an average reduction figure of 60% of the total maintenance burden may be considered reasonable. This is good news, but it must be treated cautiously because such a maintenance policy makes heavy demands upon scarce, skilled manpower. It is also estimated that only 10% of components replaced during fixed interval maintenance outages actually need to be replaced at that time. The obvious implication is that 90% of what is replaced need not be.

Such considerations, and the realisation that modern electrical machines and the processes they operate in are growing in complexity, leads one to the conclusion that continuous CM of certain critical items of plant can lead to significant benefits. These benefits accrue in:

- Greater plant efficiency,
- Reduced capitalised losses due to break-down,
- Reduced replacement costs.

The plant operator can also be updated with information on the performance of his machinery. This will help him to improve the day to day operational availability and efficiency of the plant. CM should give information relevant to both the operational and maintenance functions.

There is an added bonus in that better maintenance gives better safety.

In the longer term, CM also allows the operator to build up a data base that can be used for trend analysis, so that further improvements can be made in the scheduling of maintenance. Such information should also be used advantageously by the manufacturers and designers of plant in order to further improve product reliability. This step effectively 'closes the loop'.

In view of the above, how much needs to be spent on monitoring? This depends on the value of the process in which the machine works, and estimates vary, but are never less than 1% of the capital value of the plant being monitored. A more typical, and probably more realistic, figure would be 5% for the general run of industrial processes, whilst special requirements for high value processes, such as those found in the offshore oil and gas industry, may push a realistic figure above 10%.

## 1.3 What and when to monitor

Now that we have examined some of the advantages to be gained from a commitment to CM we can briefly address the questions, what should we monitor, and when? The question of what to monitor, has two implications:

- What machines?
- What parameters or signals?

The first part is more easily answered. In view of the capital costs involved in providing monitoring, whether it takes the form of a permanent installation with its own local intelligence, or a hand-held device used periodically by a skilled operator, it is unlikely that electrical machines with ratings less than 20 kW would benefit. There are, of course, exceptions to this where a smaller machine has a vital function in the performance of a larger system. It will pay dividends to carefully consider the implications of losing the output of an individual piece of machinery, in the context of a complete system.

Larger electrical drives, that support generating, process or production plant if a high margin of spare capacity exists, will benefit from monitoring, although perhaps not continuous monitoring. One could include induced and forced-draught boiler fan drives, boiler water feed pump drives, and cooling water pump drives in power stations, in this category. It must be borne in mind, however, that successful monitoring can allow a big reduction in the requirement for on-site spare capacity.

Machines that have a high penalty in lost output costs need to be monitored continually. Large generators naturally fall into this category since lost output can exceed £1M/day for a large machine in a high efficiency power station. A similar approach would apply to large propulsion motors and large process drive motors.

The conclusion is that there are machines to which monitoring is readily applicable, but there are other circumstances where careful assessment is needed before deciding. One must always be mindful of the scale of the maintenance burden however nor be driven to false economies on the basis that ‘nothing has gone wrong so far’. On the other hand, one must bear in mind the complexities of the monitoring system itself and its own maintenance burden. Nothing can be worse than to invest in complex monitoring equipment, which because of poor design or maintenance gives rise to large numbers of false alarms and lead to the equipment being ignored.

The parameters to be monitored are essentially those that will provide the operator and maintainer with sufficient details to make informed decisions on operation and maintenance scheduling, but which ensure security of plant operation. Automatic, online, monitoring has only recently begun to make an impact in the area of electrical machines. Traditionally quantities, such as line currents and voltages, coolant temperatures, bearing vibration levels, have been measured and will continue to be used. Other quantities, involving the sensing of pyrolysed products in cooling gases and oils, have recently been introduced, as have techniques for measuring contamination levels in bearing lubricants. Other specialist methods,

involving the accurate measurement of rotational speed, or the sensing of leakage fluxes, are being developed in order to monitor a variety of fault conditions.

As the ready availability of sophisticated electronic and microprocessor-based systems is translated into monitoring hardware, then the more variables it is possible to consider, and the more comprehensive the monitoring can be. This trend will be further accelerated as the costs of computing power fall still further, and the complexity of microprocessors increases. Such developments are essential both because of the complexity of the plant being monitored and the complexity of the monitoring signals themselves.

The question when to monitor, is more easily answered. One should monitor when it is cost-effective to do so, or when there are over-riding safety considerations to be observed. The assessment of cost-effectiveness can be a relatively complex matter, but in general terms monitoring is worthwhile when the net annual benefits are increased by its use. The net annual benefit is the difference between the gross annual benefit the annual costs including those of monitoring. The costs of monitoring include the initial investigation, purchase, and installation charges, staff training costs, costs of data acquisition and the cost of presenting the results to the operator. This expenditure can be written off over the lifetime of the monitoring system and set against the savings accrued.

As a general principle the larger the machine rating and its annual benefit the less significant will be the amortised CM.

Thus, a large 600 MW turbo-generator earning £50M/yr can readily afford a £50k/yr outlay on CM, as could a 10 MW propulsion motor for a cruise liner earning £5M/yr. However, smaller machines, such as 200 kW commuter train propulsion motors or the 20 kW electric car propulsion motors, may struggle in that justification.

But safety and maintenance consequences of commuter train failure may justify monitoring expenditure.

It is interesting that the wider application of electrical drives to aircraft, where safety is paramount, is leading to a demand for CM for such machines at ratings down to 10 kW.

Another such example is in distributed renewable energy, when wind turbine deployments were limited onshore to 1 MW there was little appetite for CM. But as offshore turbine outputs increase $>8$ MW, CM has become increasingly interesting, justified less by lost production costs but rather the need to reduce costly and dangerous offshore maintenance staff deployment.

It is sufficient to say that it is not uncommon in the right application for the capital costs of a wisely chosen monitoring system to be retrieved in the first year of its operational life. However, it is true to say that, since the first edition of this book, many more electrical machines, ranging in size from 50 kW to 1 000 MW, are now being continuously condition monitored to enable planned, reduced cost maintenance, as will be discussed in a later chapter.

Finally, it is tempting to think that, with such a degree of monitoring power becoming available, the protective and monitoring functions could be merged.

With the development of more powerful digital protection and improved signal condition and data acquisition systems (SCADA) this is happening, but care must be taken and operational experience must be established before these functions merge. It is likely that this will happen when artificial intelligence (AI) is sufficiently developed to make reliable full use of measured signals and alarms.

## 1.4 Technological timelines

When reviewing electrical machine CM it is useful to consider the timeline for electrical machine development going back to the start of the nineteenth century. On the other hand, the timeline for variable speed technology began at the start of the twentieth century and for reliability in 1940. These timelines show that:

- Principal electrical machine designs, DC and AC, were all defined by the start of the twentieth century but took another 50–60 years for their analyses to be resolved,
- DC and AC variable speed drives were envisaged from the start of the twentieth century but were initially enabled using rotating commutators for both DC and AC machines,
- This changed in the mid-twentieth century with the availability of power electronics, firstly vacuum tube valves and then semi-conductor devices,
- Reliability analysis has influenced the drives development timeline since the 1950s, following initial power electronics unreliability during the Second World War,
- Unreliable rotating commutators were rapidly superseded by reliable static commutators from the late 1970s, with the availability of more reliable, controllable power electronic switches,
- CM of electrical machines emerges in the 1980s,
- Control of speed accelerated with the development of power microprocessors in the 1980s followed by the use of digital signal processors (DSP) and field-programmable gate arrays (FPGA),
- DSP and FPGA developments also facilitated CM, housed in those processors, which progressed in the 1990s as a consequence of continuing economic changes in the electrical/electronics industry,
- Reliability analysis has progressively improved power electronic switch and controller reliability but has had relatively little effect on machine designs at the end of the twentieth century,
- However, reliability analysis has affected machine and drive operation and maintenance costs, which rose in the early twenty-first century, now influenced by the application of modern CM.

An appendix of the book gives the detailed timeline, identifying all key machine, drive and reliability technologies but Table 1.3 below provides a useful summary.

*Table 1.3 Technological timeline summary, machines, drives and reliability; refer to Drury (2009) and Chung* et al. *(2016)*

| Electrical Machines Timeline | Years | 1820–73 | 1838–73 | 1880 | 1885–90 | 1911 | 1921 | 1957 | 1950–88 | 1986 | Late 1980s | 1989 | 2013 |
|---|---|---|---|---|---|---|---|---|---|---|---|---|---|
| | Subject | Electroma-gnetism | DC Machine | Synchronous AC machine | Induction AC machine | AC variable speed machine | The diagnosing of trouble in electrical machines | AC variable-speed machine | Classic papers and books | CM of rotating electrical machines | AC variable-speed machine | Electrical insulation for rotating machines: design, evaluation, aging, testing, and repair | Analysis of electric machinery and drive systems |
| | Technology | | | Two-or three-phase stator windings and a solid rotor excited with a DC winding | One, two-or three-phase stator windings and a closed or squirrel cage rotor winding | Implemented with AC machines using a rotating commutator | Book | Implemented with AC machine using a thryistor Current Source static commutator | Machine troubles and analyses | Book | Implemented with AC machine using a PWM IGBT Voltage Source static commutator | Book | Book |

*(Continues)*

*(Continued)*

| VSD and Power Electronic Technology Timeline | | | | | | | | | | | | | | | |
|---|---|---|---|---|---|---|---|---|---|---|---|---|---|---|---|
| | Years | 1896 | 1904 | 1909 | 1911 | 1957 | | 1940–70 | 1975 | 1980 | 1980s | Late 1980s | 2000 | 2010 | 2015 |
| | Subject | DC variable-speed machine | DC variable-speed machine | Vacuum-tube rectifiers | AC variable-speed machine | Thyristor | AC variable-speed machine | AC variable-speed machine | Fast-switching semiconductor devices | Application of fast-switching semiconductor devices | IGBT | Application of IGBT | Schottky SiC diode | Advanced devices | |
| | Technology | Proposed two DC machines back-to-back using a rotating commutators | Implemented with two AC/DC machines back-to-back using a rotating commutators | Mercury arc rectifier, Vacuum-tube rectifier and Thyratron | Implemen-ted on AC machines using a rotating commutator | Invention of power drive thyristor and firing circuits | Implemented with AC machine using a thyristor current source static commutator | Implemented as an NA AC machine with shunt transformer and variable induction regulator using a rotating commutator | Invention of new fast-acting semiconductor devices | Application of GTO, GTR, power MOSFET and thyristors controlled by microprocess-ors to variable-speed drivers | Invention of the Inverse Gate Bipolar Transistor power switch | Application of GTO, power MOSFET and thyristors controlled by DSPs and FPGAs to variable-speed drivers | First Schottky SiC diode to the market | Application of SiC, MOSFETs, JFETs, BJTs andGaN power devices to variable-speed drivers. | Cost reduction of wide band-gap power devices. Improved performance of Si power devices. Intelligent powerstacks |
| | Inventor, developer, author | Ward Leonard | Kramer | Various industrial companies | Schrage | Schckley | Various industrial companies | Schwarz | General Electric | Various industrial companies | Scharf | Various industrial companies | Various industrial companies | Various Commercial companies | Various Commercial companies |
| | | | | | | Moll | | | | | | | | | |

| Reliability Timeline | | | | | | | | | | | |
|---|---|---|---|---|---|---|---|---|---|---|---|
| | Years | 1940 | 1957 | 1974 | 1975 | 1985 | 1990 | 1991 | 1995 | 2005 | 2015 |
| | Subject | Vacuum-tube devices | AGREE Report | Machines reliability | Reliability analysis | Reliability analysis | IEEE Gold Book | MIL-HNDBK 217 | MIL-HNDBK 217 superseded | Hybrid physics analysis | Reliability of power electronic convertor systems |
| | Material | | Standard | Paper | | | Book | Standard | Standard | | Book |
| | Technology | Invention of vacuum-tube devices, mass-production and first reliability engineering | Advisory group on reliability of electronic equipment report published | Operation and reliability of electrical machines. Identifies constant failure rates, $\lambda$ | System-level, reliability, safety and reliability software becomes available | Accelerated life testing, use of Bayesian statistics and six sigma | *Recommended Practice for Design of Reliable Industrial and Commercial Power Systems.* Identifies constant failure rates, $\lambda$, and hence MTBF values for electrical machines | *Military HandBook-Reliability Prediction of Electrical Equipment.* Based upon constant failure rates, $\lambda$, and MTBF | For power electronics Physics of failure (PoF) reliability analysis and varying failure rate, $\lambda(t)$ supersedes MIL-HNDBK 217F, based on constant failure rates, $\lambda$, and MTBF. However, for machines constant failure rate, $\lambda$, and MTBF still the only available guidelines | Hybrid physics statistics reliability analysis supercedes PoF for complex electronic products. Increased multiphysics simulations. | Chung *et al.* |
| | Inventor, developer, author | Various | AGREE | Dickinson, IEEE paper | Various software companies | Various industrial companies | IEEE | US Department of Defense | | Various power electronics companies | Various power electronics companies |

## 1.5 Structure of text and bibliographies

The structure of the book is organised as follows:

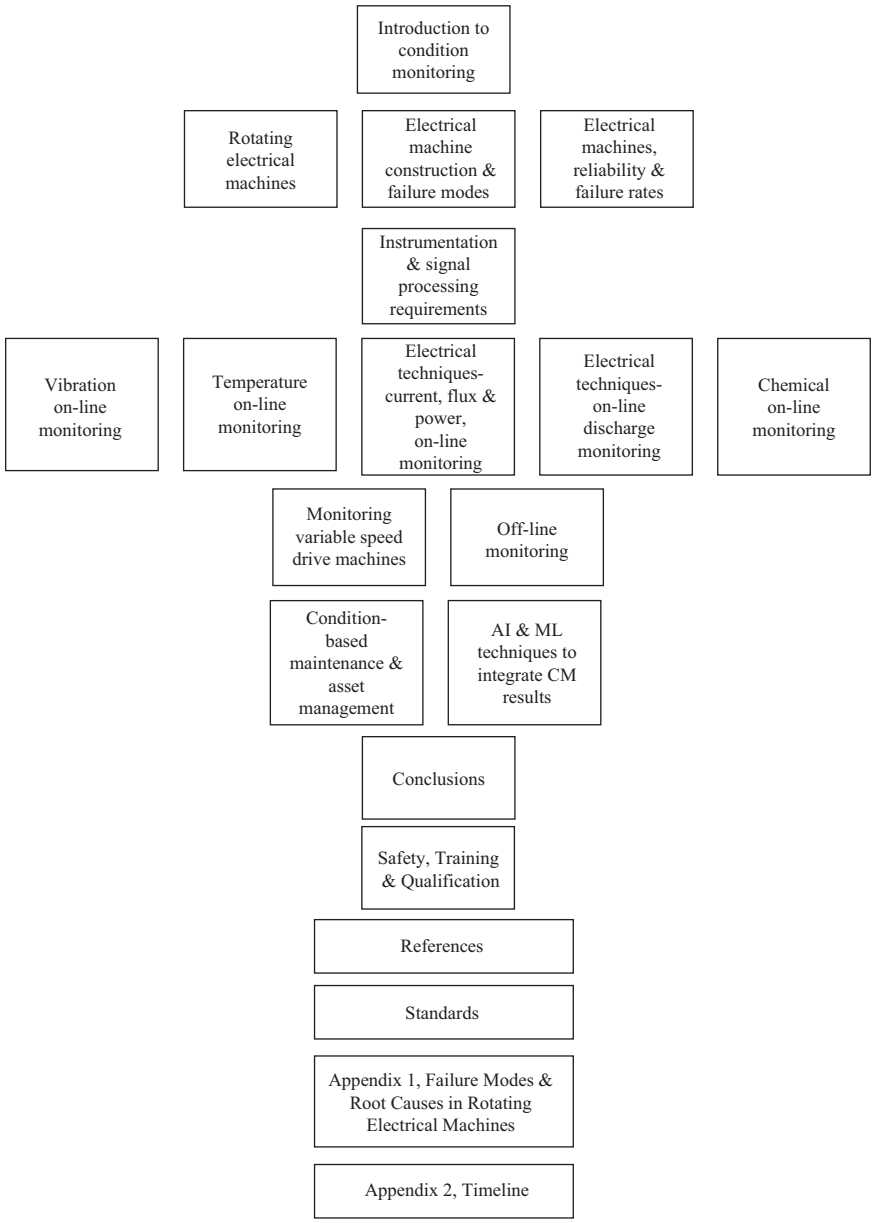

Our book includes References from the following substantial subject reviews, each taken from a different monitoring point of view:

- Penman *et al.* (1980) electrical monitoring review,
- Tavner *et al.* (1986) large motor and generator monitoring review,
- Benbouzid (1999) comprehensive review,
- Benbouzid (2000) induction motor electrical signal analysis review,
- Singh *et al.* (2003) induction machine drive CM, review,
- Nandi *et al.* (2005) motor monitoring and fault diagnosis review,
- Tallam *et al.* (2007) induction machine stator-related fault diagnosis review,
- Bellini *et al.* (2008) advances in induction machine diagnosis review,
- Tavner (2008) extension of 1986 work,
- Zhang *et al.* (2011) MV induction motor monitoring and protection review,
- Stone (2014) motor stator winding monitoring and diagnosis review,
- Riera-Guasp *et al.* (2015) machine and drive monitoring and fault diagnosis review.

To reduce the reference numbers, we have limited References to seminal books, significant IET Journal and IEEE Transaction papers and seminal conference papers only, where appropriate.

*This page intentionally left blank*

*Chapter 2*

# Rotating electrical machines

## 2.1 Introduction

The early principles of electrical machines were established from 1820 by the international inventions of Oersted, Faraday, Arago, Lenz, Wheatstone and Cook, summarised in Appendix C, culminating from 1832 to 1873 in the manufacture of DC machines by Pixii and Gramme and the first DC machine design paper, Hopkinson (1886).

The development of AC machines was also an international endeavour, starting with inventions from 1879 to 1890 by Babbage, Herschel, Bailey, Ferraris, Tesla and Dobrowlsky but the design was not harmonised for synchronous AC machines until Concordia (1908) and for asynchronous or induction AC machines until Alger (1965).

The international development of electrical machine variable-speed drives (VSDs) originally started with rotating commutator DC machines, then through a seminal paper by Ward Leonard (1896), in the mid-1900s, using AC machines with rotating commutators and then by the development of static commutators, based on Ward Leonard's principles. These were applied to AC induction and permanent magnet machines, realised in power electronics from 1923 to 1950, using the ignitron or mercury arc rectifier (MAR) and from 1950 using thyristors and then insulated gate bipolar transistors (IGBTs).

The principles of machines' CM were hinted at by Miles Walker (1929) but have been largely set out in papers and books from 1980 onwards. The CM of VSDs was proposed by Vas (1993) followed by subsequent papers, including Yang and Ran *et al.* (2010) and Riera-Guasp *et al.* (2015).

Key elements of all these developments can be seen, in year and alphabetical order, at the end of Chapter 2, in the References and Appendix B-Timelines.

Electrical machines and VSDs now permeate all areas of modern life, both domestic and industrial, and the CM of electrical machine is unique in that the all-embracing nature of the electro-magnetic field, the machine's modus operandi, enables us to infer more about operation from terminal 'performance' conditions than could be the case for non-electrical rotating plant.

Furthermore, the CM of electrical machines is dominated by the materials from which they are constructed:

- Strong but brittle ferromagnetic steel laminations, steel pole pieces and permanent magnets, the electromagnetic core,
- Conducting but ductile and mechanically weak machine conductors, the windings,

- Separated by dielectrically strong but mechanically weak and thermally vulnerable tapes, boards and resins, the insulation,
- Supported by bearings and lubricants which separate rotating from stationary parts.

These facts lie at the heart of the development and effectiveness of rotating electrical machine CM. A study of the key papers show how the subject science has evolved under these principles, first into mechanical monitoring, vibration, then into electrical monitoring, voltage and current, then into insulation monitoring and finally into the monitoring of complex machine and drive combinations.

We will first consider the structure of electrical machines and then four main types, DC machines, AC machines, synchronous or asynchronous (induction), and permanent magnet or reluctance machines, in preparation for considering how they can be monitored. In each case, we will describe their basic connection circuit, equivalent circuit for analysis and then show their magnetic field that supports the transfer of energy from stator to rotor in the case of a motor, or vice versa in the case of a generator. This approach is based on the clear French logic set out by Langlois-Berthelot (1950).

## 2.2 Electrical machines structures and types

The previous section provided a brief description of the history of the electrical machine, the main constructional components and materials from which they are made.

In this section, the detailed structure for assembly of the electrical machine is discussed and the effect upon it of different types of machine. This structure, exemplified by the clear logic of Langlois-Berthelot (1949), is demonstrated for two very different machines in Figure 2.1. Note the similarities between the 4 kW induction motor in Figure 2.1(a) and the 125 MVA synchronous generator in Figure 2.1(b).

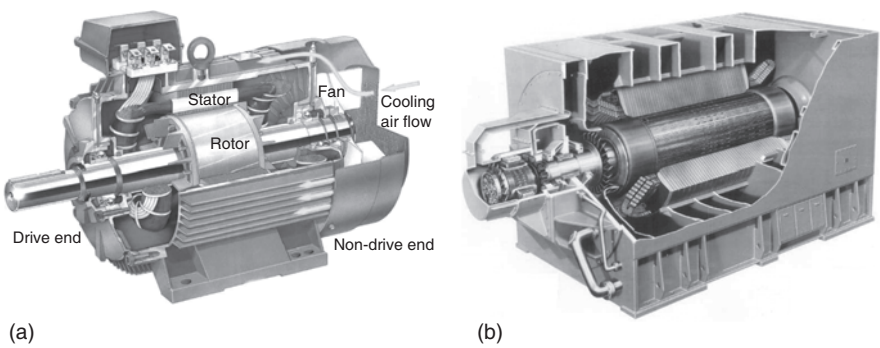


*Figure 2.1 Structure of electrical machines, stator frame, stator core and windings, rotor and bearings: (a) 4 kW induction motor and (b) 125 MVA synchronous generator*

This structure is also presented in tabular form in Table 2.1, which will form the basis for considering machine faults later in the chapter. The differences between structure for assembly and reliability will be described in Chapter 3.

Note that generators require an exciter to provide the field current for their rotor. They generally have their exciters mounted on the shaft of the main machine and a large generator can have a pilot exciter and main exciter. The main and pilot exciters are clearly visible on the left in Figure 2.1(b). Therefore, a generator may consist of two or even three electrical machines on the same shaft. This is important when carrying out a failure modes and effects analysis, in considering the number of sub-assemblies in the machine, see Chapter 4, when the number of components affects the predicted failure rate of the machine.

Table 2.1 sets out the major types of electrical machine, which shows the main constructional features of each type and factors most likely fault root causes; this is a useful reference when considering in later sections the design principles of each machine design.

Deterioration of performance or failure in service can occur due to the damage of any of these components, and the descriptions of failures at the end of this chapter show how wide-ranging these root causes can be.

However, experience shows that particular components are under specific electrical, mechanical and/or thermal stress and to a large extent those components depend on the size and type of the machine.

Table 2.2 gives a range of typical sizes for some larger electrical machines and shows some important mechanical electrical and thermal parameters in the design of electrical machines, which determine their ability to meet the conditions described in the previous sections, namely:

- Magnetic loading, T,
- Electric loading, A/mm,
- Current density, A/mm$^2$,
- Mechanical loading, rotor peripheral velocity, mm/s.

The values of these parameters in Table 2.2 give an idea of their limits in all electrical machines. What is noticeable is that magnetic flux densities are similar over huge ranges of power, power/weight ratios are relatively low and only increase in exceptionally large machines or in very small machines through the use of novel cooling or advanced materials, such as permanent magnets, but it is remarkable that very high torque densities, for propulsion motors or hydro generators, are achievable in large radius, highly rated, large machines.

Figure 2.2 summarises typical power–weight ratios over a wide range of sizes and types of electrical machine ranging from a small high-speed, air-cooled vacuum cleaner motor on the left to a massive hydrogen- and water-cooled turbo-generator on the right.

What is striking about Figure 2.2 is the relatively small range of power–weight ratios, 0.2–3.0 kW/kg, and that both small and large machines can have high power–weight ratios, occurring at low power because of high-speed and at high power by the use of more effective coolants. The limited power–weight ratio range

*Table 2.1 Types of rotating electrical machines*

| Main type of machine | Sub-types | Size range | Main constructional features | Root causes |
|---|---|---|---|---|
| DC machines | Generators | 20 kW–5 MW | Diameter ≈ length<br>Horizontally mounted<br>Medium rotational speed 500–1 800 rev/min<br>Traction or special applications | Field or armature winding electrical faults incurring consequential damage<br>Commutator faults<br>Brush-gear faults<br>Carbon dust contamination problems<br>Associated control gear problems |
| | Motors | 1 kW–2 MW | Diameter ≈ length<br>Horizontally mounted<br>Medium rotational speed 500–1 800 rev/min<br>Application to specialised variable-speed applications particularly traction, declining compared to AC VSDs | Field or armature winding electrical faults incurring consequential damage<br>Intermittent duty thermal problems<br>High-shock loading problems<br>Commutator faults<br>Brush-gear faults<br>Carbon dust contamination problems<br>Associated control gear problems |
| AC machines, synchronous | Steam and gas-turbine driven generator | c25-1 500 MVA | Length ≫ Diameter<br>Horizontally mounted<br>High rotational speed, 1 500–3 600 rev/min<br>Close circuit air or gas-cooling<br>Water-cooled stator windings in larger sizes<br>Water-cooled rotor windings in some designs<br>Fossil fuel and nuclear generation | Stator or rotor winding electrical faults incurring consequential damage<br>High-speed balance problems<br>Excitation faults exacerbate balance problems<br>Stator end winding bracing problems<br>Rotor end bell integrity problems<br>Gas-cooling circuit sealing problems<br>Water-cooling circuit sealing problems<br>High-performance oil film bearings<br>Enclosed casing means difficult to inspect frequently |

| | | | | |
|---|---|---|---|---|
| | Water turbine driven generator | c10-1 000 MVA | Diameter ≫ Length<br>Vertically or horizontally mounted<br>Low rotational speed, 80–300 rev/min<br>Air-cooled<br>Water-cooled stator windings in larger sizes<br>Hydroelectric generation | Stator or rotor winding electrical faults incurring consequential damage<br>Air-cooling and high stresses lead to discharge erosion on HV windings<br>Rotor pole integrity problems<br>High-performance oil film thrust bearing<br>Enclosed casing means difficult to inspect frequently |
| | Engine-driven generator | c10 kVA–60 MVA | Diameter ≈ length<br>Horizontally mounted<br>Medium rotational speed 500–1 800 rev/min<br>Standby, CHP, island and marine generation | Stator or rotor winding electrical faults incurring consequential damage<br>Electrical faults incur consequential damage<br>Reciprocating engines give torsional and seismic vibration problems<br>Arduous environment can cause problems |
| | Synchronous motor | 1–30 MW | Length ≈ diameter<br>Horizontally mounted<br>Wide range of possible rotational speeds 500–6 000 rev/min<br>North American technology<br>Reciprocating and turbo-compressor drives | Stator or rotor winding electrical faults incurring consequential damage<br>High-speed compressors give high-speed balance problems<br>Reciprocating compressors give torsional and seismic vibration problems<br>Stator end winding bracing problems |
| AC machines, induction or asynchronous | Generators | 100 kVA–10 MVA | Horizontally mounted<br>Medium rotational speeds 500–3 600 rev/min | Stator or rotor winding electrical faults incurring consequential damage |

*(Continues)*

*Table 2.1* (*Continued*)

| Main type of machine | Sub-types | Size range | Main constructional features | Root causes |
|---|---|---|---|---|
| | | | Becoming common in wind generation | Short air-gap drives air-gap stability problems limiting permissible bearing wear particular in high poleage, low-speed machines<br>Slip ring and brush-gear problems on doubly fed machines |
| | Motors | 0.1 kW–20 MW | Diameter ≈ length<br>Horizontally mounted<br>With VSDs wide range of possible rotational speeds 500–6 000 rev/min<br>Ubiquitous industrial workhorse | Stator winding electrical faults incurring consequential damage<br>Rotor cage electrical faults incurring consequential damage<br>High starting current limits thermal and fatigue life<br>Short air-gap dives air-gap stability problems limiting permissible bearing wear particular in high poleage, low-speed machines<br>Rotor cage integrity after many restarts<br>Slip ring and brush-gear problems on doubly fed machines |
| AC reluctance machines | Motors | 1 kW–50 kW | Diameter ≈ length<br>Horizontally mounted<br>Medium rotational speed 500–1 800 rev/min<br>Increasing application to specialised variable speed, high-torque applications | Stator winding electrical faults incurring consequential damage<br>Vibration and noise<br>VSD problems |

| | | | | |
|---|---|---|---|---|
| Permanent magnet machines | Synchronous motor | 0.5–500 kW | Length $\gg$ diameter<br>Horizontally mounted<br>High rotational speed, 500–5 000 rev/min<br>VSD applications | Stator or rotor winding electrical faults incurring consequential damage<br>Magnet damage due to heating, lack of adhesion or demagnetisation<br>High-speed balance problems |
| | Synchronous generator | 5–5 MW | Diameter $\gg$ length<br>Vertically or horizontally mounted<br>Low rotational speed, 80–300 rev/min<br>Renewable applications | Stator winding electrical faults incurring consequential damage<br>Magnet damage due to heating, lack of adhesion or demagnetisation<br>Rotor balance problems |
| AC machines, multiphase | Motors | 0.5–25 MW | Diameter $\approx$ length<br>Horizontally mounted<br>Medium rotational speed 150–500 rev/min<br>Increasing application to specialised marine high-torque, variable-speed applications | Stator or rotor winding electrical faults incurring consequential damage<br>Vibration and noise<br>VSD problems |
| AC machines, commutator | Motors | 20 kW–5 MW | Now almost obsolete in the face of power electronic VSDs applied to AC and DC machines | Stator or rotor winding electrical faults incurring consequential damage<br>Commutator faults<br>Brush-gear faults<br>Carbon dust contamination problems associated control gear problems |

*Table 2.2 Rotating electrical machine typical sizes and loadings*

| **Type of machine** | **DC permanent magnet motor** | **Air-cooled 3-phase AC induction motor** | **Air-cooled 9-phase advanced AC induction motor** | **Air-cooled 3-phase AC synchronous hydro-generator** | **Air-cooled 3-phase AC synchronous turbo-generator** | **$H_2O$- and $H_2$-cooled 3-phase AC synchronous turbo-generator** |
|---|---|---|---|---|---|---|
| Cooling type | TEFC | CACW | CACW | CACW | CACW | CHCW |
| P, MW | 0.0002 | 6.14 | 24 | 90 | 100 | 1 000 |
| Poles | 4 | 4 | 12 | 88 | 2 | 2 |
| Rev/min | 6 000 | 1 790 | 120 | 68.2 | 3 000 | 3 000 |
| Typical weight, tonnes | 0.0002 | 18 | 89 | 400 | 90 | 350 |
| Power/Weight, kW/kg | 0.88 | 0.34 | 0.22 | 0.23 | 1.11 | 2.86 |
| Magnetic loading, air-gap flux density, $T_{rms}$ | – | 0.90 | – | 1.05 | 0.94 | 1.00 |
| Electric loading, A/mm | – | 93.0 | – | 62.5 | 116.3 | 255.3 |
| Mechanical loading, rotor peripheral velocity, m/s | – | 69.5 | 14.1 | 46.3 | 139.8 | 188.5 |
| Air-gap torque density, kNm/m$^2$ | – | 140.6 | 707.4 | 140.6 | 1 518.4 | 736.8 |
| Current density, A/mm$^2$ | – | 3.9 | 3.9 | 3.7 | 2.8 | 11.1 |

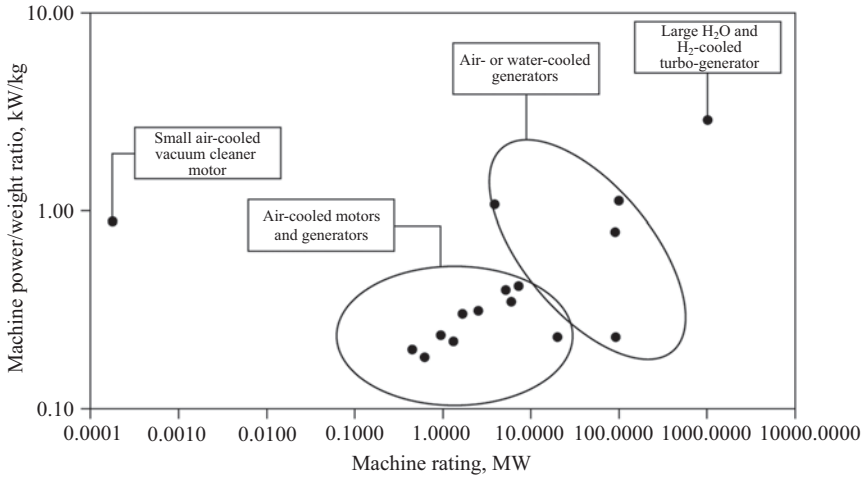


*Figure 2.2 Graphic of machine power–weight ratios against rating*

arises because of the mechanical and thermal limitations of magnetic circuit and insulation materials, not experienced by other machine types, such as diesel and petrol engines or aero and industrial gas turbines.

Based upon this range of machine power/weight and size, the following sections describe the basic structure and design principles which influence the CM of different types of machines and may affect reliability. Particular attention will be paid in these sections to show their simplified machine windings and connections, their equivalent circuits and the magnetic field that links rotor and stator.

The issues here and in the next Chapter 3 are also considered in respect of novel electrical machines in the *Electric Machines Roadmap* (2018) produced by the Advanced Propulsion Centre UK. Their report suggests that innovations are needed to improve electric traction machines power to weight ratios from their current modest 0.2–3 kW/kg to at least 7 kW/kg by 2025 and 9 kW/kg by 2035. These improvements are likely to come from the following:

- New insulation materials, see Table 3.2, Figure 3.2 and Stone *et al.* (2004),
- Better winding materials, copper, aluminium and their alloys,
- New magnetic materials, both permanent magnets and magnetic steels, see Moses *et al.* (2019) Vols 1 and 2,
- Design to tighter margins using more advanced FEA and multi-physics modelling software.

## 2.3 DC machines

All electrical machines up to the late nineteenth century were DC but, with the recent availability of power electronics, the DC machine has been slowly losing ground to the AC machine. However, DC machines continue to be the basis of

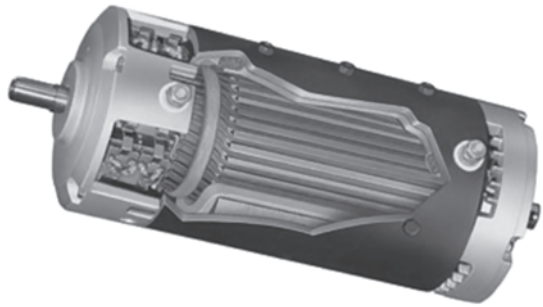

*Figure 2.3 500 W, 4-pole DC motor, section showing the stator frame and bearing housings, armature and commutator on the left*

electrical machine design and are still widely-used in precision variable speed applications. There has been a progressive movement from the use of wound field stator magnets to permanent magnets, firstly made using ferritic materials but in the last 30 years changing to more complex magnetic materials including rare earth materials and most recently high temperature superconducting coil magnets.

DC machine design is based on a simple magnetic circuit calculation method, Hopkinson (1886), and more recently on the use of magnetic field finite element analysis (FEA), Krause *et al.* (2013).

Figure 2.3 shows a typical 4-pole DC machine. Figure 2.4 gives a schematic representation of the machine, considering first windings and connections, then the equivalent circuit and finally the magnetic flux of the machine. The equivalent circuit enables the prediction of winding currents for a given voltage under steady-state load and fault conditions.

## 2.4 AC machines, synchronous

Since the advent of AC electrical supplies at the end of the nineteenth century, synchronous AC machines have been primarily used as generators but they continue to be used, albeit in smaller numbers, as high torque, fixed-speed motors in large industrial applications, such as paper-mills, cement-mills and oil production facilities.

Figure 2.5 shows a small synchronous generator, typically driven by a diesel engine, whilst Figure 2.6 shows two large machines, one a low-speed, high pole number hydro-generator, the other a high-speed, 2-pole turbo-generator.

Synchronous machine design was fixed by a seminal book by Concordia (1908) with a simple equivalent circuit, shown below.

Figure 2.7 presents the electrical circuit, equivalent circuit and magnetic flux plot of a 2-pole turbo-generator, such as shown in Figure 2.6(a), the diagrams for the multi-pole machines in Figures 2.5 and 2.6(b) would be very similar. The point of this diagram is to emphasise again the standard way electrical engineers represent electrical machines, irrespective of their size or type and that winding currents can be predicted for a given voltage under steady-state and fault conditions.

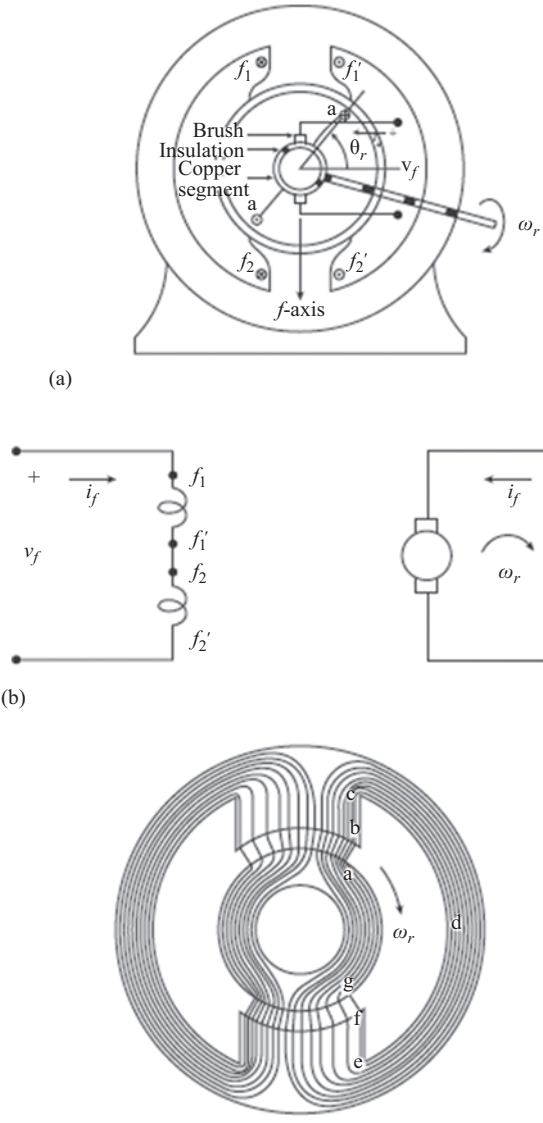


*Figure 2.4 2-Pole DC machine: (a) windings and connection diagram for a 2-pole DC machine, (b) equivalent circuit diagram and (c) consequent magnetic flux plot for a 2-pole DC machine, Hopkinson, J (1886) and Moullin (1955)*

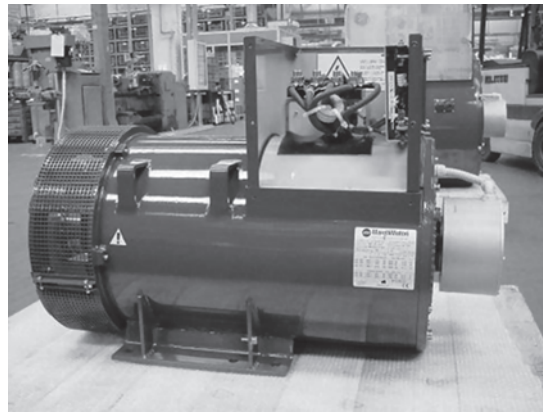

*Figure 2.5 40 kVA, 4 pole, 1 800 rev/min, 400 V, air-cooled synchronous generator for a diesel genset, pilot exciter on the right*

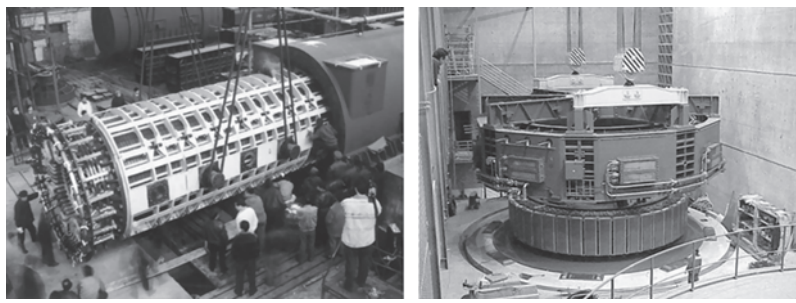

(a) (b)

*Figure 2.6 (a) 706 MVA, 2-pole, 3 000 rev/min, 24 kV, $H_2$- and $H_2O$-cooled CHCW synchronous steam turbo-generator. (b) 75 MVA, 44-pole, 136.4 rev/min, 15.7 kV, air-cooled CACW synchronous hydro-generator*

## 2.5 AC machines, asynchronous or induction

From the initial AC induction motor development in the late 1880s and the widespread application of AC electrical supplies at the start of the twentieth century, the induction or asynchronous motor has expanded in application as a universal electrical prime mover. However, fixing the design parameters proved much more difficult than for the synchronous machine but benefitted from the application of the transformer equivalent circuit, modified to take account of the secondary circuit or rotor motion, Alger (1965).

Particularly rapid growth in machine numbers occurred after the Second World War and the effectiveness of modern power electronic drives has recently

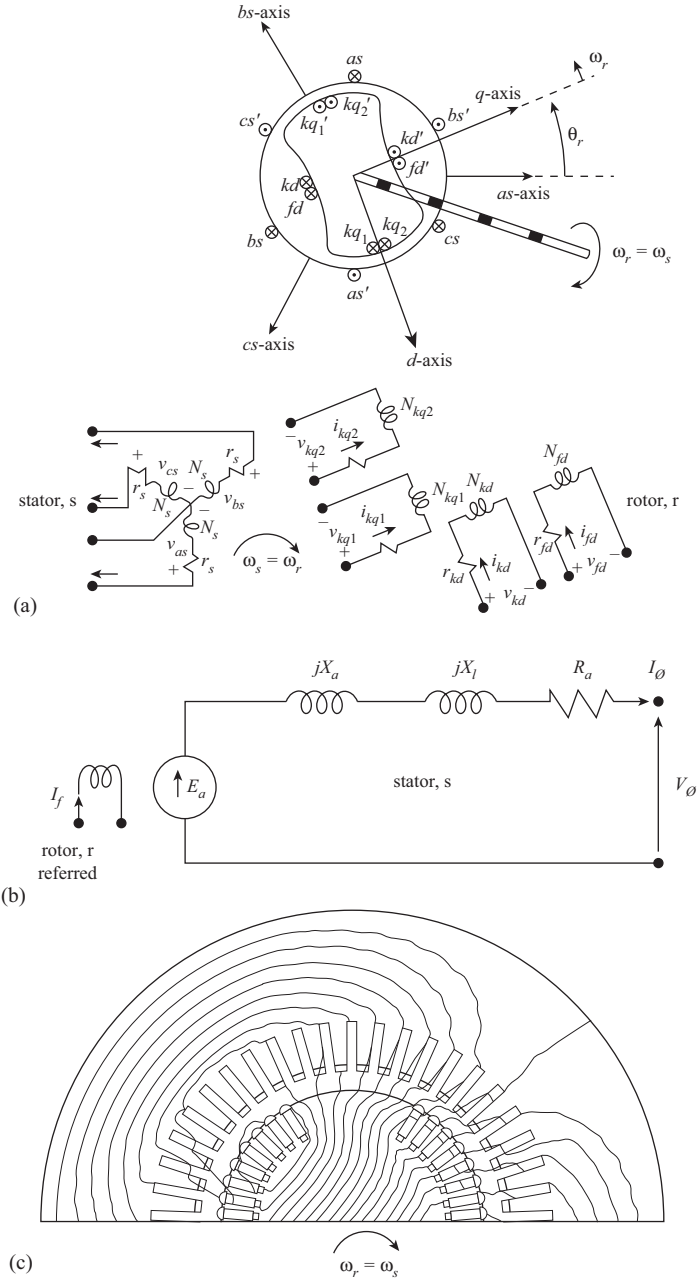


*Figure 2.7 2-Pole AC synchronous machine: (a) 3-phase a, b, c windings and connection diagram for a 2-pole DC machine, (b) single-phase equivalent diagram, rotor referred to stator and (c) consequent magnetic flux plot for a 2-pole, 3-phase, 2-pole synchronous machine, Concordia (1908)*

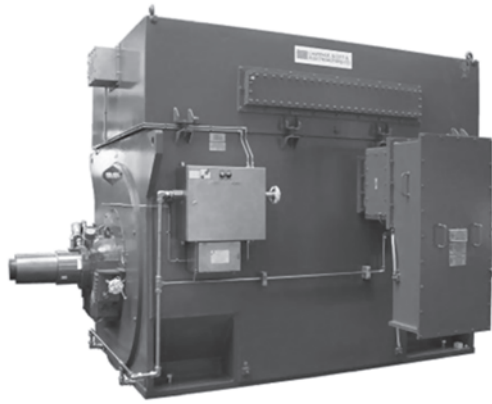

*Figure 2.8 7 MW, 11 kV, 60 Hz, 4-pole CACW AC induction motor driving a high-speed flash gas compressor for offshore oil and gas. Drive shaft on left and the water cooled heat exchanger on top of machine*

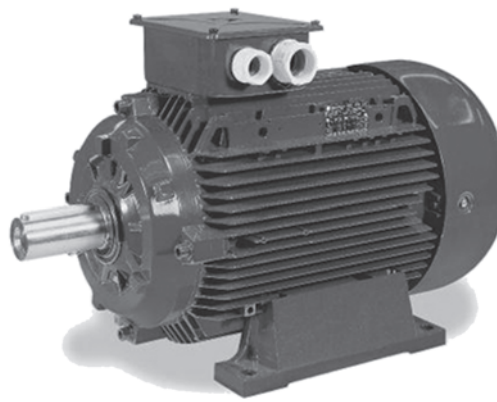

*Figure 2.9 40 kW, 400 V, 50 Hz, 4-pole TEFC AC induction motor, typically driven by a variable-speed drive*

considerably broadened their application into VSDs. Figures 2.8 and 2.9 show typical large and small induction motors.

Figure 2.10 presents in turn the electrical circuit, equivalent circuit, as perfected by Alger (1965), and magnetic flux plot of a 4-pole induction machine, such as shown in Figures 2.4 and 2.7 for DC and AC synchronous machines. Again, the purpose of this diagram is to emphasise the standard way electrical engineers represent the machines, regardless of the size or type and again that winding currents and output torques can be predicted for a given voltage under steady-state and fault conditions. Figure 2.11, taken from Krause *et al.* (2013), shows dramatic evidence of the fundamentally identical behaviour of induction motors of different

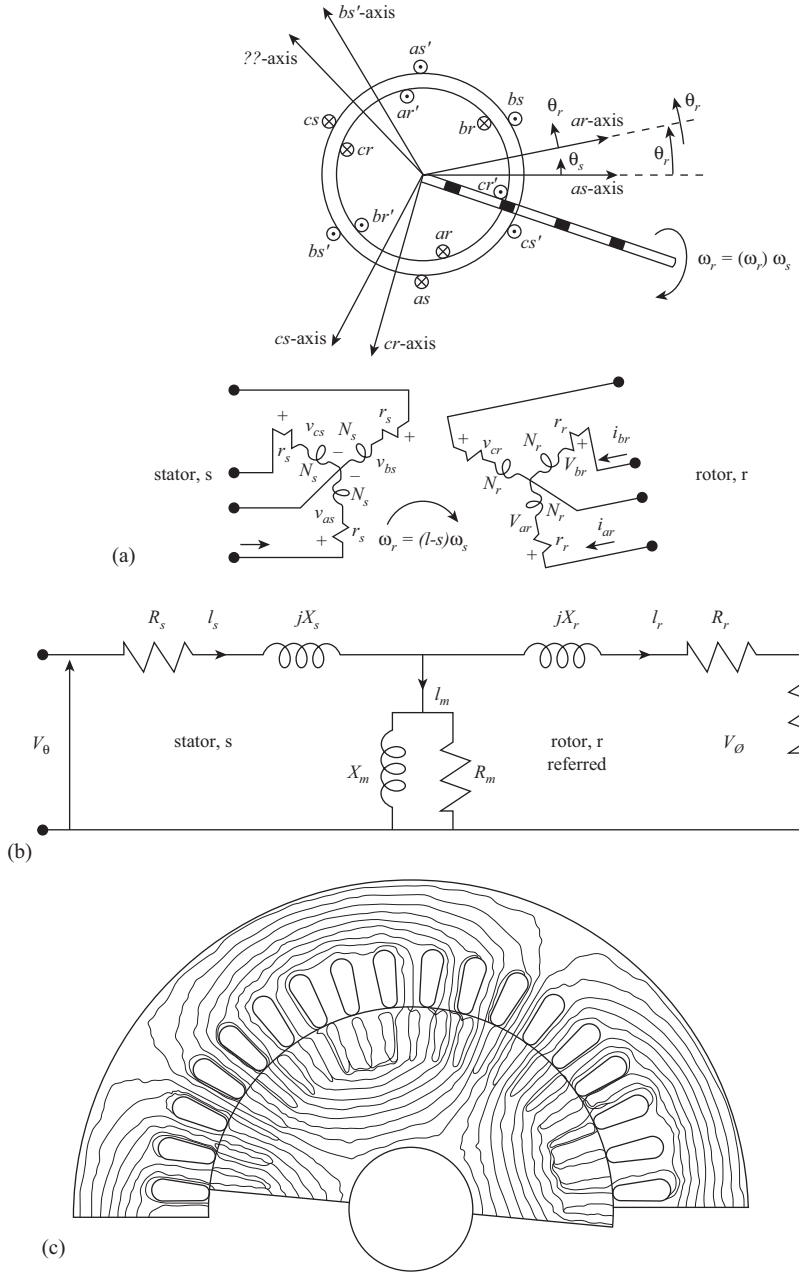


*Figure 2.10 AC induction or asynchronous machine: (a) 3-phase a, b, c windings and connection diagram for a 2-pole machine, (b) single-phase equivalent circuit diagram, rotor referred to stator and (c) consequent magnetic flux plot for a 4-pole, 3-phase, induction machine, Alger (1965)*

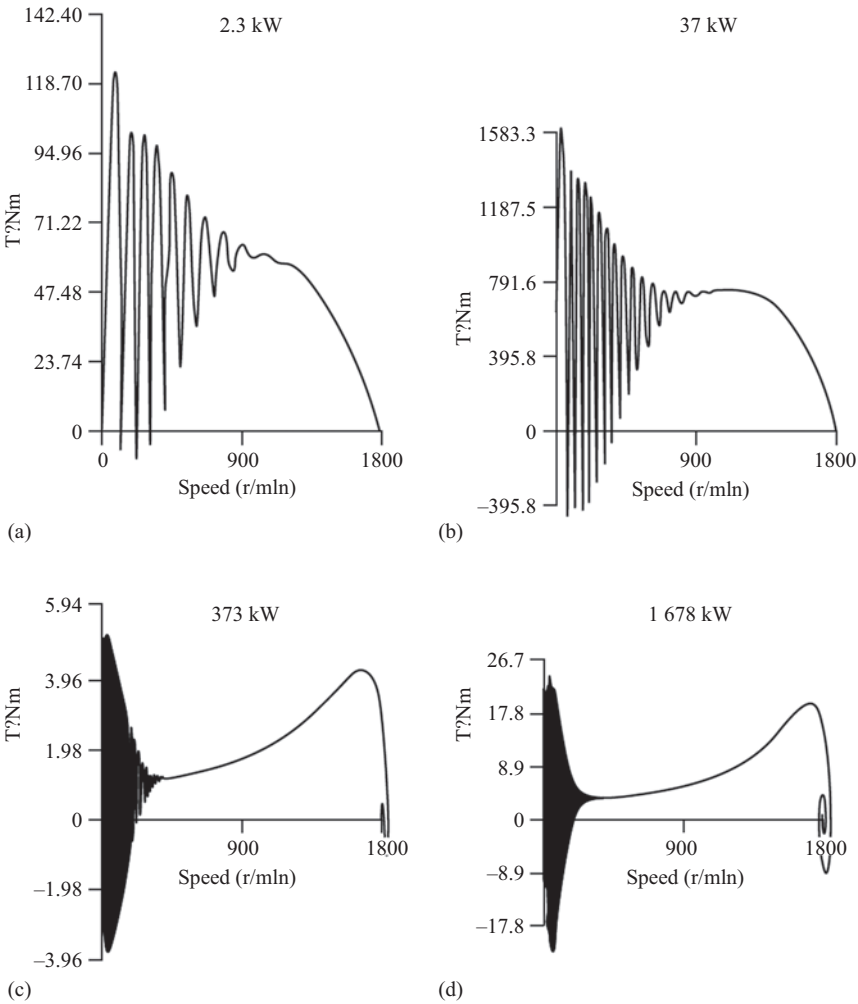


*Figure 2.11 Induction motor dynamic torque–speed curves on starting and pull-in at zero load for the four machines of increasing rating, demonstrating the similarity of form derivable from equivalent circuit, Krause et al. (2013)*

size by showing the transient starting torques, $T_e$, against no-load for four motors of increasing rating. Each torque–speed curve demonstrates the same behaviour, following the steady-state torque–speed curve, due to the properties of the rotor winding L-R circuit shown in Figure 2.10. Note the torque oscillations at start represent individual rotations of the machine, it takes many more such revolutions for larger, higher inertia machines than for smaller machines and there are larger torque reversals during the start. Furthermore, the pull-in to synchronous speed at no-load for larger machines is oscillatory but quite clear.

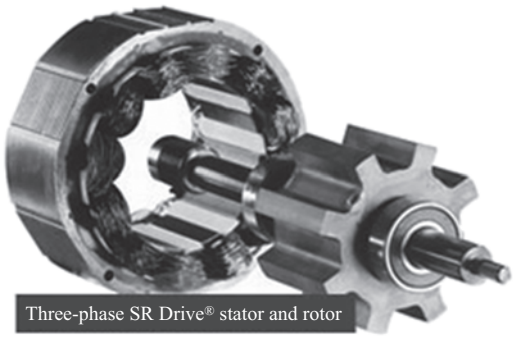


*Figure 2.12 5 kW, switched reluctance motor*

## 2.6 Permanent magnet or reluctance machines

In the 1980s, a requirement developed for a high-torque, variable speed, alternative to the induction motor, effectively a more modern version of the DC machine. This lead to the development of switched reluctance brushless drives, Lawrenson *et al.* (1980). These use shaped steel pole-pieces or permanent magnets on their rotor and switched DC supplies to their stator windings, allowing the machine to operate at variable speed. They are really a re-invention of the stepper motor, modern materials, instrumentation and electronics, achieving high torque by the use of using sharply defined pole pieces or strong, rare earth, permanent magnets. The consequence of their non-uniform air-gap is that they can also tend to be noisy. These drives have now become widely used for high torque, low variable speed, precision and traction drives.

Figure 2.12 shows a typical switched reluctance machine structure and Figure 2.13 shows the schematic, equivalent circuit and flux plot for the SR machine, similar to Figures 2.4, 2.7 and 2.10, re-emphasising the electrical machine similarities.

## 2.7 Other machine types

### *2.7.1 Multi-phase machines*

With the advent of VSDs, multi-phase stator machines with induction or permanent magnet rotors have become more attractive for high-torque motor applications, such as marine propulsion, and for direct drive slow-speed wind generators obviating the need for gearboxes.

Multi-phase stators, particularly for slower-speed applications allow the number of phases to increase above three-phase and use of parallel VSD stator connections, offering speed control and redundancy.

Lewis (2002) described a typical multi-phase machine, the advanced induction motor, a marine application shown in Figure 2.14 and a thorough review of multi-phase induction machine technology is contained in Levi *et al.* (2007).

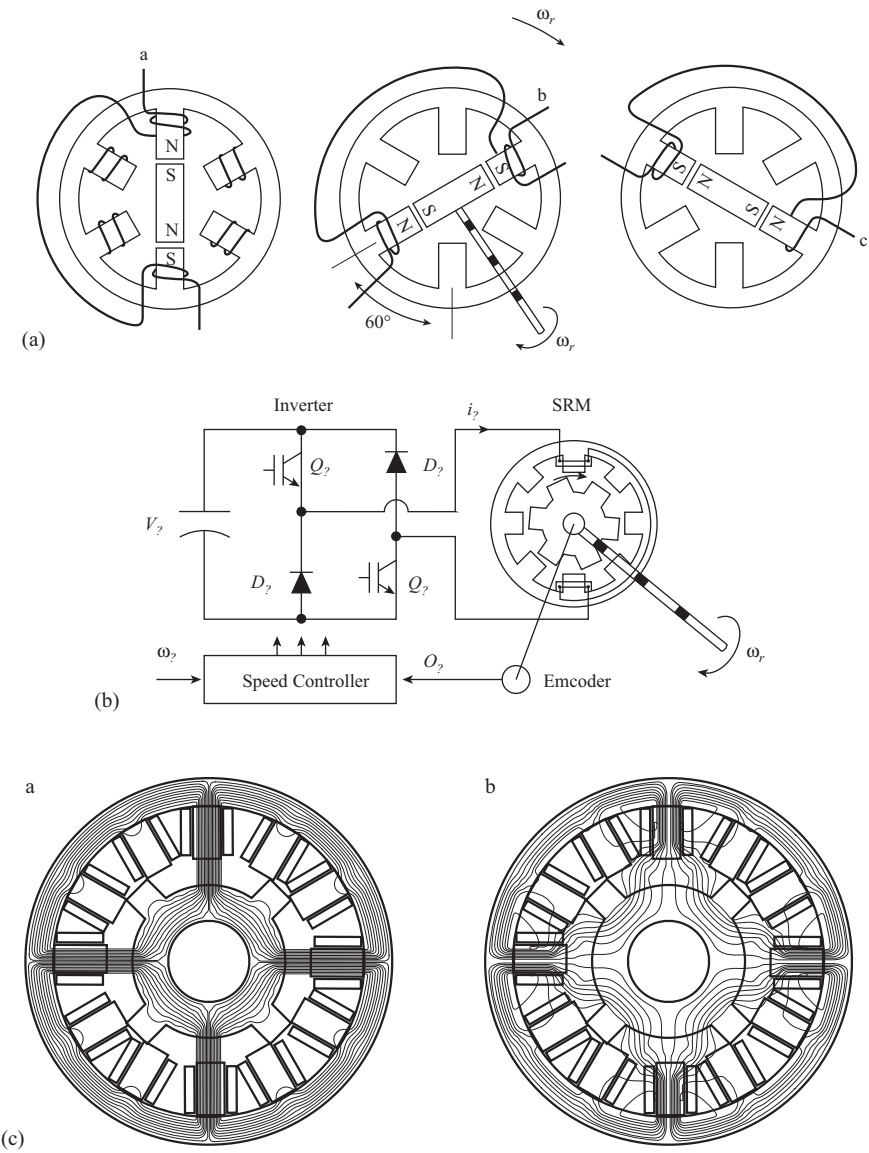


*Figure 2.13 Permanent magnet or reluctance machine: (a) 3-phase a, b, c windings and connection diagram for a 2-pole machine with 6-pole stator, (b) single-phase equivalent circuit for a 6-pole machine with 8-pole stator and (c) consequent magnetic flux plot for a 8-pole machine with 12-pole stator, operating in 4-pole mode, Lawrenson et al. (1980)*

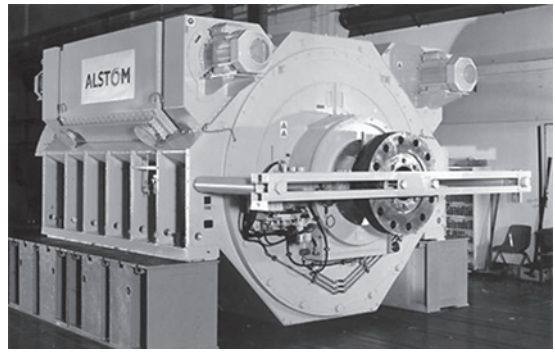


*Figure 2.14 20 MW advanced induction motor, large multi-phase, multi-pole, variable-speed AC induction motor fed by voltage-source converter for ship propulsion, Lewis (2002)*

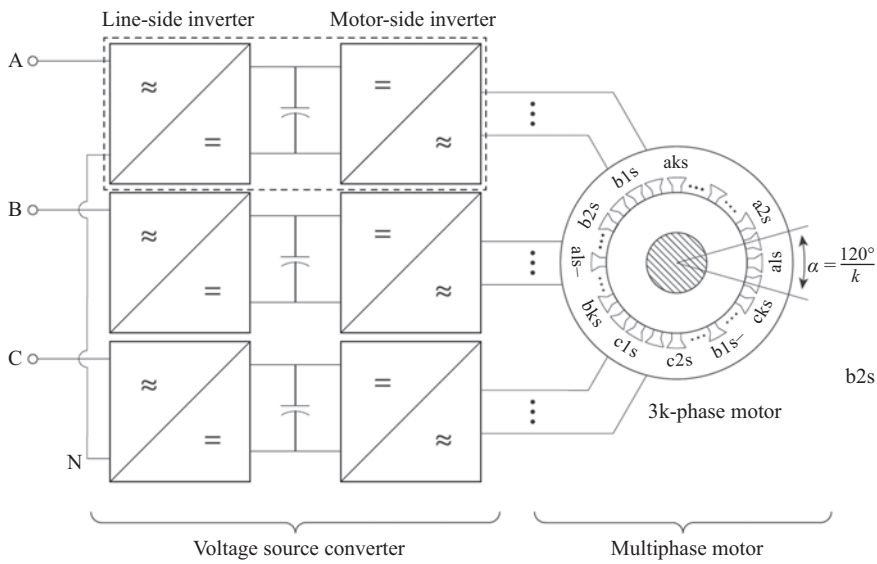


*Figure 2.15 Supply and converter for a 3k-phase, multi-pole, variable-speed AC induction or permanent magnet motor*

## *2.7.2 Doubly fed and variable-speed drive machines*

For the purpose of completeness, we want to demonstrate some basic drive types and their relevance to electrical machine CM.

An example of the connection arrangements for a multi-phase AC induction or permanent magnet machine connected to a VSD is shown in Figure 2.15. The

design circuits for a multiphase machine would be based upon the equivalent circuit model in Figure 2.10 for an induction machine or the flux plot for a permanent magnet machine.

Doubly-fed machines are AC induction motors or generators, see Figure 2.16, that have:

- Either one supply to a stator winding and the other to a rotor winding of the same pole number fed via slip-rings and a reversible, partially rated VSD. This is known as a doubly-fed induction machine (DFIM) and is widely deployed for larger wind turbine generators,
- Or two AC supplies to separate stator windings, of different pole numbers, one supply being via a reversible, partially rated VSD. This is known as a brushless doubly-fed machine (BDFIM). This is a new technology being advocated for wind turbines and some large industrial drives but has not yet been widely deployed.

The DFIM is a modern version of the wound rotor induction machine, widely used in the past as a VSD for large power stations, paper mill and cement mill plant where the speed change was achieved by varying rotor winding resistance through rotor slip-rings. Wound rotor induction machines were powerful and cheap but wasted energy in rotor resistance losses. The wound rotor induction machine's modern incarnation as a DFIM incurs no wasted power from this source, except in the converter, and allows a machine speed variation range proportional to the

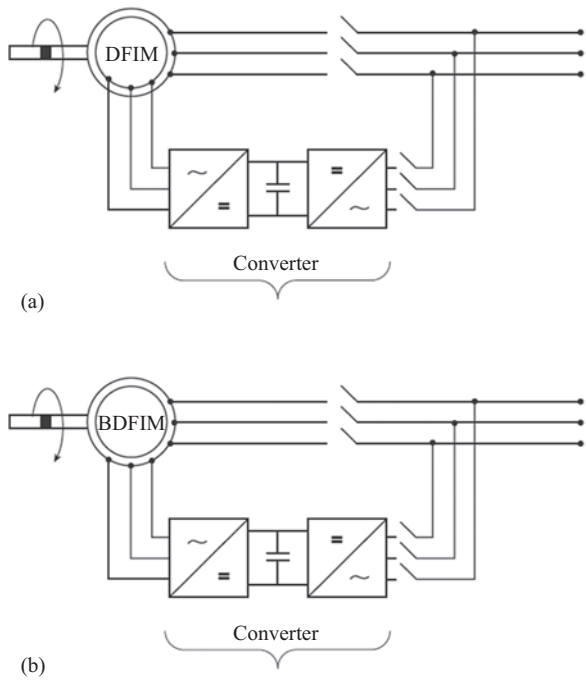


*Figure 2.16 Doubly-fed induction motors and generators: (a) slip-ring DFIM and (b) brushless DFIM*

fractional rating of the VSD converter (VSC); this has been very widely applied in the wind turbine industry.

The BDFIM is a more modern version of the DFIM with the advantage that slip-rings are avoided, but introducing complexities in machine winding design and VSD control. The equivalent circuit for the DFIM is the same as for a squirrel cage induction machine, as shown in Figure 2.8(b) and while the equivalent circuit for a BDFIM is more complex it is firmly based on that for the induction machine. Again, this means that for both the DFIM and BDFIM winding currents can be predicted under steady-state and fault condition for a given voltage.

## 2.8 Conclusions

There are currently an enormous range of VSDs being applied to electrical machines and there are a number of specialised references available for considering VSD reliability, see Appendix C-Timeline, including Yang and Ran *et al.* (2010) and Chung *et al.* (2016).

A great deal of this development is being driven by the electrification of transport, on the railway and the roads. For example, Figure 2.17 shows an example of a high-performance electric car permanent magnet motor and drive.

The conclusion of this chapter is that all electrical machines are remarkably similar in their logic and design, despite there being many different types and progressive changes in their application. However, they are all dominated by the coupling magnetic field, which is their modus operandi.

It follows therefore that their construction, failure modes and CM must derive from that fundamental mechanism, the materials which facilitate it and their operating conditions, as the following chapter will demonstrate. We will need to show how CM can take these facts into account.

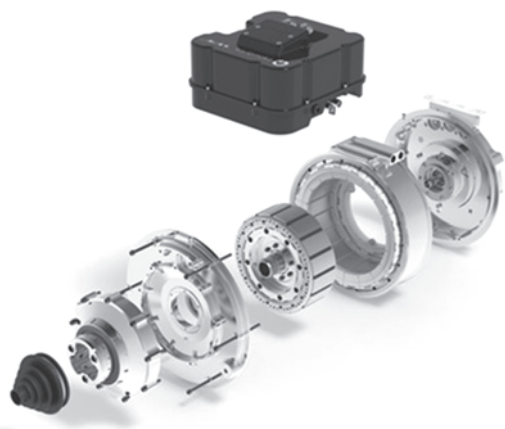

*Figure 2.17 100 kW AC permanent magnet motor and voltage source inverter for an electric-vehicle*

*This page intentionally left blank*

*Chapter 3*

# Electrical machine construction, operation and failure modes

## 3.1 Introduction

This chapter could be subtitled 'the way rotating electrical machines fail in service'. These machines convert electrical to mechanical energy, or vice versa, and achieve this by magnetically coupling electrical circuits across an air-gap that permits rotational freedom of one of these circuits. Mechanical energy is transmitted into, or out of, the machine via a drive train that is mechanically connected to one of the electric circuits.

An example of one of the largest electromagnetic energy conversion units in the world, at 1 111 MVA, is shown in Figure 3.1. The construction of electrical machines is similar, whether large or small, as shown later in the chapter and their operational weaknesses are dominated by the same principles.

The purpose of this chapter is to explain their constructional principles and the main causes of failure. The chapter is illustrated with a number of photographs to demonstrate to the reader the salient features of electrical machines.

## 3.2 Materials, strength and temperature

The magnetic and electric circuits essential to machines require materials of high permeability and low resistivity, respectively, and these are metals.

Metals with good magnetic and electrical properties do not necessarily have high mechanical strength. Indeed, the atomic structure of a good conductor is such that it will naturally have a low yield strength and high ductility. Yet the magnetic and electric circuits of the machine must bear the mechanical loads imposed upon them by the transfer of energy across the air-gap by the electromagnetic field. Furthermore, the magnetic and electrical circuits must be separated by insulating materials, such as films, fibres and resins, which have even weaker mechanical properties. Table 3.1 sets out the elastic moduli and tensile strengths of materials used in electrical machines and highlights the relative weakness of electrical steel, conductor and insulating materials. So right from the outset, there is a conflict between the electrical and mechanical requirements of the various parts of an electrical machine, which the designer must attempt to resolve.

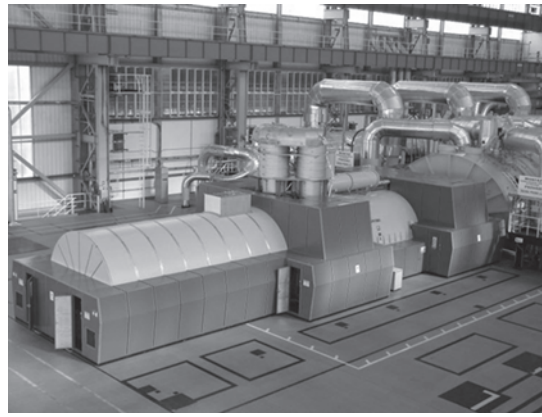

*Figure 3.1 1 111 MVA, 24 kV, 50 Hz steam turbine-driven, hydrogen-cooled, 2-pole turbo-generator*

*Table 3.1 Mechanical properties of materials used in electrical machines*

| | **Material** | **Elastic modulus, GPa** | **Tensile strength, MPa** |
|---|---|---|---|
| Structure | High tensile steel | 210 | 1 800 |
| | Structural steel | 210 | 830 |
| Core | Electrical steel | 220 | 450 |
| Windings | Copper | 120 | 210 |
| | Aluminium | 70 | 310 |
| Insulation | Epoxy-mica-glass composite | 60 | 275 |
| | Moulded organic/inorganic resin | 5 | 48 |
| | Cured phenol-formaldehyde Resins | 3 | 35 |

There is a further complication, the electromagnetic transfer of energy inevitably involves the dissipation of heat, by ohmic losses in the electric circuit, by eddy current and hysteresis losses in the magnetic circuit. The performance of the insulating materials that keep the magnetic and electrical circuits apart is highly dependent on the temperature and deteriorates rapidly at higher temperatures. Materials that can sustain these higher temperatures become progressively more expensive and their mechanical and dielectric properties are often worse than lower temperature materials. Table 3.2 classifies the common insulating materials used in electrical machines and shows the relatively low temperatures at which they are permitted to operate.

Uncertainties about the temperatures within a machine mean that the designer is forced to restrict the maximum measurable operating temperature to an even lower value than that given in Table 3.2, taken for the appropriate insulation from BS EN IEC 60085:2007, in order to provide a safety factor during operation. It is

*Table 3.2 Temperature capabilities of machine insulating materials*

| Old IEC 60085 Thermal class | Insulation materials | Max. allowable temperature, °C | Max. hot spot temperature, or relative thermal endurance index, °C |
|---|---|---|---|
| O or Y obsolete | Oleo-resinous natural fibre materials, cotton, silk, paper, wood without impregnation | 90 | >90–105 |
| A | Natural fibre materials, cotton, silk, paper and wood impregnated, coated or immersed in dielectric liquids such as oil | 105 | >105–120 |
| E | Synthetic-resin impregnated materials but not containing fibrous materials such as cotton, silk or paper or enamelled wire including phenolics, alkyds and leatheroid | 120 | >120–130 |
| B | Combinations of mica, glass and paper with natural organic bonding, impregnating or coating substances including shellac, bitumen and polyester resins | 130 | >130–155 |
| F | Combinations of mica, glass, film and paper with synthetic inorganic bonding, impregnating or coating substances including polyester and epoxy resins | 155 | >155–180 |
| H | Combinations of mica, glass, paper or asbestos with synthetic bonding, impregnating or coating substances including epoxy, polyamide or silicone resins | 180 | >180–200 |
| – | As for Class F but including Teflon | 200 | >200–220 |
| C | Combinations of asbestos, mica, glass, porcelain, quartz or other silicates with or without a high-temperature synthetic bond, impregnating or coating substance but including silicone resins or high-temperature calendered aramid papers, e.g. Nomex | 220 | >220–250 |
| – | As for Class H but including polyimide enamel or polyimide films, e.g. Kapton | 240 | |
| – | As for Class H but including polytetrafluoroethylene resins | 250 | >250 |

clear that the heat dissipated within a machine must be removed effectively if design limits are to be met.

For example, in the 1 111 MVA turbo-generator shown in Figure 3.1 with losses of the order of 12 MW, if cooling stopped the average temperature of the generator body would exceed any of the maximum permitted insulation temperatures within 12 s. The problem is exacerbated because the losses are not evenly distributed and in practice at some locations the rise in temperature will be even faster than this. So, cooling and its distribution becomes a vital part of machine design.

The health of an electrical machine, its failure modes and root causes, are ultimately related to the materials of which it is made, the mechanical and electrical stresses those materials are subjected to and particularly the temperatures they are allowed to attain in service, see Figure 3.2, taken from Table 3.2. Note that most modern machines are insulated to Class F or H standard.

In Chapter 1, we explained how electrical machines are protected by relays, which sense serious winding current disruptions and operate to trip or disconnect the machine. However, when fault currents are flowing, the machine has already failed as an electrical device. Electrical or mechanical failure modes are always preceded by deterioration of one of the machine's mechanical, electrical, magnetic, insulation or cooling components. This is so, regardless of the type of electrical machine. If that deterioration takes a significant period and can be detected by measurement, then that root cause detection will be a means of monitoring the machine before a failure mode develops. Table 3.2 and Figure 3.2 show that temperature could be one of the most effective means of root cause detection. The heart

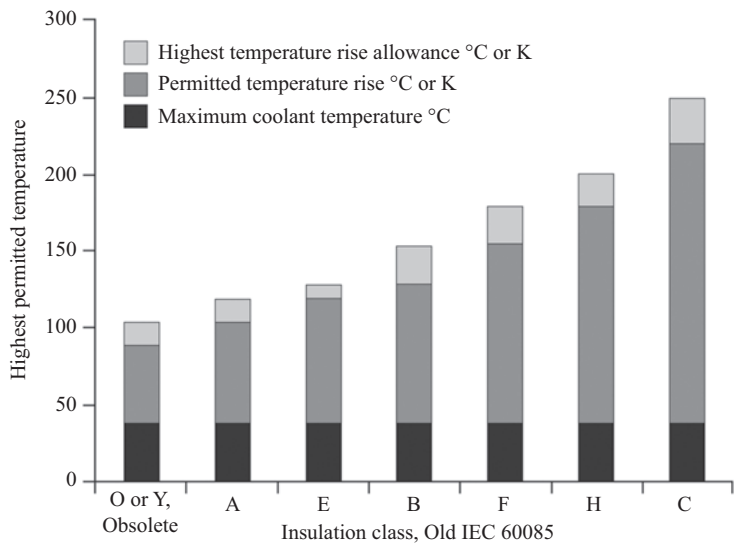


*Figure 3.2 Insulation classes, ranges of permitted temperatures, see Table 3.2*

of CM is to derive the methods to measure, as directly as possible, parameters that indicate root cause deterioration and provide sufficient warning of impending failure in order that the machine may be taken off for repair or may be tripped before serious damage occurs, see Figure 1.3.

A degree of protection could be achieved by making the protective relays especially sensitive and providing an alarm indication before tripping occurs. Experience has shown that this is a precarious mode of CM leading to false alarms and a lack of confidence in the monitoring process.

The following sections show how the construction, specification, operation and types of fault can lead to the identification of generic failure mode root causes in the machine.

## 3.3 Electrical machine construction

### *3.3.1 General*

The basic constructional features of the electrical machine are shown in Figure 3.3(a). The rotor, which usually has a relatively high inertia, is usually supported on two bearings, which may be mounted on separate pedestals or incorporated into the enclosure of the machine. Some larger, slower-speed machines incorporate a single non-drive end bearing and rely on the bearing of the prime mover or driven plant for remaining support. Rolling element bearings are used on smaller size machines where shaft peripheral velocities are low, and sleeve bearings with hydrodynamic oil films are used for larger machines. Vertically mounted machines will incorporate a thrust bearing usually at the bottom end of the enclosure. This may be a relatively modest angular contact ball bearing for a small vertically mounted pump motor but could be a large hydrodynamic oil film thrust pad Michell-type bearing for a hydro-type generator where the rotor may weigh 100 tonnes or more, see Figure 2.5(b).

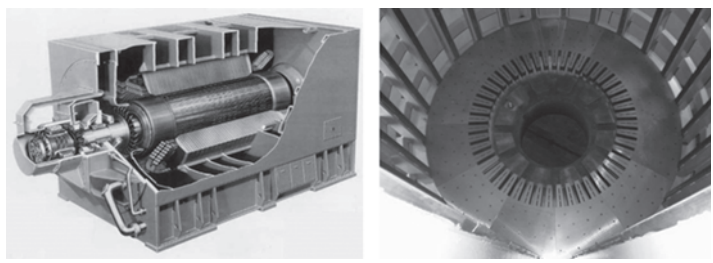

(a) (b)

*Figure 3.3 Synchronous generators: (a) medium-size, 125 MVA, 15 kV, 60 Hz, 2-pole, air-cooled, brushless excitation turbo-generator. Section showing fabricated main frame, stator core, winding, rotor and on the left machine main exciter and (b) large-size, stator core of 500 MW, 2-pole, hydrogen-cooled machine. Construction showing fabricated inner frame and segmented laminations*

### *3.3.2 Stator core and frame*

The stators of all AC machines are constructed from lightly insulated laminations of electrical steel, Figure 3.3(b) and the magnetic field rotates with respect to the stator frame and core. As Table 3.1 shows, electrical steels are strong but the silicon, alloyed to impart magnetic properties and raise resistance, weakens the material compared to structural steel, making it brittle. Furthermore, if the laminated structure is to have the cohesion necessary to transmit the load torque, and have low levels of vibration when carrying magnetic flux, it must be firmly clamped between cast or fabricated end-plates secured to the cylindrical frame into which the core is keyed. The core is constructed within the frame and compressed before the clamping plates are applied, the frame structure and its clamping are clearly visible in Figure 3.3(b). On larger machines, the clamping plates are tightened by large bolts, see Figure 3.4(a), but on smaller machines interlocking keys or even welds are used to secure the clamping plates or the core itself is welded or cleated. Large hydro-generators have very large diameter stator cores, which may be built up in segments in the factory, to facilitate transport to site and assembly there. This results in core segment gaps and a resultant magnetic potential drop between those core segments.

In a DC machine, the magnetic field is stationary with respect to the frame and core, therefore the laminated stator field poles, supporting the non-rotating DC field, are bolted to a rolled steel stator yoke which has much greater inherent strength than a laminated stator core.

### *3.3.3 Stator windings*

The stator windings of all high-voltage AC machines comprise conductor bars made of hard-drawn, high-strength copper sub-conductors that may be connected in series or parallel. Individual sub-conductors are covered with a paper or glass-based

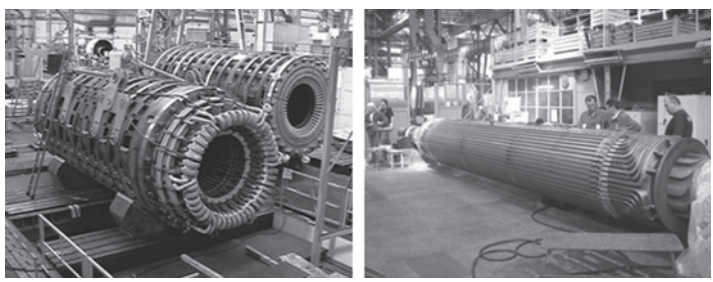

(a) (b)

*Figure 3.4 Large synchronous generator: (a) stators for two 500 MW, 2-pole, hydrogen-cooled turbo-generators. Stator nearest the camera is wound. Stator furthest from the camera is awaiting winding, (b) rotor for a 500 MW, 2-pole, hydrogen-cooled turbo-generator, showing rotor forging and rotor winding before the fitting of end bells*

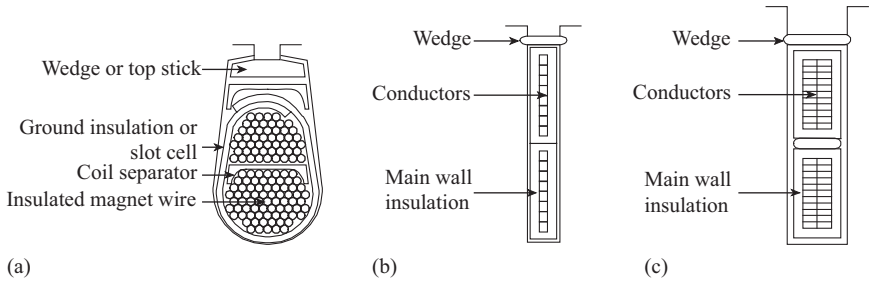


*Figure 3.5 Sectional view of slot sections 3-stator windings, not same scale: (a) a 400 V round wire winding for a 1 kW motor, (b) an 11 kV, 1.5 MW motor winding and (c) a 23 kV conductor bar for the stator winding of a large turbo-generator*

tape and the assembled bar is over-taped with a similar material impregnated on older designs with bitumen but nowadays with epoxy resins, see Figure 3.5. In the portion of the conductor bar embedded in the stator slot the insulation system is compacted by heating and pressing or it may be impregnated under vacuum and pressure. In the end winding portion where one coil is connected to another, the insulation system is not compacted and may be altered, containing less impregnant, so that it is more flexible and therefore better able to withstand the large electromagnetic forces that part of the winding experiences during a fault. An important part of the construction is the manner of the bracing of these end windings. They may be pulled back onto rigid insulated brackets, made of impregnated laminate or steel, using nylon or Terylene cord. On the largest machines, Figure 3.6(a), bracing rings of glass reinforced plastic are used with insulating bolts and the end winding is clamped within this defined and calculable structure. The exact nature of the bracing depends upon the machine rating and the relative length of the end winding, as determined by the number of pole pairs, with the proportionally largest end winding extensions being for large winding pitch 2-pole machines. The yoke or stator core is fitted into a frame and enclosure. On smaller machines and those of standard design the stator core is secured directly into a simplified design of a machine main frame, but on larger machines the core has its own inner frame, which is separate from the outer frame so that the clamped core can be removed from the enclosure for repair, Figure 3.3(b).

### *3.3.4 Rotors and windings*

The rotor design depends on the particular type of machine. AC induction and DC motors have laminated rotors where the laminations are clamped together and shrunk onto a steel shaft. Turbo-generators have large, solid, forged-steel rotors that are long and thin, Figure 3.4(b), while hydro-generators have large, short, fat rotors with laminated pole shoes bolted onto a fabricated steel spider, Figure 2.5(b). Where air or gas cooling is necessary an axial, or radial, fan may be fitted at either

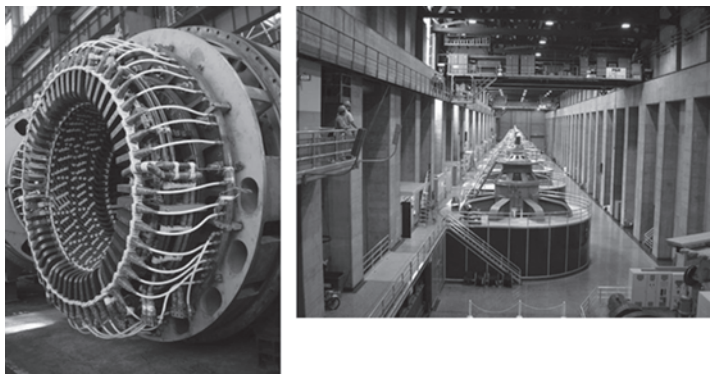

(a) (b)

*Figure 3.6 Large synchronous generators: (a) end region of a 600 MW, 2 pole, hydrogen-cooled turbo-generator with water-cooled stator windings, showing the end winding bracing structure and the hoses carrying water to the winding and (b) Generator Hall in the Grand Coulee Hydroelectric Dam, showing a number of hydro-generators, 120 MVA, 88-pole, 60 Hz, 81.8 rev/min*

or both ends of the rotor shaft. However, smaller machines rely solely on air circulation as a result of the windage of the rotor itself, which is usually slotted to accept the rotor windings, Figure 3.4(b) and larger machines contains radial air ducts, effectively an implicit fan.

Generator rotor windings are constructed of hard-drawn copper and are insulated with rigid epoxy or formaldehyde resin, impregnated into a woven material. On squirrel cage induction motors the winding may consist of lightly insulated copper bars driven into the slots in the laminated rotor or of aluminium or copper bars cast directly into the rotor. The rotor windings of a DC machine or wound rotor induction motor will be rather similar to a conventional AC stator winding described later. Typical induction motor and generator rotors are shown in Figures 2.1 and 3.12.

### *3.3.5 Enclosures*

The machine enclosure can take a wide variety of forms, depending on the manner in which the machine is cooled, and the protection needed from the environment in which it will work. Where a pressurised gas cooling system is used the enclosure will be a thick-walled pressure vessel but for simple air-cooling with an open air circuit the enclosure will consist of thin-walled ducting. Typical enclosures are shown in Figures 3.1, 3.3(a) and 3.6(b). There is an increasing demand nowadays to reduce the noise level from electrical machines and, apart from affecting the basic design of the stator and rotor cores, this is requiring specially designed enclosures with built-in noise-proofing.

### *3.3.6 Connections and heat exchangers*

Electrical connections are made to the windings via copper bus-bars or cable that leave the machine enclosure through bushings into a terminal box, the main three phase bus-bars of the 1 111 MVA generator are visible rising from the stator frame in the centre of Figure 3.1. The bus-bars may be lightly insulated to protect them against the environment. In older machines wound paper bushings were used but in modern machines bus-bars are embedded in epoxy resin and proprietary cast epoxy resin bushings are used. The electrical connections are well braced to withstand large electromagnetic forces, developed when short-circuit fault currents flow. The terminal enclosure allows the proper termination of the supply cables, or bus-bars, and must be specially designed to suit the environment in which the machine works. For example, special enclosures are required for motors that operate in inflammable areas and these incorporate baffles and seals to ensure that any flashover in the enclosure cannot ignite gas, or vapour, within or outside the terminal box.

A few machines today incorporate brush-gear for connection to the rotor windings either through steel or copper slip-rings or through a copper commutator, Figure 2.2. The commutator is a carefully designed complex component in which copper segments interlock with the rotor so that they can withstand the bursting forces acting upon them. Also, each segment must be well insulated from its neighbours, and mica is normally used for this purpose. Slip-rings are usually shrunk onto an insulating sleeve mounted on a boss on the rotor shaft, and electrical connections to the slip-rings are insulated and carefully braced to withstand the centrifugal forces upon them. Brushes will be spring-loaded and mounted in brass brush boxes, around the periphery of the rings or commutator.

The mechanical and electrical complexity and cost of the rotating commutator have been the cause of the decline of the DC machine in favour of the more reliable and easier to manufacture static commutator using power electronic switches, such as the thyristor and IGBT, mounted on the stator side external to the machine in a VSD.

Heat exchangers for the cooling system of the machine are mounted on the enclosure or may be a part of it as shown in Figures 2.7 and 2.13. They may be as simple as a finned casing to the machine to promote convective heat transfer to the surrounding air or they may be a more complex water-cooled systems, such as in Figures 2.7 and 2.13, through which the cooling gas or air is ducted.

### *3.3.7 Summary*

These descriptions show the very wide range of materials used in an electrical machine and Table 3.3 gives a summary of these based on the structure of the machine. In particular the reader should realise, both in terms of volume and cost, how important insulating materials in the overall structure of an electrical machine.

In the following section, this structure of the machine will be discussed in more detail.

*Table 3.3 Materials used in the construction of a typical electrical machine*

| Sub-assembly | Component | Materials |
|---|---|---|
| Enclosure | Enclosure | Fabricated structural steel |
| | Heat exchanger | Steel, copper or brass tube |
| | Electrical connections | Copper or aluminium bus-bar or cable |
| | Bushings | Cast epoxy resin |
| | Bearings | Steel babbitts, high tensile steel rolling elements or soft bearing alloy on bearing shells |
| Stator body | Frame | Structural steel |
| | Core | Electrical steel laminations or rolled steel yoke |
| | Core clamp | Structural steel or non-magnetic, low-conductivity alloy |
| Stator winding | Conductors | Hard drawn copper or copper wire |
| | Insulation | Mica-paper or glass or film impregnated with resin |
| | End winding support | Glass fibre structural materials and impregnated insulation felts, ropes and boards |
| Rotor winding | Conductors | Hard-drawn copper or copper wire |
| | Insulation | Mica-paper or glass or film impregnated with resin |
| | End winding support | Impregnated glass fibre rope |
| Rotor body | Shaft | Structural steel or forging |
| | Core | Electrical steel laminations or steel forging integral with shaft |
| | Core clamp | Structural steel or non-magnetic, low-conductivity alloy |
| | Slip rings | Steel, brass or copper |
| | Brush-gear | Carbon or copper brushes in brass brush-holders |

## 3.4 Machine specification and failure modes

Faults can occur because machines are incorrectly specified for the application to which they are being applied. For example, a machine may be underpowered or have an inadequate enclosure. The specification of a machine must ensure that it is of an appropriate design for the use to which it is being put.

It is a waste of time applying sophisticated monitoring techniques to a machine that is unfit for purpose. Far better, to remove the monitoring and change the machine for one that is more suited to the application.

By the same token, many operational problems could be avoided by using an over-designed machine. For example, in a hot environment it may be better to use an overrated machine, which has a substantial design margin, than push an adequately designed machine to its limit. On the other hand, it is sometimes an operational fact-of-life, especially with an expensive machine, that it must continue to operate even though it suffers from shortcomings in the original specification. In such cases effective monitoring can help to ease the burden placed upon the maintenance engineer.

The specification of a machine must reflect the mechanical, electrical and environmental conditions in which the machine will work. These matters will have a bearing on the mechanisms by which the machine may fail in service. The need for monitoring and the selection of the parameters to be monitored must be affected by these operational conditions. Table 3.4 sets out the operational conditions that should be covered by a specification, relevant to monitoring.

*Table 3.4 Operational conditions, defined by specification, which affect failure mechanisms*

| **Operational condition** | **Nature of condition** | **Detailed condition** | **Root causes and failure modes** |
|---|---|---|---|
| Mechanical | Characteristics of the load or prime mover | Duty cycle | Successive overloads may cause overheating or bearing damage |
| | | Pulsating load | May cause bearing and low cycle fatigue damage |
| | | Repeated: starting | Repeated application of high starting torques may cause excessive overheating and damage to rotor and stator end windings |
| | | Load or drive vibration | May cause high cycle fatigue damage to rotor |
| Electrical | Characteristics of the electrical system and the machine connected to it | Fast-voltage spike | May cause an insulation breakdown |
| | | Slow-voltage fluctuation | May cause loss of power and motor stall or generator pole-slip |
| | | Fast-voltage fluctuation | May disrupt the generator excitation or cause insulation failure in winding |
| | | System unbalance | May cause stator winding heating |
| Environmental | Characteristics of the environment in which the machine is being used | Temperature | High ambient temperature will cause higher machine temperatures, thus faster insulation degradation and bearing deterioration. Low ambient temperature may cause frosting and icing |
| | | Humidity | High humidity may lead to condensation and tracking damage to the insulator surfaces and corrosion of metal parts leading to susceptibility to corrosion fatigue failure |
| | | Cleanliness | Dirt from the environment may enter the machine, contaminating insulation surfaces, enhancing the propensity to tracking, fouling heat exchangers and contaminating brush-gear |

Mechanically, machines can be exposed to periods of intermittent running, frequent starting and to arduous duty cycles, where the load varies frequently between no-load and full-load with occasional overloads. These can lead to insulation degradation, bearing wear, vibration and slackening of windings, commutator or brush-gear. Similarly, a machine driving a pulsating load, such as a compressor, is going to experience heavy bearing wear, vibration and slackening of windings, commutator or brush-gear.

From an electrical supply point of view, a machine, by virtue of its location in a supply system or its task in a manufacturing process, may be subjected to a variety of transients at its supply terminals. These may be slow fluctuations in the supply voltage or even unbalance between the three phases that can cause operational problems, for example, if the machine does not have the thermal capacity to deal with the consequent overheating due to imbalance. More rapid transients in the supply voltage, however, can overstress the winding insulation because the electric stress is not uniformly distributed throughout the winding length. Modern interrupters produce very rapid voltage surges that were known to break-down Class B inter-turn insulation on the line end coils of motors, Table 3.2, but with modern Class F systems this is now rare. The most severe electrical transients a machine can receive, however, are during starting or re-switching of the supply, and part of the duty of many machines in industrial processes is to be repeatedly started and run for short periods. This will cause overheating, slackening of winding systems, movement of electrical connections and overstressing of terminal boxes.

Environmentally, there are thermal and contamination problems. The machine may run exceptionally hot, because of ambient conditions or cooling problems or simply that the machine is being operated beyond its rated limit. Each condition causes deterioration of the machines insulating materials. The machine may be operating in a dirty environment either because of the industrial process in which it is working, such as in textile or paper mills, or because it has brush-gear that produces carbon dust. If dirt can enter the main coolant circuit it may contaminate windings, bushings and electrical connections causing insulation integrity deterioration. Or it may foul coolers, seals, or bearings causing over-heating and mechanical damage. Because of ambient conditions the cooling gas may also become damp, for instance in a tropical country, or due to cooler leakage. Either of these can lead to moisture condensation on the electrical insulation and connections giving a reduced insulation resistance.

A machine needs to be designed to meet the environmental, mechanical and electrical disturbances it is likely to encounter during its life but any monitoring scheme that is installed should be directed towards detecting the untoward effects of these disturbances.

## 3.5 Insulation ageing mechanisms

### *3.5.1 General*

Electrical insulation faults are a significant contributor to rotating machine failures. Industry studies indicate that up to one-third of rotating machine failures, Table 4.2 can

be attributed to stator winding insulation problems. Therefore, they deserve consideration before we consider failure modes in general. However, it should be borne in mind that although the final failure mode may be electrical breakdown of a dielectric component, but the underlying mechanism driving the breakdown may be driven by thermal, mechanical or environmental stress as well as electrical factors. This section will cover the basic stresses that affect the performance of stator winding, stator core and rotor winding insulation systems on operating machines as well as discussing the roles that design, operation and maintenance have on the life of the equipment.

Insulation systems are classified into Types I or II where different insulation materials apply.

- Type I materials are usually organic, such as polyamide-imide or polyester with a polyamide-imide overcoat and the rated voltage is below 700 V,
- Type II will rely on mica using mica paper tape for coil insulation and mica-based ground-wall insulation to withstand PD.

Insulation in service is exposed to high temperature, high voltage, vibration and other mechanical forces, as well as some adverse environmental conditions. These stresses can act together or individually to degrade insulation materials or systems. Thermal ageing of insulating material due to high temperatures has been most studied, and is perhaps best understood. The mechanism may be treated as a chemical rate phenomenon, described by the Arrhenius relationship, and includes loss of volatiles, oxidation, de-polymerisation, shrinkage and embrittlement. In actual service, loss of insulation system integrity is aggravated by cyclic and transient mechanical forces, which cause relative movement and abrasion of insulation. Furthermore, insulation subjected to high voltage can degrade due to PD activity. Eventually, the stresses will so weaken the insulation that puncture occurs and the conductor is connected to earth. Thus, although the final result is electrical failure, the root cause may be the result of a non-electrical stress. In general, the higher the electrical stress or temperature, the more rapidly insulation will age. In the discussion to follow, each of the above stresses, thermal, electrical, mechanical and ambient conditions will be described in generic terms. The exact details of which the critical mechanisms are very much dependent on the type of equipment and service conditions.

### *3.5.2 Thermal ageing*

Thermal ageing occurs when the temperature of the insulation is high enough to cause the electrical and mechanical properties of the insulation to degrade. Cycling of the temperature can also induce mechanical stresses causing deterioration, even if the temperature alone is insufficient to cause damage, for example the loss of the copper/insulation bond in the stator windings of rotating machines as a result of successive conductor heating and cooling.

The operating temperatures of inorganic insulating materials, see Table 3.2, for example, porcelains and glasses, are limited by the reversible changes of conduction, dielectric loss or strength, or softening, or the danger of fracture due to

differential thermal stresses. Organic materials suffer irreversible changes at high temperatures. Generally, the temperature limit of the machine will restrict deterioration to what is acceptable over the equipment design life, except when the temperature rise in service is of short duration then immediate changes, such as softening, may occur. Typical obvious symptoms are shrinkage, hardening, spontaneous cracking or crazing, loss of strength, embrittlement, discolouration, distortion and, in extreme cases, charring. These effects are generally due to, or accompanied by:

- Loss of weight resulting from the evaporation of volatile components,
- Oxidation or pyrolysis to form volatile substances or gases such as CO and $CO_2$, water and low molecular weight hydrocarbons,
- Excessive cross-linking.

### *3.5.3 Electrical ageing*

#### 3.5.3.1 General

Electrical ageing occurs when the electric stress applied to insulation causes deterioration. Although electric stress due to DC and transient voltages can cause ageing, AC voltage is normally the most severe. It should be noted that the insulating materials used in practical equipment operate well below their inherent breakdown strength. Consequently, electrical ageing of insulation usually occurs as a result of the presence of faults in the material, for example, gas voids due to imperfect impregnation, resulting in PD or incorrect lay-up of fibre components. The following are the electrical ageing mechanisms that can be induced by the principal power frequency voltage or by transient surge voltage from power system disturbances.

#### 3.5.3.2 Partial discharges

In general, deterioration from PD will occur in insulation that has voids created during manufacture or by thermal or mechanical ageing in service. The direct impingement of discharges on insulation surfaces will cause decomposition of solid insulation. PD only occurs in machines with disturbances associated with local peaks of electric stress, depending on air pressure, humidity and machine voltage. In general, in normal ambient conditions at the sea level, PD does not occur at sinusoidal winding phase voltages less than 3 kV. Each individual PD represents a charge transfer of picocoulombs (pC), however there may be many PDs in each voltage half-cycle, see Figure 3.7.

Therefore, they depend upon voltage, environmental conditions, machine design, particularly of the winding insulation, and application. Over time, they can damage the machine insulation.

#### 3.5.3.3 Surface tracking and moisture absorption

Electrical surface tracking is the formation of conductive or carbonised paths over an insulation surface, caused by AC electrical stress. When an insulating surface collects dust and moisture it can become conducting. The conduction current can

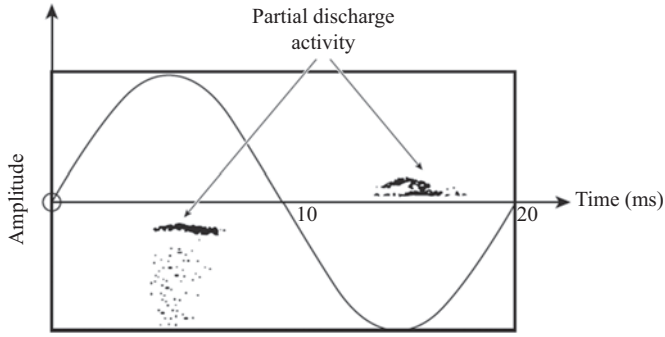


*Figure 3.7 Example of PD activity during a voltage cycle*

become large enough to swamp the effects of capacitance currents, in that case the voltage distribution is no longer determined by capacitances, as for a clean surface, but depends on how the conductance varies over the surface. The pollution film is never uniform, and conduction through the film causes drying out that is most rapid in the regions of highest resistivity. Drying out then causes a further increase in resistivity in these regions, so the effect is cumulative and eventually a dry band is formed across the insulation. Most of the surface voltage appears across this dry band, flashover then occurs over the dry band, constituting a partial break-down. An arc is formed in the air adjacent to the dry band, this arc can do one of the following three things:

- Extinguish rapidly,
- Stabilise and continue to burn,
- Or extend in length until it bridges the insulation causing complete breakdown.

In the final stages, the arc may grow slowly, by thermal drying, a reversible process, or it may propagate rapidly and irreversibly due to the stress concentration at the arc root. Arcs on polluted insulation can propagate and cause failure at working stresses of 0.02–0.04 kV/mm. Such low stress should be compared with the average insulation breakdown stress of 3 kV/mm for uniform fields and 5 kV/mm for point-plane gaps in air.

#### 3.5.3.4 Transient voltages

Transient or surge voltages can result from a number of causes such as lightning strikes, switching operations due to faults or from the power electronic devices feeding the machine, in the case of VSDs. Normally, insulation systems are designed and qualified to withstand lightning and switching surges, however, faster transients, such as those associated with drives or gas insulated switchgear operations, have been known to cause failures due to the non-uniform voltage distribution resulting from steep-fronted surges. Consequently, part of the design process requires knowledge of the electrical environment, the surge environment, in which the equipment will be operating. Transient events can also cause failure in older

equipment that has been subject to several years of thermal, electrical, mechanical, or ambient ageing.

### *3.5.4 Mechanical ageing*

Mechanical stress is a major direct or indirect contributor to many insulation system ageing mechanisms. Mechanical ageing is principally produced by the relative motion of insulating components and results from mechanical and electromagnetic forces, resonances, inadequate wedging and bracing, flexing, abrasion and environmental factors that affect the mechanical properties of the insulation. These are particularly prevalent in the stator end windings of larger machines.

### *3.5.5 Environmental ageing*

The contamination of insulation systems by water, oils, or chemicals can cause insulating materials to degrade mechanically and electrically. Thermal ageing will also proceed at a faster rate in air than in relatively inert atmospheres such as hydrogen or carbon dioxide. The effects of moisture or water absorption are well known. The most common ageing effect is the worsening of insulation electrical properties and a general tendency to poorer mechanical performance. In practice, the severity of problems, caused by the presence of moisture in the insulation, is dependent on the type of insulation system. Older insulation systems, containing organic binders and bonding varnishes, are more susceptible to mechanical degradation from water absorption than modern systems containing inorganic binders and synthetic resins such as epoxy. However, polyester-based materials can lose their electrical and mechanical properties in wet environments. Hydrolysis is a mechanism by which moisture causes rupture of the chemical bonds of the insulation. This tends to cause delamination and swelling of the insulation exposing it to the risk of failure due to thermal, electrical or mechanical factors.

Oils, acids, alkalis and solvents can also attack certain insulating materials and bonding agents. Again, organic materials are more likely to suffer significant deterioration. Contamination of insulating materials with dust can result in electrical failure due to surface tracking.

There are a number of high-voltage applications, such as coolant circulator motors within nuclear power station reactor containment areas, where radiation levels can be high. If acceptable insulation life is to be achieved, the insulation systems used must contain materials with a high radiation resistance to prevent rapid mechanical deterioration of mechanical properties. Materials such as ceramics, mica and glass are known to be only slightly affected by the radiation levels encountered in these areas. Organic materials, on the other hand, are strongly affected by the ionising radiation while polymers with aromatic rings, such as polyamides, will tolerate higher doses without deterioration. Because of the susceptibility of organic materials to radiation damage, great care is required in selecting and qualifying insulation materials and systems for use in these environments. The principle sources with which the designer is concerned are $\gamma$-rays and neutrons that interact with insulating materials to produce the damaging electrons.

The two molecular changes that may be produced by radiation in an organic insulation are cross-linking of molecular chains and bond scission, or cutting, of polymer chains. Cross-linking builds up the molecular structure, initially increasing tensile strength, but then reduces elongation and eventually results in the loss of impact strength. This changes rubbery or plastic material into hard, brittle solids.

Scission breaks down the molecular size, reduces the tensile strength and usually adversely affects other properties.

In outdoor applications, attention should be paid to the resistance of insulation to degradation by ultraviolet light that can also result in material embrittlement.

### *3.5.6 Synergism between ageing stresses*

Typically, the operating environment of most rotating machines results in two or more of the above ageing mechanisms being present at the same time. Interactions between the stresses may be complex and result in unexpected consequences. The complexity introduced by a combination of stresses is one of the reasons that most insulation materials, systems and sometimes components are subjected to sequential application of individual stresses in prescribed multi-factor ageing test cycles. Multi-factor ageing of insulation materials, which tries to represent these insulation system operating conditions, is performed on sample insulation components in some cases, however, the results require significant analysis, see the 'Standards' section at the end of this book.

An understanding of the synergistic effects between ageing stresses is central to the design of any CM program since it will affect the selection of the hardware and the interpretation of the data derived from these sensors and measuring instruments.

## 3.6 Insulation failure modes

### *3.6.1 General*

From the preceding sections, it can be seen that the means by which electrical machines fail depends not only on failure modes, which will be discussed in Chapter 4, but also on the type of machine and the environment in which it is working. However, it is possible to identify certain basic failure mechanisms that apply to all machines. We must then identify the early root causes of these faults because it is by detecting root causes that monitoring becomes practicable and beneficial.

Any fault involves a failure mechanism, progressing the initial fault to the failure itself. The time taken for such a progression will vary, depending on a wide range of circumstances. What is important, however, is that all faults will have early indicators of their presence and it is here that monitoring must seek to look and act. Also, any fault is likely to have a number of possible causes and is likely to give rise to a number of early indications. A typical route to failure is shown in Figure 1.3.

In this and the following section, we give a description of the ailments with which electrical machines are afflicted. A detailed schedule of failure mechanisms for electrical machines is given in Appendix A where the failure modes and root

causes for electrical machines are elaborated. By a study of Appendix, the reader can identify what parameters would be worth monitoring in order to give an early indication of a particular fault. However, the general overview in the Appendix may fail to give the reader a clear image of the faults he/she may encounter on his/her machines.

Therefore, we will describe in these sections a number of specific machine failure modes that draw out the factors that need to be considered in any monitoring system. Most of these incidents have been taken from the authors' experience, so detailed references do not exist. However, various electrical machine users have tried to record their own failure statistics and typical results are summarised in Dickinson (1974), Barker *et al.* (1982), O'Donnell (1985) and Tavner *et al.* (1986).

Insulation faults present some of the most challenging problems for electrical machines, so this section starts with the major insulation failure modes of electrical machines and then follows with other failure modes.

## *3.6.2 Stator winding insulation*

### 3.6.2.1 General

Stator winding insulation is affected by all of the aforementioned thermal, electrical, environmental and mechanical stresses, however, the extent to which these stresses will cause problems in the short or long term, in normal operation, will depend on factors such as the operating mode and type of ambient cooling conditions. For example, air-cooled machines tend to be subject to higher rates of thermal ageing compared to generators with direct liquid cooling of the stator winding. Furthermore, generators with this type of cooling usually operate in a compressed hydrogen atmosphere thus eliminating oxidation.

### 3.6.2.2 Delamination and voids

Stator winding insulation is a laminated system consisting of numerous layers of mica-paper tape on a fibre-glass backing material impregnated and consolidated with a synthetic resin, usually epoxy or polyester-based. The stator windings of rotating machines built prior to 1970 are likely to contain a bituminous resin instead of epoxy or polyester. Further, these older insulation systems tend to employ large flake mica rather than mica-paper. Consequently, the results derived from any CM tool that is focused on stator winding insulation must be viewed in the context of the differences in these materials. While the older, thermoplastic resins flow at relatively low temperatures, around 70 °C, causing resin migration leading to void formation and embrittlement of the main ground-wall insulation, the high mica content provides significant resistance to PD deterioration. Further, the propensity of bitumen-based insulation to soften at elevated temperatures permits the ground-wall to conform to the walls of the stator core slot and render a degree of self-healing. The lack of this property in modern, thermoset insulation systems based on synthetic resins has resulted some problems to be discussed below. Consequently, the use of age as a reliable index of machine health is not supported.

Voids or delaminations in the ground-wall insulation of stator windings may result from the manufacturing process and/or operating stresses. The presence of voids in new stator windings, although not desirable and should be minimised, does not necessarily imply that the winding be rejected or that it is not fit for the design life intended. Application of various diagnostic tests, such as PD and dielectric loss, as well as potentially destructive overvoltage tests aid in the production of stator windings with minimal void content. During the life of the machine, these initial delaminations, or those initiated by thermal, mechanical or electrical stress may result in the growth of voids prone to PD. The probability that a void will be subject to PD is governed by a number of factors such as void dimensions, electrical stress, pressure, temperature and the presence of initial electrons to cause discharge inception.

A PD is so called because it represents a gas breakdown between the two dielectric surfaces or between a conductor and a dielectric surface. Details of the physics of the process can be found in Pedersen *et al.* (1991). PD, similar to any gas breakdown, results in the emission of heat, light, sound as well as the production of electrons and ionic species. Depending on the energy of the discharge, erosion of the void walls will result causing growth of delamination and potentially failure in the long term. However, from a practical perspective, stator winding failure caused by internal void discharge is very uncommon and is not considered by manufacturers and users of rotating machines to be a significant problem. There are two principle reasons why void discharge does not lead to rotating machine failure:

- Presence of mica, a material extremely resistant to electrical discharge attack, forces PD erosion to occur only in the organic binding resin component. Consequently, the electrical breakdown path must follow a very circuitous route from the initiation site to the grounded core steel before failure can result. Typically, the initiation point is located at the edge of the copper conductor stack. Thus, the time-to-failure for such a process is very long, in the order of decades.
- Application of on-line PD monitoring equipment as well as advances in the interpretation of the data produced by these tools. Use of PD monitoring equipment has enabled machine users to better determine the condition of stator winding insulation in operating machines and to take corrective action at early stages, however, refer to Sections 11.6 and 11.7. Although there is little maintenance available to remediate the presence of voids in the ground-wall insulation, actions such as maintaining the integrity of the slot support system or reducing the operating stresses on the machine may arrest the process of PD delamination.

Thus, although void discharge has been and continues to be, a subject of intense study by academic and other research organisations, failure of stator winding insulation from this mechanism is of low probability. The use of PD measurement may be of value, however, because PD is a symptom of other stator winding deterioration mechanisms that can cause failure (Figure 3.8). These mechanisms will be discussed below, therefore PD can provide a useful history of machine winding insulation.

*Figure 3.8 Corona discharge on an end winding knuckle of an HV induction motor, over time this will result in winding insulation PD damage*

### 3.6.2.3 Slot discharge

Slot discharge or high-energy discharge is a very damaging deterioration mechanism found generally, but not absolutely exclusively, in air-cooled machines. Left undetected or uncorrected, failure from this type of mechanism can result in a relatively short period of time, two to three years. Slot discharge is the term used to describe a discharge occurring between the surface of the stator coil or bar and the grounded core steel. Generally, this mechanism results from a loss of good electrical contact between the insulated bar or coil surface and the stator core. Rotating machines rated above 3.3 kV employ a resistive coating applied to the slot portion of the stator coil or bar to promote good electrical contact with the core. Deterioration of this coating or loss of contact between bar surface and core steel can lead to conditions favourable for slot discharge.

The key to preventing slot discharge is to minimise the differential movement between the stator winding and core (Figure 3.9). Consequently, significant effort is expended by machine manufacturers and users to maintain the integrity of the slot support system, that is the tightness of the stator wedges that restrain the winding in the slot.

During the transition from thermoplastic to thermoset insulation systems a significant increase in slot discharge problems on large air-cooled machines was observed by Lyles *et al.* (1993).

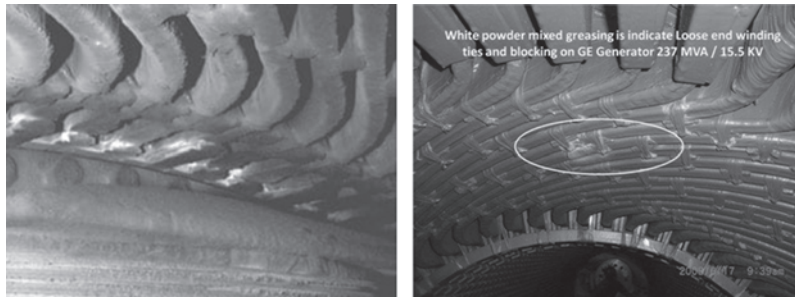


(a) (b)

*Figure 3.9 Examples of PD damage on HV stator windings: (a) stator slot emergence due to corona shield damage and (b) between the end winding coils*

The failure modes of large hydro generators were described by Evans (1981). In those cases, the new hard insulation systems did not conform well to the stator slot unlike the older thermoplastic insulations. Consequently, significant vibration of the stator winding was encountered that lead, during operation, to cyclical isolation of the stator bar or coil surface from the core steel. The resultant loss of electrical contact with the grounded core at one or more points along the coil or bar surface caused the surface potential on the bar to rise to line-to-ground potential. If this potential was sufficient to break down the gas gap between bar and core steel, then a high-energy discharge would result. Over a period of time, these discharges would erode the resistive surface coating leaving isolated non-conducting areas that further exacerbated the problem since these locations would become capacitively charged resulting in further discharge and erosion of the ground-wall insulation itself.

A further mechanism leading to slot discharge in machines with apparently good bar-core steel contact resulted from abrasion of the resistive coating and the creation of isolated, insulating patches on the bar or coil surface Jackson *et al.* (1982) and Wilson (1991). Wilson (1991) identified the critical conditions leading to slot discharge for this case and also demonstrated analytically that the problem could also occur throughout the winding and not be limited to the high-voltage coils or bars. This finding was borne out by experience in the field that found visual evidence of slot discharge damage at, or close to, the neutral point of the windings of large hydraulic generators as described by Lyles *et al.* Parts I and II (1994).

Slot discharge can be identified using on-line PD measurements. The PD behaviour of slot discharge tends to be characterised by:

- Large magnitude pulses with a predominance of one polarity depending on how the measurement is accomplished.
- The position of the occurrence of the PD pulses may vary over the power frequency cycle since the discharge is occurring between a capacitively

charged surface and the core steel and these surfaces are, due to vibration, not at well-defined positions with respect to one another.
- Rapid increase in PD magnitudes over a relatively short period of time, such as doubling of pulse magnitudes over six months.

The production of ozone in open-ventilated air-cooled machines is both a symptom of slot discharge and ultimately a life-limiting fault in itself. Ozone is a strong oxidising agent and will have a negative effect on the insulating and conducting materials. However, very often those machines that are producing excessive ozone are removed from service and rewound because the concentrations of ozone exceed the limits prescribed by health and safety legislation for workers.

#### 3.6.2.4 Stator end windings

From the perspective of electrical insulation, the end-windings of rotating machines are prone to environmental and mechanical rather than electrical ageing. Assuming that factory and/or acceptance overvoltage tests have demonstrated that the end-winding clearances have been properly designed and manufactured, the key problem areas for end-windings are:

- Surface contamination. The design and testing of the clearances in end-windings are performed from the context of clean and dry insulating surfaces. However, air-cooled machines, especially motors, often operate in ambient conditions containing high levels of conducting contaminants such as salt, cement dust, lubricating oil and brake dust. Over time, and in the presence of moisture, these conductive layers distort the electrical field in the end-winding and lead to surface tracking. This deterioration mechanism if not corrected may lead to serious problems including the phase-to-phase failure of the machine. PD measurements can be used to detect the presence of contaminated end-windings.
- Internal voids. Until relatively recently, the end-winding portion of stator bars and, especially, stator coils tended to be taped manually rather than by machine as is the case in the slot cell. Consequently, the insulation of the end-winding region is prone to contain voids or delaminations. The presence of such faults is not as critical as for the slot cell of the winding because the electrical stress in this area is relatively low.
- Mechanical aspects. The end-winding structure of a rotating machine, especially for large turbo-generators, represents several challenges for designers. Apart from electrical clearance, the major issues are minimising the vibration and differential movement. Modern synthetic insulation systems are quite rigid and thus prone to cracking either due to long-term cyclic fatigue in normal operation or transient events causing end-winding distortion such as a close-in transformer fault. Unfortunately, while the behaviour of insulating materials in this region of the machine is considered of significant interest, relatively little work has been done to develop a similar understanding of the creep and fatigue properties that exist for metals.

#### 3.6.2.5 End-winding stress grading

End-winding stress grading systems tend to be found on machines rated 6.6 kV and above. Their role is to reduce the electric field at the surface of the stator bar or coil where it exits the core slot. Without application of such a material, there is a high probability of surface discharge or even flashover from the capacitively charged insulating surface back to the core steel. The functionality of the stress grading system may be compromised by the surface contamination or improper design and processing of the interface between the end-winding grading and slot stress control systems. In the latter case, a combination of electrical and thermal effects can cause erosion of the junction between the two systems, potentially resulting in an increase in surface discharge activity. While this fault can appear serious, the discharges tend to be transverse to the surface resulting in a low probability of machine failure due to this mechanism. Empirical evidence indicates that when the junction between end-winding and slot stress control systems has been completely disrupted, and the electrical contact lost, the surface discharges cease.

#### 3.6.2.6 Repetitive transients

Variable-speed drives based on electronic inverters are widely applied on low voltage, <1 000 V, motors. Insulation problems have been experienced on these largely random wound machines resulting in failures. The bulk of the failures have been attributed to electrical discharges in the end-windings of these machines. The steep-fronted surges generated by the IGBT devices employed in these drives may cause transient voltage-doubling that exceeds the electric field required to cause breakdown in the air around the end-windings. The insulation systems employed in random wound machines, typically polyester-based enamels and Daglas, have poor discharge resistance and are thus prone to failure in the presence of such discharges. Steps to mitigate this problem include better design of the winding, to minimise the areas of high electrical stress, consideration of the length of cables used to connect to the motors, to reduce the probability of voltage doubling, the use of multi-converter topologies, and the use of metal-oxide loaded enamels to grade the winding electric stress.

High-voltage motors, employing form wound stator windings, are less prone to the deterioration mechanism described above although some consideration is being given to the behaviour of the resistive slot stress control material under repetitive transient conditions.

### *3.6.3 Stator winding faults*

#### 3.6.3.1 Winding faults (All machines)

It is clear that the insulation system is potentially one of the intrinsically weakest components of an electrical machine, both mechanically and electrically and in the earliest days of machine construction insulation faults were excessively frequent as Miles Walker (1929) described.

However, as described above, modern techniques of winding manufacture, using thermosetting resin or vacuum pressure impregnated insulation, provide systems that

are mechanically tough and electrically sound. Nonetheless, modern machines use drives insulation systems to their thermal, mechanical and electrical limits. However, there are very few incidences of failures on machines due simply to ageing of insulation. A very thorough review of root causes of failures and failure modes in insulation systems and conducting components is given in Stone *et al.* (2014).

An example of a generator winding failure is shown in Figure 3.10 and the final puncture of the insulation system was the result of accelerated ageing due to an over-temperature in the adjacent generator core.

An exception to this may be on air-cooled, highly rated hydro-generators where epoxy mica insulation has failed due to erosion of the insulation in the slot portion as a result of discharge activity, primarily because of the rigidity of epoxy mica systems, the large forces on such large conductor bars, the high dielectric stress on the windings and the fact that these machines are air-cooled.

However, failures due to isolated insulation faults do occur. These are due to manufacturing faults, such as voids or foreign bodies, embedded in the main wall insulation, or penetration of the insulation by foreign material, such as oil or metal, from elsewhere in the machine.

Whether insulation failure occurs due to ageing or the action of an isolated fault, the indications are similar in that there will be an increase in discharge activity in the machine culminating in an insulation puncture like the shown above.

Faults can also occur in low voltage windings, which are generally dipped in varnish and do not experience high voltage discharge. Figure 3.11 shows a typical failure in a round wire winding that is varnish impregnated showing the effect of moisture contamination and tracking that has eaten away part of the winding slot liner causing a fault to earth.

### 3.6.3.2 Winding conductor faults (Generators)

These faults are again generally confined to large generators where the current densities are such that the stator winding is electrically, thermally and mechanically

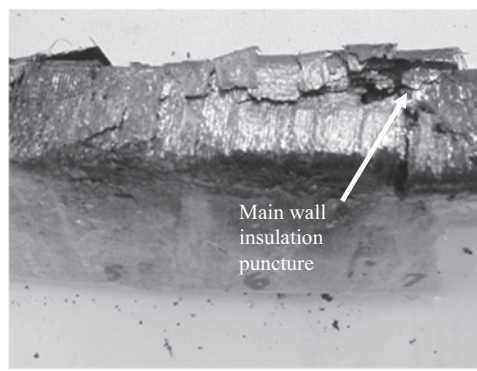


*Figure 3.10 Stator fault in a 15 kV generator winding, showing the main-wall insulation punctured in the top right as a result of core overheating*

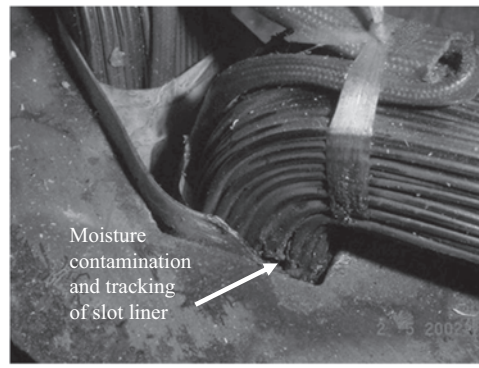


*Figure 3.11 Stator fault on a 200 V exciter winding, showing the effect of moisture contamination and tracking*

highly stressed. It is normal to subdivide the conductor into a large number of sub-conductors and to insulate and transpose them to minimise winding losses. In the most modern machines the transposition is distributed throughout the conductor length employing the Roebel technique. This gives a uniform current distribution and minimises the voltages between sub-conductors. Older machines, however, have the transpositions made in the end winding at the knuckle joint and quite large voltages, up to 50 V rms, can exist between sub-conductors. If severe, mechanical movement of the winding occurs during operation and the sub-conductor insulation fails then sub-conductors can short together causing arcing. A number of older machines have failed in the United Kingdom and the United States due to this arcing, which in the worst cases has eroded and melted other sub-conductors, pyrolysing the main wall insulation of the conductor bar. If this happens in the slot portion, or near to other earthed metalwork, then an earth fault can occur but if not, it is possible for the debris, ejected from the burnt area, to produce a conducting path between electrical phases of the winding leading to the more serious phase-to-phase fault, as shown in Figure 3.12(b). Sub-conductor arcing has also been initiated by fatigue failure of sub-conductors, where the conductor bar emerges from the core or enters a water box, due to excessive and winding vibration. The consequences of such a failure are very similar to those of a sub-conductor short. When this arcing takes place in a machine with hollow water-cooled sub-conductors, perforation of a sub-conductor occurs and, since they are usually arranged so that there is an excess of cooling gas pressure over the water, this leads to a leakage of gas into the water cooling system.

The early indicators of such faults are arcing activity within the winding and the pyrolysing of insulation. Although the fact that burning is taking place deep within a conductor bar usually means that, initially at least, only small quantities of particulate and gaseous matter produced by the burning are released into the cooling gas circuit. Where water-cooled sub-conductors are present the fault causes a leakage of gas into the winding cooling system.

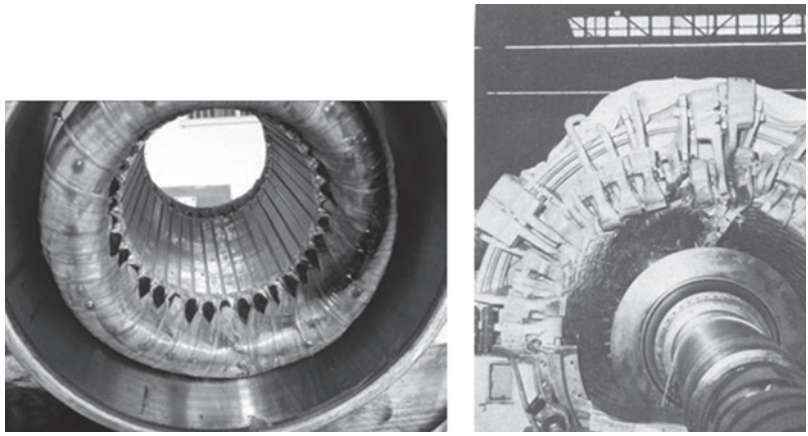

(a) (b)

*Figure 3.12 Stator winding faults: (a) overheating of 20 kW, 415 V induction motor LV stator winding due to inter-turn shorts and (b) stator sub-conductor fault on 588 MVA, 23 kV, 50 Hz turbo-generator winding, stator conductor bars ejected into the air-gap, disrupting the end winding*

### 3.6.3.3 Winding inter-turn faults (All machines)

A common failure mechanism on machines employing multi-turn stator coils is break-down of the turn insulation, see Figure 3.12(a). The resultant short-circuit between the copper turns causes a significant circulating current to flow in the coil leading to rapid deterioration and failure. Turn failures tend to be very destructive involving burning of the insulation and localised melting of the copper conductors. Often, failures resulting from breakdown of the inter-turn insulation are inferred from the location of the puncture, typically at or near the core exit, and the electrical position in the winding, typically the first or second coil from the line end.

During the 1980s, an EPRI study investigated the reasons for an apparent increase in the number of turn failures experienced by North American utilities. Initially, the increase in breakdowns was attributed to the increase in use of vacuum circuit breakers as replacements for conventional magnetic air circuit breakers. The steep-fronted, high-magnitude transients generated during operation of the vacuum circuit breaker was considered to exceed the capability of the turn insulation. However, the EPRI study concluded that the principal reason for the perceived increase in turn insulation failures was inadequate turn insulation. Those machines that incorporated dedicated turn insulation consisting of either mica-paper tape or double Daglas were found to have superior capability to withstand the steep-fronted surges imposed by vacuum circuit breakers as well as being able to withstand the rigours of steady-state operation at power frequency. The use of dedicated turn insulation provides abrasion resistance in the event of differential movement between turns due to thermal or thermo-mechanical ageing.

Early detection of the onset of conditions likely to lead to breakdown of inter-turn insulation may be possible using PD methods and/or techniques based on axial leakage flux detection, investigated by Penman *et al.* (1980). With regard to PD-based methods, a significant practical problem is that although the deterioration of the inter-turn insulation can, in principle, be detected, attributing the detected signals to this deterioration mechanism in the presence of PD pulses originating from other faults is practically impossible.

#### 3.6.3.4 End winding faults (All machines)

A considerable amount of effort over the whole range of machines has gone into the design of end winding structures. The first objective is to restrain the end winding against the large forces on the winding during transient loading or faults and the second is to cushion the conductor bars against the smaller forces during steady, continuous running. End winding movements are larger on the older, less rigid, bituminous mica insulation system but then that system, because of its softness, was more able to withstand the steady fretting action of normal running than the hard epoxy-mica systems. In either case end winding movements in normal operation are quite significant and can be as much as a few millimetres on a large turbo-generator.

Faults occur in the end winding when the bracing structure slackens, due to torsional and lateral vibration, either as a result of a succession of unusual overloads or because of an extended period of continuous running at high or overload. In some cases, end winding insulation becomes cracked, fretted or worn away. In the limit, a full line to line fault can lead to a catastrophic failure of the end winding as shown in Figure 3.12(b). On the largest machines, fatigue failure of conductors can occur when the winding becomes slack enough to permit a significant amount of conductor movement during normal operation or during the much larger forces of starting or re-switching. In addition, seismic excitation of the relatively weak end winding structure can occur in applications with inherent vibration where the machine is mounted on a flexible foundation and this has been a major cause of end winding failures in the offshore industry.

Foreign bodies inside a machine, such as steel washers, nuts or small portions of insulation, get thrown around by the rotor. Damage is caused by these objects, usually in the stator end winding region, where the insulation is damaged by impact or eroded by debris worming into the insulation under the action of electromagnetic forces. The early indications of problems are an increase in end winding vibration and the possibility of electrical discharge activity to nearby earth planes.

#### 3.6.3.5 Winding coolant system faults (Large machines)

Many large machines employ direct or indirect liquid-cooling of the stator windings to permit operation at higher energy densities. In the vast majority of cases, the coolant medium is water, however, a small number of designs use oil. Consequently, there is a risk that the coolant path will deteriorate resulting in the release of water, of varying levels of purity, on to insulating or high-voltage components resulting in deterioration and potentially failure of the machine.

Large steam turbo-generators employ direct liquid-cooling of the stator windings in that demineralised water flows through hollow sub-conductors. Most designs, whether single or two-pass, use a manifold at one or both ends of the winding that connects to the individual stator bars using insulated (Teflon) hoses, see Figure 3.6(a). Catastrophic failure of the hose or the connection of the hose to the bar or manifold will result in water impinging on the stator winding. Depending on the condition of the water, such an event may not cause an immediate stator earth ground alarm or fault, however, the coolant loop pressure and stator winding temperature will be affected. Smaller leaks would likely result in gas-in-coolant alarms and potentially gas-locking.

Some types of turbo-generators employ a plenum that connects a group of stator bars directly to the water circuit without the use of hoses. The plenum consists of cast insulating epoxy components, mechanical failure of which will cause loss of the coolant circuit and water impingement on the stator winding.

Other sources of potential water leaks onto the stator winding include faults in the hydrogen coolers. In this case, water is likely to have a relatively high conductivity and would have a high probability of causing a stator ground fault alarm and ultimately fault.

Water leaks into the bulk of the stator winding insulation can also occur. This water ingress has been observed on liquid-cooled stator windings using the clip design where the connection of the stator bar to the coolant system is affected. Pinhole leaks appear after a few years of service and moisture propagates along the brazed joint until contact with the strand insulation. The moisture further wicks into the insulation degrading the dielectric properties. Two principle root causes for moisture ingress into stator winding insulation.

- Crevice corrosion, resulting from chemical reaction between the coolant water and the braze material that
- Deficiency in the quantity of brazing material; the initial brazed joint is tight, but over time vibration and thermal stresses cause voids in the braze to connect creating a channel for the water.

In principle, the presence of a leakage channel in the brazed region should result in a gas-in-coolant alarm. However, the insulation covering the water box is very tight and hydrogen does not migrate easily through it. Therefore, water box leaks detected in this way are rare.

Water ingress in the insulation wets the material to up to ten times the initial moisture level. Another consequence of water ingress in the ground-wall insulation is a drop in insulation resistance. This resistance decay can be quite slow. It is considered that it takes about 5 years for water to migrate and cause a significant insulation drop. This is the main mechanism for stator winding failure due to water box leaks. Several stator earth fault failures are due to water ingress and thus to water box leaks. So far, water box leak detection methods have been based on detecting one of the consequences of the water ingress. However, no reliable on-line method has been developed.

In addition to problems caused by coolant leaks, serious damage can be caused by blocking of the coolant flow in stator windings. Depending on the location and number of plugged sub-conductors catastrophic failure due to overheating can occur rapidly. Other than blockages caused by foreign material entering the coolant loop and gas locking, flow restrictions can result from the deposition of copper oxide deposits. These deposits may result from poor control of stator water chemistry.

Plugging or flow restriction of the coolant medium in the hollow sub-conductors of liquid-cooled stator windings can have serious, if not catastrophic, implications for the reliable operation of large steam turbo-generators. Significant efforts have been, and continue to be, expended on understanding the fundamental mechanisms resulting in coolant flow restriction. Apart from loose debris in the coolant circuit, the predominant cause of blockage is corrosion of the copper conductors resulting in the deposition of copper oxides that tend to clog the small aperture hollow sub-conductors. Consequently, much of the work in this field has focused on the chemistry of the coolant water.

Unfortunately, for some utilities plugged sub-conductors are already a reality, resulting in the derating of units and/or the implementation of complex flushing and cleaning procedures. Again, many organisations are pursuing work to understand and optimise these remedial actions. Consequently, significant work is underway, or has already been performed, to understand the plugging mechanism and the means to prevent or remedy it. These efforts are necessary to enable utilities to maximise reliability and availability of their generators. However, there is a third aspect to this problem, namely, for those utilities experiencing over-heating due to plugged sub-conductors, how best to manage the situation so as to minimise the revenue loss while ensuring that the stator winding suffers no undue loss-of-life.

Unfortunately, early detection of stator bar overheating due to plugging is complicated because of, in many cases, the dearth of sufficient temperature and flow data. Even where significant quantities of temperature data exist, such as on hose-type machines with thermocouples on the outlets, the location of the temperature sensor with respect to the hot spot increases the difficulty of successful early plugging detection. Some organisations have recognised this problem and have attempted to address it by detailed thermohydraulic modelling of the stator winding and/or the implementation of post-processing of the temperature.

Notwithstanding the above efforts, operators of large steam turbo-generators presently lack tools to objectively assess the risks associated with operating machines with known, or possible, sub-conductor plugging.

### *3.6.4 Rotor winding faults*

#### 3.6.4.1 General

Rotor windings of synchronous machines are insulated with epoxy-glass laminates or polyester-based materials (Nomex). Rotor windings of large squirrel cage induction motors generally consist of lightly insulated copper bars driven into the laminated slots in the case of large machines rotor or die-cast aluminium or copper

cages for smaller machines. The principal stresses of concern to rotor windings are due to thermal expansion and centrifugal mechanical forces.

### 3.6.4.2 Winding faults (Induction motors)

Faults on the rotor windings of induction motors have not been easy to detect because there is not necessarily an electrical connection to the winding and it is difficult to measure the low frequency currents induced in the rotor winding. Although the rotor winding of a squirrel cage induction motor is exceptionally rugged, faults do occur particularly on the larger machines especially when they are subjected to arduous thermal and starting duty causing high temperatures in the rotor and the high centrifugal loadings on the end rings of the cage, see Figure 3.13.

Faults may occur during manufacture, through defective casting in the case of die-cast rotors, or poor jointing in the case of brazed or welded end rings. Such a fault results in a high resistance, which will cause overheating, and at high temperature the strength of the cage will be impaired. Cracking may then occur in the rotor bar and indeed usually takes place at the cage end rings where the bars are unsupported by the rotor core. Similar faults can occur because of differential movement of the cage in the rotor slots, because of a succession of periods of high temperature running and shutdowns. This can lead to distortion and ultimately cracking of the end rings and the associated bars. It should be remembered that the bars must provide the braking and accelerating forces on the end ring when the motor changes speed. If the motor speed fluctuates, because of the changing load or as part of the normal duty cycle, then high-cycle fatigue failures can occur at the joints between bars and ring. If the motor is repeatedly started, then the exceptional starting forces may lead to low-cycle fatigue failure of the winding component.

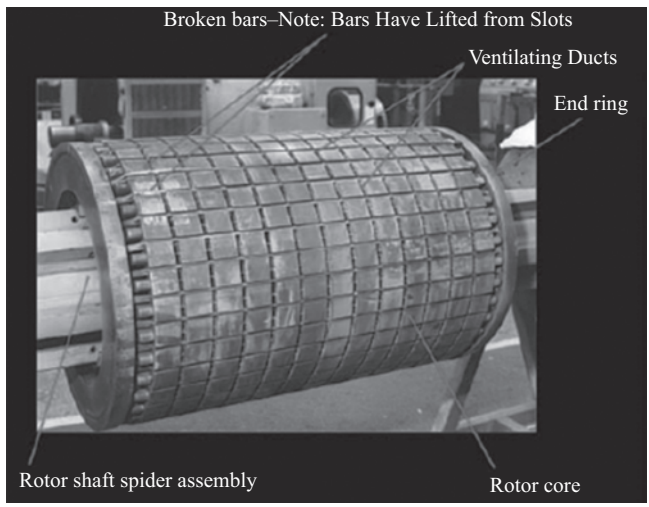


*Figure 3.13 Rotor cage fault in a 1.5 MW squirrel cage induction motor*

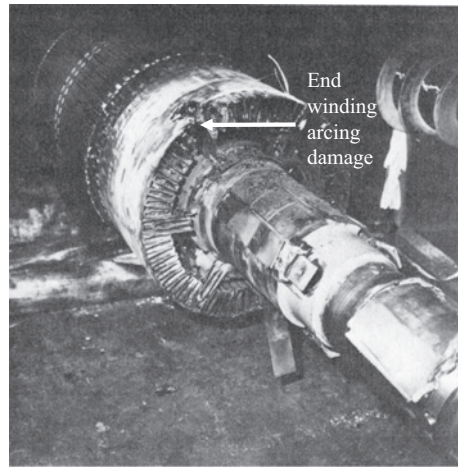


*Figure 3.14 Rotor winding fault in a 3 MW slip ring induction motor, showing the arcing damage between the phases in the winding end region*

The early indications of these faults are pulsations in the speed, supply current, stray leakage flux and vibration of the machine.

The rotor windings of wound rotor induction motors are of rather similar design to the stator winding of the motor except that the end windings must restrained against centrifugal forces by steel wire or woven glass fibre banding rings. Damage to the windings usually occurs in the end region due to centrifugal forces on the crossovers and connections of the winding causing shorts between turns. These faults are similar to the problems experienced on the rotor windings of high-speed turbo- generators. An additional difficulty encountered with the wound rotor machine is that of ensuring balance between the phases of the external resistors connected to the winding via the slip rings. These resistors are usually water-based and can become unbalanced with time, then the currents flowing in the rotor windings will be unbalanced and overheating will occur. This can lead to the rapid degradation of rotor winding insulation and ultimately failure such as shown in Figure 3.14. The problem is difficult to detect because the rotor currents are at the very low slip frequency and one must detect the relatively small changes in those currents.

### 3.6.4.3 Winding faults (Turbo-generators)

The rotor winding insulation and bracing system in turbo-generators must be designed to withstand the extremely high centrifugal forces present during operation. An inter-turn short-circuit can occur between rotor turns due to puncture or cracking of the turn insulation. The current that subsequently flows between turns creates localised heating and the probability of further shorted turns. This disturbance of the current flow will cause an asymmetry in the flux in the machine causes unbalanced magnetic pull (UMP) leading to vibration of the rotor and this

can be compounded when the asymmetric heating leads to thermal bending of the rotor. Two and four pole totally enclosed machines are particularly prone to these problems especially if they have a short air-gap that will have a reduced coolant gas flow and therefore rotor temperatures can be higher. Differential movement between turns and fretting action in the rotor winding can produce copper dust may also increase the probability of turn shorts. This phenomenon occurs because of the cyclic movement that a large winding experiences relative to the rotor. The movement is partly caused by self-weight bending of the rotor and thermal cycling. This problem can also be exacerbated by the long periods of barring or turning gear. During this type of very low-speed operation, there are little or no centrifugal forces that act to lock the key internal rotor components in place and hence minimise the differential movement.

If an insulation fault occurs between the winding and rotor body, then a ground fault current flows that can be detected by an earth leakage relay. The ground fault current is limited such that a single ground fault is not serious, but a second ground fault can result in very large circulating currents. A second ground fault can cause an arc to be struck at the fault location not only causing winding damage but also severe damage to the rotor forging, see Figure 3.15. The early indications of these faults are distortion of the air-gaps flux and associated stray leakage flux around the machine and an increase in bearing vibration.

Therefore, the early indications of these faults are usually excessive transverse bearing vibrations, although attention has also focussed on measuring the torsional oscillations of the shaft itself, see Chapter 8.

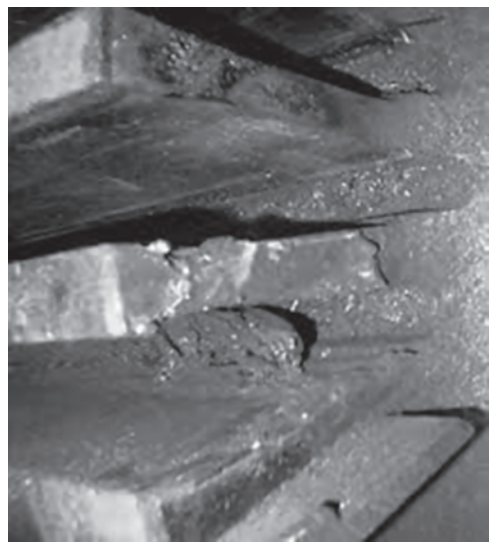

*Figure 3.15 Rotor winding earth fault on a 2-pole turbo-generator, showing resultant damage to rotor forging*

*Figure 3.16 Failure of DC armature winding close to the commutator*

#### 3.6.4.4 Winding faults (DC machines)

DC machines encounter particular difficulties in their armature, where the AC winding is directly connected to the commutator and electrical action between brushes and commutator segments can lead to high temperatures and the production of carbon dust. A common problem with DC armature windings is failure between conductors close to the commutator connection, Figure 3.16 shows just such a failure, possibly aggravated by the accumulation of carbon dust under the banding that provides the centripetal force to retain the winding in place close to the commutator connections.

## 3.7 Other failure modes

### *3.7.1 Stator core faults (Turbo- and hydro-generators)*

A core fault is a rare event, Figure 3.17, which usually only occurs in the largest turbine-driven generators where the laminated steel cores are sufficiently massive, and carry a sufficiently high magnetic and electric loading, see Table 2.2. They can occur anywhere in the laminated steel core of large rotating electrical machines but are more common in the stator core, see Tavner *et al.* (2005). A core fault initiates when core-plates are electrically connected together, either because of an insulation failure between them, or as a result of physically imposed short circuits due to various causes including foreign bodies. These connections circulate additional currents in the core, coupling the main flux, leading to additional losses and heating, further weakening core-plate insulation and expanding the fault. The fault is then at a zone in the core that is overheated, buckled and electrically interconnected.

*Figure 3.17 Core fault in the stator core of a 660 MW turbo-generator*

This can expand, melting material, leading to the catastrophic runaway of the fault and creating a cavity in the core, continuing until the main conductor insulation is damaged and the machine is disconnected for an earth fault. Core faults generally occur some distance from the main conductors and final disconnection frequently occurs after irreparable damage has been done to the core and conductors.

A number of large generators worldwide have experienced this problem, mainly as a result of damage to their stator cores during manufacture or rotor insertion, when laminations became shorted together, and the application to the core of transient high flux conditions.

### *3.7.2 Connection faults (HV motors and generators)*

Faults in the connections of electrical machines are very unusual in the lower voltages < 1 000 V rms but become more common at higher voltages where the dielectric stress on the bushings and forces on the conductors increase.

Insulation failures also occur from time to time on the bushings that carry the electrical connections through the machine enclosure. On a turbine-type machine these are mounted in the pressure-tight casing and therefore have to withstand the operating pressure of the machine. Failure of a bushing can occur either due to mechanical stresses or vibration on the conductor passing through the bushing, causing it to crack, or debris being deposited on the exposed surfaces allowing it to track electrically, as described in Section 3.6.3.3. Again, the early indication is an increase in discharge activity.

Figure 3.18 shows damage to a high-voltage switchgear bushing, similar to that used in HV machines, where moisture and contamination have allowed a

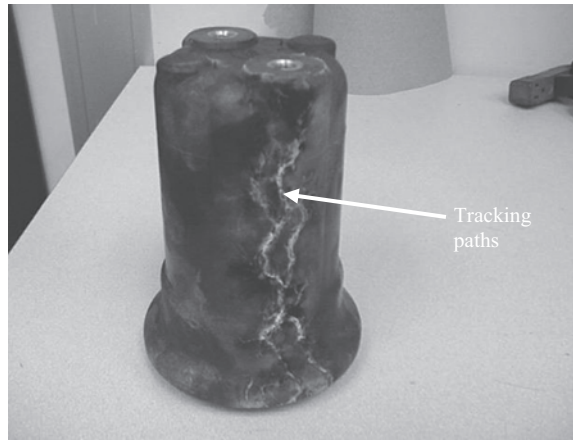


*Figure 3.18 Tracking damage on cast resin bushing similar to that used for high-voltage motor and generator connections*

conductive film to form on the surface of the bushing and severe surface tracking has taken place. The high dielectric stress on the surface of the bushing has allowed tracking to take place over an extended period of time, probably many months and even more than a year. This kind of damage tends to occur where bushings are exposed to the environment outside the machine. It is rare inside the machine unless there is a cooling liquid leak combined with solid contamination circulating in the inner cooling circuit. This kind of damage can be diagnosed by physical inspection, PD measurements or thermography.

### *3.7.3 Water coolant faults (All machines)*

In machines with water-cooled heat exchangers, it is possible for coolant blockage or failure to occur, either in the pipework leading to the heat exchanger or in the heat exchanger itself. This can be the result of pipework debris being circulated in the water system, although it should be removed by filters fitted close to the inlet of the machine or due to negligence when cooling systems or machines are maintained. The normal vibration of a machine in service can excite resonances in an improperly designed cooling pipework system and this can cause fatigue failure of a pipe and loss of coolant. The early indications of these kinds of fault are indicated by high conductor or cooling water temperatures, leakage from the water system and pyrolysing insulation leading eventually to damaging discharge activity that will be electrically detectable at the machine terminals.

### *3.7.4 Bearing faults (All machines)*

Rolling element, sleeve and pad bearings are used in rotating machines as guide and thrust bearings and fail when the load upon the bearing is excessive or its lubrication fails. The choice of bearing and the lubrication used depends upon the

load borne and the shaft speed, Table 3.4 gives a summary of the curves involved in the choice, based upon a prospective bearing life of 10 000 h, and this can be helpful when considering fault conditions. A good summary of bearing selection is given in Neale (1973) and shown in Figure 3.19.

Bearing failure is usually progressive but ultimately its effect upon the machine is catastrophic. Failure is accompanied by a rising temperature at the bearing surface, in the lubricant and in the bearing housing, which are detectable by temperature sensors. An important consequence of bearing deterioration for electrical machines is the rotor becomes eccentric in the stator bore causing a degree of

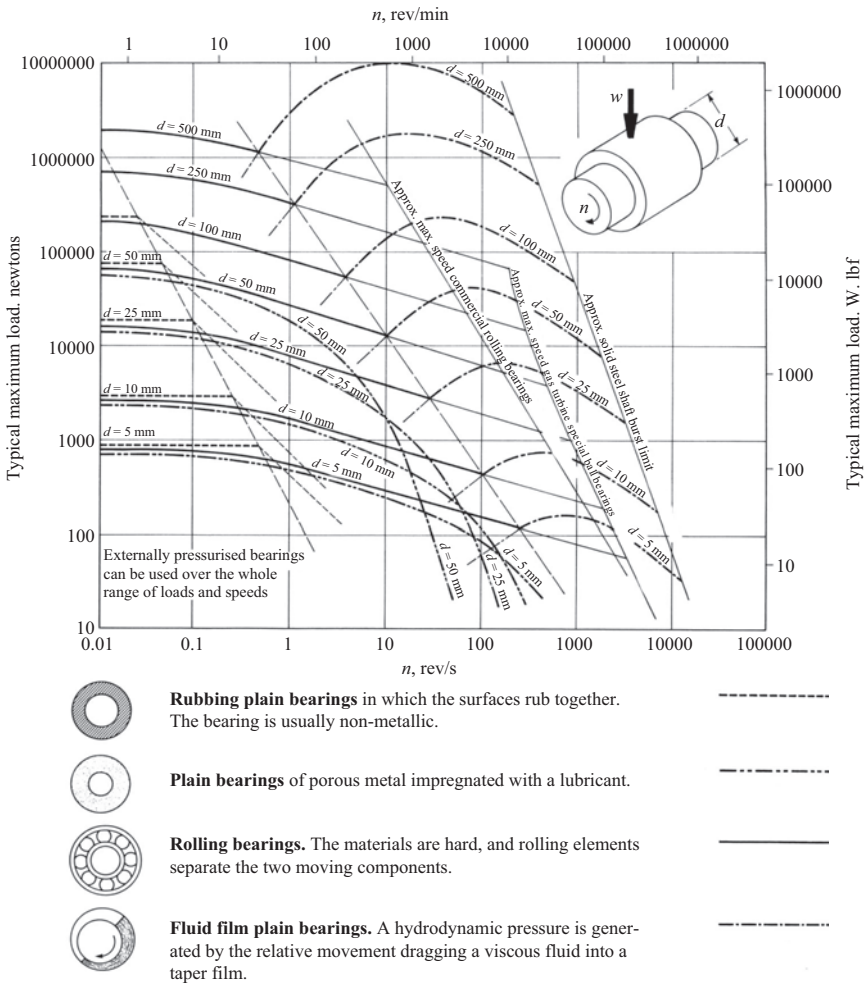


*Figure 3.19 A summary of the bearing selection criteria for all machinery*

static and/or dynamic eccentricity, disrupting the fine balance between the magnetic forces of adjacent poles, causing UMP and placing more load on the bearing. This also causes an increase in vibration as the shaft dynamics are affected by the altered air-gap and bearing stiffness.

Bearings can also be damaged by the flow of shaft currents as described in the following section.

### *3.7.5 Shaft voltages (Large machines)*

Electrical machines can generate voltages in their shafts due to an unbalance in the magnetic circuit of the machine, see Tavner (2008). The shaft voltage can circulate current through the bearings of the machine and this leads to bearing damage.

Voltages on small machines can be of the order of 500 mV rms but in larger machines they can be 5–10 V rms.

There is a considerable literature about shaft voltages and manufacturers design machines to minimise their effects by insulating one bearing of the machine and providing a shaft ground to allow the shaft voltage to be monitored.

The damage that occurs to bearings depends upon the type of bearing. In general, a rolling element bearing is more susceptible to the effects of shaft voltages, exhibiting electro-erosion, see Figure 3.20(a).

Sleeve bearings have higher impedance and resistance to damage but can also be affected by electro-pitting action consequent upon the intermittent flow of shaft current through the bearing oil firm, see Figure 3.20(b). However, the bearings of machines supplied from a VSD may experience more energetic electrical action, but this is dealt with in Chapter 11.

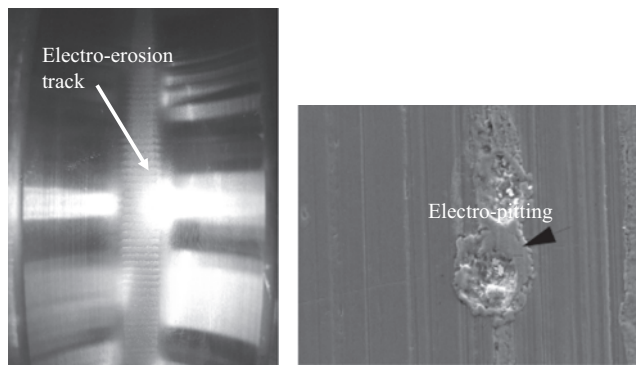


*Figure 3.20 Bearing electrical damage: (a) electro-erosion damage in race of a rolling element bearing due to the flow of shaft currents and (b) electro-pitting damage to a bearing sleeve due to the flow of generator shaft currents*

## 3.8 Conclusions

This chapter has shown the common structure present in electrical machines regardless of their type or size.

The construction of electrical machines has also been demonstrated with an indication of the effect of operational service on failure modes.

The importance of the insulation system of the machine has been considered and discussed.

Finally, typical failures in service have been shown to identify the most common failure modes that an engineer will encounter, starting with those originating in the insulation system but then expanding to consider other sources.

A set of failure modes root causes is set out in Appendix A and these demonstrate how faults could be detected in their early stages by monitoring appropriate parameters.

In the next chapter we will describe reliability analysis that will connect root causes to failure modes and shows how CM can be directed to address particular components in the electrical machine.

*Chapter 4*

# Reliability of machines and typical failure rates

## 4.1 Introduction and business of failure

Chapter 3 described the construction and operation of electrical machines and the way they fail in service.

We now move towards identifying what CM is needed to detect those faults.

All machines, plants and animals are subject to fault processes and natural degradation of health, similar to that plotted in Figure 1.3. Plants and animals have a cellular structure, incorporating growth and self-repair mechanisms, dependant on their genes, a subject of intense research in the biomedical sphere to promote health and prolong life.

However, machines of human construction do not have these benefits, but there are many similarities.

Electrical machine reliability is fundamentally dependent on:

- Design: by virtue of materials, rating and load, which may subject a machine to excessive torques, temperatures, voltages or currents; variability or discontinuity in the driving or driven machine load and varying ambient environment, including machine temperature, dependant on cooling and lubrication quality and contamination,
- Application: may be benign at a constant load; such as base-load generators or rapid load application and sudden reversals of power; such as a traction machine, or sudden operation at overvoltage or overload; such as a submarine propulsion motor, or stochastic changes of load, voltage and ambient conditions due to the natural environmental changes; such as in a wind or tidal turbine,
- Physics: torque being developed by **thermodynamically reversible** electromagnetic, electrostatic and mechanical processes, but accompanied by the **irreversible loss** processes in windings ($\alpha$ to $I^2R_{\text{wind}}$), core ($\alpha$ to $V^2/R_{\text{core}}$), insulation ($\alpha$ to $V^2/R_{\text{ins}}$), bearings ($\alpha$ to $\omega r_{\text{brg}}F_{\text{brg}}$) and coolant ($\alpha$ to $\Delta Tf_c$), due to the changing currents, voltages, speeds, forces and temperatures. These **irreversible processes** constitute the **electrical, mechanical, thermal and chemical root causes** of degradation, wear, corrosion and fatigue leading to yield, described in Chapter 3, which can be mitigated by design but ultimately interfere with energy conversion.

In time, these root causes accumulate to trigger the machine failure modes, a stochastic integration process, worsening machine reliability and leading to machine failure, Figure 4.1 repeated from Chapter 1.

The impact of these effects on electrical machine reliability is the subject of this chapter.

CM has previously been seen as the province only of those who analyse fault signals and interpret results.

However, interpretation must be informed by causality and the authors' view is that an important change in CM over the last 40 years is ensuring that it is firmly directed towards detecting and prognosing real machine failure root causes. In so doing, successful CM directly addresses, at the earliest practicable stage, machine unreliability and, more importantly, gives the operator a prognosis, which can be used to improve the availability.

By this means modern machine reliability theory, CM and prognosis, for human-made machines attempts to mimic living gene self-repair mechanisms.

The reliability to date of our surface and air transport and electrical generation systems confirm their effectiveness.

This chapter sets out the mathematical and numerical issues controlling this causality.

## 4.2 Definition of terms

In considering the progression to failure of machinery, we must remind ourselves of the definitions of a number of useful terms, already used, as follows:

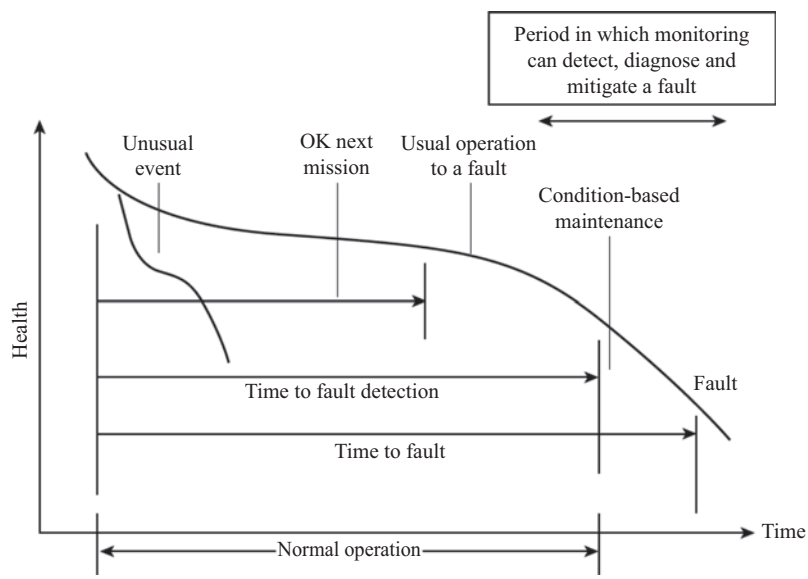


*Figure 4.1 Progression of an electrical machine to failure showing the benefit of CM*

- Failure is when the electrical machine fails to perform its energy conversion function. Failure is complete and does not imply partial functionality.
- Failure mode is the manner in which final failure occurred. For example,
  - Insulation failure to ground,
  - Or structural failure of a shaft.
- Root cause is the manner in which the failure mode was initiated. For example, for the two cases above:
  - Overheating of the insulation could be the root cause leading to the failure mode of insulation failure to ground,
  - Or excessive shock torque being applied to the shaft could be the root cause leading to the failure mode of structural failure of the shaft.
- Failure mechanism is the physical manner in which a failure process progresses from the root cause to the failure mode. For example, in the two cases above:
  - Overheating causes degradation of the insulation material leading to reduced voltage withstand capability,
  - Excessive shock torque on the shaft causing yield and an increase in stress in the remaining parts of the shaft leading to a progressive and ultimately catastrophic yield of the component.
- Root cause analysis, RCA, is an analysis following failure of the failure modes and underlying root causes.
- Duration of the failure sequence is considered in this book to be the time from root cause to failure mode. This may be a period of seconds, minutes, days, months or weeks and can depend on:
  - Failure mode itself,
  - Operating conditions of the machine,
  - Ambient conditions.
- Reliability, $R$, is the probability that a machine can operate without failure for a time $t$ and in this book is generally quoted as a percentage. A high reliability machine has few failures, a high mean time between failure, a high-percentage reliability and a low failure rate. The reliability as a function $R(t)$ is sometimes known as the survivor function because it indicates what proportion of the starting population survives at a particular time $t$. A word definition of reliability would be 'the probability that a system will operate to an agreed level of performance for a specified period, subject to specified environmental conditions'.
- Availability, $A$, is the probability that a machine will be available to operate for a time $t$ and in this book is generally quoted as a percentage. A high-availability machine has only short periods of time shutdown due to failure or maintenance.
- Failure intensity, $\lambda(t)$, is the rate at which failures occur in a machine, sometimes called the hazard function and this varies through machine life. However, experience shows that for complex objects, such as an electrical machine, the failure intensity generally develops, after an early period of operation, into a constant failure rate, $\lambda$, and in this book is generally quoted as

*failures/machine/year*. It is the objective of machine maintenance engineers to keep the failure rate low, constant and predictable.

- Time to failure, TTF, is the time measured from the instant of installation of the machine to the instant of failure. The mean time to failure, MTTF, is the expected value of successive TTFs. MTTF does not include the time to repair as a result of a failure. The MTTF is usually given in hours.
- Mean time to repair, MTTR. Time to repair, TTR, is the time measured from the instant of first failure to the instant when the machine is available for operation again. The MTTR is the average of successive TTRs and can be averaged over a number of machines in a population. The MTTR $= 1/\mu$ is usually given in hours.
- Under the hypothesis of minimal repair, that is a repair that brings the unit back to the condition before failure, time between failure, TBF, is the time measured from the instant of installation of the machine to the instant after the first failure when the machine is available for operation again. The mean time between failures, MTBF, is the average of successive TBFs and can be averaged over a number of machines in a population. MTBF is the sum of the MTTF and MTTR. The MTBF or $\theta = 1/\lambda$ is usually given in hours.
- Failure mode and effects analysis, FMEA, is a subjective analysis tool, defined by the international standard, BS EN IEC 60812:2018, that uses a qualitative approach to identify potential failure modes, their root causes and the associated risks in the design, manufacture or operation of a machine.

Reliability theory has developed as set out in the Timeline Table 1.3 and in more detail in Appendix B, but summarised here as:

- Early anecdotal information,
- Followed by mathematical reliability representations, set out in the following section,
- Realisation that failure intensity, $\lambda(t)$, particularly failure rate, $\lambda$, and its inverse MTBF helps to identify when repairs hints at the difference between availability and reliability,
- Development of MIL-HNDBK 217, *Military Handbook: Reliability Prediction Of Electronic Equipment*, prescribing the mathematical reliability representations and tests to be used for electronics development,
- Understanding that repair intensity, $\mu(t)$, particularly repair rate, $\mu$, and its inverse MTTR help identify the mean repair time needed emphasises the importance of availability over reliability,
- Realisation that the variation of failure rate, $\lambda(t)$, was more significant for electronics than simple failure rate, $\lambda$, and that physics of failure (PoF) is important, leading to the supercession of MIL-HNDBK 217. This issue is more significant for power electronics than machines, which still conform to earlier notions of reliability.

## 4.3 Root cause and FMEA

### *4.3.1 General*

The sequence from operation to failure for a specific failure mode in a typical sub-assembly or component of a machine is shown in Figure 4.1 but could be explained diagrammatically in Figure 4.2, in this case for a main shaft and the sequence is from root cause through failure mode to failure.

The duration of a failure sequence depends on the failure mode, the operating condition of the machine and the ambient condition in which it is operating. Figure 4.3 shows this process for a failure mode whose statistic can be described by a normal distribution.

- Figure 4.3(a) shows progression from reliable to non-reliable operation rapidly at the 50% life point for a fast fault. The probability of failure rises sharply close to this point, the area under the curve being equal to 1 because in the life of the machine there is 100% probability of failure.
- Figure 4.3(b) repeats the progression for a medium speed fault.
- Finally, Figure 4.3(c) repeats the progression for a slow fault.

This process of RCA and FMEA is at the heart of CM.

If a failure sequence is like Figure 4.3(a), very rapid, then effective CM is impossible. This is the situation for failure modes that actuate the electrical protection, where final failure mode action maybe seconds or even only a few mains cycles. However, if the failure sequence is days, weeks or months, like the slow fault in Figure 4.3(c), then CM has the potential to provide early warning of impending failure and the ability to continue operating the machine before failure and maintain it to avoid failure. Therefore, CM must concentrate on those root causes and failure modes that exhibit a failure sequence of substantial duration and our ability to detect its initiation and progress is crucial to successful CM.

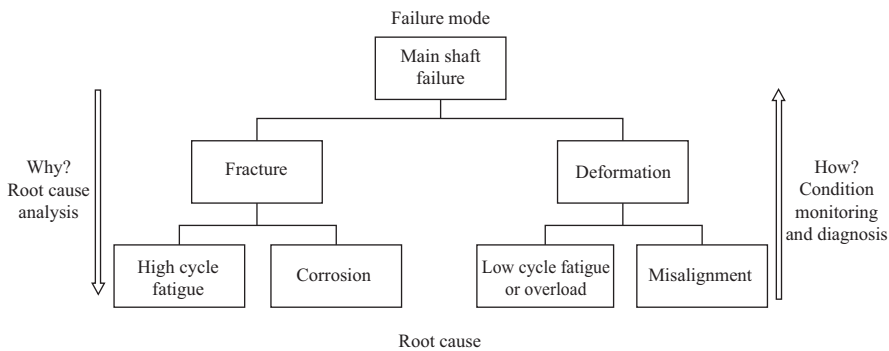


*Figure 4.2 Cause-and-effect diagram showing the relationship between the failure sequence and RCA for a main shaft failure initiated by low or high cycle fatigue*

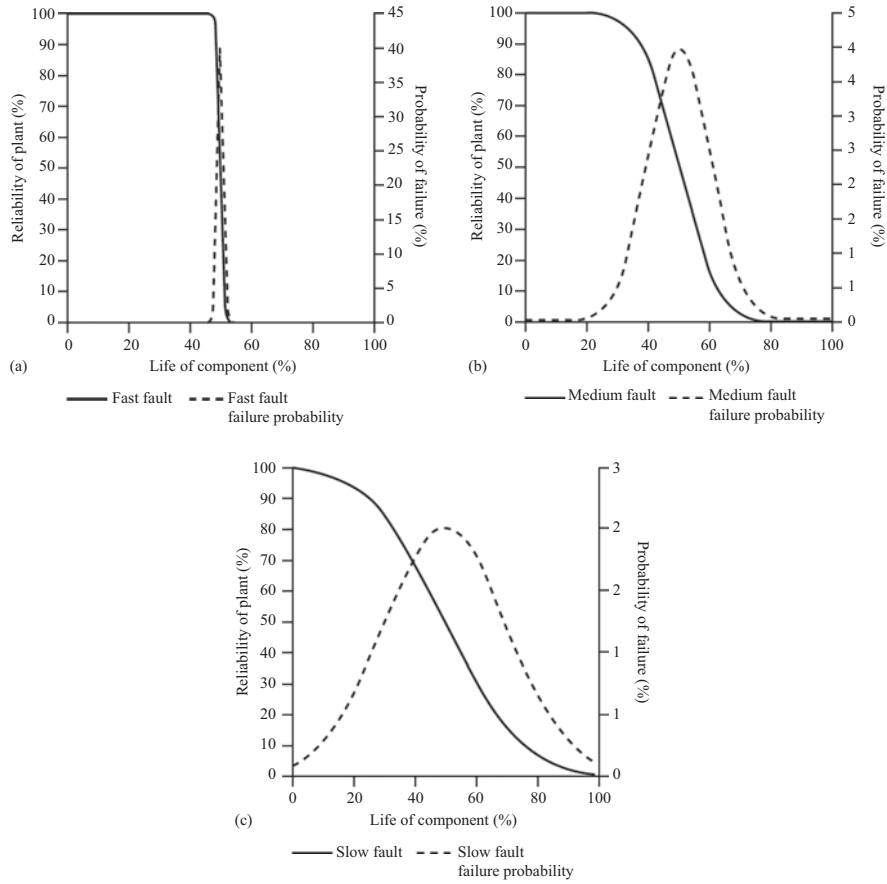


*Figure 4.3 The failure sequence showing operability falling with time as a fault progresses: (a) fast speed fault, (b) medium speed fault and (c) slow speed fault*

### *4.3.2 Typical root causes and failure modes*

It is important to distinguish between root cause, which initiates a failure sequence and could be detected by CM, and a failure mode that terminates it but cannot be predicted.

After a failure, operators are used to tracing the sequence back from the failure mode to the root cause, in order to determine the true cause of failure. That is the process of RCA or asking why a failure occurred, see BS EN IEC 60812:2018.

On the other hand, the designer of a CM system must keep in mind the need to predict the reverse of that process, tracing how a failure develops, as shown in Figure 4.2.

On this basis the authors propose, see Chapter 3, the most common root causes and failure modes for rotating electrical machines. They are similar to the root

causes and failure modes identified in *IEEE Gold Book* (1997) and Thorsen *et al.* (1995) and could be related to the more detailed failure modes analysis developed by Bonnett *et al.* (1992) for induction motors, in particular.

It is surprising how few root causes and failure modes there are and a reader should note that these are generic and could be applied to many different machine sub-assemblies and components.

The following are key examples and a complete set of failure modes and root causes for different types of electrical machines is given in Appendix A.

### *4.3.3 Root causes*

- Defective design or manufacture,
- Defective material or component,
- Defective installation,
- Defective maintenance or operation,
- Ambient conditions,
- Overspeed,
- Over-load,
- Low cycle fatigue or shock load,
- High cycle fatigue or excessive vibration,
- Component failure,
- Excessive temperature,
  - Winding overtemperature,
  - Bearing overtemperature,
- Excessive dielectric stress, steady or transient,
- Debris or dirt,
- Corrosion.

### *4.3.4 Failure modes*

- Electrical:
  - Core insulation failure,
  - Stator winding insulation failure,
  - Rotor winding insulation failure,
  - Brush-gear failure,
  - Slip-ring failure,
  - Commutator failure,
  - Control failure,
  - Electrical trip,
- Mechanical:
  - Bearing failure,
  - Rotor mechanical integrity failure,
  - Stator mechanical integrity failure,
  - Fan failure,
  - Cooler failure.

## 4.4 Reliability analysis

Component failure modes and the failure sequence described in Section 4.3 are controlled by statistical processes in the components, such as insulation degradation or degradation of metal components due to fatigue. These processes govern the transition from operation to failure exemplified by Figure 4.3. This process is the subject of detailed texts on reliability such as Billinton *et al.* (1992). Each component failure mode will have its own probability density function that derives from its own physical processes.

For example, the shape of the probability density function for winding insulation deterioration depends on the ambient and operating temperatures, deteriorating slowly as the insulation degrades with time. Whereas the probability density function for shaft fatigue would show a rapidly rising trend as fatigue cycles are accumulated.

The mathematical function, $f$(t), for a component failure mode probability density function should have the flexibility to represent a wide range of major failure modes, such as are present in most machinery. A flexible function that is available for this work is the Weibull function:

$$f(t) = \frac{\beta}{\theta}\left(\frac{t}{\theta}\right)^{\beta-1} e^{-\left(\frac{t}{\theta}\right)^{\beta}} \tag{4.1}$$

The instantaneous failure rate, $\lambda(t)$, or hazard function of a component in a population of components can be obtained from $f(t)$ because:

$$\lambda(t) = \frac{f(t)}{R(t)} \tag{4.2}$$

where $R(t)$ is the reliability or survivor function of a population of components, which for a Weibull distribution would be given by:

$$R(t) = e^{-\left(\frac{t}{\theta}\right)^{\beta}} \tag{4.3}$$

Therefore:

$$\lambda(t) = \frac{\beta}{\theta}\left(\frac{t}{\theta}\right)^{\beta-1} \tag{4.4}$$

which can be simplified to:

$$\lambda(t) = \alpha\beta t^{\beta-1} \tag{4.5}$$

where $\beta$ is a shape parameter and $\alpha$ is a scale parameter equal to $1/\theta^{\beta}$ and reduces to $1/\theta$ when $\beta = 1$, where $\theta$ is the MTTF of the component and $\approx$ MTBF. This expression is a very powerful mathematical tool to understanding the behaviour of components, sub-assemblies and complete machines from a reliability point of view.

Figure 4.4 shows the effect on the probability of failure of a component for different values of $\beta$, in this case life is expressed in arbitrary units.

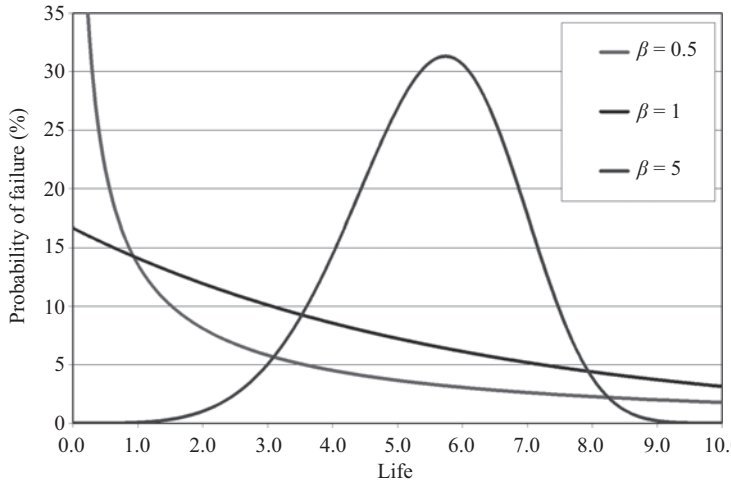


*Figure 4.4 Variation in the probability density function of failures to a component, showing the effect of different degradation processes at work*

So, for example, the curve with $\beta = 0.5$ could describe the behaviour of a population of rolling element bearings whose probability of failure decreases progressively with time as the bearing and grease runs in.

On the other hand, the curve with $\beta = 2$ or 5 could describe the behaviour of an insulation component subjected to increased degradation with time and temperature.

Figure 4.5 shows the hazard or failure intensity function using (4.5) for such components against life. The bearing component shows a failure rate decreasing steadily with time, whereas the insulation component shows an increasing failure rate.

The complete failure intensity function for a population of components varies over time as shown in Figure 4.6. Each phase of the segregated failure rate curve is represented by (4.5), for different values of the shape parameter, $\beta$. When components are assembled into sub-assemblies and thence, for example, into a complete electrical machine, the aggregated component failure mode sequences result in a composite failure intensity function curve, such as Figure 4.6, derived from (4.5).

Failure intensity, Figure 4.6 is a combination of three curves representing three stages of a population's operation:

- Early life ($\beta < 1$): stage is also known as infant mortality or burn-in, where the failure rate falls as the components prone to early failure are eliminated.
- Useful life ($\beta = 1$): stage represents normal operation of the system, when the failure intensity is a constant failure rate over an extended period of time.

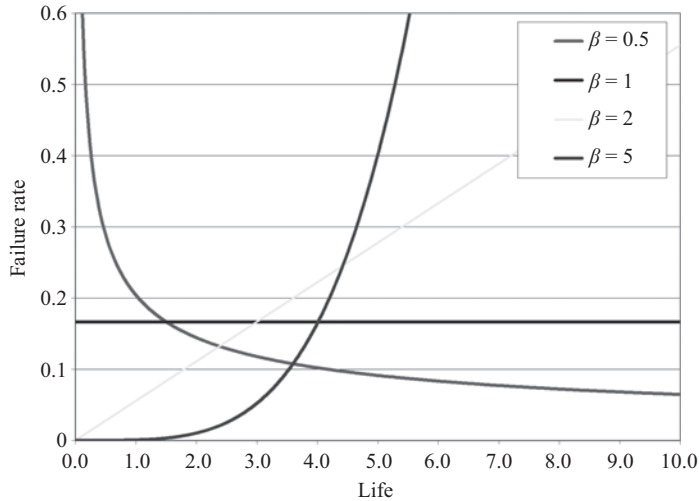


*Figure 4.5 Variation in the hazard function of a population of components for different underlying the probability density functions, showing the effect of different degradation processes on the deterioration of failure rate and therefore on the reliability*

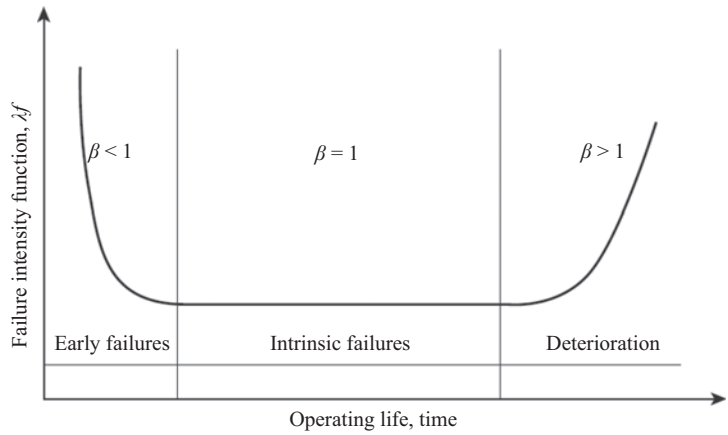


*Figure 4.6 Aggregate hazard or failure intensity function for a population of components or sub-assemblies forming a complete electrical machine, known as bath-tub curve, showing the effect of shape function β at the start and end of a machine's life*

- Wear-out ($\beta > 1$): stage represents increasing system failure intensity, occurring towards the end of its useful life, due to the deterioration of the individual components that start to fail in increasing numbers.

However, components of machinery do not always follow the typical bath-tub form. The authors have noted how complex electronic equipment does not often

exhibit infant mortality symptoms. This is because such sub-assemblies are subjected to automatic and accelerated life testing on completion of manufacture, before delivery, specifically designed to minimise the number of early life failures.

In another way, electrical insulation systems do not tend to show a low, constant, mid-life failure rate but a rather gradual worsening in failure intensity over the whole life, as the insulation material steadily deteriorates with ageing, as shown in Figure 4.5 with $\beta = 2$.

However, the hazard function or failure intensity of the bath-tub curve is instructive for those engaged in CM because they demonstrate the character of failure modes, which CM needs to detect, and the different phases of a machine's life.

The low, constant, mid-life failure intensity becomes a constant failure rate, the bottom of the bath-tub, and is achieved partly by good machine component design and manufacture but its base value can be reduced and duration extended by maintenance and in turn by monitoring.

So, the shape of the failure intensity bath-tub for a complex engineering plant is dependent upon the maintenance and monitoring regime that is adopted as set out in Chapter 1.

## 4.5 Machine structure

The structure of a machine is an important factor in the cause-and-effect diagram and in the aggregation of failure mode probability density functions, as described in the previous section.

We may consider that structure to be simply the assembly structure of individual components into sub-assemblies and then the aggregation of those sub-assemblies into a complete machine. This could be exemplified by the exploded diagram of the machine and was discussed in Chapter 2, see, for example, Figure 2.9.

Billinton *et al.* (1992) concluded that the relevant structure is not assembly but that due to the reliability dependence of components, where the failure of one component in the structure may not incur the failure of the machine, for example, due to redundancy. This affects the makeup of the cause-and-effect diagram, which is the structure relevant to CM, and is governed by causality rather than assembly.

The structure for a sub-assembly can be built up from the cause-and-effect diagrams of individual components to give a cause-and-effect diagram for the sub-assembly, such as is shown in Figure 4.7. The assembly structure for a typical electrical machine is shown in Figure 4.8 and may be adequate in some cases but is not necessarily correct for the assessment of failure modes. Compare Figure 4.8 to the diagram in Figure 2.12.

A simple example of the two aspects of this issue could be the lubrication pumps of a large turbo-generator. It is customary to introduce redundancy into this plant by providing 2 off, 100%-rated, main and standby, AC motor-driven lubrication pumps with a third 100%-rated, DC motor-driven pump to provide

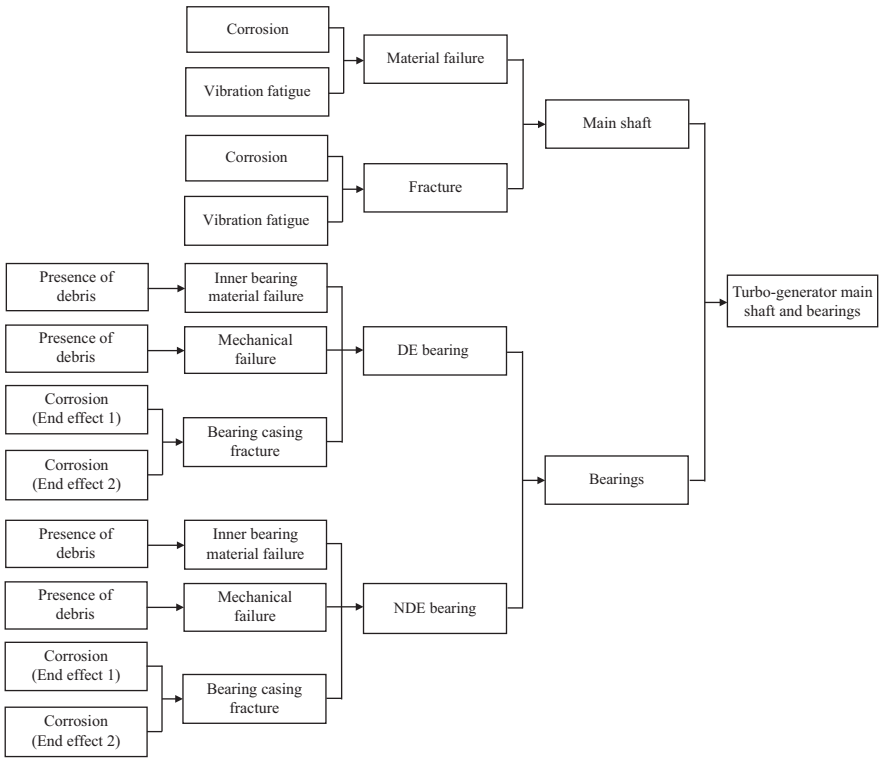


*Figure 4.7 Example of a cause-and-effect diagram for a simple sub-assembly, main shaft of a turbo-generator*

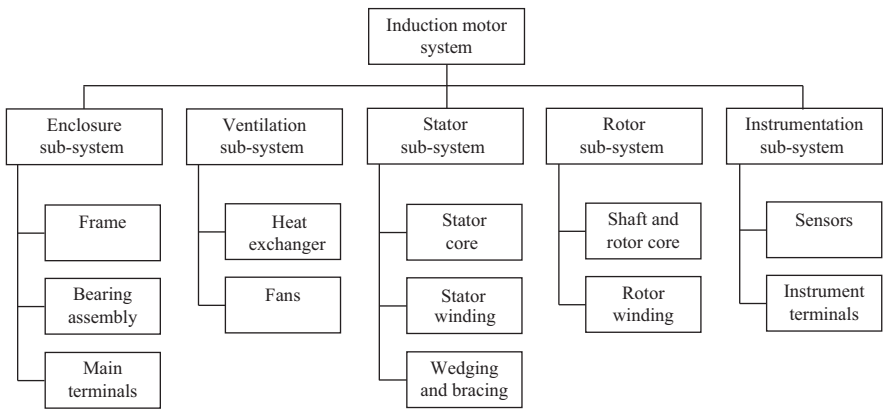


*Figure 4.8 Example of a typical electrical machine structure diagram, see Figure 2.12*

emergency power from a battery, when AC power fails. In this case, it is not legitimate simply to add the cause-and-effect diagrams in series or to add the failure mode probability functions of the three pumps, since a large turbo-generator can operate with any one out of three pumps functioning. The correct approach is to consider the three systems in parallel and take account of the probability density functions in the same way.

## 4.6 Typical failure rates and MTBFs

The approach of this chapter can be put into context by considering the failure rates and MTBFs of typical electrical machines.

Such data can be notoriously difficult to find but some information, particularly about MTBF, is available from the reliability surveys, mostly conducted in the United States under the auspices of the IEEE, Dickinson (1974), O'Donnell (1985), Albrecht *et al.* (1986), Bonnett *et al.* (1992) and IEEE Gold Book (1997). Information about the life of electrical machines has also come to light from experience in the Defence Industry, where reliability predictions are a contractual requirement of equipment purchase, see Tavner *et al.* (1999). Finally, information is available from the wind industry about generators being fitted to the wind turbines being installed in increasing numbers, where fault data is recorded sufficiently frequently to deduce the life curves of typical electrical machines and their reliability, see Spinato *et al.* (2006).

The MTBF can be a deceptive quantity. It is intended to represent the prospective life of the machine, assuming it has a constant failure rate, as shown in the constant failure rate region of Figure 4.6. Then one could consider that there would be a 50% probability of failure before the MTBF and 50% probability of failure afterwards. However, machines can have a failure rate that improves with time and then it is possible that a higher proportion of failures could occur before the MTBF. However, a well-maintained machine is expected to be operating in the constant failure rate region, in which case MTBF gives a good indication of prospective life, which engineers can appreciate without being overwhelmed by any statistical interpretation.

Table 4.1 extracts the data from a number of surveys of electrical machines and gives the failure rates and MTBFs for a range of machines, showing a remarkable degree of consistency with MTBFs ranging from 18 to 33 years, if a year is assumed to contain 8 766 h operation. Table 4.1 also gives an idea of the significance of each survey by noting the number of machines surveyed and the number of failures recorded.

It should be noted that the large surveys are dominated by the induction motors because of their ubiquity.

Results have also been added for machine converters since so many drives, particularly with induction motors, now include VSD converters, the latter results having been taken from the wind industry, the largest sector to release such reliability figures.

*Table 4.1 Typical measured or predicted failure rates and MTBFs, for electrical machines and converters, from literature*

| Machine or converter type | | No. of machines in the survey | Machine years in survey | No. of failures in survey | Failure rate, $\lambda = 1/\text{MTBF}$ (failures/machine/year) | MTBF (h) | Source of data |
|---|---|---|---|---|---|---|---|
| Electrical machines | Large steam turbo-generators | Unknown | 762 | 24 | 0.032 | 273 750 | Dickinson (1974), IEEE Gold Book (1997) |
| | Induction motors, 601–15 000 V | Unknown | 4 229 | 171 | 0.040 | 216 830 | Dickinson (1974), IEEE Gold Book (1997) |
| | Motors > 200 HP generally MV and HV induction motors | 1 141 | 5085 | 360 | 0.071 | 123 740 | O'Donnell (1985), IEEE Gold Book (1997) |
| | Motors > 100 HP generally MV and HV induction motors | 6 312 | 41 614 | 1 474 | 0.035 | 247 310 | Albrecht *et al.* (1986) |
| | Motors > 11 kW generally MV and HV induction motors | 2 596 | 25 622 | 1 637 | 0.064 | 137 110 | Thorsen *et al.* (1995) |
| | Wind turbine generators < 2 MW | Various predictions based on measured wind industry data | 44 785 | 4 389 | 0.098 | 89 387 | Spinato *et al.* (2006) |
| Variable speed drives | Soft starter for induction generator | | – | – | 0.063 | 139 000 | Chung *et al.* (2016) |
| | LV partially-rated converter for DFIG | | – | – | 0.121 | 72 400 | |
| | 3-axis pitch converter for DC motors | | – | – | 0.195 | 44 900 | |
| | MV fully-rated converter for induction generator | | – | – | 0.402 | 21 800 | |
| | MV fully-rated converter for permanent magnet generator | | – | – | 0.738 | 11 900 | |

The striking message from Table 4.1 is that electrical machines are generally more reliable than VSD converters, i.e. they have a lower failure rate, $\lambda = 1/\text{MTBF}$. However, experience shows that because of VSD modularity $\text{MTTR} = 1/\mu$ is lower than for an electrical machine, because faulty VSD modules can be rapidly exchanged to restore converter reliability.

The distribution of failures within an electrical machine structure is also important because it should guide the application of CM. Table 4.2 gives another analysis of failures based on the literature used in Table 4.2 and three important areas of the machine are identified: stator-related, primarily the winding; rotor-related, including slip rings and commutators; bearing related. Remaining failures are grouped as other. The failure data comes from different surveys and whilst these surveys are not necessarily complementary they are substantial and show a consistent failure significance in descending order of importance:

- Bearings,
- Stator-related,
- Rotor-related.

The relative importance of failures is affected by the size, voltage and type of machine under consideration. In particular, the relative weighting of stator-to-rotor winding failures does depend upon the type and size of machine under consideration.

For example, small, low-voltage induction machine failures, exemplified by the first two columns of Table 4.2, are dominated by bearing faults, as LV windings experience very few faults. Smaller machine bearings are usually rolling element and their reliability depends heavily on the standard of maintenance. Induction machines show a much lower number of rotor winding or squirrel cage faults compared to stator winding faults, because of the ruggedness of cage construction. But larger, HV machines, exemplified by the next three columns of Table 4.2, receive a higher proportion of failure modes on the stator winding, due to dielectric stress and vibration root causes and this can rise to be of a similar significance to bearing faults. Large machine bearings are also usually of sleeve construction and with constant lubrication are generally more reliable than bearings in smaller machines. Table 4.2 also shows that other component failure modes, for example, in the cooling system, connections and terminal boxes, become more significant on larger machines.

An interesting aspect of this analysis is the attention being paid in published literature to different machine failure mechanisms. The authors have used the search engine IEEEXplore to consider Trans IEEE and Proc IEE/IET papers only in the period 1980 to date and searched the metadata under the following headings:

- Broken bars in induction motor rotor cages, 35 papers,
- Discharge activity in MV and HV stator windings in motors and generators, 9 papers,
- Stator winding faults excluding discharge activity in motors and generators, 19 papers,
- Bearing faults in electrical machines, 17 papers.

*Table 4.2 Distribution of failed sub-assemblies in electrical machines obtained from literature*

| **Sub-assemblies** | **Predicted by an OEM through FMEA techniques, 1995–97*** | **MOD Survey, Tavner *et al.* (1999)** | **IEEE large motor survey,1985,O'-Donnell (1985)** | **Motors in utility applications, Albrecht *et al.* (1986)** | **Motor survey offshore and petrochem, Thorsen *et al.* (1995)** | **Proportion of 80 journal papers published in IEEE and IEE/IET on these subject areas over the past 26 years** |
|---|---|---|---|---|---|---|
| Types of machines | Small- to medium-LV motors and generators <150 kW, generally squirrel cage induction motors | Small LV motors and generators < 750 kW, generally squirrel cage induction motors but also DC machines | Motors >149 kW, generally MV and HV induction motors | Motors >75 kW generally MV and HV induction motors | Motors >11 kW generally MV and HV induction motors | All machines |
| Bearings | 75% | 95% | 41% | 41% | 42% | 21% |
| Stator related | 9% | 2% | 37% | 36% | 13% | 35% |
| Rotor related | 6% | 1% | 10% | 9% | 8% | 44% |
| Other | 10% | 2% | 12% | 14% | 38% | 0% |

*Private communication from Laurence, Scott & Electromotors Ltd.

The spread of this collection of 80 publications is shown distributed alongside the relevant failure areas in Table 4.2.

It shows that much more publishing effort has gone into the study of the less prevalent, but calculable, rotor faults than into the more prevalent, but perhaps more mathematically challenging, bearing faults.

Induction motor rotor cage faults can be detected through perturbations of the air-gap magnetic field, see Chapter 9. The distribution of journal papers towards those faults is probably due to the fact that the air-gap field is scientifically interesting, analytically tractable and cage induction motors are very numerous.

Bearing faults, on the other hand, involve a more complex interplay of mechanical and electrical physical effects. However, bearing faults lead to air-gap eccentricity and the effect on the resultant magnetic field is also tractable, although more complex than the effect of rotor cage faults.

Some of the lessons learnt from rotor cage fault detection, combined with the study of the effect of eccentricity on the air-gap magnetic field can be applied to the detection of bearing faults and this topic is returned to in later chapters. It is interesting that the study of eccentricity effects in induction motors, the most numerous electrical machines, can also be elicited from literature survey above and that recorded that 36 papers have addressed the subject since 1980. Some of these papers address the issues of noise and speed control but that number demonstrates the attention that is beginning to focus on this important issue because of the application of VSDs to these machines.

## 4.7 Conclusions

This chapter has shown that causality must be the guiding principle when applying CM to electrical machines.

First, the operator must be aware first of the failure modes and then the root causes for the machine being considered for CM.

Second, causality must be traced through prospective failure sequences, possible by the use of cause-and-effect diagrams. The probability of failure of a component of a machine can be described by a probability density function for that component. The resultant hazard function curves for each component in a sub-assembly can be aggregated to give a prospective life curve for that sub-assembly and can then be aggregated to give the life curve of the machine. The aggregation of cause-and-effect diagrams and hazard functions needs to be done with care, taking account of the assembly structure of the machine and the reliability dependence of components. From the aggregate hazard function, a model for the complete machine could be derived.

Third, CM needs to address the root causes that have a slow failure sequence to the failure mode and this information can be derived from knowledge of the failure modes in operation in an electrical machine.

In Chapter 1, we proposed three different courses of maintenance action:

- Breakdown maintenance, implying uncertainty and a high spares holding,
- Fixed-time interval or planned maintenance, implying extended shutdown or outage periods and lower availability,

- Condition-based maintenance, CBM, implying low spares holding but maintenance planned based on the monitored information leading to high availability.

Real engineering plant demands a flexible combination of maintenance regimes based on the above.

This chapter has shown that by addressing failure modes that are slow to mature, CM could significantly affect the detection of faults before they occur. CM can then form part of planning fixed-time interval maintenance (ii) and will be at the heart of maintenance for method (iii).

Prior to determining the type of equipment and frequency of monitoring, some consideration should also be given to whether the cost of implementing such a program is justified. Factors involved in this decision may include:

- Replacement or repair cost of the equipment to be monitored,
- Criticality of the plant to safe and reliable operation,
- Long term future of the facility in which the equipment is installed.

Assuming that consideration of the above points indicates that the expenditure is justified, the following points will aid in determining how the CM programme should be implemented.

- Design,
- Manufacture,
- Installation,
- Operation,
- Maintenance.

In the majority of cases, the end users of rotating machines are dealing with existing plant and will have to consider all five of the points identified above. This task is complicated because often there is very little design information, the manufacturer may no longer exist and installation, operation and maintenance records may be incomplete. The paucity of information can lead to the assumption that the age of the equipment indicates the need for more rigorous monitoring. However, this is not always the case since the refinement of design tools and the constant pressure on manufacturers to reduce costs has, in some cases, lead to decreased design margins.

The practicability of these approaches for electrical machines depends upon the application of the machine and the engineering plant it serves. That is the basis of this book and the fault Mechanisms and root causes, dealt with in this and the previous chapter, which CM must deal with are set out in Appendix A.

In the next chapter, we describe the signal processing and instrumentation needs for CM.

*Chapter 5*

# Signal processing and instrumentation requirements

## 5.1 Introduction

An electrical machine CM system involves the measurement of operating variables of the plant being monitored, and interpretation as well as management of the acquired data. In many plants, measurements are already used for control and protection. From a cost perspective, it would be ideal if such measurements can also be used for CM. However, knowledge of the limitations of the existing measurements and understanding of the difference between the objectives of control, protection and CM is important, as will be discussed later in the book.

One feature of CM, described in Chapter 3, is to detect the impending faults at an early stage, capturing weak signatures in measurements that are usually mixed with noise. Furthermore, some impending faults may manifest themselves in non-electrical variables that are not usually used in control or protection.

Before getting into the details of the instrumentation elements, we need to view a CM system from a higher level where the functionality of different parts of the system can be more clearly described. By doing this, it should be possible to identify the common elements of a CM scheme, irrespective of the system detail.

In essence we are saying that an engineer examining occasional meter readings, with a view to producing an operational and maintenance strategy, is involved in a procedure that is analogous to a sophisticated CM system.

In view of this analogy, we believe that the following tasks are essential elements in a CM system, see Figure 5.1:

- Measurement or transduction task, sensing of primary variables,
- Data acquisition task, conversion of sensed variables into digital data in CM system,
- Data processing task, identifying information buried in data,
- Diagnostic task, acting on processed data.

Tasks (i) and (ii) are usually carried out whilst the monitored plant is operating. Tasks (iii) and (iv) can be performed off-line and the results of these tasks may not be fed back immediately to the plant operators. This is a non-intrusive approach of CM.

In contrast, it is possible to use an intrusive approach in which a signal is injected into the plant being monitored and the response is used to indicate the plant

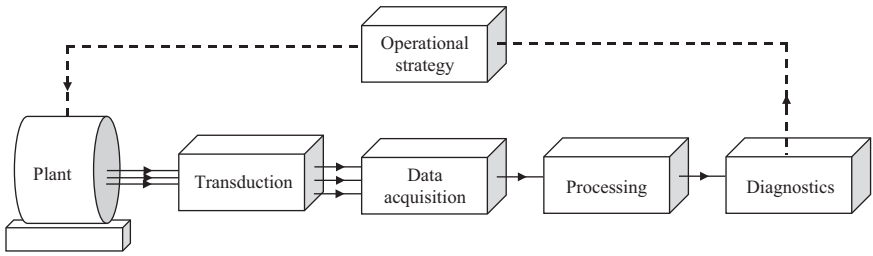


*Figure 5.1 Monitoring tasks*

status. This is particularly attractive in plants involving power electronic converters that generate monitoring signals and are very fast acting.

As of now, we will confine our description to the non-intrusive approach.

In each of the above four tasks, human intervention is possible, and often desirable. Indeed, in some cases these tasks may be entirely carried out by the operator. Let us return to the analogy of the engineer collecting his meter readings, and trying to identify the tasks. The meter deflections or the numbers displayed on the panels will naturally be in response to measurements made elsewhere in the plant being monitored and may be picked up by currents transformers (CTs), voltage transformers (VTs), thermocouples or accelerometers, for example.

This is the transduction task and is normally performed automatically as it is difficult for the human operator to act in anything but a qualitative way in fulfilment of this task. That is, he/she may be able to tell if one piece of plant is hotter than another but little else. Having that said, it often relies on a human operator to ensure the reliability of the transduction task.

The data acquisition task could be simplified to the action of the engineer writing down a series of readings from each meter, together with information regarding time, load, ambient conditions and location of the plant being monitored. In our example, this would be wholly under human control. The periodicity of the observations will depend on the plant characteristics.

The processing task corresponds to the analysis of the readings in the same way. It may be considered appropriate to average several readings, for example, and to present them in a way that allows easy comparison with other data. This phase can vary greatly in complexity and it demands significant computing power in automatic systems. We shall return later to more common processing techniques merely noting now the use of methods such as spectral analysis, time averaging, auto- and cross-correlation.

The diagnostic task operates on the results of the processing task in order to recommend actions that hopefully will result in improved operational readiness and performance, and improved maintenance scheduling. Again, returning to our simple analogy, on the basis of examining the average meter readings and comparing them with the manufacturer's operational limits, say, the engineer decides, for the next plant shutdown, which items of machinery must be overhauled or replaced.

He/she arrives at this judgement on the basis of experience and the data available as a result of collecting and processing readings and having access to the manufacturer's data on operational limits. For the manufacturer to set the operational limits, a relationship between the plant condition and the signature during operation should already have been established. Understanding of the mechanism of fault development is particularly useful in determining such threshold values. The diagnostic task is mostly carried out with significant input from human operators, but with the development of knowledge-based expert systems or other forms of artificial intelligence, full automation of this phase can be realised.

Recent development of communication technology, for example, in fibre-optics and semiconductor sensing devices, allows the data acquired to be sent to a central point or to the manufacturer for processing and analysis. With the current trend of restructuring in many industrial sectors, the responsibility of plant CM has also started to change; operators, asset owners and manufacturers may all have different parts to play with manufacturers taking more responsibility than traditionally. Depending on application, a plant can be equipped with CM functionalities as a selling point. As manufacturers cannot schedule plant shutdowns, the central position of the operator could hardly be replaced. Here we are mainly interested in the technical aspects of CM. The trend towards through-life costing of plant means that manufacturers are more closely involved with the operator in managing plant beyond the warranty period and this opens up and increased market for service work, which can be sustained by CM activity.

In Figure 5.1, we summarised the four tasks associated with the CM and indicate the obvious step of closing the loop as an aid to improve the operational performance.

We must now examine the first two of the four CM tasks in some detail, both in a general way and as they apply to electrical machines. Data-processing task will be developed next in Chapter 5 while the diagnostic task will be delayed to later in the book. At all times we must be mindful that the monitoring activity is aimed at reaping the benefits to be gained by closing the loop identified in Figure 5.1.

Broadly speaking, the data-processing task for these signals is that part of the monitoring activity where data, which has been collected and suitably formatted, is operated upon or otherwise transformed so that a diagnosis of plant condition can readily be made. As we have mentioned previously, it is here that the most significant scope for automation exists. Indeed, to perform many of the data-processing functions now commonly used in CM, considerable computational effort will be required. Processing may be done on or offline and this choice will predominantly depend upon whether the monitoring system is one that operates on a continuous basis, or not. It also depends on understanding how quickly monitored faults can develop. Usually CM on a continuously operating plant and on faults that can develop quickly should process the obtained data online. However, this distinction may not be clearly drawn. Modern data acquisition units now permit data to be obtained from a running plant and analysed at a different location without any significant time delay.

In the past, dedicated signal analysers were applied to analogue signals from the transduction process, to obtain the spectra that could indicate the occurrence

and level of signal components at particular frequencies. Their use has now been almost completely replaced by general computer algorithms acting on data acquired in the digital format.

There are two fundamental objectives in signal processing:

- Filtering out the noise present in measurements,
- Extracting signatures which can indicate the health condition.

Although computer software packages are commercially available for digital signal-processing applications and can be used for CM of electrical machines, it is important to fully appreciate the characteristics of the different algorithms in order to avoid unreliable results, leading to misinterpretation of the plant condition. Requirements of such algorithms and their limitations must be clearly understood. For such a reason, this chapter describes in greater detail some of the more important numerical techniques used for signal processing in CM.

Perhaps the simplest form of signal processing is one in which the magnitude of the raw incoming signal is examined on a regular basis, as a function of time. In fact, this is essentially the basis of all visual inspection techniques or trend analysis, which involves active collection of data by personnel. The processing, in such cases, may consist of a comparison of the current record with the previous value or with some preset, or predetermined, threshold. This process is simple to automate, even when many hundreds of inputs are being monitored. The processor is simply required to associate the incoming reading with a particular item of plant. If the incoming data is to be trended, to examine the lead up to an atypical event, then a data storage medium is essential. There is the trend to use company-wide intranet for data storage, backup and sharing, as part of an asset management system, Sabin *et al.* (2017). It is very easy, when monitoring many inputs, to accumulate exceedingly large volumes of data, so it is desirable to automatically refresh the data storage so that after a given period of time the data storage elements either transfer their contents to bulk storage media, or are overwritten by the incoming data stream.

When a plant malfunction is detected, a common practice is to annunciate the event and discontinue data storage on that channel or continue for a specified period. In this way the diary of events leading up to the malfunction is preserved for subsequent examination, if required.

The above example of magnitude detection implies that plant condition information is seeded in the event of a change of signals from the plant. Indeed, the variation of signals usually tells us the change of condition. Variation of a signal in the time domain can be more saliently expressed as components in the frequency domain. Therefore, spectral analysis is naturally a very common technique of signal processing used in CM. Spectral analysis is effective when applied to steady-state periodic signals, which is usually the case when monitoring machine faults that gradually develop. In recent years, higher-order spectral analysis has been used to make use of phase information and improve the signal-noise ratio. We will describe first and higher-order spectral analysis techniques in this chapter. Sometimes a CM technique may also be applied to transient or non-stationary signals. However, it is

normally the case that the condition signatures are highly dependent on the machine operating condition which varies with time. Some signals, such as partial discharge, even change within a fundamental mains cycle during periodic operation. Therefore, correlation analysis which is a powerful tool in revealing buried relationships between signals and identify the causes and consequence of a plant fault will also be described. Sometimes a CM technique may also be applied to transient and non-stationary signals. Wavelet transform techniques that have more recently been developed will then be described for this objective, followed by a description of signal processing techniques based on modelling. The chapter is completed by instrumentation and signal condition techniques commonly used in electric machine CM.

## 5.2 Spectral analysis

Spectral analysis is the name given to describe methods that transform time signals into the frequency domain. The spectral representation of a time signal is therefore a collection of components in the frequency domain, each with a specific frequency, amplitude and phase angle. The transformation is achieved using the techniques of Fourier analysis whereby any periodic signal, $g$, of period $T$, has:

$$g(t) = g(t + T) \tag{5.1}$$

This can be represented by equally spaced frequency components *G(f):*

$$G(f_k) = \frac{1}{T}\int_{-T/2}^{T/2} g(t)e^{-j2\pi f_k t}dt, \quad k = 0 \pm 1, \pm 2, \tag{5.2}$$

where the subscript $k$ indicates the $k$th harmonic of the fundamental frequency $f = 1/T$. The harmonic represents a sine wave at the harmonic frequency whose amplitude and phase angle can be determined from (5.2). The original time domain signal can be reconstructed by summing all the harmonic components as shown below in (5.3).

$$g(t) = \sum_{k=-\infty}^{\infty} G(f_k)e^{j2\pi f_k t} \tag{5.3}$$

We see that a continuous periodic time function can therefore be represented as a discrete series in the frequency domain. The advantages are immediately apparent; our continuous input can be approximately represented to the required accuracy by a finite and often a small set of numbers. As we are going to illustrate in some later chapters, many faults give rise to harmonic components that are normally non-existent or of insignificant amplitudes. Spectral analysis compacts the data significantly at the cost of computation time, and allows the trend of change to be more easily recognised.

Because it is often necessary to digitise the transducer signals for onward transmission to the processing unit in a monitoring system, the incoming data is also sampled in time. That is, it is represented as a series of discrete values at

equally spaced instants in time, in a similar fashion to the frequency domain representation of a continuous time signal. Under these conditions, the equivalent statement of (5.2) becomes,

$$G(f_k) = \frac{1}{N}\sum_{n=0}^{N-1} g(t_n)e^{-j2\pi nk/N} \tag{5.4}$$

The corresponding inverse transform is:

$$g(t_n) = \sum_{k=0}^{N-1} G(f_k)e^{j2\pi nk/N} \tag{5.5}$$

In these expressions, we see that the frequency is effectively sampled at the discrete frequencies $f_k$ whilst the time signal is sampled at instant $t_n$. We therefore have a means of representing a discrete time function by a set of discrete values in the frequency domain. This transformation is known as the discrete Fourier transform (DFT). In practice, this transformation is carried out using the fast Fourier transform (FFT) technique, which is an extremely efficient way of achieving a DFT by constraining the number of time samples to a power of 2 and decomposing the transformation into a number of smaller transformations which are then combined to produce the result, Bateman *et al.* (2002). The number of calculation steps is significantly reduced, usually by orders of magnitude, to permit real-time signal processing of large data size, and this is also important for the accuracy when capturing weak condition signatures because the total round-off error is reduced.

When sampling a continuous signal, the total sampling length, the observation interval must be taken into consideration. The entire sampled data is automatically treated as one period in spectral analysis. If the signal is not strictly periodic or the sampled data does not precisely represent an actual period, then harmonic distortion may occur because the periodic waveform created by the sampling process may have sharp discontinuities at the boundaries. This effect may be minimised by windowing the data so that the ends of the data block are smoothly tapered. Common window functions include Bartlett, Hanning, Hamming and Blackman windows, see Madisetti *et al.* (1998). The original sampled data is multiplied with the window function before FFT is applied to generate the frequency domain spectrum, as shown in Figure 5.2. What we obtain is not a true spectral representation of the original time domain signal, but the effect of boundary discontinuities is attenuated. A way to view the windowing technique is that the finite sampling process itself has already windowed the true waveform with a rectangular window. Applying an additional window will give a more desirable result that minimises frequency domain distortion.

Another way often used in practice is to increase the length of the sampled data block, by increasing the observation interval. This lowers the fundamental frequency assumed in the spectral analysis. For a given sampling rate, the observation interval is proportional to the number of samples taken for the FFT. With increased observation interval, the harmonic distortion due to the discontinuity at boundaries

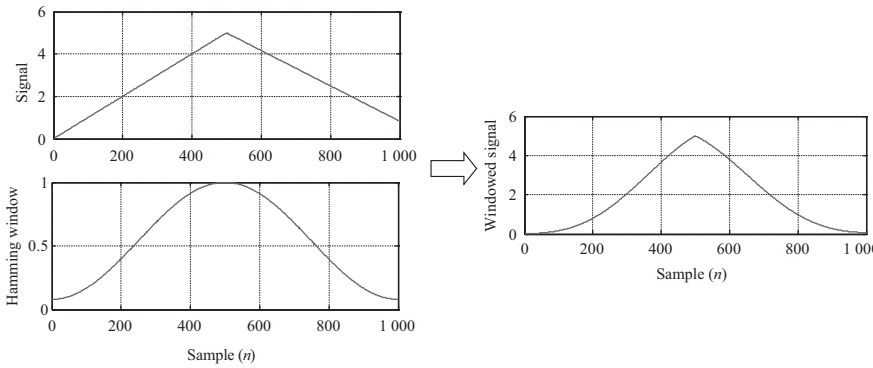


*Figure 5.2 Illustration of window function*

tends to concentrate in the low-frequency range; their contribution in the high-frequency range is reduced. It must be understood that the finite observation interval always results in a fundamental limit on the frequency resolution. Lengthening the observation interval increases the frequency resolution in the resultant spectrum.

Since FFT only provides components at discrete harmonic frequencies, which are integer multiples of the fundamental frequency, there is always the risk that the target component for CM is at a frequency that is between two-integer harmonic frequencies. This means that not all frequencies can be seen by the FFT, due to the so-called 'Picket fence' effect, disregarding the length of the observation interval. In such a case, the energy of the components unseen by the FFT slips through the Picket fence and leaks into the harmonics that are seen by the FFT. Several algorithms, including polynomial estimations, have been developed to detect the target component from the harmonics that have been identified by the FFT. For example, Figure 5.3 shows how the energy of harmonics of unity amplitude of a machine current signal at 59.83, 59.85 or 59.87 Hz could leak to components at 59.6, 59.7, 59.8, 59.9, 60 and 60.1 Hz that are at the FFT output frequencies, and this depends on the sampling scheme used. Details of the algorithms to estimate the components at intermediate frequencies, as a reverse process of what is shown here, can be found in Durocher *et al.* (2004). In CM of rotating electrical machines, the target frequency component in a signal is usually dependent on the speed of the machine that may vary continuously depending on the load condition. As a result, the target frequency is unlikely to be a multiple integer of the fundamental frequency determined by the length of the observation interval.

A final point that we would like to highlight here is the risk of aliasing that can occur in the spectral analysis. More and more electrical machines nowadays are connected to power electronic converters, which generate switching harmonics. High-frequency harmonics exist in both machine current and vibration signals that may be used for CM. Figure 5.4 illustrates the cause of aliasing. Suppose the original continuous time signal has a spectrum shown in Figure 5.4(a). The sampled discrete time data then will have a spectrum shown in Figure 5.4(b) where the

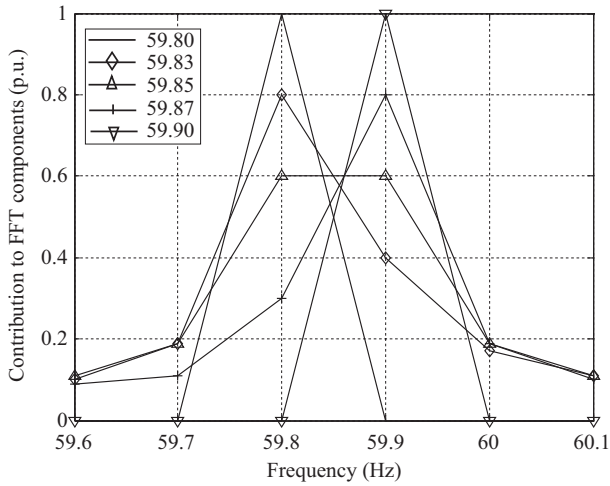


*Figure 5.3 Illustration of picket fence leakage*

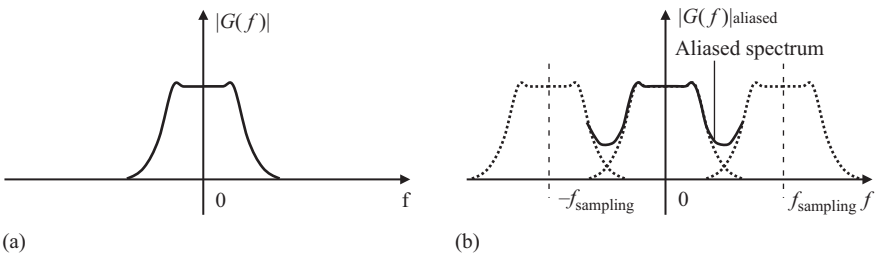


*Figure 5.4 Occurrence of aliasing: (a) true spectrum and (b) aliased spectrum*

original spectrum is duplicated according to integer multiples of the sampling frequency, see Flankin *et al.* (1998). If the sampling frequency is lower than the Nyquist frequency that is twice of the highest frequency in the signal, as shown in Figure 5.3, then aliasing occurs. In this case, some harmonic components in the spectrum obtained by performing FFT on the sampled signal are due to aliasing or sampling effects rather than real components of the original continuous time signal.

Consider an example. Figure 5.5(a) shows the stator current of an induction motor fed by a PWM (pulse-width-modulation) voltage source inverter with a symmetrical PWM switching frequency of $f_{sw} = 2.5$ kHz. The current is now sampled also at a rate of 2.5 kHz and the result is shown in Figure 5.5(b). The sampling rate may be considered natural because it coincides with the internal clock of the controller that generates the PWM pulses. Suppose that the output fundamental frequency of the inverter is $f_o = 10$ Hz. The actual current then contains a fundamental component and harmonics at $f_{sw} \pm 2kf_o$, where $k = 1, 2, 3 \ldots$, giving harmonics at 2 480 Hz, and 2 520 Hz, due to the modulation process in the

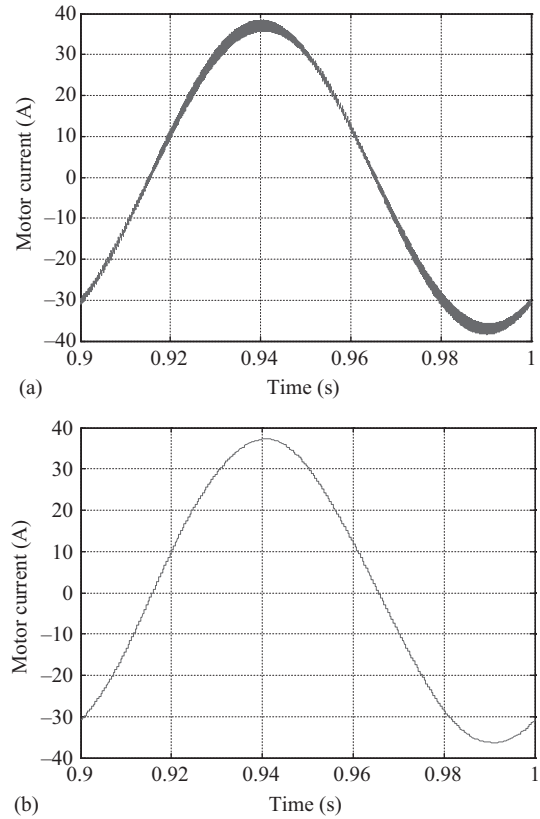


*Figure 5.5 (a) Inverter-fed motor current and (b) sampled motor current*

inverter Mohan *et al.* (2003). A section of the true spectrum is shown in Figure 5.6 (a), the corresponding spectrum of the sampled current Figure 5.5(b) is shown in Figure 5.6(b). The 2 480 Hz and 2 520 components in the original spectrum, after being shifted downwards by 2.5 kHz, have contributed to the 20 Hz component in the aliased spectrum that may be misinterpreted in CM and therefore should be taken care of. The 40 Hz component is caused by the same mechanism. The effect of sampling also depends on the instant of a sample is taken in a PWM switching cycle, see Jintakosonwit *et al.* (2002).

If the sampling rate cannot be further increased, then a common practice is to physically filter the signal and limit its frequency bandwidth before sampling. This anti-aliasing filter can prevent unrealistic components being introduced to the resultant spectrum. In general, the filter bandwidth and the sampling rate afterwards should be determined after knowing the target frequencies that are to be extracted for the purpose of CM.

As will be shown later in the book, spectral analysis is the foundation of CM techniques for induction machines, based on measurement of the stator current, i.e.

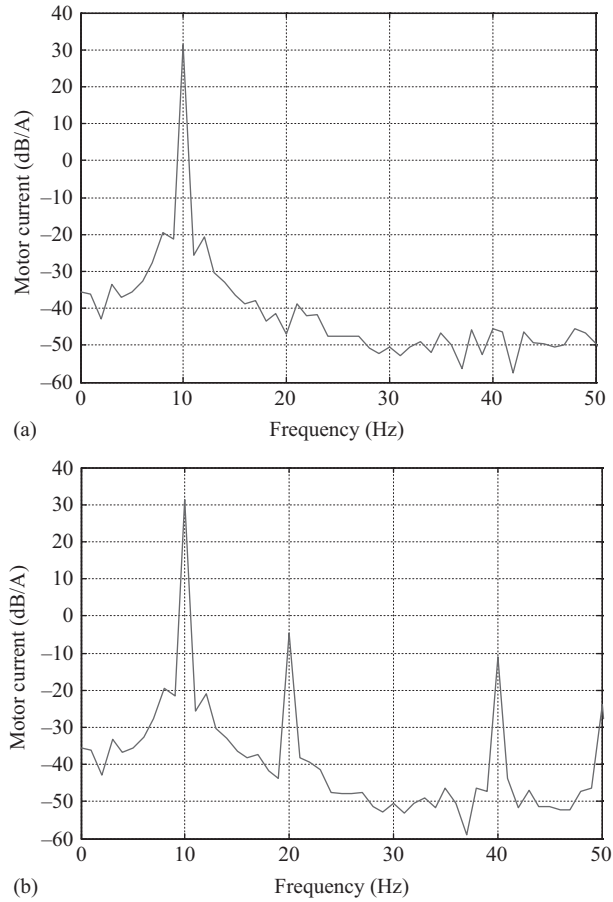


*Figure 5.6 Effect of sampling on inverter-fed motor current spectrum: (a) true spectrum of motor current and (b) spectrum of sampled motor current*

machine current signature analysis (MCSA). Later development normalised the spectrum with respect to the supply frequency, slip and the rated current so that the condition signatures can be easily identified Sapena-Bano *et al.* (2010). It is also common to plot the amplitude in dB to highlight the weak signatures.

## 5.3 Higher-order spectral analysis

Higher-order spectral analysis is a relatively new technique for CM. The first-order spectral analysis as described in the previous section makes little use of the phase information of the Fourier harmonic components. This can be taken into account in higher-order spectral analysis and the signal-noise ratio can be consequently improved Arthur *et al.* (2000).

For first-order harmonic components defined by (5.2), a second-order power spectral density (PSD) at frequency $f_k$ can be defined as:

$$P(f_k) = G(f_k)G^*(f_k) \tag{5.6}$$

where $G^*(f_k)$ is the complex conjugate of $G(f_k)$. Extending this definition to third- and fourth-order measures gives birth to the bispectrum $B(f_1,f_2)$ and trispectrum $T(f_1,f_2,f_3)$ as shown below.

$$B(f_1,f_2) = G(f_1)G(f_2)G^*(f_1+f_2) \tag{5.7}$$

$$T(f_1,f_2,f_3)) = G(f_1)G(f_2)G(f_3)G^*(f_1+f_2+f_3) \tag{5.8}$$

From (5.7) and (5.8), we may see that, unlike the PSD $P(f_k)$, the bi-spectrum and tri-spectrum are functions of more than one frequency index and, further, we may also see that they are complex quantities, that is they contain both magnitude and phase information about the original sampled time signal. In contrast, $P(f_k)$ is only of real values.

We can appreciate the value or potential of such higher-order spectral analysis by looking into what happens during some typical faults that causes electromagnetic disturbances in the machine. For example, a broken rotor bar fault in an induction motor will usually give rise to harmonics at two frequencies $f_1$ and $f_2$ in the air-gap flux density, with phase angles $\phi_{f_1}$ and $\phi_{f_2}$. A vibration signal is likely to be related to the flux according to a quadratic function, see Onadera *et al.* (1993). As a result, the vibration signal that can be acquired through an accelerometer contains harmonics at frequencies $f_1$, $f_2$ and $f_1 + f_2$ due to the quadratically non-linear relationship. Their phase angles will be $\phi_{f_1}$, $\phi_{f_2}$ and $\phi_{f_1+f_2} = \phi_{f_1} + \phi_{f_2}$, showing a quadratic phase coupling that can be easily indicated by a peak in the bi-spectrum of the vibration signal at the bi-frequency, $B(f_1,f_2)$, where the associated bi-phase $\phi(f_1,f_2)$ tends to zero. Faults of other types that cause flux components at different frequencies can be similarly detected provided that the target frequencies are known. Higher-order spectral analysis can be used when multiple faults exist in the machine so that more signature frequencies can be identified with a high signal-to-noise ratio, by exploiting the property of phase coupling. Examples of using higher-order spectral analysis for CM of induction machines are shown in Arthur *et al.* (2000).

## 5.4 Correlation analysis

This is a time-domain technique. Correlation between two signals, in the time domain, is a process mathematically very similar to that of convolution. The auto-correlation function provides a measure of the similarity between a waveform and a time-shifted version of itself, whilst the cross-correlation function refers to two different time functions.

The auto-correlation function of a time signal $f(t)$ can be written as,

$$R_{ff}(\tau) = \int_{-\infty}^{\infty} f(t-\tau)f(t)\mathrm{d}t \tag{5.9}$$

The function $f(t - \tau)$ is delayed version of $f(t)$, by a time $\tau$. Essentially, the process may be thought of as one signal searching through another to find similarities.

If $R_{ff}(\tau)$ is plotted against $\tau$, then the result is a correlogram. If the signal tends to repeat, the correlogram plot will give a peak indication when $\tau$ is around the time that takes the signal to show some repetition. Therefore auto-correlation is a powerful tool to identify the repeating features that can be hidden in a signal mixed with noises and disturbances.

Figure 5.7 illustrates the principle. The time signals are shown in Figure 5.7(a) and (b), and the resulting correlogram in Figure 5.7(c). It is apparent that signals exhibiting a periodic similarity, which may be difficult to extract from a background of noise, can be identified using this technique.

The cross-correlation function of two different signals $f(t)$ and $h(t)$ may be written as,

$$R_{fh}(\tau) = \int_{-\infty}^{\infty} f(t - \tau)h(t)\mathrm{d}t \tag{5.10}$$

The similarity between correlation and convolution is now clearly seen. For example, the convolution of the two time functions $f(t)$ and $h(t)$ would be expressed as,

$$g(t) = \int_{-\infty}^{\infty} f(t - \tau)h(\tau)\mathrm{d}\tau \tag{5.11}$$

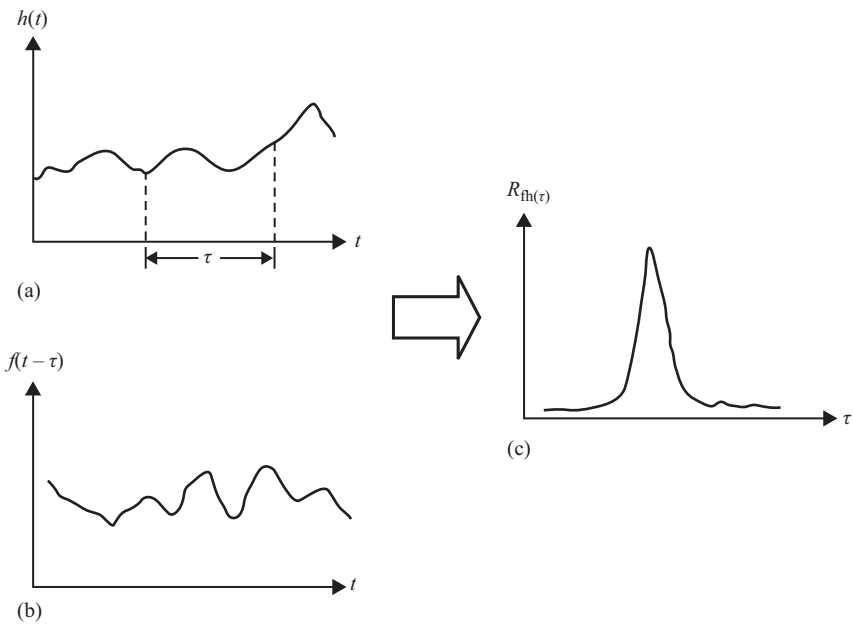


*Figure 5.7 The use of correlation functions*

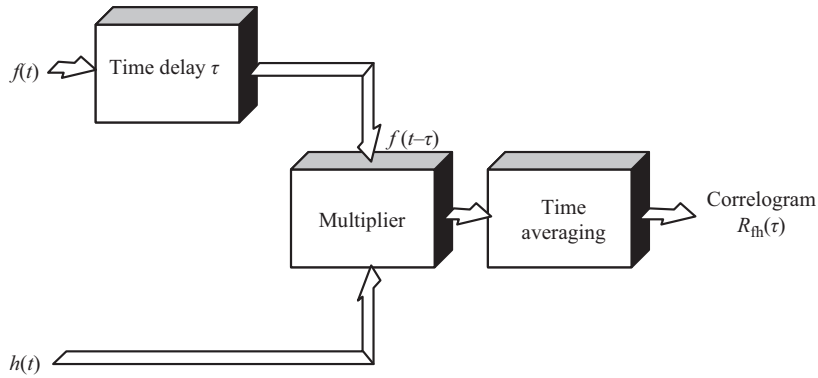


*Figure 5.8 Implementing the measurement of correlograms*

The only difference is that one of the time functions is effectively reversed.

Like the auto-correlation function, the cross-correlation function can also be used to recover both the amplitude and phase of signals lost in a noisy background. If two signals are inherently related but are phase shifted due to transmission delay in the system or modulated by physical processes in the system, cross-correlation can reveal the similarity between these signals, which are then confirmed to be due to the same cause. Because of such a property, correlation functions are particularly suitable to monitor faults like bearing degradation, PD activity on worn transformers, including their on-load tap changers, which have intermittent effects during operation Yazici (2004) and Kang *et al.* (2001). Correlation functions provide a means of relating the CM signatures to the causes of faults. Correlation functions can also be used to exclude the effects of factors that may not have direct implication on the plant condition, for example, known variations of load or changes of ambient temperature.

If we redefine (5.10) in a slightly different way, that is let the cross-correlation function between two signals $f(t)$ and $h(t)$ be

$$R_{fh}(\tau) = \lim_{T\to\infty} \frac{1}{T}\int_0^T f(t-\tau)h(t)\mathrm{d}t \tag{5.12}$$

it is easy to see how the correlation process can be realised in a numerical algorithm. Figure 5.8 illustrates the activity schematically; the time-averaging operation required will be described in the next section.

## 5.5 Vibration signal processing

### *5.5.1 General*

Vibration monitoring requires a number of specialised techniques and two of these techniques shall be briefly mentioned here. Although they are beginning to establish themselves as powerful diagnostic tools, their acceptance and application, is limited now primarily to the diagnosis of faults in gearboxes.

### 5.5.2 Cepstrum analysis

Mathematically, the cepstrum, $C(\tau)$, a function described as the inverse Fourier transform of the logarithm of the power spectrum of the function; that is if we define the power spectrum, $P_g(f)$, of a function $g(t)$ as:

$$P_g(f) = F\{g(t)\}^2 \tag{5.13}$$

then the corresponding cepstrum is:

$$C(\tau) = F^{-1}\{\log_e P_g(f)\} \tag{5.14}$$

where $F$ and $F^{-1}$ represent the forward and backward Fourier transforms, respectively, described in Section 5.2. Therefore $P_g(f)$ is the power spectrum of the time signal $g(t)$, which is also defined in (5.6). The dimension of the parameter $\tau$ in (5.14) is time and is introduced by the inverse Fourier transform; hence we can display the magnitude of the cepstrum with respect to time intervals in the same way as the spectrum can be illustrated with respect to frequency. The logarithm is employed so that the harmonic components in $P_g(f)$ that have relatively low amplitudes are also taken into account; their existence is amplified. The inverse Fourier transform in (5.14) tries to reconstruct the time signal but only highlights the time instants when considerable activities are occurring.

From this, the repetition of the activities can be identified as demonstrated next. The use of the cepstrum has found favour in examining the behaviour of gearboxes because such items of equipment tend to produce many families of side-bands in their vibration spectra, due to the variety of meshing frequencies and shaft speeds that may be present. Figure 5.9(a) shows the power spectrum of a gearbox vibration signal, containing harmonic side-bands that are spaced according to some pattern. We hope to identify such a pattern in order to derive information about the condition of the gearbox and the cause of fault if present. Figure 5.9(b) shows the cepstrum calculated from the power spectrum using (5.14), with $\tau$ progressing from 0 to a cycle. The horizontal axis here is practically time and the spikes correspond to the instants when significant activities are present in the original time signal. It is clear that the activities repeat predominantly according to two time periods, marked as A and B, respectively, in Figure 5.8(b). By measuring the periods (8.083 and 19.6 ms), we know that the fundamental repetition frequencies are 123.75 and 51 Hz. We can then further infer that the power spectrum of Figure 5.9(a) contains two sets of harmonic side-bands that are separated by 123.75 and 51 Hz, respectively, as illustrated in Figure 5.9(c).

So, the cepstrum essentially highlights multiple periodicity in complex signals, and hence identifies clearly various families of side-bands. The identification of various side-bands in a rich signal may be practically impossible using spectral analysis, but as Figure 5.9 shows the cepstrum easily picks them out.

We note in passing that although the horizontal scales of the cepstrum are in seconds it is usual practice to refer to the horizontal quantity as frequency, the peaks in the cepstrum as harmonics and the process as liftering. This is done to firmly identify the methodology with that of spectral analysis. If this technique can

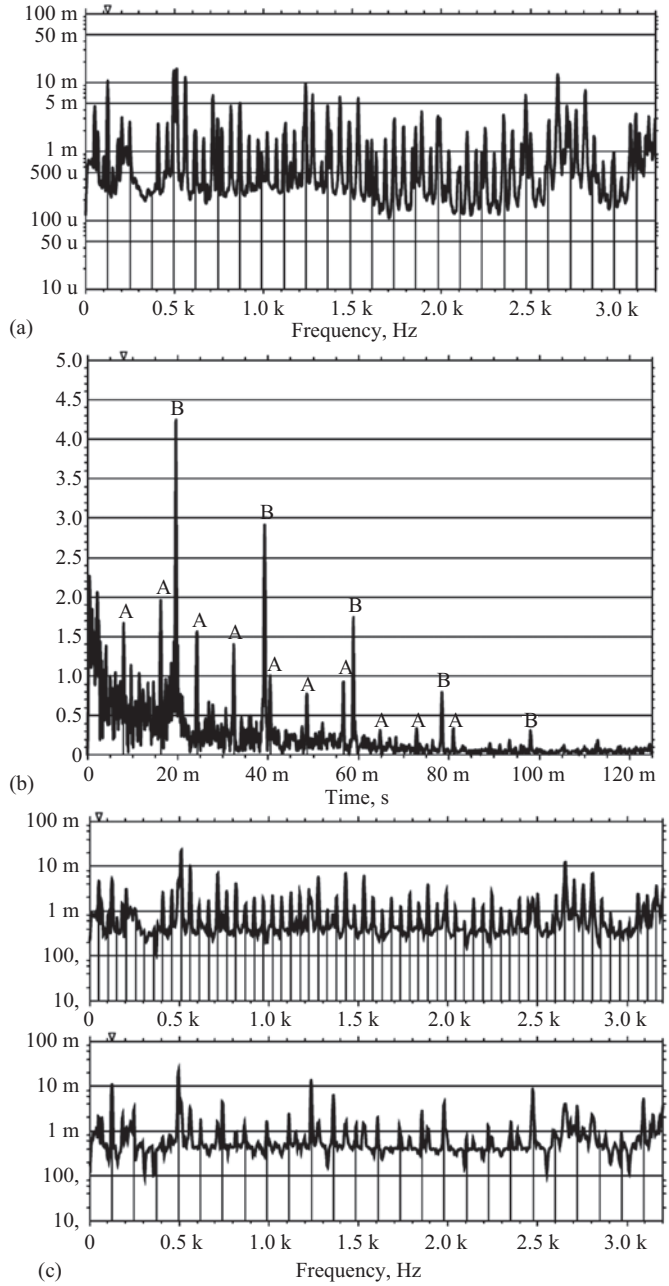


*Figure 5.9 Gearbox vibration spectra and associated cepstra: (a) power spectrum of the gearbox, (b) cepstrum of the gearbox and (c) liftered spectra*

identify side-bands with ease, then it may hold significant possibilities for the identification of faults in induction machines, particularly when they are fed from harmonic-rich inverters. To the best of the authors' knowledge, no work on this application has yet been reported but it may yet prove to be a fruitful path to follow. Its disadvantages lie with the technique complexity. It is a 'post' spectral analysis tool, in much the same way as spectral analysis is generally employed once one's suspicions are aroused by anomalies in time domain signals taken using overall level monitoring.

### *5.5.3 Time averaging and trend analysis*

In Figure 5.7, the need for signal averaging was noted during the practical computation of correlation functions. The averaging technique has found considerable favour in its own right for the detection of faults in gear boxes and rolling element bearings. It achieves this by simply averaging a large number of samples, taken successively from the same transducer or an upper stream numerical process, with each sample carefully timed to the same period. With rotating plant the rotational period of the element under inspection is usually chosen. In this way, noise generated elsewhere in the system is effectively smoothed out, and the signals due to faults that exhibit a cyclic pattern over the chosen period are enhanced.

Averaging can be implemented using one of the many transient signal capture techniques. For example, if it is necessary to take the average of 1 000 records, say, then each record must be captured and then stored for a simple average to be obtained on a point-by-point basis. This is an inefficient technique since it requires large amount of digital storage. It is possible to reduce this requirement significantly by approximation and defining the average of a sampled quantity $x_n$ as,

$$\bar{x}_n = \bar{x}_{n-1} + \frac{x_n - \bar{x}_{n-1}}{n} \tag{5.15}$$

In (5.15), $n$ is the record number, $x_n$ is the value for the $n$th record, and $\bar{x}_n$ and $\bar{x}_{n-1}$ are the average values up to the $n$th and $(n-1)$th records, respectively. Using this technique it can be seen that only two records need to be stored at any given time, yet the truly moving average is still calculable. The corresponding saving of digital memory is obvious, but it has been gained at the expense of requiring more rapid processing hardware, particularly if the period of each record is short. This problem is not always significant, particularly as fast processors are becoming more easily available in embedded systems. Time averaging is seldom applied to a signal that changes very quickly with time. For example, it should not be used for time-domain voltage and current signals. Time averaging is usually applied to a signal that indicates the level of a signature in the frequency domain, for example, the rms value of the voltage or current. Time averaging helps to avoid the effect of random, background noise in that signal. It is nearly always possible to choose records with suitable gaps between them. It is however of paramount importance to ensure that each record is properly synchronised. In addition to time averaging that filters out the random noise in the measurement, it is often necessary to perform some trend analysis to capture the change of a CM signature in a relatively long

period of time. Auto-regression models in time series analysis Morris (2001) and Stack *et al.* (2004) can be applied for the purpose on monitoring developing fault.

The usefulness for time-averaging techniques in monitoring electrical machines is somewhat limited although it is effectively the technique described by Tavner *et al.* (1986) for detecting rotor cage faults by speed variation. It may also prove helpful for drive systems where the effect of a gearbox, excluding the input shaft and bearings, can be removed using this technique.

## 5.6 Wavelet analysis

We do not attempt to present even an overview of the rich subject of wavelet transform; interested readers are referred to Flordin (1999), for example. But there is an increasing interest in developing CM techniques based on signal-processing methods using the wavelet transform. This is primarily because of the limitations of conventional spectral analysis based on Fourier series. For example, spectral analysis assumes that a signal is periodic and the harmonic components are obtained as an average over the entire observation interval; there is no information about the local variation of a signal at a certain frequency during a particular short period of time. Faults of an intermittent nature, such as mechanical faults in an electric machine drive train, cause intermittent, non-stationary, oscillatory signals; see, for example, Lin *et al.* (2003). If the oscillatory signature lasts for only a relatively short period each time it occurs, it may easily be masked if spectral analysis is applied over a long observation interval. Also capturing such a signature may require a high sampling rate that may not be acceptable to sample the signal for a long period of time; a flexible sampling scheme is desirable. For the reasons to be shown next, wavelet transform will be more suitable in such a case. It can employ a long window and low sampling rate for a low frequency component in the signal, and at the same time a short window and high sampling rate for a high frequency component. Furthermore, wavelet transform exhibits time–frequency localisation and globalisation, which gives a more precise description of the signal, providing more informative data for CM.

It is true that CM is usually applied to steady-state signals, even the signature carried by the signals may be of an intermittent nature. However, it has been realised that sometimes the target signature can be too difficult to separate from the dominant fundamental signal. For example, a broken rotor bar fault in an induction machine causes side-band current components whose frequencies are only slightly different from the fundamental frequency, the difference depending on the slip, which is normally very small in the steady state. It has been suggested by Zhang *et al.* (2003) and Douglas *et al.* (2004) that a more effective method is to detect the current signatures during start-up of the machine when slip is large. However, the transient current during start-up is not a stationary and periodic signal. Conventional spectral analysis would give erroneous results in this case. Again, wavelet transform, due to its time-frequency localisation property, can be a more suitable technique to extract the signatures from transient currents.

Fourier analysis uses sine waves of different amplitudes, frequencies and phase angles to synthesise a periodic signal. Wavelet transform expands this concept by considering that a time domain signal, not necessarily periodic, can be reconstructed using a series of small waveforms that can be transitioned and scaled in time. Such small waveforms, which are called wavelets, no longer need to be periodic, like sine waves. As an example, for a time signal $f(t)$, and a chosen basic mother wavelet function $\psi(t)$, the corresponding wavelet transform, $W(a,b)$, is defined as:

$$W(a,b) = \frac{1}{\sqrt{a}} \int_{-\infty}^{\infty} f(t)\psi^* \left( \frac{t-b}{a} \right) dt, a > 0, -\infty < b < \infty \tag{5.16}$$

where $a$ is the scaling factor of time while $b$ is the time-shifting parameter in the mother wavelet function and $\psi$ is defined below. The mother wavelet function is usually chosen as an oscillatory waveform that decays in both directions from the centre of the wavelet, as shown in Figure 5.10. So, the parameters $a$ and $b$ in (5.16) therefore scale the mother wavelet frequency and shift the centre of the mother wavelet, respectively. For a given instant $t = b$, if the signal $f(t)$ contains significant oscillation at a frequency coinciding with $1/a$, then the integration shown in (5.16) will result in a significant output. Because the mother wavelet decays in both directions away from the centre $t = b$, what happens to the signal $f(t)$ long time before $t = b$ or after $t = b$ does not matter. Therefore, wavelet transform provides the local frequency information in signal $f(t)$ around $t = b$. As parameter $b$ is varied, the $f(t)$ is scanned through in terms of time. As parameter $a$ is changed, signatures at different frequencies in the signal are revealed.

The decaying rate of the mother wavelet is usually selected to depend on the scaling factor $a$. If $a$ is small so that the corresponding frequency is high, then the

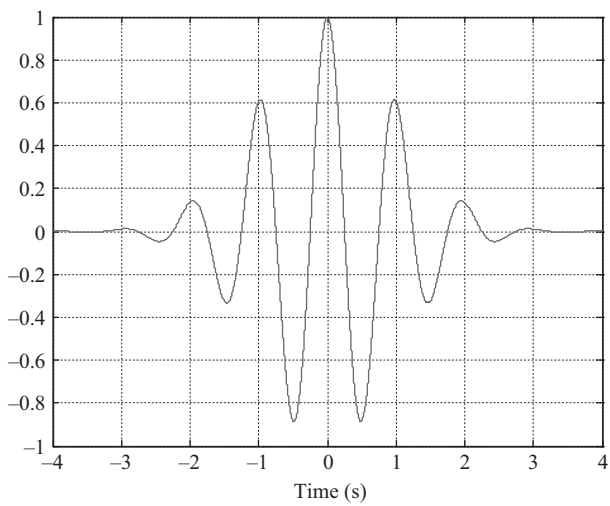


*Figure 5.10 A mother wavelet function*

decaying rate can be fast. If $a$ is large corresponding to a low frequency, then the decaying rate is slow. In this way, wavelet transform exhibits the property of multiple resolutions. The low-frequency information, which is present for a relatively long period of time in the signal, and the high-frequency information, which exists for a short period of time, can be obtained simultaneously. A most commonly used mother wavelet function, whose real part waveform is partially shown in Figure 5.10, is the Gaussian function and this is described below in (5.17).

$$\psi(t) = e^{-t^2/2}[\cos(2\pi t) + j\sin(2\pi t)] \tag{5.17}$$

It is obvious that wavelet transform as defined in (5.16) can be calculated numerically in a similar way to that shown in Figure 5.8, further taking into account the complex number nature of the mother wavelet function. It is however important to note that wavelet transform may involve different sampling rates and different observation lengths. It is therefore important to keep synchronisation in the sampling scheme. As $\psi(t)$ is complex, from the output of wavelet transform $W(a,b)$ both amplitude and phase information can be retrieved.

For the sake of being complete, (5.18) gives the inverse wavelet transform where:

$$C(\psi, v) = \int_0^\infty [\psi^*(v)\psi(v)/v]\mathrm{d}v.$$

$$f(t) = \frac{1}{C}\int_0^\infty \int_{-\infty}^\infty \frac{1}{a^2\sqrt{a}} W(a,b)\psi\left(\frac{t-b}{a}\right)\mathrm{d}b \cdot \mathrm{d}a \tag{5.18}$$

Figure 5.11(a) shows a measured starting current signal of an induction motor taken from Ran *et al.* (1996). It was found that transient torsional vibration was excited during the direct-on-line starting of the motor. The natural frequency of the mechanical shaft was known to be 22 Hz. Research showed that the torsional vibration could be indicated in the motor stator current as side-band components at 28 and 72 Hz, assuming a supply frequency of 50 Hz. As the starting current was transient and non-stationary, wavelet transform was applied to the current signal and the result is shown in Figure 5.11(b). The development of the 28 Hz component is clearly observed while the 72 Hz component is shadowed by the fundamental, see Yacamini *et al.* (1998).

## 5.7 Model-based information extraction

The above is to extract the information from the available data. In practice, the measurement of some variables may not be that straightforward. The dynamics of the instrumentation system may need to be considered and some quantities ideal for CM may not be directly accessible. For example, the temperature of permanent magnets on the high-speed rotor may be important information when operating safety critical permanent magnet machines, see Feng *et al.* (2018). Also, thermal conductivity in parts of a machine system may better indicate the cooling system

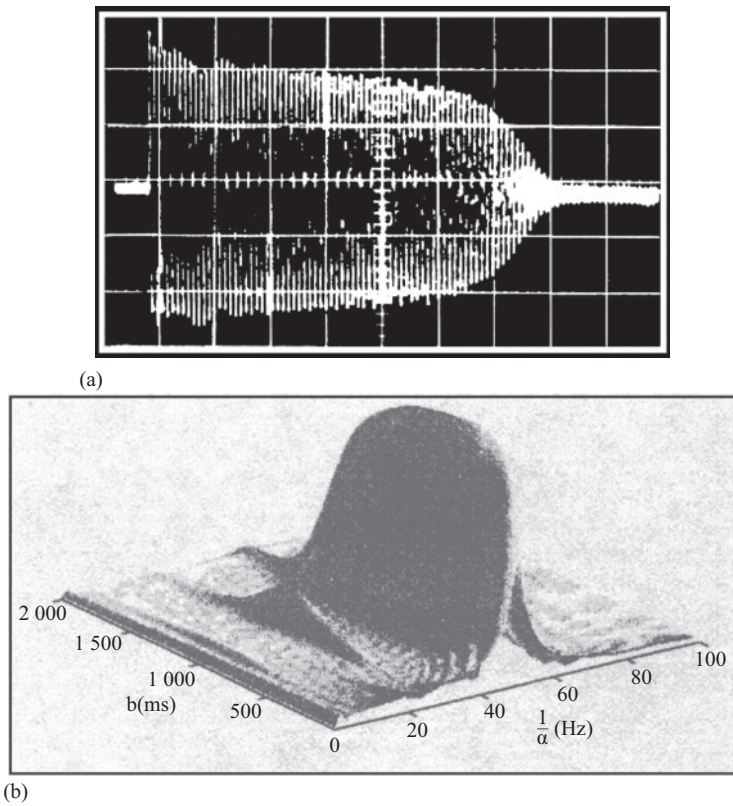


*Figure 5.11 Monitoring the onset of torsional vibration during the start-up of a downhole motor pump set. Taken from Yacamini et al. (1998) and Ran et al. (1996)*

condition than temperature measurements themselves. In all these cases, the target quantities need to be derived from data that are subject to modelling and/or measurement errors. In recent years, there has been a trend to develop more insightful and precise CM for electric machines using a mode-based approach, which complements the more traditional data-driven approach.

### *5.7.1 Kalman filter*

Kalman filter is traditionally used to estimate the unmeasurable state variables in a dynamic system, and is executed numerically in discrete time-steps, see Dutton *et al.* (1997). The estimation is based on measurable input and output signals that are polluted by random noises. In the discrete time domain, the system model is:

$$x_{k+1} = \varnothing x_k + u_k + w_k \tag{5.19}$$

$$y_{k+1} = Cx_k + v_k \tag{5.20}$$

where $x$ is the variable to be estimated, while $u$ and $y$ are the measured input and output, respectively. Subscript $k$ is the time-step, and $w$ and $v$ are noises. In applications, these quantities can be of high dimensions and the linearised model is characterised by the matrices $\varnothing$ and C.

Our task is to estimate $x$ at step $k + 1$, given the input and output measurements up to step $k$. Kalman filtering is a recursive process which breaks down the estimation into two steps: 'predict' and then 'correct'. The estimate from step $k$ to step $k + 1$ is denoted as $\widehat{x}_{k+1|k}$; then $\widehat{x}_{k+1|k+1}$ is the final estimate given measurement at step $k + 1$. Starting from $\widehat{x}_{0|0}$, at each time-step $k$, the variable is predicted for the next time-step $k + 1$ using the first model equation:

$$\widehat{x}_{k+1|k} = \varnothing\widehat{x}_{k|k} + u_k \tag{5.21}$$

This is used to predict the measurable output using the second model equation:

$$\widehat{y}_{k+1} = C\widehat{x}_{k+1|k} \tag{5.22}$$

When output measurement $y_{k+1}$ becomes available, its difference with $\widehat{y}_{k+1}$ is used to correct the prediction for $x$, as:

$$\widehat{x}_{k+1|k+1} = \varnothing\widehat{x}_{k|k} + u_k + K_{k+1}\left(y_{k+1} - \widehat{y}_{k+1}\right) \tag{5.23}$$

where $K_{k+1}$ is the Kalman gain which is updated step by step to minimise the variance of the estimate $\widehat{x}_{k+1|k+1}$. The procedure to determine $K_{k+1}$ can be found in Dutton *et al.* (1997) and it reflects the statistic characteristics of noises $w$ and $v$. Both the linearised system model and the noise characteristics can be updated with time. The Kalman filter is indeed adaptive, Dutton *et al.* (1997), extracted from which Figure 5.12 shows the response of a Kalman filter for a second-order

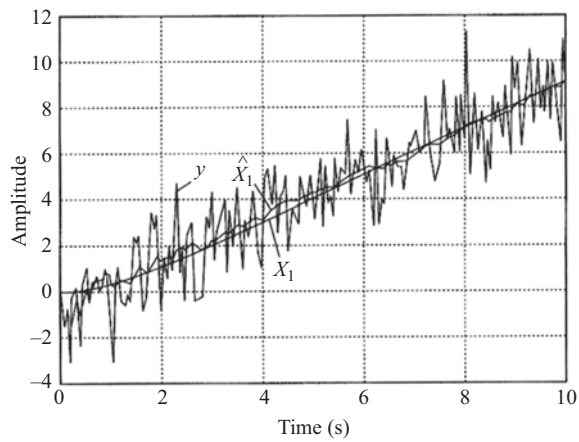


*Figure 5.12 Noise rejection by Kalman filter from Dutton et al. (1997)*

dynamic system where an internal variable $x_1$ is estimated step by step as $\hat{x}_1$. In this case, the output $y$ is actually measuring the internal variable $x_1$ but subject to considerable white random noise as shown in the Figure 5.12. The Kalman filter has effectively rejected the noise present in the transient process.

### *5.7.2 Observer*

Strictly speaking, the concept of an observer is not part of signal processing in the normal sense, but of extracting information by modelling. While filtering works on signals that are directly measured or indirectly estimated, an observer is more suitable for updating model parameters which change as the monitored system ages. Since CM focuses on the early stages of fault development, sometimes it can be assumed that the model structure remains the same, and only the parameters need to be updated. This is usually acceptable for early stages of cooling degradation, in both machines and power electronic systems, for example, Xiang *et al.* (2011), Gerstenkorn *et al.* (2017). Figure 5.13 shows a block diagram to estimate a thermal resistance value based on measurements of temperatures and power losses, following the concept of a Luenberger observer, see Dutton *et al.* (1997). The thermal resistance value is updated according to the difference between the measured temperature and the temperature estimated by the electro-thermal model of the system; a proportional-integral-derivative (PID) algorithm can be employed to update the parameter and the process can be extended to cases with multiple parameters to be updated. The objective here is to minimise the difference between the model output and the actual measurement. As long as the parameter changes slowly, the numerical process can be stable. As shown in Xiang *et al.* (2011), an advantage of using the thermal resistance as a health condition signature rather than using the measured temperature itself is that it is more constant and insensitive to the change of the operating point. The estimation of some internal temperatures can be achieved by Kalman filtering to mitigate random measurement errors.

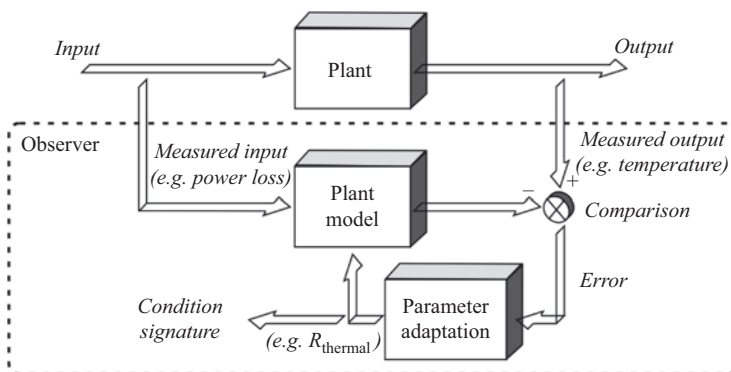


*Figure 5.13 An observer for condition monitoring*

## 5.8 Temperature instrumentation

Temperature is widely monitored in electrical drives and generators. For example, it is common to find temperature sensing used to monitor specific areas of the stator winding, core and cooling fluids of large electrical machines such as turbo-generators. Such measurements can only give indications of gross changes taking place within the machine but they are extremely effective if mounted and monitored in carefully selected sites. When temperature measurement is combined with information about machine load and ambient conditions, it provides very valuable monitoring information. Bearing temperatures are commonly monitored on drive trains and, together with vibration sensing, temperature measurement provides the standard approach to the assessment of the condition of these elements. The typical techniques and sites for temperature measurement in an electrical machine are described in Chapter 8. Here, we describe the three principal methods of measuring temperature electronically:

- resistance temperature detection (RTD),
- thermistors,
- thermocouples.

Each type has acceptable areas of application, which we will now briefly investigate.

The RTD uses the resistance change of a metal to indicate temperature change. Platinum and nickel is usually used because they are retardant to corrosion and because they have sensitive resistance vs. temperature characteristics, as shown in Figure 5.14, where $R_0$ is the resistance of the device made of the metal at 0 °C, see Morris (2001). An RTD can be made by either winding insulated metal wire around

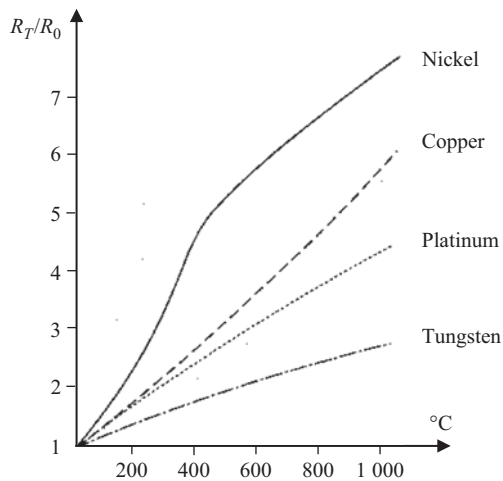


*Figure 5.14 Typical temperature–resistance characteristics of metals*

a thin cylindrical former or by evaporating a thin coating of the metal on an insulating, usually ceramic, substrate. Figure 5.15 shows a commercial sensor enclosed in a thin stainless steel tube for protection. Such devices are widely used for gas and liquid temperature measurement applications up to 1 000 °C and are the usual choice for electrical machine manufacturers for insertion between winding conductors in machine slots.

RTD devices are constructed generally to a base resistance of 100 Ω at 0 °C and have the advantage of being linear over a wide operating range. They have very good accuracy and precision but have, however, a relatively low sensitivity. They are generally used in a 4-wire configuration of Wheatstone bridge, but 2- or 3-wire operation is also possible. The circuit converts the change of resistance into the change of output voltage.

Figure 5.16 shows a Wheatstone bridge circuit for an RTD device made of platinum. The RTD device has the following temperature–resistance relationship: $R_T = R_0(1 + \alpha T)$, where $R_T$ is the resistance in Ω and $T$ is the temperature in °C.

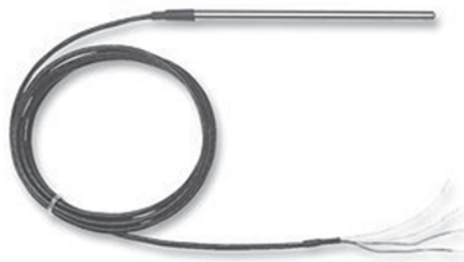

*Figure 5.15 An RTD device*

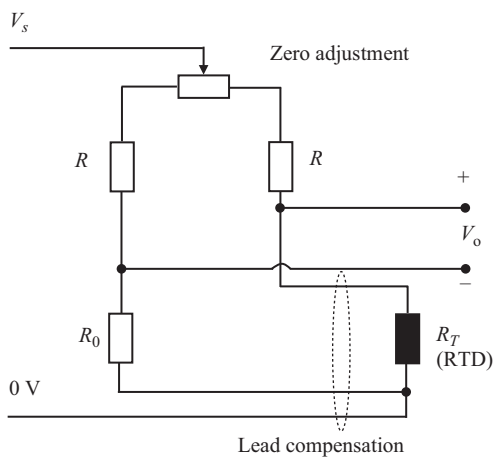


*Figure 5.16 Wheatstone bridge circuit for an RTD*

$\alpha_r = 0.00385/°C$, $R_0 = 100\ \Omega$ and the power supply to the circuits is $V_s = +15$ V. Ignoring the zero adjustment resistance, Table 5.1 shows the output voltage calculated for two resistance values: $R = 5\ 530\ \Omega$ and $R = 48\ \Omega$. The overall sensitivity and linearity between 0 °C and 100 °C are then derived. The sensitivity is defined as the ratio of change of output to the change of input while the linearity is defined as the deviation from the straight line between the two end points of the whole range, that is from 0 to 100 °C.

It is clear that increasing the value of $R$ causes the sensitivity to be reduced but the linearity to be improved. The self-heating error is reduced as the value of $R$ is increased. The Wheatstone bridge arrangement allows the lead resistance to be easily compensated as shown in the figure.

Temperature measurement using thermocouples is based on the well-known Seebeck effect whereby a current circulates around a circuit formed using two dissimilar metals, when the metal junctions are held at different temperatures. If a break is made in one of the wires, then a voltage is generated across the break, which increases with the temperature difference between the junctions. One junction is held at a temperature that can be easily measured to allow the so-called reference junction compensation. By doing this the need for a carefully controlled reference junction temperature is avoided and a device with effectively only a single junction result. Some typical junction materials and their associated operating ranges and outputs are given below in Table 5.2, derived from standard

*Table 5.1 Response of a Wheatstone bridge RTD circuit*

| $T$ (°C) | $R_T$ (Ω) | $V_0$ ($V$ @ $R = 5\ 530\ \Omega$) | $V_0$ ($V$ @ $R = 48\ \Omega$) |
|---|---|---|---|
| 0 | 100 | 0 | 0 |
| 20 | 105.79 | 0.0204 | 0.24 |
| 40 | 115.54 | 0.0406 | 0.46 |
| 60 | 123.24 | 0.0606 | 0.66 |
| 80 | 130.89 | 0.0804 | 0.84 |
| 100 | 138.5 | 0.1 | 1.0 |
| Sensitivity | | 0.001 V/°C | 0.01 V/°C |
| Linearity | | 0.6 °C error | 6 °C error |

*Table 5.2 Ranges, outputs and sensitivity of thermocouple junction materials*

| Type | Junction materials | Range (°C) | Output at 100 °C (mV) | Sensitivity at 30 °C (mV/°C) |
|---|---|---|---|---|
| E | Chromel/constantan | −279/1 000 | 6.317 | 0.0609 |
| J | Iron/constantan | −210/1 200 | 5.268 | 0.0517 |
| K | Chromel/alumel | −270/1 370 | 4.095 | 0.0405 |
| N | Nicrosil/nisil | −270/1 300 | 2.774 | 0.0268 |
| T | Copper/constantan | −240/400 | 4.277 | 0.0407 |

thermocouple tables. Multiple thermocouples can be cascaded to form a thermopile of higher sensitivity.

Figure 5.17 shows thermocouples being bonded on the coils of an air-cored axial flux permanent magnet motor in an electric vehicle for CM. It is essential to use the correct leads when extending the wires to the point where the output voltage is measured. As the thermocouple output is already in the form of a voltage, there is no need to use additional circuit such as a Wheatstone bridge for signal conversion. However, downstream devices are still generally required for amplification and reference junction compensation. Figure 5.18 shows a reference junction temperature compensation circuit using an LM35 integrated circuit (IC) whose output voltage is 0 V at 0 °C and increases at a rate of 10 mV/°C. A voltage divider is included to cause an approximately 40 μV/°C voltage gradient across resistor $R_2$ that forms part of the measured output voltage. The voltage across $R_2$ will then compensate the voltage developed across the cold junction marked as '3' in Figure 5.18, assuming that the cold junction is at room temperature around 30 °C.

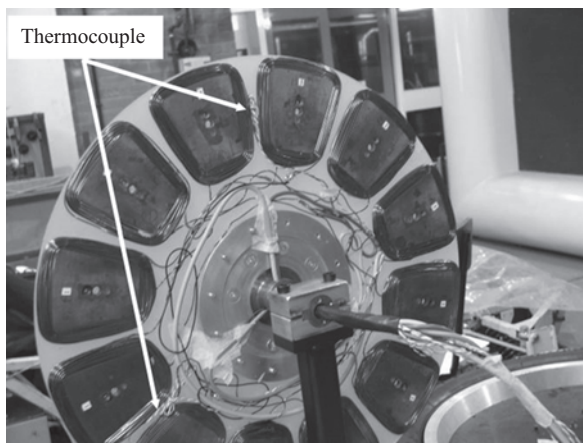


*Figure 5.17 Thermocouples to monitor coil temperature in a permanent magnet wind turbine generator*

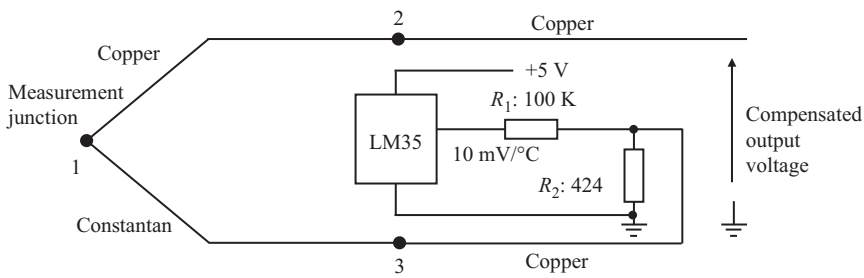


*Figure 5.18 Reference junction compensation for a thermocouple*

When appropriate, the sparking welding technique can be used to cause a thermocouple junction directly on a metallic surface.

The working life of thermocouples depends on the working temperature and the physical dimensions of the junction materials, but for copper/constantan and chromel/alumel, which are most widely used in electrical machine CM, they are be expected to survive for many years.

Provided the quality of the signal conversion circuit, the performance of RTD temperature transduction is very good; it is however relatively expensive. Thermocouples usually offer slightly reduced performance at much more modest cost. We noticed that the changes of output involved in both types of temperature transducers were small. Another type of temperature transducer we wish to briefly mention is the thermistor that provides coarse but very sensitive response. Thermistors are manufactured from the blends of metal oxides of cobalt, iron, titanium and nickel, which are fired like clays into small discs or beads that may be encapsulated in resin or enclosed in protective brass tubes. They are also available in the form of washers for easy mounting. Figure 5.19 shows a range of commercial thermistors.

Thermistors exhibit a large change in resistance as a function of temperature. In addition to sensitivity, they also have the advantages of high stability, fast response, and very small physical size. Typically a glass bead device will have a diameter in the order of 0.25 mm, whilst flake thermistors are produced in thickness down to 0.025 mm with cross-sections of 0.5 $\times$ 0.5 mm. The size advantage means that the time constant of thermistors operated in sheaths is small. But the size reduction also decreases the heat dissipation capability and so makes the self-heating effect of greater importance. Thermistors are generally limited to 300 °C, above which level the stability reduces. They do not provide a linear output and this

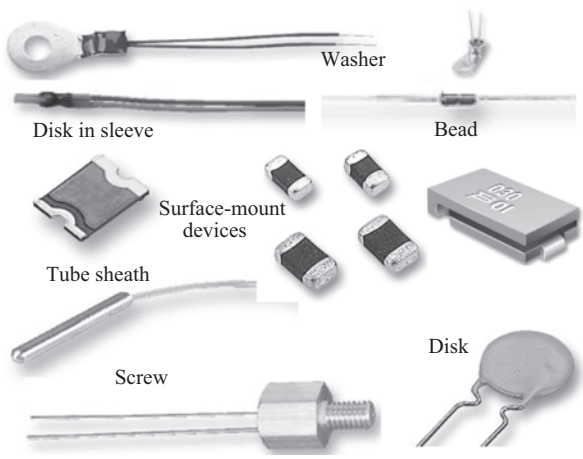


*Figure 5.19 Commercial thermistors. Source: EPCOS Inc. & Tyco Electronics Corp*

must be taken into account. For this reason, it is also difficult to control the consistency between samples of thermistors, implying that the precision achievable is relatively low. A thermistor is usually used as a logic switching device to operate an alarm when the temperature exceeds a preset limit and are inexpensive.

Figure 5.20 shows four typical temperature–resistance characteristics of thermistors. The nominal values of resistance 10, 20, 30 or 100 kΩ are defined for a room temperature of 25 °C. We note that the vertical axis is in logarithmic scale implying that the change of resistance with temperature is indeed significant. Since the accuracy of the device is hardly high and the characteristic may also slightly drift after long-time thermal cycling, the signal conversion scheme adopted for a thermistor is usually quite simple; in most applications, a voltage divider will be more sensible than a Wheatstone bridge circuit, helping to keep the overall cost down.

Semiconductor temperature transducers in the form of ICs have found more applications, Morris (2001). Their design results from the fact that semiconductor diodes have temperature sensitive voltage–current characteristics. With external power supply and internal feedback mechanisms, transistors in the IC can be made to produce an output current or voltage that is proportional to the absolute temperature. A voltage is developed as the current flows through a fixed resistor. The use of IC temperature sensors is limited to applications where the temperature is within a −55 to 150 °C range. Their errors are typically ±3%, quite low indeed. They are very inexpensive and therefore have been used in large quantities to monitor the temperature distribution of equipment featuring large dimensions, such as pipes and cables. We have described reference junction compensation. Such ICs can also be used for that purpose.

Other techniques such as quartz thermometers, fibre-optic temperature sensing, infrared thermography can be used to achieve high accuracy, fast response or provide non-contact and spark free solutions. They are generally more expensive than the techniques described above and have not been widely used in CM of

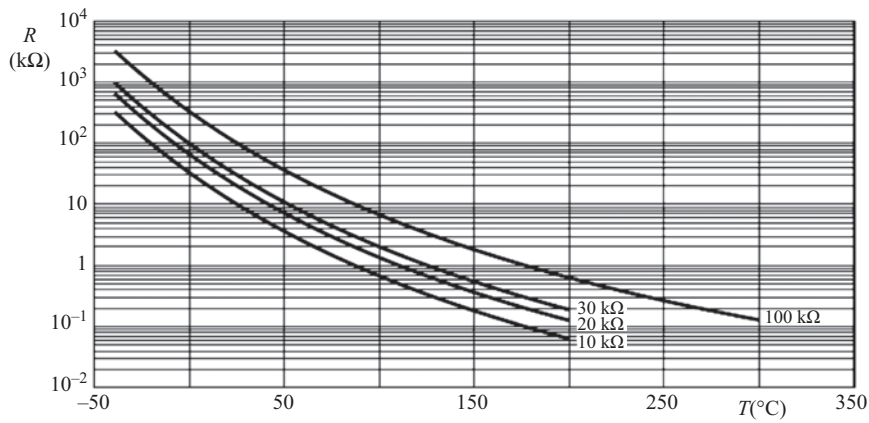


*Figure 5.20 Thermistor characteristics*

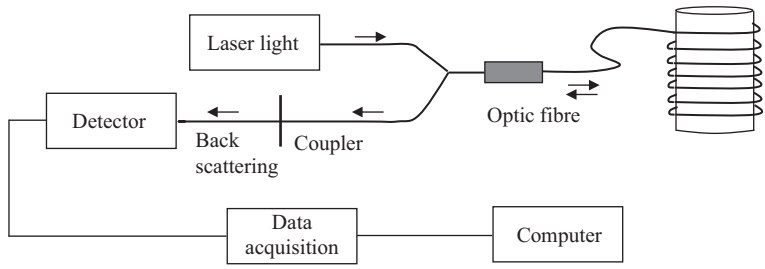


*Figure 5.21 Principle of fibre-optic temperature sensing*

electrical machines. However, in cases where the value of the monitored equipment greatly exceeds the cost of the transducers, such techniques are now increasingly being used. For instance, fibre-optic temperature sensing has been applied to identify hot spots in switchgear, transformers and more recently synchronous generators, see Morris (2001) and Miyazaki *et al.* (2003). For this reason, we now outline the principle and characteristics of such a technique, indicating its advantages and limitations.

Figure 5.21 shows the basic concept of fibre-optic temperature sensing. When a laser pulse is injected into the optic fibre, it is subject to scattering as it travels and the back scattered pulse is returned as shown in the principle of optical time domain reflectometry (OTDR), Miyazaki *et al.* (2003) and Rogers (1982). The back-scattered light consists of a Rayleigh component, a Brillouin component and a Raman component, which differ in wavelength. Thermally influenced molecular vibration causes the Raman-scattered component to change and therefore it is sensitive to temperature. According to the time when the signatures in the back-scattered light are received, the temperature along the optical fibre can be detected. Therefore, fibre-optic temperature sensing can be a naturally distributed method. Spatial resolution is typically in the 1 m range in terms of the fibre length. By winding the optic fibre around the body whose surface temperature is to be measured, better spatial resolution in terms of physical body dimensions can be achieved, see Kher *et al.* (2004). Using a technique called fibre Bragg grating (FBG), distributed temperature sensing can be multiplexed with strain and displacement measurements in the same fibre-optic system, as to be described later in this chapter. The temperature resolution is typically <0.1 °C in the range from 0 °C to a few hundreds of °C. The response time of fibre-optic temperature sensing can be 1 ms to 2 s.

## 5.9 Vibration instrumentation

### *5.9.1 General*

In Chapter 8, we will discuss in detail the techniques available and the applicability of vibration monitoring. This is particularly useful for monitoring the condition of components in the mechanical drive of electrical machines, such as gearboxes, shaft couplings, bearings and rotor unbalance. More recent work has extended that

*Table 5.3 Matching vibration transducer to the required frequency range, Mills (2010)*

| Transducer | Typical transducer output response | | | | | |
|---|---|---|---|---|---|---|
| | **0–2 Hz** | **2–5 Hz** | **5–200 Hz** | **0.2–1 kHz** | **1–2 kHz** | **2–20 kHz** |
| Displacement | Good | Good | Good | Fair | Poor | Nil |
| Velocity | Fair | Good | Good | Good | Fair | Poor |
| Accelerometer | Poor | Fair | Good | Good | Good | Good |

to the extraction of condition information from electrical variables such as current, vibration sensing, including acoustic noise, and it remains a most important monitoring technique for the operators of electromechanical plant. Its use is extremely widespread and has reached a high degree of sophistication. It revolves around the measurement of three quantities that are related by numerical integration or differentiation:

- displacement,
- velocity,
- acceleration.

Which quantity one should measure depends on the size of the plant being monitored, and the frequency range in which one is interested. Generally, machines of similar type and size have a more or less constant vibrational velocity. Also, as the vibration frequency increases it is likely that displacement levels fall, but acceleration levels rise. This suggests that with increasing frequency it is better to progress from a displacement device to a velocity transducer and ultimately to an accelerometer.

The frequency ranges of various transducers are shown in Table 5.3.

As a guide, the approximate frequency ranges of vibration transducer applications are shown graphically in Figure 5.22; it is useful to appreciate that an integration process to obtain velocity attenuates measurement noise whilst differentiation to obtain acceleration amplifies it.

Care must be exercised, however, when monitoring systems with small moving masses, for in such circumstances transmitted forces may be small and the accelerometer mass may be significant compared to the body mass. Here, displacement will usually provide the best indication of condition.

We can now characterise the vibration transducers according to the quantity they measure.

### *5.9.2 Displacement transducers*

Here, we confine ourselves to non-contact displacement probes or proximeters. This excludes some capacitive and low-frequency inductive devices such as a linear-variable differential transformer LVDT. One type of non-contact device that is used in CM operates by using a high-frequency current/voltage source to

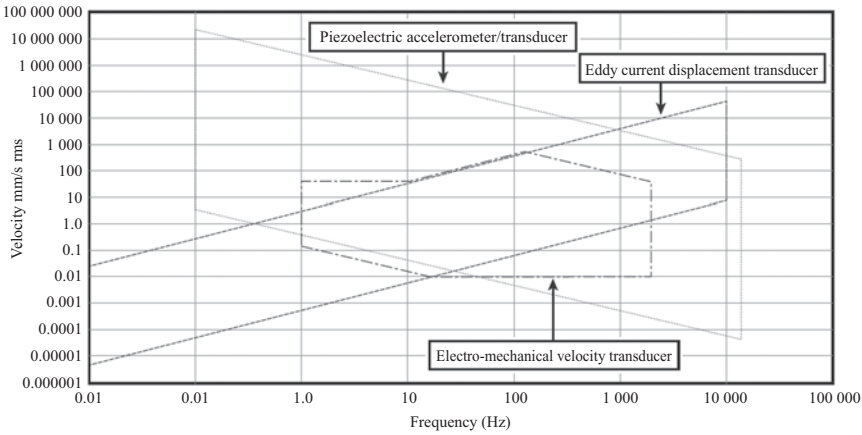


*Figure 5.22 Normal frequency range applicabilities for vibration transducers, Mills (2010)*

generate an electromagnetic field at the probe tip. The system energy, due to eddy currents in the target, is dependent upon the local geometry of the area surrounding the probe tip. If the system energy changes, for example, when the target surface, which is ferromagnetic and electrically conductive, moves with respect to the probe, then the system energy also changes. This change is readily measured as the change of voltage/current in the high-frequency excitation circuit is related to the displacement of the target surface from the probe tip. It should be noted that such systems measure the relative motion between the probe and the target; hence the vibration of the housing in which the probe is mounted is not readily measured by this technique. Figure 5.23 shows the operation of a proximity probe.

Sensitivities in the order of 10 mV/μ displacement are easily achievable with displacement probes, and they find wide application in situations where heavy housings ensure small external movements. The measurements of shaft eccentricity and differential movements due to expansion are therefore most easily achieved using displacement transducers. The same principle has been used to develop devices that effectively measure rotational displacement or speed by sensing the passage of keyways on the shafts, these are sometimes called key phasors.

As mentioned previously, displacement is most effectively measured at the lower frequencies even though the frequency range of eddy current systems can extend above 10 kHz. They are relatively robust transducers and the driving and detection circuits are straightforward. Essentially the high-frequency signal applied to the probe is modulated by the passage of the target, and the demodulated signal used as the measurement quantity. Consideration of Figure 5.22, which illustrates the basic displacement measurement principle, shows us that the output of the system will depend not only on the displacement between the probe and the target, but also on the material from which the target is made. This is because the eddy current reaction of the target, and hence the system energy, is dependent upon the

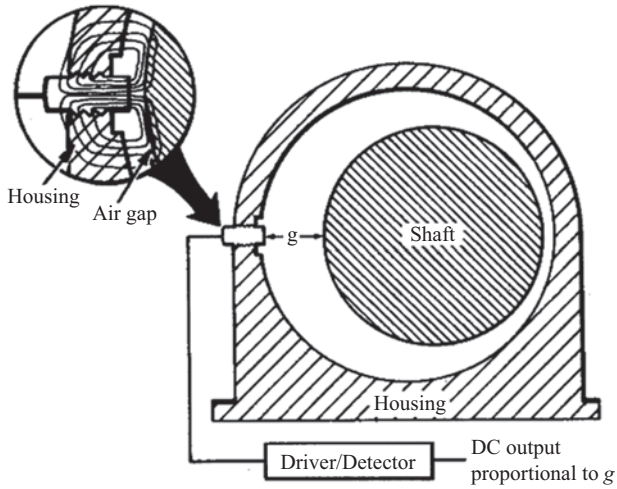


*Figure 5.23 Operation of a proximeter probe*

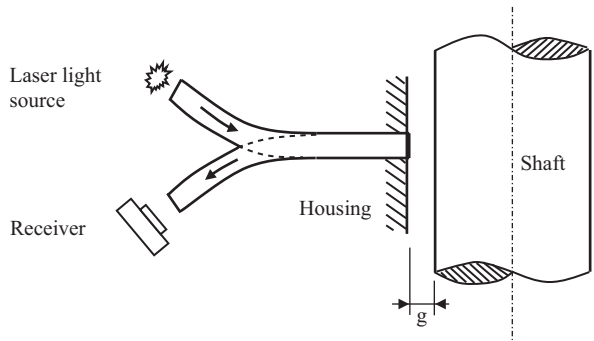


*Figure 5.24 Principle of fibre-optic proximetry*

conductivity and/or permeability of the material. Proximity probes must therefore be calibrated for each target material. Care must also be taken when mounting the probe to ensure that electrically conducting and magnetic surfaces around the probe tip do not cause unnecessary disturbance of the applied high frequency field and that the target surface is smooth with no surface or magnetic disturbances.

Another non-contact device uses a fibre-optic, which detects the light reflection and compares it with the injected light to determine the distance between the reflection surface and the optic fibre end. This is illustrated in Figure 5.24. The result is converted into a voltage signal using a photodiode in the receiver. The contact-free measurement range is up to 0.3 mm with typical resolution of 0.01 mm. There are other fibre-optic displacement sensors based on an FBG that can have a larger measurement range. However, they usually require contact to the

target surface; temperature compensation may also be necessary as the displacement is translated into strain for measurement, see Iwaki *et al.* (2000). In general, fibre-optic devices are intrinsically immune to electromagnetic noise problems.

### *5.9.3 Velocity transducers*

Rotational speed in electrical machine systems is usually measured for the purpose of control. Optical encoders are now used as common practice. They effectively derive the speed information by counting the position rotated per unit time. The optical encoder, which when in use is attached to the rotating shaft, carries a disk cut in slits. A light source and a receiving device are aligned on both sides of the disk. Light pulses are caused on the receiver, which are converted into electrical pulses by a photo-sensitive transistor. Such an encoder is very suitable to interface with a digital control system. The angular resolution is typically 0.18° corresponding to 2 000 pulses per revolution. Linear encoders are commercially available. However, application of such optical encoder for vibration measurement has been limited to very low-frequency range because position variation is hardly enough when the vibration frequency is high.

High-precision electromagnetic resolvers can also be used to obtain the rotational information from a drive shaft.

For vibration measurement, velocity is most usefully sensed in the frequency range from 10 Hz to 1 kHz. This is usually achieved in an analogue manner by designing a spring mass system with a natural frequency less than 10 Hz, and letting the mass take the form of a permanent magnet, as illustrated in Figure 5.25. The device is responsive regardless of the range of displacement involved in vibration. The magnet is then surrounded by a coil that is securely attached to the housing. Whenever the housing is placed in contact with a vibrating surface, the housing and coil move with respect to the magnet and cause an EMF to be induced in the coil, in accordance with the expression:

$$e = \ell B v \tag{5.24}$$

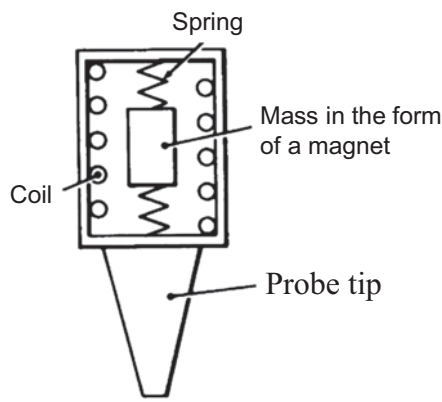


*Figure 5.25 Principle of an electromagnetic velocity probe*

where $e$ is the induced EMF, $\ell$ the effective length of the conductor in the coil, $B$ the radially directed flux density, which is ideally constant and $v$ is the velocity in the axial direction.

This transducer is relatively delicate but has the advantage of producing an output signal that is relatively large, and therefore requires little or no signal conditioning. Modern electromagnetic velocity transducers are designed using computer-aided design software including finite-element analysis to ensure the quality of dynamic response in the target frequency range.

### *5.9.4 Accelerometers*

Nowadays, however, velocity and displacement are commonly measured using accelerometers, the required parameters being derived by integration. Accelerometers are rigidly fastened to the body undergoing acceleration. For each accelerometer there is a sensing axis aligned with the direction of the acceleration that is intended to be measured. Accelerometers produce an electrical output that is directly proportional to the acceleration in the sensing axis. The output should be low if the acceleration is applied at 90° to the sensing axis; the non-zero output is due to cross-sensitivity.

The piezoelectric device has become almost universally accepted as the transducer to use for all but the most specialised of vibration measurements. The piezoelectric crystals act as both the spring and damper in the accelerometer that is consequently very small and light in weight. The piezoelectric accelerometer is physically much more robust than the velocity transducer and has a much superior frequency range. This has become more important as CM techniques involving frequencies well above 1 kHz have been adopted.

The construction of a typical piezoelectric accelerometer is illustrated in Figure 5.26.

When it is subject to vibration, the seismic mass, which is held against the piezoelectric crystal element, exerts a force upon it. This force is proportional to the acceleration. Under such conditions, the piezoelectric crystal, which is usually a polarised ceramic material, generates a proportional electric charge across its faces.

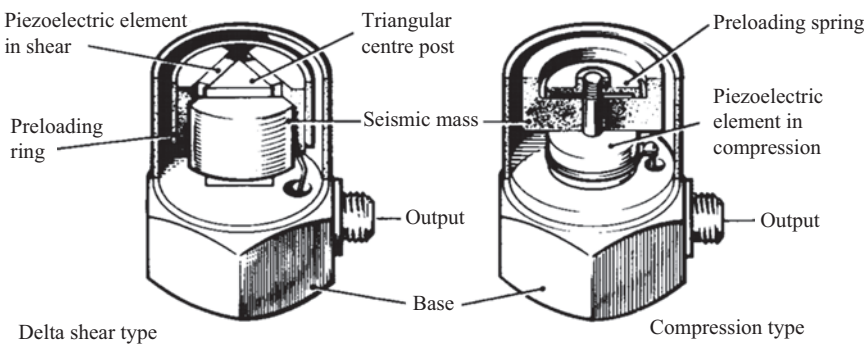


*Figure 5.26 A piezoelectric accelerometer. Source: Bruel and Kjaer*

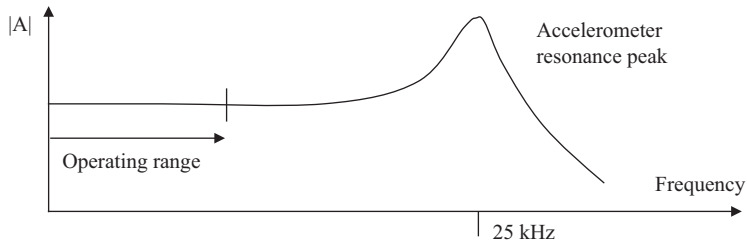


*Figure 5.27 Accelerometer response*

The output can then be conditioned using a charge amplifier and either incremental velocity or displacement signals recovered by integration. The device has the obvious advantage of generating its output without an external electrical source being required. As the electrical impedance of a piezoelectric crystal is itself high, the output must be measured with a very high-impedance instrument to avoid loading effects. Integrated circuit piezoelectric devices have become available with a high-impedance charge amplifier resident in the accelerometer encapsulation. In recent years, integrated accelerometer circuits, which include more than one sensing axis, have been developed to permit 2D and 3D measurements.

When using piezoelectric accelerometers it is important to realise that, unlike proximity probes, the natural frequency of the device is designed to be above the usual operating range. A typical frequency response is shown in Figure 5.27. This limits the useful operating range to around 30% of the natural frequency. Also, because the output is low at low frequencies the normal range of application of accelerometers is approximately 1 to 8 kHz, although small devices may have ranges extending beyond 200 kHz and integrated amplifier allows measurement at nearly DC.

There is an extremely wide range of piezoelectric accelerometers available today, from very small devices that will measure shocks of high acceleration, in excess of $10^6$ ms$^{-2}$, to large devices with sensitivities greater than 1 000 pC/ms$^{-2}$. Highly sensitive devices, on the other hand, have to be physically large so as to accommodate the increased seismic mass required to generate the high output. In all cases, however, care must be taken when mounting accelerometers since they can be easily destroyed through over-tightening.

Table 5.4 below provides a short summary of the area of application of each of the vibration transducer types discussed above.

## 5.10 Force and torque instrumentation

One of the most common ways of measuring force is to use a strain gauge, a simple device that comprises a long length of resistance wire formed into a zigzag shape and securely bonded to a surface that will alter shape elastically under the action of the force. When the gauge is stressed under the action of the force, the cross-section and length of the wire changes so that its resistance alters. In recent years, wire-type gauges have largely been replaced by metal foil or semiconductor types.

*Table 5.4 Application of vibration-monitoring techniques*

| Application | Transducer type |
|---|---|
| Motor pump drives | Velocity or acceleration |
| Motor fan drives | Displacement or velocity |
| Motor connected to the gearbox with rolling element bearings | Acceleration |
| Motors and steam, gas or hydro-turbine-driven generators with oil film bearings | Displacement |
| Overall vibration levels on all the above machines | Velocity |

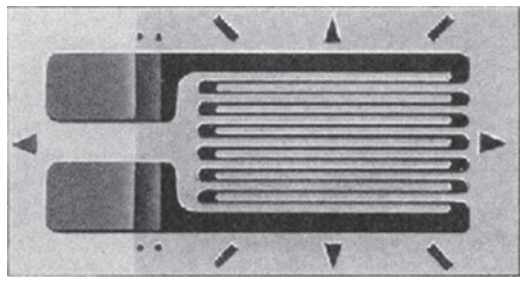

*Figure 5.28 A metal foil-type strain gauge*

Figure 5.28 shows a metal foil-type strain gauge; the material used is typically the 'advance alloy' made of copper, nickel and manganese. Cutting a foil into the required shape is much easier than forming a piece of wire into the required shape, and this makes the devices cheaper to manufacture.

The input–output relationship of a strain gauge is expressed by the gauge factor, $G$, which is defined as the relative change in resistance, $R$, for a unit value of strain, $\varepsilon$, that is:

$$G = \left(\frac{\Delta R}{R_{\text{nominal}}}\right) \Big/ \varepsilon \tag{5.25}$$

Strain gauges are manufactured to various nominal values of resistance, of which 120, 350 and 1 000 Ω are the most common. The typical maximum change of resistance in a 120 Ω device would be 5 Ω at maximum deflection. The resistance of the gauge is usually measured by a bridge circuit and the strain and hence force is inferred from the bridge output measured. The maximum current that is allowed to flow in a strain gauge is in the region of 5 to 50 mA, generally small to limit the self-heating effect.

In order to measure forces, strain gauges need to be applied in a particular arrangement, examples of which are shown in Figure 5.29. Within the same stressed structure, usually some strain gauges are subject to tension while other two

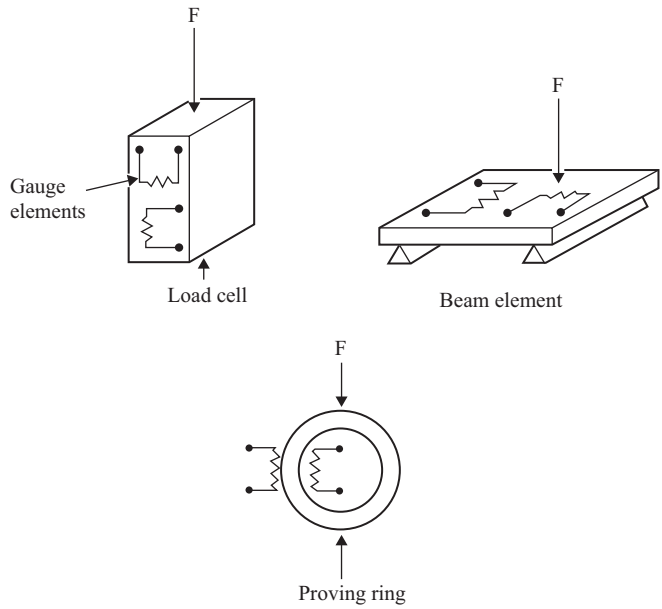


*Figure 5.29 Arrangement of strain gauges to measure the force*

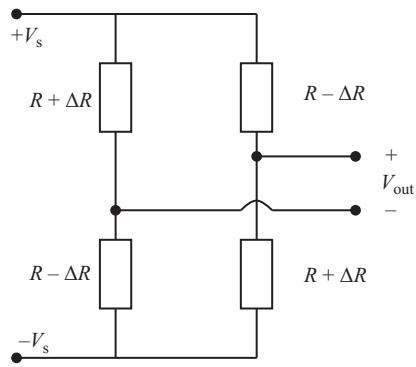


*Figure 5.30 Wiring of strain gauges in a Wheatstone bridge*

are subject to compression. Consequently, the resistance of some strain gauges increases while that of others decreases. Figure 5.30 shows a common way of wiring four strain gauges into a Wheatstone bridge where the increased and decreased resistance alternates to maximise the output sensitivity. Note that the voltage supply to the Wheatstone bridge circuit is ±Vs rather than between 0 and 2 Vs. This is to avoid common mode voltage in the output that can cause common mode errors in the down-stream circuits.

Force transducers of this type are routinely used to measure forces ranging from a few Newtons to huge tonnes of force. Care must be taken to either operate

*Table 5.5 Other strain measurement methods*

| Method | Principle of operation | Remarks |
|---|---|---|
| Fluidic load cells | Force applied to a diaphragm causes pressure. | Pressure signal must then be converted to an electrical output. |
| Optical encoder | Twisting torque causes displacement across the two ends of a shaft. | High resolution needed. Usually applied on long shaft such as in turbine-generators. |
| Fibre-optic | Some fibre-optics exhibit the property to rotate the transmitted light in proportion to the stress applied to the fibre. | Careful phase measurement needed. Expensive but highly accurate. |
| Magneto-elastic | The magnetic properties of some ferromagnetic materials depend on the mechanical stress the material is subject to. | Expensive but accurate. Special precaution needed to screen devices. |

them at a constant temperature or properly compensate for the effects due to expansion. Modern strain gauge bridge systems, to measure $\Delta R$, may be self-balancing with automatic read out.

It is immediately apparent that such devices can be used to measure torques applied to shafts but if the shaft is in motion the additional problem of extracting the signal must be faced. This may be done using instrumentation grade slip rings attached to the shaft, or by suitable noise-free telemetry. Telemetry systems in the electrically noisy environment around electromechanical machinery can be difficult to implement. Alternatively, contact free inductive magneto-elastic or FBG torque transducers can be used that work on the change of the material permeability or the reflection of polarised light. Table 5.5 outlines a few such strain measurement methods that, although still relatively expensive, are becoming increasingly popular owing to the computing power available for the compensation of temperature and/or nonlinearity effects. For instance, Sihler *et al.* (2005) described a case of using an inductive torque transducer in a synchronous generator system to monitor the occurrence of sub-synchronous resonance and this enables the control system to provide damping using active compensation, this subject is dealt with in more detail in Chapter 8.

In this section, we have simply outlined the most common means of measuring force, and it is an area that is extremely well established and highly developed. The use of specific techniques for particular applications can be found by searching the large literature associated with force measurement. Some helpful references are Beihoff (1999) and Gao *et al.* (1999).

## 5.11 Electromagnetic instrumentation

The basic electrical quantities associated with electromechanical plant are readily measured by tapping into the existing CTs and VTs that are always installed as part

of the protection system. These are standard and therefore need not be considered further here.

There can be a requirement, however, to measure the magnetic flux density in, or around, electrical machines. This is not normally measured for control or protection. For the purpose of CM, this can be done in one of the two ways. Either a simple search coil is used, or a Hall-effect device may be more appropriate. These two options are different in nature since the search coil is a passive device whereas the Hall-effect device is not. On the other hand, only the search coil has the capacity for significant energy storage and the risk of sparking; therefore in areas that may present an explosion hazard, such as on offshore oil rigs or refineries, their use must conform to current safety standards. The search coil induced EMF, $e$, is given by the expression:

$$e = \omega BAN \tag{5.26}$$

where $\omega$ is the frequency of the normal component of flux density, $B{\cdot}A$ is the effective cross-section of area of the coil and $N$ the number of turns in the coil. Such devices cannot detect DC fields and at very high frequencies their output may be limited by the self-screening effects due to the parasitic capacitance between turns.

Coils can be produced by evaporating copper directly onto surfaces, in the appropriate position, or by evaporating them on to insulating materials such as Mylar, which can then be bonded to the appropriate surface. These techniques are extremely useful if the coil is to be used inside an electrical machine, where the coil must not be allowed to move into the air-gap and risk damage to other areas of the machine.

As previously mentioned, if the coil is to be placed in a hazardous area then it is not the output of the coil that is important, it is the possibility of an unwanted input that must be considered. The energy stored in a coil is given by the expression:

$$E_e = (1/2)LI^2 \tag{5.27}$$

where $L$ is the inductance of the coil, and $I$ the current flowing in it. The stored energy $E_e$ can be reduced by ensuring that either $L$ is low or $I$ is limited. For a high signal output, $L$, which is a function of the number of turns, $N$, should be reasonably high. Therefore, one must limit $I$, usually by a large resistance of the coil. It is then important that the input impedance of the downstream circuit is high. If this is the case, the voltage measured across the terminals of the search coil indicates the EMF and hence the flux density, without much effect of the coil resistance or inductance. A search coil is often made of thin wire so the coil resistance is high; the input impedance of the downstream circuit should be significantly higher. Suitable buffering to the signal conditioning amplifier is sufficient to allow operation in most areas.

The Hall-effect device does not suffer from such disadvantages so long as the required power supply to the device is suitably isolated, but it is by nature only able to provide a measurement of flux density over a very small area. Figure 5.31 shows the basic principle of operation of the Hall-effect element. When a current $I$ flows

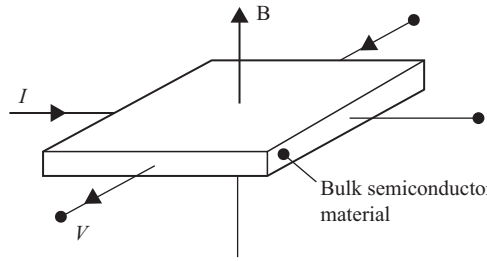


*Figure 5.31 The Hall-effect principle*

through the Hall device in perpendicular to an applied magnetic-filled strength $B$, the electrons are crowded to front surface due to Lorentz force causing a transverse voltage across the device. The output voltage, $V$, is related to the applied current, $I$, and the field, $B$, by:

$$V = \frac{kIB}{nq} \tag{5.28}$$

where

$q$ = electron charge,
$n$ = the number of charge carriers per unit volume in the semiconductor,
$k$ = a constant,
$k/nq$ = Hall constant of material.

In measuring the magnetic field, the current is established and regulated by a power supply.

Hall-effect devices have the advantage of being able to measure down to DC, and can be made in extremely small sizes. Since Hall effect can be established in less than a nanosecond, the response bandwidth of a Hall-effect transducer can be easily over 100 MHz.

We said at the beginning that current and voltage measurements are usually obtained from CTs and VTs. This is often the only option we have for large generators in power plants. For small- and medium-size electric machines, for example, motors in most VSDs, it is often more common to measure both current and voltage using Hall-effect transducers. Figure 5.32 shows a board with three Hall-effect current transducer channels and a board with three Hall-effect voltage transducer channels. The operating principle of the transducer is still that shown in Figure 5.31. Commercial Hall-effect current transducers require voltage supply to establish the current while the magnetic field is set up by the current to be measured. This allows contact free arrangement as the conductor carrying the current passes through the Hall transducer that is shaped in a ring. Hall-effect transducers are also available for measuring voltage, where the voltage is turned into weak current through a large ohmic resistor, say 100 kΩ. Both current and voltage measurement using Hall-effect transducers requires on-board signal conditioning to set the ratio.

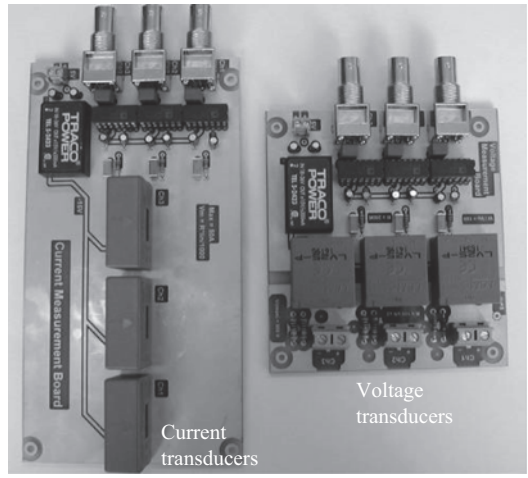


*Figure 5.32 Hall-effect current and voltage transducers*

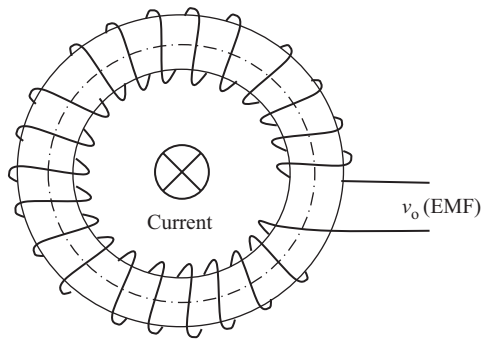


*Figure 5.33 Illustration of a Rogowski Coil measuring current in a bus-bar*

Another current transduction technique used for CM of electrical machines is the Rogowski coil whose operating principle is similar to that of a search coil. However, a Rogowski coil is specifically arranged to provide features that are desirable in some applications. As shown in Figure 5.33, a Rogowski coil is an air-cored toroidal coil that can be placed around a conductor that may carry current. An EMF is induced by the alternating magnetic field. Since there is no saturable magnetic component in the coil, the total magnetic field is strictly proportional to the current that excites it and the net effect of any current external to the toroidal coil is always zero. To complete the Rogowski coil current transducer, the induced EMF is electronically integrated so that the output from the integrator, properly initialised, is a voltage that accurately reproduces the current waveform. Rogowski coils are often used to capture the high-frequency spikes in the neutral current that may be used to interpret internal faults or PD in an electrical machine, see Xiao

*et al.* (2003). Conventional CTs are not suitable for this purpose due to more limited bandwidth and possible core saturation.

## 5.12 Wear and debris instrumentation

In many electrical machines, we can derive crucial condition information from fluid lubricant and coolant. For example, bearing damage accounts for at least 50% of rotating electrical machine failures, see Chapter 3 and Durocher *et al.* (2004). As the bearing wears, we would naturally expect to detect debris in the lubricant. Similarly, when internal faults such as PDs occur in the machine, we would expect that the coolant would be contaminated. Chemical methods of monitoring the wear and contamination will be discussed in detail in Chapter 6. For completeness, we will here briefly describe the physical techniques of debris measurement in line with the transduction task in monitoring. The most common method of doing this is to use a so-called debris sensitive detector. Such a detector depends on the lubricating fluid being continually passed through a device that is sensitive to the presence of particular material. This is commonly achieved using either an electrical transducer to measure the electrical changes in inductance, capacitance, or conductivity, or optically by measuring changes in turbidity of the lubricant.

The principle of operation of the electrical techniques is essentially the same. The lubricant and debris pass through a small chamber that can alternatively be part of a conductive circuit, the dielectric in a capacitor, or part of a magnetic circuit, in order to measure the changes in conductivity, capacitance or inductance, respectively. AC power supply is usually needed when detecting the change of capacitance or inductance.

All of these devices can give good indications of general levels of wear, and dramatic indications of the occasional large pieces of debris. Such transducers are both complex and expensive, and require careful and regular attention. Figure 5.34 shows a scheme of measuring the change of inductance, which is most widely used in practice. An inductive coil is placed around the tube carrying the fluid that may contain metallic debris. The inductance of the coil is detected using a high-frequency

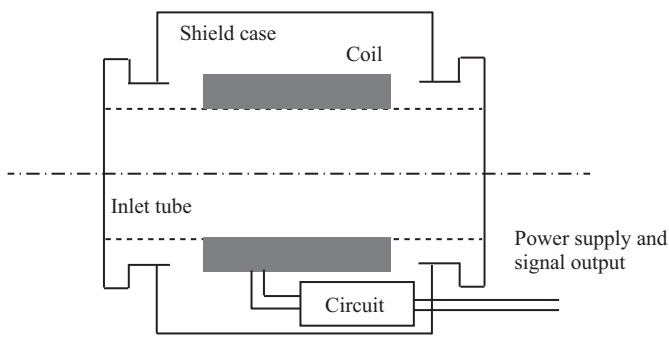


*Figure 5.34 Structure of an inductive debris detector*

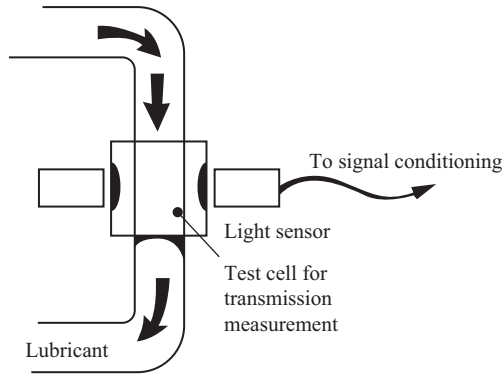


*Figure 5.35 Arrangement for an optical debris sensor*

oscillating circuit. Ferromagnetic debris in the oil increases the coil inductance and hence decreases the resonant oscillating frequency of an LC circuit. If the metallic debris is non-ferromagnetic, the high-frequency inductance of the coil tends to reduce due to eddy current induced in the debris, see Whittington *et al.* (1992).

Optical monitors generally operate by sensing either a loss of transmission of light through a test cell, or by detecting light scatter from the particular matter (known as the Tyndall effect), as shown in Figure 5.35.

Maintenance of optical systems is minimal, and they may be used on a wide variety of fluids. They are subject to spurious output, however, if the lubricant becomes aerated to any significant degree. Being more suitable for detecting fine particles in the fluid, they are however unable to differentiate between harmful and non-harmful particulate matters. Optical and electrical detectors are often used in combination in CM applications.

## 5.13 Signal conditioning

Signals from sensing devices will often require some type of modification before they are transferred for data acquisition and signal processing. This requires local signal conditioning circuits that usually employ analogue devices. The modification may be amplification or averaging, for example. In noisy environments, it is often necessary to filter the outputs of the transducers. Figure 5.36 shows two typical signal conditioning circuits using operational amplifiers, and their input–output relationships under ideal conditions. Their operation is explained thoroughly in many text books. Figure 5.37 shows a buffer amplifier circuit that can avoid the effect of the resistance of the leads. This allows transmission of analogue signals over distances up to 100 m using the screened cables.

We have already discussed in previous sections that many transducers output a differential voltage signal by using a Wheatstone bridge whose loading capability is very small, that is the current drawn from the bridge should ideally be zero.

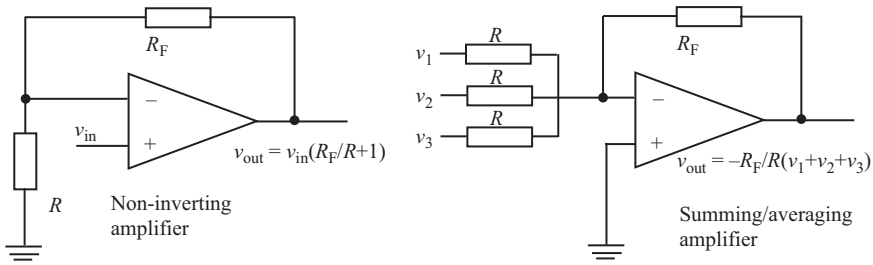


*Figure 5.36 Two commonly used amplifier circuits*

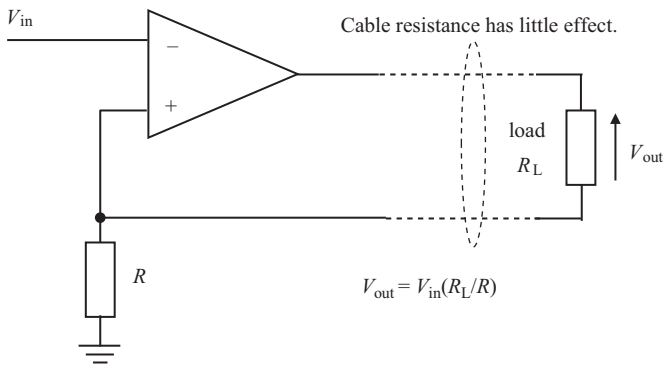


*Figure 5.37 Buffer amplifier circuit for signal transmission*

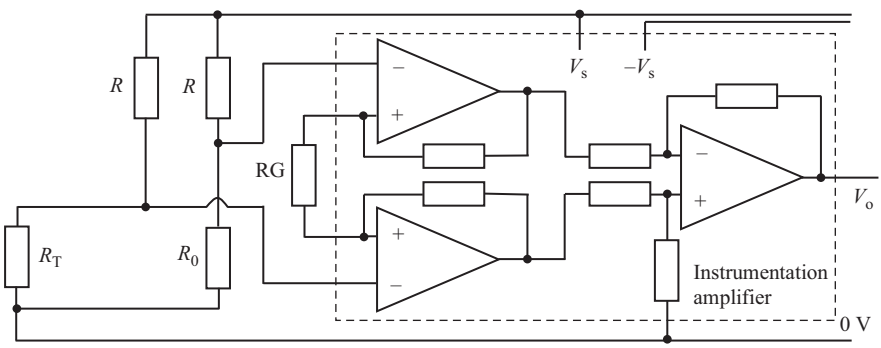


*Figure 5.38 Instrumentation amplifier*

Furthermore, we often would like to turn the differential voltage into a voltage signal referenced to the common ground with the rest to the circuit. This can be achieved by an instrumentation amplifier, as shown in Figure 5.38, and an RTD temperature transducer. The entire circuit is usually made in a single chip and value $R_G$ can be tuned externally to adjust the overall gain of amplification.

More generally, great care must be taken with regard to the cabling and termination of transducers and equipment to reduce noise problems. Cables should be of high quality and routed through unexposed areas wherever possible, so as to avoid the possibility of accidental damage. If many channels coexist in the same transmission corridor, care must be taken to avoid common impedance coupling between channels by segregating power from signal cables and ensuring that cables cross at right angles where EMC isolation is important. In most cases, twin-screened twisted pairs should be used to couple a transducer to the primary data acquisition unit to avoid induction from low-frequency fields <500 Hz. Screened co-axial cables are suitable to screen from high frequency fields >100 kHz. Optical fibre cabling is now robust and therefore a frequently used alternative, particularly when high noise immunity is essential. These issues are particularly important when CM electrical machines supplied from harmonic rich converters. Communications between the primary data acquisition unit and the processing system should also be established via a high-integrity low-noise link to avoid any chance of data corruption, or interruption.

## 5.14 Data acquisition

The precise nature of the data acquisition techniques used is usually determined by the subsequent algebraic manipulations that will be performed on the data sets produced by the transduction process. It is not really possible, therefore, to separate these two tasks fully, in most cases. What is of paramount importance, however, irrespective of the complexity of the monitoring system, is the fidelity of the information received by the processing unit. Transmitted or recorded data must be sufficiently noise-free to comply with the demands of the monitoring system, and must be wholly consistent. If this is not the case then the whole data set, perhaps spanning several months, may be effectively corrupted and therefore useless. In complex systems handling many inputs, either continuously or on a sampled basis, it is usual to have the processing system remote from the plant. In such cases some degree of local data conversion may be advisable. For example, the signals taken from a group of machines in adjacent locations may be routed to a nearby collection point that digitises the incoming signals and identifies them for onward transmission to the central system. In noisy environments it may even be desirable to digitise signals at the measurement point, and then forward them to a gathering point.

Figure 5.39 illustrates a preferred structure for a fully automatic system. The basic data acquisition system shown above is broken down into three, concatenated functions: multiplexing, sampling and holding, and analogue-to-digital conversion (ADC). An analogue multiplexer directs different signal channels for downstream processing and allows the channel identity to be passed through. The use of a multiplexer is essential if a large number of channels are to be monitored, and can be appropriate even for small numbers of channels because it allows the use of a single high quality ADC, rather than recourse to many lower grade devices. Commercial multiplexers can now accommodate many channels. An ADC turns an

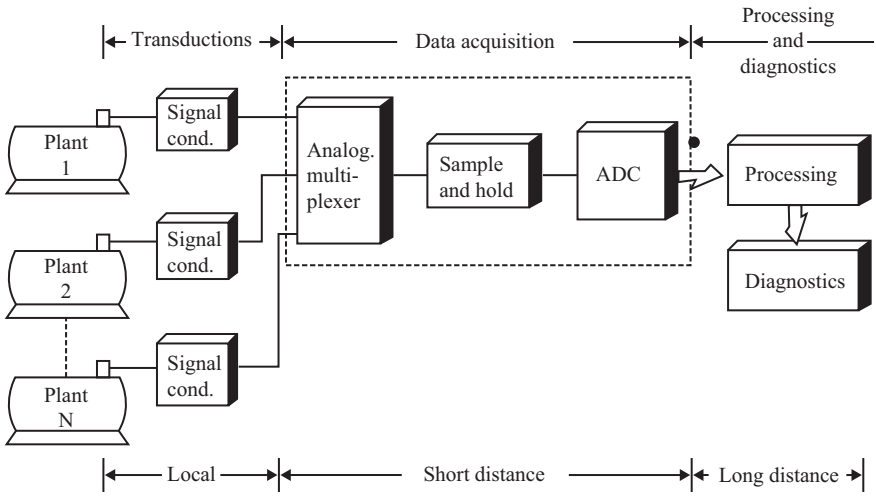


*Figure 5.39 General arrangement of data acquisition*

*Figure 5.40 A commercial data acquisition device to interface to a PC. Source: Adept*

analogue voltage signal into a digital number that can be recognised by the computer according to a defined comparison scheme or scaling factor. During conversion time, the input analogue signal is sampled and the sample is held constant. Resolution of the ADC, which affects the sensitivity of the CM system, depends on the number of bits. Since CM aims to capture weak signals at early stages of impending faults, high sensitivity is desirable. A 12-bit ADC has a resolution of 1 in 4 096 and typically completes conversion in less than 0.01 μs. The switching rate of the multiplexer can therefore be in the range of 10 MHz, adequately high to avoid any significant time lag between the multiplexed channels.

General purpose data acquisition units, designed in line with the above generic structure, are now commercially available and have naturally been used for CM purposes. For example, Figure 5.40 shows a 16 channel, 32 bit acquisition board that can interface with a standard PC by USB and operate in a specific software

environment. This is a suitable choice provided that the use of a dedicated PC can be arranged. Other options, such as LabVIEW, are also available, which normally provide output channels to implement some simple control actions.

In data acquisition, it is important to determine how often the signal is sampled and how many samples are kept for further processing. This is an area where mistakes can be easily made and we have provided some guidelines in this chapter to avoid them. Here, we just stress that the Shannon sampling theorem must be observed. The theorem states that the sampled data can be used to faithfully reproduce a time-varying signal provided that the sampling rate is at least twice the highest frequency present in the signal. This minimum sampling rate is called Nyquist frequency. Given a sampling rate, the total number of samples kept for signal processing implies the duration during that the signal is sampled. This duration determines the frequency resolution that a spectrum analysis performed on the data can give. For example, if a signal is sampled for 1 second, the frequency resolution is 1 Hz.

## 5.15 Conclusions

This chapter has described the signal-processing methods now available for computer monitoring electrical machines and the wide range of instrumentation and processing techniques used to monitor machines.

Modern techniques and methods have been shown and the next chapters show how the signals from these have been applied to provide CM information.

The following chapters will therefore describe the major temperature, chemical, mechanical and electrical techniques available for monitoring.

*This page intentionally left blank*

*Chapter 6*

# Online temperature monitoring

## 6.1 Introduction

As has been described in Chapter 2, the limits to the rating of electrical machines are generally set by the maximum permissible temperature that the insulation can withstand. Indeed, the performance testing of machines, before they leave a manufacturer's works, is dominated by the measurement of winding or embedded temperatures and the need to achieve temperature rises within the appropriate standards. The measurement of temperature therefore has an important role in the monitoring of electrical machines and the following describes how this can be done using the measurement techniques described in Chapter 4.

There are three basic approaches to temperature monitoring:

- to measure the local temperatures at points in the machine using embedded temperature detectors (ETDs),
- to use a thermal image, fed with suitable variables, to monitor the temperature of what is perceived to be the hottest spot in the machine,
- to measure the distributed temperatures in the machine or the bulk temperatures of coolant fluids.

These approaches demonstrate the fundamental difficulty of thermal monitoring, which is resolving the conflict between point temperature measurements that are easy to make, but give only local information, and bulk temperature measurements that are more difficult and run the risk of overlooking local hot-spots.

The following three sections show how these approaches can be applied practically.

## 6.2 Local temperature measurement

This can be done using thermocouples, RTD or ETDs whose characteristics are described in Chapter 4. To monitor the active part of the machine, they are usually embedded in the stator winding, and in the stator core. They can also be located in the bearings, to detect hot running. The choice of location requires careful consideration during the specification stage of the machine. For example, temperature detectors embedded in the stator winding need to be located close to its hottest part, which may be in the slot portion or end winding portion, depending on the

thermal design of the machine. Or for a machine with an asymmetrical cooling arrangement they should be located at the hottest end of the machine. Some guidance as to where ETDs should be located is given in Chalmers (1988) and this is summarised in Figure 6.1. It should be noted that when ETDs are fitted in

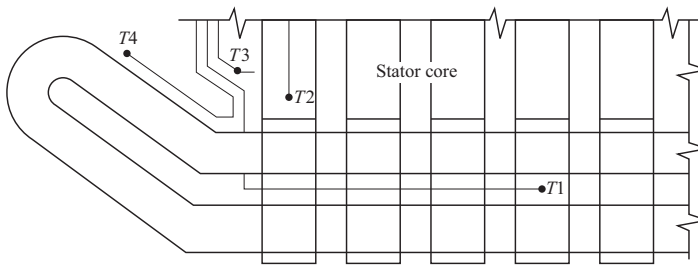


(a) Embedded between conductors in the slot portion (*T*1)
Embedded in core pack laminations (*T*2)
Mounted on potentially hot components such as pressure plates (*T*3)
Embedded on conductors in the end winding portion (*T*4)

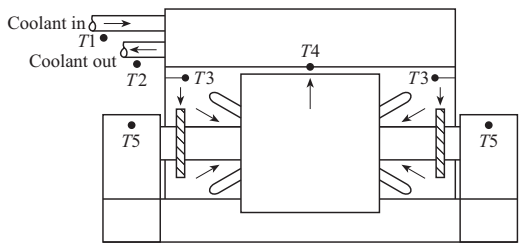


(b) Water or air inlet to the heat exchanger (*T*1)
Water or air outlet from the heat exchanger (*T*2)
Re-entry air to the machine from the heat exchanger (*T*3)
Exhaust air from the machine to the heat exchanger (*T*4)
Bearing temperatures (*T*5)

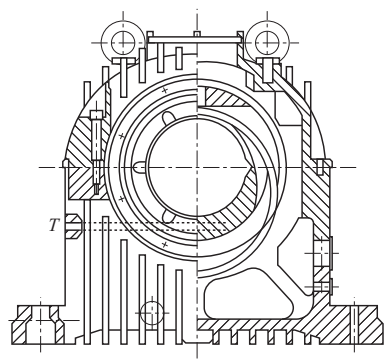


(c) Bearing temperature (*T*)

*Figure 6.1 Location of temperature detectors in electrical machines*

bearings, precautions must be taken to ensure that the bearing insulation is not breached.

The weakness of these methods is that thermocouples and RTDs are metallic devices and cannot be located on the hottest active component, the winding copper, because they need electrical isolation. On a winding, the devices have to be embedded in the insulation at some distance from the copper itself, see Figure 6.2(a). As a result, the measured temperature will not necessarily be that of the winding itself but an image of it, as shown in Figure 6.2(b). The heat flow per

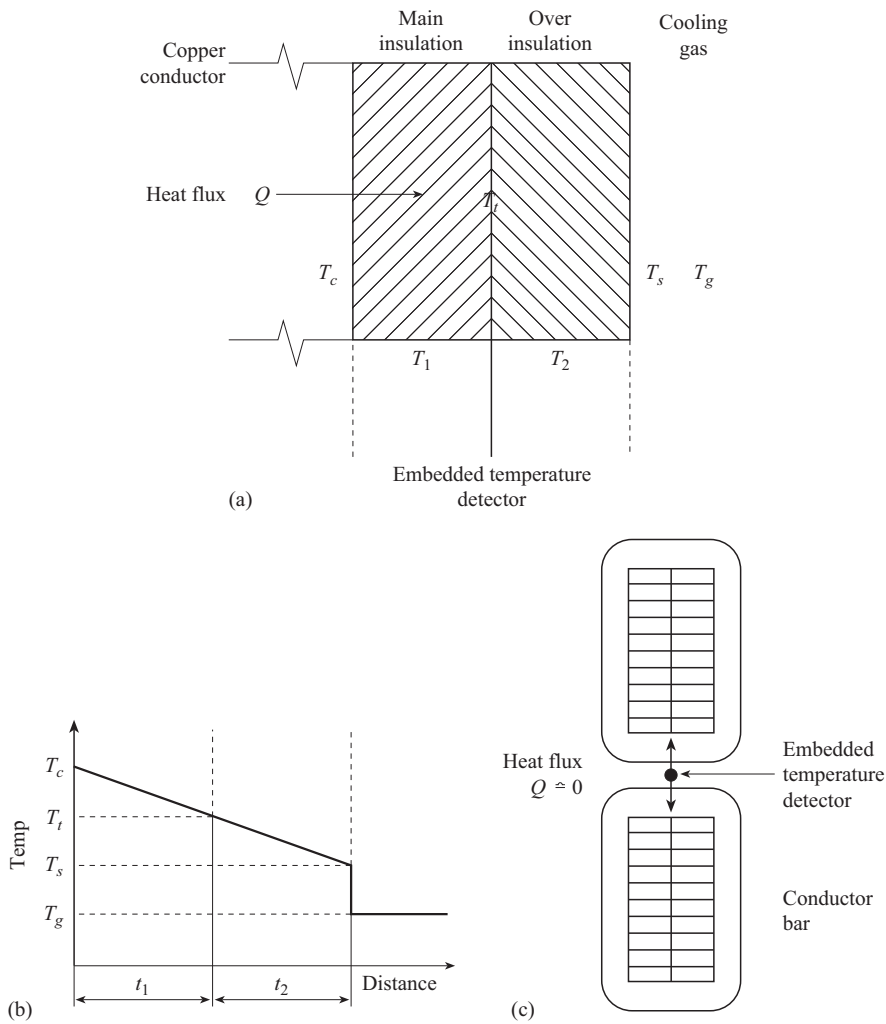


*Figure 6.2 Effect of embedding a temperature detector away from an active part: (a) asymmetrically ETD, (b) temperature detection from (a), and (c) symmetrically ETD*

unit area, $Q$, through the insulation system can be described by simple conduction equations as follows:

$$Q = h\left(T_s - T_g\right) = \frac{k}{t_2}(T_s - T_t) = \frac{k}{t_1}(T_c - T_t) \tag{6.1}$$

where

- $t$ is the insulation thickness,
- $T$ is the temperature,
- $k$ is the heat transfer coefficient through an insulating material,
- $h$ is the heat transfer coefficient from the insulation surface.

Eliminating $T_s$ between the first two expressions gives:

$$T_t = T_g + Q\left(\frac{t_2}{k} + \frac{1}{h}\right) \tag{6.2}$$

Therefore, we have:

$$T_t = T_g + (T_c - T_t)\left\{\left(t_2 + \frac{k}{h}\right)\Big/ t_1\right\} \tag{6.3}$$

$$T_t = \frac{T_g + T_c\left\{\left(t_2 + \frac{k}{h}\right)/t_1\right\}}{1 + \left\{\left(t_2 + \frac{k}{h}\right)/t_1\right\}} \tag{6.4}$$

So:

$$T_t \approx T_c \quad \text{if } T_g \ll T_c \text{ and } \left(t_2 + \frac{k}{h}\right)\Big/ t_1 \gg 1, \text{ i.e. if } t_2 + \frac{k}{h} \gg t_1 \tag{6.5}$$

So, the measured temperature $T_t$ will approach the temperature of the hottest active component $T_c$ if the thickness of insulation, $t_2$, applied over the ETD is sufficient compared to the main insulation. This problem does not occur for devices embedded in the slot portion, between two conductors, as shown in Figure 6.2(c), where there is a low heat flux between the active copper parts. But it is an important difficulty when monitoring end winding temperatures in that case the thickness of over-taped insulation, $t_2$, needs to be substantial if sensible readings are to be obtained.

It would be very desirable to develop a temperature monitoring device that can be affixed to a high voltage winding and give electrical isolation. Such a device was developed in the 1980s for power transformers, comprising a small phial of liquid that had a high vapour pressure that varied widely with temperature. The phial was affixed to the high voltage winding whose temperature was required. The pressure in the phial was then monitored through a non-conducting silicone rubber tube and the temperature was derived electronically from the pressure measurement. The device was applied, on a trial basis, to operational transformers where it performed satisfactorily.

More widespread modern methods of measuring temperature on high-voltage components have also been developed using fibre-optic techniques, as described in Chapter 4 and are shown in Figure 6.3. A particular design using the dependence of the polarisation of light on the temperature of a material is described by Rogers (1986).

Light from a laser is transmitted to the device and is passed through a polarising prism before being launched into a fibre maintained at the temperature to be measured. This material introduces a rotation of the light beam that is dependent on temperature. The beam is reflected back through the fibre and polariser and is relaunched with a light amplitude proportional to the polarisation that has taken place in the fibre. By arranging two passes through the fibre, the polarisation is rendered insensitive to electrical or magnetic field effects.

A modern approach to temperature monitoring, based on that proposed by Rogers (1986), Rogers (1999) and Kher *et al.* (2004), has been developed for electrical machines by Mohammed *et al.* (2016) using FBG sensors, initially embedded in stator winding motorettes to test the approach. The technique has produced very promising results, Figure 6.4 shows a test coil design and Figure 6.5 shows the fitting arrangement, giving operators the opportunity to have a full thermal map of a stator winding in operation. The approach has been applied to a working TEFC induction motor with an enamelled round wire stator winding, see Mohammed *et al.* (2018).

The temperature measurements described in this work have all been on machine stationary parts so far and on many machines the thermal design is stator-critical, so the hottest spot will be located there. But many machines are rotor-critical, particularly larger induction motors, because under stall conditions the rotor losses are very large, and the temperatures can rise rapidly to values that could damage the rotor integrity. On such machines there may well be no apparent deterioration after one or two stalls, but should this occur repeatedly there will be a weakening of rotor bars and/or end rings that may result in premature mechanical failure. In the past, there have been various crude methods of measuring rotor temperatures for experimental purposes, using heat-sensitive papers or paints, or thermocouples connected through slip rings. Until recently, however, there has not

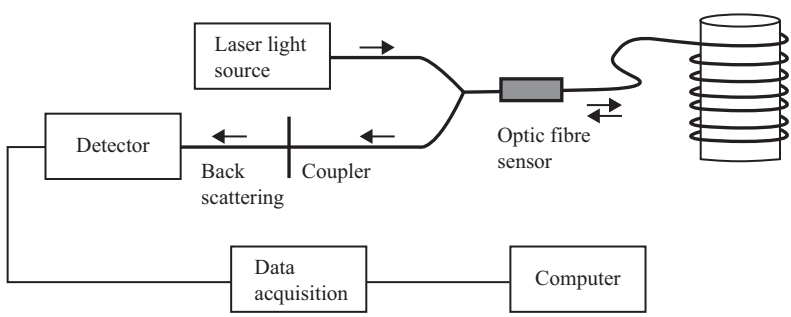


*Figure 6.3 Principle of fibre-optic temperature sensing*

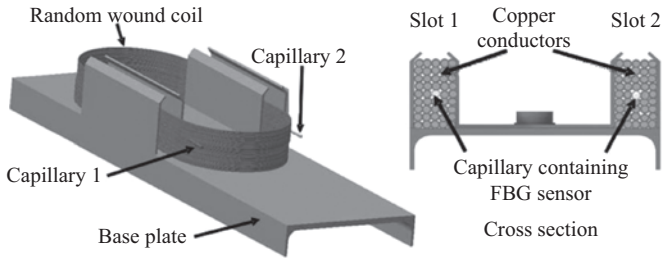


*Figure 6.4 Test coil design, manufacture and the IEEE motorette rig, Mohammed et al. (2018)*

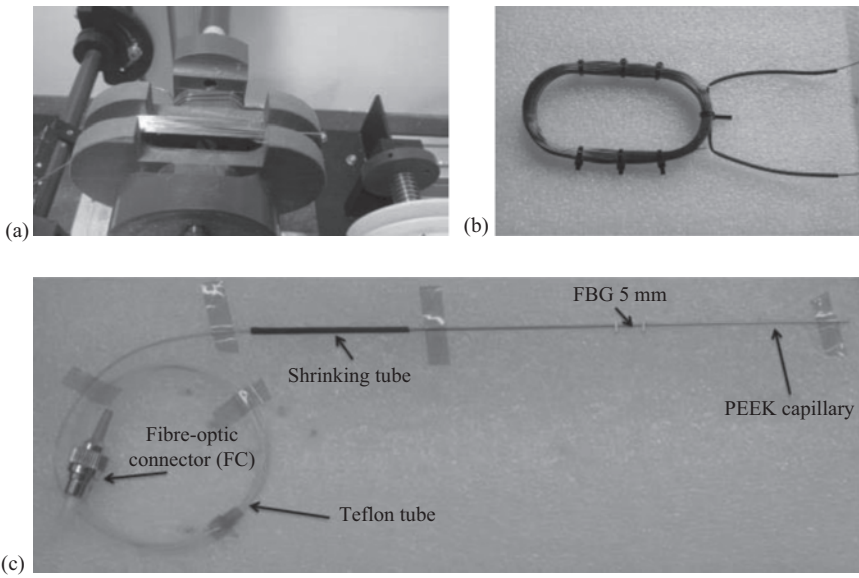


*Figure 6.5 Arrangement of FBG winding temperature sensor, Mohammed et al. (2018): (a) motorette rig with an FBG embedded test coil, (b) winding bobbin and (c) test random wound coil*

been a method sufficiently reliable to use for monitoring purposes. Siyambalapitiya *et al.* (1988) described a device for monitoring eight thermocouples, multiplexing the signal on the rotor, then optically coupling to the stator and decoding in a DSP. These techniques have now been adopted widely, using modern blue-tooth technology, particularly for prototype experimental work on induction motors, see Hou *et al.* (2012), but such methods have not yet been widely deployed for regular CM, but Hou *et al.* (2012) and Kumar *et al.* (2018) give guidance on the latest methods for this type of work.

## 6.3 Hot-spot measurement and thermal images

Local temperature measurements give the machine operator considerable confidence that he/she knows the operating temperature of key points in the machine, but there is always the nagging suspicion that temperature detectors may not be located at the hottest point. This problem has long been recognised in power transformers where it is extremely difficult to obtain even embedded winding temperatures, because of the need for EHV isolation and the great thickness of electrical insulation necessary, so thermal images of the hot spot temperature are used. The thermal image consists of a dial-type thermometer with its bulb immersed in the region where the transformer oil is hottest. A small heating coil, connected to the secondary of a current-transformer, serves to circulate around the bulb a current proportional to the load current and is such that it increases the bulb temperature by an amount equal to the greatest winding-to-coil temperature gradient. The indicator therefore registers an approximation to the hot-spot temperature.

The thermal image technique has not received wide application on rotating electrical machines, although it deserves to. The availability of a thermal image hot-spot temperature of machine could be used for motor monitoring and protection purposes, as proposed by Zocholl (1990), Milanfar *et al.* (1996) and Mellor *et al.* (1991), who proposed a technique for small, totally enclosed, forced-cooled, induction motors where a thermal model of the machine is configured in a DSP that is fed with signals proportional to the ambient air temperature and the stator winding current. The model can calculate the predicted temperatures at a variety of key points in the machine. Stator core, stator winding slot or stator end-winding representation must be programmed solely using the design information for the machine. The instrument is designed to produce an analogue voltage that is proportional to several temperatures at the hottest points.

Mellor *et al.* (1991) have used the device on two totally enclosed fan-cooled (TEFC) machines and compared the predictions of the thermal image with. The measured temperatures in the stator end-winding were found to be the hottest point in this design of the machine. Figure 6.6 shows the comparison of results for those two machines when they have been put through very severe duty cycles and it can be seen that the comparison between modelled and measured results is extremely good. The device has been designed to be part of the thermal protection of a motor but it could equally well be used for monitoring a machine for operational purposes, particularly, for example, on a crucial machine located in an inaccessible position, where hot-spot measurements may be difficult to obtain.

## 6.4 Bulk measurement

In the electrically active part of the machine, even when hot-spot locations are known or hot-spot temperatures can be surmised from a thermal image, there is still a desire to obtain a bulk indication of the thermal state of the machines. This can be

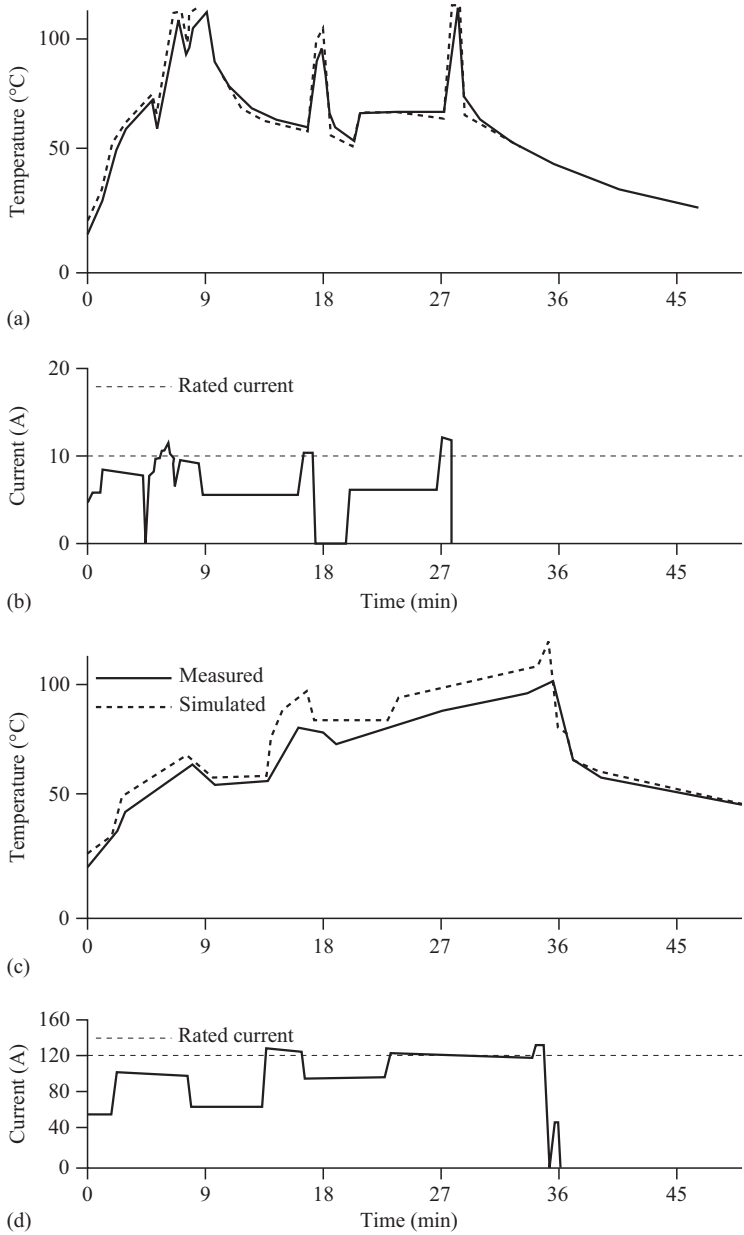


*Figure 6.6 Comparison between measurements and the predictions of a thermal image of an electrical machine: (a) comparison for 5.5 kW induction motor, (b) duty cycle for (a), (c) comparison for 7.5 kW induction motor and (d) duty cycle for (c). Taken from Mellor et al. (1991)*

found from the measurement of the internal and external coolant temperature rises, obtained from thermocouples located, for example, as shown in Figure 6.1. This is done on most larger machines, but it is normal for coolant temperatures to be displayed and rare for the point values to be subtracted to give the temperature rise directly. An increase in temperature rise from such a device would clearly show when a machine is being overloaded or if the coolant circuits are not performing as they should. But the method is insensitive to localised over-heating in the electrically active parts of the machines. Therefore, considerable effort has been devoted, as an alternative to the thermal image, to devising methods whereby single indications of high temperature can be obtained from a device that is embedded in the bulk of the machine.

Lengths of signal cable using heat-sensitive semi-conducting material as the insulation have been proposed but most effort has been devoted to the use of optical fibres. Brandt *et al.* (1982) have described various methods, including simple point measurements on high-voltage components, using the optical fibre for isolation purposes. But they have also described how, using the temperature sensitive properties of fibre optics, a continuously sensitive fibre could be embedded in the machine, adjacent to the high voltage copper, to detect localised overheating anywhere in the winding and yet provide a single indication. The method proposed would utilise the black body radiation in the optic 1 fibre, alongside the hot spot, being transmitted back to the detector and being used to determine the hottest point along the fibre's length. Such a device would therefore need to be embedded in the machine during manufacture and as yet a practicable instrumentation scheme has not been devised.

An interesting approach to monitoring temperature in a variable-speed induction motor by Chen *et al.* (1994) is described briefly in a later chapter.

## 6.5 Conclusions

This chapter shows that temperature measurement yields valuable bulk indications of the condition of an electrical machine using simple sensors and narrow bandwidth (<1 Hz), low data rate signals and, because temperature limits the rating of a machine, overtemperature is a valuable CM signal. Temperature detection has repeatedly been shown to be an effective global monitoring technique for electrical machines, but has been neglected as a monitoring method.

Temperature measurement is usually done in traditional and rather antiquated ways, there are some simple changes that could be made in existing practice to make more sense of temperature measurement. These changes are partly in the area of sensing but also in the area of signal processing and in particular the importance of presenting temperature rise to the operator, rather than absolute temperature. There are also advances in the application of modern sensors becoming available, which will allow the temperature measurements to be made closer to the active parts of a machine, and these should be exploited.

An important conclusion of this work is that the availability of new FBG temperature sensors gives the potential for much greater distributed electrical

machine temperature measurements. This will be more essential if power/weight ratios are to rise to 7 kW/kg by 2025 and 9 kW/kg by 2035, as proposed by the Electric Machines Roadmap (2018). Such rating improvements may well depend in future of better CM and these authors propose that this could be done by a closer integration between the temperature monitoring proposed by Mohammed *et al.* (2018) and the thermal modelling proposed by Mellor *et al.* (1991). Perhaps this could be achieved in the future using the AI methods proposed in Chapter 14.

*Chapter 7*

# Online chemical monitoring

## 7.1 Introduction

The insulating materials used in electrical machines are complex organic materials, which, when they are degraded by heat or electrical action, produce a very large number of chemical products in the gas, liquid and solid states. Lubrication oils also carry not only the products of their own degradation but also those from the wear of the bearings and seals they cool and lubricate.

Techniques to provide early warning of the deterioration of electrical machines should include the measurement of these complex degradation products where they can be accessed in the machine.

## 7.2 Insulation degradation

What are the mechanisms by which insulation can be degraded? Well, the table in Appendix A shows how important excessive temperature and therefore thermal degradation is as a failure mode and this is largely determined by the thermal performance of the insulation. The insulation consists in the main of organic polymers, either natural forms such as bitumen, or more commonly nowadays, synthetic epoxy resins, and Chapter 2, Section 2.7.2 has described the majority of the failure modes associated with insulation degradation. The thermal degradation of these materials is a complex process. However, as the temperature of the insulation rises above its maximum permitted operating value, approximately 160 °C, volatiles used as solvents in the insulation manufacture start to be driven off as gases. Then the heavier compounds making up the resin may reach their boiling point. The gases so produced are generally the heavier hydrocarbons such as ethylene. As the temperature rises further, above 180 °C, chemical decomposition of the resin components starts. A supersaturated vapour of the heavier hydrocarbon decomposition products then forms in the cooling gas close to the high temperature area of insulation. Rapid condensation of that vapour occurs as the cooling gas leaves the hot area producing condensation nuclei that continue to grow in size by further condensation until they reach a stable droplet size. These droplets, usually called particles, are of submicron size and form what would commonly be called smoke. The precise materials given off depend primarily on the insulation material being heated but also on the cooling gas of the machine. The binder material of the

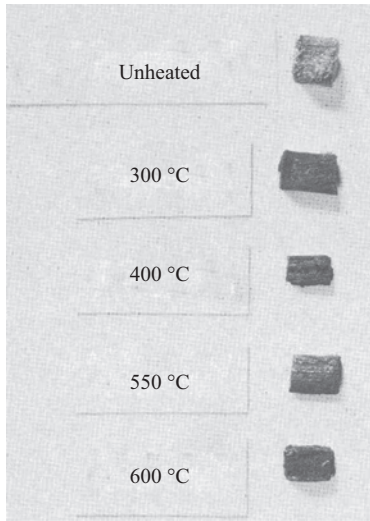


*Figure 7.1 Heating of phenolic impregnated wood insulating material*

insulation, whether it be wood, paper, mica or glass fibre, can usually withstand much higher temperatures, but eventually as 400 °C is reached, they start to degrade and char, releasing gases such as carbon monoxide and carbon dioxide, drawing oxygen from the cooling gas, if it is air, or from the degradation of the complex hydrocarbon in the resin. Figure 7.1 shows a piece of phenol-impregnated wood insulation from a turbo-generator, progressively raised to higher temperatures in hydrogen. Up to 300 °C, one can see the effects of the resin material being decomposed and driven off, but the wood binder still retained its strength. Above 400 °C, the binder has degraded by charring and no longer has significant mechanical strength.

Pyrolysing activity therefore gives rise to a wide range of liquid droplets, solid particulates and gases, which together make up the smoke being driven off from the insulation.

Electrical discharge activity, within or adjacent to the insulation system, can also degrade the insulation releasing particulate and gaseous chemical degradation products. The very high temperature associated with sparking breaks down the hydrocarbon compounds in the insulation to form acetylene. It also breaks down the oxygen in the cooling gas, if it is air, to give ozone. Furthermore, continuous discharge activity gradually carbonises and erodes the insulating material to produce, on a smaller scale, the degradation products that result from more widespread overheating.

## 7.3 Factors that affect detection

Before considering the different methods of detecting chemicals within an electrical machine it is necessary to understand the factors that affect the detectability.

Consider Figure 7.2(a), which shows the machine within its enclosure, the rate of change of concentration of a detectable substance can be determined by the following equation:

$$\begin{aligned}&\{\text{Rate of change of concentration of a detectable}\\&\quad\text{substance in the cooling circuit of a machine}\} =\\&\{\text{Specific production rate of detectable}\\&\quad\text{substance} - \text{leakage rate from the machine}\}/\{\text{machine volume}\}\end{aligned} \tag{7.1}$$

$$\frac{\mathrm{d}C}{\mathrm{d}t} = \left\{\frac{\dot{\nu} - \frac{VC}{\tau_r}}{V}\right\}$$

where

- $V =$ the machine volume
- $C =$ the volumetric concentration of the substance concerned
- $\tau_r =$ a leakage factor
- $\dot{\nu} =$ the volumetric rate of production of the detectable substance.

When leakage is low, $\tau_r$ is effectively a residence time constant for the substance in the machine enclosure. The rate of production, $\nu$, is related to the volume of material being overheated, and its chemical composition. This variable is in fact a function of time $\nu(t)$. So, the equation could be rewritten as:

$$\frac{\mathrm{d}C}{\mathrm{d}t} + \frac{C}{\tau_r} = \frac{\dot{\nu}(t)}{V} \tag{7.2}$$

$$\left(D + \frac{1}{\tau_r}\right)C = \frac{\dot{\nu}(t)}{V} \tag{7.3}$$

The complementary function for this equation is:

$$C = A\exp\left(-\frac{t}{\tau_r}\right) \tag{7.4}$$

The particular integral is:

$$C = \frac{(\dot{\nu} - \dot{\nu}_b)\tau_r}{V} \tag{7.5}$$

where

$$\dot{\nu}(t) = \dot{\nu} + \dot{\nu}_b$$

- $\dot{\nu} =$ a step increase in the volumetric rate of production,
- $\dot{\nu}_b =$ the background rate of production of the substance.

When $t = 0$, $C = C_b$, the background concentration, then:

$$C_b = \frac{\dot{\nu}_b\tau_r}{V} \quad \text{and} \quad A = \frac{\dot{\nu}\tau_r}{V} \tag{7.6}$$

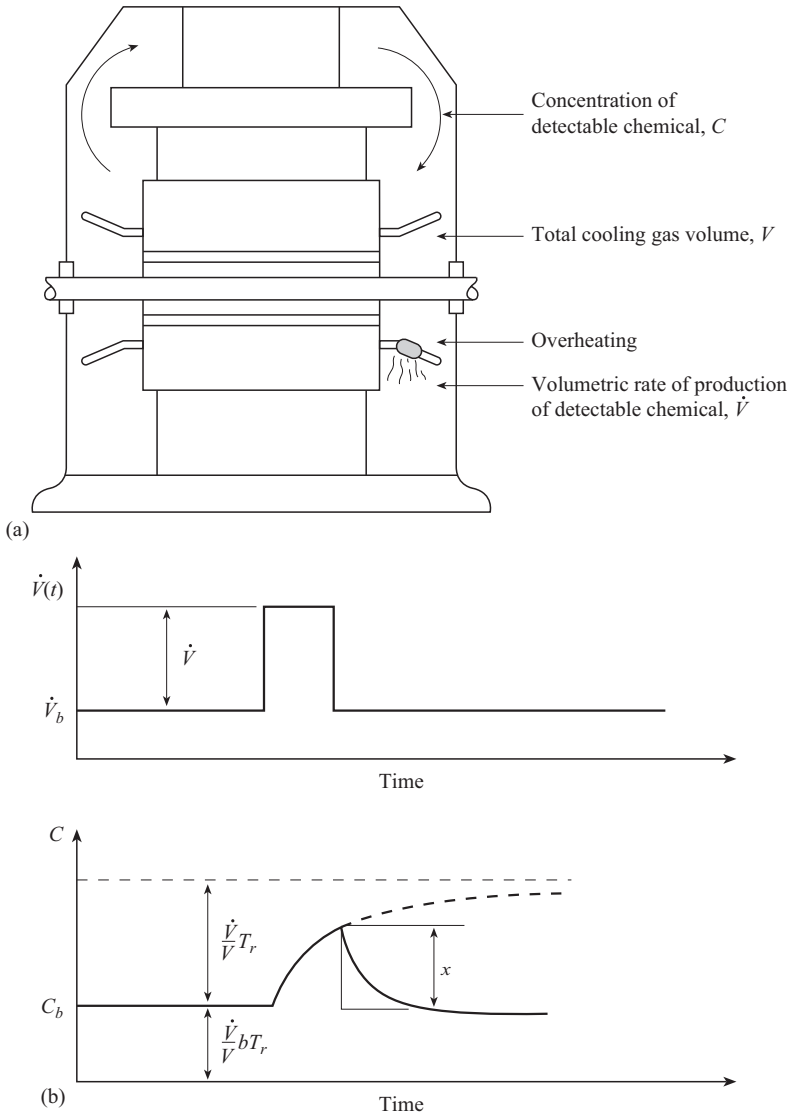


*Figure 7.2 The concentration of detectable chemicals in coolant gas of an electrical machine: (a) cross-section of the machine and (b) response of the concentration of detectable chemical to a step change in the rate of production of that chemical*

$$\therefore C = \frac{\dot{v}\tau_r}{V}\left(1 - \exp\left(\frac{t}{\tau_r}\right)\right) + \frac{\dot{v}_b\tau_r}{V} \tag{7.7}$$

From (7.7), it is possible to determine how the detectable concentration depends upon the design of the machine, the nature of the overheating it is suffering from,

and the concentration of material involved. Figure 7.2(b) will help to explain this. A machine with a tightly sealed and pressurised cooling system, such as a turbo-generator, will have a long residence time, $\tau_r$, of many hours, the background concentration level of the detectable substance, $C_b$, will be high. On the other hand, the concentration level, which can be reached after an extended period of overheating, will also be correspondingly high. But if the length of the overheating incident, $\tau_o$, is short compared to the residence time, say a few minutes, then the concentration will not build up to a significant level compared to the background. A machine with an open cooling circuit will have a short residence time, $\tau_r$, of perhaps merely a few seconds. So, the background concentration will be low and there will need to be a large volumetric production, $V$, from an overheating incident to produce a large increase in concentration $C$. But the concentration level will respond rapidly to any overheating.

Detectability of overheating depends upon:

(i) A large signal-to-noise ratio. That is, the magnitude of the indication ($X$ in Figure 7.2(b)), must be large compared to the background, $C_b$,
(ii) A long duration of indication.

The larger the signal-to-noise ratio of the indication and the longer its duration, the easier it will be to detect. These two conditions can be considered mathematically:

For a large signal-to-noise ratio, (i) above, $\dot{\nu} \gg \dot{\nu}_b$ and $X \gg \frac{\dot{\nu}_b \tau_r}{V}$
Now

$$X = \frac{\dot{\nu}}{V}\tau_r\left(1 - \exp\left(\frac{\tau_0}{\tau_r}\right)\right)$$

where $\tau_0$ is the duration of the overheating incident
So

$$\left(1 - \exp\left(-\frac{\tau_0}{\tau_r}\right)\right) \gg \frac{\dot{\nu}_b}{\dot{\nu}}$$

$$\therefore \left(1 - \frac{\dot{\nu}_b}{\dot{\nu}}\right) \gg \exp\left(-\frac{\tau_0}{\tau_r}\right)$$

That is

$\dot{\nu}$ must be $\gg \dot{\nu}_b$ and $\tau_0 > \tau_r$

Or

$\dot{\nu}$ must be $> \dot{\nu}_b$ and $\tau_0 \gg \tau_r$

For a long duration of indication, (ii) above, $\tau_0 \gg \tau_r$
The time constant, $\tau_0$, depends on:

- the type of fault causing the overheating,
- the extent of the fault,

- the nature of the material being overheated,
- the nature of the substance being released and detected.

So, for example, a small intermittent shorted turn in the rotor winding of a large turbo-generator will produce heating for only a few minutes and the increase in concentration of detectable substances in that time will be small because of the long residence time, $\tau_r$, in such a machine. On the other hand, overheating in a terminal connection or due to excessive stray losses will operate for many hours and produce a substantial indication.

The effect of the substance being detected can be considered as follows. An insulation material that is heated at a steady but relatively low temperature of say 190 °C will produce a considerable amount of hydrocarbon gases over a long period of time, up to 2–3 h, until those gases are all driven off. Particulates will also be formed but these will have a short lifetime in the enclosure because of recombination and condensation, say 10–15 min. If the insulation is raised to higher temperatures the production of copious quantities of gases will take place over a much shorter period of time and will stop before charring commences. If the machine is air-cooled, large amounts of carbon monoxide and carbon dioxide will also be produced, if overheating takes place over a long period of time, because production of those gases continues even during charring.

All these factors need to be taken into consideration when deciding which of the following techniques should be applied to a particular machine to detect a certain type of fault.

## 7.4 Insulation degradation detection

It can be concluded from Sections 7.1 to 7.3 that insulation degradation can be monitored chemically by detecting the presence of particulate matter in the coolant gas or by detecting simple gases, like carbon monoxide and ozone, or more complex hydrocarbon gases, like ethylene and acetylene. Let us consider these approaches in turn.

### *7.4.1 Particulate detection – core monitors*

Detecting the smoke given off from degrading insulation appears the simplest and most general of all techniques, since proprietary smoke detectors already exist using an ion chamber to detect the smoke particles. An example is shown in Figure 7.3. As the cooling gas of the machine enters the ion chamber it is ionised by a weak radioactive source. The gas then flows through an electrode system to which a polarising voltage is applied.

The free charges in the gas are collected on the electrode and flow through an external electrometer amplifier circuit, which produces an output voltage proportional to the ion current. When heavy smoke particles enter the chamber, they too are ionised and their greater mass implies a lower mobility compared to the gas molecules, so as they enter the electrode system the ion current reduces. Therefore

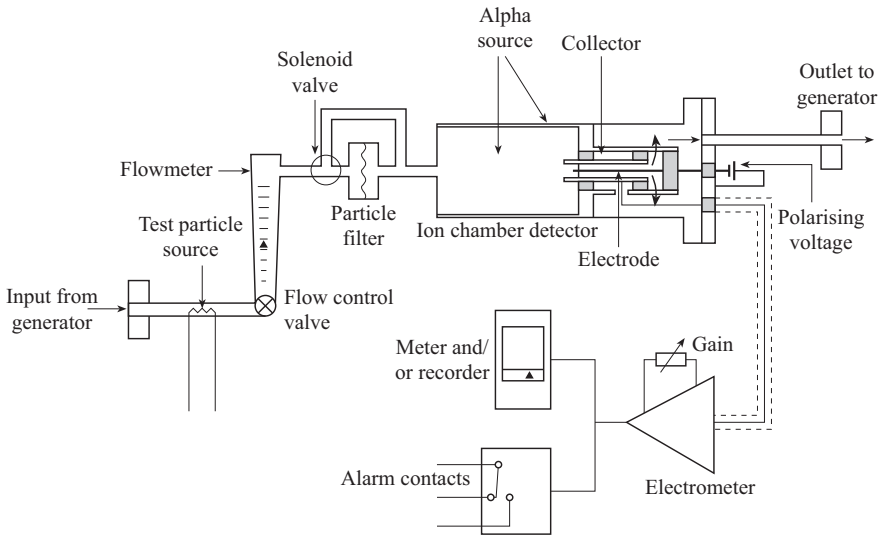


*Figure 7.3 Diagram of a basic core monitor. Taken from Carson et al. (1978)*

the smoke is detected by a reduction in the output voltage from the electrometer amplifier. Skala (1966) described an ion chamber specifically designed to detect the products of heated insulation and this was applied to a large turbo-generator by Carson *et al.* (1973).

The primary impetus for this work was the need to provide early warning of core faults referred to by Tavner *et al.* (1986) and Tavner *et al.* (2005), which the larger sizes of turbo-generators started to experience in the early 1970s. A core fault can involve substantial quantities of molten stator steel and, hitherto, the fault could only be detected when the melt burnt through the stator winding insulation and caused an earth fault. It was hoped that the core monitor could detect the degradation of the insulation between the steel laminations at an earlier stage in the fault. The lifetime of pyrolised particles in the closed hydrogen cooling circuit of a large generator is 15 to 30 min after which time the particulates are deposited onto the exposed surfaces of the machine. So, a single instance of insulation overheating should lead to a reduction of core monitor ion current for a period of time of this order. Figure 7.4 shows typical core monitor responses. When a core fault is occurring, the overheating continues over a longer period and it has been shown by Carson *et al.* (1973) that the core monitor does respond to this and other forms of insulation overheating. Core monitors are available from several manufacturers. The sensitivity of the device depends upon the ion chamber design but experimental figures for the monitor described in Carson *et al.* (1973) show that it will produce a response ranging from 85% to 95% of full-scale deflection when 100 $cm^2$ of lamination insulation is pyrolised, depending on the material. An area is quoted because the production of particulates is primarily a surface effect.

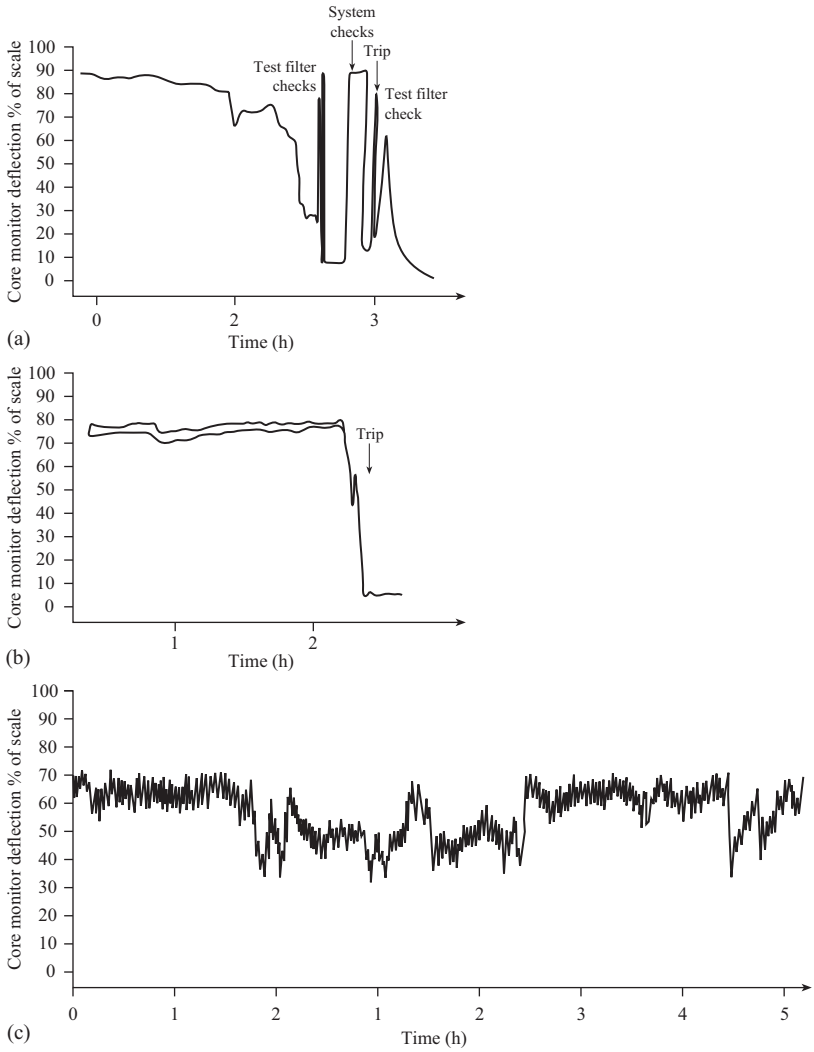


*Figure 7.4 Typical core monitor responses: (a) machine with overheating conductor bar, (b) machine with a core fault and (c) machine with no overheating but heavy oil contamination*

The device, however, does have some practical difficulties:

(i) Monitor output fluctuates with cooling gas pressure and temperature,
(ii) Monitor responds to oil mist that may be present in the circuit of any hydrogen-cooled machine due to faulty hydrogen seals, see Carson *et al.* (1978),
(iii) Monitor is non-specific; that is, it cannot distinguish between the materials being overheated.

Items (i) and (ii) affect the background signal from the monitor, which any signal due to damaging over-heating must exceed. Figure 7.4(c) shows a typical core monitor trace from a machine affected by oil mist. Item (iii) affects the attitude of a machine operator to an alarm from the core monitor, since there will be less confidence in the monitor if it is not known from that part of the machine the detection originated.

A more advanced monitor, described by Ryder *et al.* (1979), has been devised to overcome problems (i) and (ii) by using a differential technique. This monitor consists of two identical ion chambers in series in the gas flow line with an intermediate particulate filter between them. The monitor displays the difference between the ion currents in the two chambers and thereby eliminates fluctuations due to pressure and temperature.

The sensitivity of a core monitor to oil-mist can be reduced if the ion chamber is kept at an elevated temperature (Figure 7.5). It has been proposed that oil mist is only produced by overheating, so that its detection may be useful, and the use of heated ion chambers was not initially encouraged, however, current thinking is that heated ion chambers are essential for reliable detection. However, the amount of oil in a turbo-generator casing varies widely and can be particularly high. In this case it has been found that there can be frequent false core monitor alarms, so the use of a heated ion chamber gives a significant advantage. In order to completely vaporise an oil mist, it is necessary to raise the ion chamber temperature above 120 °C. The monitor described in Ryder *et al.* (1979) has heated ion chambers and the authors' experience, using these set to 120 °C, was that they gave an adequate protection against spurious oil mist indication. Using a heated ion chamber also means that

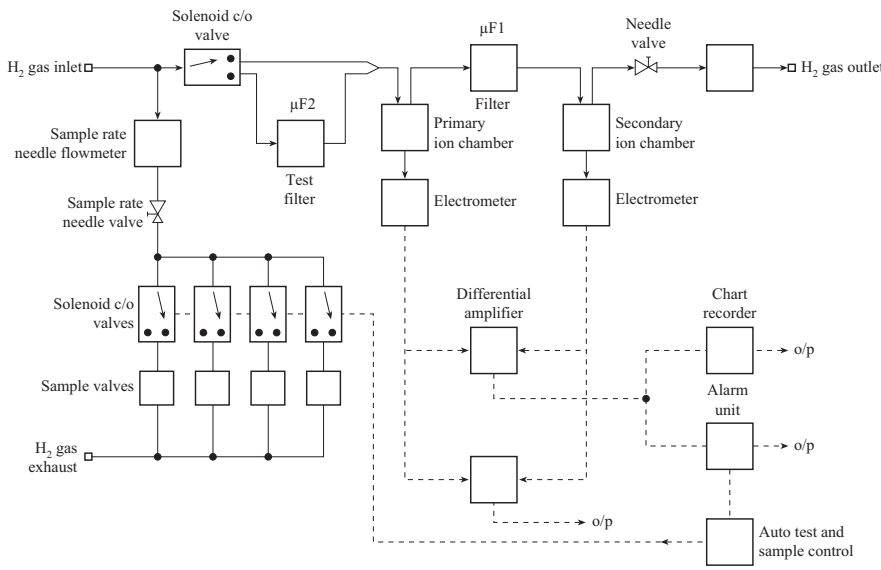


*Figure 7.5 Diagram of a differential core monitor with heated ion chambers*

some of the droplets produced by over-heating will be vaporised, or at least reduced in size, and this must result in a consequential loss of sensitivity. However, laboratory tests can quantify this loss of sensitivity, which at 120 °C has been shown to be 20%. Braun *et al.* have shown more recently by careful tests, the deleterious effects of using heated ion chambers on the core monitor sensitivity, see Ryder *et al.* (1979).

The use of core monitors in the early 1970s was advocated in the United States as a panacea for the early detection of major core and winding faults. Since then, however, although there have been some notable detection successes, such as those traces shown in Figure 7.4(a) and (b), there have also been false alarms, many caused by oil mist, see Figure 7.4(c).

The authors are not aware of the core monitor being used on air-cooled machines, or machines without a closed cooling circuit at all, although, apart from the short time constant of the indication from the monitor, there seems to be no reason why it should not be used for these applications. Experience has shown that the core monitor cannot be relied upon, on its own, to give incontrovertible evidence of an incipient fault. It is a valuable device that does detect pyrolised insulation, but its indications need to be considered alongside those of other monitoring devices. In particular, the core monitor needs to be complemented by an offline technique to chemically analyse the particulate material causing the detection, as described in the following section.

### *7.4.2 Particulate detection – chemical analysis*

Many authors have advocated taking a sample of the particulate material when a core monitor indicates an alarm. In order to collect a detectable amount of particulate matter within a short time, it is necessary to have a very large gas flow-rate through the filter. This is achieved by venting the pressurised casing of the machine through the filter to atmosphere. There is not such close agreement about the method of analysis, however. Carson *et al.* (1973) described a method whereby the pyrolysis products are collected upon a small charge of silica gel and are then released into a gas chromatograph upon the application of strong heat. This technique is applicable only when sampling is carried out immediately upon detection of local overheating. This is because it is designed especially to collect the particulates and heaviest pyrolysis products, which are present for only a limited time in the gas, sometimes for only a few minutes. There is also a problem with the gas chromatographic analysis of the pyrolysis products as these contain a very large number of different organic compounds and the resultant chromatogram is difficult to interpret, Figure 7.6 taken from Dear *et al.* (1977) gives an example. The most arduous test would be to distinguish the products of pyrolised insulation from the overheated oil that is generally present in any electrical machine. Further work on this from Dear *et al.* (1977) on the gas released from pyrolisation is shown in Figure 7.7. Some have used a mass spectrometer in association with the gas chromatograph on the particulate matter, to obtain precise identification of individual compounds. But the problem then arises of how to distinguish between the very

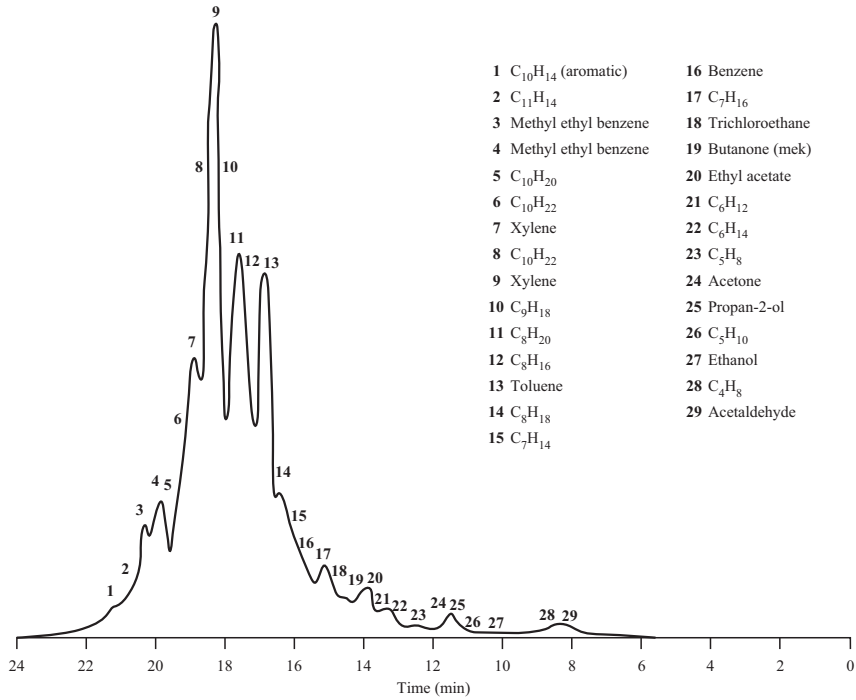


*Figure 7.6 Gas chromatogram of generator hydrogen impurities described from a Tenax GC pre-column. Taken from Dear et al. (1977)*

large numbers of organic compounds that are obtained and how to associate a pattern of compounds with the over-heating of a particular insulation material but as yet this has not proved practicable. We shall return to this in the analysis of the gas released in pyrolisation.

An alternative is to reduce the amount of chemical information obtained from the pyrolysis products by using detection techniques that are less sensitive or only sensitive to pyrolysis products. One technique makes use of the fact that many organic materials fluoresce when irradiated with ultraviolet light. The resultant UV spectrum is far less complex than the chromatogram produced by the same compounds going through a gas chromatograph. Figure 7.8 gives an example taken from Ryder *et al.* (1979), which should be compared with Figure 7.7. The filter is illuminated by a UV lamp, of a given wavelength, and the fluorescent light from the collected organic particles can be viewed with a UV spectrometer. It has been claimed that pyrolised insulation can be clearly distinguished from oil by this technique, to date a commercial version is not available.

It must be stressed that despite the various techniques described here, to the authors' knowledge there is, as yet, no definitive way to identify conclusively material collected on a core monitor filter. A way out of this difficulty was sought by tagging components in the machine with compounds, which when overheated

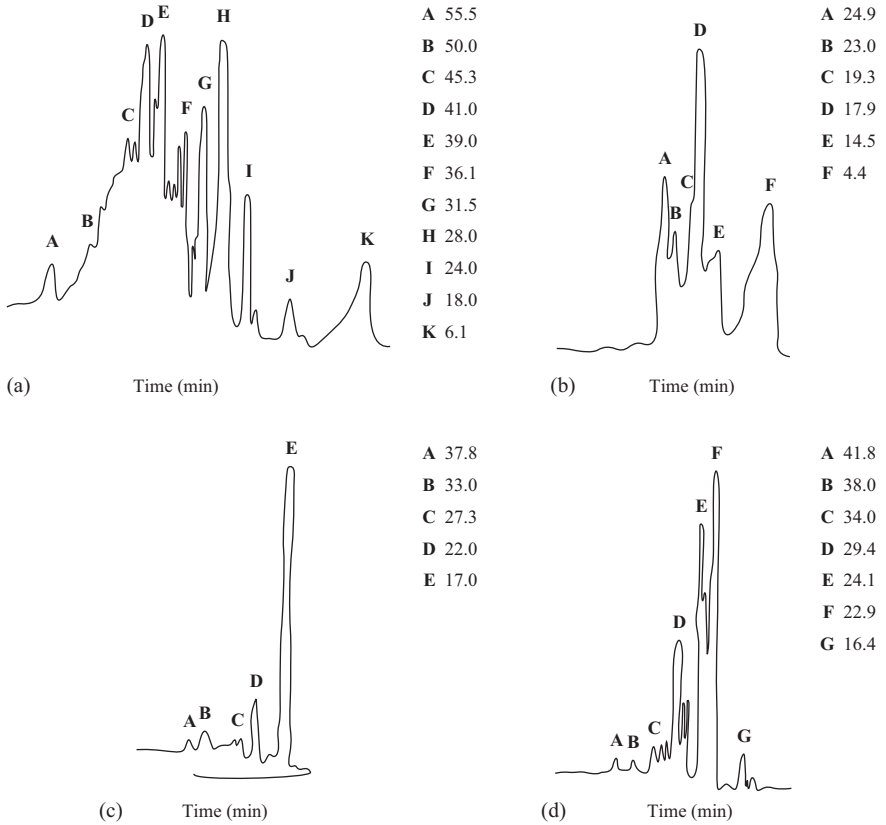


*Figure 7.7 Comparison of gas chromatograms taken from the pre-column samples from hydrogen-cooled generators with overheating of various insulation components: (a) main wall insulation, (b) epoxy rating, (c) alkyd enamel paint and (d) generator hydrogen coolant gas background. Taken from Ryder et al. (1979) © IEEE (1979)*

give off material with easily identifiable chemical compositions. This technique has been used in the United States by Carson *et al.* (1973).

### *7.4.3 Gas analysis offline*

An alternative to detecting and analysing the particulate matter is to detect the gaseous products of pyrolysis, such as the hydrocarbon gases or carbon monoxide and carbon dioxide in the cooling gas. There may be two advantages in doing this. First from Section 7.2, it is clear that some gases are given off at lower temperatures, before particulates, so an earlier warning of overheating may be given. Second, in a closed cooling circuit, where particulates have a short lifetime of only 15–30 min, gaseous products will have a much longer lifetime of many days,

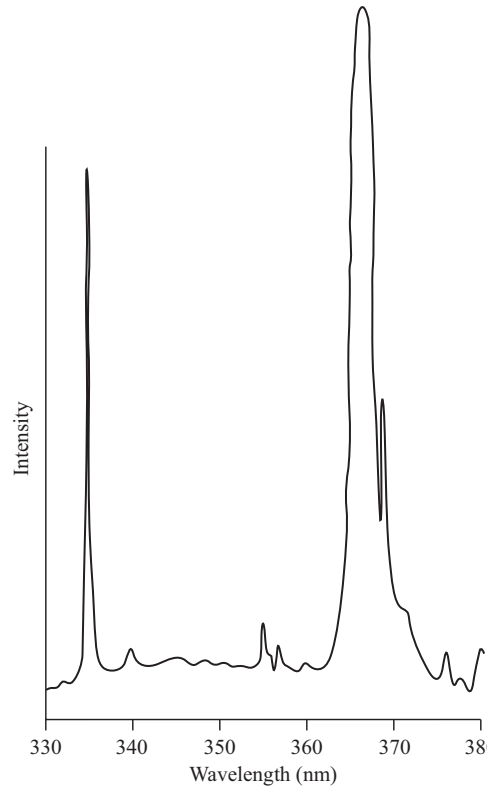


*Figure 7.8 Typical ultraviolet spectrum of hydrogen impurities due to pyrolised insulation. Taken from Tavner et al. (1986)*

depending upon the coolant gas leakage factor, $\frac{1}{\tau_r}$, so it will not be necessary to detect simply a short-term change. On the other hand, whereas the concentration of particulates will be zero in the absence of burning insulation, there will always be a small and possibly variable background concentration of gases, due to impurities in the make-up, and this will effectively determine the threshold for the detection of burning by this technique.

The gas analysis method, which has received attention for large hydrogen-cooled generators, uses a gas chromatograph and flame ionisation detector (FID) to measure the total hydrocarbon content in the hydrogen. Early work showed that most organic compounds present in the cooling gas could not be detected without a concentration technique. A number of such techniques have been reported but the most widely used is a pre-column method in which the impurities are absorbed on a gas chromatographic stationary phase contained in the short tube.

Another offline method of gas detection that has been used in modern large air-cooled machines is to measure the ozone concentration to detect the onset and progress of slot discharge erosion caused by PD activity. Large epoxy insulated

windings in an air-cooled environment experience this problem, which can lead to major insulation failure, see Chapters 2 and 10. The technique has been successfully used on large hydro generators, which operate at stator voltages as high as 24 kV in an air-cooled environment, where stator winding bars are subjected to high slot forces and PD activity is consequent upon mechanical damage, leading to the production of ozone gas. The ozone concentration in the coolant air can be measured by taking a gas sample and using a Draeger tube.

### *7.4.4 Gas analysis online*

The advantage of performing gas analysis continuously online is that, because of the long residence times of gases due to overheating in the cooling system, it may be possible to obtain earlier warning of incipient damage to the machine. The disadvantages are the inherent complexity of continuous chemical gas analysis equipment and the difficulty of translating the analysis into a single electrical signal.

Bearing in mind the experience of Kelley *et al.* (1976), shown in Figure 7.9, a continuous monitor was devised for application to hydrogen-cooled generators, using an FID to measure the total organic content of the hydrogen. This is the type of detector used in chromatography for the detection of organic species. The generator hydrogen gas is introduced into a hydrogen/air flame. The flame forms part of an electrical circuit and normally presents a very high resistance. When organic species are introduced organic ions containing carbon are formed and the resistance

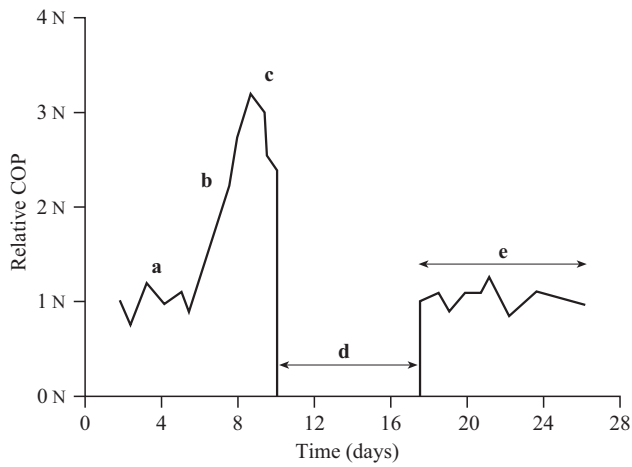


**a** 1 N is equivalent to normal concentration of organic product (COP)

**b** Significant increase in COP accompanied by a core monitor deflection

**c** Core monitor alarm, load reduction initiated

**d** Unit off line for inspection and maintenance

**e** Generator synchronised, COP back to normal

*Figure 7.9 Plot of concentration of organic products during and after a generator overheating problem*

of the flame decreases linearly with the amount of organic compound introduced. The device is very sensitive and can detect increases as small as 0.2 parts per million by volume (vpm). But its usable sensitivity is reduced because of the presence of background levels of organic compounds that can be 10–50 vpm with a variability of ±20%. However, one considerable advantage of the continuous monitor over the core monitor is that it shows the trend of any increase in the products of over-heating, as shown in Figure 7.10. The total organic content is measured in vpm of methane ($CH_4$) equivalent. However, Figure 7.10 also shows the very considerable background level against which faults need to be detected. The sensitivity of the monitor has been calculated theoretically based upon the methane equivalent content of typical insulation materials.

This shows that the pyrolysing of 24 g of insulation would produce about 32 l of methane equivalent hydrocarbons, which on a large hydrogen-cooled generator (500 MW) would give a concentration of about 15 vpm of methane equivalent on the FID. The amount of hydrocarbons produced depends not only on the temperature of the insulation but also on the part being overheated. The mass of insulation per unit volume in the laminated core is relatively small. Whereas, on a winding if overheating takes place a very large proportion of the volume involved will be insulation and this will give a correspondingly large indication on the FID. Overheating would be considered to be serious if the rate of increase of total organics exceeded 20 vpm/h.

An alternative to the FID detector, for the detection of organic content in hydrogen, has been proposed using a commercial photoionisation detector (PID) for flammable gases. The detector contains an ultraviolet lamp that ionises the gas stream as it passes through. A potential is applied across electrodes in the detector and the conductivity is measured as in the FID. The device detects the heavier hydrocarbon compounds in the gas stream and it has been shown that a fault involving over-heating of about 2 g of organic material would produce a deflection of 1 or 2 vpm on the device fitted to a large generator. Typical background levels of 7–10 vpm were measured.

More recent work by Sorita *et al.* (2000) using a quadrupole mass-spectrometer on the gases evolved from faults has identified methods for analysing and classifying faults from turbo-generator faults.

On air-cooled machines an overheating incident will produce a large volume of carbon monoxide and carbon dioxide as well as the light hydrocarbon gases. An instrument has been produced to detect overheating by measuring the carbon monoxide concentration. The instrument contained an auxiliary pump that drew air, through tubes from a number of motors that are being sampled, to a commercial infrared detector. The detector measured the carbon monoxide content using the principle that the vibration of the carbon monoxide molecule corresponds with a known wavelength in the infrared region.

Within a totally sealed motor enclosure, the air should recirculate with a long residence time, $\tau_r$, but because of leaks in a practical enclosure, a substantial proportion of the total volume of air is exchanged with the environment every minute. Thus, any carbon monoxide in the cooling stream produced by overheating will be

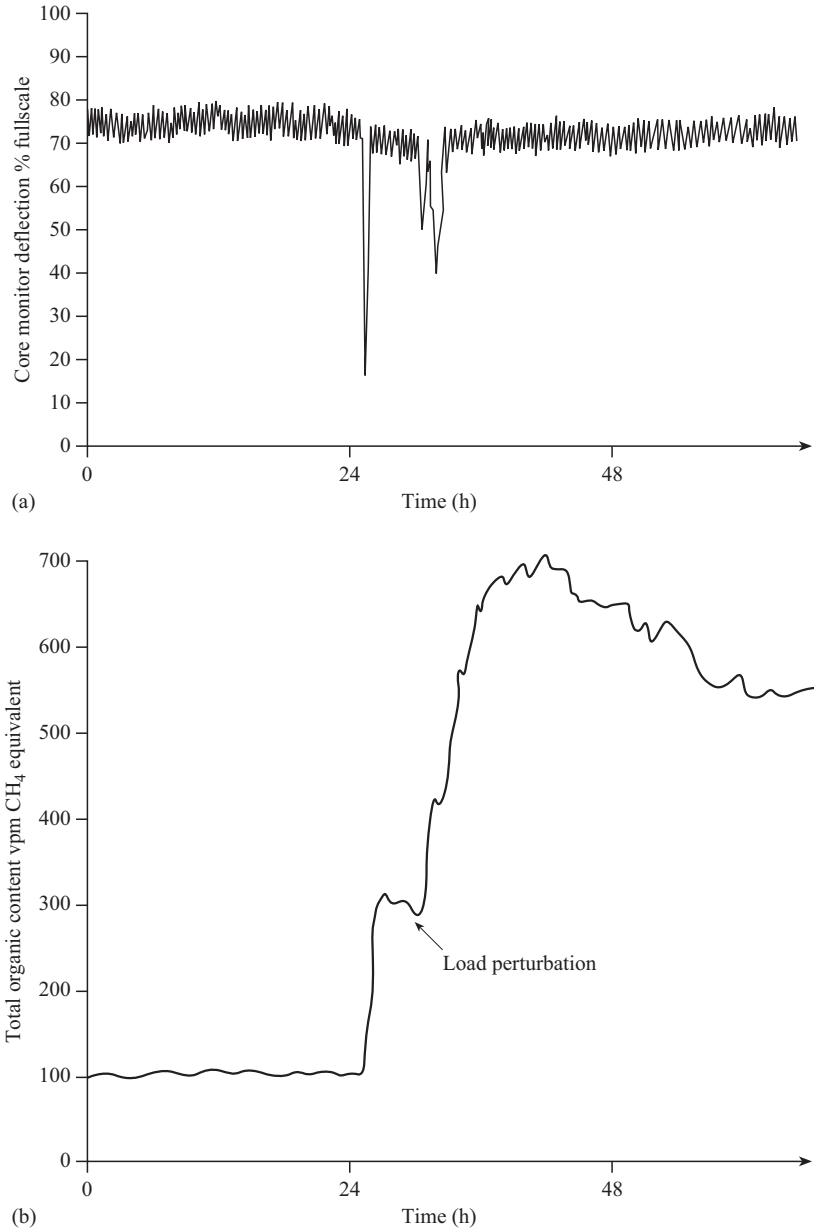


*Figure 7.10 Comparison of the traces from a continuous gas monitor with the response of a core monitor on a 500 MW alternator following an over-heating incident: (a) core monitor response and (b) continuous gas response*

diluted fairly rapidly. This is in contrast with the detection problem in the sealed cooling system of a hydrogen-cooled generator. However, the infrared analyser was capable of detecting concentration of carbon monoxide down to less than 1 vpm. Calculations have shown that 180 g of insulation heated to 300 °C will introduce a 1.5 vpm rise in the concentration of carbon monoxide in the cooling air. Therefore, the analyser has sufficient sensitivity to detect localised overheating on motor windings.

## 7.5 Lubrication oil and bearing degradation

The shafts of smaller electrical machines are supported by ball or roller bearings lubricated with grease and faults in such bearings could be detected by shock pulse techniques as described in Chapter 8. But high-speed machines above about 300 kW and low-speed machines above about 50 kW use oil-lubricated rolling element bearings and still larger sizes need sleeve bearings with a continuous oil supply. A number of authors including Evans (1978) and Bowen *et al.* (1976) have suggested that the continuous monitoring of that oil supply could provide early warning of incipient problems either in the oil itself or in the bearings.

The normal mode of failure of rolling element bearings is by fatigue cracking of the rolling elements or their raceways, although other wear mechanisms like fretting, scuffing and abrasion will also generate debris. For white-metalled sleeve bearing failures are not usually progressive. Debris is likely to be released in short bursts when the bearing is transiently overloaded or if an oil-film momentarily ruptures. Quite substantial damage can be tolerated whilst the bearing continues to be fed a copious supply of cooled lubricating oil. Nevertheless, there are many potentially damaging situations that could be diagnosed by analysing the lubricating oil including fatigue failure or cavitation at the white metal surfaces and corrosion in the lubrication system. Any incipient bearing failure is likely to lead to local heating and degradation of the lubrication oil at the wear site.

A particular problem associated with electrical machines is the flow of currents through bearings and oil films, which pit the bearing surface, producing metallic debris and degrading the lubrication oil. This sort of activity is caused by magnetically induced shaft voltages induced within the machine, whose cause and effects are summarised very thoroughly by Verma *et al.* (1981). Photographs of this type of damage are shown in Chapter 2, Figure 2.14(a) and (b).

The two approaches that could be used on the lubrication oil to detect these various types of incipient failure activity are therefore:

- the detection of oil degradation products,
- the detection of bearing degradation products or wear debris detection.

## 7.6 Oil degradation detection

The chemical detection of oil degradation has been used most effectively for the CM of transformers, see Rogers (1978), where the oil is used for insulating and

cooling purpose and is sealed within the transformer enclosure. But in that case the mechanisms of degradation are clearly defined, being distinguished by the different temperatures reached. The technique is offline gas-chromatograph analysis of the transformer oil, done at regular intervals during the plant life. Such rigorous analysis is necessary to distinguish between the complex products produced in the oil. But the mechanisms involved in bearing oil degradation are not so clearly defined and the analysis that would be necessary would be more complex and less easily prescribed. However, standard offline oil analysis procedures are available commercially but the authors do not know of any programmes that have experienced particular success with electrical machines. The typical parameters to be screened in bearing oil analysis are given in Neale (1973).

## 7.7 Wear debris detection

### *7.7.1 General*

The offline monitoring of wear debris in lubricating oils has been widely used for some time, particularly for rolling element bearings and gears, in the military and aviation fields. This has particularly made use of the ferromagnetic attraction of debris particles. In fact, passive magnetic plugs fitted to lubricating oil sumps have been used, for many years, to collect ferromagnetic debris and regular inspection gives an aid to indicate when full maintenance should be carried out on helicopter gearboxes. But these techniques have now advanced so that online detection of the debris content in oil is possible. Work has also been done to extend the capabilities of online detection so that other debris, produced for example from the soft material of white-metal bearings, can be detected. These techniques are described in the following two sections. When reading these sections it should be borne in mind that oil is supplied to the bearing from a closed-loop lubrication system, which will contain oil filtration equipment. That equipment will remove a proportion of any debris entrained so that, following a wear incident, the concentration of debris will increase and then decay away as the filters do their work. Thus, the ability to detect wear debris is dependent upon volume and residence time factors similar to those that control the detectability of chemicals in cooling gas, as described in Section 7.3.

### *7.7.2 Ferromagnetic techniques*

The normal mode of failure of rolling element bearings is by fatigue cracking and spalling of the rolling elements or raceways producing fragments up to a millimetre or more in size in the oil. An online device has been developed that can be inserted into the full-flow oil line from a bearing and count the number of ferromagnetic particles present in the oil flow, with a certain size band. The detector is based on the induction unbalance principle used in metal detectors. A pair of carefully screened coils surround the oil line and form two arms of an AC bridge circuit. Magnetic or conducting particles entrained in the flowing oil cause the bridge to

unbalance, first on one side of null, as the particle approaches the device, and second on the other side of the null as the particle recedes. Figure 7.11 shows a section through the sensor as described in Chapter 4 and by Whittington *et al.* (1992). The phase of the bridge unbalance enables ferromagnetic particles to be discriminated from other conducting particles. The sensitivity of the system varies according to the shape of the particles but for approximately spherical particles the sensitivity can be adjusted to separately record the passage of particles at two size levels, small from 200 μm to 2 mm in diameter, in an oil flow velocity of 1 to 12 m/s, that is an oil flow of up to 20 l/s. The output is in the form of a counter reading in each of the two size ranges and the output could be made available to a data acquisition system. This robust device has been widely used on jet engine installations, where its performance in a high temperature, pressure and vibration environment has been proved. There is no record, however, of this device being used on an electrical machine.

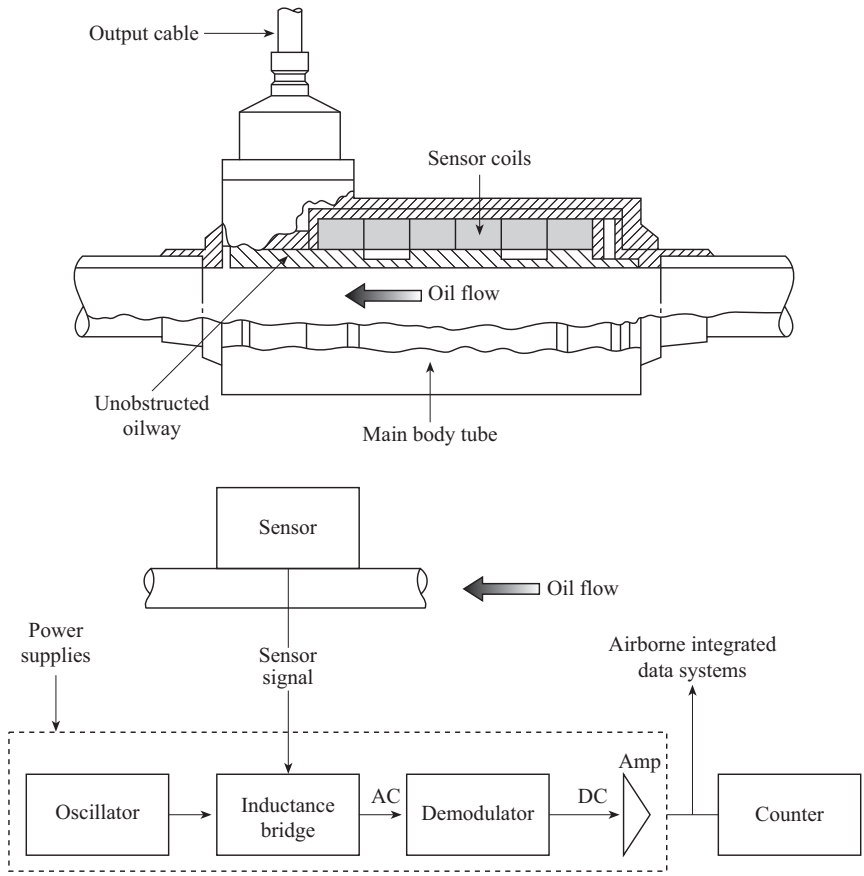


*Figure 7.11 Structure of a inductive debris detector*

A device that can produce a greater amount of information about ferromagnetic wear debris is the instrumented magnetic drain plug. Conventional magnetic plugs usually consist of a bar magnet with a pole projecting into the lubricating oil. In an instrumented plug, it is necessary to measure the change in field strength at the magnet pole as debris is collected. Because of the difficulties of measuring those changes a horseshoe magnet has been adopted instead of the bar magnet. As particles are attracted to the gap between the poles of the magnet they increase the field within the gap, while at the same time increasing the total flux in the magnetic circuit. Two differentially connected, matched field sensors, sampling each of these fields, can thus give additive, particle-dependent signals, whilst cancelling out fluctuations due to temperature and magnetic field strength. Figure 7.12 shows the arrangement of the device. Another device, an instrumented oil drain plug, gives an analogue voltage proportional to; the amount of debris deposited, the rate of accumulation of debris and the temperature of the oil. The device can detect masses of ferromagnetic debris attracted to the pole pieces ranging from 10 to 600 mg, with a resolution of 10 mg in an oil flow velocity of 0.1 to 0.5 m/s.

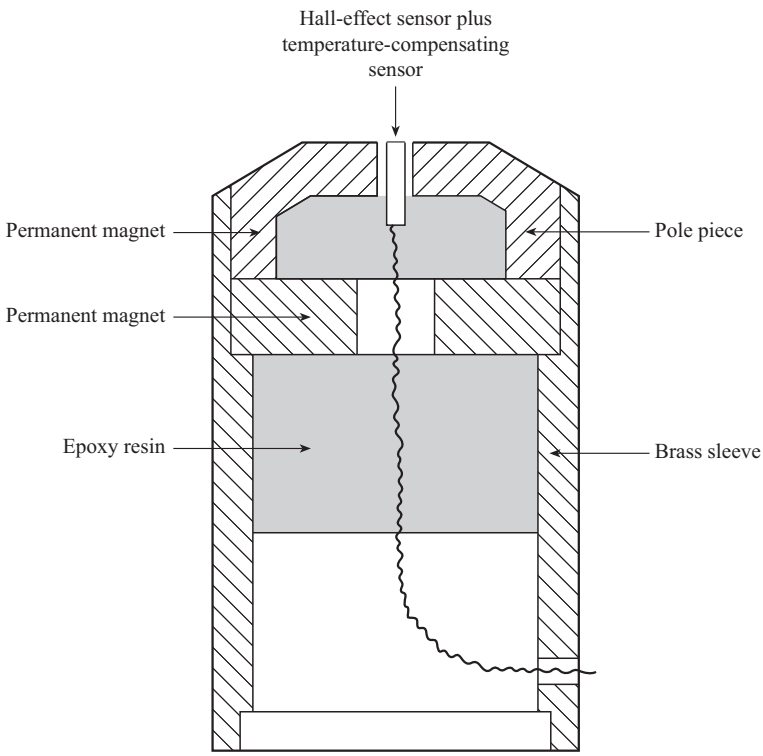


*Figure 7.12 An instrumented magnetic drain plug*

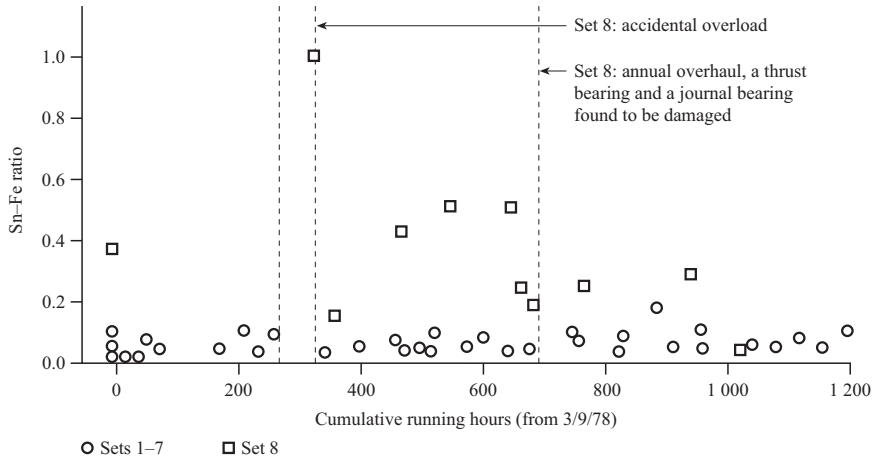


*Figure 7.13 Ratio of tin-to-iron in the oil filter deposits from eight 60 MW turbo-generator sets. Taken from Lloyd et al. (1981)*

### *7.7.3 Other wear debris detection techniques*

The ferromagnetic techniques described in the previous section are appropriate for rolling element bearings but not for the white-metalled sleeve bearings that are used on larger electrical machines. Lloyd *et al.* (1981) have investigated the problem of detecting wear in the bearings and hydrogen seals of large turbo-generator sets. They describe an investigation that characterised the debris circulating in the oil system of a number of 60 MW turbo-generators and correlated the results with plant condition. A major feature in this correlation was the presence of white-metal in the machine bearings that typically contain 85% tin.

The results of their investigation showed that by determining the ratio of tin-to-iron in the debris an operator could see how much bearing damage was occurring, compared to normal running wear; see Figure 7.13. However, if information was available about running time, monitoring of tin content alone would be adequate.

Lloyd *et al.* (1981) then proceeded to investigate how the oil system could be automatically monitored to provide early warning of bearing damage. In particular, they considered X-ray fluorescence (XRF) detection and the measurement of the electrical properties of the oil. Their investigation showed that XRF would be feasible but would be prohibitively expensive as an online technique.

## 7.8 Conclusions

This chapter has shown that chemical and wear analysis have been demonstrated to be effective global monitoring techniques for electrical machines which can produce narrow bandwidth (<1 Hz) signals. Chemical degradation of insulating materials and lubricants is detectable and can give bulk indications of the condition

of an electrical machine. This is particularly important when it is considered how central insulation and lubrication integrity are to the long-term life of a machine.

However, the detectability criteria for these techniques are difficult and the chemical analysis processes involved are complex and expensive and the quantity of data generated by chemical analysis currently confine their application to only the largest machines in the case of the winding or the core, this tends to throw the user back towards lower cost, more pervasive modern thermal monitoring techniques, eg FBG, described in Chapter 6. However, the disadvantage of point temperature techniques compared to chemical methods is that they cannot provide an overview.

*Chapter 8*

# Online vibration monitoring

## 8.1 Introduction

An electrical machine, its support structure and the load to which it is coupled, form a complex electromechanical system. It can receive impulsive excitations that vibrates it at its own natural frequency, or it can be forced, by the exciting air-gap electromagnetic field or torque spectrum of the driven or driving machine, at many different frequencies. These frequencies may cause the machine to emit an unacceptably high level of acoustic noise, or cause progressive mechanical damage, due to high cycle fatigue, which ends in a machine failure mode.

Consequently, a great deal of effort has been applied to try to determine the principal sources of vibration in electrical machines, and a large literature, spanning nearly one hundred years, has accumulated. A representative selection of papers and articles is included in the references.

The principal sources of vibration in electrical machines are:

- Stator core response to the attractive force developed magnetically between the rotor and stator,
- Rotor dynamic behaviour transmitted to the bearings as the machines rotates,
- Shaft-bearing responses, influenced by the machine structure and foundation support, to vibration transmitted from the rotor,
- Stator end winding responses to the conductor electromagnetic forces.

These four areas are interrelated; for example, bearing misalignment or wear can result in eccentric running, which will in turn stimulate stator and rotor vibration modes, furthermore air-gap-induced radial vibration is coupled to the end-windings, which are effectively embedded encastré in the stator core.

Before examining the specific monitoring techniques, we shall first look at the characteristic features of the frequency responses of the machine elements listed above.

## 8.2 Stator core response

### *8.2.1 General*

The stator and its support structure comprise a thick-walled cylinder, slotted at the bore, resting inside a thin-walled structure, which may be cylindrical for smaller or

gas-pressurised machines but is usually of box structure for larger air-cooled machines. A stator in its cylindrical support structure is illustrated schematically in Figure 8.1. Analysis of a three-dimensional structure such as this, in response to the complex imposed force distribution, is a formidable problem, even for powerful numerical techniques. Fortunately, the main features of the response can be developed using simplified models.

Jordan (1950) and Alger (1965) considered the machine to be reducible to an infinitely long, thin-walled, cylinder representing the stator core. This simplification allows a qualitative assessment of response to be made. A fuller treatment of the mechanical system is provided by Erdelyi *et al.* (1956) and Yang (1981) gave a detailed analysis of stator displacements, taking into account higher frequency effects due to slot passing.

The forces acting on the stator core are the result of the interaction between the air-gap flux wave and the currents flowing in the windings embedded in the stator slots. The forces acting on the end winding are due to the interaction between the end region leakage flux and the winding currents.

It is apparent, therefore, that the precise nature of the applied force waves will be a function of the form of the current distribution and the geometry of the air-gap and end regions. Disturbances to either, due to rotor eccentricity or damaged areas of the rotor or stator windings, for example, will alter the harmonic components of

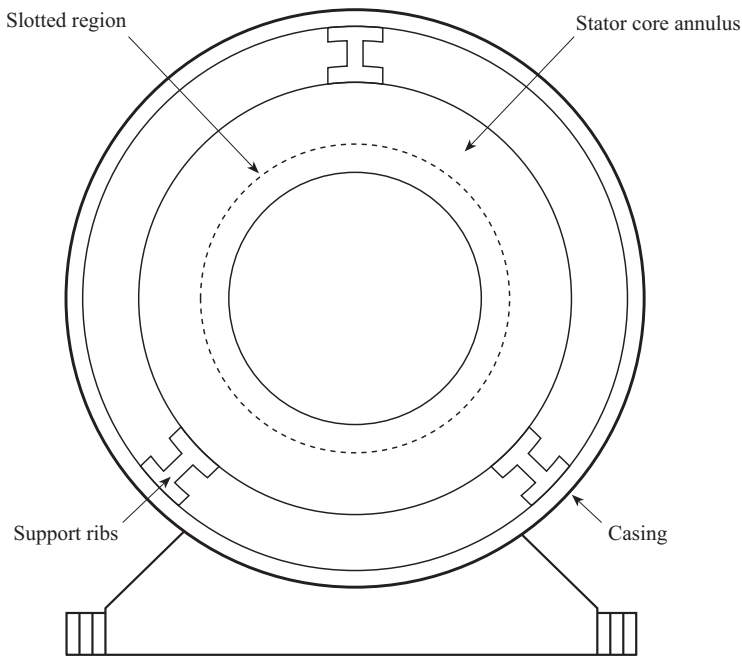


*Figure 8.1 A machine stator and its supporting structure*

the force wave and initiate a different response from the stator core, particularly if the applied forces stimulate any of the natural modes of the system.

### *8.2.2 Calculation of natural modes*

For a simple thin-walled cylinder of infinite length the radial and peripheral displacements, $u_r(\theta, t)$ and $u_\theta(\theta, t)$, of the structure at a radius fixed at the mid-wall value, may be written as:

$$u_r(\theta, t) = \sum_{n=\text{even}}^{\infty} \{a_n(t) \cos(n\theta) + b_n(t) \sin(n\theta)\} \tag{8.1}$$

And:

$$u_\theta(\theta, t) = \sum_{n=\text{even}}^{\infty} \{c_n(t) \cos(n\theta) + d_n(t) \sin(n\theta)\} \tag{8.2}$$

If it is further assumed that the deformations are inextensible:

$$\frac{\partial u_\theta}{\partial \theta} = -u_r \tag{8.3}$$

Then:

$$c_n = \frac{b_n}{n} \text{ and } d_n = -\frac{a_n}{n}$$

During deformation by the deflections in (8.1) and (8.2), the system accumulates volumetric elastic strain potential energy, $V_\ell$, per unit length given by the expression:

$$V_\ell = \frac{1}{2} \int_{-\pi}^{\pi} \frac{EJ}{(1 - \nu^2) r^2} \left[ \frac{\partial^2 u_r}{\partial \theta^2} - u_r \right] \mathrm{d}\theta \tag{8.4}$$

where

$E$ = Young's modulus of the material,
$\nu$ = Poisson's ratio of the material,
$J$ = the polar moment of inertia of the core cylinder.

Equation (8.4) reduces to:

$$V_\ell = \frac{\pi}{2} \frac{EJ}{(1 - \nu^2) r} \sum_{n=1}^{\infty} \left(1 - n^2\right)^2 \left[ {a_n}^2(t) + {b_n}^2(t) \right] \tag{8.5}$$

Timoshenko (1974) shows that the kinetic energy of the system, $T_\ell$, per unit length is given by:

$$T_\ell = \frac{w}{2g} \int_{-\pi}^{\pi} \left( {\dot{u}_r}^2 + {\dot{u}_\theta}^2 \right) \mathrm{d}\theta \tag{8.6}$$

where $w$ is the weight per unit length per unit circumferential angle of the cylinder and $g$ is the acceleration due to gravity. Substituting (8.1) and (8.2) into (8.6) gives:

$$T_\ell = \frac{\pi w}{2g} \sum_{n-1}^{\infty} \left(1 + \frac{1}{n^2}\right) \left[\dot{a}_n{}^2(t) + \dot{b}_n{}^2(t)\right] \tag{8.7}$$

If it is necessary to include the vibration of the core, enclosure and frame building bars of the machine, then these can also be incorporated. So, for example, the total elastic strain energy, $V_\ell$, would be given by:

$$V_\ell = V_E + V_S + V_F \tag{8.8}$$

where the subscripts $E$, $S$ and $F$ refer to the enclosure, the stator core and the frame building bars, respectively.

The total kinetic energy of the system would be given by:

$$T_\ell = T_E + T_S + T_F \tag{8.9}$$

However, the calculation of these quantities for the enclosure and frame structures is complex. The equation of motion can now be formulated. It is given for free vibration by the Euler–Lagrange equation:

$$\frac{\partial}{\partial t}\left(\frac{\partial T_\ell}{\partial \dot{a}_n}\right) - \frac{\partial V_\ell}{\partial \dot{a}_n} = 0 \tag{8.10}$$

If the forced vibration response is required directly, then the right-hand side of (8.10) becomes a forcing function. For example, if we are interested in the system response to the $m$th harmonic of the radial force wave $f(\theta, t)$, the forcing function becomes the work function, $W$, given by:

$$W = \sum_{m=1}^{\infty} f_m(\theta, t)\, u_{rm}(\theta, t) \tag{8.11}$$

Generally, $f_m(\theta, t)$ has the form of travelling wave:

$$f_m(\theta, t) = F_m \cos(\omega_m t - m\theta) \tag{8.12}$$

Erdelyi *et al.* (1956) show how the Rayleigh–Ritz method can be used to solve (8.10) to yield the natural frequencies of the system, under the assumption that time variations are harmonic. That is, the coefficients $a_n(t)$ and $b_n(t)$ are given by:

$$\begin{aligned} a_n(t) &= A_n \sin \omega_n t \\ b_n(t) &= B_n \sin \omega_n t \end{aligned} \tag{8.13}$$

Under this assumption, (8.10) becomes a polynomial in $\omega_n$ whose roots give the natural frequencies. Some of the natural circumferential mode shapes of the radial vibration of the stator are shown in Figure 8.2.

Besides these circumferential modes, it is also possible for the radial vibration of the stator to vary as a function of machine length. The mode shapes for a

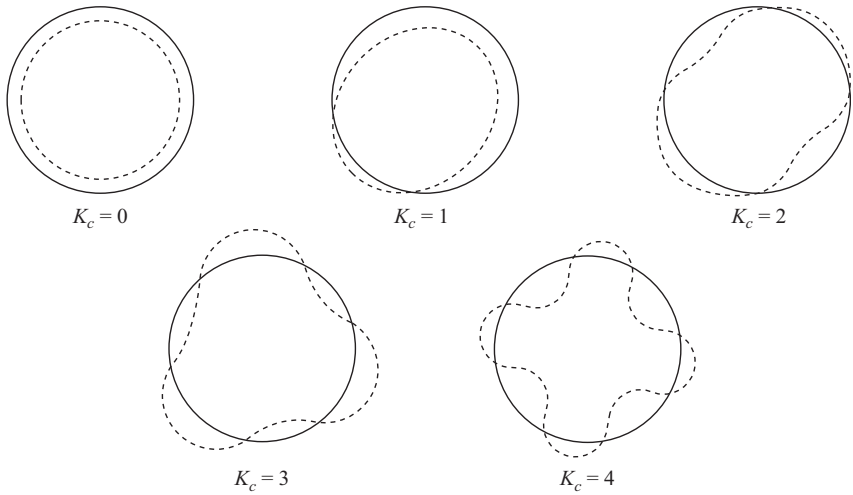


*Figure 8.2 Radial mode shapes of a stator in a circumferential direction*

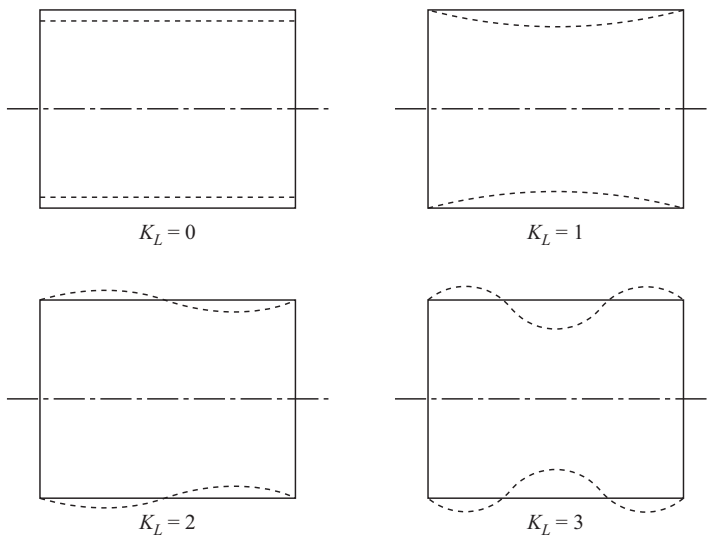


*Figure 8.3 Radial mode shapes of a stator in a longitudinal direction*

cylinder vibrating in this way are illustrated in Figure 8.3. In practice, however, only the $k_L = 0$ case need be considered for machines of normal proportion. Very long machines may exhibit vibrations at the higher modes, but the most important mode shapes are those due to the circumferential radial vibrations. It is easily recognised that the cases for $k_C = 0$ and $k_L = 0$ and are identical.

Approximate formulae for the natural frequencies of a simple single ring stator have been reported by Yang (1981) in the form given here. For $k_c = 0$, the corresponding natural frequency $f_0$ is given by:

$$f_0 = \frac{1}{2\pi r_{\text{mean}}}\left[\frac{E}{\rho}\left\{\frac{w_y}{w_y + w_t + w_i + w_w}\right\}\right]^{\frac{1}{2}} \tag{8.14}$$

where $\rho$ is the density of the core, and $w_y$, $w_t$, $w_i$ and $w_w$ are the weights of the core yoke, teeth, insulation and windings, respectively, $r_{\text{mean}}$ is the mean radius of the core, excluding the teeth. For $k_c = 1$, the natural frequency $f_1$ is given by:

$$f_1 = f_0\left[\frac{2}{1 + \frac{{t_0}^2 S}{12{r_{\text{mean}}}^2}\left\{\frac{w_y}{w_y + w_t + w_i + w_w}\right\}}\right]^{\frac{1}{2}} \tag{8.15}$$

where $t_0$ is the radial thickness of the stator core annulus and $S$ is a constant related to the stiffness of the winding, insulation and slot components:

$$S = 1 + \frac{N_s}{2\pi J r_{\text{mean}}}\left(\frac{w_t + w_i + w_w}{w_t}\right)\left(\frac{1}{3} + \frac{t_0}{2h_t} + \left(\frac{t_0}{2h_t}\right)^2\right)a_t {h_t}^3 \tag{8.16}$$

where

$N_s$ = number of stator slots,
$J$ = the polar moment of inertia of the core,
$a_t$ = cross-section of area of the teeth,
$h_t$ = tooth depth.

The higher natural frequencies, $f_m$, may be calculated from:

$$f_m = \frac{f_0 t_0 m(m^2 - 1)G(m)}{\frac{2}{3} r_{\text{mean}}\sqrt{(m^2 + 1)}} \tag{8.17}$$

where the function $G(m)$ is given by:

$$G(m) = \left\{1 + \frac{\frac{{t_0}^2}{12{r_{\text{mean}}}^2}(m^2 - 1)\left\{m^2\left(4 + \frac{w_y M}{w_y + w_t + w_i + w_w}\right)\right\}}{(m^2 + 1)}\right\}^{-\frac{1}{2}} \tag{8.18}$$

It is clear that the calculation of the natural frequencies of complex mechanical structures, as represented by the stator core and frame of an electrical machine, is a difficult matter.

However, this could be resolved experimentally by carrying out separate mobility tests of the stator and rotor components and then a mobility test of the composite assembly. By these means, it is possible to determine the modes of the structure.

### *8.2.3 Stator electromagnetic force wave*

In order to anticipate changes in stator core frame and winding vibrations due to electrical or mechanical anomalies in the machine, it is important to determine the exciting forces. The problem of calculating the forces exerted on the stator and rotor reduces to calculate the flux density $\bar{B}$ in the air-gap of the machine. This can be achieved using numerical techniques, such as the finite element method, and requires that a solution be found to the following equation for the machine:

$$\bar{\nabla} \times \bar{\nabla} \times \bar{B} = \sigma\left(\bar{v} \times \bar{B} - \mu \frac{\partial \bar{B}}{\partial t}\right) \tag{8.19}$$

where $\sigma$ is the electrical conductivity of the region, and $v$ is the velocity of the rotor, relative to the travelling flux wave produced by the stator. The solution of (8.19), even in the two dimensions, representing a cross-section in the radial and circumferential directions of the machine, requires significant computational effort if the slotting of both rotor and stator are to be taken into account. If good accuracy is required, however, it is the only suitable path to follow, using a detailed explanation of the solution of (8.19) for a linear machine, using the finite element technique.

The finite element method can be used to account for any distribution of windings, and any radial or peripheral geometrical variations, simply by increasing the complexity of the model. However, there are limits to the accuracy of finite element modelling determined by the accuracy of the precise manufacturing data. These methods are essentially numerical and therefore quantitative.

However, a qualitative assessment can be more valuable than a full analysis and this is readily achieved, in certain circumstances, using simpler, although less accurate methods.

If the rotor and stator surfaces are assumed to be smooth then it is possible to solve (8.19) in the radial and circumferential plane analytically, provided the motion term is neglected. This approach allows the effect of individual conductor currents to be accounted for. Hague (1962) and Stafl (1967) both used separation of variable techniques to calculate air-gap flux densities for a variety of configurations.

Many authors have examined the important sources of unbalanced magnetic pull (UMP) and the effect it has on vibration. Swann (1963) showed how it is possible to calculate the harmonics introduced into the flux wave due to rotor eccentricity. He does this by using a conformal transformation to re-centre the rotor. In addition, Binns *et al.* (1973) identified the role of static eccentricity in the production of UMP. A review of a considerable amount of previous work on UMP may be found in the report by Rai (1974).

Perhaps the simplest, generally useful method of gaining a qualitative assessment of the flux wave form was that used by Yang (1981). Here, the flux wave is calculated by simply multiplying the stator magnetomotive force distribution, $F_1$, due to the winding currents, by the permeance, $\Lambda$ of the air-gap:

$$\Phi = F_1 \cdot \Lambda \tag{8.20}$$

Binns (1968) suggested that this procedure had limited accuracy, but within the limitations suggested by Lim (1951) the technique is valuable, since it can easily accommodate geometrical effects and anomalies in winding arrangements. Williamson *et al.* (1980) later proposed an analytical permeance-wave method for calculating the harmonic impedances of a machine and thereby, by the use of harmonic equivalent circuits, it was possible to predict machine rotor torques. These and other authors have subsequently, successfully used this method, sometimes incorporating finite element solutions, to allow for three-dimensional components that are not tractable by the analytical method. Using such techniques it has been possible to analyse the effects of winding faults and rotor eccentricity on the flux density in the air-gap.

Vas (1993) made the point in his book about the all-embracing nature of the electro-magnetic field in the energy conversion process, stressing the importance of the air-gap flux density in electrical machine monitoring. This relates to the emphasis in the published literature to date on the effect of more tractable faults on the air-gap field.

The permeance variation, taking account of the relative motion of the rotor with respect to the stator, can be expressed in the form of an infinite series of harmonics. If both the rotor and stator surfaces are slotted, then the permeance wave has the form:

$$\Lambda(\theta_1, t) = \sum_{m=1}^{\infty} \sum_{n=1}^{\infty} \widehat{\Lambda}_{m,n} \cos\left[mN_r\omega_{\mathrm{rm}}t - (mN_r \pm nN_s)\theta_1\right] \tag{8.21}$$

With $\widehat{\Lambda}_{m,n}$, the peak amplitude of the permeance wave defined above:

$m$ and $n$ = integer slot harmonics
$N_s$ and $N_r$ = number of stator and rotor slots, respectively,
$\omega_{\mathrm{rm}}$ = mechanical angular speed of the rotor.

Similarly, the instantaneous MMF, $f_1$, in the stator air-gap can be expressed as an infinite series of space and time harmonics. The result, which can be found in standard texts, is,

$$f_1(t) = \sum_{\ell=1}^{\infty} \sum_{q=1}^{\infty} \widehat{f}_{s,\ell,q} \cos\left[\ell\omega_{\mathrm{se}}t - qp\left(\theta_1 - \frac{\alpha_s z}{L}\right) - \varphi_{\ell q}\right] \tag{8.22}$$

$\widehat{f}_{s,\ell,q}$ = the stator MMF wave components of the form $NI$ with $\ell$ time harmonics and $q$ space harmonics
$q$ = the order of the stator winding MMF space harmonic
$\ell$ = the order of the supply time harmonics
$\omega_{\mathrm{se}}$ = the angular frequency of the electrical supply
$z$ = the longitudinal distance from the centre of the machine
$L$ = the active length of the core
$\alpha_s$ = the skew angle of the stator
$\phi_{\ell q}$ = the phase angle of the stator MMF wave $F_{s,\ell,q}$

$p$ = the number of pole pairs

Similarly the rotor MMF, referred to the stator, can be expressed as:

$$f_2(t) = \sum_{\ell=1}^{\infty}\sum_{q=1}^{\infty}\widehat{f}_{r,\ell,q}\cos\left[\ell s\omega_{\text{se}}t - qp\left(\theta_2 - \frac{\alpha_r z}{L}\right) - \varphi_{\ell q}\right] \tag{8.23}$$

where

$s$ is the slip of the rotor with respect to the stator magnetic field,

$\widehat{f}_{r,\ell,q}$ = the rotor MMF wave components of the form $NI$ with $\ell$ time harmonics and $q$ space harmonics.

The total MMF can be found by adding (8.22) and (8.23), and the flux wave calculated by multiplying this sum by the result of (8.21).

Yang (1981) shows that the effect of eccentricity can be incorporated by modifying the permeance wave expression (8.21). He proposes the following expressions for dynamic and static eccentricity, stator permeance variations, $\Lambda_{s,\text{ecc}}$ due to static eccentricity being:

$$\Lambda_{s,\text{ecc}} = \sum_{n=1}^{\infty}\Lambda_{0,\text{ecc}}\cos n\theta_1 \tag{8.24}$$

Stator permeance variations, $\Lambda_{d,\text{ecc}}$, due to dynamic eccentricity:

$$\Lambda_{d,\text{ecc}} = \sum_{n=1}^{\infty}\widehat{\Lambda}_{0,\text{ecc}}\cos\left(\omega_{\text{ecc}}t - n\theta_1\right) \tag{8.25}$$

where $\omega_{\text{ecc}}$ is the angular velocity of the eccentricity.

These expressions can be combined with (8.21) to give the permeance wave for the complete system, and the flux wave found in the manner outlined above. Ovality of the stator bore can be accounted for in a similar manner. The expressions and methodology outlined here provide a general and relatively simple method of calculating the harmonics of the flux wave acting on the stator so that its response can be determined. The radial and tangential forces applied to the core can be calculated from the flux density using the method of Maxwell stresses, as described by Carpenter (1959) from the radial and tangential stresses given by, $\sigma_r$ and $\sigma_\theta$:

$$\sigma_r = \frac{{B_r}^2}{2\mu_0} \quad \text{and} \quad \sigma_\theta = \frac{{B_\theta}^2}{2\mu_0} \tag{8.26}$$

where $B_r$ and $B_\theta$ are the amplitudes of the radial and tangential flux density waves, respectively, calculated from the MMF and permeance waves that when integrated give (8.20).

## 8.3 Stator end winding response

The end winding structure of an electrical machine has a relatively low stiffness or compliance but relatively high, non-linear damping coefficients due to frictional

contact between adjacent conductors in the structure. The stiffness may be increased by improved methods of bracing, which are used in large turbo-generators or induction machines with more onerous starting duties. The motion of the stator end winding is excited by two mechanisms:

- Seismic excitation of the coils, as encastré beams, by the ovalising displacements of the stator core and displacement of the machine by its environment,
- Electromagnetic forces on the coils themselves due to the currents flowing in them.

The magnetic field of this condition was considered by Ashworth *et al.* (1961) and the consequent forces by Brandl (1980). The dynamics of the end winding are complex, partly because of its complicated geometry but also because of the distributed nature of the forces applied to it and the non-linear coefficients of its response. The resultant displacements are at twice the electrical supply frequency, $f_{se}$, and it is necessary to carry out a very thorough analysis to determine the mode shapes of the structures. The dynamic behaviour has been described by Ohtaguro *et al.* (1980). Again, when the analysis is difficult, experimental determination of the structure can be obtained by mobility tests to determine the modal response of the structure.

A number of utilities have installed triaxial accelerometers on the end winding structures of large turbo-generators to monitor the amplitudes of $2f_{sm}$ vibrations at widely-spaced intervals of time in order to check that the end winding has not slackened. Displacements of end windings on large turbo-generators of from 1 to 10 mm are quite usual during normal running, even with modern epoxy insulation systems, and this can lead to fretting of the insulation, slackening and dielectric damage.

Because of this end winding, monitoring on the very largest synchronous machines is now being considered for regular online measurement but caution must be taken as it requires very specialist interpretation to determine from accelerometer signals where end winding slackening has occurred, so that remedial action can take place.

Experience from the work to date on this issue suggests that the measurement of individual displacements is less important than determining any change in the vibration eigen values of the end winding structure. In that case weakness in structural stiffening could be identified and bracing tightened at the next major outage to resolve the issue.

However, on smaller machines, for example, induction motors, the displacements are not large, but they do require special prediction techniques, especially for larger motors in the oil and gas production industry, as described Williamson *et al.* (1988), and for measurement, see Campbell *et al.* (1984). This is particularly important during design for arduous starting conditions when induction motor winding currents can be very large and displacements could be significant.

## 8.4 Rotor response

We now consider the motion of a rotor in response to:

- Transverse force excitation, due to self-weight, mechanical unbalance, shaft whirling, dynamic or static electro-magnetic UMP due to eccentricity or a combination of all four,
- Torsional torque excitation, due to the prime mover drive or electromagnetic torque reaction.

Transverse forces are due to asymmetries in the machine, whilst torsion is primarily due to the driving torque, however, both may be affected by electrical or mechanical faults in the machine itself or electrical or mechanical system disturbances outside the machine.

An important issue is the response of the machine to these applied excitations. There will also be a coupling between torsional and transverse effects due to the transfer function or stiffness between these axes of the machine, so torsional effects, like current faults in rotor and stator windings, can cause transverse effects, like vibrations, and vice versa.

### *8.4.1 Transverse response*

#### 8.4.1.1 Rigid rotors

In order to examine the response of a rotor to unbalanced forces, a distinction must be drawn between the rigid and flexible rotors. Rigid or short rotors may be considered as a single mass acting at the bearings, and it has been shown that the displacement, $u$, of the rotor and its bearings can be modelled by the differential equation:

$$(M + M_s)\frac{\mathrm{d}^2u}{\mathrm{d}t^2} + c\frac{\mathrm{d}u}{\mathrm{d}t} + ku = mr{\omega_{\mathrm{rm}}}^2 \tag{8.27}$$

where

$M$ = mass of the rotating system,
$m$ = equivalent unbalance mass on the shaft,
$M_s$ = support system mass,
$r$ = effective radius of the equivalent unbalanced mass,
$c$ = damping constant of the support system,
$k$ = stiffness of the support system.

For sinusoidal motion the peak displacement, $\widehat{u}$, is given by the solution to (8.27), and is:

$$\widehat{u} = \frac{mr\left(\frac{\omega_{\mathrm{rm}}}{\omega_0}\right)^2}{(M + M_s)\sqrt{\left\{\left(1 - \left(\frac{\omega_{\mathrm{rm}}}{\omega_0}\right)^2\right)^2 + 4D^2\left(\frac{\omega_{\mathrm{rm}}}{\omega_0}\right)^2\right\}}} \tag{8.28}$$

With $\omega_0$, the natural frequency of the rotor support system, and $D$ the damping factor are given by:

$$\omega_0 = \sqrt{\frac{k}{(M + M_s)}}$$
$$D = \frac{c}{2\sqrt{k(M + M_s)}} \tag{8.29}$$

If the displacement is divided by the specific unbalance $e$, given by:

$$e = \frac{mr}{M}$$

Then the behaviour of the displacement, $u$, as a function of frequency is as shown in Figure 8.4. The degree of residual unbalance is denoted by the quantity $G = e\omega_{\mathrm{rm}}$ and the permissible limits are provided by international standard ISO 1940-1:2003, as shown in Figure 8.5.

For electrical machinery, the appropriate quality grades are towards the lower end of the values shown in Figure 8.5. For example, $G = 2.5$ is generally applicable to machines of all sizes, and $G = 1.0$ for special requirements.

### 8.4.1.2 Flexible rotors

For long slender rotors operating at higher speeds, as in two pole machines, particularly large turbo-generators that have restricted rotor radii, the foregoing analysis is insufficient and the distribution of unbalance must be considered. Again, Campbell *et al.* (1984) show how it is possible to calculate the natural frequencies of general problems of a rotor with a flexural rigidity $EJ$, and mass per unit length

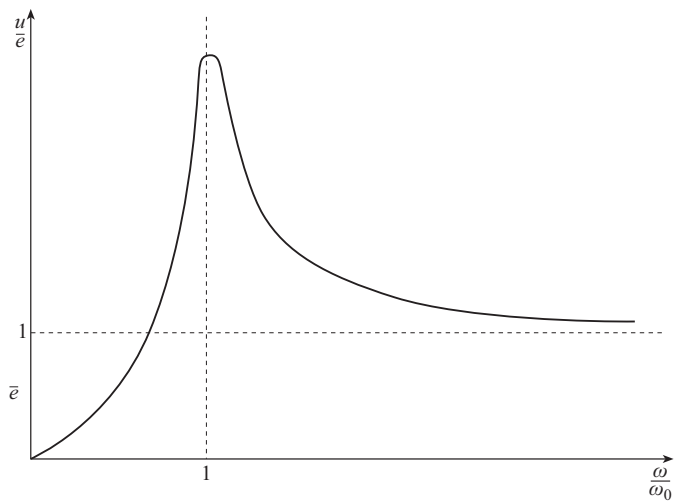


*Figure 8.4 Displacement per specific unbalance versus normalised frequency*

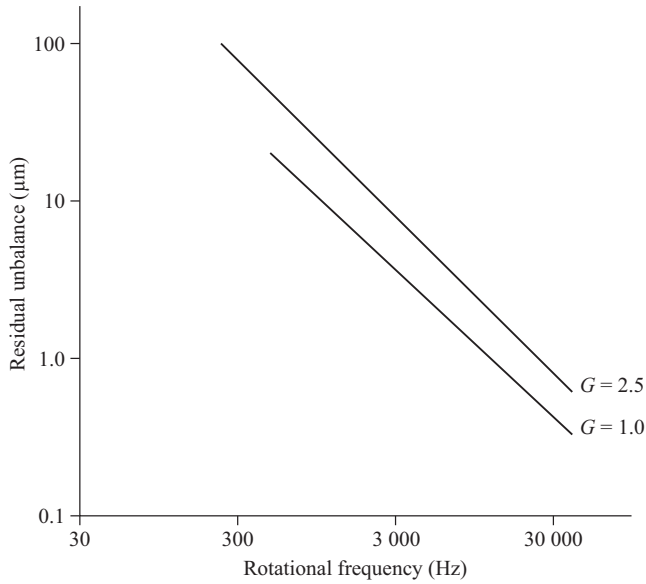


*Figure 8.5 Extract from ISO 1940-1:2003 permissible limits to residual unbalance*

$m$, which are both functions of axial location, $z$. The displacement $u$, for any $z$, is given by the solution of:

$$\frac{\partial^2}{\partial z^2}\left(EJ(z)\frac{\partial^2 u}{\partial z^2}\right) - {\omega_{\mathrm{rm}}}^2 m(z)u = \sum_{n=1}^{\infty} f_n \tag{8.30}$$

where $f_n$ is the unbalance forcing function and:

$$2\pi f_n = \omega_n = \int m(z){g_n}^2(z)\mathrm{d}z \tag{8.31}$$

With $g_n(z)$ the $n$th solution of (8.30). The solution for coupled systems comprising several rotors, consisting of the electrical machine and the machine it is driving or driven by, is extremely complex. It is usual to assume that the stiffness of couplings between rotors is low and rotors may be considered to be decoupled from one another, allowing them to be considered individually as described above.

The mode shapes for the rotor shafts will also depend upon the nature of the bearing supports for the shafts. For example, Figure 8.6 shows the effect of hard and soft bearings on the first and second modes for a single flexible rotor.

The results for higher modes are readily deduced from these examples. For nearly all electrical machine vibrations, for which monitoring would be appropriate, the bearings may be considered to be hard, although Smart *et al.* (2000) have shown how the influence of foundations should be taken into account when studying the transverse vibration behaviour of a large machine.

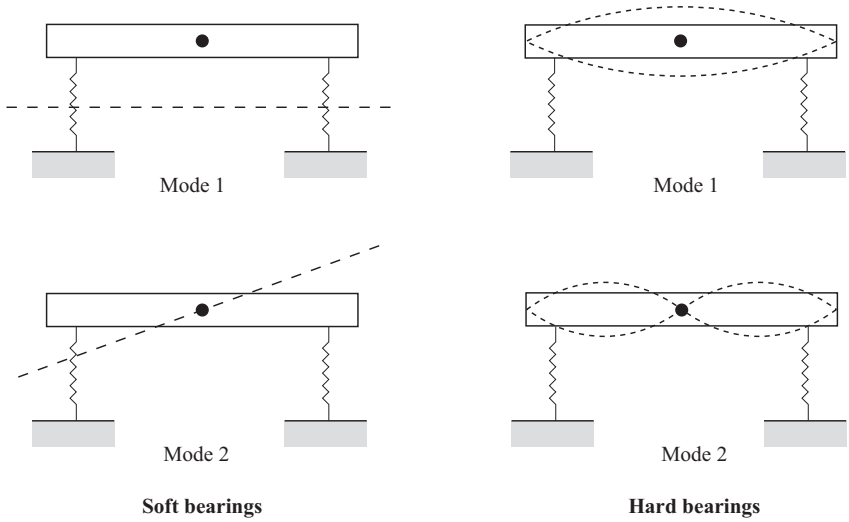


*Figure 8.6 Rotor mode shapes for hard and soft bearings*

The international standard limits shown in Figure 8.5 are applicable to rigid rotors operating well below their critical speed. For flexible rotors it has been suggested that the allowable eccentricity can be modified so that the same standard applies. Dimentberg (1961) uses the correction:

$$e_{\text{flexible}} < e_{\text{rigid}} \left( 1 - \left( \frac{\omega_{\text{rm}}}{\omega_0} \right)^2 \right) \tag{8.32}$$

where $\omega_0$ is the first critical speed of the rotor. This, however, is only applicable for rotors running at less than $\omega_0$, that is a hypo-critical machine. When the machine is operating above $\omega_0$, it is a hyper-critical machine.

In general, large 2-pole turbo-generators and some induction motors are hyper-critical machines but most multi-pole machines are hypo-critical.

### *8.4.2 Torsional response*

The torsional oscillatory behaviour of a large rotating electrical machine and its driven machine or prime mover can be complicated. For example, in a large turbo-generator, the electrical machine links a complex prime mover to a large interconnected electrical network in which large quantities of energy are being transported. The possibility of forced torsional oscillation in the rotor of a turbo-generator is significant because of its great length and relatively small radius. The nature of such oscillations will depend upon the form of the disruptions that occur in the mechanical or the electrical system. Disturbances in the electrical system are particularly important since it has been reported that they can limit shaft life due to fatigue, see, for example, Walker *et al.* (1975), Walker *et al.* (1981) and Joyce *et al.* (1980).

Cudworth *et al.* (1984) have developed a computational model for a turbo-generator shaft that is very general, and allows a wide variety of fault conditions to be investigated. The electrical system is represented in phase variables and takes into account as many static and rotating electrical elements as may be required. For the mechanical system, the lumped parameter model illustrated in Figure 8.7 is used. The shaft damping and steam damping effects on the turbine blades are represented by variable viscous dampers, and material damping is also included.

The waveform shown in Figure 8.8 is representative of the results achievable using a model, such as the one described above. This shows the oscillations in shaft

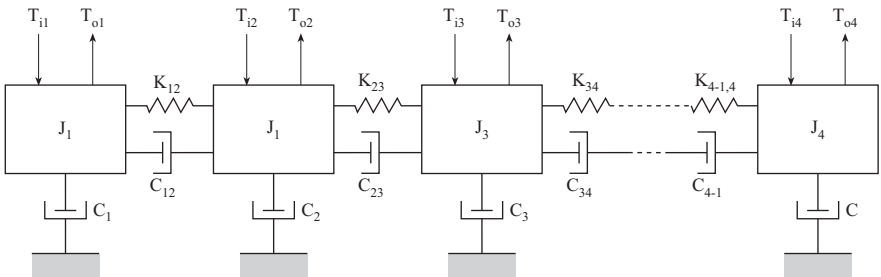


*Figure 8.7 A lumped parameter model to determine torsional response*

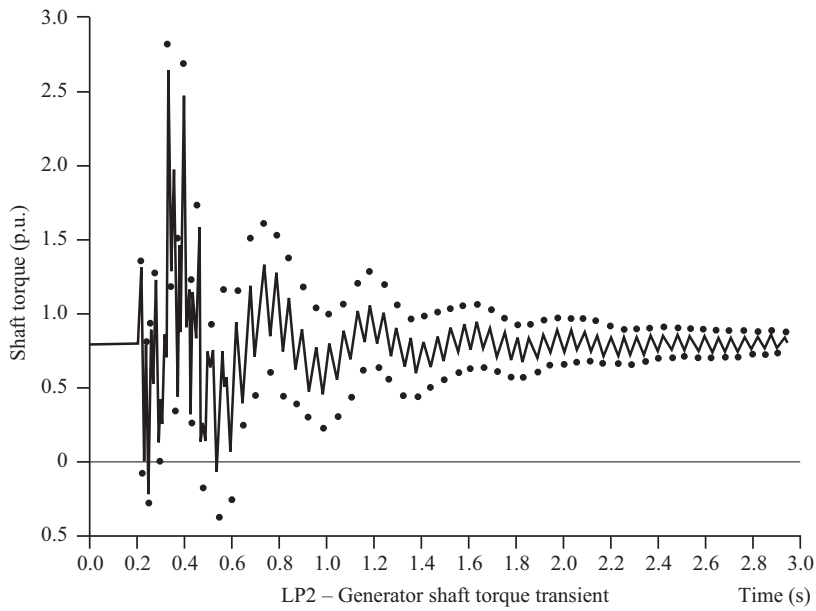


*Figure 8.8 Calculated shaft torque transients using a turbo-generator rotor lumped parameter model, dots show the permissible limits of calculation error*

torque of a 500 MW turbo-generator following a phase-to-phase short circuit on the transmission system. The lower level oscillations persist for some considerable time after the major transient has largely died away and this has obvious implications for the fatigue life of the shaft. It is advisable to monitor such events, and methods for doing so will be discussed later in this chapter.

## 8.5 Bearing response

### *8.5.1 General*

Rotor vibration force is transmitted to the stator via the air-gap magnetic field and the bearings in parallel.

Therefore, it is important to consider the response of the bearings to that vibration force so that its effect is not confused with vibrations generated by faults within the bearings themselves.

Rotor vibration force will cause vibration of the rotor relative to the housing and an absolute vibration of the bearing housing.

This action must be considered for both rolling element bearings and oil-lubricated sleeve bearings.

### *8.5.2 Rolling element bearings*

A schematic view of a typical rolling element bearing is shown in Figure 8.9 and these are fitted to machines of output generally below 300 kW, which constitute the vast majority of electrical machines.

Rolling element bearing failure is the most common failure mode associated with smaller machines. Because of their construction rolling element bearings

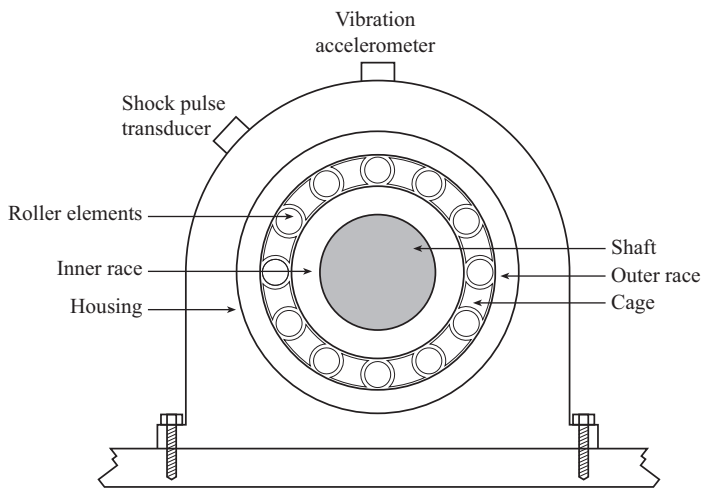


*Figure 8.9 Rolling element bearing assembly*

generate precisely identifiable vibration frequencies. Also, since the oil or grease film is very thin the relative motion between the housing and the shaft is small. It is therefore possible to detect on the stator side the vibrations associated with the bearings using an accelerometer mounted directly on the bearing housing, $\omega_{\mathrm{sm}}$.

The characteristic frequencies of rolling element bearings depend on the geometrical size of the various elements, and can be found in many texts; see Collacott (1979), for example. Table 8.1 summarises these frequencies and their origins.

Besides the frequencies given in Table 8.1, there will also be higher frequencies generated by elastic deformation of the rolling elements themselves, and the excitation of the natural modes of the rings that comprise the inner and outer races. These effects will, however, be secondary to the principal components defined here. The magnitudes of the components given in Table 8.1 are often lost in the general background noise when the degree of damage is small, but because of their precise nature they present an effective route for monitoring progressive bearing degradation. A simple instrument can be devised using an accelerometer mounted on the bearing housing to detect the amplitude of vibration at these characteristic frequencies. Once the characteristic frequencies have been calculated, it is possible to enhance the performance of the instrument by the use of highly selective filters and weighting functions, so as to be able to identify bearing faults at an earlier stage.

When monitoring the vibration due to rolling element bearings it is prudent to obtain a good vibration baseline. This is because once the bearing becomes worn

*Table 8.1 Characteristic transverse mechanical angular frequencies produced by rolling element bearings*

| **Fault** | **Stator transverse mechanical frequency, $\omega_{\mathrm{sm}}$ (rad/s)** | **Comments** |
|---|---|---|
| Outer race | $\omega_{\mathrm{sm}} = \frac{n_b}{2} \cdot \omega_{\mathrm{rm}} \cdot \left(1 - \frac{d_b}{D_b}\cos\varphi\right)$ | Rolling element passing frequency on the outer race |
| Inner race | $\omega_{\mathrm{sm}} = \frac{n_b}{2} \cdot \omega_{\mathrm{rm}} \cdot \left(1 + \frac{d_b}{D_b}\cos\varphi\right)$ | Rolling element passing frequency on the inner race |
| Rolling element | $\omega_{\mathrm{sm}} = \frac{D_b}{2d_b} \cdot \omega_{\mathrm{rm}} \cdot \left(1 - \left(\frac{d_b}{D_b}\right)^2 \cos^2\varphi\right)$ | Rolling element spin frequency |
| Train fault | $\omega_{\mathrm{sm}} = \frac{1}{2} \cdot \omega_{\mathrm{rm}} \cdot \left(1 - \frac{d_b}{D_b}\cos\varphi\right)$ | Caused by an irregularity in the train |

**Definitions**

$n_b$ = number of rolling elements
$\omega_{\mathrm{rm}} = \frac{2\pi N}{60}$ mechanical rotational frequency (Hz)
$\omega_{\mathrm{sm}}$ = mechanical vibration frequency on the stator side
$N$ = rotational speed (rev/min)
$d_b$ = rolling element diameter
$D_b$ = rolling element pitch
$\phi$ = rolling element contact angle with races

significantly the vibration spectrum it emits becomes more random again, although at a higher baseline than for a good bearing. If no baseline is available and no history has been built up and the background noise has risen, then it will be impossible to detect specific faults.

Machinery will also have a degree of unbalance, which will modulate the characteristic frequencies of the bearings and produce side-bands at the rotational frequency. Vibration monitoring is highly suitable for rolling element bearings, although it is complex but has gained wide acceptance throughout the industry. See Stack *et al.* (2004) for a description of the process to classify rolling element bearing faults.

### *8.5.3 Sleeve bearings*

In sleeve bearings, the shaft is supported by a fluid film pumped, by the motion of the shaft, at high pressure into the space between the bearing liner and the shaft. Because of the compliance of the oil film and the limited flexibility of the bearing housing, vibrations measured at the housing may be of low amplitude. Also, because the liners of the bearing will inevitably be a soft material such as white metal, small faults are very difficult to identify by measuring the absolute vibration of the housing. These factors point to the use of displacement transducers as being the most effective tool, but they will only be useful at the lower frequencies. Higher frequencies, for example, multiples of the rotational frequency, are best measured with an accelerometer mounted on the bearing housing.

It is worth bearing in mind, however, that as the bearing load increases, due to an increase in rotor load, the oil film thickness decreases with a commensurate decrease in bearing flexibility. This increases the vibration detectable at the bearing housing and allows more information to be derived from the measurement.

An important concern for sleeve bearings is the onset of instability in the oil film. This can result in oil whirl and subsequently oil whip, in response to unusual loading of the bearing. Figure 8.10 shows the forces acting upon the shaft in a sleeve bearing, and illustrates that the shaft is supported by a wedge of oil just at the point of minimum clearance.

The oil film is circulating at a speed of approximately half the shaft speed, but because of the pressure difference on either side of the minimum clearance point, the shaft precesses at just below half speed. This motion is termed oil whirl and is a direct result of the pressure difference mentioned above, which comes about due to viscous loss in the lubricant. Instabilities occur when the whirl frequency corresponds to the natural frequency of the shaft.

Under such conditions, the oil film may no longer be able to support the weight of the shaft. Details of the mechanisms involved in oil whirl, and its development into the more serious instability called oil whip, which occurs when the shaft speed is twice its natural frequency, are given by Ehrich *et al.* (1984). Care must be taken, therefore, that either the machine does not operate at a speed higher than twice the first critical speed of the rotor shaft, or if it must, then oil

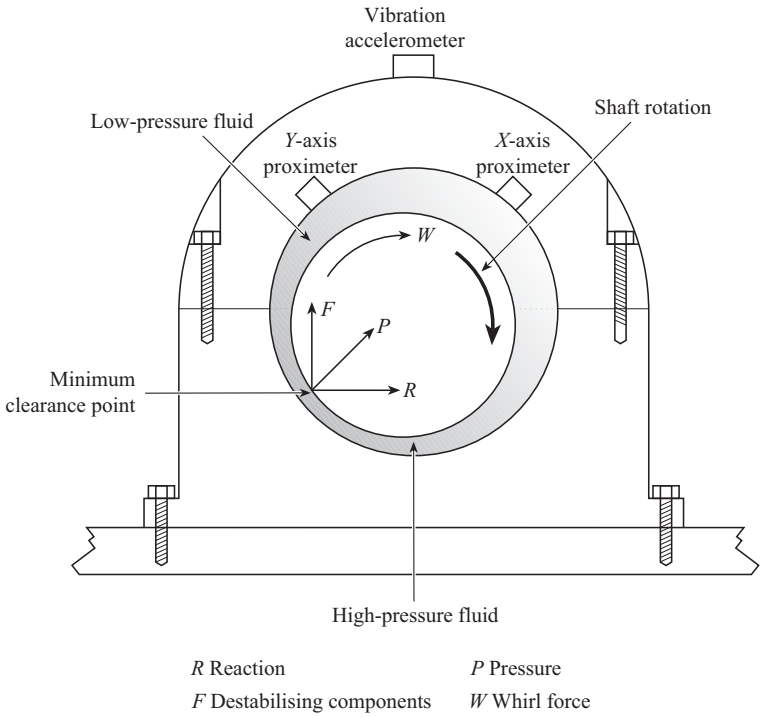


*Figure 8.10 Forces acting upon a shaft in a sleeve bearing*

whirl must be suppressed. The following frequency, $\omega_{sm}$, is identified in the literature as caused by oil whirl:

$$\omega_{sm} = (0.43 \text{ to } 0.48)\omega_{rm} \tag{8.33}$$

## 8.6 Monitoring techniques

Now that we have discussed the ways in which transverse and torsional vibration can be produced in electrical machines, and we have outlined, in Chapter 3, the principal analytical tools at our disposal to measure the effect of vibration, we can proceed to show how vibration can be used to monitor the health of machines.

For electrical machine CM, it is important to recognise that mechanical and electrical faults excite the machine structure in different ways. For example,

- Mechanical faults like self-weight, mechanical unbalance and shaft whirling will excite transverse motion in the machine frame, detectable by vibration sensors.

- Dynamic or static electromagnetic UMP due to eccentricity, which may be caused by bearing wear, will also excite transverse motion in the machine frame, detectable by vibration sensors.
- Electrical faults in stator or rotor windings will excite torsional motion in the shaft that will be detectable in the torque signal but not necessarily by vibration sensors, unless the activity is coupled to transverse motion by asymmetries in the machine frame.

Because many faults can be identified by more than one method, and because the internationally agreed standards and limits relate not to specific items of plant, but to the form of analysis to which measurement is subjected, we shall use the measurement treatment as the generic identifier. We shall also be principally concerned with so-called online monitoring, that is, we are interested in techniques that can be applied to machinery that is running and in the predictive power of the monitoring rather than simply the ability to merely intercept faulty conditions when they become serious enough to cause damage. There may often be some commonality between these objectives.

### *8.6.1 Overall level monitoring*

This simple form of monitoring is the most commonly used technique, although as an aid to diagnosis of faults in electrical machines its efficacy is limited. The measurement taken is simply the rms value of the vibration level on the stator side of the machine over a selected bandwidth. The usual bandwidth is 0.01–1 kHz, or 0.01–10 kHz, and in practice the measured parameter is usually vibration velocity taken at the bearing cap of the machine under surveillance. The technique has found favour because over the years a considerable experience has been built up to relation overall vibration monitoring levels to machinery failure modes. This has resulted in the publication of recommended vibration standards for running machinery. These standards do not give diagnostic information, but simply indicate the overall health of machinery at a given vibration level. Many operators use such information to develop a strategy for maintenance scheduling.

The guidance given in the past by the German Vibration Standard VDl 2056 is illustrated below in Table 8.2, however the relevant up-to-date standard is ISO 10816-1:1995. These criteria are based solely on machine rating and support systems, and utilise a 0.01–1 kHz bandwidth. Essentially it recommends that when vibration levels change by 8 dB or more care must be exercised, and when the change exceeds 20 dB action should follow. These limits can be relaxed, however, if a subsequent frequency analysis shows that the cause of the increase in level is due to a rise in the higher frequency components. In such cases, changes of 16 and 40 dB, respectively, may be more appropriate. A section of the specification, as it relates to electrical machines, is given in Table 8.3. Group K signifies smaller, quiet running plant, Group M is medium-sized plant and Group G is the larger, noisier plant.

This reflects that electrical machines, when uncoupled from their prime mover or driven plant, are generally low-noise, low-vibration machines.

*Table 8.2 Vibration standard VDl 2056*

| Vibration velocity (mm/s rms) | Vibration velocity (dB, ref $10^{-6}$ mm/s) | Group K, smaller, quiet running plant | Group M, medium-sized plant | Group G, larger, noisier plant |
|---|---|---|---|---|
| 45 | 153 | Not permissible | Not permissible | Not permissible |
| 28 | 149 | | 20 dB (×10) | |
| 18 | 145 | | | |
| 11.2 | 141 | | | Just tolerable |
| 7.1 | 137 | | Just tolerable | |
| 4.5 | 133 | Just tolerable | | Allowable |
| 2.8 | 129 | | Allowable | |
| 1.8 | 125 | Allowable | | Good |
| 1.12 | 121 | | Good | Large machines with rigid and heavy foundations whose natural frequency exceeds machine speed |
| 0.71 | 117 | Good | Medium machines 15–75 kW or up to 300 kW on special foundations | |
| 0.45 | 119 | Small machines up to 15 kW | | |
| 0.28 | 109 | | | |
| 0.18 | 105 | | | |

*Table 8.3 Vibration limits for maintenance as given in CDA/MS/NVSH107*

| Type of plant | New machines | | Worn machines, full-load operation | |
|---|---|---|---|---|
| | 100–1 000 h life (mm/s rms) | 1 000–10 000 h life (mm/s rms) | Service level (mm/s rms) | Immediate overhaul* (mm/s rms) |
| Boiler auxiliaries | 1.0 | 3.2 | 5.6 | 10.0 |
| Large steam turbine | 1.8 | 18.0 | 18.0 | 32.0 |
| Pump drives | 1.4 | 5.6 | 10.0 | 18.0 |
| Motor-generator set | 1.0 | 3.2 | 5.6 | 10.0 |
| Fan drives | 1.0 | 3.2 | 5.6 | 10.0 |
| Motors in general | 0.25 | 1.8 | 3.2 | 5.6 |

*These levels must not be exceeded in any octave band.

Another useful set of criteria was given in the Canadian Government Specification CDA/MS/NVSH107, no longer issued. This specification relates primarily to measurements taken on bearings, and it is here that overall level measurement is most commonly employed. This specification has a broader bandwidth than VDl 2056, namely 0.01–10 kHz, but still relies on the overall velocity vibration measurement.

The strength of the overall vibration level technique is its simplicity. It requires only the simplest of instrumentation applied to the stator side of the machine, and

because of this it is a common feature in many installations. It also provides an ideal method for use with portable instruments, but it makes heavy demands upon technical personnel. The sensitivity of the technique is also low, particularly when a fault is at an early stage, and there is little help on offer to aid diagnosis without further sophisticated techniques being employed.

Neale (1973) indicates that it may be possible to affect a limited diagnosis by taking two overall level measurements, $V_a$, the peak vibration velocity in mm/s and $X$ the peak to peak displacement in μm. These quantities are then used to define the parameter, $F$, as follows:

$$F = \frac{0.52NX}{V_a} \tag{8.34}$$

where $N$ is the speed in rev/min of the machine. Then the interpretations in Table 8.4 are appropriate.

### 8.6.2 Frequency spectrum monitoring

The key to vibration monitoring diagnostics is the frequency spectrum of the signal, and the past decades has seen a remarkable increase in the range and sophistication of techniques and instrumentation available for spectral analysis.

There are various levels of spectral analysis commonly used, and these may be regarded as a continuum extending from the overall level reading to the narrow band with constant frequency bandwidth presentation, as shown in Figure 8.11.

In the octave band and 1/3 octave band techniques, the spectrum is split into discrete bands, as defined by Figure 8.12. The bands are, by definition, such that when the frequency is scaled logarithmically the bands are of equal width. The constant percentage band is one which is always the same percentage of the centre frequency, whilst the constant frequency bandwidth is an absolutely fixed bandwidth form of analysis that can give very high resolution, provided the instrumentation is of a sufficiently high specification.

The effect that the change of bandwidth has on the processed signal output highlights precisely why the narrow band technique is superior to the overall level technique as a diagnostic tool. For example, a certain transducer may provide an output PSD that may be interpreted in the ways shown in Figure 8.13. It is apparent that the components around frequency $f_1$ dominate the overall level reading, and the shape of the 1/3 octave result. Important changes, say at $f_2$ and $f_3$ or the presence of other components, could go largely unnoticed, except by the use of narrow band

*Table 8.4 Diagnosis using the overall level measurements based on Neale*

| Value of $F$ | Trend | Fault |
|---|---|---|
| $F < 1$ | Decreasing | Oil whirl |
| $F = 1$ | Steady | Unbalance, indicative of eccentricity or perhaps faulty rotor |
| $F > 1$ | Increasing | Misalignment, static eccentricity |

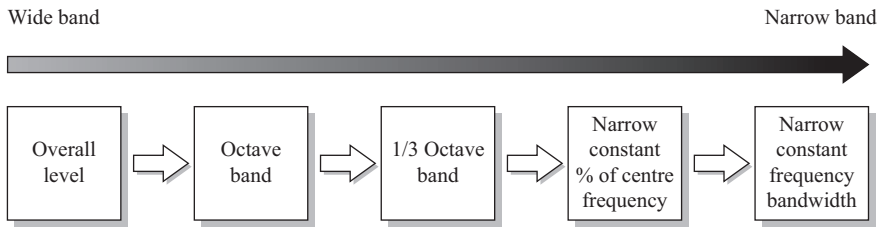


*Figure 8.11 Levels of spectral analysis*

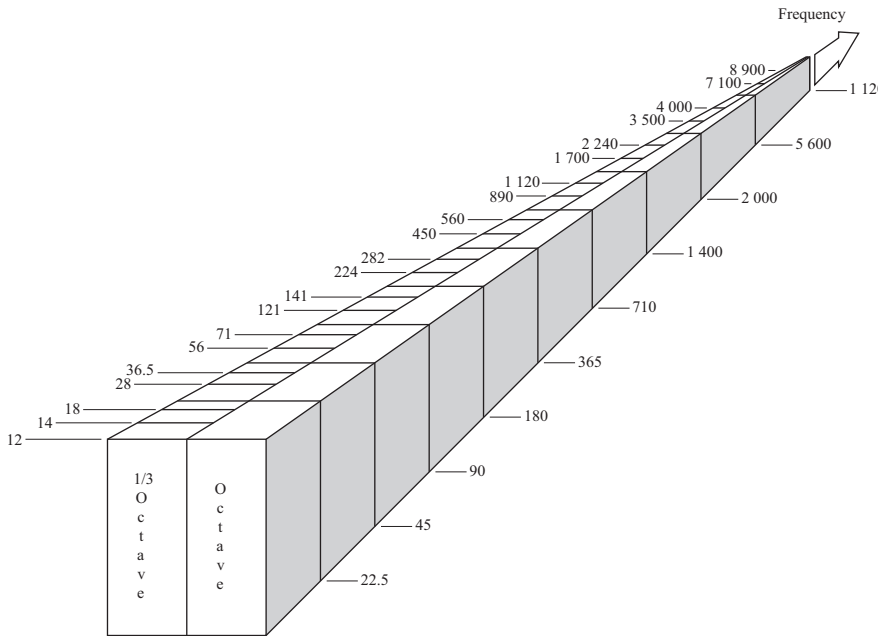


*Figure 8.12 Octave and third octave bands*

methods. This is crucial because the flexibility of the mechanical system may be such that important components are masked by those closer to resonances in the mechanical structure of the machine.

The narrow band spectrum also allows the operator to trend the condition of the machine most effectively. This requires that an initial baseline spectrum is taken and subsequent spectra are compared with it. The use of digitally derived spectra means that the results of such comparisons can be computed quickly since the spectra reduce to a simple sequence of numbers at discrete frequencies, as closely spaced as required within the limitations of the instrumentation. In this way, criteria such as VDl 2056 can be applied for each frequency. Because of the large amounts of data generated using narrow band methods, it is frequently convenient

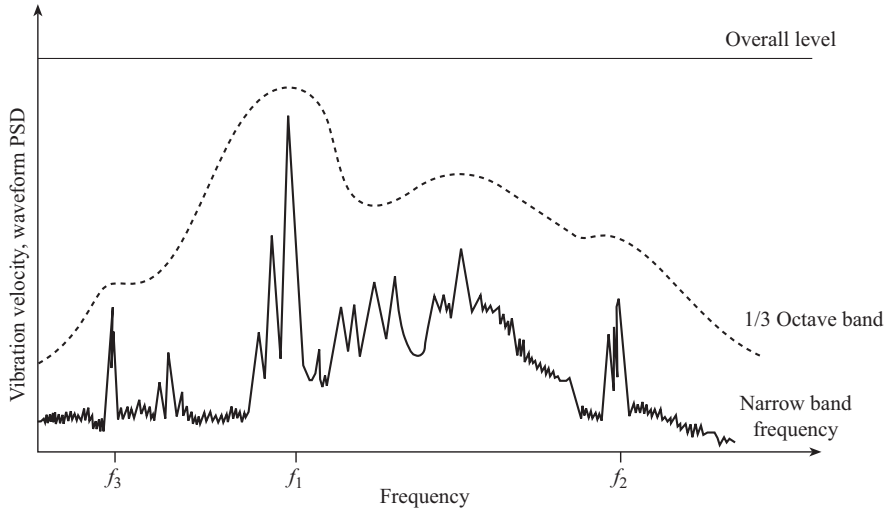


*Figure 8.13 Effect of change in bandwidth on the spectral response*

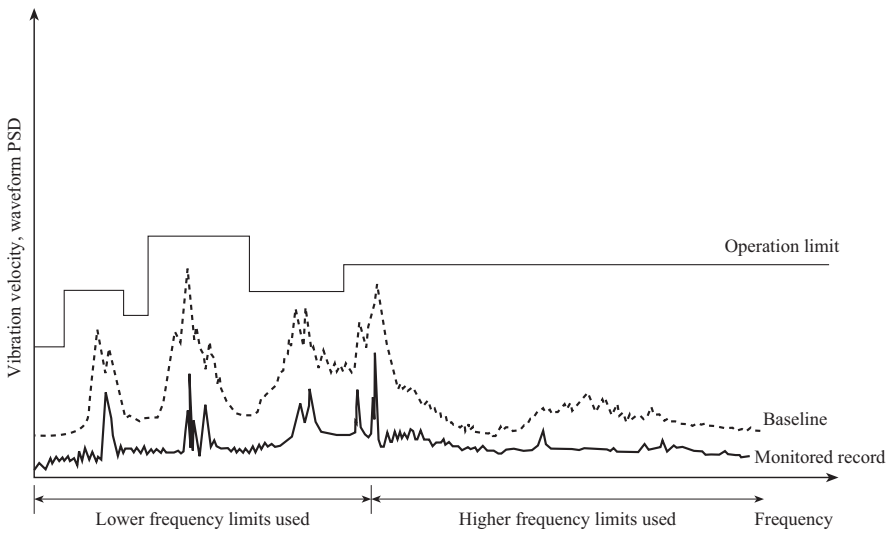


*Figure 8.14 Operational envelope around a spectral response*

to predetermine the operational limits, on the basis of one of the vibration standards, and to construct an operational envelope around the baseline spectrum. This can take account of the wider limits allowable at higher frequencies, and can be used to automatically flag warnings when maintenance limits are reached. The basis of this technique is illustrated in Figure 8.14, where the baseline is set at the

maximum value of vibration expected and the operational envelope at which trips are initiated, is set above this. The techniques described thus far, in this section, are relatively general. In order to identify not just unsatisfactory overall performance, but to pinpoint specific problems, it is necessary to examine discrete frequencies, or groups of frequencies, as indicated earlier in this chapter. Induction motors in particular require a high degree of frequency resolution applied to their vibration signals since the speed of rotation is close to the electrical supply frequency. This tends to generate side-bands spaced at $s$ and $2s$ around the harmonics of the supply frequency, where $s$ is the slip frequency of the machine.

The application of vibration monitoring for fault diagnosis in large turbo-generators has been described by Mayes (1994) and computer analysis techniques that can be applied offline to vibration data collected online are described by Herbert (1986), some of the detail of analysis and the effect of the foundation response to the machine excitation is given by Smart *et al.* (2000).

### *8.6.3 Faults detectable from the stator force wave*

Using the techniques in the previous section and verifying by measurement, it has been shown that UMP can excite stator side vibration components at 1, 2, and 4 times the supply frequency. Dynamic unbalance and coupling misalignment also produce this effect; see Rai (1974) and Dorrell *et al.* (1997).

The last reference also suggests that even orders of the fundamental occur in the frame vibration spectrum due to inter-turn winding faults on the stator. Dorrell *et al.* (1997) use the principal slot harmonics as an indicator of eccentric running. They use the transverse mechanical angular frequency, $\omega_{\mathrm{sm}}$, measured on the stator frame, excited by radial forces, given by Yang (1981) and others as:

$$\omega_{\mathrm{sm}} = \omega_{\mathrm{se}}\left[(nN_r \pm k_e)\frac{(1-s)}{p} \pm q\right] \tag{8.35}$$

where

$n$ = an integer,
$q$ = space harmonic of the stator winding MMF, 1, 3, 5, 7, ...,
$k_e$ = the so-called eccentricity order number, which is zero for static eccentricity and a low integer value for dynamic eccentricity.

They report tests on a machine with a 51 slot rotor ($N_r$) and a 4-pole, 3-phase stator, which exhibits an increase in frame vibration levels of 25 and 17 dB at the frequencies 1 104 and 1 152 Hz due to the introduction of 50% dynamic eccentricity.

There are strong indications that frame vibration can be used to monitor a variety of fault conditions, particularly in induction machines. Caution must be exercised, however, for vibration transmitted from adjacent, or coupled, plant may excite a natural mode in the machine, while a forced component from a fault within the machine may be sufficiently different from any natural frequency to cause only a slight response.

This effective signal-to-noise ratio for the detection of faults by frame-borne vibration can be quantified using the notion of system flexibility, or mobility, the flexibility being regarded as the sum of the modal responses of the machine, and the vibration experienced by the machine is the product of the exciting force wave and this flexibility. See Smart *et al.* (2000) for an explanation of the interaction of the foundation response of a turbo-generator to the exciting effect of unbalance during a rundown.

A number of authors have reported the identification of various vibrational frequencies associated with faults in induction machines, including Rai (1974), Hargis *et al.* (1982), Dorrell *et al.* (1997) and Nandi *et al.* (2005). It has been suggested that, on a machine supplied at $f_{se} = 50$ Hz, vibration at or near 50, 100 and 200 Hz is indicative of eccentricity, but the picture is confused because other anomalies also manifest themselves by the production of such frequencies, for example, misalignment and dynamic unbalance. Dorrell *et al.* (1997) showed that on a machine supplied at $f_{se} = 50$ Hz, the stator frame vibration will exhibit 100, 200, and 300 Hz components due to an inter-turn winding fault or supply voltage unbalance, including single phasing. They also show that higher order harmonics occur in the stator frame vibration, due to eccentricity, as derived from (8.35). However, the exact arrangement of the drive, and the nature of the coupled load, may be of critical importance, since transmitted vibration may mask the frequency that one is hoping to measure.

Vibration can occur in electrical machinery as a result of both electrical and mechanical action. Finally, Trutt *et al.* (2001) carried out a theoretical review of the relationships that should exist between electrical winding parameters and the mechanical vibration of AC machine elements under normal and faulted operating conditions.

Table 8.5 has been compiled to distil the information to be found in these various references.

### *8.6.4 Torsional oscillation monitoring (IAS)*

As we have seen previously in Section 8.4.2, there may be a specific need to monitor the torsional behaviour of a long thin shaft such as on a turbo-generator. The direct approach to this problem would be to mount suitable strain gauges on the shaft, together with suitable telemetry, to transmit the gauge output from the rotating reference frame. This has only been done for experimental purposes and is not appropriate for long-term use due to the harsh operational conditions the transducers would need to withstand. An indirect method of monitoring the torsional responses of shafts have been outlined by Walker *et al.* (1981), in which the twist of the shaft system is measured by comparing the angular displacement of the non-drive end of the high-pressure turbine shaft with that of the non-drive end of the generator exciter. The air-gap torque produced by the machine is calculated directly from the monitored electrical quantities. The monitor has a modular construction, the two principal elements being concerned with the capture of the mechanical, or torque transient and electrical transient. The torque transient capture

*Table 8.5 Mechanical frequency components related to specific machine faults*

| | | Rotational angular frequency of the rotor, $\omega_m$ (rad/s) | Transverse vibration angular frequency on the stator, $\omega_{sm}$, rad/s | Comments |
|---|---|---|---|---|
| **Mechanical faults** | Oil whirl and whip in sleeve bearings | – | $\omega_{sm} = (0.43 \text{ to } 0.48)\omega_{rm}$ | Equation (8.33). Pressure-fed lubricated bearings only. |
| | Damage in rolling element bearings | – | $\omega_{sm} = \frac{n_b}{2} \cdot \omega_{rm} \cdot \left(1 - \frac{d_b}{D_b}\cos\varphi\right)$<br>$\omega_{sm} = \frac{n_b}{2} \cdot \omega_{rm} \cdot \left(1 + \frac{d_b}{D_b}\cos\varphi\right)$<br>$\omega_{sm} = \frac{D_b}{2d_b} \cdot \omega_{rm} \cdot \left(1 - \left(\frac{d_b}{D_b}\right)^2 \cos^2\varphi\right)$<br>$\omega_{sm} = \frac{1}{2} \cdot \omega_{rm} \cdot \left(1 - \frac{d_b}{D_b}\cos\varphi\right)$ | Common source of vibration. Also frequencies in the range 2–60 kHz due to element resonance. Rolling element bearing faults can also be diagnosed by the shock pulse method. |
| | Static misalignment of rotor shaft in a synchronous machine | $\omega_{rm} = \omega_{se}/p$ | $\omega_{sm} = 2p\omega_{rm}$ | Causes static eccentricity. |
| | Unbalanced mass on the rotor of a synchronous machine | | $\omega_{sm} = \omega_{rm}$ | Very common. Unbalance causes dynamic eccentricity of the rotor, see below. |
| | Dynamic eccentricity in a synchronous machine | | $\omega_{sm} = \omega_{rm}$ | Dynamic eccentricity causes UMP in an electrical machine. |
| | Dynamic displacement of shaft in bearing housing in a synchronous machine | | $\omega_{sm} = \omega_{rm}, 2\omega_{rm} \ldots$ | Causes dynamic eccentricity. Generates a clipped time waveform, due to shaft motion being limited by bearing constraint, therefore produces a high number of harmonics. |

*(Continues)*

*Table 8.5* (*Continued*)

| | | Rotational angular frequency of the rotor, $\omega_m$ (rad/s) | Transverse vibration angular frequency on the stator, $\omega_{sm}$, rad/s | Comments |
|---|---|---|---|---|
| | General expression for static and dynamic eccentricity in an induction machine | $\omega_{rm} = (1 - s)\, n\omega_{se}/p$ | $\omega_{sm} = \omega_{rm}[(nN_r \pm k_e)(1 - s) \pm pk]$ | Equation (8.35). Side-bands at plus or minus slip frequency may occur and components due to UMP, see above. |
| | Commutator faults in a DC machine | – | $\omega_{sm} = 2pk_c\, \omega_{rm}$ for lap wound $\omega_{sm} = 2k_c$ $\omega_{rm}$ for wave wound | Unbalanced rotor components also generated. |
| **Electrical faults** | Broken rotor bar in an induction machine | $\omega_{rm} \pm \frac{2ns\omega_{se}}{p}$ | $\omega_{sm} = \left(\omega_{rm} \pm \frac{2ns\omega_{se}}{p}\right)$ | Difficult to detect because of the small amplitude. Current, speed or leakage field have better detection levels. |
| | Stator winding faults induction and synchronous machines | – | $\omega_{sm} = p\omega_{rm}$ , $2p\omega_{rm}$, $4p\omega_{rm}$ … | Problems can be identified as of electrical origin by removing supply and identifying change. Cannot differentiate winding fault types on vibration alone, current monitoring also necessary. |

**Definitions**

$\omega_{sm}$= mechanical vibration frequency on the stator side
$\omega_{se}$ = electrical supply frequency
$N_r$ = integer number of rotor slots
$N$ = rotational speed in rev/min
$f\omega_{rm} = \frac{2\pi N}{60}$ mechanical rotational frequency, Hz
$\omega_{rm} = \omega_{se}/p$ for a synchronous machine
$\omega_{rm} = (17-s)\omega_{se}/p$ for an asynchronous machine
$s$ = asynchronous machine rotor speed slip, 0–1

$p$ = pole pairs
$n$ = an integer,
$k_e$ = eccentricity order, zero for static eccentricity, low-integer value 1, 2, 3 … for dynamic eccentricity
$k$ = space harmonic of the stator winding MMF, 1, 3, 5, 7…
$n_b$= number of rolling elements
$d_b$ = rolling element diameter
$D_b$ = rolling element pitch
$\phi$ = rolling element contact angle with races
$k_c$ = number of faulty commutator segments

unit is triggered by any sudden increase in the air-gap torque, or by sudden changes in the shaft angular vibration velocities. Similarly, the electrical transient is captured in response to any sudden change in the value of the line currents. The captured data can then be transmitted for further analysis and evaluation, Figure 8.15 refers. The software receives the captured data and determines the torsional response of the shaft and the associated impact on the fatigue life of the set. The results obtained in this way can be used to plan maintenance intervals on the basis of need, rather than risk catastrophic failure when there has been a high level of system disturbances between fixed outages.

The monitoring of torsional oscillations can also be used to detect faults in induction motors. The speed of an induction motor driving an ideal load should be constant. Perturbations in load and faults within the rotor circuit of the machine will cause the speed to fluctuate. If the rotor is defective the speed fluctuation will occur at twice slip frequency. This is because the normally torque-producing slip frequency currents that flow in the rotor winding are unable to flow through the defective part. In effect the speed fluctuations complement the twice slip frequency current fluctuation described in Chapter 9. A defective induction machine with a rotor of infinite inertia will have twice slip frequency current fluctuations and no speed variation, whereas a low-inertia rotor will exhibit speed fluctuations but no current fluctuation. This method developed by Gaydon was reported by Tavner *et al.* (1986) and has been investigated further as the instantaneous angular speed method (IAS) by Ben Sasi *et al.* (2004), a typical measurement result being shown in Figure 8.16.

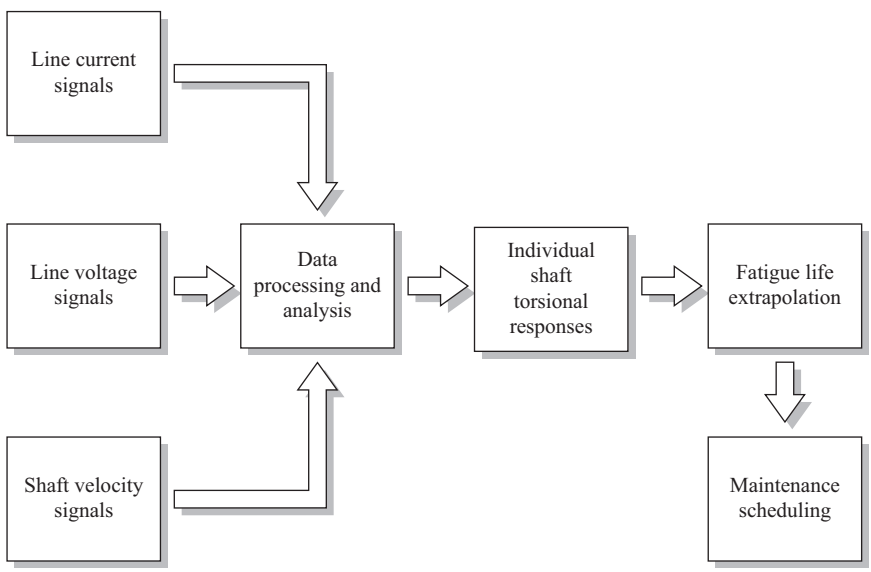


*Figure 8.15 Functional description of the torsional oscillation monitoring system*

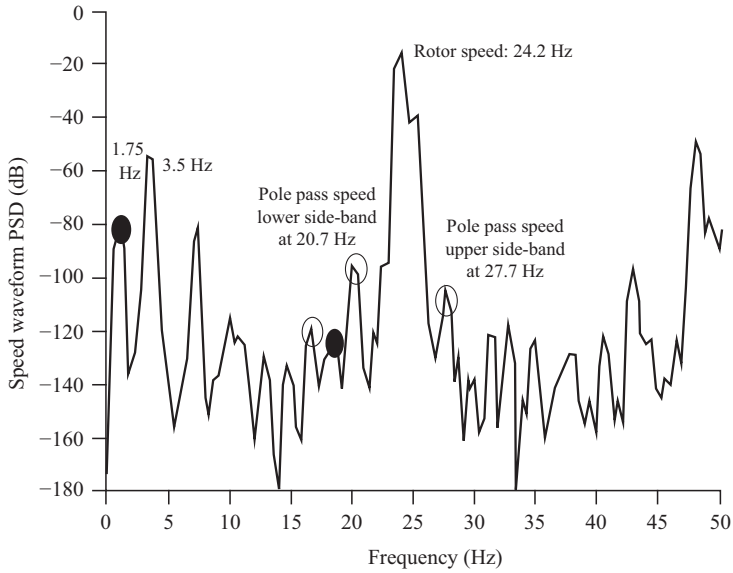


*Figure 8.16 Rotor speed spectrum (IAS) from an induction motor with a rotor bar fault. Taken from Ben Sasi et al. (2004)*

This work has been added to recently by Shahriar *et al.* (2018), who detected machine rolling element bearing faults by the detailed analysis of both IAS and MCSA, proposing the former as effective for detecting rolling element defects, see Figure 8.17 but note the very small amplitude of the detection signals, which would be an enormous problem for machine operators.

### *8.6.5 Shock pulse monitoring*

The shock pulse method is used exclusively for detecting faults in rolling element bearings and is based on the principles described in Section 8.5.2. Since the largest proportion of electrical machine failures are ascribable to bearing problems, see Chapter 3, and the majority of machines are smaller than 300 kW then this technique is important for a large number of machines. As a rolling element bearing deteriorates, the moving surfaces develop small pits or imperfections and the interaction between such surfaces generates mechanical stress waves, or shock pulses, in the bearing material, which propagate into the frame and structure of the electrical machine. These shock pulses are at ultrasonic frequencies and can be detected by piezoelectric transducers with a strong resonant frequency characteristic tuned to the expected frequency of the pulses at around 32 kHz. To increase the sensitivity of the electronic conditioning of the transducer is tuned to this resonant frequency. A peak hold circuit enables the maximum value of the shock pulse to be recorded, which is taken to be a measure of the condition of the rolling

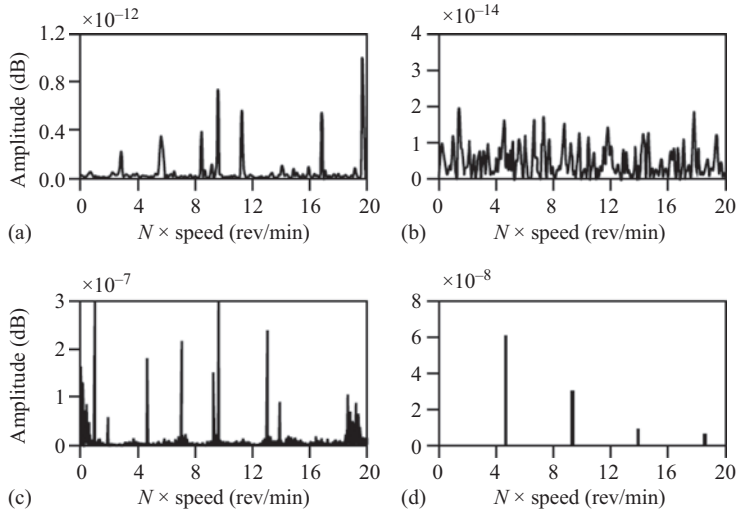


*Figure 8.17 IAS detection of induction motor rolling element bearing defects from Shahriar et al. (2018): (a) small defect at 6 rev/min, (b) small defect at 120 rev/min, (c) large defect at 6 rev/min and (d) large defect at 120 rev/min*

element bearing. This condition of the bearing is assessed by defining a quantity known as the shock pulse value, SPV, defined as:

$$\text{SPV} = \frac{R}{N^2 F^2} \tag{8.36}$$

where $R$ = the shock pulse meter reading,

$N$ = shaft speed in rev/min,
$F$ = factor relating to bearing geometry.

Low values indicate bearings in good condition. Generally the technique is best used in conjunction with the overall vibration level monitoring, and Table 8.6 can be used to give qualitative guidance on the bearing condition.

Tandon *et al.* (1992, 2007) describe the development of rolling element bearing monitoring including vibration, acoustic and shock pulse methods. There is a technique for assessing the thickness of the oil or grease film in the rolling element bearing, based on the experimental evidence that the shock pulse value increases, in approximately the manner shown in Figure 8.18, as a function of the percentage of dry contact time per revolution. The dry contact time was measured by monitoring current flow between the inner and outer races of a test bearing and current flow taken as an indication of dry contact.

Stack *et al.* (2004) classify motor bearing faults illustrating the unpredictable and broadband nature of the effects produced, emphasising its significance, because a

*Table 8.6 Shock pulse interpretation*

| Overall vibration level trend | Shock pulse value trend | Comments |
|---|---|---|
| Low and rising | Remains low | No bearing damage |
| Low and rising | Low but rising at the same rate as the overall vibration level | Bearing damage likely |
| Low and rising | High value but constant | Bearing damage but another problem is causing rising vibration |

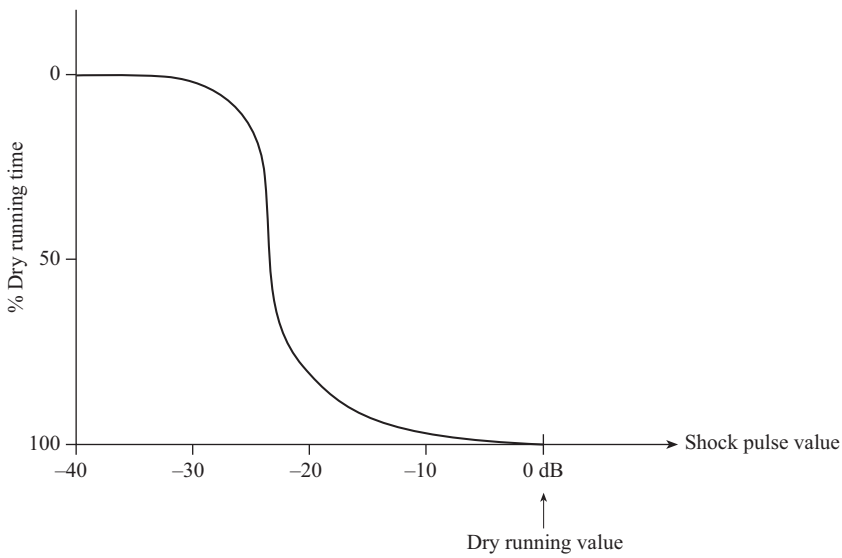


*Figure 8.18 Shock pulse value as a function of dry running time per revolution*

successful bearing CM scheme must be able to reliably detect all classes of faults. So, the quantitative evaluation of bearings using the shock pulse method remains difficult.

## 8.7 Conclusions

Vibration and associated mechanical measurement has been at the heart of rotating machine monitoring. However, electrical machines are generally low-vibration devices, yet they may be coupled to high-vibration prime movers or driven plant via flexible couplings and mounted on separate foundations via resilient mounts. The excitation of electrical machine vibration is generally mechanical unbalance or harmonic electromagnetic forces originating from the machine

air-gap. The response of the machine to these exciting forces depends on the precise coupling and mounting of the machine.

Vibration monitoring and shock pulse analysis are non-invasive but use a number of specialised sensors and broad bandwidth, complex analysis. The precise selection and location of sensors is very important.

However, because of its wide application in other rotating machines vibration analysis has established itself as a reliable and widely accepted technique for electrical machines and shock pulse analysis also, particularly for bearings, because it is capable of differentiating between mechanical and electromagnetic excitation forces and this is invaluable in detecting root causes before they develop into failure modes. Motor speed has been analysed using IAS to detect rotor electrical faults but has not been widely used by the operators.

The following chapters will show the close relation between vibration and electrical monitoring of the machine.

*This page intentionally left blank*

*Chapter 9*

# Online current, flux and power monitoring

## 9.1 Introduction

Chapter 1 explained that electromechanical protective relays were the earliest electrical technique for monitoring motors. The technology of these devices is dated, their purpose was exclusively to detect gross perturbations in the electrical quantities at the terminals of the machine to protect against catastrophic damage. They are now largely being replaced by digital protection devices detecting the voltage and current perturbations, as described in Chapter 1, see Figure 1.2.

Within the machine, the magnetic flux varies, circumferentially in the air-gap, periodically in space and, for an AC machine, periodically with time, as described in Chapter 8. Under ideal conditions, this magnetic flux waveform will be symmetrical but electrical faults in the machine will distort it. Rotor faults could be detected by the electrical sensors fixed to the rotor, and stator faults could be detected by electrical sensors fixed to the rotor. Faults on either rotor or stator disrupt the radial and circumferential patterns of flux in the machine causing changes to the power being fed to the machine, which can detected via its terminal 'performance' quantities, voltage, current and power, measured outside the machine to give an indication of its condition. Each disturbance probably represents a power of <mW, but they do indicate the health of the machine and affect its operation. In effect monitoring, these disturbances are a detailed more and prolonged process than can be detected by a digital protection relay.

In the following sections, we describe a number of these techniques.

## 9.2 Generator and motor stator faults

### *9.2.1 Generator stator winding insulation detection*

The most significant technique in this area is online discharge detection, which is dealt with in Chapter 11.

### *9.2.2 Stator current monitoring for stator faults*

This work, mostly concerned with motors, is connected to the earlier work described in Chapter 8 on the effect of faults on vibration, which also considered rotor eccentricity but now extended to consider stator winding faults, see the works

by Rai, R. B. (1974), Schlake *et al.* (1981), Hargis *et al.* (1982), Hargis (1983), Dorrell *et al.* (1997) and Nandi *et al.* (2005). This work is also closely associated with the detection of rotor winding faults described in Section 9.4.3. The theoretical work, verified by laboratory experiments, was started by Penman *et al.* (1994) and continued with Penman *et al.* (1996), who concentrated primarily on stator winding faults.

Thomson *et al.* (1998) and Thomson *et al.* (1999) then took up the practical application of this work to machines in industrial applications but with the particular intention to detect rotor eccentricity, which could indicate the deterioration of machine bearings, one of the common failure modes of electrical machines, set out in Chapter 3.

### *9.2.3 Brush-gear fault detection*

Brush-gear, in those machines that use it, requires a steady maintenance commitment if good performance with minimum of sparking is to be maintained. Poor performance can be detected by measuring brush or brush-holder temperature, but a more direct method would be to detect the radio frequency energy generated by sparking, as described by Michiguchi *et al.* (1983). They used a wide bandwidth dipole antenna connected to an RF amplifier with a bandwidth from 10 to 100 MHz, the output of which was rectified and the processing electronics measured the area under any pulses of RF power that enter the monitor as a result of sparking activity at the brushes. The monitor thereby produces a chart record showing the average area of sparking pulse and Michiguchi *et al.* (1983) related this to a spark number indicating an intensity of sparking. Maintenance staff can use this indication to decide when brushes should be changed.

### *9.2.4 Rotor-mounted search coils*

We have not found any techniques reported for detecting stator faults by search coils mounted upon the rotor. No doubt the usefulness of this technique would be affected by the need to mount expensive instrument slip rings on the rotor, however that could be mitigated by modern work, see Kumar *et al.* (2018), to extract the signals from the rotor by wireless technology. Its effectiveness will be limited by the reliability of the measurement equipment, which from experience measuring shaft voltages, as will be described in this chapter, can be notoriously poor.

## 9.3 Generator rotor faults

### *9.3.1 General*

The rotors of large turbo-generators are particularly highly rated because of the large mechanical and electrical stresses placed upon them, in particular, the high centrifugal forces on the winding and the relatively high temperatures attained in the winding insulation. Consequently, that part of the machine is particularly prone to faults that, as Chapter 2 has said, tend to develop over a long period of

time. The rotor is also relatively inaccessible both for obtaining signals during running and for removal for repair if a fault is detected. These facts, taken together with the high value of turbo-generator plant, have meant that monitoring techniques for generator rotors have been developed to a high degree of sophistication. Some of the techniques described below are also applicable to smaller output machines, but have yet to become fully accepted.

### *9.3.2 Earth leakage faults on-line*

A single earth leakage fault on a generator rotor winding is not serious in itself, because it cannot cause any damage as the earth leakage current is limited to leakage resistance of the excitation supply. However, if two well-separated earth faults occur then large currents can flow, leading to significant damage to the winding, its insulation and the rotor forging. The aim of a rotor earth fault detector is to apply a DC bias voltage to the rotor winding and monitor the current flowing to the rotor body via an alarm relay, see Figure 9.1(a). If such an alarm occurs many utilities would consider that the machine should be shut down so that the rotor can be investigated. However, operational pressures are such that this is often not possible, and it is necessary to continue running the unit. The next step then is to monitor the earth leakage current and manually trip the unit if there is any further increase, indicative of a second earth fault.

An alternative method is to use a potentiometer fed to earth via a sensitive galvanometer making a bridge circuit, as shown in Figure 9.1(b). As the earth fault location alters or a second fault occurs, the bridge unbalances and an indication occurs on the meter. The problem is that the second earth fault may arise close to the location of the first fault and the resultant change in earth leakage current may not be particularly large.

A more sensitive indicator of the onset of a second earth fault is the resistance of the winding to earth, measured from either terminal. Such a technique has been described using two voltmeters, $V_1$ and $V_2$, as shown in Figure 9.1(c). When the switch is open the fault position, $K$, defined as the fractional position up the winding from the negative slip ring, can be calculated as:

$$K = \frac{V_1}{V_1 + V_2} \tag{9.1}$$

When the switch is closed to A, the voltages $V_1$ and $V_2$ will change by an amount depending on the fault resistance, $R_f$, and the current flowing through the fault, $I_f$, so that now the apparent position $K'$ is given by:

$$K' = \frac{V_1'}{V_1 + V_2'} \tag{9.2}$$

From the apparent change in fault position $\Delta K = K' - K$, the voltage across the fault resistance can be calculated and finally the fault resistance itself. This procedure can be repeated, by connecting the voltmeters to the other terminal of the

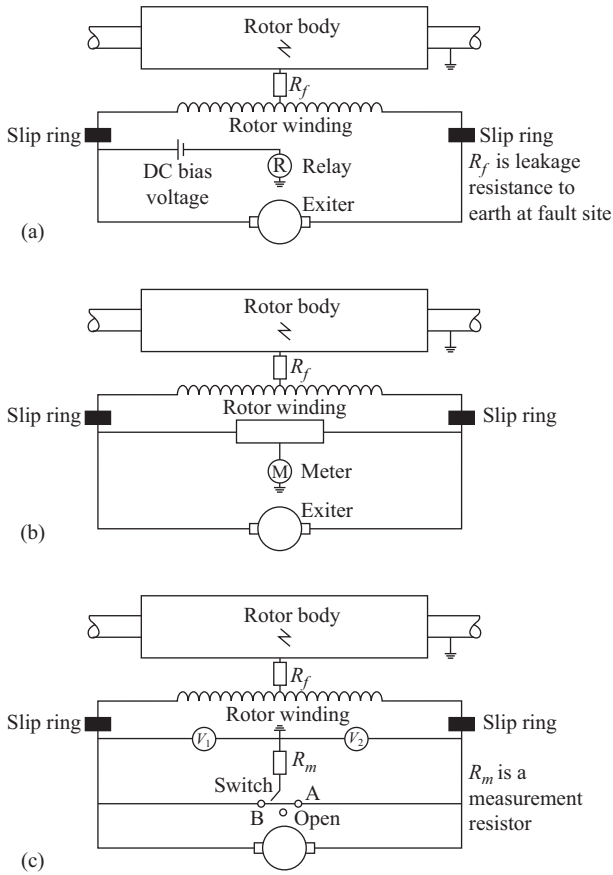


*Figure 9.1 Detecting rotor earth faults: (a) use of an earth leakage relay, (b) monitoring of an existing earth fault using a potentiometer and (c) monitoring for a second earth fault by measuring resistance to earth from each end of the winding*

winding, by closing the switch to B. The choice of terminal connection is governed by the initial fault position, the objective being to optimise the measurement of the fault resistance, $R_f$. The scheme can be implemented using a microprocessor-based unit, which makes the measurement at each terminal of the winding at approximately one second intervals, processes the results and presents information for the operating staff as well as initiating relay indications if necessary.

## *9.3.3 Turn-to-turn faults on-line*

### 9.3.3.1 Air-gap search coils

Turn-to-turn faults in a generator rotor winding may lead to local overheating and eventually to rotor earth faults. In addition, the shorting of turns causes unequal

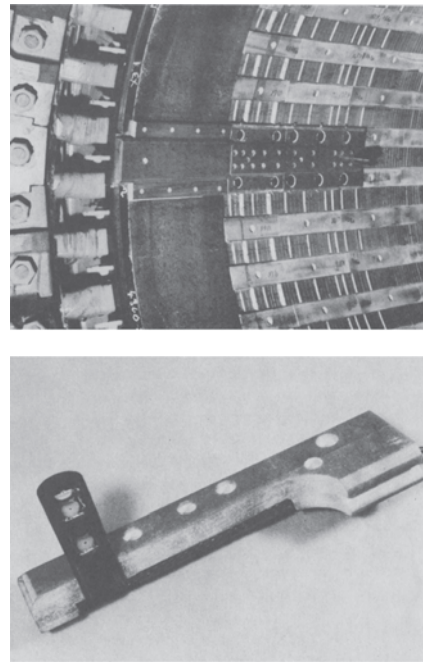

*Figure 9.2 Photographs of two typical search coil installations in large generators*

heating of the rotor leading to bending and an unbalanced pull, which together cause increased vibration as described by Khudabashev (1961). Such faults can be detected offline by the method of recurrent surge oscillography (RSO), described in Section 9.3.4, but a way of detecting them online was first described by Albright (1971) using a stationary search coil fitted in the air-gap of the machine. The search coil, of diameter less than the tooth-width of the rotor, is fixed to the stator usually in the air-gap, and detects either the radial or circumferential component of magnetic flux. Examples of two types of air-gap search coil installation are shown in Figure 9.2.

Figure 9.3 shows typical waveforms obtained from a radial search coil in a two-pole generator operating on load.

A normal two-pole rotor will have an even number of winding slots and will produce a radial flux wave, $B$, in the air-gap as follows:

$$B = \sum_{n=1,3,5,\ldots} B_n \sin n\omega t + \sum_{m\,\text{even}} B_m \sin m\omega t \tag{9.3}$$

This is the normal MMF wave tooth ripple.

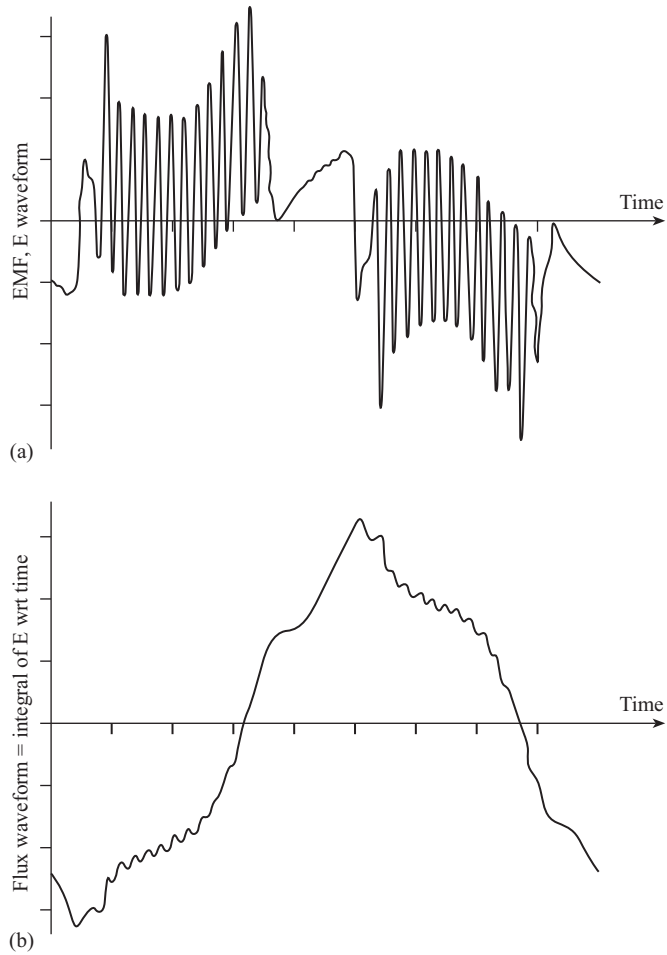


*Figure 9.3 Typical voltage and flux waveforms obtained from a generator air-gap search coil: (a) search coil voltage waveform and (b) flux waveform obtained by integrating (a)*

The search coil normal EMF waveform per turn of the search coil will be:

$$e_{\text{normal}}(t) = A\frac{\mathrm{d}B}{\mathrm{d}t} = \underbrace{\sum_{n=1,3,5,\ldots} An\omega B_n \cos n\omega t}_{\text{normal MMF wave}} + \underbrace{\sum_{m\,\text{even}} Am\omega B_n \cos m\omega t}_{\text{normal tooth ripple MMF wave}} \tag{9.4}$$

where $A$ is the effective search coil area. The $n$ odd harmonics are due to the wave shape of the MMF wave in the air-gap and are dependent upon the spread of

winding slots over the rotor pole pitch. The $m$ even harmonics are due to the rotor tooth ripple that is present in the voltage waveform.

When a shorted turn occurs two things happen. First, it disturbs the MMF distribution, causing low-order even harmonics or an asymmetry in the flux and search coil voltage waveforms. Second it disrupts the $n$th-order slot ripple harmonics. This is shown in the search coil faulty waveform as follows:

$$\begin{aligned} e_{\text{fault}}(t) = & \sum_{n=1,3,5,\ldots} An\omega B_n \cos n\omega t \\ & \text{normal MMF wave} \\ & + \sum_{\ell=2,4,6,\ldots \text{ dependent on fault location}} A\ell\omega B_\ell \cos \ell\omega t \\ & \text{fault asymmetric MMF wave} \\ & + \sum_{m \text{ even}} Am\omega B_m \cos m\omega t \\ & \text{normal tooth ripple MMF wave} \\ & + \sum_{p=\pm1,\pm3} A(m+p)\omega B_n \cos(m+p)\omega t \\ & \text{fault tooth ripple MMF wave} \end{aligned} \tag{9.5}$$

The heights of the corresponding peaks and troughs in the ripple will change so that the search coil voltage will no longer be symmetrical about zero.

In principle, the changes in the heights of the peaks and troughs can be used to determine the number and location of any shorted turns and this is what Albright (1971) did in his original paper. He identified faults by measuring the peak heights of the ripple from stored oscilloscope waveforms, recorded under open and short circuit test conditions. He did not consider that waveforms obtained with the generator on load could provide the sensitivity required to detect shorted turns. Since that time a considerable number of large steam turbine-driven generators have been fitted with air-gap search coils and a great deal more experience has been obtained of detecting shorted turns. The detection technique has therefore been refined to deal not only with the different types and locations of search coils but also to detect shorted turns under both off-load and on-load conditions.

New techniques have been developed utilising a digital storage oscilloscope connected to the search coil to give an initial indication of the development of an inter-turn fault. Secondly, more detailed analysis techniques can then be performed offline on the stored and downloaded waveforms to positively identify and locate the faults. The online method measures the sum of the first four even harmonics of the search coil waveform. The purpose is to identify any asymmetry in the MMF waveform caused by shorted turns. The monitor produces an analogue signal on a chart recorder and the monitor can be adjusted so that any increase above a preset level gives an alarm, which can be used to initiate a more detailed analysis. The setting of that preset level depends upon the generator itself, its history and the type of search coil fitted. Again, one is faced with the problems of determining background levels.

The three main methods of detailed analysis of the search coil waveforms yield the following results:

- the difference between the search coil voltage waveform and a delayed version of itself,
- the amplitude of the increments in the tooth ripple in the search coil voltage waveform, using the method of Albright (1971),
- the flux waveform by integrating the search coil voltage waveform.

Before these can be done, the waveform is Fourier analysed into its real and imaginary components. It has been shown that the waveform obtained from a search coil at one radial position in the air-gap can be modified to predict the waveform if the coil were at another position closer to the rotor. This is particularly helpful for coils fitted close to the stator surface, where the rotor tooth ripple may be very small. It also allows results from different sizes and designs of machines to be compared on a common basis. The difference waveform can be calculated from the digitised components of the search coil voltage and this waveform can be plotted out to show the presence of a fault as shown in Figure 9.4.

The incremental voltages are calculated by measuring the voltage height between the peaks and troughs of each tooth ripple associated with each pole of the winding and the heights are measured on the side of the ripple furthest from the pole face. These incremental voltages can be plotted out as a histogram over the rotor surface together with a histogram of the differences between the voltages over one pole and the next, as shown in Figure 9.5.

The flux waveform is found by integrating the voltage waveform. Distortions of the flux waveform can be brought to light either by direct inspection or by carrying out the difference procedure described above for the search coil waveform.

Computer simulations and the practical experience of measuring search coil voltage waveforms suggest that the magnitude of the asymmetry in the search coil waveform produced by a fault depends upon the load as well as the location and number of shorted terms. This is because the degree of saturation affects the magnitude of the rotor tooth ripple, which varies with load and with position around the rotor circumference. In the absence of saturation, the asymmetric component would be expected to be proportional to rotor current. However, magnetic saturation of the shorted turn has a significant effect, so that for some loads and locations of shorted turn the magnitude of the asymmetry actually decreases with increasing rotor current.

### 9.3.3.2 Circulating current measurement

An alternative way of monitoring shorted turns, which is still under development, uses the stator winding itself as the search coil. The principle of this technique, first suggested by Kryukhin (1972), has been developed and fitted to a number of generators in the United Kingdom. This technique makes use of the fact that in large two-pole generators, each phase of the stator winding consists of two

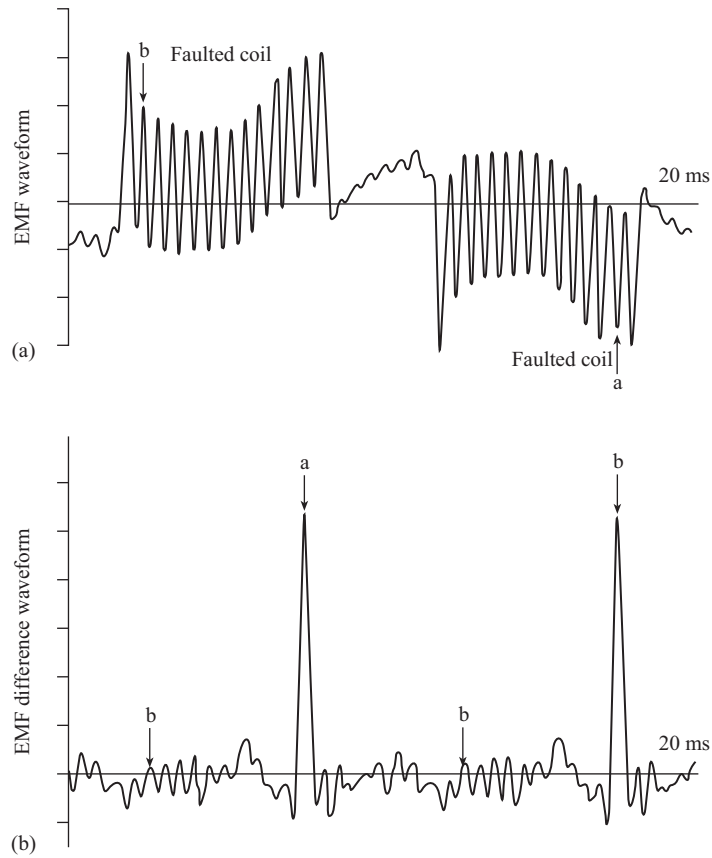


*Figure 9.4 Effect of delaying and adding the waveform from a search coil fitted to a faulty machine: (a) predicted search coil voltage close to the rotor surface and (b) difference waveform obtained by delaying (a) half a cycle and adding*

half-phase windings in parallel. Any asymmetry in the rotor MMF will induce counter-MMF currents in the stator winding with a twice fundamental frequency, which will circulate between the half-phases. The presence of shorted turns is detected by measuring those even harmonic currents. The size of the currents depends upon the severity of the shorted turns, the coupling between rotor and stator and the impedance of the stator winding to the currents. This approach has been developed by others with supporting analysis, for example, by Poyhonen *et al*. (2003), but has been subsumed into the analysis of induction motors, which for some reason appears more popular to researchers than synchronous generators, despite the fact that very large amounts of capital are invested in the latter machines.

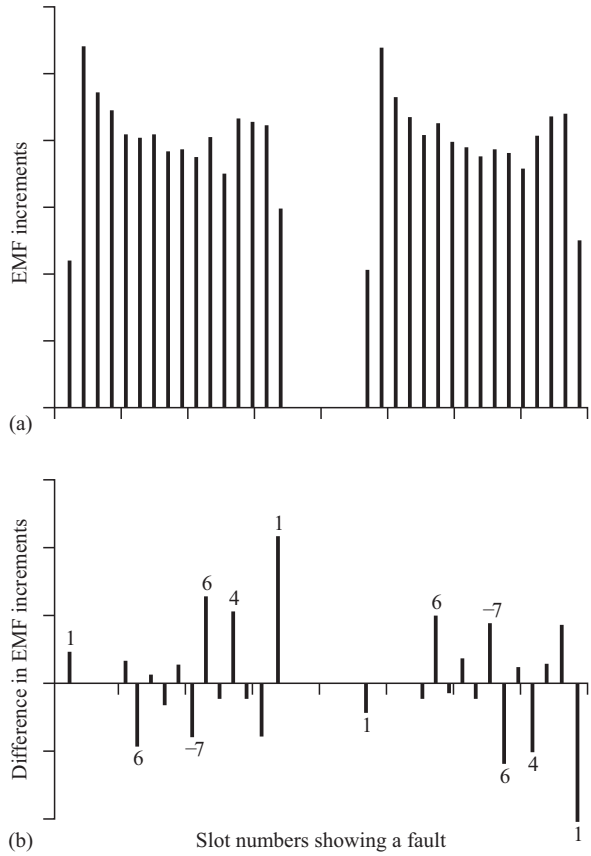


*Figure 9.5 Method of incremental voltages proposed by Albright (1971): (a) incremental voltages obtained from the previous figure and (b) differences in incremental voltages between the poles obtained from (a)*

It can be shown that the EMF, $e(t)$, induced across a stator half-phase winding, due to a single shorted turn, spanning an angle, $2\beta$, on a two pole rotor is given by:

$$e(t) = \frac{4\mu_0\omega}{\pi Cg} NI\, r_{\text{air-gap}} L \sum_{n=1,3,5,\ldots}^{\infty} \frac{1}{n} k_{wn} \sin n\beta \cos(n\omega t) \tag{9.6}$$

where

$NI$ is the ampere-turns of the short
$\omega$ is the rotational frequency
$N$ is the number of stator turns in series per half-phase
$r_{\text{air-gap}}$ is the mean radius of the air-gap
$L$ is the active length of the rotor

$C$ is the Carter factor to account for slotting
$g$ is the width of the air-gap
$\beta$ is the half-angle subtended by the shorted turn
$n$ is the harmonic number
$k_{wn}$ is the stator winding factor for the $n$th harmonic.

The EMF induced in the opposite half-phase winding, on the same phase, will be of the same form but the term $\cos(n\omega t)$ will be replaced by one of the form $\cos(n\omega t - n\pi)$. The odd harmonics of the EMFs in the two half-phases will therefore be of the same sign and so when the half-phases are connected in parallel they will aid one another, forming the terminal voltage due to that shorted turn. The even harmonics will be of opposite sign and so will drive the circulating currents between the half phases. The currents are flowing in the stator winding, rotating at the same speed as the rotor, effectively replacing the rotor shorted turn. The second harmonic circulating current that flows in the stator, $i_{2C}$, can be related to the second harmonic EMF, $e_2$, induced by the shorted turn, providing the second harmonic impedance, $X_2$, of the winding is known. Now, the impedance to second harmonic currents, $X_2$, is given by:

$$X_2 = X_{m_2} + X_{\ell_2} \tag{9.7}$$

where

$X_{m_2}$ is the second harmonic magnetising reactance
$X_{\ell_2}$ is the second harmonic leakage reactance.

For a typical large machine, it has been shown that $X_2 = 0.516$ pu. Therefore, for a single shorted turn spanning an angle of $2\beta$ on the rotor the second harmonic current circulating in the stator winding is approximated by:

$$i_{2C} = \frac{e_2 \sin 2\beta}{0.516} \tag{9.8}$$

The currents are detected using air-cored Rogowski coils wrapped around the winding and a diagram of an online monitor for doing this is shown in Figure 9.6.

An advantage of this new technique, compared to air-gap search coils, is that the current transducers can be installed without the need to remove the rotor from the generator. For many generators the half-phase windings are joined within the cooling pressure casing in a fairly restricted space that requires special arrangements to gain access. But on some machines, the half-phase windings are joined outside the casing, so fitting of the Rogowski coils becomes simpler. Care must of course be taken to provide appropriate high-voltage insulation and electrostatic screening between the Rogowski coil and the conductor.

A disadvantage of the circulating current method, however, is that it does not give information on the turn location, whereas the air-gap search coil method does.

Neither the air-gap search coil nor the Rogowski coil methods appear to have been applied to multi-pole hydro-type generators or even 4-pole turbine-type machines. No doubt applications will evolve as operational circumstances demand them.

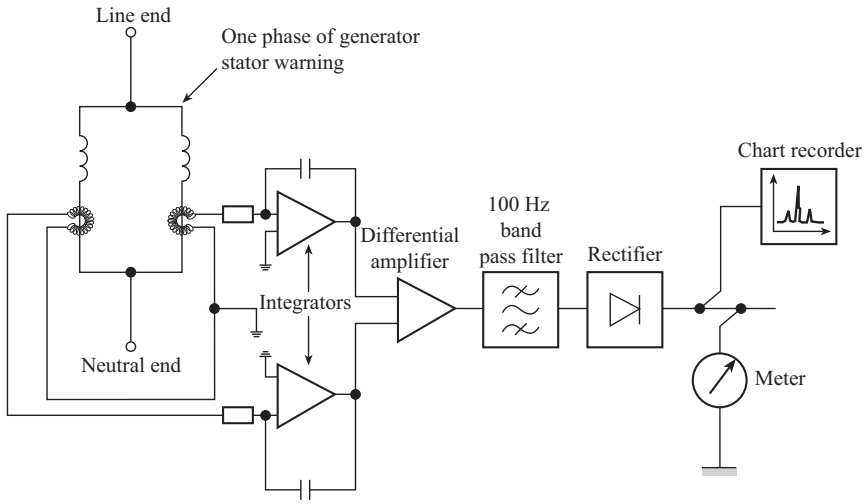


*Figure 9.6 Continuous monitor for use on circulating current Rogowski coils*

## 9.4 Motor rotor faults

### *9.4.1 General*

The rotors of other electrical machines can be highly stressed, though perhaps not to the same degree as turbo-generators. Table 2.4 from Chapter 2 shows that large induction motors can have mechanical, electrical or magnetic loadings higher than larger machines and squirrel cage or wound rotors have had problems, as the experience of Tavner *et al.* (1986) shows. A number of both electrical and mechanical techniques have been developed to monitor these problems. This section deals with the electrical techniques.

### *9.4.2 Air-gap search coils*

The work on air-gap search coils, described in Section 9.3.2, was all on turbo-generators but there is no reason why such methods could not be successfully applied to smaller machines. Indeed Kamerbeek (1974) successfully used the method experimentally on small induction motors but for measuring torque rather than machine faults. A paper by Seinsch (1986) then applied this technique to induction motors using a distributed coil on the stator.

### *9.4.3 Stator current monitoring for rotor faults (MCSA)*

Although the technique of using a stator search coil has not been widely used, it is possible to use the stator winding itself as a search coil, in a somewhat similar way to the method described for generators in Section 9.3.3. Any rotor fault in an induction motor will cause a characteristic swing in the supply ammeter reading, which maintenance staffs have come to recognise as indicating that trouble is on its

way. Careful measurement of the stator current will therefore enable such a fault to be monitored.

The current drawn by an ideal motor should have a single component of supply frequency. Changes in load will modulate the amplitude of the current to produce side-bands. Faults in the rotor circuit will generate a side-band below the supply frequency and displaced from it by twice the slip frequency.

This effect was described in Hargis *et al.* (1982), Hargis (1983), the references in Tavner *et al.* (1986) and an explanation is given here. A motor winding with $p$ pole pairs and supply frequency $\omega_{se}$ produces a fundamental stator radial MMF wave, $f_1$, at mechanical angle $\theta_1$ containing odd harmonics only. Consider the fundamental MMF wave:

$$f_1(t) = N_1 I_1 \sin(\omega_{se} t - p\theta_1) \tag{9.9}$$

where

$N_1$ is the number of stator turns
$I_1$ is the stator current.

The angle, $\theta_2$, on the rotor is given by:

$$\theta_2 = \theta_1 - \omega_{rm} t \tag{9.10}$$

where

$\omega_{rm}$ is the angular speed of the rotor
the rotational speed $N = 60\omega_{rm}/2\pi$.

So that for a $p$ pole rotor the rotor sees the MMF:

$$f_1(t) = N_1 I_1 \sin((\omega_{se} - p\omega_{rm})t - p\theta_2) \tag{9.11}$$

This MMF rotates forward with respect to the rotor at the slip speed, however, under normal circumstances the rotor carries induced currents, which establish a fundamental rotor MMF wave, $f_2$, to counter the stator MMF and moving at the same speed:

$$f_2(t) = N_2 I_2 \sin((\omega_{se} - p\omega_{rm})t - p\theta_2) \tag{9.12}$$

If the rotor has a fault, such as a broken bar, the MMF due to the rotor current is modulated by $\sin 2p\theta_2$ so that:

$$f_2(t) = N_2 I_2 \sin((\omega_{se} - p\omega_{rm})t - p\theta_2)\sin 2p\theta_2 \tag{9.13}$$

Therefore, for a $p$ pole-pair machine:

$$f_2(t) = \frac{N_2 I_2}{2}\{\cos((\omega_{se} - p\omega_{rm})t - 3p\theta_2) - \cos((\omega_{se} - p\omega_{rm})t + p\theta_2)\} \tag{9.14}$$

Referring this MMF to the stator, as the counter to (9.11), using (9.10) gives:

$$f_1(t) = \frac{N_2 I_2}{2}\{\cos((\omega_{se} + 2p\omega_{rm})t - 3p\theta_1) - \cos((\omega_{se} - 2p\omega_{rm})t + p\theta_1)\} \tag{9.15}$$

Which if we use the fractional slip $s = \left(\frac{\omega_{se} - p\omega_{rm}}{\omega_{se}}\right)$ for a $p$ pole pair induction machine gives:

$$\theta_2 = \theta_1 - \frac{(1-s)}{p}\omega_{se}t \tag{9.16}$$

$$f_1(t) = \frac{N_2 I_2}{2}\{(\cos(3-2s)\omega_{se}t - 3p\theta_1) - (\cos(1-2s)\omega_{se}t - p\theta_1)\} \tag{9.17}$$

Note that these fundamental MMF wave equations (9.11) and (9.17) echo (8.22) and (8.23) in Chapter 8, where all harmonic MMFs were considered in the excitation of stator core vibrations by the air-gap MMF wave acting on the bore of the core.

Now, the first component of MMF in (9.17) induces zero sequence EMFs in the three phase stator winding, because it contains $3\omega_{se}t$ and $3\theta_1$, and gives rise to no current contribution from the supply. The second component of MMF, however, induces a proper 3-phase set of currents at the normal supply frequency but contains a component, or side-band, $2s\omega_{se}$ below that frequency.

This is the twice slip frequency modulation of the supply current that is seen as the swing on the ammeter reading. Such a cyclic variation in the current reacts back onto the rotor to produce a torque variation at twice slip frequency that, if the rotor does not have an infinitely high inertia, gives rise to the $2sp\omega_{rm}$ variation in speed or $2s\omega_{se}$ variation in mechanical vibration, that can also be used for fault detection as described in Chapter 8, Section 8.6.4. This speed effect reduces the lower side-band, $(1-2s)\omega_{se}$, current swing and produces an upper side band at $(1+2s)\omega_{se}$, enhanced by modulation of the third harmonic flux in the stator and it can be shown that other side-bands at $(1 \pm 2ns)\omega_{se}$ are also found. The ratio of the lower side-band amplitude to the main supply frequency component gives a straightforward indication of the extent of rotor damage, as first described by Jufer *et al.* (1978).

The supply current can be monitored very easily, without interfering with the machine, simply by fitting a clip-on CT or Rogowski coil around the supply cable to the motor or around the cable of the protection CT used to monitor the motor current, see Figure 9.7. The normal procedure is to use a spectrum analyser package in a PC connected via an A/D converter to the CT. Surveys of the supply currents to a number of motors can be taken at regular intervals, or when a fault is suspected. Figure 9.8(a) and (b) shows the PSD for the current from two identical machines. The motor in Figure 9.8(a) had a rotor fault corresponding to three fractured cage bars, shown by spectral components at about 48, 49, 51 and 52 Hz, that is a slip frequency of 0.5 Hz for $n = 1$ or 1 Hz for $n = 2$ and a slip $s$ of 1%, with side-bands described by $(1 \pm 2ns)f_{se}$. The lower side-band due to the MMF modulation can clearly be distinguished from the supply frequency and an estimate of the fault severity can be made by taking the ratio between the amplitudes of the lower side-band and the fundamental frequency. Because the current measuring technique looks into the motor from the terminals it is also possible to see beyond the electrical circuits and detect faults on the mechanical load train, such as worn gear teeth, which the motor is driving. Figure 9.8(b) shows a wider frequency range current spectrum from the motor, with no $(1-2s)$ component, indicating rotor

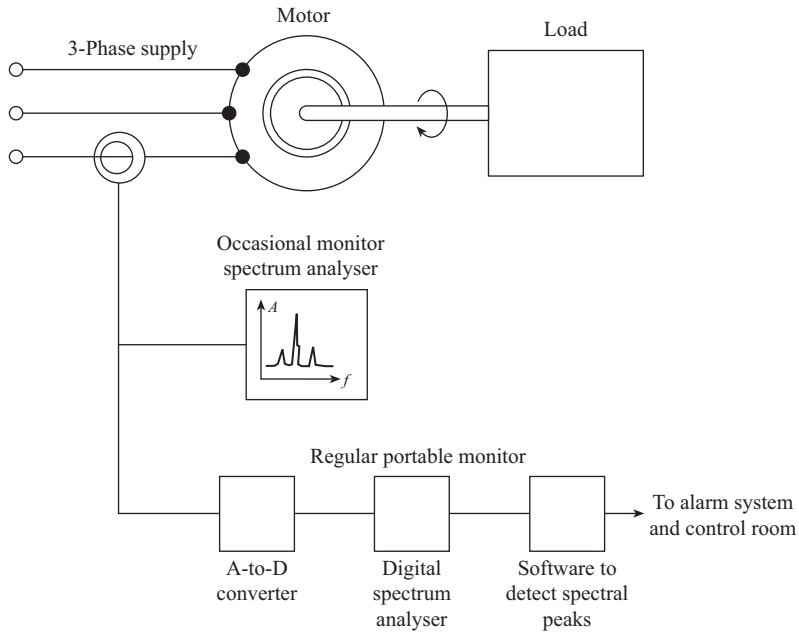


*Figure 9.7 Detecting side-bands in the supply current of an induction motor*

damage, but other side-bands due to the motor driving a load through a damaged gear-box.

Interpretation of the current spectrum requires a relatively skilled operator to carry out a machine survey and it cannot be considered as continuous monitoring. The normal practice would be to carry out a survey whenever ammeter swings indicate that a problem is imminent. Where motors of high value are at risk, more frequent monitoring may be necessary and in extreme cases of great operational importance, such as in a nuclear power station or online oil and gas plant, continuous monitoring could be considered.

Detection can be more difficult when the motor speed is varying rhythmically because of the driven load, such as on a belt or mill drive, or if the frequency variation is significant, for example, on a relatively small power system.

The technique has stimulated a surge in investigations in the literature as analysts seek to describe the precise conditions under which faults can be detected, examples include Menacer *et al.* (2004) and Li *et al.* (2006), who make a comparison between current, vibration and acoustic methods of detection.

Appendix B gives a draft guide to the application of the MCSA method.

### *9.4.4 Rotor current monitoring*

The rotor circuits of wound rotor motors are usually poorly protected in most installations. Faults in brazed joints and slip-ring connections have sometimes

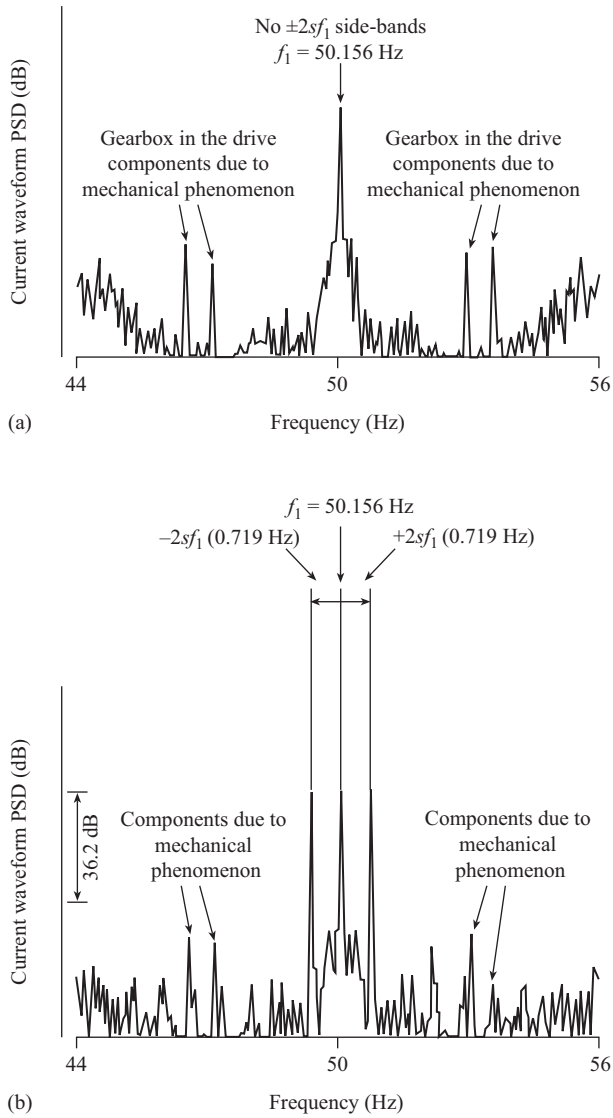


*Figure 9.8 Supply current spectra from induction motor drive trains: (a) with a fault in an attached gearbox and (b) with a rotor cage defect. Taken from Thomson et al. (2001)*

caused severe damage because they have not been detected promptly. Overheating of rotors can also be caused by current imbalance in the external resistors or circuits connected to the slip rings. The low frequency of these currents makes measurements with conventional CTs inaccurate. Faults of these types were some of the reasons that encouraged the development of proprietary leakage flux technique that

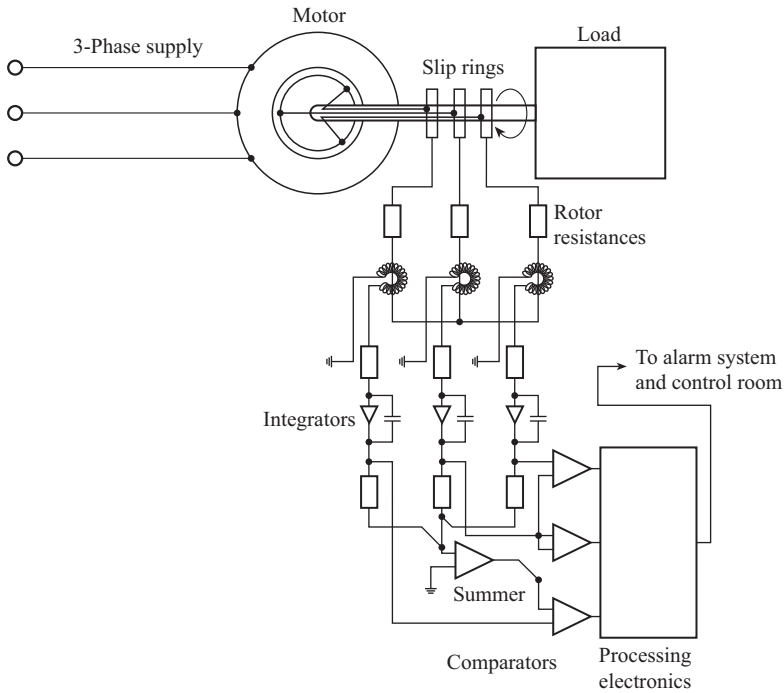


*Figure 9.9 Continuous monitor of rotor current in a wound rotor induction motor*

is described later in Section 9.5, see Rickson (1983). However, low-frequency currents can be measured accurately by Rogowski coils. These have been used to monitor the rotor resistance currents in variable speed wound rotor motors as shown in Figure 9.9. The signals from the Rogowski coils are integrated to give a voltage proportional to rotor current. These signals are summed to give the mean current in all three phases of the rotor and are compared to the individual phase currents. Processing electronics then detects whether severe unbalance is present and provides amplitude and alarm signals to the control room. The approach described in Penman *et al.* (1980) was based upon a protection philosophy, in that indications from the monitor are used to trip the machine. In practice, however, the instrument has been used to provide monitoring indications that assist in determining when motors should be taken out of service for repair.

## 9.5 Generator and motor comprehensive methods

### *9.5.1 General*

The reader should be able to see, both from the 'Introduction' section to this chapter and the methods that have been described, that electrical techniques have much in common. There would seem to be some advantage in devising a single

electrical technique that is capable of detecting all electrical faults, whether they are on the rotor or stator. Trutt *et al.* (2001), Kohler *et al.* (1999) and Sottile *et al.* (2002) have advocated this generalised approach to the monitoring of the terminal 'performance' quantities of induction machines and Sottile *et al.* (2006) have applied the same technique to three phase synchronous generators.

We describe below four techniques that detect faults by measuring the effect they have on the machine terminal 'performance' quantities.

### *9.5.2 Shaft flux*

Shaft flux, or more generally axial leakage flux, occurs in all electrical machines. It is produced because no machine can be constructed with perfect symmetry. There will always be, for example, slight differences in the reluctance of magnetic circuits due to building tolerances, core-plate anisotropy, and plate thickness variation, see Tavner *et al.* (2005). This asymmetry is reflected in the impedances presented by the various phase groups, or coils in the machine stator, and will cause slight variations between the currents flowing in the coils. It is also the cause of homopolar fluxes in the machine shaft that can lead to shaft voltages as described in a later section.

This asymmetry, together with small differences in the electrical properties of the conductors, and variations in the physical disposition of the conduction in both the active length and end regions of machines, will give rise to a net difference between the currents flowing in one section of the end winding when compared with the corresponding section diametrically opposite. The imbalance leads naturally to a net axial flux component. A similar argument can be applied to the rotor circuits; hence one can expect to measure axial flux, even in machines that are in 'perfect health'.

It is a simple extension of the above to consider what happens when certain fault conditions arise in a machine. Faults, such as winding short circuits, voltage imbalance, and broken rotor bars, represent severe disruptions to the internal symmetry of the machine. It is logical to conclude, therefore, that the effect on the production of axial flux will be readily observable. Any gross change of magnetic circuit conditions, such as the formation of an eccentric air-gap due to bearing wear, will, by the same token, be reflected with a corresponding change in axial leakage flux.

The purpose of axial flux monitoring is therefore to translate observed differences in the nature of the axial leakage flux into an indication of fault condition. The production of such fluxes in squirrel cage rotor induction machines was studied by Jordan (1964) and Jordan *et al.* (1965) with particular emphasis on the changes occurring due to static eccentricity, Erlicki *et al.* (1971) showed that it is possible to detect the loss of a supply phase through axial flux monitoring.

In the 1970s in the United Kingdom, a large power station boiler auxiliary induction motor, equipped with two stator windings for two-speed operation, was operating on one winding with a shorted turn on the idle winding. Circulating currents in the faulty idle winding, induced by the energised winding, caused degradation of the insulation, charring and the generation of flammable gases, see Section 7.2. Eventually these gases entered the terminal box, ignited, bursting the

terminal box and causing a fatality. This incident galvanised interest in the United Kingdom in motor monitoring, because it was quickly realised that the faulted idle winding could have been detected by monitoring the axial leakage flux of the machine, particularly by mounting a search coil around the rotor shaft.

Rickson (1983) developed a protection device based on this principal. Penman *et al.* (1980) showed that more discrimination could be achieved between a variety of fault conditions by carefully processing the axial flux signal and this initiated their work on machine CM.

The technique relies upon examining the changes in the spectral components of the axial flux. These components arise as described below. Since the fluxes are produced by winding currents, the frequency of these flux components must be related to the frequencies of the currents. Rotor currents are also induced by the air-gap flux, so the net air-gap flux will be modified as a result. While the rotor is at rest the air-gap field results solely from the currents flowing in the stator; hence only the time harmonics present in the line currents will appear in the axial flux. Once the rotor moves, however it does so with an angular speed, $\omega_{rm} = (1 - s)\omega_{se}/p$, with respect to the stator, where $p$ is the number of pole pairs in the machine. The air-gap flux components will consequently be frequency filtered. For example, in the normal three-phase stator winding, the air-gap field produced, $b_{\text{stator}}$, can be approximated up to the seventh harmonic by the form:

$$b_1(t) = \widehat{B}_1 \cos(\omega_{se}t - p\theta_1) + \widehat{B}_5 \cos(\omega_{se}t + 5p\theta_1) - \widehat{B}_7 \cos(\omega_{se}t - 7p\theta_1) + \cdots \tag{9.18}$$

We can transform this expression into a frame of reference moving with the rotor by considering Figure 9.10, which shows the relationships between a fixed point in the stator and a fixed point on the rotor:

$$\theta_2 = \theta_1 - \omega_{rm}t \tag{9.19}$$

But for an induction machine with $p$ pole pairs:

$$\theta_2 = \theta_1 - \frac{(1 - s)}{p}\omega_{se}t \tag{9.20}$$

Using these expressions, it can be shown that the $n$th term of the air-gap field in the stator frame is:

$$b_{n1}(t) = \widehat{B}_n \cos[(1 \pm (1 - s)n\omega_{se}t) \pm np\theta_1] \tag{9.21}$$

The rotor frame expression corresponding to (9.18) is:

$$b_2(t) = \widehat{B}_1 \cos(s\omega_{se}t - p\theta_2) + \widehat{B}_5 \cos((6 - 5s)\omega_{se}t - 5p\theta_2) - \widehat{B}_7 \cos((7s - 6)\omega_{se}t - p\theta_2) + \cdots \tag{9.22}$$

The first air-gap harmonic produces currents at $s$ times the supply frequency, the fifth air-gap harmonic produces time frequencies of $(6 - 5s)$ times and so on.

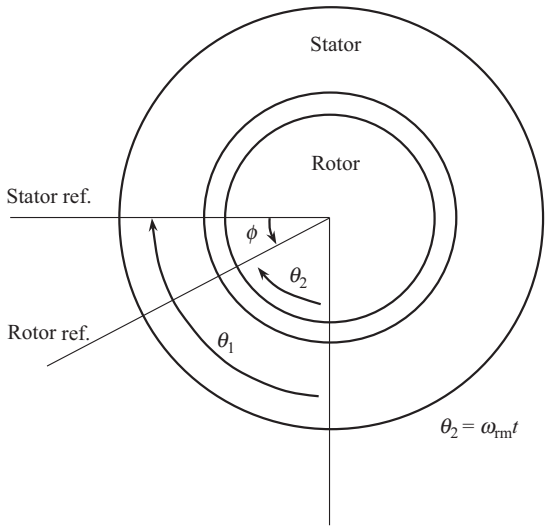


*Figure 9.10 Rotor and stator frames of reference*

It is now apparent that the axial flux spectrum is rich in harmonics, even in a well-constructed, healthy machine. Moreover, because fault conditions, such as shorted turns, loss of phase, eccentricity and so on, cause changes in the space harmonic distributions in the air-gap, such conditions will be accompanied by a corresponding change in the time harmonic spectrum of axial flux. Furthermore, by effectively using the stator winding as a search coil to detect rotor faults, and the rotor winding to detect stator faults, it is possible to gain insight into the harmonic changes to be expected for a given fault condition.

Let us follow a typical fault condition through the diagnostic procedure. If we assume that an inter-turn short circuit exists in the stator winding then this condition can be represented as a single pule of MMF, similar to that shown in Figure 9.11, results. The components of the stator air-gap field $b_{\text{stator}}$ generated by this distribution are:

$$b_1(t) = \sum_{n=1,3,5,\ldots} \widehat{B}_n \cos(\omega_{se}t \pm n\theta) \tag{9.23}$$

The $n$th component in the rotor frame will therefore be:

$$b_{n,2}(t) = \widehat{B}_n \cos\left[\left(1 \pm (1-s)\frac{n}{p}\right)\omega_{se}t \pm n\theta_2\right] \tag{9.24}$$

These harmonics will induce currents in the rotor circuits, and because there are asymmetries in the rotor magnetic and electric circuits, they will appear as additional components in the spectrum of axial flux.

Table 9.1 at the end of the chapter summarises the angular frequency components arising in the axial flux.

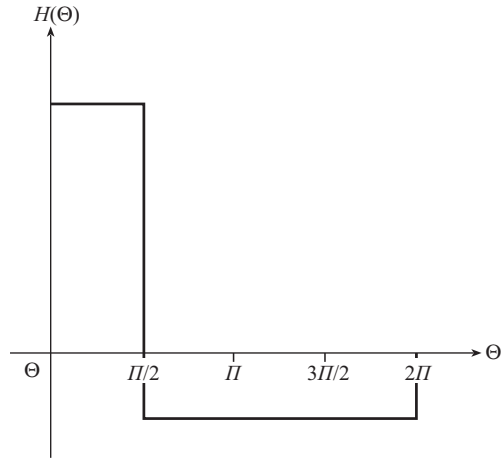


*Figure 9.11 MMF due to a single fully pitched coil*

*Table 9.1 Axial flux angular frequency components related to specific induction machine asymmetries (9.24), taken from Vas (1993)*

| | **Space harmonic of the stator winding MMF** | | | |
|---|---|---|---|---|
| | $k = 1$ | $k = 3$ | $k = 5$ | $k = 7$ |
| | **Angular frequency components (rad/s)** | | | |
| **Stator asymmetry** | $s\omega_{se}$ | $(3s - 2)\omega_{se}$ | $(5s - 4)\omega_{se}$ | $(7s - 6)\omega_{se}$ |
| | $(2 - s)\omega_{se}$ | $(4 - 3s)\omega_{se}$ | $(6 - 5s)\omega_{se}$ | $(8 - 7s)\omega_{se}$ |
| **Rotor asymmetry** | $s\omega_{se}$ | $(3 - 2s)\omega_{se}$ | $(5 - 4s)\omega_{se}$ | $(7 - 6s)\omega_{se}$ |
| | $(2s - 1)\omega_{se}$ | $(4s - 3)\omega_{se}$ | $(6s - 5)\omega_{se}$ | $(8s - 7)\omega_{se}$ |

Figure 9.12 illustrates the comparable results from a small four-pole squirrel cage induction machine using the technique. Only the spectral components below 500 Hz are shown, but faults, such as inter-turn short circuits, broken rotor bars, or negative phase sequence in the supply, are visible in the spectra and have been identified.

The axial flux monitoring technique is still embryonic but essentially it requires the collection of an axial flux signal, using a search coil wound concentrically with the shaft of a machine. This signal is then spectrally analysed and on the basis of the appearance of certain harmonic groups a decision is made as to the condition of the machine. The attractions of the method are that it is completely non-invasive and a single sensor can be used for a variety of fault types. It is, however, a complex technique requiring specialised equipment and is, as yet, relatively untested.

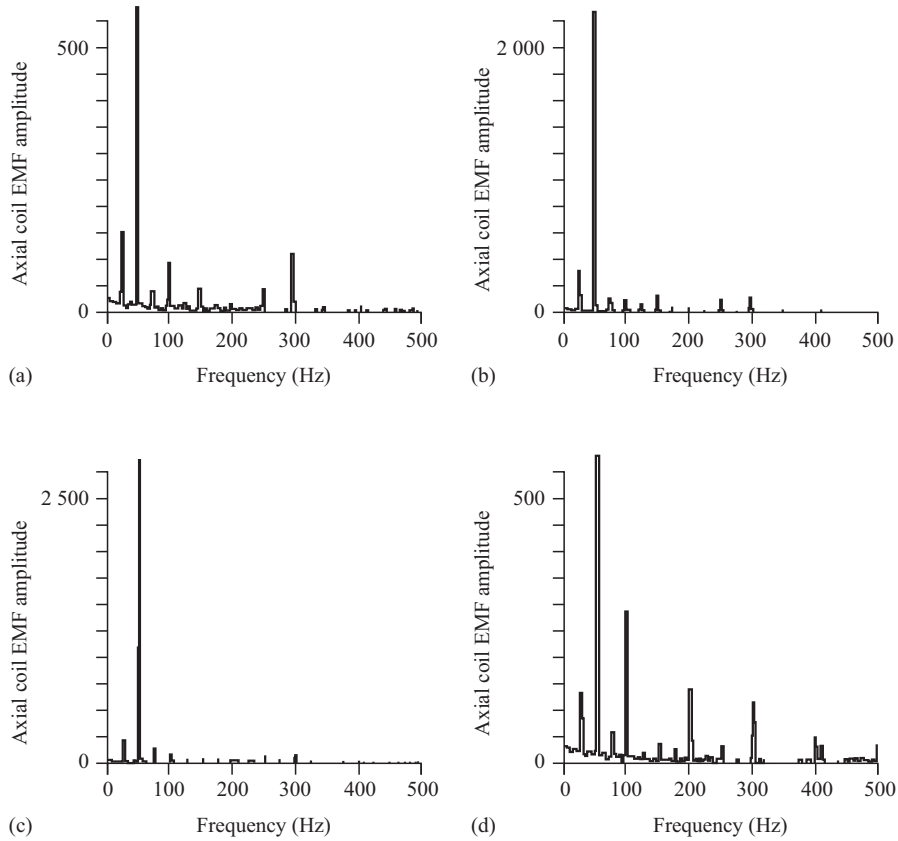


*Figure 9.12 Typical spectra taken at identical gains from an axial flux search coil fitted to an experimental motor: (a) good rotor, no faults, no load, (b) broken rotor bar, no other faults, (c) good rotor, large stator shorted turn 1 A, no load and (d) good rotor, small stator negative phase sequence, no load*

Little further work has been done on this technology since its inception in the 1980s, therefore it cannot be recommended to operators. However, some new industrial application, such as traction, electric cars or aerospace, could make it exceptionally appealing because of its ease of fitting and universality.

### *9.5.3 Stator and rotor currents*

Stator current has been shown in Sections 9.2.2 and 9.4.3 to be a viable CM technique. The results of Figure 9.10(a) have also shown that it also has the capability to look beyond the electrical machine itself and detect faults in the mechanically driven load. A further example of fault detection in the driven machine by current analysis was shown, for a VSD downhole pump, in Figure 5.10 by Yacamini *et al.*

(1998) and Ran *et al.* (1996), where the wavelet analysis was used to deal with the non-stationary behaviour of the signal.

There is now a more extensive literature on the current analysis method including Joksimovic *et al.* (2000) and Stavrou *et al.* (2001), who investigated the fundamental magnetic field effects on the air-gap, Bellini *et al.* (2001) and Bellini *et al.* (2002), who give a good account of the present state of the art, together with Henao *et al.* (2003) and Henao *et al.* (2005).

Table 9.2 summarises the angular frequency components that can be detected in the stator current and their relation to machine faults.

### *9.5.4 Power*

Work by Trzynadlowski *et al.* (1999) showed that the power spectrum may be an effective monitor of machine health and it may simplify some of the complexities of the stator current and axial flux spectra. This was a technique pioneered by Hunter *et al.* (1982) but also considered more recently on wind turbine induction generators by Watson *et al.* (2010). The process can be considered as follows, instantaneous power, $p_1$, delivered to or from a three-phase machines is given at the stator terminals by:

$$p_1(t) = \sum_{q=1}^{3} \sum_{n=1}^{\infty} \sum_{m=1}^{\infty} \widehat{V}_{nq} \sin(\theta_{nn}) \widehat{I}_{mq} \sin\left(\theta_{mm} + \varphi_{mq}\right) \tag{9.25}$$

where $\theta_{nn}$ or $\theta_{mm}$ are defined as follows:

$$\theta_{\ell k} = \ell \omega_{se} t + (q-1)\frac{2\pi k}{3} \tag{9.26}$$

where

$\widehat{V}_{nq}$ is the peak of the $n$th harmonic of the phase voltage in the $q$th phase assuming that the phase voltages are angularly spaced by $2\pi/3$
$\widehat{I}_{mq}$ is the peak of the $m$th harmonic of the phase current in the $q$th phase assuming that the phase currents are angularly spaced by $2\pi/3$
$q$ is the phase number
$n$ is the voltage harmonic number
$m$ is the current harmonic number
$\phi_{nq}$ is the phase angle between the phase current, $\widehat{I}_{nq}$, and the phase voltage, $\widehat{V}_{nq}$.

If the load on the machine is perfectly balanced between the three phases and the voltages and currents contain no harmonics, then the expression for instantaneous power reduces to:

$$p_1(t) = \widehat{V}_1 \widehat{I}_1 \sum_{q=1}^{3} \sin(\theta_{11} + \varphi) \tag{9.27}$$

$$p_1(t) = \frac{\widehat{V}_1 \widehat{I}_1}{2} \sum_{q=1}^{3} \left\{\cos\varphi - \cos\left(\theta_{2,2} + \varphi\right)\right\} \tag{9.28}$$

*Table 9.2 Electrical angular frequency components related to specific electrical machine faults*

| | | Current | Flux | Power |
|---|---|---|---|---|
| | | Angular frequency components (rad/s) | | |
| **Mechanical faults** | Oil whirl and whip in sleeve bearings | $\omega_{se}(0.43 \text{ to } 0.48)/p$ | | $\omega_{se}(1 + (0.43 \text{ to } 0.48))/p$ |
| | Unbalanced mass on the rotor of a synchronous machine | $\omega_{se}/p$ | $\omega_{se}/p$ | $\omega_{se}(1 + 1/p)$ |
| | Dynamic eccentricity in a synchronous machine | $2\omega_{se}/p$ | $2\omega_{se}/p$ | $\omega_{se}(1 + 2/p)$ |
| | Dynamic displacement of shaft in bearing housing of a synchronous machine | $\omega_{se}/p$, $2\omega_{se}/p$, ... | $\omega_{se}/p$, $2\omega_{se}/p$, ... | $\omega_{se}(1 + 1/p + 2/p + \cdots)$ |
| | Static misalignment of rotor shaft in a synchronous machine | $\omega_{se}/p$, $2\omega_{se}/p$, $3\omega_{se}/p$, ... | $\omega_{se}/p$, $2\omega_{se}/p$, $3\omega_{se}/p$ ... | $\omega_{se}(1 + 1/p + 2/p + \cdots)$ |
| | Static and dynamic eccentricity in an induction machine | $\omega_{se}\left\|(nN_r \pm k_e)\frac{(1-s)}{p} \pm k\right\|$ | $\omega_{se}\left\|k_e\frac{(1-s)}{p} \pm k\right\|$ | $\omega_{se}\left\|1 + k_e\frac{(1-s)}{p} \pm k\right\|$ |
| **Electrical faults** | Broken rotor bar in an induction machine | $\omega_{se}\left\|1 \pm \frac{2ns}{p}\right\|$ | $s\omega_{se}$ ... $(2s - 1)\omega_{se}$ ... | $2ns\omega_{se}/p$ $2n(1 - s)\omega_{se}/p$ |
| | Stator winding faults in a synchronous machine | $\omega_{se}$, $2\omega_{se}$, $4\omega_{se}$, ... | $\omega_{se}$ | $\omega_{se}$, $3\omega_{se}$ |
| | Stator winding faults in an induction machine | $\omega_{se}$, $2\omega_{se}$, $4\omega_{se}$, ... | $s\omega_{se}$ ... $(2 - s)\omega_{se}$ ... | - |
| **Electrical and mechanical faults, Zappala *et al.* (2019)** | Stator or rotor winding and mechanical faults in a wound rotor induction machine | $\omega_{se}\left\|\eta\frac{(1-s)}{p} \pm k\right\|$ | – | $\omega_{se}\left\|j \pm \eta\frac{(1-s)}{p} \pm k\right\|$ |

Definitions
$\omega_{sm}$ = stator mechanical vibration frequency
$\omega_{se}$ = stator electrical supply frequency
$N_r$ = integer number of rotor slots
$N$ = rotational speed (rev/min)
$f\omega_{rm} = \frac{2\pi N}{60}$ mechanical rotational frequency (Hz)
$\omega_{rm} = \omega_{se}/p$ for a synchronous machine
$\omega_{rm} = (1 - s)\omega_{se}/p$ for an asynchronous machine
$s$ = asynchronous machine rotor speed slip, 0–1
$p$ = pole pairs
$n$ = a positive integer
$k_e$ = eccentricity order, zero for static eccentricity, low integer value 1, 2, 3, ... for dynamic eccentricity $\eta = (nN_r \pm k_e)$
$j$ = supply harmonics
$k$ = space harmonic of the stator winding MMF, 1, 3, 5, 7,...

The second term in brackets sums to zero because the three-phase components are spaced in phase at $4\pi/3$ rad. The net balanced power delivered to or from the stator of the machine is therefore as expected:

$$P_1 = \frac{3}{2}\widehat{V}\widehat{I}\cos\varphi \tag{9.29}$$

Consider the case where the peak phase voltages are balanced and include harmonics, $V_n$, but the phase currents are unbalanced and also include harmonics. (9.27) can be rewritten in terms of the peak positive, negative and zero sequence harmonic currents, $\widehat{I}_{+m}, \widehat{I}_{-m}$ and $\widehat{I}_{0m}$, respectively, as follows:

$$\begin{aligned} p_1(t) = \sum_{n=1}^{\infty}\sum_{m=1}^{\infty}\widehat{V}_n \sin(\theta_n)\{&\widehat{I}_{+m}\sin\big(\theta_{+m}+\varphi_{+m}\big) \\ &+ \widehat{I}_{-m}\sin(\theta_{-m}+\varphi_{-m}) + \widehat{I}_{0m}\sin(\theta_{0m}+\varphi_{0m})\} \end{aligned} \tag{9.30}$$

where in this case:

$$\begin{aligned} \theta_n &= n\omega_{se}t \\ \theta_{+m} &= +m\omega_{se}t \end{aligned}$$

Equation (9.30) reduces to:

$$\begin{aligned} p_1(t) = \sum_{n=1}^{\infty}\sum_{m=1}^{\infty}\{ &\frac{\widehat{V}_n\widehat{I}_{+m}}{2}\left[\cos\big(\theta_{(m-n)(m-n)}+\phi_{+m}\big) - \cos\big(\theta_{(m+n)(m+n)}+\phi_{+m}\big)\right] \\ &+ \frac{\widehat{V}_n\widehat{I}_{-m}}{2}\left[\cos\big(\theta_{-(m-n)(m-n)}+\phi_{-m}\big) - \cos\big(\theta_{-(m+n)(m+n)}+\phi_{-m}\big)\right] \\ &+ \frac{\widehat{V}_n\widehat{I}_{0m}}{2}\left[\cos\big(\theta_{(m-n)-n}+\phi_{0m}\big) - \cos\big(\theta_{(m+n)n}+\phi_{0m}\big)\right]\} \end{aligned} \tag{9.31}$$

When $m = n$, a DC contribution is made to the power in each phase as shown in (9.29). For harmonic components of power, however, because of the presence of the phase factor, $(q-1)2\pi/3$, a contribution to the power only occurs when $(m-n)$ or $(m+n)$ are multiples of 3, or are triplens. These contributions will be at $\pm(m-n)\omega_{se}t$ or $\pm(m+n)\omega_{se}t$, depending on whether the positive or negative sequence currents are contributing to the power.

From inspection of the last term in (9.31), it can be seen that there will be no zero sequence contribution to the ripple in instantaneous power. This is because for all values of $n$, the term in $(q-1)2\pi/3$ in $\theta$ ensures that the summation over three phases always comes to zero.

An application of these equations to the power CM of an electrical machine would be a three-phase induction motor with a broken cage. We already know from Table 9.1 that at a fundamental supply voltage angular frequency of $\omega_{se}$ the fundamental supply current will contain components at $(1 \pm 2s)\omega_{se}$.

Therefore for the first and $(1 - 2s)$th harmonics of voltage

$$\pm(m - n)\omega_{se} = \pm 2s\omega_{se}$$
$$\pm(m + n)\omega_{se} = \pm 2(1 - s)\omega_{se}$$

So, the power spectrum due to the fundamental supply voltage will contain components at $2s\omega_{se}$ and $2(1 - s)\omega_{se}$.

An example of this was simulated by Trzynadlowski *et al.* (1999), as shown in Figure 9.13, for a 6-pole induction motor with a damaged rotor fed at $f_{se} = 60$ Hz

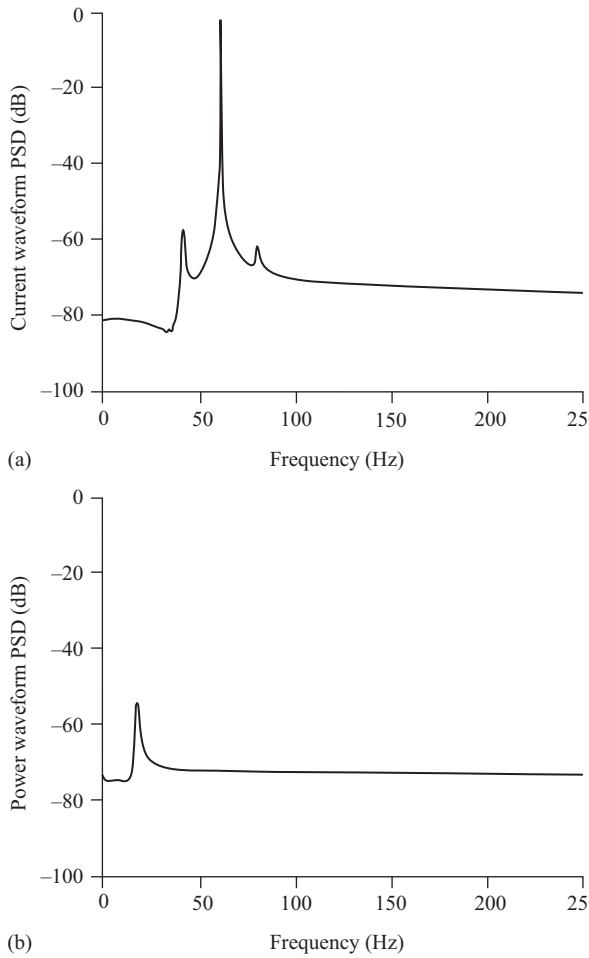


*Figure 9.13 Spectra from a simulation of an induction motor with broken rotor bars: (a) the upper curve shows the current spectrum with the typical fault side-bands and (b) the lower graph shows the power spectrum with the fault side-band shifted down to DC*

with a very large slip at this operating condition of 15.8%, therefore the side-bands on the current PSD spectrum due to damage are positioned above and below the 60 Hz fundamental, at 41 and 79 Hz, whereas on the power PSD spectrum the damage side-band is positioned at 19 Hz.

### *9.5.5 Shaft voltage or current*

Many electrical power utilities have attempted to monitor the voltages induced along the shafts of electrical machines in the hope that they may be a useful indicator of machine core or winding degradation and because they can give rise to large shaft currents, which are damaging to bearings.

Figure 9.14 shows how a voltage can be induced between contacts sliding on a rotating machine shaft whenever fluxes in the machine are distorted, either from the normal radial and circumferential pattern, or from the normal axial pattern. These sliding contacts may be the result of rubs on defective bearings or seals or could be brushes placed to detect flux distortion. The brushes would normally be placed at either end of the machine to embrace the complete shaft flux circuit. If a fault, such as a rotor winding shorted turn, produces a rotating distortion of the field in the radial and circumferential plane then an AC or pulsating shaft voltage results. If a fault produces a distortion of the field in the axial direction, then this gives rise in effect to a homopolar flux that produces a DC shaft voltage. In steam-turbine driven machines, shaft voltages can also be produced by electrostatic action, where the impingement of water droplets on turbine blades charges the shaft. Verma *et al.* (1981) have given a full report on the mechanisms for the production of shaft voltages and currents and the faults they may indicate. Methods of monitoring shaft voltages usually include making AC and DC measurements of the voltage and sometimes analysing the harmonic content of the waveform. Verma proposed a comprehensive shaft voltage monitor and Nippes (2004) a more up-to-date version.

Our experience, however, is that shaft voltage has not proved to be a useful parameter for continuous monitoring. The voltage is difficult to measure continuously, because of the unreliability of shaft brushes, particularly when they are

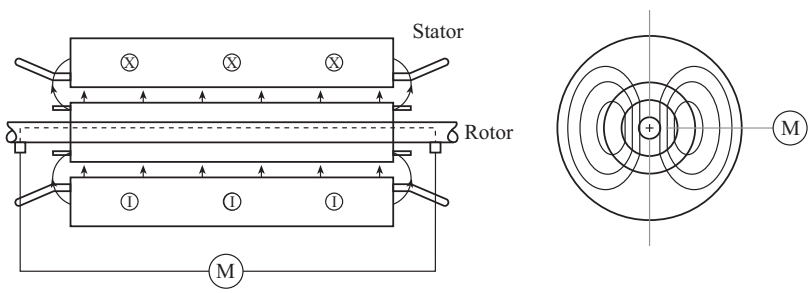


*Figure 9.14 Production of shaft voltages due to asymmetries in the magnetic field of the machine*

carrying only a small measurement current. In addition, it has been shown by authors' colleagues that any damage to the core and winding would need to be substantial before a significant variation in shaft voltage occurred.

This should not detract, however, from the normal regular maintenance procedure of measuring shaft voltages at bearing pedestals, from time to time, in order to check the pedestal insulation and to confirm that there is no tendency for large shaft currents to flow.

### *9.5.6 Mechanical and electrical interaction*

As can be seen in Section 9.6.4, there is considerable commonality between the approaches described in this section and those of Chapter 8, concerned, respectively, with the electrical and mechanical responses to faults in the electrical machine.

This commonality arises from the air-gap magnetic field and it will be important for future CM strategies on electrical machines to have a clear understanding of the link between the electrical and mechanical root causes of faults and their effect on the air-gap field.

Mechanical engineers will tend to look for faults via the vibration spectrum and electrical engineers will look via the current, flux or power spectra.

The reality is that all these spectra are closely coupled as set out in these chapters and it may be better to look for some faults via the vibration signal and for others via the flux, voltage, current or power signals.

A great deal more work has been done recently on mechanical and electrical interaction, particularly on generators used by wind turbines by Ibrahim *et al.* (2018) and Zappalá *et al.* (2019), who used particularly precise electrical and mechanical transducers to establish the consequences of mechanical and electrical interaction from faults.

These papers substantially increase earlier knowledge from Rai (1974), Hargis *et al.* (1982), Dorrell *et al.* (1997) and Nandi *et al.* (2005), showing that both mechanical and electrical measurements, torque, speed, vibration, current and power, detect fault air-gap field effects and their electrical and mechanical consequences.

A number of contributors, including Zappalá *et al.* (2019), describe how mechanical spectra are noisier than corresponding electrical spectra, partly due to instrumentation sensitivity but also because mechanical signals are influenced not only by air-gap excitation but by the machine frame response as well, see Chapter 8, which may mask fault responses.

However, experienced machine operators have high confidence in mechanical monitoring, for example, speed and vibration, and these can be combined with less understood, though stronger, electrical signals, power and current, to enhance their credibility, this will be dealt with in a later chapter.

In Table 8.6, we gave a summary of the lateral vibration angular frequencies caused by various faults.

In Tables 9.1 and 9.2, we now give a similar summary respectively of current and flux angular frequencies caused by various faults.

## 9.6 Conclusions

This chapter has shown that electrical techniques are powerful tools for the CM of electrical machines, particularly axial leakage flux, current and power, offering the potential to provide a general CM signal for the machine.

The availability of high-quality, digitally sampled, mechanical vibration and electrical terminal 'performance' data from electrical machines opens the possibility for more comprehensive monitoring of the machine and prime mover or driven machine combinations. However, these signals generally require broad bandwidth (>50 kHz) and a high data rate for adequate analysis. Therefore, the principal difficulty of applying these techniques is the complexity of the necessary spectral analysis and interpretation of their content.

This situation is made more difficult if VSDs are involved because time-domain signals may no longer be stationary and will also be polluted by harmonics from the power electronic drive, see Chapter 5.

Comprehensive monitoring of an electrical machine can be achieved by measuring shaft flux, current, power and electrical discharge activity. These are broad bandwidth (generally >50 kHz) signals requiring complex analysis.

Shaft flux, current and power signals are capable of detecting faults in both the electrical and mechanical parts of a drive train. Shaft voltage or current is an ineffective CM technique for electrical machines.

Shaft flux monitoring is non-invasive and uses a single sensor, but it is complex to analyse and untested in the field.

Current monitoring is also non-invasive, but uses existing sensors and has established itself as MCSA, a reliable and widely accepted technique for machine monitoring. This technique is demonstrated at work in an AI example in Chapter 14.7. Power monitoring is also non-invasive, uses existing sensors but requires less bandwidth (<10 kHz) and less complex spectral interpretation to detect faults but is not yet widely accepted, so it deserves investigation for future development.

*This page intentionally left blank*

*Chapter 10*

# Online partial discharge (PD) electrical monitoring

## 10.1 Introduction

Chapter 9 discussed about the perturbations to current, flux and power at the terminals due to faults in the machine, the electro-magnetic effect.

However, something else is at work in high-voltage electrical machines and that is perturbations to the voltage and current wave fed to the machine as a result of electrical disturbances or discharges in the insulation system, the dielectric effect.

PD occurs only in high-voltage machines with disturbances occurring at local peaks of electric stress. In general, in normal ambient conditions at sea level PD does not occur at winding phase voltages greater than 3 kV. Each individual PD represents a charge transfer of picocoulombs (pC), with an individual energy of pJ, a power of <pW, however there may be many PDs in each voltage half-cycle. Therefore, dependant on machine design, particularly winding insulation, application, voltage and environmental conditions, over time these PDs can damage the machine insulation.

This chapter deals with a more specialised, higher bandwidth electrical terminal 'performance' analyses than considered in Chapter 9, which have the potential to detect those discharge activities present in high-voltage machine winding insulation.

One of the reasons discharge monitoring has received so much attention is because the insulation system lies at the heart of every electrical machine and its deterioration can be relatively slow, as described in Chapters 3 and 4. Therefore, it should be a good target for CM, however, there are numerous very high-frequency events occurring embedded within complex winding and insulation systems, which any monitoring method must be able to detect and locate.

## 10.2 Background to discharge detection

Discharge behaviour is complex and can be categorised in the ascending order of energy and damage as:

- Corona discharge,
- PD,

- Spark discharge,
- Arc discharge.

A well-made insulation system will exhibit low-level corona discharge on the surface of the insulation at AC voltages above 3 kV to ground, see Figure 3.8. If there are voids inside the body of the insulation system, those voids will also exhibit PDs at the points in the voltage cycle when the local electric field strength exceeds the Paschen curve level for the gas in the void at that temperature. Neither that surface or body activity is necessarily damaging unless the activity is sufficiently powerful to degrade the insulation system, as can occur thermally or chemically, Chapters 6 and 7. This activity can progressively worsen depending on the quality of the insulation, the local strength of the field and the mechanical, thermal and electrical conditions to which the material is subjected. There are certain parts of high-voltage winding insulation systems that are particularly vulnerable to discharge activity, namely:

- Stator slot wall where PD activity can erode and damage the main wall insulation.
- Slot emergence where coils emerge from the earth protection of the slot and the insulation system is exposed to surface discharge activity.
- End winding surfaces, which can be subjected to damaging discharge activity, particularly at the phase separation regions, when the surface is wet or dirty or both.

A study of the failure mechanisms in Chapter 3 shows that electrical discharge activity is an early indicator of many electrical faults in machine stators, the activity is also be related to the remanent life of the insulation system.

The accurate detection of discharge activity could therefore give valuable early warning of failure and could provide information about the remaining life of the insulation.

Electrical discharges are transitory, low energy disturbances that radiate electromagnetic, optical, acoustic and thermal energy from the discharge site. That conducted energy causes perturbations to the waveforms of the voltage and current both within the machine and at the machine terminals. The earliest applications of PD detection were to isolated insulation components, such as transformer and high-voltage machine bushings or most successfully to the stop joints in oil-cooled EHV cables, see Wilson *et al.* (1982), where the insulation under inspection is close to the coupling circuit and is energised solely at the phase voltage of the cable.

After successful application on cable stop joints the method was then applied to the windings of HV turbo- and hydro-generators. However, an electrical machine winding, see Figure 10.1, represents a much more complex insulation system than a stop joint.

For example,

- The insulation is distributed throughout the length of the winding, which may represent many hundreds of meters in length,
- It is energised with a distributed potential, applying full-line voltage between the winding ends but zero voltage at the neutral point,

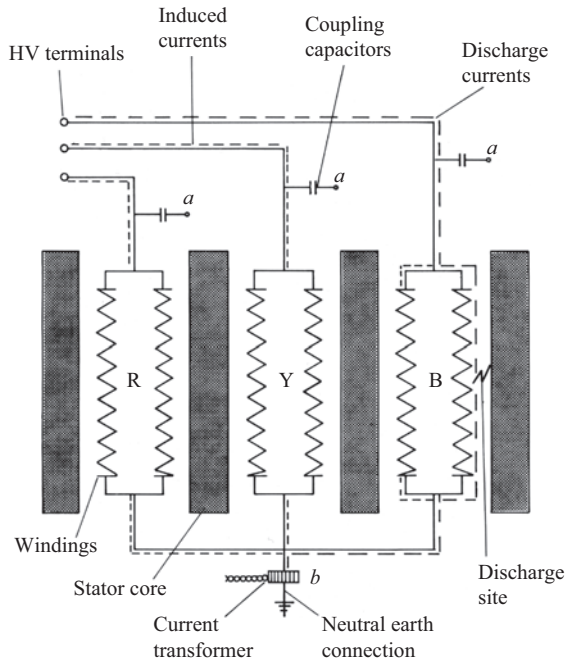


*Figure 10.1 Complex structure of a machine stator winding*

- The winding is complex from a propagation point of view:
  - Containing propagation path bifurcations:
    - at coil connections,
    - where sections of the winding are connected between phases,
    - where individual phases consist of parallel paths,
  - It also contains many surge impedance transitions throughout its length, see Figure 10.2:
    - as it enters and emerges from the slot,
    - as the coupling varies between winding components, in slot and end winding portions,
    - as it connects to the main terminals of the machine.

The following description traces the development of electrical machine winding PD detection up to the present day and demonstrates the value of and difficulties of discharge detection techniques.

## 10.3 Early discharge detection methods

### *10.3.1 RF coupling method*

The earliest work, summarised by Godwin *et al.* (1979), described a technique developed by Westinghouse in the United States to detect the presence online, of

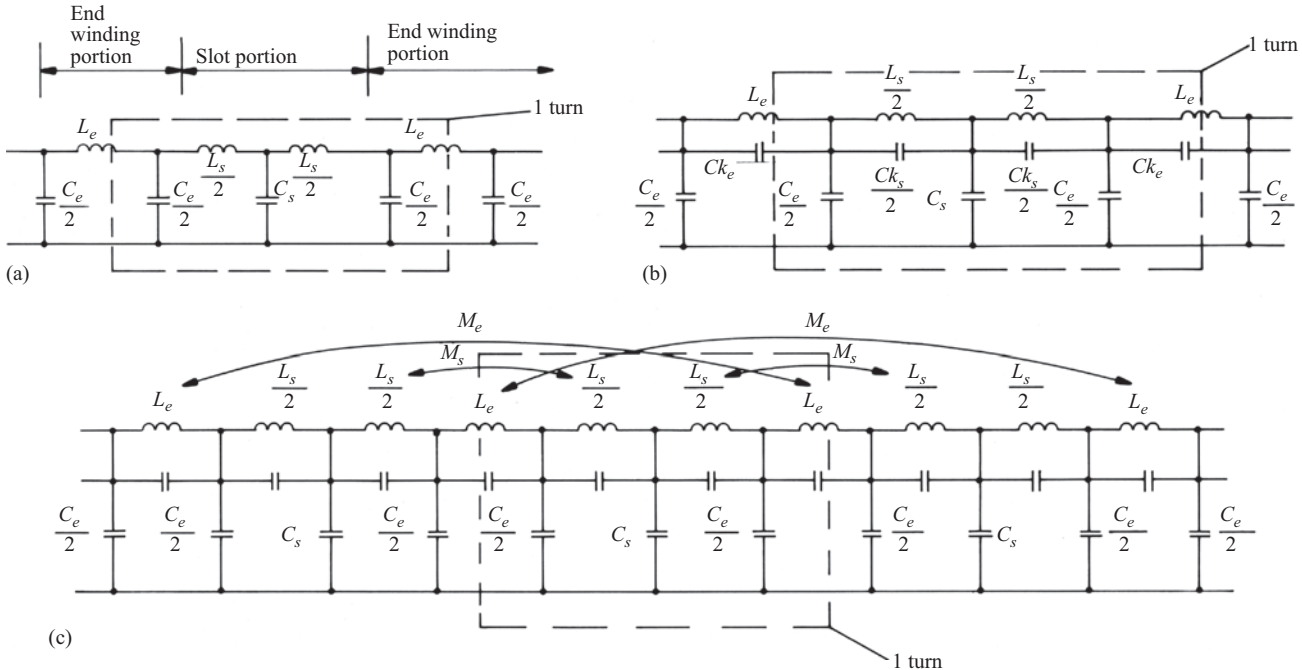


*Figure 10.2 Electrical structure of one turn of a typical stator winding and complex coupling arrangements: (a) simple model, one turn represented by a tee; (b) increased complexity, one turn represented by a series of tees and (c) further complexity, with core and end winding coupling approximated*

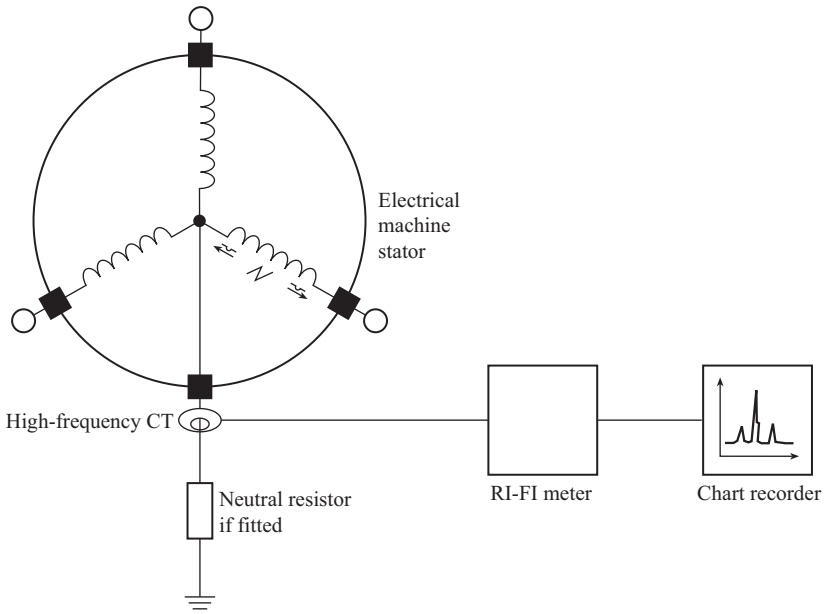


*Figure 10.3 Detection of discharge activity in a generator. Taken from Emery et al. (1981) © IEEE (1981)*

sub-conductor arcing in the stator windings of large steam turbo-generators, by measuring perturbations in the winding current. Arcing activity produces very wide-band electro-magnetic energy, some of which propagates into the neutral connection of the star-connected winding. Emery *et al.* (1981) used a ferrite-cored RF current transformer (RFCT) wrapped around the neutral cable to couple to this activity, which he detects using a quasi-peak, radio interference field intensity (RIFI) meter, as shown in Figure 10.3. The neutral cable was chosen a good measurement location because it is a low potential with respect to ground and because arcing at any location in the generator causes RF current to flow into the neutral lead.

The radio frequency CT (RFCT) has a frequency response from 30 Hz to 30 MHz and the RIFI meter has a narrow bandwidth of ~10 kHz centred at about 1 MHz. The centre frequency is nominally tuned to match resonances in the winding that the arcing activity excites; the RIFI meter effectively measures the average peak energy received by the instrument. The RFCT and RIFI meters are proprietary items and a simple monitoring system can be assembled using these components. Westinghouse also developed a specialised RF monitor based on this technique that is fully described in Emery *et al.* (1981). The monitor interface with a remote panel located in the machine control room and provides a permanent record of arcing activity, with alarm indications to the operator when a severe increase occurs. Godwin *et al.* (1979) had shown, with later details by Emery *et al.* (1981) and

Harrold *et al.* (1986), positive proof of the detection, not only of sub-conductor arcing, but also of sparking in other parts of steam-turbine-driven generators. However, the change in signal level when arcing occurs, from the RIFI meter tuned to 1 MHz, is not dramatic. An increase of <50% of the unfaulted indication is typical and this makes the setting of alarm levels for such a monitor difficult.

Timperley (1983) used this technique and applied it not only to steam turbo-generators but also to hydro-generators in the American Electric Power service. He appears to have used wider bandwidth quasi-peak RIFI instruments connected to the neutral RFCT because he analyses the received signal in both the frequency and time domains. Using the technique he has shown some evidence of the detection of slot discharge activity on hydroelectric machines and other forms of unexpected corona activity.

### *10.3.2 Earth loop transient method*

Wilson *et al.* (1982), in the United Kingdom, devised a similar technique to that of Emery *et al.* (1981) as a cheap method of detecting discharge activity online in a wide range of high-voltage plant. Initially it was applied to a relatively small, identifiable section of insulation, such as a stop joint in an oil-insulated EHV cable, and was known as an earth loop transient monitor. It has since been applied to the insulation of generator and motor stator windings and aims to look for PD activity in the bulk of the winding. It uses a Rogowski coil, wrapped around the neutral cable of the machine winding, and the detector is a narrow band instrument that measures the average peak energy received by the instrument as shown in Figure 10.4. The Rogowski coil is an air-cored solenoidal search coil that is closed on itself round a current carrying conductor. The manufacture of these coils was patented in the UK by Ward *et al.* (1993) and they are called Rogowski coils to distinguish them from their ancestor, the Chattock potentiometer, which is not a wrap-around coil as needed for current measurements. The frequency response of the Rogowski coil is relatively wide but the detector has a narrow bandwidth of ∼15 kHz centred at a value determined by the application and the background radio noise, but usually for a generator or motor winding this would be 1 MHz.

The monitor is calibrated in pCs and is provided with alarm circuits, so that when the discharge level exceeds a warning threshold an alarm signal can be transmitted to the plant control room. Wilson *et al.* (1982) explained that when applying this technique to a distributed insulation system, such as a machine winding, care must be taken in the calibration, because energy may be propagated to the instrument from a number of different discharge sites in the insulation simultaneously. Geary *et al.* (1990) provided a theoretical model for the manner in which energy, in the frequency band detected by the instrument, is propagated from the discharge site in to the winding neutral and he has shown how this propagation depends critically on the configuration of the winding and the size of the stator core, as described in Section 10.2.

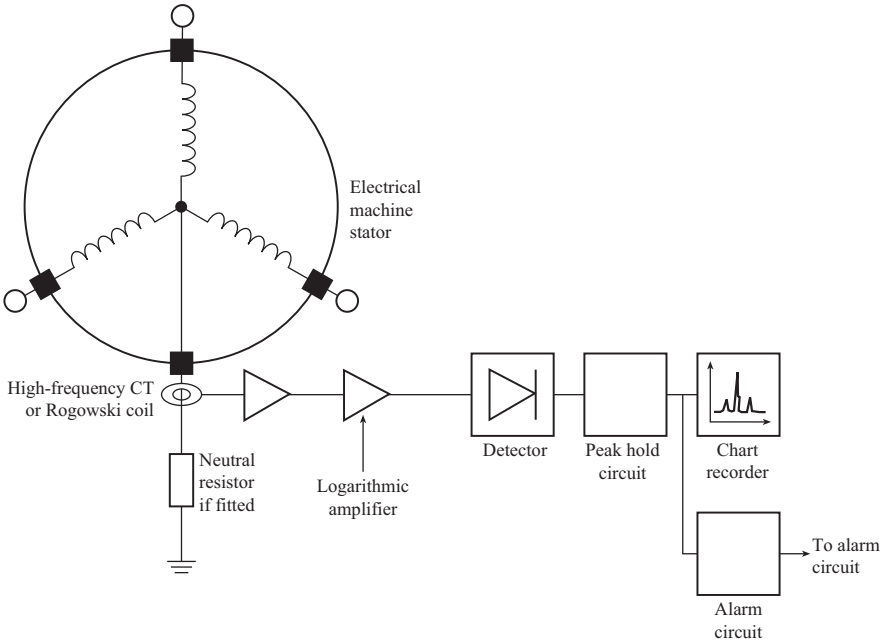


*Figure 10.4 Continuous monitor of discharge activity using an earth loop transient monitor. Taken from Wilson et al. (1982)*

### *10.3.3 Capacitive coupling method*

An alternative technique, where perturbations in voltage waveforms are detected at the machine terminals, has been described by Kurtz *et al.* (1979) and applied primarily to hydro-generators in Canada aimed at detecting the slot discharge activity with which these high-voltage air-cooled windings are afflicted. Connection to the winding is made through coupling capacitors connected to the line terminals of the machine as shown in Figure 10.5. Discharge pulses are coupled through these capacitors to a specialised pulse height analyser, which the analyser electronics captures up to 80 MHz, sufficient to capture PD pulses with rise times of the order of 1 to 10 ns. In the early days of this technique capacitative couplers had to be connected to the machine during an outage but in a later publication Kurtz *et al.* (1980) describe how capacitative couplers can be permanently built into the phase rings of the machine so that the measurements can be made without service interruptions. In addition, these permanent couplers are also intended to ensure that discharge activity from the electrical supply system, to which the machine is connected, is rejected. However, the pulse height analysis of discharges by this method is still carried out at intervals during the life of the machine rather than continuously online. Kurtz *et al.* (1979) and (1980) have not shown how the electromagnetic energy from a discharge site is propagated through the winding to the coupling capacitors but have shown empirically that the method is capable of

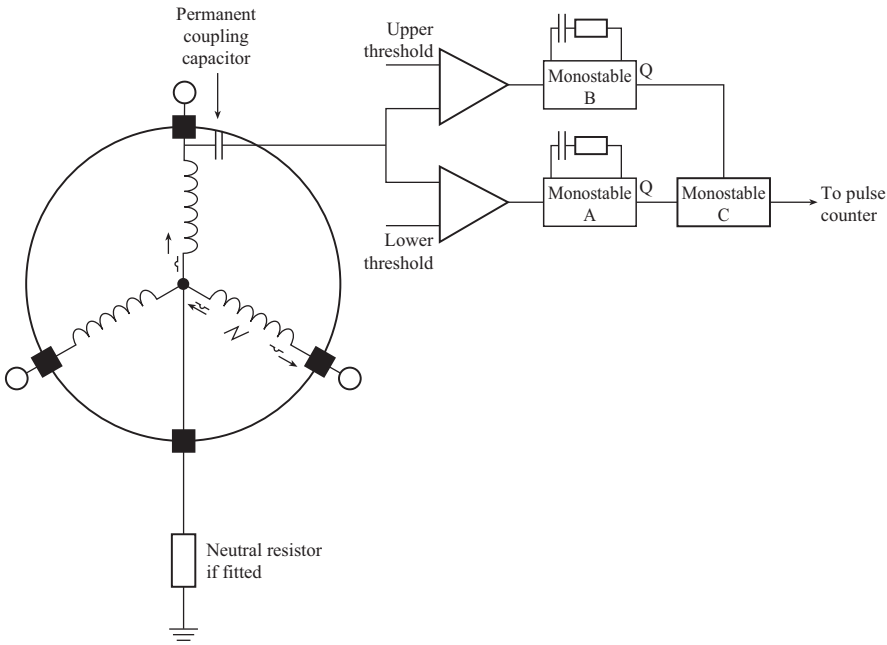


*Figure 10.5 Detection of discharge activity using a coupling capacitor. Taken from Kurtz et al. (1980)*

detecting slot discharges and the steady deterioration of winding insulation with time.

### *10.3.4 Wide-band RF method*

The techniques for detecting insulation deterioration described in Sections 10.3.1–10.3.3 operate at relatively low frequencies (1–80 MHz) and detect the electromagnetic energy propagated along the winding to the neutral or line end connections, see Tavner *et al.* (1986). They are generally known in North America as electromagnetic interference (EMI) detection methods.

In any healthy machine, there will be a background of corona and PD activity that will vary from machine to machine and also varies with time. Tavner *et al.* (1986) described a technique, developed by Malik, following the approach of Emery *et al.* (1981) and Harrold *et al.* (1986) but demonstrating that more damaging discharge pulses, such as sparking or arcing, have faster rise-times than background corona and PD activity and therefore produce a wider frequency band of electromagnetic energy (10–350 MHz). This work showed that if this energy is detected, at as high a frequency as possible, the ratio of damaging discharge signals to background activity is increased, see Figure 10.7. Frequencies of electromagnetic energy >4 MHz propagate from the discharge site by radiation from the winding, not by propagation along the winding as in the case with the lower

frequency techniques. This radiation can be detected by a radio frequency (RF) aerial located either inside the enclosure of the machine or outside, close to an aperture in it. The technique is similar to that proposed by Michiguchi *et al.* (1983) for detecting the faults in brush-gear. A monitor for detecting damaging turbo-generator stator winding sub-conductor arcing activity was described based on this idea, as shown in Figure 10.6. It receives the energy from an aerial and amplifies it before detection. The monitor contains a band-pass filter tuned above the cut-off frequency of background activity (~350 MHz), avoiding interference from nearby radio or radar stations, to the part of the spectrum that is of interest. The output of the monitor is a chart record that shows the instants in time at which the energy due to damaging discharge activity exceeded a threshold value. This threshold can be set according to the level of background activity in the machine.

The monitor has been used successfully on large operational steam-driven turbo-generators, where the aerial was fitted outside the cooling casing by mounting it close to the neutral point connection bushing. The instrument positively identified proven sub-conductor arcing and has been shown to detect other forms of damaging discharge activity. Its advantage over the other techniques is that by detecting at higher frequencies the signal-to-noise ratio of damaging activity to background is larger and this makes it much easier to determine alarm settings for the instrument, as shown in Figure 10.7.

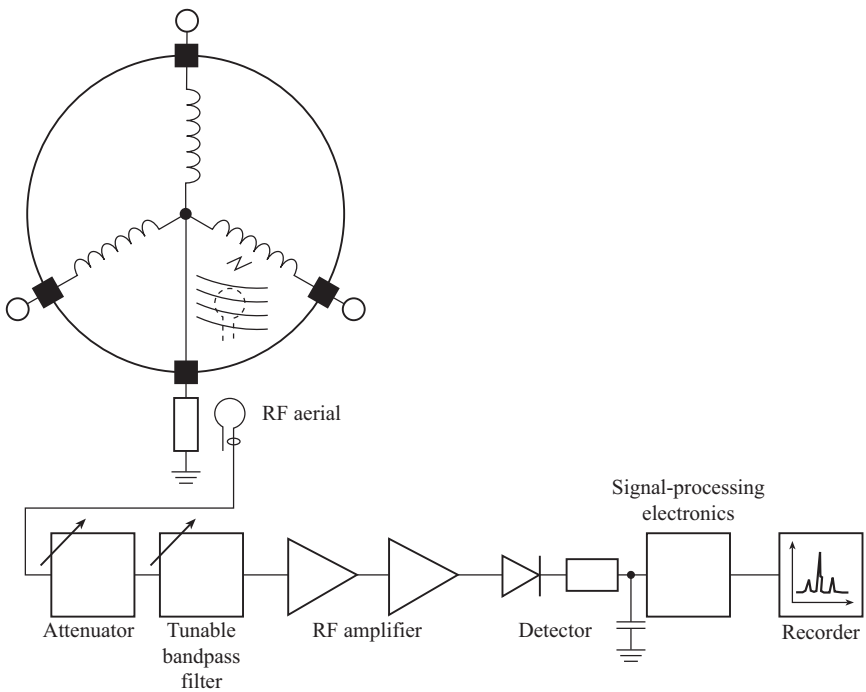


*Figure 10.6 Detection of damaging discharge activity using RF energy*

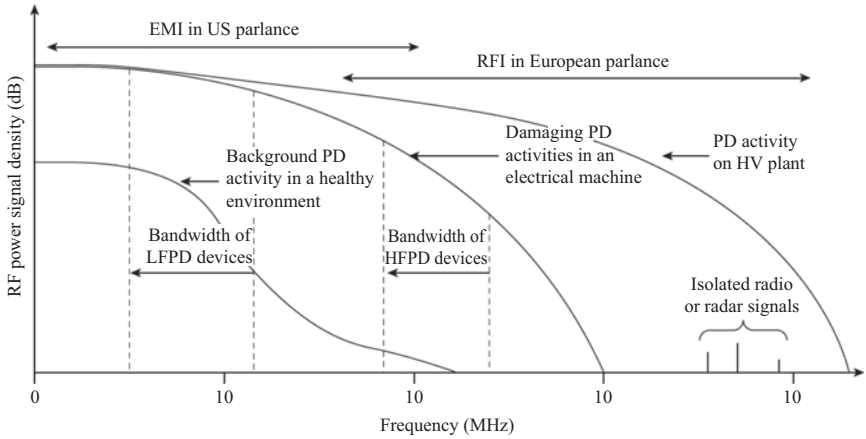


*Figure 10.7 Radio frequency energy from background and damaging discharge activity*

On the other hand, the received signal loses information so the relationship to discharge pC magnitude and time is lost and the method is subject to interference from commercial radio and radar transmissions, although these can be screened out when their specific frequencies are known.

This wide-band RF data collection technique is similar to that currently used in monitoring PD activity in large sub-stations with various spatial aerial/sensor arrangements and generally termed RFI detection, see Figure 10.7. However, in the case of PD monitoring in large sub-stations, with spatial sensor arrangements, more sophisticated time and frequency domain data processing allows preservation of some relationship between pC magnitude, timing and location. So far, this has not been possible in electrical machines.

### *10.3.5 Insulation remanent life*

Besides identifying specific faults, PD detection and measurement has held out the possibility of determining the insulation system remanent life and this has occupied a considerable amount of the literature as described by Stone *et al.* (2014). This process requires measurements of insulation resistance, polarization index, capacitance, dissipation factor tip-up, PD magnitude, and discharge inception voltage as well as online PD activity and is a difficult and elusive objective.

## 10.4 Detection problems

Lower-frequency work (1–80 MHz), called EMI in North America, involving propagation along a homogeneous conductor, suggests that a discharge site can be located by timing the arrival of discharge pulses received at a number of different sensors. This has now been demonstrated, as shown in the next section on modern techniques, but reflections at each discontinuity in the winding or variation in its

insulation and connection, see Figure 10.2, make pulse identification at the terminals extremely difficult. Low-frequency RFCT devices (EMI) produce an output calibrated in pCs of discharge activity, because the response can be related directly to the amplitude of a discharge calibration pulse. This allows the user to see the measured activity in discharge terms so that he can decide what level of activity he considers to be damaging. Various PD detectors have been investigated, including the portable Tennessee Valley Authority (TVA) probe and discharge locator (DL), by Sedding *et al.* (1989) and the stator slot coupler (SSC), Sedding *et al.* (1991), which can be mounted above the stator conductor in the slot beneath the wedge, see Figure 3.4. These confer some advantages in enabling the operator to locate the discharge activity.

The Rogowski coil developed by Ward *et al.* (1983) was shown to be easier to fit than the RFCT but initially suffered from low sensitivity and for a time was little used, but Rogowski coil and amplifier design has now improved, they are therefore commercially available and have become industrially accepted, they are now widely used for the detection of PD activity.

More recently PD measurement has also been made using a standardised capacitive coupler, a robust power engineering component based on the Canadian experience of Kurtz *et al.* (1979) and Stone *et al.* (1992), whose capacitance $C$ can easily be calibrated in $Q_m$, the discharge value in millivolts across the coupler, where $Q_m$ in millivolts $= Q/C$, where $Q$ is the discharge value in pC.

The higher signal-to-noise potential of wideband RFI techniques at frequencies (100 MHz–1 GHz) described in Section 10.3.4 has been investigated further by Stone *et al.* (2014) and from this work there would appear to be the potential for discharge site location by the use of directional aerials. But at the frequencies involved, the dimensions of such an aerial, diameter from 0.6 to 6 m, would be impracticably large for use in electrical machines and in any case the complex machine structures cause reflections and local resonances would disrupt that location. However, this method has been used successfully in transformers using three or more RF sensors located in positions on the surface of the transformer tank to triangulate the location of defects. This work has then led to the development of wide-ranging substation and HV plant PD detection described above.

Ultrasonic detection of the noise emitted from discharges has also been demonstrated on switchgear sites and transformers to be a more effective fault locator than PD methods in rotating electrical machines. So despite the potential of wideband RF techniques their lack of location ability means that the technique has now largely been superceded for the rotating machines.

It must be made clear at this stage that there is less value in being able to detect discharge activity if, when the machine is taken out of service, that activity is impossible to locate. It would be preferable to allow damaging discharge activity to continue until it had reached such a pitch that the damage was observable, see Figures 3.8 and 3.9. This highlights the problem of what constitutes a significant level discharge activity.

In all PD detection systems, it is necessary to shield the desired PD activity signal from the external noise, either due to PD activity in the connections and

*Table 10.1 Probability distribution of $Q_m$ in mV from a database of results from a set of air-cooled machines using 80 pF capacitive couplers, taken from Stone et al. (2014)*

| | | Machine-rated voltage | | | |
|---|---|---|---|---|---|
| | | **2–5 kV** | **6–9 kV** | **10–12 kV** | **13–15 kV** |
| Cumulative probability (%) | 25% | 8 | 29 | 34 | 50 |
| | 50% | 20 | 70 | 77 | 113 |
| | 75% | 63 | 149 | 172 | 239 |
| | 90% | 228 | 288 | 376 | 469 |

switchgear of the electrical machine or due to sparking in brush-gear or harmonic activity due to nearby power electronics. In some cases, when the electrical machine is connected to the system via a lengthy, low-discharge XLPE cable, that provides the necessary filter, but it is not always so. These noise and calibration issues are dealt with by Geary *et al.* (1990), Stone *et al.* (1992), Wood *et al.* (1993), Campbell *et al.* (1994) and Kemp *et al.* (1996).

Another fundamental problem for all PD detection systems is that the discharge activity of identical windings in different machines exhibit large variations in background activity, due to variations in ambient conditions, differences in insulation manufacture and homogeneity and in noise conditions. Therefore, one cannot say with any certainty what the background discharge activity for a winding should be, and this activity will vary naturally with time, regardless of whether any damaging activity is taking place.

An example of PD detection results taken from a database of a number of air-cooled machines in the US, measured using capacitive couplers, is shown in Table 10.1, which shows the percentage cumulative probability of PD variations, measured in $Q_m$ millivolts, with rated voltage between machines. Thus, for a rating of 13.8 kV, 25% of machines had a $Q_m$ <50 mV and 90% had a $Q_m$ <469 mV, therefore if a measurement of $Q_m$ of 500 mV occurred in such a machine, the operator knows that it has a PD higher than 90% of all similar machines.

## 10.5 Modern discharge detection methods

Modern online discharge detection methods for rotating electrical machines have developed from the early work described in Section 10.3, improved to resolve some of the problems described in Section 10.4 and can now be divided into two techniques:

- The hydro-generator partial discharge analyser (PDA), based on Section 10.3.3 above, see Figure 10.8 and Lyles *et al.* (1993).
- The motor or turbo-generator analyser (TGA), based on Sections 10.3.1 and 10.3.2, which adopts a variant of the PDA to improve the signal-to-noise

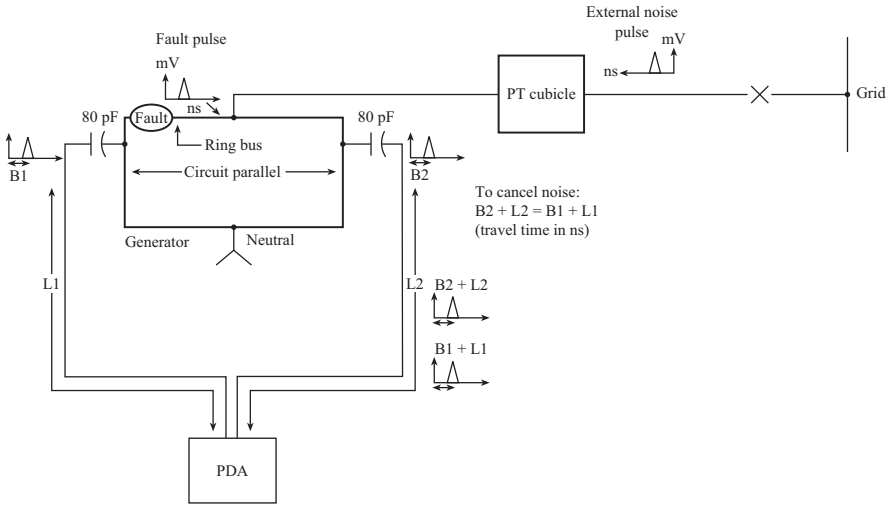


*Figure 10.8 Diagram of the coupler connections and electronics for the PDA. Taken from Lyles et al. (1993) © IEEE (2004)*

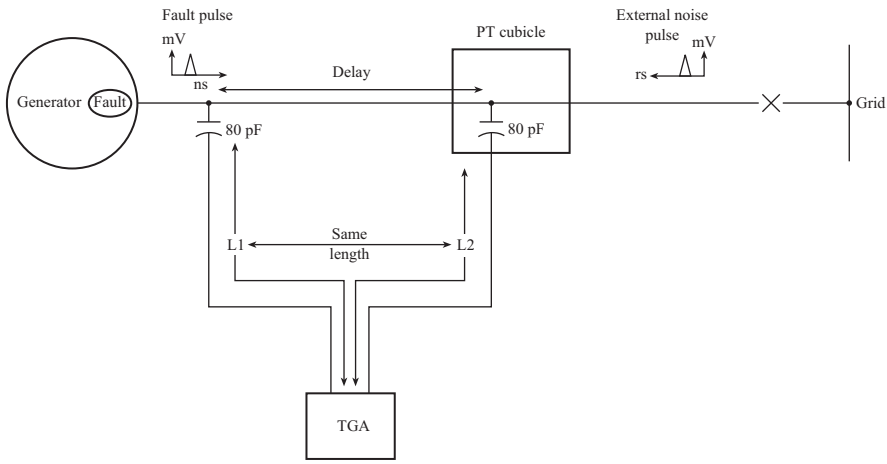


*Figure 10.9 Diagram of the connections and electronics for the turbine generator analyser (TGA). Taken from Stone et al. (1996) © IEEE (2004)*

ratio of PD detection on windings of the types found in motors and turbo-generators, see Figure 10.9. Experience with this technique is described in Stone *et al.* (1996).

A standard has also been devised, IEEE Std 1434 (2014), to regularise the measurement of PD on rotating machines.

Work continues to improve PD detection methods, including work on lower voltage, 4 kV, motors by Tetrault *et al.* (1999), work on large machines by Kheirmand *et al.* (2004) and an example of an insulation monitoring system that detects insulation leakage currents by measuring machine terminal voltages on an induction motor by Lee *et al.* (2005).

Perhaps, the most exciting recent development in PD electrical machine detection results from the application of expert systems or AI to the classification of discharge occurrences, as described by Contin *et al.* (2011). Electrical machine insulation failure mode descriptions in Chapters 3 and 4 showed that PD occurs at specific points in a stator winding insulation and at specific times in the voltage waveform. On a test 13.8 kV stator coil, Contin has shown that by fast recording and storage of individual PDs, then classifying their duration, frequency content and whether they occur in the positive or negative voltage half-cycle. Then it should be possible to infer their location and detect the onset and progress of damage at known sites of insulation weakness. Figure 10.10, taken from Contin *et al.* (2011), shows how this could be possible, segregating coil PD into separate types and locations, A and B.

In this way the electrical machine PD problem, of a distributed insulation energised by varying potential over great length, could be resolvable by the use of powerful expert systems or AI. However, authors of this book recommend that we must not underestimate the scale of extending such an approach to a full-scale,

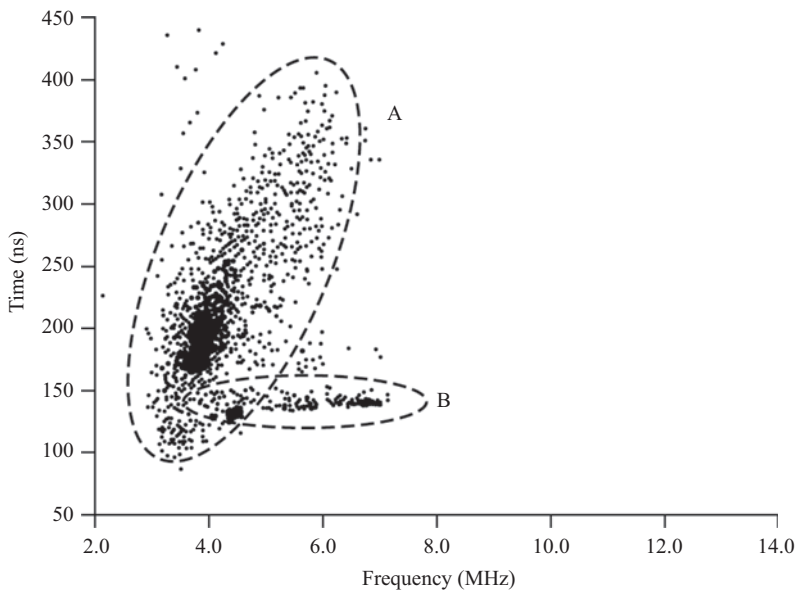


*Figure 10.10 Time–frequency segregation of PD, showing separate types and locations, A and B. Taken from Contin et al. (2011) © IEEE*

realistically manufactured winding, exposed to moisture and oil contamination in an operating environment where stator voltages may alter with time.

## 10.6 Conclusions

Discharge measurement has shown itself to be the most problematic electrical method of electrical machine CM. It requires special sensors, wide bandwidth (>100 kHz) and very complex analysis for fault detection. It can only be recommended where a specific and costly high-voltage failure mode is being searched for in a known location on a large machine.

It addresses one of the most vital parts of the electrical machine, it can detect global effects, including possibly remanent life of the machine insulation and it does give a long warning before failure occurs. Yet, the analysis of Chapter 4 shows that, with modern materials, the proportion of machine failures due to insulation faults are now less than a third. Furthermore, the detection methods rely on the most advanced signal processing to extract useful indications, which are then open to wide interpretation by PD measurement experts.

This has made it extremely difficult to increase the confidence of machine operators in the value of this type of monitoring because of their need to refer to differing expert opinion.

PD monitoring was first applied to isolated insulated components, such as bushings and cable stop joints where it had and continues to have a vital role to play. Its greatest impact to date has been on transformers, sub-station plant, gas- and air-insulated switchgear, where specific Failure Modes in particular locations are being searched for using both wide-band RFI and narrow-band EMI techniques, with support from acoustic measurement.

However, when applied to the distributed, multi-path, multi-connection, variably stressed insulation system of an electrical machine winding, shown in Figures 10.1 and 10.2, it has a much more difficult task.

These methods have been valuable on large machines such as hydro-generators where stator winding fault locations are limited to particular machine ends and their connections, allowing the precise location of sensor couplers, the tailoring of signal processing to that failure mode and where the asset value justifies the application of complex techniques.

Work still continues to develop this method, including the use of AI, see Chapter 14, to determine the overall deterioration of a winding insulation system but that objective has not yet been reached.

However, the most thorough treatise to navigate this complex but promising technology is undoubtedly Stone *et al.* (2014).

*This page intentionally left blank*

*Chapter 11*

# Online variable speed drive machine monitoring

## 11.1 Introduction

VSDs are being applied to increasing numbers of electrical machines of all types. This edition of the book was prepared on the basis that it includes the specific problems of condition monitoring VSDs. Electrical machines in VSDs have been reported to be less reliable than those fed direct-on-line from the grid mains, see Montanari (2017). This is because the voltage supply imposes extra stresses when synthesised by a power electronic converter; in particular, the voltage waveform contains fast switching edges with high d$V$/d$t$. Two main problems, both of a wear-out nature, have been an industry focus:

- Stator winding insulation failures,
- Drive-side shaft-bearing failures.

These are more likely to occur when an old machine which has been in service is retrofitted with a variable voltage and frequency supply to achieve speed control and improve the energy efficiency.

Our focus here is on drive systems using voltage source converters (VSC) where the DC link is capacitively smoothed. Two-level pulse-width-modulation (PWM) is usually used in low-voltage drives for machine voltages up to 690 $V_{rms}$ line–line. Multi-level converters may be used in MV drives for motors up to 11 kV, see Stone *et al.* (2014). In addition to voltage source converters, there are also current source converters with an inductively smoothed DC link for large motors rated at tens of MW. Harmonics and inter-harmonics in the inverter output and machine windings also increase machine stresses through electrical, thermal and mechanical effects.

Growing areas of VSD application are electric traction, including rail and electric vehicles, where both induction and permanent magnet motors are used but reliability and CM are obviously important. Another area that has become substantial in recent years is renewable power generation, particularly wind turbine systems with induction, doubly fed induction or permanent magnet generators. Reliability and maintainability have become increasingly important as more variable speed wind turbines are deployed offshore. In this chapter, we will outline some major and common issues of electrical machines in VSDs or generator systems and describe the available techniques for monitoring the major fault

mechanisms which are new to VSDs. The working principles of these techniques will be analysed to understand their capabilities and limitations.

## 11.2 Operation and fault mechanisms

It is useful here to identify the key mechanisms that CM could detect from VSD drives:

- When supplied from a VSD all terminal 'performance' quantities of the electrical machine, voltage, current, power and axial flux will be polluted by harmonics generated by the drive. Filtering this pollution will be essential to obtaining a good signal-to-noise ratio with CM signals from such a machine,
- If the speed of the drive remains constant for substantial periods of time, then spectral analysis of flux, voltage, current, power or vibration, as described in Chapters 8 and 9, can still be done provided that the results are interpreted for the speed and base frequency when the measurements were made,
- However, if the speed is varying then non-stationary techniques, such as spectrograms over short time intervals, wavelets or Wigner–Ville techniques, dependent on the rate of change of speed, will need to be used with the monitoring signals because the spectra will not be stationary,
- If speed is varying under control in-loop action then the frequency content of monitoring signals will be affected by the bandwidth of the controller, as described by Bellini *et al.* (2000). In this case, it is possible for the drive controller to suppress fault harmonic signals in the flux, voltage, current, power or vibration. However, Bellini *et al.* (2002) have shown that it is still possible to extract CM information from signals derived inside the controller, and in Bellini's example this was done from the direct axis current, $i_d$.

Chen *et al.* (1994) demonstrated a CM system for variable-speed induction motors using the power line as his communication channel. This is a brave attempt to achieve universal monitoring and wisely the author has avoided monitoring the electrical signals but concentrated upon monitoring winding temperature.

### *11.2.1 Insulation degradation mechanisms*

Figure 11.1 shows the insulation structure of random and form wound stator windings. Proper insulation strengths need to be maintained between phase windings, between winding conductor and core through a semiconductive coating and the ground-wall insulation, between turns of the same phase and between core lamination sheets. In operation, the insulation tends to age through four types of stresses:

- Thermal,
- Electrical,
- Ambient, environmental,
- Mechanical.

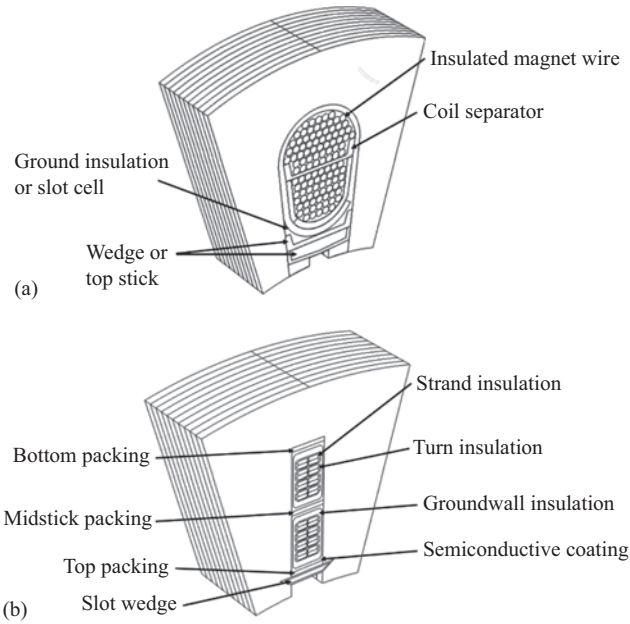


*Figure 11.1 Stator winding insulation structure: (a) random-wound winding and (b) form-wound winding*

These are collectively referred to as TEAM. Compared to an AC machine with a pure sinusoidal supply, an inverter supply exacerbates these stresses. The inverter type used most widely is the voltage source inverter operated in the PWM mode. The additional impacts of such a voltage supply are:

- The amplitude of the voltage applied to the machine is determined by the DC link voltage rather than the phase angle in a fundamental cycle,
- Without over-modulation, the DC link voltage must be higher than the peak value of the fundamental line–line voltage on the AC side,
- As a result, the winding insulation is constantly subject to high transient electric field levels, which can also affect PDs that may occur, see Montanari (2017).

Chapter 3 stated that in normal ambient conditions at the sea level PD does not occur at sinusoidal winding phase voltages <3 kV. However, presence in a VSD output high d$V$/d$t$ switching edges in the output waveform excite high-frequency resonances, depending on the inverter machine connection cable and distributed winding characteristics. As a result, even higher peak voltages can be expected, particularly near the machine terminals and the high-frequency alternating electric field inside the insulation material induces power loss which can cause increased temperature rise, Stone *et al.* (2014). However, modern LV 2- or 3-layer polyimide winding wire coatings can resist the effects at phase voltages up to 3 kV. There is

increasing intent, with multilevel converters, to apply higher voltages to larger machines, particularly in the expanding wind power and traction environments, so we can expect an increase in issues of winding insulation degradation in these industries.

Supply harmonics in the relatively low-frequency range can cause mechanical vibrations as well as additional power losses in the windings and magnetic cores, see Tsypkin (2017). This tends to loosen the lamination structures and cause abrasion against the winding insulation. It is particularly harmful when an excitation frequency coincides with a core or winding structural resonance.

Since the mid-1990s, industry has tried to understand and manage the additional stresses arising from inverter supplies. From a winding insulation point of view, the most important modification is perhaps to use a semi-conductive coating in the slot section of the coil to prevent discharge in the air pockets between the coil and core. However, it has been discovered that this coating itself can degrade over time, due to diverted leakage current flow, Sharifi *et al.* (2010) or due to abrasion Tsypkin (2017). Cost permitting, the semiconductive layer has been used more widely in high-reliability machines to eliminate locally high electric fields, see Barater *et al.* (2017).

Figure 11.2(a) shows the discharge activities detected and related to the phase angle of 50 or 60 Hz sinusoidal voltage. When the same machine was supplied from a PWM voltage source inverter, the pattern of PD is then changed to that shown in Figure 11.2(b); see Montanari (2017). Now the PDs tend to occur around switching edges of the inverter voltage and occur at higher amplitudes due to the voltage ringing effect. However, the switching edges introduce noise which makes the measurement more difficult.

The consequence of insulation degradation or failure is increased winding leakage currents, or an eventual short circuit which sits in a strong and alternating magnetic field. An unchecked fault current flows in the machine but cannot easily be detected by differential or over-current relays. This may quickly lead to overheating and destruction of the machine. With an inverter supply, the supply current may also increase upon insulation breakdowns. This can prevent further damage to the machine but will inevitably lead to a whole system shut-down.

### *11.2.2 Bearing current discharges*

The damaging effect of bearing currents on a VSD machine system is now widely known. The bearing current consists of many pulses corresponding to inverter switching actions. They may be of a conduction nature in which case the current is not harmful. But at a high rotating speed, lubricant films are formed to act as insulation between the bearing rollers and the races. The bearing then behaves more like a capacitor. The bearing current spikes can be constantly induced by the high $\mathrm{d}V/\mathrm{d}t$ edges in the common mode nature between the inverter phases, or DC link, and the ground, or motor frame. The current can be of a capacitive nature across the insulation layers formed by the lubrication oil film. The current through the bearing can also be of a resistive nature when metallic contacts are present between the

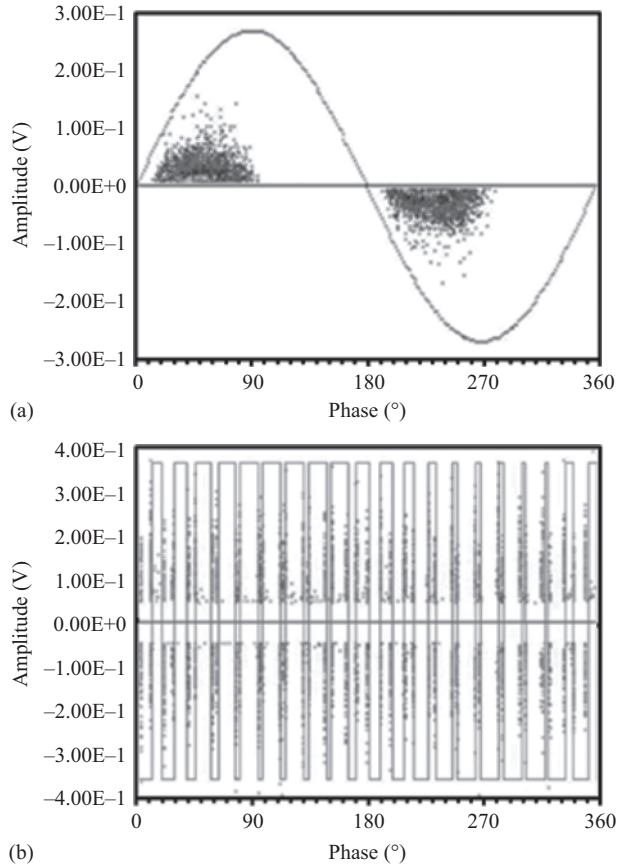


*Figure 11.2 Measured motor PDs, from Montanari (2017): (a) sinusoidal mains supply and (b) PWM inverter supply*

rollers and races. Actual damage is caused by the discharges or dielectric breakdown in the oil film, causing electric discharge machining and chemical changes in the lubricant, see Erdman *et al.* (1996). The corresponding bearing current is no longer caused by the d$V$/d$t$ but by too great an instantaneous voltage across the lubricant film, resulting in a discharge spark in the lubricant. Depending on the film thickness, dielectric breakdown occurs with a threshold voltage, across the film, in the order of 5–30 V, see Muetze *et al.* (2011).

Consequently, the surfaces of both the bearing rollers and races will roughen more quickly with a voltage source inverter supply, causing damages to other parts in the mechanical drive train. Figure 11.3(b) shows a micrograph image of a bearing race subject to the discharge bearing current effects. The traces caused by normal running of the ball roller, indicated by 1, and the spots caused by discharges, indicated by 2, are clearly distinguishable and the discharge spots or micro

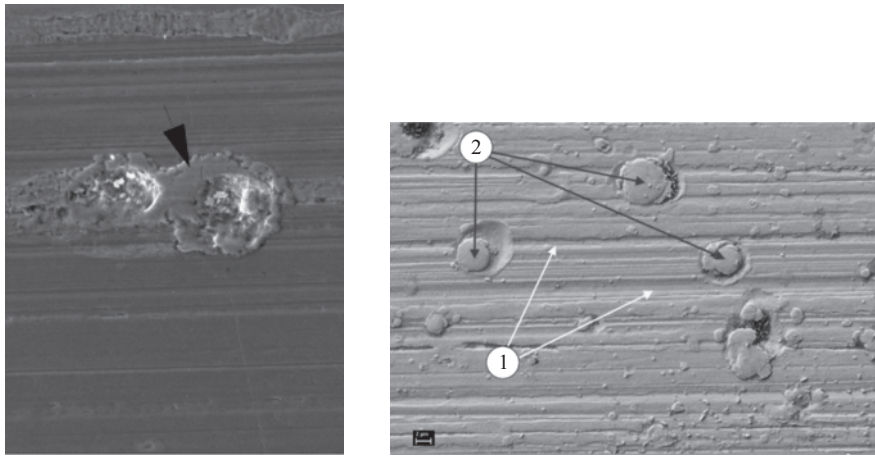


(a) (b)

*Figure 11.3 Comparing bearing effects of conventional shaft currents with fast dV/dt VSD currents: (a) photograph showing sleeve-bearing electro-pitting due to the flow of mains frequency generator shaft current and (b) micro-graph showing 1. ball-bearing race wear and 2. micro-pitting, due to fast dV/dt VSD currents, source: SKF*

craters, will be harmful during normal running. Compare both the images in Figure 11.3(a) and (b) to see the different effect of electro-pitting product of a sleeve bearing by mains frequency bearing current, see earlier Figure 3.19, with the discharge product of high frequency VSD d$V$/d$t$. The surface roughness in Figure 11.3(b), due to VSD d$V$/d$t$, affects the lubrication film as well as the nature of the discharge taking place. It has been reported that the discharge activities depend on the operating condition of the drive system, and the health condition of the bearing itself, Muetze *et al.* (2011).

Figure 11.4 shows the possible paths of VSD-bearing currents, see Chen *et al.* (1998):

- Common mode current through capacitive coupling,
- Circulating current due to the distribution gradient of the common mode current in the axial dimension,
- Discharge-bearing current due to high electric field strength.

The voltage across a lubricant film causes the discharge, may be initiated by the other two current modes. In some systems, brush-slip ring kits can be used to bypass the bearing and prevent the damaging discharge. But many low-voltage motors do not have such an arrangement which, in the presence of a shaft voltage, may also be undesirable because a large circulating current would be constantly present. A choke, or filter, may be used to damp the common mode bearing current, provided that this does not introduce high earthing resistance between the inverter

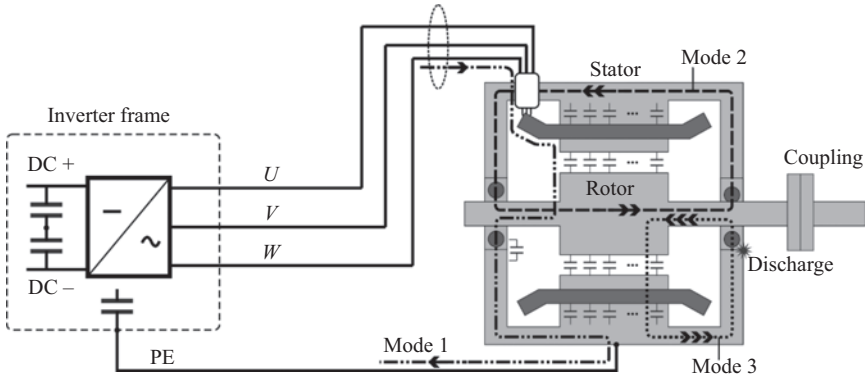


*Figure 11.4 Possible paths of VSD-bearing currents*

and motor frames, see Ogasawara *et al.* (1996). But this adds to cost and usually impedes the drive performance in other aspects.

In addition to these specific ageing-to-failure mechanisms, motors fed by inverters are also subject to degradation common in mains-fed motors.

It has also been recognised that many motors fed by inverters are under speed or torque control which are implemented by inner current loops. The controller structure and response would inevitably affect the CM signatures extracted from motor current and/or vibration measurements. The chapter will also provide a discussion on this issue.

## 11.3 Bearing current discharge detection

In a VSD motor, the presence of high-frequency current spikes coupled to the bearings from the winding supply can be an issue. Almost every switching event in the inverter will excite such a current spike if the bearing is not bypassed by a brush-slip ring kit or the inverter modulation scheme is modified to reduce common mode voltage. From a CM point of view, the bearing discharge current needs to be detected and collected for data analysis, because this type of current is damaging to bearing surfaces and the chemical composition of the lubricant. It is therefore important, Ran *et al.* (1998), to understand the features of the two different types of bearing current:

- Discharge-bearing current,
- High-frequency bearing current, caused by inductive coupling.

Figure 11.5 compares these two types of bearing current. They are both attributed to inverter switching common mode voltage, but are related to different parts of the common mode voltage waveform. While the high frequency is caused by switching edge $dV/dt$ and is oscillatory in nature, the discharge-bearing current is associated with insulation breakdown as the voltage build-up across the lubricant

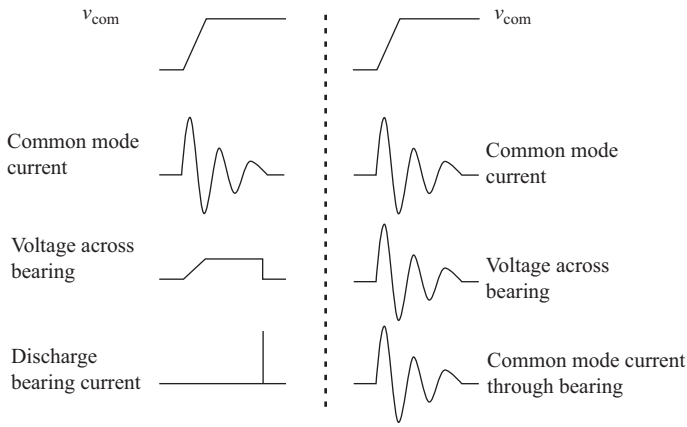


*Figure 11.5 Features of discharge- and switching-induced bearing current*

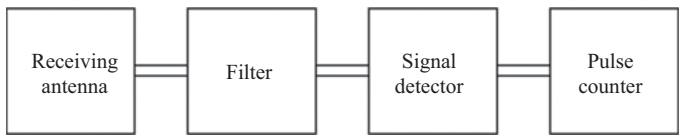


*Figure 11.6 Detection scheme of discharge-bearing current*

film exceeds the critical value, which is ~4 kV/cm and affected by contamination and moisture, Niskanen *et al*. (2014).

A condition for the discharge bearing current to occur is that lubricant oil or grease films have been formed between the bearing ball/race interface. There is no longer an ohmic path for current to flow. Even under this condition, high-frequency bearing current caused by inductive coupling, and excited by d$V$/d$t$, can still flow but its amplitude will be much smaller. The oscillating frequency of this current is typical in a range from 100 kHz to a few MHz depending on the size of the machine and the length of the cable, see Ran *et al.* (1998). Although the drive system will radiate electromagnetic waves, the efficiency of the system as a transmitter antenna is low in this frequency range. In contrast, the discharge bearing current is the result of an activity similar to that in spark gap. The signal frequency is much higher and hence can be more efficiently radiated out, typically in the range of 90–400 MHz, Zhang *et al.* (2015). Such differences in amplitude and frequency band can be used to differentiate these two types of bearing current spikes which can be detected using a receiver antenna, as shown in Figure 11.6, from Muetze *et al.* (2011) and Niskanen *et al.* (2014). The RF antenna has consistently been placed at the drive end of the machine.

To analyse the detected discharge bearing current spikes, the strength of the signal and the frequency of occurrence can be correlated to the drive system operating parameters. The signals are particularly sensitive to the shaft speed and

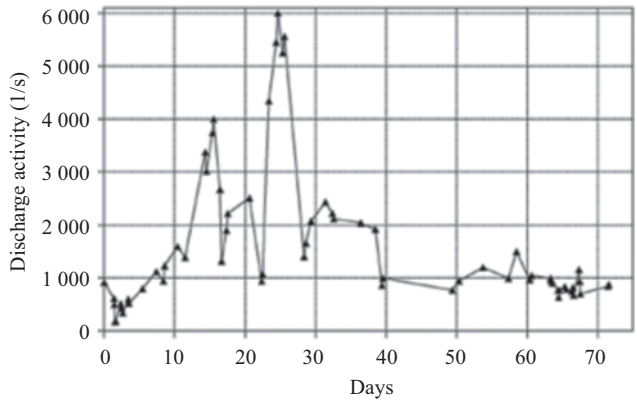


*Figure 11.7 Discharge activities in operation*

bearing temperature. Figure 11.7 shows a set of measured discharge activities over an extended period of time when the motor speed and temperature may be changing, Muetze *et al.* (2011). It is worth pointing out that in a VSD machine without forced ventilation, the temperature changes with shaft cooling fan speed.

Figure 11.7 shows the detection results of discharge activities, i.e. number of discharges, over a relatively long experimental time period and large variations of discharge activity were observed. Classification of the discharge activities in terms of RF signal strength may help to extract bearing condition information. More specific capture of bearing current events, representing transition between the conductive and capacitive bearing modes during operations could also be used to more clearly indicate what is happening inside the bearing.

In spite of such progress and the general knowledge about causes of discharge bearing currents, more investigation and particularly experience are needed to define the threshold values for bearing monitoring. This requires further understanding of the impact of discharges and ideally the establishment of a lifetime model. Implementation in combination with other monitoring techniques such as vibration signature and lubricant chemical analyses would be entirely appropriate, although the latter are monitoring the consequences rather than the cause of the damage.

## 11.4 Insulation degradation detection

### *11.4.1 PD measurement*

According to the winding insulation system, electrical machines are categorised into Type I or II where different insulation standards apply. Type I machines use organic insulation, such as polyamide-imide or polyester with a polyamide-imide overcoat. The rated voltage is usually below 700 V and is in general random wound, which is prone to inter-turn insulation degradation under an inverter supply. Type I machines are not supposed to withstand PD during operation because of the

very thin organic insulation on the wire, see Yang *et al.* (2012). Therefore, the procedure to guarantee insulation performance is offline testing to determine the repetitive partial discharge inception voltage (RPDIV) as described in standards such as IEC 60034-18-41. The standard defines the experimental procedure, measurement method and pass or failure criterion. For both phase-to-ground and phase-to-phase voltages, the switching spikes are measured using wide bandwidth differential voltage probes, and the values at which repetitive PD occurs are compared with the maximum DC link voltage in normal operation, for a two-level inverter. A pulsed voltage generator is needed to vary the amplitude and the rise-time of the test voltage applied to the machine and this could be another voltage source converter. The machine under test is temporarily taken out of service. The ratio is then used to judge whether the machine can pass the test; the higher the RPDIV the better. The procedure allows to check, step-by-step, phase-to-ground and turn-to-turn insulation health conditions, see Tozzi *et al.* (2010).

Detection of PD is also a commonly used technique for online monitoring the insulation condition of electrical machines particularly Type II machines which include hybrid organic/inorganic insulation and usually have form-wound windings for medium-voltage levels. Normally, Type II insulation will use mica paper tape for the coil insulation and have a mica-based ground-wall insulation system to withstand the PD expected during voltage impulses, see Stone *et al.* (2014). Figure 11.3 has previously shown the slot structure and the insulation components in a Type II machine, see Stone *et al.* (2014) and Zoeller *et al.* (2017).

Detecting PD in a noisy environment is challenging and can lead to false diagnosis, Chapter 10 refers. PD, as the partial breakdown of gas or liquid inclusions in a solid insulation material, tending to produce high-frequency electromagnetic signals which can be picked up using an ultra-high frequency antenna or a wide bandwidth (up to 1 GHz) current probe placed in the neutral or leakage current path. Modern digital signal processing is now being used to identify the true PD bursts and reject the noise pick-up, see Cavallini *et al.* (2003). Furthermore, the true PD signals can be classified as due to internal discharge, surface discharge or corona by analysing the signal characteristics in terms of its shape in the time domain, frequency components and its correlation with the supply voltage. Such results of classification can give insight into the degradation process and hence are valuable from prognosis and maintenance points of view. A time-domain signal is associated with each possible PD event. The signal needs to be sampled at a very high sampling rate because the signals are typically in the frequency range of hundreds of MHz. Therefore, a triggered sampling and analysis scheme, as shown in Figure 11.8 is recommended so that each event is processed immediately and the storage is only needed for the classified type and strength of each true PD event. The results can then be used for trend analyses, etc.

For a machine with a sinusoidal supply, it has been found that PD activities tend to concentrate around certain phase angles of the associated supply voltage. For an VSD machine, it is important to understand that PD may occur with different patterns, as shown in Figure 11.2. The frequency of PD occurrence is no longer clearly related to the fundamental voltage phase angle. Figure 11.9 shows

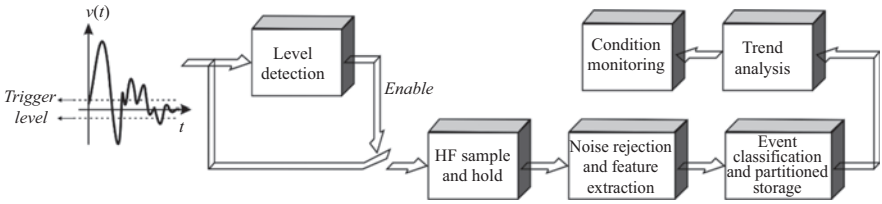


*Figure 11.8 A triggered sampling and signal-processing scheme*

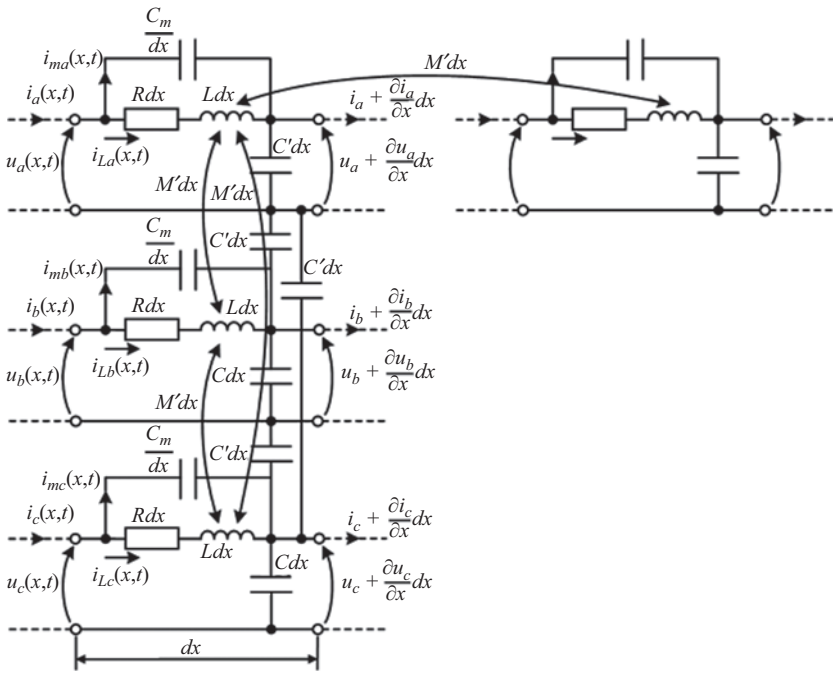


*Figure 11.9 Element of a distributed winding model*

part of a possible equivalent circuit of the stator windings of an induction machine which could be used to estimate the high-frequency voltage and current response, Clerici *et al.* (2010), compare with Figures 10.1 and 10.2 in the chapter on PD propagation. The windings are indeed a distributed system with mutual magnetic and electrostatic coupling between different winding sections. When a sudden change of voltage is applied to the terminal, depending on the switching edge ($dV/dt$), resonance will lead to uneven distribution of electric field inside the machine, triggering PD activities. Figure 11.2 showed the PWM waveform of one machine phase. If all three phases were shown, it would be possible to see that the PD activities are more likely to occur following rather than prior to a switching event in the inverter. This, if confirmed, could be used to reject some random noises.

### 11.4.2 Capacitance and dissipation factor measurement

While PD detection monitors the motor insulation ageing development from a microscopic point of view, the degradation can also be detected using macroscopic signatures. Increases of stray capacitance and dissipation factor are usually used to signify the degradation of either groundwall insulation or turn-to-turn insulation. The change of such parameters can be 20%–25% before the end of the lifetime, see Zoeller *et al.* (2017). Some of the online monitoring techniques can simply use the same voltage and current sensors that are also used to control.

Figure 11.10(a) shows the connection of an induction motor drive, with the neutral point of the star-connected machine floating. The common mode voltage and current are calculated as:

$$I_{\text{com}} = (I_a + I_b + I_c) \tag{11.1}$$

$$V_{\text{com}} = (V_a + V_b + V_c)/3 \tag{11.2}$$

where the high-frequency common mode current is regarded as being driven by the common mode voltage to flow through the leakage path including the stray capacitance across the groundwall insulation. The obtained current and voltage signals are then subject to a Fourier series analysis, and the frequency-domain

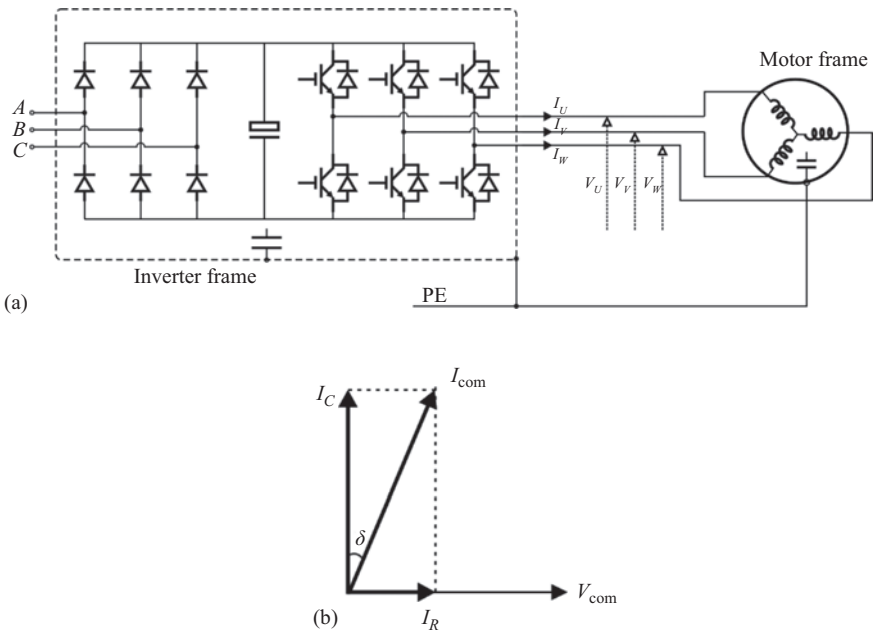


*Figure 11.10 Insulation degradation detection by common mode capacitance and dissipation factor: (a) measurement arrangement and (b) phasor diagram*

components are used to further calculate the equivalent capacitance $C_{eq}$ and dissipation factor $DF$:

$$C_{eq} = I_{com}(j\omega)/(3\omega V_{com}(j\omega)) \tag{11.3}$$

$$DF = \frac{I_R}{I_{com}} \times 100\% \tag{11.4}$$

where $I_{com}(j\omega)$ and $V_{com}(j\omega)$ are the amplitudes of the harmonic components of the common mode current and voltage, respectively, at angular frequency $\omega$ (rad/s). $I_R$ is the vector component of the harmonic current in-phase with the harmonic voltage, as shown in Figure 11.10(b), see Zhang *et al.* (2015).

Selection of the frequencies for calculation should be carefully considered. With PWM switching, the harmonic frequencies in the common mode voltage and hence current are around integer multiples of the switching or carrier frequency $\omega_c$ (rad/s), modulated by the output supply frequency to the motor $\omega_o$, see Ran *et al.* (1998). Therefore, we recommend to use:

$$m\omega_c \pm n\omega_o,\ m = 1 \text{ and } n = 0, 1, 2, \ldots \tag{11.5}$$

With $m = 1$, we recommend focusing on the relatively low excitation common mode signal frequencies. This is because at very high frequencies, the distributed parameter effects of the machine, shown in Figure 11.10(a), become dominant invalidating the assumptions for (11.3) and (11.4), although a spectral monitoring approach could be used to directly analyse the leakage current spectra in the MHz range, see Zoeller *et al.* (2017). In this regard, further validation and modification may be necessary with future high switching frequency inverters built on wide band-gap power semiconductors.

### *11.4.3 Built-in winding insulation degradation detector*

Zhang *et al.* (2015) reported that more than 30% of machine failures can be traced to the winding insulation, whereas this book suggested in Section 4.6 from the earlier work 13%–37% could be associated with stator windings. With the wider onset of the use of VSDs, it is not surprising that these proportions are rising.

It is logical to enhance or build-in redundancy in the insulation system, particularly for high reliability applications. Barater *et al.* (2017) describes a design of permanent magnet surface mounted motor system using polymer cable for the stator winding. This is for aerospace application where the expected reliability is very high. Figure 11.11 shows the structure of the winding cable. Two semiconductive layers are used to smooth the electric field distribution and avoid local extreme stresses. As the semiconductive layers follow the cable to form the stator winding, the outer semiconductive layer forms another set of winding phases which have almost the same inductance values as the main copper winding but with higher resistances. These winding phases are not connected to the inverter output but their neutral point can be connected to the centre-tap of the DC link, as shown in Figure 11.11(a). Now if degradation occurs in the cable insulation layer, a leakage

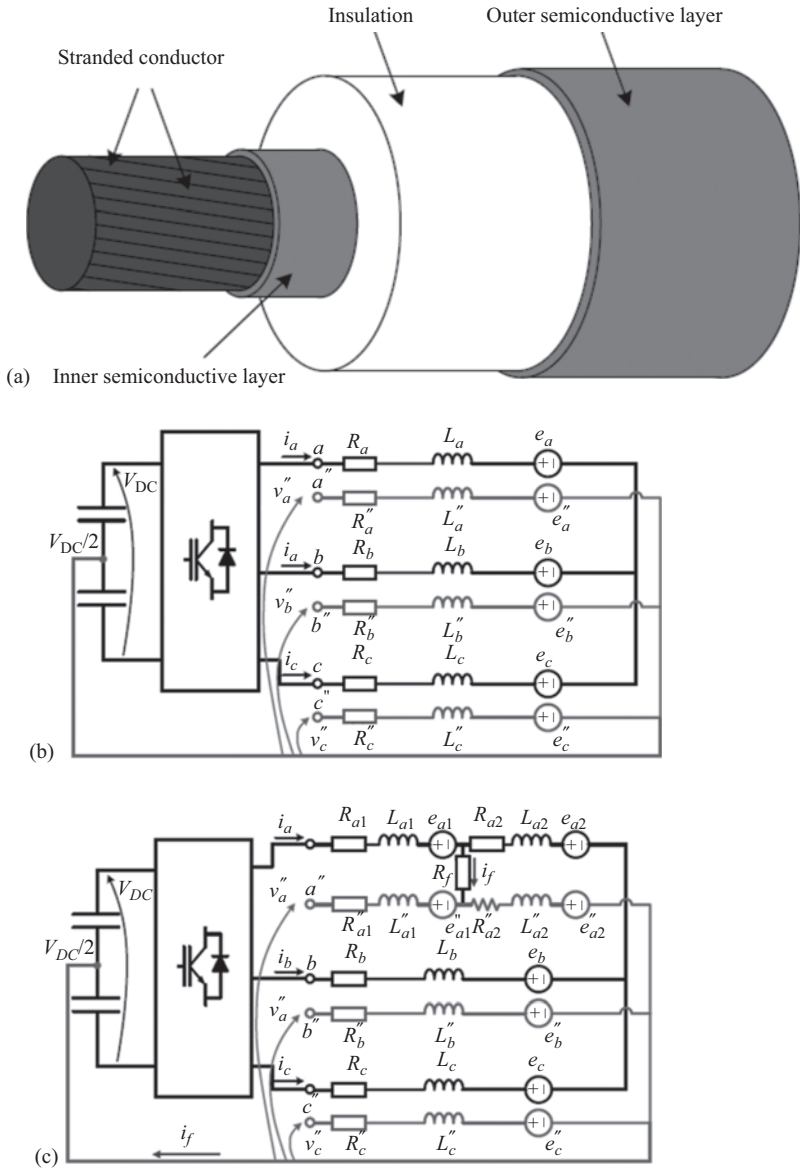


*Figure 11.11 Detection scheme built in system design: (a) cable insulation structure for machine winding, (b) circuit model for healthy motor and (c) circuit model for degraded motor*

path is formed as shown in Figure 11.11(b). The main machine model is now noticeably modified and the response in normal control would then change. CM can therefore be achieved in the control loops. Without the double semiconductive layers, such a single insulation failure would not be detectable. The inverter supply is also a necessity for the detection scheme to work.

This is an example of building the possibility of CM in the system design, which also enhances the winding insulation performance.

## 11.5 Control in-loop machine fault detection

Vector- or field-oriented control of induction or permanent magnet machines is now widely available in industrial drives. Figure 11.12 shows the block diagram of a typical control scheme for an induction machine where the voltage applied to the machine terminals, by the inverter output, is determined by the speed or torque demand while the internal flux amplitude is usually maintained constant, also by the inverter control. Therefore, the typical control block diagram has two loops, for speed/torque control and flux control.

A feature of vector- or field-oriented control is that it depends upon the machine model and parameters. The model equations are used to calculate the output voltage of the inverter. Numerical observers are built into the controller to update the model parameters. If condition degradation causes the machine to deviate from the model known to the controller, the parameters will be updated and this is usually different from the normal variation of the machine parameters due to temperature or slight saturation of the core. The unusual variation of parameters, often accompanied by currents exceeding limits, can be used to indicate the machine condition. Such a method was first suggested by Ran *et al.* (1998) for conducting EMC investigations, then for machine monitoring by Bellini *et al.* (2000).

Although machine phase current under closed-loop control is subject to control limits, this is usually intended for protecting the inverter rather than the machine. However, machine insulation breakdown, such as an inter-turn short circuit fault or core faults may cause internal circulating currents which do not appear externally to the machine. CM needs to detect such situations and rotor unbalance, VSD in-loop control allows us to do this.

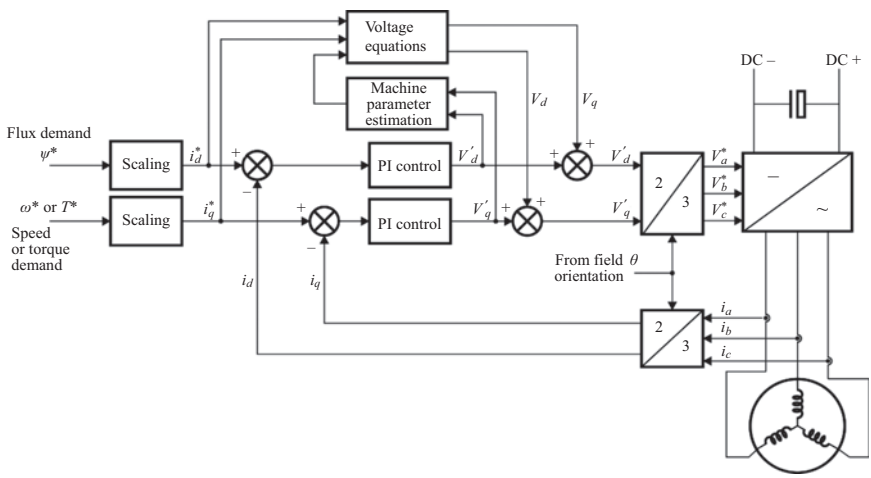


*Figure 11.12 Vector control block diagram for an AC machine*

Using the method of detection VSD control in-loop based on Bellini *et al.* (2000), described above, Zaggout *et al.* (2014) developed current and power monitoring methods for detecting wind turbine DFIG rotor unbalance. This was based on Chapter 9, Figure 11.13, albeit on a test rig with limited experimental results. Under both fixed and variable speed conditions, Zaggout was able to monitor rotor winding unbalance by measuring rotor current converter feedback signals, $i_d$ and $i_q$ from Figure 11.14, comparing his result against a control simulation. In so doing during variable speed operation he obtained the benefit of the closed loop gain, as recommended by Bellini *et al.* (2002), increasing the fault

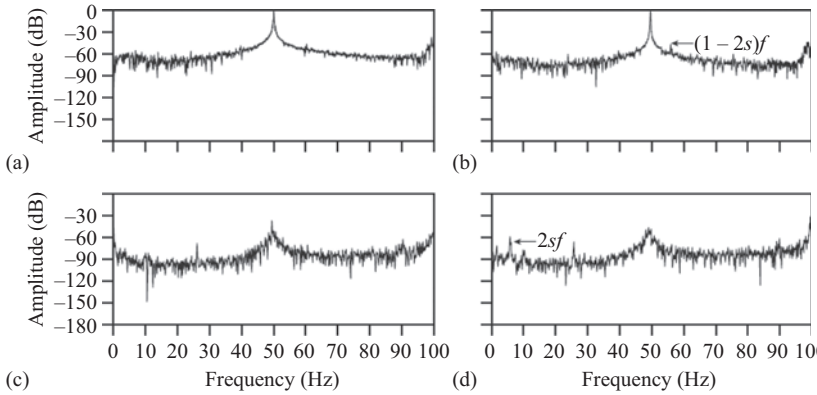


*Figure 11.13 Measured healthy and faulty stator current and power spectra from a DFIG with an unbalanced rotor fault, Zaggout et al. (2014): (a) current healthy, (b) current faulty, (c) power healthy and (d) power faulty*

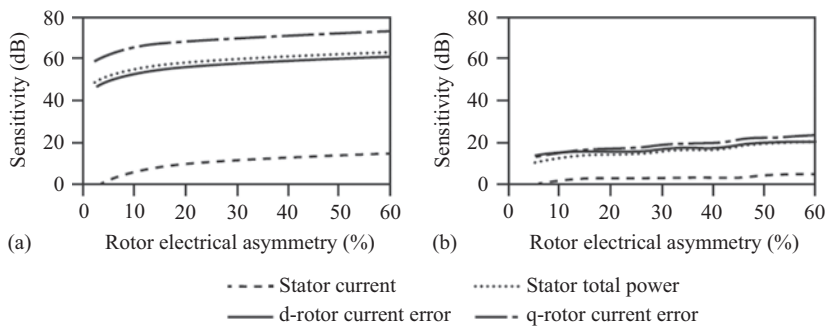


*Figure 11.14 Detectability of a DFIG unbalanced rotor fault from simulated or measured stator current and power signals, noting increased detectability with $i_d$ and $i_q$, Zaggout et al. (2014): (a) simulated and (b) measured*

detectability and detection confidence, Figure 11.14, although the measured results proved less significant than the simulation.

This is a considerable step towards in-loop monitoring of VSD-fed machines, proposed by Bellini *et al.* (2000).

Turning now from the issue of bearing or rotor un-balance faults to those in the laminated core of a machine, Figure 11.15 shows the path of circulating current following an inter-laminar fault in the stator core of an AC machine, see Wittek *et al.* (2010).

Traditionally, stator cores are checked against such a fault during maintenance, see Chapter 12. A test AC voltage is applied to excite the stator core using loop turns as shown in the figure. The power loss is measured and the leakage flux pattern is plotted around the core using a Rogowski coil, see Chapter 12. The changes against historical record are used to indicate the inter-laminar insulation degradation. This usually requires the rotor to be removed therefore is only used for large machines during overhauls. Online monitoring of inter-laminar insulation usually relies on chemical techniques, the cost and sensitivity of which can be questionable for many drive machines in the kW range.

Figure 11.16(a) shows a technique for a VSD-fed machine which senses stator core loss under pulsating rather than rotating flux excitation, hence capable of monitoring stator core inter-laminar faults, see Wittek *et al.* (2010) and Lee *et al.* (2010).

Such a testing mode can be built into the VSD control scheme shown in Figure 11.12, with the speed reference set to zero, during which the rotor does not need to rotate. A pulsating component is added to the flux reference whose angle stepped around the machine frame to check different angular sections of the stator core. Figure 11.16(b) shows a test result indicating a rise of core loss when the test flux is aligned at about $\theta = 3\pi/2$ with respect to the stator core, suggesting a core fault at this position.

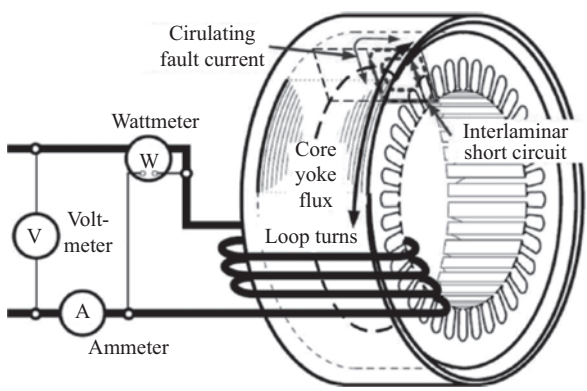


*Figure 11.15 Offline test for a stator core fault*

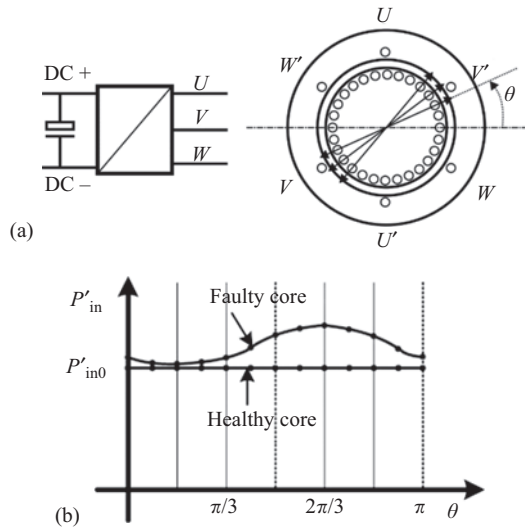


*Figure 11.16 Using VSD control in-loop to detect a core fault, Lee et al. (2010): (a) applying pulsating stator core flux, stepped through angular positions and (b) core loss test results*

## 11.6 Conclusions

This chapter has presented specific CM methods, which can detect issues to which VSD-supplied machine are susceptible:

- Insulation PD,
- Bearing current discharge,
- Control in-loop detection of rotor unbalance or stator core defects.

The fast-switching edges produced by VSDs exacerbate the first two mechanisms in VSD-fed machines but VSD control in-loop signals clearly enable improved detection of rotor winding unbalance and the continuous monitoring of progressive stator core deterioration due to interlamination breakdown due to those fast-switching edges.

*Chapter 12*

# Offline monitoring

## 12.1 Introduction

Offline techniques were excluded from the first and second editions partly because the authors felt that online techniques were more important. At the conception of this edition, however, the institution asked that offline techniques should be included for completeness and the authors have added this chapter to widen their earlier focus.

Many offline techniques, but not all, focus on machine-winding insulation systems and it would be reasonable to classify the areas for offline monitoring as follows:

- Stator core related,
- Stator winding related,
- Rotor core and winding related.

As a general principle, offline methods seek to measure 'design' parameters such as reactance or resistance, whereas online methods seek to measure 'performance' parameters from electrical machine terminal, recalling the comment by Jones (1967).

There is an extensive literature on offline monitoring of non-rotating electrical machines, i.e. transformers, and this is summarised in Abu-Siada, Ed (2018), some of whose techniques are similar to those set out here.

The methods are summarised in the following sections but the authors refer in particular to Stone *et al.* (2014) for their thorough coverage of individual tests.

## 12.2 Stator core

### *12.2.1 General*

The integrity of large stator cores became an operational issue in the early 1970s as machine sizes, air-gap flux densities and stator current loadings rose, see Table 2.2 and Figure 2.2. In particular, magnetic loadings above 1 T and electrical loadings above 100 A/mm can lead to faults in the associated core of large turbo-generators, see Figure 2.5(a), and large hydro-generators, see Figure 2.5(b). An example of such a fault is shown in Figure 3.17.

The first paper to describe core faults was by Tavner *et al.* (2005) and the following summary is taken from it. A core fault has the approximate shape of a

cylindrical ellipsoid in the stator core with its major axis perpendicular to the core-plate. Under extreme conditions, melting of core-plate material occurs within the ellipsoid and a cavity is formed. A core fault may be initiated by:

- Core constructional defects,
- Thermal factors,
- Electrical factors,
- Operational factors, such as over-fluxing, pole-slipping or foreign bodies introduced into the machine air-gap during operation,
- A core fault may not grow immediately after it is initiated and its growth can be influenced by a complex interplay of electromagnetic, mechanical, thermal, material and constructional factors, which may not be operative at the time of initiation but worsen with the passage of time.
- A core fault grows axially in the core along its major axis. The radius of the cavity increases with length but this is not the main axis of growth because that is limited by core cooling.
- A core fault grows axially until heating at the circumference of the cavity damages the main stator winding insulation, causing a stator earth fault and tripping, or the core fault extends to the core end.

Three mechanisms have been identified which control core faults:

- Core faults tend to if the initiating defect is $>1$ cm in diameter,
- Mechanism I, yoke flux diversion, which circulates current within the fault,
- Mechanism II, yoke flux linking, which circulates current between the fault and the core frame and this is the most powerful core fault growth mechanism but appears to be active in relatively few faults. It can be limited or eliminated by introducing a high resistance between the stator core and its frame and some manufacturers do this.

The currents flowing in a core fault can be as large as the current circulated in the core frame by the core leakage flux, that is up to 20 kA. The tendency of a laminated core to be subject to core faults can be reduced by maintaining the highest quality of core construction by:

- Ensuring correct core-plate insulation quality and thickness,
- Deburring individual core-plates,
- Avoiding introduction of particularly metallic foreign bodies into the core construction,
- Applying uniform and adequate clamping pressure to the stator core,
- Carrying out a recorded visual and electromagnetic/thermal inspection on completion of core build,
- Insulating the core frame from the core can eliminate the effect of the yoke flux linking mechanism, once a fault is initiated,
- Lowering the magnetic loading below 1T to reduce the effect of the yoke flux diversion mechanism, but this has to be consistent with other machine design requirements,

- Lowering the electrical loading below 100 A/mm will reduce a risk of core faults, however, if this limit has to be exceeded for larger machines, for design reasons, it will be necessary pay closer attention to core-plate insulation quality and cooling intensity to reduce core fault risk,
- Providing radial cooling ducts in the core with high-resistance/insulating duct spacers to resist the axial growth of the fault. This approach is as yet unknown in the industry and would involve expensive materials,
- Ensuring that the machine is not operated at an excessive field or armature current and consequently core flux density and is not subjected to pole slipping,
- Early warning of core faults during an operation can be given by the use of core monitors, see Chapter 8.

Operators realised that the early signs of core damage can be detected by thorough core tests. Stator cores are subjected to a high flux test (HFT) during manufacture using infrared thermography to identify hotspots in the bore and ends of the core. Manufacturer's certificates to this effect are available in machine data packs. Initially when core fault problems occurred in the 1970s, HFTs were conducted in the field but were costly and time-consuming, because of the need to have a controllable high-voltage supply and the need to wind large capacity cables through the core, see Figure 12.1.

However, when a core is energised the disturbance to the magnetic potential around the core bore, due to a fault, should be detectable, even at low flux densities.

Low-voltage stator core testing method development was therefore initiated on 2-pole turbo-generators in the 1970s and 1980s, Bertenshaw (2014) has given a good summary of these different techniques which evolved as follows. El CID, Sutton (1980), was the first and still dominant LV method. In this test, the stator

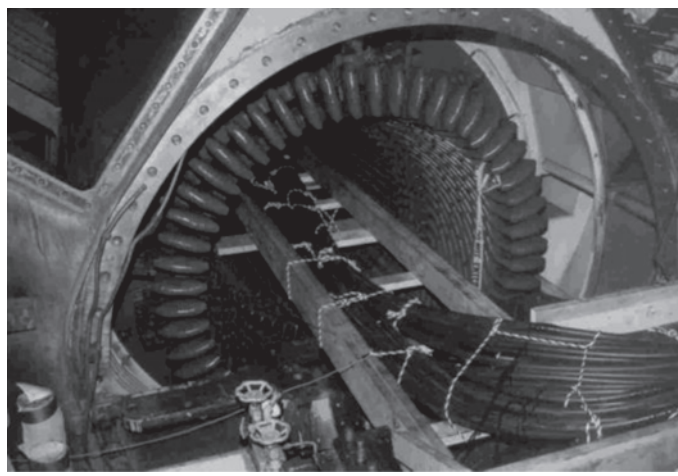

*Figure 12.1 High flux test (HFT) on a 2-pole air-cooled turbo-generator stator*

core is circumferentially magnetised by current, $I_e$, at rated frequency but at 5% of rated flux. A Chattock potentiometer or search coil, from which the Rogowski coil, Figure 5.32, was developed, is used bridging one slot and two teeth, together with an axial calibration search coil, to detect the disturbance to the magnetic potential across the slot and teeth, see Figure 12.2. The detection is the in-phase component, $\delta$, of the magnetic potential disturbance, caused at the core bore by the fault and detected by the Chattock potentiometer.

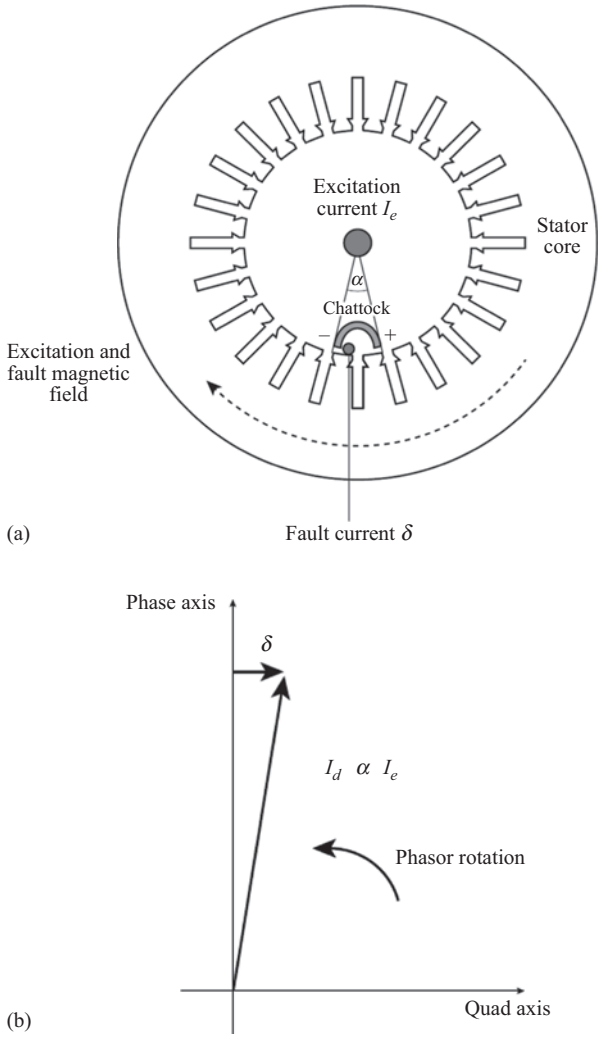


*Figure 12.2 Principle of LV stator core test: (a) application of the excitation, $I_e$, and position of Chattock potentiometer and (b) phasor diagram of El CID, showing the detection signal, $\delta$ and its relation to the Chattock potentiometer detection current, $I_d$, and the excitation current, $I_e$*

The test provides hard copy of the Chattock potentiometer axial position, as it moves through the core, and the measured magnetic potential, $I_d \alpha I_e$, across each slot and adjacent teeth, corrected for phase by the axial search coil signal, to form the detection signal, $\delta$. These test results involve some calibration and interpretation.

The following methods are derivatives and possible improvements of El CID:

- ABB DIRIS method,
- ICEMENERG PROFIM method,
- GE Racer method,
- Siemens SMCAS method,
- Russian EMK method.

The following sections describe briefly the application of LV stator core testing methods to turbo-generators and hydro-generators.

### *12.2.2 Turbo-generators*

El CID-type methods were initially applied to large 2- or 4-pole turbo-generator stator cores of rating 200 MW or greater, Figure 12.3(a) and (b).

### *12.2.3 Hydro-generators*

It became apparent in the 1990s that there were significant issues applying LV stator core testing methods like El CID to large, slow speed, multi-pole, large diameter hydro-generator machines in service, as shown in Figure 12.3(c), despite the fact that there is a pressing operational need to confirm the integrity of such cores. The specific problems experienced were as follows:

- Large diameter stator cores, segmented to facilitate on-site assembly, resulting in core segment gaps and a magnetic potential drop between those segments, causing anomalies in the compensation of the detection signal, $\delta$, close to those segment gaps,

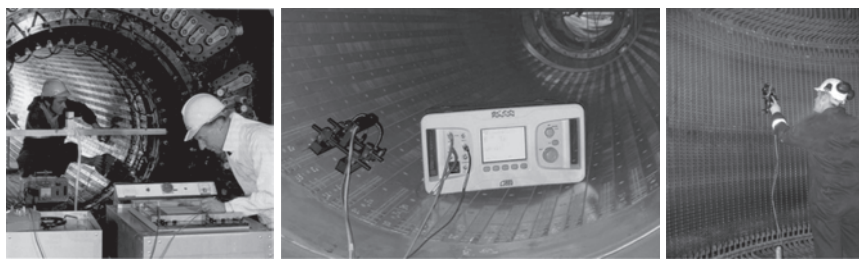

(a) (b) (c)

*Figure 12.3 El CID stator core tests being undertaken: (a) original testing on a 500 MW turbo-generator, 1980, J Sutton on the left, (b) modern version of testing a turbo-generator and (c) modern version of testing a hydro-generator*

- Presence in the stator of large numbers of parallel winding circuits, resulting in circulating currents induced in parallel stator windings when the core is magnetised by ring excitation, Figure 12.2. This can obscure the signal, $\delta$,
- Large size rotors, difficult to remove for inspection resulting in LV stator core testing over sections of the stator core with a rotor pole piece removed to allow Chattock potentiometer access to the stator core air-gap. This can result in unusual detection signals, $\delta$.

These issues were explained by Ridley (2007), based upon a previous work by Sutton (2008) and Bertenshaw (2014), and organised by analysing phasor diagrams from El CID results, see Ridley (2017).

## 12.3 Stator windings

### *12.3.1 Summary of offline tests*

Table 12.1 sets out the offline stator winding tests.

### *12.3.2 Frequency response analysis*

Frequency response analysis (FRA) testing of transformer windings has been used for some years, see Jayasinghe *et al.* (2006) and Abu-Siada (2018), as a means of determining winding location changes, particularly because transformers can undergo severe short circuits, due to grid conditions, causing primary or secondary windings to move significantly axially with respect to the laminated core. The method applies a test voltage to the transformer winding and sweeps the frequency of that voltage over a predetermined range to identify changes in the impedance spectra, resulting from winding positional changes with respect to the core.

Some consideration has been given to applying such methods to turbo-generator and hydro-generator windings for measuring their impedances under transient operational conditions, see Sen *et al.* (1956).

This was later proposed, following transformer experience, as a method for determining stator winding movement, especially after a machine had sustained a severe service fault. However, the method has not progressed into practical application, simply because in rotating electrical machines both stator and rotor windings are mounted within steel slots, where winding movement is physically more restricted than between the concentric windings and core of a transformer. Rotating machine winding movement does occur but is only significant in the end windings, where weaker electromagnetic fields are in play than in a transformer, so consequential winding forces and movement are proportionally smaller.

## 12.4 Rotor windings

### *12.4.1 Summary of offline tests*

Table 12.2 sets out the offline rotor winding tests.

*Table 12.1 Offline stator winding tests, based on Stone et al. (2014)*

| Name of the test | Description | Difficulty to perform | Effectiveness | Relevant standards |
|---|---|---|---|---|
| Insulation resistance (IR) | Apply DC voltage for 1 min to measure the leakage current | Easy | Only locates contamination or serious defects | IEEE Std 43:2013 |
| Polarisation index (PI) | Ratio of 1 min and 10 min IR readings | Easy | | |
| DC high potential | Apply high DC voltage for 10 min | Easy | Only locates serious defects | IEEE Std 95:2002 |
| AC high potential | Apply high AC voltage for 10 min | Moderate due to the need for a large AC transformer | More effective than DC high potential | NEMA MG-1:2016orBS EN IEC 60034-27-4:2018 |
| Capacitance | Apply low or high voltage to measure the winding capacitance to earth | Moderate | Moderately effective at finding thermal or water leak problems | – |
| Dissipation or power factor | Apply low or high voltage to measure the insulation loss | Moderate | | IEEE Std 286:2000orBS EN 60034-27-3:2016 |
| Power factor tip-up | Differences in insulation loss from high to low voltage | Moderate | Effective to find the widespread thermal or contamination problems in stator winding | |
| Offline PD | Directly detect PD voltages at rated winding voltage | Difficult | Finds most stator winding problems except end winding issues | IEEE Std 1434:2014 |
| Surge comparison | Apply simulate voltage surge | Difficult to determine if a puncture occurs in the stator winding insulation | Effective for finding inter-turn insulation problems in stator winding | IEEE Std 522:2004 |
| Blackout test | Apply high AC voltage to the stator winding and look for the discharges during the blackout | Moderate | Effective for identifying the discharges due to contamination problems | IEEE Std 1434:2014 |
| Wedge tightness | Tap wedges to identify the looseness | Moderate | Effective for identifying loose stator winding coils | – |
| Slot side clearance | Insert feeler gauge between stator coil and slot side | Easy when wedges removed | | – |

*Table 12.2 Offline rotor winding tests, based on Stone et al. (2014)*

| Name of the test | Description | Difficulty to perform | Types of rotor winding | Effectiveness | Relevant standards |
|---|---|---|---|---|---|
| Insulation resistance (IR) | Apply DC voltage for 1 min to measure leakage current | Easy | All types | Only locates contamination or serious defects | IEEE Std 43:2013 |
| Polarisation index (PI) | Ratio of 1 min and 10 min IR readings | Easy | All types | | |
| DC high potential | Apply high DC voltage for 10 min | Easy | All types | Only locates serious defects | IEEE Std 95:2002 |
| AC high potential | Apply high AC voltage for 10 min | Moderate due to the need for a large AC transformer | All types | More effective than DC high potential | NEMA MG-1:2016orBS EN IEC 60034-27-4:2018 |
| Open circuit | Measure the generator output voltage as a function of field current to identify the shorted rotor turns | Moderate, repeat of commissioning open circuit test | All types | Effective only for generators. Needs comparison with commissioning measurement | BS EN IEC 60034-2-1:2014 |
| Impedance | Apply 50 or 60 Hz current and measure *V*/*I* at different speeds to find turn short circuits | Moderate | All rotors with slip rings | Effective | – |
| Pole drop | Apply 50 or 60 Hz current and measure voltage drop across each | Easy | Salient pole rotor winding | Only finds short circuits present even when the rotor is stopped | – |
| Surge test | Find turn and ground faults by measuring discontinuities in surge impedance | Difficult | Round rotor windings | Effective if close to a dead short circuit | – |

### *12.4.2 Synchronous rotor surge tests*

Surge techniques have been used for many years by transformer manufacturers for locating turn-to-turn and earth leakage faults in transformer windings. Turbo-generator manufacturers have used similar techniques for pin-pointing faults in their rotor windings, as a quality control check immediately after a rotor has been assembled. Work in the United Kingdom showed that such a technique can be used to detect both earth leakage and turn-to-turn faults on generators during their service lives, originally using a mercury-wetted contact relay or now a fast electronic switch to develop recurrent, rapid rise-time surges (approximately 20 ns) injected into the winding between the slip-ring and the earthed body of the rotor. Figure 12.4(a) shows this recurrent surge generator, which is switched on and off at

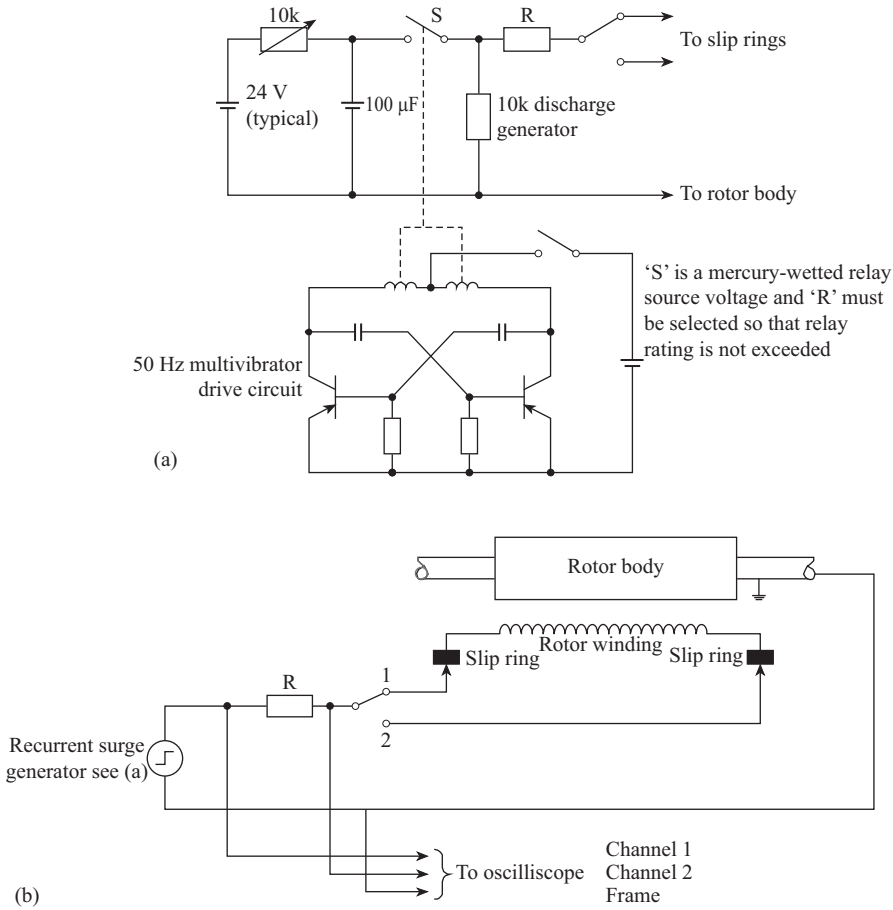


*Figure 12.4 Arrangements for obtaining an RSO from a rotor winding: (a) recurrent surge generator and (b) connection of the recurrent surge generator to a rotor winding*

a frequency of 50 Hz, while Figure 12.4(b) shows the connection of the generator to the rotor winding. The winding approximates to a simple transmission line where the propagation is dominated by the geometry and insulation of the winding conductor in the rotor slot. Mutual coupling between turns of the winding will cause dispersion but this effect has been found to be small in solid steel rotors. When the surge is injected at one end it has a magnitude determined by the source impedance, $R$, of the recurrent surge generator and the surge impedance of the winding, $Z_o$. The surge propagates to the far end of the winding in a time, $t$, determined by the length and propagation velocity of the winding. The surge is reflected at the far end, its magnitude determined by the reflection coefficient, $k_r$. For a winding with the far end open-circuited, $k_r = +1$ and with it short-circuited $k_r = -1$. The reflected surge returns to the source and if the source impedance equals the surge impedance of the winding ($k_r = 0$ at source), it is absorbed without further reflection. This is shown in Figure 12.5.

When an insulation fault to earth, or a turn-to-turn fault, is encountered, this reflection pattern will be disrupted and may be observed on the oscilloscope. The pattern on the oscilloscope is known as a recurrent surge oscillograph (RSO) and this has become the name of the technique. The rise time of the surge will affect the method's sensitivity and must be less than the propagation time of the surge-front through a single winding turn for sharp reflection to occur.

Figure 12.4(b) shows the results obtained from the practical application of this method. The source impedance $R$ was adjusted to be equal to the winding surge impedance and a surge of between 10 and 100 V was applied with a rise time of 20 ns.

The surge was injected into each end of the winding, with the far-end open-circuited, and two reflection traces were obtained as shown in Figure 12.5(b) (i) and (ii), either of which should be compared to the ideal response of Figure 12.5(a) (i). The results show the distortion of the trace as a result of dispersion and the lack of surge sharpness. Faults are indicated by superimposing the two traces and observing any deviations between them, as shown in Figures 12.5(b) (ii) and (iii).

Earth faults may be located, approximately, by taking the ratio of the times for reflections from the fault and from the end of the winding. Similarly, the electrical length of the winding can be estimated by measuring the time for the surge to make a single pass through the winding. This can be done by short circuiting the far-end of the winding to obtain a trace like Figure 12.5(a) (ii). Any shortening of the length indicates that shorted turns are present in the winding.

The surge impedance of a rotor winding lies between 20 and 30 Ω. A deviation becomes observable on the RSO trace when the impedance to earth of the fault is a significantly small multiple of the surge impedance. In general, the technique can detect faults with impedances to earth of less than 500–600 Ω. Similarly, the technique can detect a turn-to-turn fault that has a resistance significantly less than the surge impedance, say in the order of 10 Ω down to zero.

To carry out RSO measurements, the generator must be isolated, the field de-energised and the exciter connection disconnected. It is known that many rotor faults are affected by both gravitational and centrifugal forces upon the conductors

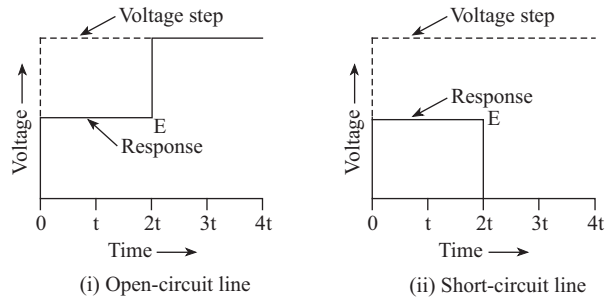


(i) Open-circuit line (ii) Short-circuit line

t - time to traverse one length of the winding
E - start of reflection from winding end

(a)

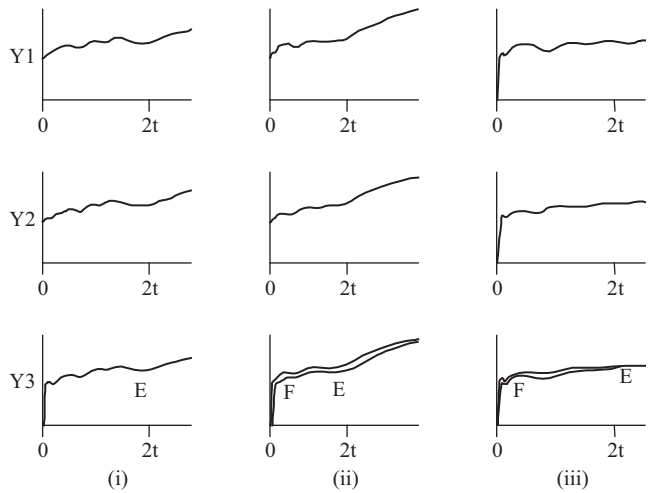


X = 10 μs/div
Y1 = slip ring 3 to earth
Y2 = slip ring 4 to earth
Y3 Y1 and Y2 superimposed
E - start of reflection from winding end (open circuited)

X = 10 μs/div
Y1 = slip ring 1 to earth
Y2 = slip ring 2 to earth
Y3 Y1 and Y2 superimposed

X = 5 μs/div
ditto

RSO for faulted rotor winding

F - start of reflection from fault
Speed rpm
Winding type: progressive

RSO for healthy rotor winding

(b)

*Figure 12.5 Ideal and typical practical RSOs obtained from generator rotor windings: (a) ideal response of generator rotor windings and (b) typical responses for generator rotor windings*

during rotation, so it is common to carry out the tests stationary, at barring and at speed for comparison purposes. The test has now been applied by many utilities as a routine technique for assessing the operational state of machine windings, although it is clear it cannot be used for brushless machines without the rotor being stationary.

The advantages of the technique are that with the oscillographs it provides a permanent record of the state of a rotor throughout its service life and it can detect both earth and inter-turn faults before their resistance falls to a value where large fault currents flow. Experience has shown that the deterioration of a winding can be assessed by a comparison between oscillographs obtained from the same rotor. It is not possible, however, to make comparisons between oscillographs from different rotors, even if they are of the same design, because of the effects on the surge propagation of quite small variations between the insulation and rotor body properties of different rotors.

The disadvantages are that it detects faults of high resistance and is unable to differentiate between faults that are operationally significant and those that are not. Also, it cannot be used online, testing the winding under truly operational mechanical and thermal conditions. This is in contrast to the effectiveness of the air-gap search coil or circulating current method that can provide online information. There a number of modern references that cover this and other techniques including Ramirez-Nino *et al.* (2001) and Streifel *et al.* (1996).

## 12.5 Conclusions

Offline testing for electrical machines has developed considerably over the last 30 years and this is represented in the summary tables above but also in the availability of a number of internationally recognised standards. But a review of the tables shows that the most developed off-line techniques are associated with the stator cores and windings and rotor windings of larger turbo-generators and hydro-generators. Not all offline tests are easy to perform and many cannot duplicate operational conditions.

In many ways, the authors suggest that offline testing, particularly for larger machines, provides the background diagnostic information which should be used to direct the focus of subsequent online CM.

*Chapter 13*

# Condition-based maintenance and asset management

## 13.1 Introduction

The primary objectives of CM are to provide early detection of faults and advanced warning of failure so that preventative action can be taken. For late detections of severe faults, this action might be to shut down the machines before catastrophic failure. However, a more valuable approach is to schedule maintenance in advance of failure. So far, this book has been concerned with the process of early detection through CM. Greater benefits can be achieved from CM if the information from sensors and systems is used to inform and schedule maintenance, allowing planned shut-downs so that the life of plant, of which the electrical machine forms a part, can be extended whilst the durations and impacts of shut-downs are reduced. This is the process of CBM, first described in Chapter 1. It is important to note that it would be unusual to consider only the electrical machine within a system when applying CBM planning since the benefits of an improved strategy will only be realised by an approach that encompasses the whole plant or system. Hence, this chapter includes examples of electrical machines in context, particularly conventional power generation and wind energy. However, further benefits can be realised if decisions on maintenance scheduling are taken to reduce total life-cycle costs of the whole machine and plant it serves. This requires an estimate of the variable costs of operating and maintaining the plant throughout its life and, increasingly, reliable performance measures, such as energy production, against which to evaluate costs. With this knowledge, the plant or asset owner can operate, maintain, or dispose of that asset on the basis of the information available from these processes. This is asset management. This chapter describes how CBM, life-cycle costing and asset management could be applied to rotating electrical machines.

## 13.2 Preventative maintenance

Preventative maintenance demonstrates how the costs of CM can be justified in terms of the influence of CM on plant failure. Preventative maintenance is generally performed at fixed intervals, much as a car is serviced after a given time

period or number of miles. The purpose is to prevent the majority of failures based on likely component or system lifetimes. This approach has a lot of value, particularly in cases where confident estimates of average lifetimes are known with certainty, courtesy of large populations. Some failures will still occur, but most will be prevented through maintenance or replacement of non-repairable parts. However, such an approach is unlikely to be optimal. Figure 13.1 shows the degradation of three systems over time, each degrading at a different rate (fast, average or slow) but being maintained at a fixed preventative maintenance interval. The preventative maintenance interval could be assumed to be optimised for the average case to coincide with deterioration reaching a particular threshold. The fast-deterioration system fails before the fixed-interval preventative maintenance action occurs, resulting in down-time and, potentially, catastrophic or cascading failure. The slow-deterioration system is maintained far in advance of likely failure, meaning that maintenance actions are being conducted unnecessarily. Both cases will lead to additional or unnecessary costs. These costs can justify the installation of CM systems to allow maintenance to be planned and conducted on the basis of machine condition and not simply after, for example, a given number of operational hours.

An extension of the basic preventative maintenance approach is perhaps better described as reliability-centred maintenance. The problem of system components aging at different rates has been considered by various authors. A particular example for electrical machines is given in Queiroz (2017). Here, a criticality value is estimated for the various system components based on eight criteria:

- Health, safety and environment,
- Cost of lost production,
- Time between potential failure detection and the moment of functional failure,
- Repair costs,
- Ease of access to the equipment manufacturer,
- Redundancy level,
- Ease of access to workforce,
- Age of equipment.

Each of these eight criteria are assigned an importance factor relative to each of the other criteria to form a prioritisation matrix. After applying weights to the criteria and their factors, the time between maintenance for high-criticality system components is calculated from their failure rates. A similar approach is taken for medium-criticality and low-criticality systems. Effectively, the method groups components by importance and allows operators to conduct preventative maintenance at different time intervals for different groups of components.

This approach is moving the operator towards CBM in that maintenance scheduling is now based on an estimate of likely condition, estimated based on experience. It does not yet incorporate information describing the current state of components or systems.

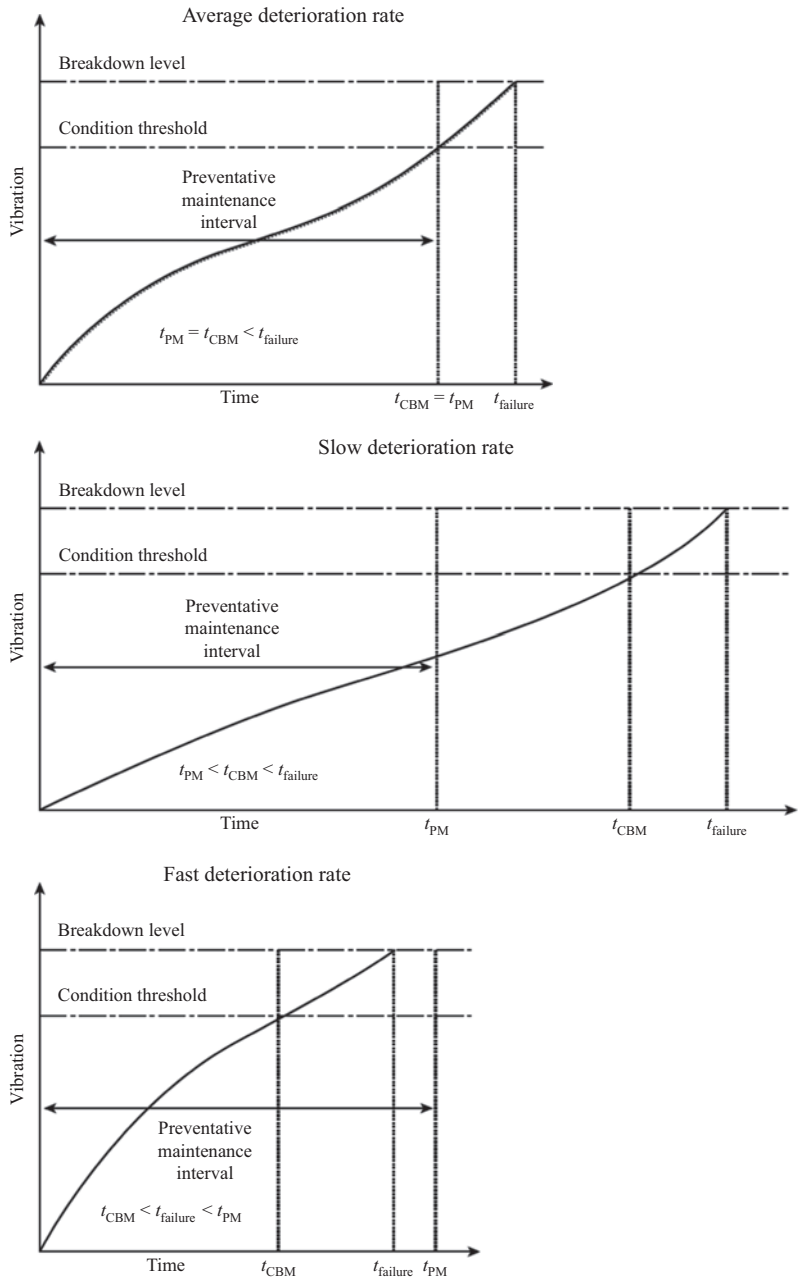


*Figure 13.1 Advantage of CBM, which can extend or reduce preventative maintenance intervals by providing extended warning of deterioration in machine condition*

## 13.3 Condition-based maintenance

CBM is a process of planning plant maintenance on the basis of machine condition information obtained through CM and, in some cases, inspection. Rao (1996) provided a description of CBM in terms of the expected outputs of the approach: lower maintenance costs, higher availability, reduced severity of in-service failures. CBM requires the application of specifically-designed software to specific pieces of plant within a clearly-defined plant structure. The software receives condition data from the plant and collates this to present it in a way that assists maintenance engineers in planning maintenance actions.

### *13.3.1 Signals and data for condition-based maintenance*

The data which CBM software needs to record when monitoring rotating electrical machines and making maintenance decisions includes signals of global significance to the machine alongside any application-specific monitoring signals. Globally-important signals are largely related to operational conditions and include:

- Running hours,
- Number of starts and stops, particularly for induction motors and standby generators,
- Cumulative kWh (energy) consumption or generation over time.

There are more targeted signals which might also be considered to be of global significance for electrical machines, including:

- Power, current and voltage,
- Speed,
- Torque.

Examples of specific monitoring signals to enable confident and precise detection and diagnosis include:

- Bearing or frame vibration with time at specified positions, related to likely fault conditions,
- Winding and bearing temperatures with time,
- Shaft vibration with time,
- Winding discharge level, for high-voltage machines.

Examples of sensor and system configurations are available on the websites of most CM system manufacturers. To take just one example, Brüel and Kjær Vibro provides a diagram of its monitoring system applied to a hydro-electric power plant, and it is interesting to observe the large number of sensors and measurements related to the electrical generator alone, Figure 13.2, as well as the faults detected using these:

- Four absolute and four relative vibration sensors,
- Tachometer,
- Air gap length, magnetic flux and partial discharge,
- Lubrication/bearing temperatures.

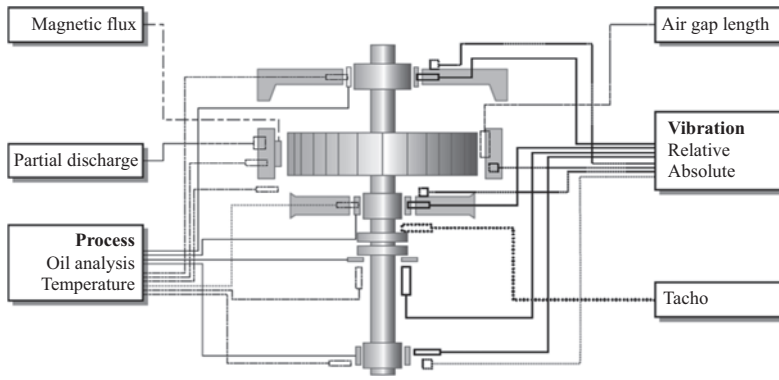


| | | Vibration | Air gap | Magnetic flux | Process values |
|---|---|---|---|---|---|
| Mechanical and bearing | Unbalance | ✓ | | | |
| | Misalignment | ✓ | | | |
| | Rotor rub | ✓ | | | |
| | Foundation problems | ✓ | | | |
| | Loose bearings | ✓ | | | |
| | Oil and lubrication | ✓ | | | |
| | Stator/rotor bar problems (loose, shorted) | | ✓ | | |
| Generator | Stator bar/core vibration | | | | |
| | Air gap abnormalities | | ✓ | ✓ | ✓ |
| | Rotor/stator out-of-roundness | | ✓ | | |
| | Loose/shorted stator bars | | | ✓ | |

*Figure 13.2 Outline of Brüel and Kjær Vibro condition monitoring system applied to a hydro-electric generator*

These signals will be acquired or sampled in different ways depending on the particular application. Some will be recorded continuously to allow detailed evaluation against time or operating condition. Other signals, particularly high-frequency vibration or electrical discharge measurements, might be sampled at specified internals or under specific operational conditions to allow direct comparison with historic observations.

There are numerous data acquisition systems and approaches that can support the data requirements of CBM. Many of these are specific to particular machine types or applications; however, there are common themes to their operation. Most data for CBM planning is collected by SCADA systems. These systems are present in most large-scale electrical machine applications in some form, either for generic plant monitoring (e.g. speed, power and temperature) or to collect more specific condition-related information (e.g. vibration and shaft position). Whilst raw data might be sampled at high frequencies, SCADA systems tend to down-sample or resample the raw data to provide averaged or instantaneous values at given

intervals, typically every few minutes or, at most, every second. In some systems, additional information can be extracted to add detail to the averaged values, including standard deviations, maxima and minima. To provide an idea of the range of systems available in just one operational environment, Chen (2014) presented a review of SCADA systems for wind turbines reporting on 26 systems of varying type. Several of these are simply data acquisition systems that allow operators to visualise the data from different wind turbines and farms. Ten of the systems were developed by industrial software companies while six were developed in-house by wind turbine manufacturers. The majority of the surveyed systems include some form of data processing, either through simple trending and time-series analysis or through artificial intelligence methods as discussed in Chapter 14.

Whilst much of the data required for CBM planning can be acquired through SCADA systems, there are cases where independent CM systems are installed to either perform a function that is perhaps specific to a particular machine or to collect more detailed information from existing sensors. Most modern CM systems have developed from systems for high-frequency vibration monitoring and spectral analysis. An example of this is the SKF CM system that was developed for vibration monitoring of bearings and gears in conventional applications before being extended incrementally to accept other signals, such as oil debris counts, for application to wider technologies, such as variable-speed drive wind turbines. Again, there is an extensive range of systems available. To return to the wind turbine example, another survey conducted in 2014 identified 36 CM systems specifically for wind turbine application, mainly focused on rotating electrical machines and gearboxes, Crabtree (2014). A suitable monitoring system must be selected for any given application depending on the systems that are of interest within that application.

### *13.3.2 Targeted monitoring*

As described in Section 13.2, preventative maintenance strategies can benefit from planning maintenance based on the criticality of a given system component. It is logical to take a similar approach when considering which systems should be monitored and by what means in order to achieve CBM. Wear of carbon brushes in electrical machine brush gear, for example, can be monitored by considering spring pressure, machine speed, rotor current, brush material, slip ring surface finish and temperature. However, brushes and similar components are perhaps unlikely to wear in a consistent manner and deteriorate steadily over time, except in very exceptional circumstances. Brushes are also relatively low cost components so the costs of monitoring hardware, data communication and processing software development are unlikely to be justified. Here, a fixed-interval maintenance approach is most likely to be cost-effective.

Conversely, large generator bearings are expensive and their wear is likely to be driven and accelerated by abnormal conditions. The consequences of failure are also more significant as bearing failure could lead to catastrophic generator failure and shaft damage, for example. In this case, there is likely to be a compelling

financial argument for vibration or temperature-based CM and investment in the required monitoring hardware and software.

Machine-related electronic systems, such as power converters, may offer a particular challenge. They are likely to be critical to plant operation but their failure modes can easily develop without significantly or obviously affecting operation. Functional failure might therefore appear to occur quite suddenly with little advanced warning. Figure 13.3 illustrates this concept for mechanical and electronic components. Mechanical components generally degrade noticeably and steadily over an extended period of time, allowing fault signatures to develop and be observed in monitoring signals such that operators can be confident that failure is not imminent. The performance of electronic components, however, may not be obviously degraded until just before failure, meaning that monitoring systems

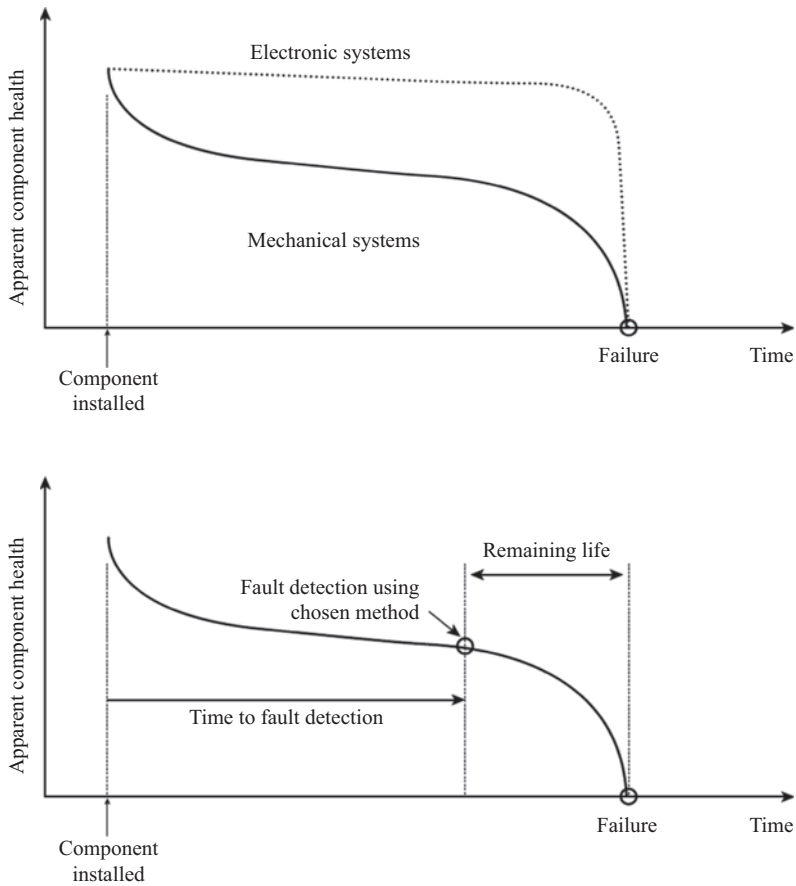


*Figure 13.3 Detectability of faults in mechanical and electronic systems. Large-scale electrical systems such as windings are likely to follow the mechanical curve*

might struggle to provide advanced warning of failure despite the criticality of the systems to electrical machine operation.

For large systems which comprise multiple sub-systems or components, manual monitoring is likely to be impractical, especially where multiple signals are recorded, so operators must either select components for monitoring based on a criticality list or invest in automated signal and alarm handling software to reduce the complexity of the incoming data and information. This requires a strong cost justification.

## 13.4 Economics of maintenance strategies

Maintenance is a costly activity and can contribute significantly to the costs of operating any plant. Ultimately, any costs incurred will affect the price of the plant output. Consequently, any maintenance strategy must be justified against certain criteria, the specific details of which will depend on the particular application. For example, a coal crushing and handling plant in a conventional power station might be critical to overall plant operation and the resulting risk to energy production, extended down-time and reduced production leading to lost revenue, is likely to justify the presence of a permanent maintenance team rather than a complex, remote monitoring system. Some plant scenarios will have a relatively simple cost justification: the high cost of a single failure justifies a monitoring system with human involvement to interpret data. Other situations are more complex and require detailed life-cycle cost models to understand the benefits, or otherwise, of different monitoring and maintenance strategies.

### *13.4.1 Basic economic justification*

Before considering detailed studies of the economic benefits, or otherwise, of CBM, it is worth considering by intuition whether or not an operator is likely to benefit from applying CBM strategies to their particular plant. There are certain plant characteristics that will generally yield benefits when CBM is applied instead of a reactive or preventative strategy. Beneficial characteristics that are likely to justify the costs of monitoring and CBM include applications with:

- Very high plant repair or replacement cost,
- Significant risk of common-mode or cascading failure,
- Challenging accessibility,
- Continuous operation that is critical to wider plant operation,
- High component lead times, or where carrying spares cannot be justified,
- High down-time costs, such as significant lost production or financial penalties.

It is unlikely, for example, that an easily accessible, low cost electrical system will justify the cost of CBM on its own. However, if this system supports a major plant function, the effects of its failure on wider plant operation may well justify the

costs of CBM. Kerres *et al.* (2015) examine these effects by considering a 660 kW onshore wind turbine under three maintenance strategies:

- Run to failure, corrective maintenance,
- Annual inspections,
- CBM.

Under the corrective maintenance strategy, components are only replaced once failure has occurred. With annual inspections, component replacement is carried out if a defect is observed. To understand the effects of CBM, a CM system is modelled with an assumed detection success rate of 90% while the time of detection is modelled as a random variable. The study assumes that there are no false-positive detections.

Figure 13.4 shows probability distributions of lost energy sales for the three scenarios from Kerres *et al.* (2015). As the maintenance approach shifts from corrective to condition-based, the probability of high lost sales reduces. Logically this means that the probability of lower lost sales increases. However, this clear shift does not have a dramatic effect on the overall cost of maintenance and lost production; due to the relatively low failure rates of generators and gearboxes, the corrective and CBM strategies are remarkably similar in cost, being 1060k SEK

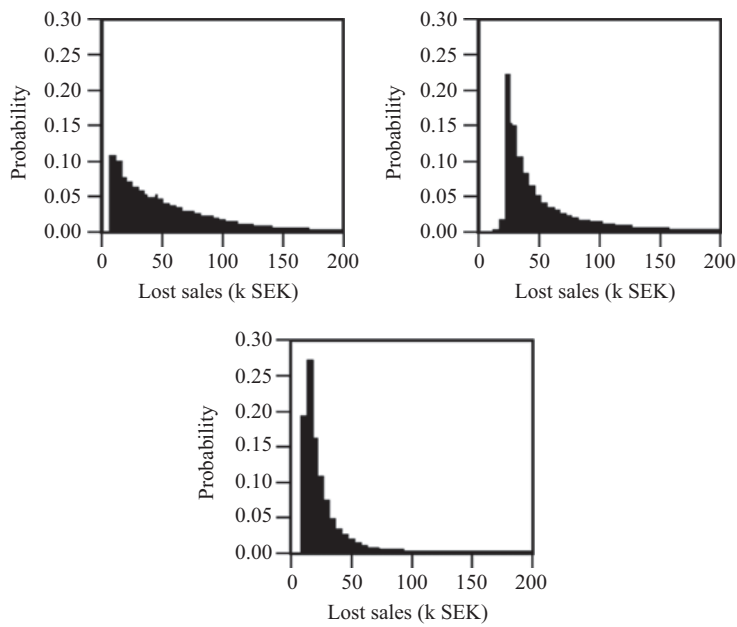


*Figure 13.4 Probability of lost energy sales due to the generator and gearbox failures under: (top left) corrective maintenance; (top right) annual inspections; (bottom) CBM; based on Kerres et al. (2015)*

(Swedish Krone) and 1057k SEK, respectively. This is a result of the ease with which the machines can be accessed for inspection and maintenance. Kerres *et al.* (2015) compare these findings with a similar study by Andrawus (2008) and observes that any such study is highly sensitive to the factors listed earlier in this section, specifically component lead times and accessibility. This is a complex issue even for conventional electrical machine applications. In conventional power stations, accessibility is largely irrelevant to cost estimates. On the other hand, the large machines in conventional stations, perhaps 600 MW rather than 600 kW, means that spares may not be carried and lead times could be significant. The costs of lost production will also increase:

- A 24-h period of down-time for a 6 MW offshore wind turbine with a high capacity factor of 40% might lead to energy production losses of 58 MWh valued at around £5k,
- A 600 MW conventional unit at 80% usage over 24 h would lose 11 520 MWh, valued at around £1M.

### *13.4.2 Life-cycle costing*

Life-cycle costing, also called whole-life costing, is a technique used to establish the total cost of ownership of plant throughout its lifetime. This includes plant capital, installation, monitoring and maintenance costs. It is a structured approach to managing all cost elements and can be used to produce a spend profile over the anticipated plant lifetime. The subject was initially hampered by a lack of international standardisation; however, standards have now existed for some time. IEC 60300-3-3:2017 provides the latest guidance.

A detailed life-cycle costing can be used to help managers decide upon the most appropriate maintenance option by evaluating the effects of, for example, break-down, planned or CBM on long-term costs. The accuracy of any such costing diminishes as it projects further into the future, so it is most valuable as a comparative tool when the same long-term assumptions are applied to all the options. The resulting analysis might not be accurate, but it will allow the impact of different options to be compared.

Life-cycle costing is an innovation of the last 30 or 40 years, reflecting a desire from plant owners to maximise the value of returns from their investments by sweating their assets. It is born of an operational environment where the costs of initial capital investment and operations and maintenance labour are high. It is used in developed countries as they attempt to compete with developing countries with lower labour costs.

On a more industry-specific level, life-cycle costing is used in privatised national utilities, like railways, water and gas, as private operators attempt to deliver profitability in a highly regulated environment. Most recently, it has become essential in electrical power generation applications where cost of energy is critical to the funding and success of a project in a changing market. Forms of distributed generation, for example, are particularly sensitive to operations and

maintenance costs, as previously mentioned, since the financial and reputational losses resulting from individual failures do not provide an implicit justification for significant expenditure on monitoring equipment.

However, life-cycle costing offers a further benefit beyond the relatively simple economics of failure; it raises the possibility of creating measurable extensions to plant life by reducing overall costs through investment of initial capital into monitoring systems and the application of CBM to reduce through-life costs.

Life-cycle costing has also developed in other industries, for example defence where high weapon programme costs force governments to demand better field performance, and also aerospace, where the costs of failure due to loss of business and litigation can be terminal for private companies.

In order to achieve life-cycle benefits, it is necessary to:

- Understand the life-cycle costs and devise a management system to control them,
- Monitor machine condition,
- Maintain the machine on the basis of condition where possible,
- Assess long-term plant condition on the basis of monitoring signals and manage that plant accordingly.

One relatively recent application for which life-cycle costing is of utmost importance is offshore wind, where complex electrical systems surround critical rotating machines in a hostile and inaccessible environment. A particular paradox for maintenance and machine lifetime is that the highest energy capture and revenue returns are achieved at the windiest and most challenging sites, meaning that reliability and maintenance issues are the driving factors in operational planning.

For any electrical energy generation plant, whether conventional or renewable, the regulatory environment and consequent competitive contracting means that cost of energy is often the metric against which projects are evaluated. This in turn means that any life-cycle costing to justify the selection of monitoring systems, maintenance methods and, in fact, machine type is driven by a complex combination of reliability analyses, energy resource/capture estimations and maintenance models. As mentioned, long-term estimation of any of these variables is likely to be challenging and imprecise; however, a comparative study can be conducted by applying consistent assumptions and parameters to all models.

The difficulty of this cost estimation is borne out by a comparison of different studies of levelised cost of energy (LCOE) from wind by capital and operational expenditure (OPEX). Figure 13.5 shows six studies conducted by various major industry stakeholders, Crabtree *et al.* (2015). The contribution of OPEX to LCOE varies from 25% to 40%, depending on which components each study included in its estimations. The LCOE calculation includes initial capital cost, the lifetime costs of operations and maintenance, a fixed charge rate and, importantly, the annual energy production, each of which are sensitive parameters. However, comparisons within each study are possible by ensuring that parameters are comparable between cases.

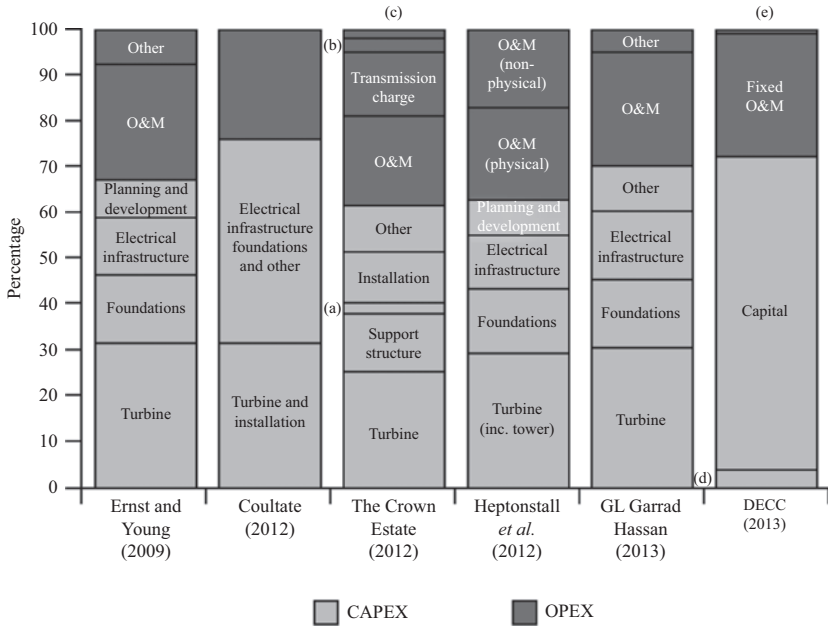


*Figure 13.5 Offshore wind LCOE breakdown by CAPEX and OPEX from six studies, Crabtree et al. (2015): (a) array cables, (b) decommissioning, (c) seabed rent, (d) pre-development and (e) variable O&M*

### *13.4.3 Cost–benefit analysis of condition monitoring for CBM*

There is a clear opportunity for CBM to reduce these OPEX costs. Remote CM and, preferably, automated fault detection could reduce the number of manual inspection visits and could lead to more targeted maintenance actions, McMillan *et al.* (2008), Andrawus (2006). A reduction in the number of physical visits to site is also beneficial from a safety point of view. There is, of course, a risk element to this approach whereby undetected failures could cause significant maintenance actions to be required so the success rate of the CM system must be factored into any estimation of cost benefit. This point has been the subject of a number of studies for wind energy applications. Wind energy provides an excellent demonstration of the importance of CBM due to its delicate cost balance.

The ability of a CM system to detect faults can be represented in calculations in a number of ways. A detailed analysis is provided by May *et al.* (2015), who model a wind turbine's electrical and mechanical systems as a hidden Markov model. Numerous texts on Markov modelling are available however the concept is relatively simple to explain, even if the reality of modelling is more challenging. At any point in time, the electrical and mechanical systems can be healthy or faulty

*Table 13.1 Indicative condition monitoring costs for a wind turbine machine, May et al. (2015)*

| | **Vibration** | **Oil** | **Acoustic** |
|---|---|---|---|
| Capital cost | £6 550 | £9 200 | £8 150 |
| Annual costs | £570 | – | – |

*Table 13.2 Lifetime savings resulting from CBM using condition monitoring, May et al. (2015)*

| **Drive train monitoring system** | **Lifetime saving compared to fixed-interval maintenance** |
|---|---|
| Vibration only | £12 000 000 |
| Vibration and oil sensing | £19 100 000 |
| Vibration and acoustics | £18 900 000 |
| Vibration, oil and acoustics | £20 300 000 |

and the probability of moving between these states depends on the failure rate ($\lambda(t)$) and repair rate ($\mu(t)$) of components. As an aside, this instantly introduces two other factors on which CBM justification relies: the reliability of systems and the ease with which they are repaired. If the Markov model determines that a system has failed, an additional layer decides whether or not that failure is observable by the CM system. This is effectively governed by a detection rate. The model also allows false positives to be observed. These are occasions when the system is healthy, but the monitoring system believes it has detected a fault.

Example CM costs for typical electrical machine and drive train systems are given in Table 13.1. Using these values and their hidden Markov model, May *et al.* (2015) demonstrated clear benefits of using CM systems to inform a CBM strategy over the 20-year lifetime of a 20-turbine, 60 MW offshore wind farm. The lifetime savings compared to fixed-interval maintenance of using various combinations of different drive train monitoring systems for CBM are given in Table 13.2. Figure 13.6 illustrates the effect of CM system detection rate on lifetime savings and demonstrates that savings can be achieved even when a monitoring system has a detection rate of only 60%.

### *13.4.4 Asset management*

In general, the approaches discussed throughout this chapter are the component parts of the process of asset management. This is a business, rather than an engineering, process which provides a forecasting framework for decision-making based on the behaviour or performance of an asset. Asset performance is itself derived from economic and engineering data. Asset management incorporates an economic assessment of trade-offs between alternative investment options and uses

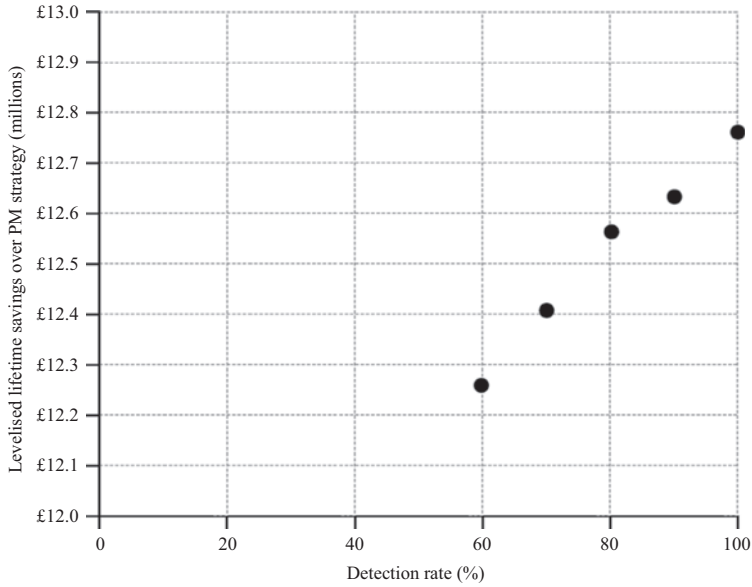


*Figure 13.6 Savings due to condition monitoring and CBM against detection rate for a wind drive train and structural condition monitoring system, May et al. (2015)*

this information to make cost-effective investment decisions. In the context of this book, the degree to which CM should or should not be applied depends on performance. The value that can be obtained from its use is a key factor in many asset management decisions for electrical machines and related power and drive train systems. Hodges (1996) provided an introduction to asset management and a prediction about its progress past the turn of the last century, which proved to be quite accurate, see Figure 13.7, the implication of which is that asset management is a step change approach to maintenance and planning. It includes corrective maintenance, CBM and life-cycle costing to produce the best support for machines and their operators.

Proactive asset management exploits CM to assess the conditions of assets, to control their operation and plan maintenance, replacement or disposal. In particular, it ensures that maintenance work is carried out only when needed but before assets deteriorate. The ultimate aims are to avoid costly failure and maximise the return on investment by developers and operators. Asset management is now standard practice and developing industries are driven towards it because of:

- Changes in the economic environment and pressure from investors and shareholders,
- Changes in public expectations,
- Advances in instrumentation and computing technology.

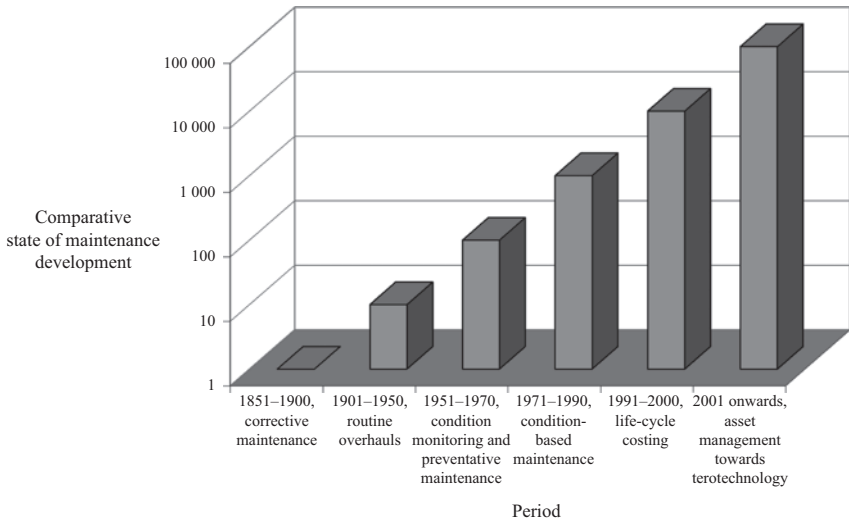


*Figure 13.7 Development of maintenance, condition monitoring, CBM, life-cycle costing and asset management, based on Hodges (1996)*

The issue of public expectation is an interesting one which could form the basis of a lengthy text in its own right. Public expectation has a particular influence over power generation and transmission owners and operators. Increases in the cost of electricity are publicly opposed (both by the public and by government) so operators must sweat aging assets using asset management techniques.

Comprehensive specialist software is essential to expert asset management, building upon software used for CBM and extending it to a network of assets or plant. Software must incorporate life-cycle costings, asset health and performance information, and management information and be capable of presenting this engineering and financial information to business managers and decision-makers in a way that assists in planning maintenance, replacement or disposal of the assets.

Asset management reflects a level of long-term care for engineering plant that is closer to the healthcare of human beings by a general practitioner. It is a long way from breakdown maintenance and requires a significant management and resource commitment in itself. In conventional electrical engineering, the greatest advances in asset management have been made with transmission assets; Brown *et al.* (2005) have given an overview as has Morton (1999). The degree of progress towards industrialisation of the process is indicated by the relatively small number of academic studies in recent years, suggesting that operators are now considering asset management as standard practice. Transmission assets for which most progress has been made, in relation to CM, include:

- Transformers, using transformer gas-in-oil analysis, Dominelli *et al.* (2006),
- Transformer windings, using partial discharge data, Judd *et al.* (2002),
- Transmission line, using voltage and current monitoring, Zhang *et al.* (2014).

It is not surprising that transformer monitoring has been so successful. Its major advantages over other electrical machines are that there are no moving parts and that the transformer is completely contained within its tank. This contained environment means that techniques of global significance to the transformer, such as gas-in-oil analysis, partial discharge and acoustic detection, are highly effective for asset management. These techniques are particularly applicable to a life cycle and CBM approach.

The application of asset management techniques to electrical machines in large power stations is now standard although it is worth noting that these assets are of such importance that shut-downs at regular intervals are scheduled to prevent major failures in the mechanical systems. In such a critical operational environment, where the costs of failure are extremely high, key components, such as turbine generator rotors, can be monitored and spares held to be installed in faulty machines when CM signals suggest that precautionary measures need to be taken. This is a standard practice, with Kohler *et al.* (1999), for example, providing details of the possibilities over 20 years ago.

Modern electrical industries have followed suit. Large hydroelectric power stations have very similar operational characteristics to conventional plant, in terms of scale, types of machines and the impact of failure, so are able to adopt similar practices. Wind energy, the dominant form of renewable energy in Europe, has developed from small-scale, onshore wind farms of only a few 600 kW wind turbines into a multi-billion pound business featuring Megawatt-scale offshore wind turbines in farms of some GW. Onshore, reactive or breakdown maintenance was, initially, the standard approach to maintenance but as the industry developed, installing larger turbines and increasing energy production, CM techniques from other industries began to be adopted. By 2007, before the development of large-scale offshore wind, the certification body Germanischer Lloyd, now DNV GL had been established, with the issue of certification guidelines for wind turbine CM systems, GL (2013). As the preface to those guidelines says, the importance of CM to wind energy was recognised as early as 2003, suggesting the industry had learned from other electrical industries and was targeting asset management from the start. By 2010, the first IEC standard for collecting CM data from wind turbine systems was issued, BS EN IEC 61400-25-6:2016. Asset management in offshore wind is now standard and has allowed developers and operators to dramatically reduce the cost of electricity from offshore wind in Europe to well below the industry target of £100/MWh.

## 13.5 Conclusions

The era of CBM, life-cycle costing and asset management is firmly upon us yet there are remarkably few published results to confirm the efficacy of techniques when applied to rotating electrical machines across different industries.

There are, however, studies of the application of CBM and asset management which demonstrate that significant value can be obtained through the application of

such techniques. The greatest value is always likely to be obtained in the higher risk industries, whether these are physical failures or financial penalties and loss risks, and these industries with remote assets; conventional power generation and offshore wind are good examples of these risk categories. Applying CM to detect progressive deterioration in remote or high-risk assets has been shown to be valuable by a number of academic studies and is showing through in industrial metrics, such as cost of energy reduction.

Monitoring techniques that will have the greatest impact are those which monitor the most critical components, such as those which may cause cascading failures through the plant or catastrophic damage. Studies have shown these monitoring signals to include 'performance' parameters of global significance, such as:

- Electrical power and current for electrical condition;
- Winding, coolant and bearing temperature rise for thermal condition;
- Speed, torque and vibration, for rotor, bearing & structural dynamic condition.

Life-cycle costing studies have demonstrated the importance of selecting the most suitable CM approaches for the particular situation by estimating the life-cycle value of applying techniques individually and in various combinations. To ensure that asset management can be successfully achieved, the metrics against which maintenance and monitoring scenarios are assessed should reflect the needs of the particular situation, whether it be reducing the cost of energy produced or maximising plant throughput.

Asset management using CM is now essential to the success of any large, capital-intensive project and should be considered from the outset.

*This page intentionally left blank*

*Chapter 14*

# Application of artificial intelligence techniques to CM

## 14.1 Introduction

In earlier chapters of the book, we have presented various CM techniques. It can be seen that most faults have predictable symptoms during their development, from root cause to failure mode, which can be detected by mechanical, electrical, electromagnetic, optical or chemical sensors.

CM has to establish a map between the input signals and output indications of the machine condition. Classifying the machine condition and determining the severity of faults from the input signals have never been easy tasks and they are affected by several factors.

Return to our simple analogy in Chapter 5 of an engineer collecting data and acting on that data. Until recently, it was believed that in the final, diagnostic stage experienced human engineers can still out-perform most computerised CM systems. This has become questionable in recent years, as the successes of AI continues to surprise, usually pleasantly, human beings versus a machine in the AlphaGo game being one of the most convincing examples, see Lee (2018). It has been recognised that CM of electrical machines together with prognostics and health management (PHM) could be an ideal field for AI because of the 'mapping' feature of the problem.

Intelligence is about information acquisition and decision-making based on the information acquired. Behind this is usually a knowledge base and inference engine to make use of that knowledge. When the knowledge had to be provided by a human, it was easy to argue that AI could not replace human intelligence entirely. However, if the development of knowledge is part of intelligence, one can reasonably imagine that a computerised system might be more capable of extracting the knowledge from the data which could be overwhelmingly large by a human standard Xin *et al.* (2018).

As for decision making, a CM system should provide, in a progressively more specific order, the following functionalities:

- Raise an alarm when necessary,
- Predict the remaining machine useful life,
- Plan maintenance.

Except for alarms, the other two CM outcomes, prediction and maintenance planning, require considerable intelligence, taking account of in-service stress and holistic approach consequences. This is a high-dimensionality optimisation problem subject to many variable and uncertainty combinations. An automated AI system could be extremely capable of decision-making in the case of such complexities.

It is of course the human benefit that decision-making process should try to maximise. This is almost a philosophical point which this book cannot address. But it is a matter of fact that experienced engineers have been retiring, while new, complex electrical machine systems continue to appear, providing services in new environments and usually with very low safety margins Barater *et al.* (2017). In such circumstances, the importance of AI-based CM techniques cannot be stressed enough, and this must be the future trend for CM electrical machines, especially in environments where more machines are being incorporated into VSD systems, rich in data, and being applied to high-integrity environments such as electric vehicles, rail traction and ship propulsion.

One application area of importance in utility and process industries, including water and electricity suppliers, is asset management, see Chapter 13. Electrical machines are inevitably applied to other apparatus, pumps, fans, generators and propulsion systems. A feature here is the widespread use in those systems of sensors transferring large amounts of data, made possible only by recent IT technology developments, see Sarantakos *et al.* (2017) and Sabin *et al.* (2017). The objective of asset management systems is to manage reliability, warranty and maintenance costs and to defer new asset investment. AI-assisted electrical machine CM will be an essential ingredient for power and process asset management systems. In recent years, there has been considerable effort to develop AI systems that can play a role that is currently performed by humans in electrical machines monitoring. This is important for at least two reasons:

- Electrical machines, both motors and generators, are now used as elements in larger systems where operators may be inexperienced in their design,
- Human experts can be subject to influences that make quick and consistent judgement impossible, particularly in systems with many machines. Correct judgement may also depend on the expert knowledge and experts may not be available at the time of faults.

AI can take different forms, but the core problems are ‘learning’ and ‘classification’. Learning can be from existing knowledge or raw data that contains knowledge. An educated AI-system can then be used to classify a set of input data that may or may not be directly covered in the learning process. It is classification that is related to the CM outcome and to decision making. In this chapter, we will present the fundamental concepts of machine-based learning and classification.

We start from the simple case of looking at multiple signals at the same time, multi-parameter monitoring.

We then progress to the more complex case of programming existing knowledge to scan the input data so that a classification can be achieved. This is the

structure of an expert system that mimics experienced engineers. Presentation of knowledge and heuristic reasoning are key parts of an expert system, whose limitations are:

- Adaptation of the knowledge base usually needs human intervention,
- System cannot easily handle complex numerical calculation, which may not be clearly formulated.

We then recognise that some human knowledge is inherently vague and uncertain, but this can be a strength when dealing with complex situations. Fuzzy statements and fuzzy reasoning can be used to enhance such expert systems.

Finally, we progress to the use of ANNs (artificial neural networks) which, with on-line training, which can learn and obtain knowledge through data-mining.

For CM of electrical machines there have been two traditional AI approaches, see Lee (2018).

'Rule-based' methods that mimic mathematical transforms using symbolic or Expert Systems attempting to teach computers to 'think' by a series of logical rules.

'Neural network' methods that mimic the human brain's underlying architecture to deduce relationship from a wide range of given data.

The first method can advance if simple mathematical expressions are available, which is clearly possible from the data in Tables 9.1 and 9.2 for IAS and MCSA.

On the other hand, the second method requires:

- Large amounts of wide ranging and relevant data,
- A strong algorithm with a narrow domain,
- A concrete goal.

In the early stages of development of CM, the model-based approach provided insights into the physical mechanisms giving rise to CM signatures. The data-driven approach has been used to conduct the trend analyses but has struggled to interpret the signal significance.

Nowadays, there is little doubt that a sensible way is to combine both so that more informative results can be obtained under operational uncertainties, see Garcia-Escudero *et al.* (2017).

## 14.2 Multi-parameter monitoring

A step on the path to the use of AI for CM is to compare and contrast multiple CM signals on the same machine, which was called multi-parameter monitoring by Tavner *et al.* (1986). Figures 14.1–14.3 show three different examples of this type of fault detection using the disparate signals, as follows:

- Figure 14.1(a) and (b) used two different chemical monitoring methods to show detection of a stator core fault in a 500 MW turbo-generator using a core monitor, $S_d$, or smoke detector, and a total organic matter gas detector, VOC. These signals are the result of core overheating and related to generator MW

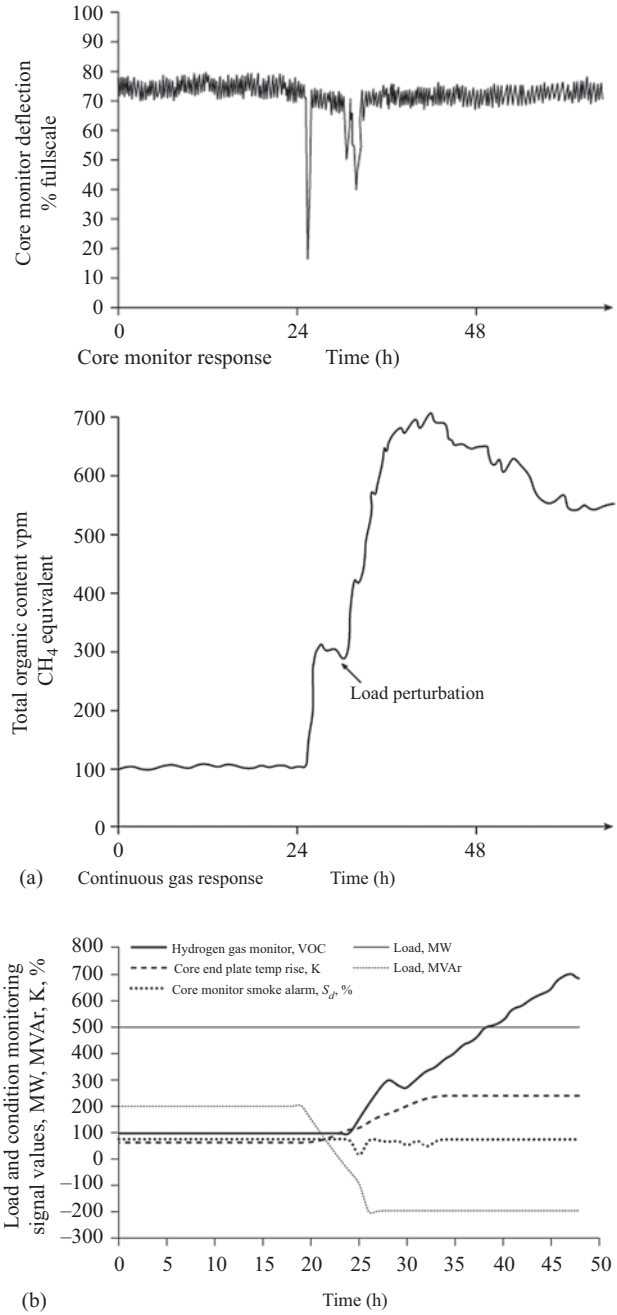


*Figure 14.1 Multi-parameter monitoring of a 500 MW 2-pole turbo-generator stator: (a) comparing in hydrogen coolant core monitor smoke, $S_d$, % and total gas organic measurement, VOC and (b) load perturbation from full-load lag to lead power factor, triggering core end-plate temperature rise, K, and consequent internal smoke, $S_d$, and VOC increase. Taken from (a) above*

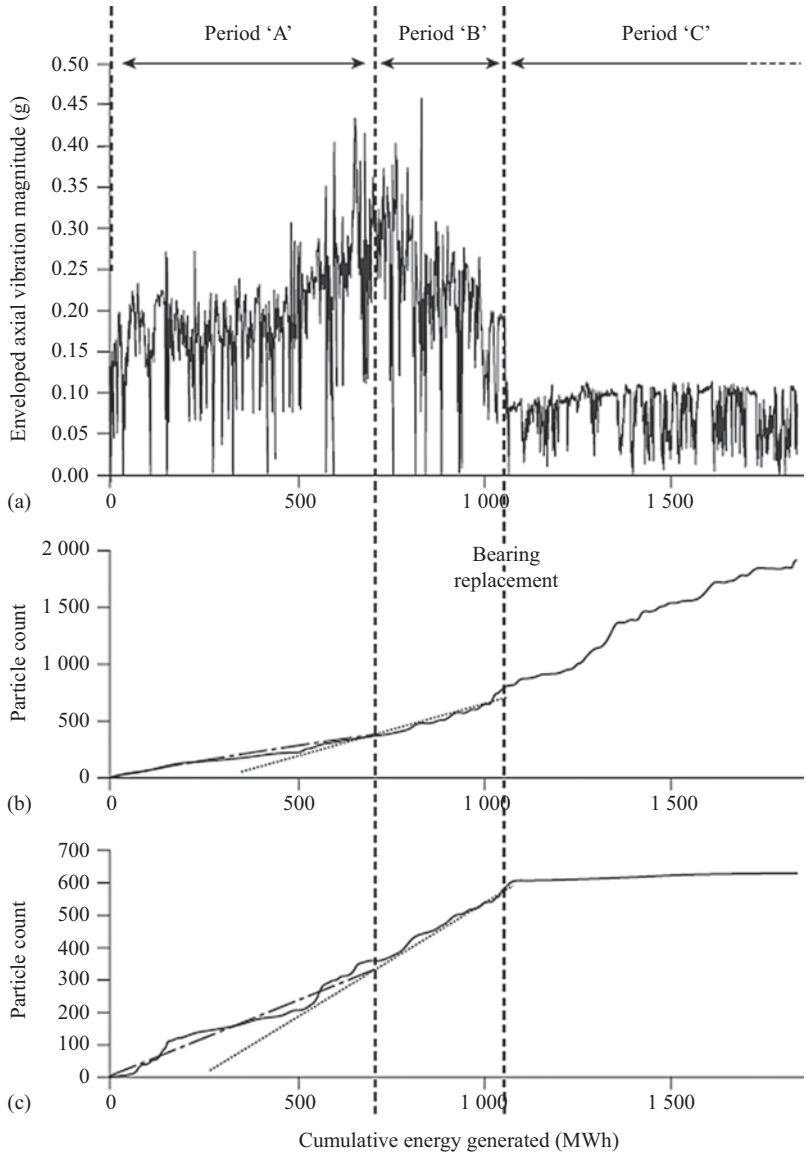


Period A: rolling element bearing wear, vibration increases
Period B: collapse of rolling element cage
Period C: replacement of rolling element bearing and cage without filtering the lubrication oil

*Figure 14.2 Multi-parameter monitoring a WT 6-pole generator gearbox rolling element bearing fault, comparing bearing vibration and gearbox oil particulate measurements*

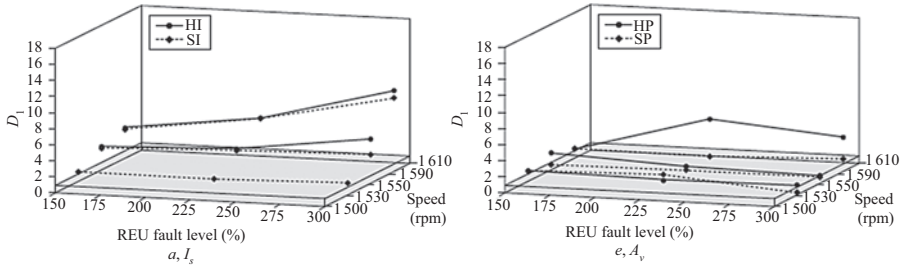


Comparing current, $I_s$, and vibration, $A_v$,signals from a rotor-faulted (REU) DFIG generator at increasing loads

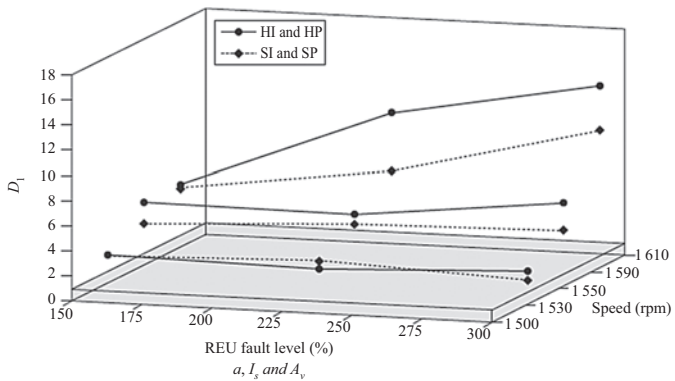


Data fusion of $I_s$ and $A_v$ signals on a rotor-faulted DFIG generation at different loads with comparison of signals to improve REU detectability

*Figure 14.3 Multi-parameter monitoring of a WT DFIM 4-pole generator rotor fault, comparing stator current, $I_s$, and bearing vibration, $A_v$, with data fusion over a range of fault levels and generator loads*

and MVAr load and core temperature rise, K, see Ryder *et al.* (1979) and Tavner *et al.* (1986),

- Figure 14.2 monitoring a WT 6-pole generator gearbox bearing fault using both bearing vibration, $A_v$, and gearbox oil debris, $O_g$, to measure the progression to failure, Feng *et al.* (2012),
- Figure 14.3 monitoring a wind turbine DFIG using both stator current, $I_s$ and stator-bearing vibration $A_v$ to measure rotor unbalance, see Zappalá *et al.* (2019). Note the similarity of this work too that by Shahriar *et al.* (2018) on rolling element bearing analysis comparing IAS and MCSA results but those authors did not realise that this method can lead to increased detectability and detection confidence.

In each of the three cases, Figures 14.1–14.3, electrical machine fault conditions were monitored simultaneously by disparate chemical, temperature, electrical or mechanical CM signals, indicating fault presence and progression. In each case the combination of disparate signals delivered a higher detectability and increased detection confidence.

This book's authors propose that much greater management confidence can be placed on diagnosis from disparate CM signals than reliance on one measurement method alone, this has been the basis for multi-parameter monitoring and should form a significant part of an expert system for the AI of electrical machines and CM.

## 14.3 Expert systems

Expert systems were perhaps the first AI techniques applied to CM. Although modern asset management systems are more sophisticated, expert systems are usually an important component in such systems, Ma *et al.* (2015).

An expert system treats the CM of an electric machine like a medical doctor diagnosing a patient. Some surface evidence is used to form hypotheses about the machine condition, i.e. the possible faults. Then further evidence is searched to narrow down the judgement and increase the confidence when a more specific judgement is made. When engineers do this, they apply their knowledge. In an expert system, such knowledge should now be represented in a way that can be interpreted by a computer. This is not an easy task, however, because the knowledge is usually heuristic in nature, based on 'rules of thumb' rather than absolute certainties. Furthermore, human knowledge has complex linguistic rather than precise numerical structures, and most of it is almost subconscious. There is no doubt that we need to obtain a substantial amount of knowledge in order to build an expert system that provides usable CM outcome. Close interaction between machine experts and software engineers is necessary.

The knowledge to be used in the expert system can be represented in a number of ways:

- Frame-based systems, representing knowledge in data structures called frames which describe the typical situations or instances of entities,

- Semantic networks, representing knowledge in a graphical structure where nodes represent concepts and beliefs about the system while arcs represent relationships between these concepts and beliefs,
- Rule-based systems, representing the knowledge as 'If-Then' rules in the computer memory, see Birmingham *et al.* (1986).

All representations have been used but the rule-based knowledge scheme is probably the most common in practice. Typically, the rules will not have certain conclusions; there will be just certain degree of certainty that the conclusion will hold for given input conditions. Statistic methods are used to determine these certainties [14.9]. Figure 14.4 shows the general architecture of a rule-based expert system.

Declarative and imperative knowledge need to be represented as rules:

- Declarative knowledge tells the expert system what it could believe, with a degree of certainty. For example, a negative sequence component above a certain level in the input current of an induction machine implies stator winding shorted turn fault or unbalanced supply,
- Imperative knowledge, on the other hand, tells the expert system what to do next, e.g. looking into the data which may indicate that supply imbalance is not in fact present.

This gives rise to the ability for heuristic reasoning. Human experts are distinguished not only by the quantity of knowledge that they possess but also by the way that the knowledge is applied skilfully. For the reason described at the beginning of this section, an expert system for CM needs to perform both forward and backward reasoning.

A feature of the architecture shown in Figure 14.4 is that case specific data and the general knowledge base are separated. This allows the expert system to be used in different cases, provided that the rules in the knowledge base are adequate. They

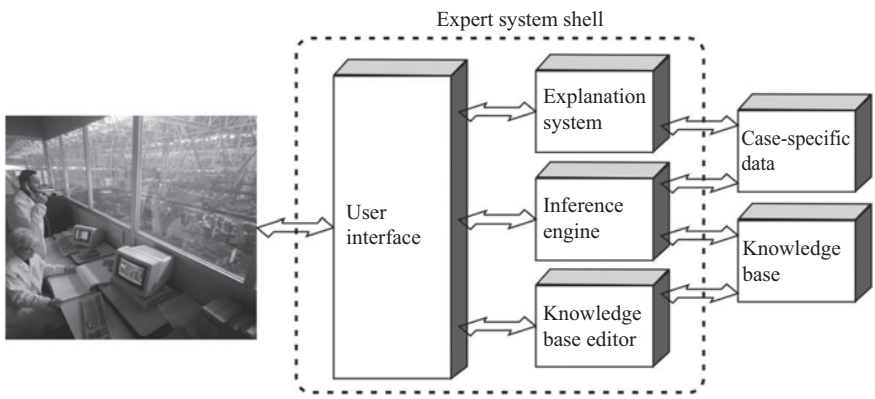


*Figure 14.4 Expert system architecture*

are both separated from a more general part of the architecture called expert system shell. We can usually find commercial shell software with appropriate characteristics, to develop the expert system by programming rules into the system and setting the user interface. The shell shown here has an explanation sub-system which allows the expert system to explain its reasoning to the user. The knowledge base editor allows the rules to be modified when necessary and hence makes the expert system developed maintainable.

Stone *et al.* (1997) developed an expert system for monitoring stator insulation in generators and motors. The majority of stator windings, rated 4 kV or above, fail as a result of gradual electrical insulation deterioration. We have described in Sub-section 3.6.3 the dominant mechanisms leading to stator winding insulation failure. It can be seen that several interacting factors, including high electric field, vibration, over-heating and moisture contamination, are involved in the degradation process and insulation failure can occur in different parts of the winding. As some factors cause air pockets in the winding insulation structure, PD occurs leading to further damage to the insulation. PD can therefore be monitored, from the stator terminals or neutral ground, to indicate the insulation condition. The main measurement techniques have been described in Section 10.2. PD signals are generally high frequency spikes, in 100 MHz range, which can be easily confused with noise from adjacent machines or that caused by adjacent switchyard and switchgear arcing or corona activities. Expert knowledge is important to ensure the reliability of the PD measurement data, by checking, for example, the d$V$/d$t$ rate. Stephan *et al.* (2003) confirm this by showing that the measurement data can be badly contaminated by loose brush-gear contacts, meant to ground the generator shaft. They also show that the data reliability can be improved by considering the correlation of PD events with the phase angle of the generator terminal voltage; however, this becomes more complicated in machines fed from variable frequency drives. Given the reliability of the acquired PD data, conclusions can only be drawn based on the trend analysis, comparison with other generators in the power plant, maintenance record, earlier off-line test results, present operating point, vibration and temperature measurement, visual inspection and fleet experience, etc. Such aspects are best taken into account using expert knowledge, represented in rules, as it is extremely hard to establish algorithmic solutions to the problem.

The output of an expert system gives an index of the health condition of the machine in one aspect or overall, which is expressed as a relative position between good and bad. This can be used in comparison with other machines to determine the one that is most in need of maintenance. An expert system usually provides a list of mechanisms which might be occurring. The probabilities of such mechanisms may be indicated, and these are estimated statistically using expert experience and knowledge. Other auxiliary information may also be displayed to further aid the operator, Stone *et al.* (1997).

In practice, expert systems can be made modular with each module focusing on one aspect of the machine condition. Modules are then integrated to provide entire machine monitoring. Figure 14.5 shows the architecture of a system for steam turbine synchronous generators. Interactions between different modules are taken

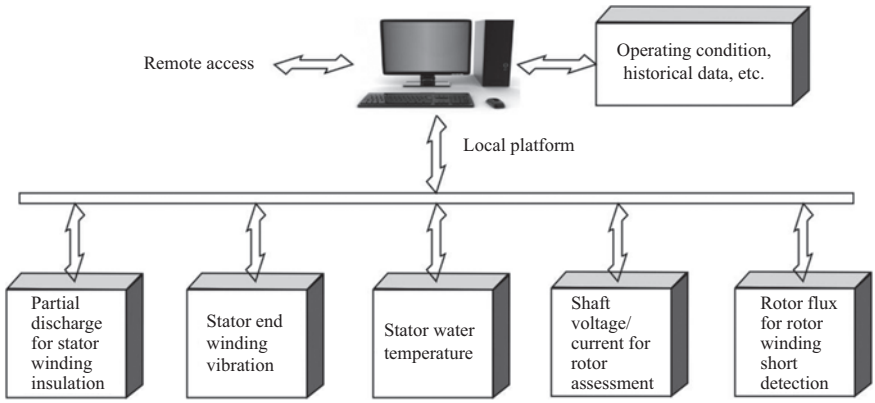


*Figure 14.5 Configuration of a modular expert system*

into account and these modules may overlap in their functionalities. For example, the condition of shaft grounding can affect PD as mentioned above. High end-winding vibration may indicate looseness in the end-winding support which among other things can cause cracks in the end winding corona protection, leading to PD in this region, by including an end-winding vibration monitoring module additional information is provided. Combining information from all the modules in a synchronised manner allows for correlation and check for plausibility of different effects, see Stephan *et al.* (2003).

## 14.4 Fuzzy logic

To some engineers, the health condition signatures described previously in this book may imply that CM could be carried out in an unambiguous manner. But this is unfortunately not usually realistic in practice. Taking stator winding shorted turn fault in an induction motor as an example, an obvious signature would be the negative sequence component in the input current, or acoustic vibration measured on the motor frame. Assuming a balanced voltage supply and perfect manufacturing of the machine, such signals can be confidently associated with the stator winding fault as described in Chapter 9. However, supply imbalance and manufacturing imperfections always exist; a brand new machine will inevitably show some negative sequence current and vibration. Unless we have already defined the threshold values, the information we acquire could be better described as 'negative sequence current quite large'. The condition of the machine that is being monitored can therefore also be described in a linguistic manner. For instance, the machine is not necessarily 'good' or 'bad', but may fall into some intermediate range, fuzzy logic is therefore suitable in such cases.

In fuzzy logic, input signals for CM are associated with certain membership functions. A membership function allows a quantity to be associated with a linguistic variable to a certain degree of truth or confidence. For example, Figure 14.6

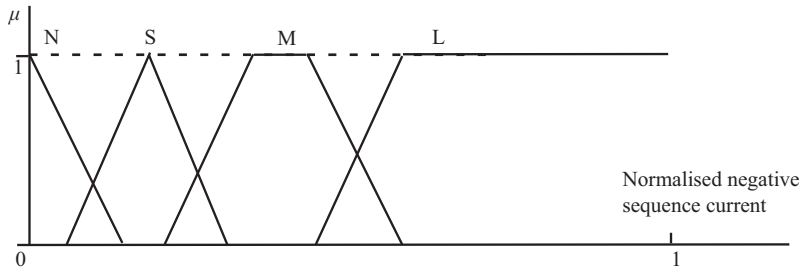


*Figure 14.6 Illustration of membership functions for induction motor negative sequence current*

shows membership functions for the negative sequence current measured on an induction motor that is running in the steady state. The horizontal axis is the negative sequence current normalised to the rated current. The vertical axis indicates how the negative sequence current is associated to four linguistic variables denoted as 'negligible (N)', 'small (S)', 'medium (M)' or 'large (L)'. Therefore, four membership functions are proposed.

In Boolean logic, the current would be judged either 'true' or 'false' with respect to any of the linguistic variables. But in fuzzy logic, such a concept is extended to allow the current to be associated with these linguistic variables to any degree between 0 (fully false) and 1 (fully true). The same input value is mapped to more than one membership functions, implying that different statements can be simultaneously true but to different degrees of truth. For example, a negative sequence current may be judged as 'medium' by a degree of 0.6 while at the same time as 'large' by a degree of 0.3. It is also considered not being 'negligible' or 'small' if the corresponding membership function values are zero. Other input signals, for example, negative sequence supply voltage, can also be represented in this way, as fuzzy sets by means of membership functions.

Different membership function shapes can be chosen. Obviously, the construction of the membership functions requires significant insight into the physical meaning of the signals and the linguistic variables selected. Practical experience and experiments in the laboratory or industrial environments are usually the only way to gain such insight, see Benbouzid *et al.* (2001). However, there is no doubt that fuzzy logic does provide an alternative and powerful tool of information representation and processing.

Associating input signals with membership functions is called fuzzification. The power of fuzzy logic is more evident during the operation and inference stages, which derive new results which then progressively provide more precise information about the actual machine condition. As in Boolean logic, basic fuzzy logic operation includes 'AND', 'OR' and 'NOT'. But instead of producing 'true' or 'false' as an outcome, fuzzy logic operations result in a degree value (between 0 and 1) to which the combined statement of the logic operation is true. For example, consider the two statements:

- A: motor negative sequence current is 'small' with a membership function value of 0.7,
- B: negative sequence supply voltage is 'negligible' with a membership function value of 0.5.

One way to define a fuzzy logic 'AND' operation is to use the smaller value of the involved membership functions. Therefore, the degree of the following statement being true is 0.5.

(A) AND (B): (negative sequence current is 'small') and (negative sequence voltage is 'negligible')

A fuzzy logic 'OR' operation may be similarly defined by using the maximum (greater) membership function value while fuzzy logic 'NOT' operation may be defined as $1 - \mu$, where $\mu$ is the membership function value of the operand statement involved.

Fuzzy inference is applied to the statements, with or without fuzzy logic operators, to imply the degree to which a consequent statement is supportable. This usually takes the form of 'If-Then' rules. For example, one of the many rules that could be used in a CM system for stator winding shorted turn fault detection could be expressed as:

Rule (i): If [(negative sequence current is 'small') and (negative sequence voltage is 'negligible')] Then (shorted turn fault is present)

Because the condition or antecedent of this rule is not 100% true, the output statement, which is also linguistic, is not 100% true either. For the output statement, we are not particularly interested in the extent to which it is true. What it means to the actual machine condition is of more importance. We apply a procedure called fuzzy implication for this purpose. The process is illustrated in Figure 14.7. In the final plot, the horizontal axis is fault severity, e.g. a measure of inter-turn resistance during fault development, which may be normalised. It may be considered that the shaded area represents a probabilistic distribution of the fault severity.

There may be several rules associated with the same output statement and a CM system may have several output statements regarding the machine condition. For instance, another rule output statement could be 'shorted turn fault is serious', while the input signals are also associated with different membership functions.

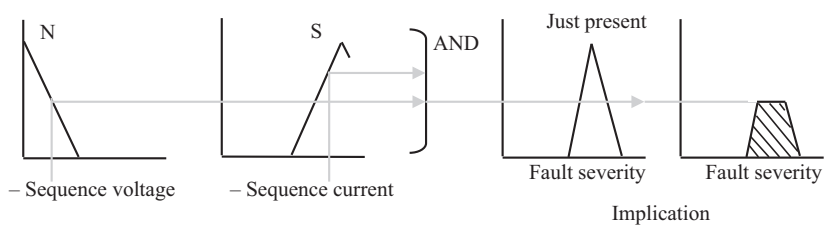


*Figure 14.7 Illustration of application of fuzzy inference to negative sequence current caused by an induction motor winding fault*

All rules are scanned by a fuzzy logic inference engine, generating the corresponding output implications which are aggregated to form a single overall fuzzy set regarding the shorted turn fault severity. The order of all the rules being executed does not matter, since the aggregation procedure should always be commutative.

Three ways of aggregation are commonly applied to the output implications of all the rules: maximum selection, probabilistic OR i.e. $a + b - ab$, and summation. Weighting factors can be introduced to reflect the relative importance of each rule. A de-fuzzification procedure can then be used to obtain a single normalised index for the particular fault severity that is being monitored. One way is to calculate the centroid of the aggregated overall distribution.

Caldara *et al.* (1997) describe a fuzzy diagnostic system for a linear induction motor drive, the expert system having a configuration outlined in Figure 14.8.

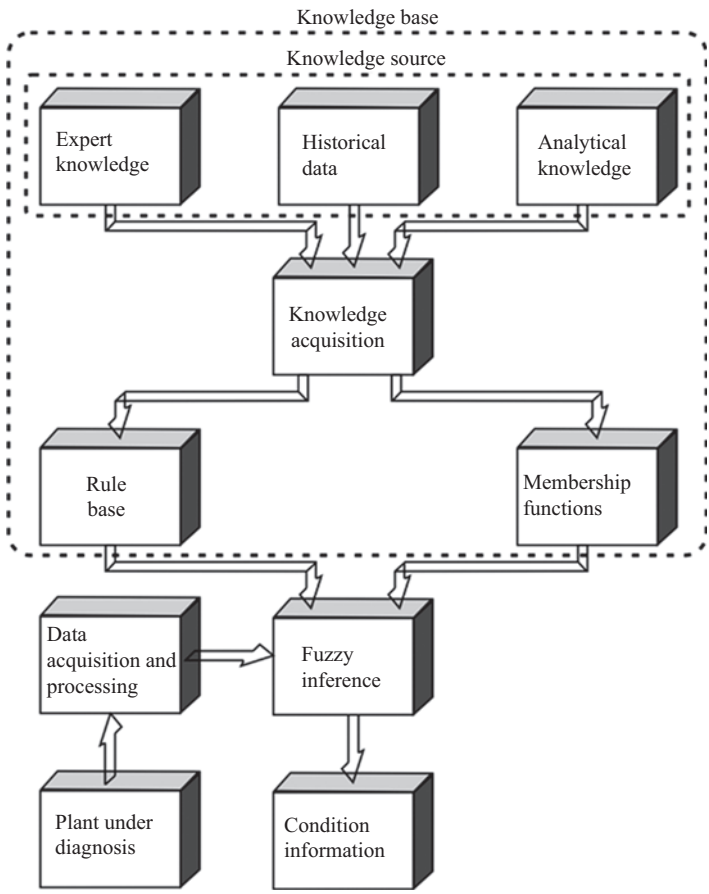


*Figure 14.8 Block diagram of a fuzzy diagnostic system*

## 14.5 Machine learning using ANNs

### *14.5.1 What can be learned for CM?*

Machine learning, as a subset of AI, is to acquire knowledge by using pattern recognition and inference with as little human intervention as possible. In CM of electrical motors or generators, the targeted knowledge generally includes that in two related aspects:

- Extraction of measurement features or signatures, and derivation of a quantitative relationship between the health condition and such signatures,
- Understanding of electrical machine degradation dynamics and health condition as affected by in-service stresses and the health condition itself.

Such knowledge could be obtained from experimental or operational data, and machine learning is to establish algorithms for this purpose. An adequate number of data samples need to be available to facilitate the learning process. In most cases, the data size can be increased by aggregating electrical machines of the same design in similar fleets, for example, the electrical generators in different wind farms.

A difficulty is to define the machine condition. An unhealthy condition could be set according to events occurred in the past, see Qiu *et al.* (2015). But ultimately it should be defined based on the remaining useful lifetime, RUL, Krummenacher *et al.* (2018), that is the second aspect of machine learning listed above. In many cases, the measured signature itself contains information about the remaining useful life as shown in Figure 14.9, taking a single dimension of the health condition and a single condition signature as example.

It is a general phenomenon that as the system or component ages, the rate of degradation also increases under the same operating condition. This is implied in the empirical laws of the physics-of-failure, such as the Arrhenius rate law, see Lai *et al.* (2016), which states that the rate of a chemical reaction process, $k$ driven

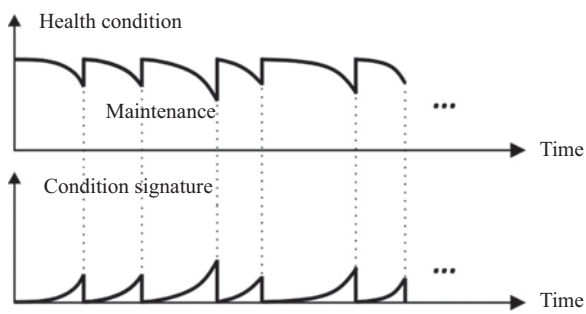


*Figure 14.9 Health condition and condition signature changes between maintenance cycles*

by temperature, increases with the temperature $T$ according to an exponential relationship:

$$k = Ae^{-E_a/RT} \tag{14.1}$$

where $A$ is a constant, $E_a$ the activation energy and $R$ the ideal gas constant.

This is directly relevant to insulation degradation in electrical machines because dielectric loss usually increases and heat dissipation reduces as the insulation degrades, leading to a rise of temperature. Other degradation, for example, rotor eccentricity, also tends to exacerbate the relevant ageing mechanisms through e.g. unbalanced magnetic pull, see Dorrell (2011).

Based on such understanding about the significance of measured condition signatures, particularly their rates of change with respect to time and in-service duties, the condition of the electrical machine in the corresponding aspect can be assigned a seriousness value, for example:

- Healthy condition, no degradation,
- Minor degradation which requires occasional attention, long RUL,
- Modest degradation which requires continuous attention, modest RUL,
- Serious degradation which requires close attention, short RUL,
- Very serious degradation which requires immediate action, virtually no RUL.

### *14.5.2 Supervised learning through ANN*

ANNs have been used for many different applications, and have become the most widely used tool in machine learning in general. The results of signal processing and fuzzy logic operations can be used as the input to the ANN. The output can often be a direct estimate of the remaining useful life of the component or electrical machine being monitored, under its in-service stresses, as defined above. In recent years, ANN has also been used for feature extraction from the raw transducer data as a time series, see Krummenacher *et al.* (2018). This reduces the need for traditional signal processing, to some extent.

The feature of ANNs that is attractive in CM is their capability of representing complicated, nonlinear relationships through a large number of simple and identical algebraic operations. Of all neural network structures, the multi-layered perceptron (MLP), trained using the back-propagation (BP) algorithm, is one of the earliest and perhaps most widely used. MLP training can be viewed as a gradient descent optimisation and therefore, to analysts, it possesses a high degree of credibility, although the local minimum problem needs to be dealt with during the training process, see Penman *et al.* (1994).

Figure 14.10 shows an MLP network that was used in an early development by to detect the number of broken rotor bars in induction motors, see Filipetti *et al.* (1995). The network consists of an input layer that accepts six signals:

- Slip ($s$, no unit),
- Slip as a ratio to the rated slip ($s/s_r$, no unit),

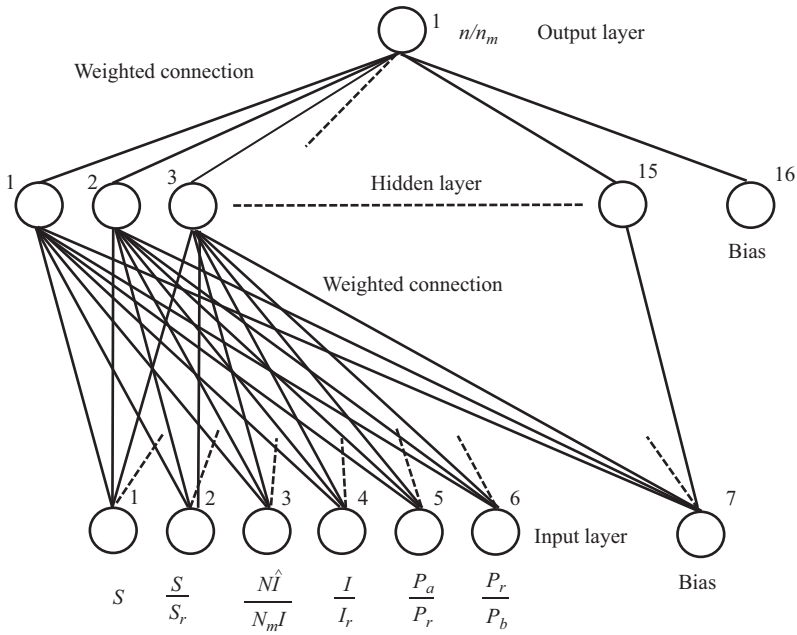


*Figure 14.10 A neural network structure for broken rotor bar detection*

- A quantity dependent on the $(1-2s)f$ current $\widehat{I}$: $(N\widehat{I})/(N_m I)$, where $I$ is the fundamental current and $N$ the total number of rotor bars that is normalised to a maximum bar number, say $N_m = 100$,
- Fundamental current $I$ as a ratio to the rated current $I_r$,
- Input power $P_a$ as a ratio to the rated power $P_r$ and finally,
- Rated power $P_r$ as a ratio to a selected base power $P_b$, say $P_b = 100\,\text{kW}$.

Above the input layer is a hidden layer of 15 neurons which perform the same algebraic operation. Setting the number of hidden neurons is empirical and often requires 'trial and error' iterations. One common nonlinear function that is performed by the hidden neurons is the sigmoid 'squashing' function and the output of each hidden neuron is calculated as:

$$F(x_i) = \frac{1}{1+e^{-x_i}},\ i = 1,\ 2, \ldots, 15 \tag{14.2}$$

where $x_i = \sum_{j=1}^{7} w_{ij} u_j$ is the weighted summation of all the input signals towards the hidden neuron $i$. $w_{ij}$ represents the weight from input $j$ to hidden neuron $i$, and $u_j, j = 1,\ 2, \ldots, 7$, represents the inputs.

This neural network also has an output layer consisting of only one neuron, which calculates for an estimation for the number of broken bars as a ratio to a maximum broken bars number, which was arbitrarily set to $n_m = 10$. The calculation is based on the same function as (14.2) and there are also weighting gains

from the hidden neurons to the output neuron. In Figure 14.10, there are two bias nodes which affect the hidden and output neurons directly. The bias nodes can be manually set for calibration purposes.

In order for a neural network, so structured, to have the intelligence that we wish, it must go through a learning process. This is to find proper values for the weights in the connections. This requires data from practical recording, experiments or detailed simulation models which can represent machine defects with high fidelity. The learning process of an MLP network, like the above, usually requires supervision in which the data are all labelled, i.e. the meaning of the output is explicitly stated, as described in sub-section 14.4.1. In this case, the number of broken rotor bars is always known in the data set. In other words, the desired output for a given input pattern should be explicitly stated in the learning process. The data set should cover both the normal and fault conditions the neural network will encounter. The weights are adjusted in the learning process until the error is minimised. A typical fitting error function is the sum-of-squared error as shown below, where $N_{\text{data}}$ is the total number of input–output pairs in the data set to be learned.

$$\text{Error} = \sum_{i=1}^{N_{\text{data}}} \{\text{Output}_{\text{calculated}} - \text{Output}_{\text{desired}}\}^2 \tag{14.3}$$

A way of adjusting the weights is to use the back-propagation (BP) training algorithm detailed by many authors including Halpin *et al.* (1997). In this algorithm, the error regarding the final output of the neural network is used to modify the weights based on a sensitivity-like principle. How quickly the weights can be modified is controlled by the two parameters: the learning rate and momentum, which can help avoid a local minimum problem or aid convergence. The weights closest to the output layer are modified first and the error is gradually propagated

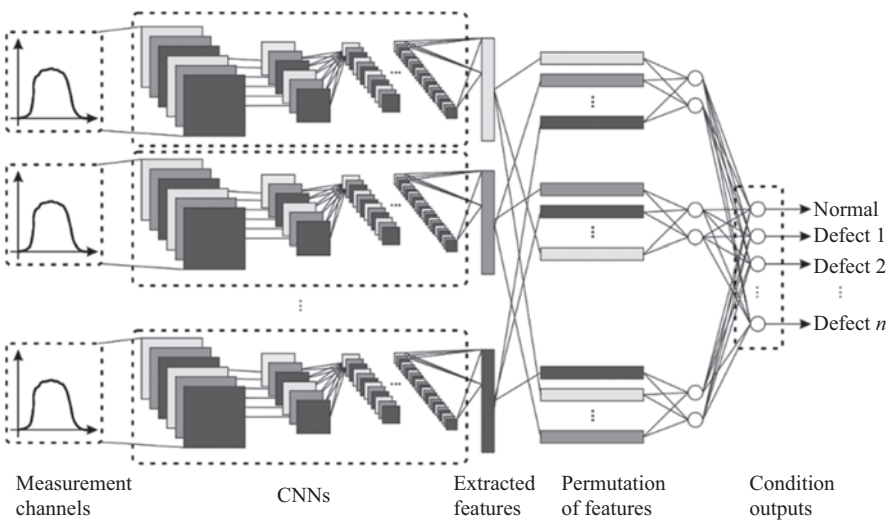


*Figure 14.11 Structure of a multi-channel neural network system for CM*

back towards the input layer to modify other weights. The procedure is iterated until the overall error defined in (14.3) is minimised.

This is for one failure mechanism. In an electrical machine, several failure mechanisms could co-exist and progress simultaneously. Figure 14.11 shows a system of multiple ANNs working together to provide monitoring and prognosis, see Krummenacher *et al.* (2018). Returning to our analogy of medicine, examination of a patient usually includes different parts of the body. In the structure shown in Figure 14.11, different ANNs, which are multi-layer convolutional neural network (CNN) type, Sze *et al.* (2017), and will pick up symptoms of different failure mechanisms that can also be cross-coupled. Therefore, the features extracted from each measurement by a CNN, e.g. temperature, vibration or current, are then treated together by another downstream neural network to analyse the cross-coupling between these failure mechanisms. Each network, CNN or MLP network at the output stage, can be trained individually.

### *14.5.3 Unsupervised learning*

A neural network can also learn unsupervised, see Penman *et al.* (1994). Unsupervised learning, compared to supervised system, provides a significantly different neural network approach to identification of abnormal conditions. The system can proceed through the learning stage without provision of classifications for each input set of data, whereas the connection weight adaptation in the MLP network is driven precisely by just such knowledge. The possibility of training a network on a set of data , with no labelled inputs and outputs or only a fraction of which are labelled clearly, offers significant advantages for electrical machine systems in unfamiliar environments with unclear ageing-to-failure mechanisms, such as renewal energy systems in early deployment stages. However, to interpret such outputs and use them for classification, knowledge of the training data set is still required. Nevertheless, unsupervised networks require fewer training iterations, since they do not require exact optimisation for their decision-making.

The unsupervised network implementation described here is based on the well-known Kohonen feature map, presented in the 1980s, derived from observation of the human brain cerebral cortex fine structure, and created during algorithm learning which promotes self-organisation. Kohonen's algorithm mimics such processes. It creates a vector quantiser by adjusting the weights from common input nodes to the output nodes, which are arranged in a two-dimensional grid like network, as shown in Figure 14.12. Such a map is usually from a higher-dimensional input space into a low-dimensional output space.

As shown in Figure 14.12, $n$ inputs $x_1, x_2, \ldots, x_n$ are mapped onto $m$ output nodes $y_1, y_2, \ldots, y_m$ which have been arranged in a matrix, for example, dimensioned $5 \times 5$. Each input unit $i$ is connected to an output unit $j$ through weight $w_{ij}$. The continuous valued input patterns and connection weights will give the output node $j$ continuous-valued activation value $A_j$:

$$A_j = \sum_{i=1}^{n} w_{ij} x_i = W_j X \tag{14.4}$$

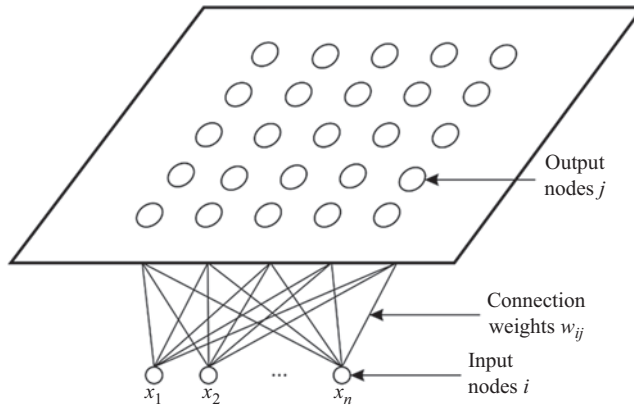


*Figure 14.12 Structure of a self-organising feature map*

where $X = [x_1, x_2, \ldots, x_n]$ is the input vector and $W_j = [w_{1j}, w_{2j}, \ldots, w_{nj}]^T$ is the connection vector for output node $j$.

A competitive learning rule is used, choosing the winner $c$ as the output node with weight vector closest to the present input pattern vector:

$$\|X - W_c\| = \min_j \|X - W_j\| \tag{14.5}$$

where $\|\|$ denotes the Euclidean distance, or norm between the two vectors. Both the input and connection vectors are normalised.

It is noted that the data presented for the learning purpose consist only of inputs not outputs. When an input pattern is presented to the neural network without specifying the desired output, the learning process will find a winning output node $c$ according to (14.5), and subsequently updates the weights associated with the winning node and its adjacent nodes. The weights are updated in such a way so that if the same input is presented to the network again immediately afterwards, the winning output node will still fall into the same neighbourhood of the output node picked up earlier, and with an even greater winning margin when (14.5) is used to select the winning node this time. In other words, the feature of the input pattern is enhanced by updating the corresponding connection weights. A typical learning rule is:

$$\begin{cases} \Delta w_{ij}^{(k)} = \alpha^{(k)} \left[ x_i^{(k)} - w_{ij}^{(k)} \right] \\ w_{ij}^{(k+1)} = w_{ij}^{(k)} + \Delta w_{ij}^{(k)} \end{cases}, \; j \in N_c \tag{14.6}$$

where superscript $k$ denotes the number of the input pattern presented for learning. $N_c$ denotes the neighbourhood around the winning node $c$ with respect to the present input pattern. $\alpha^{(k)}$ is the learning rate that is used in this step of learning.

As more input patterns are presented for the network to learn, the learning rate gradually decreases to guarantee convergence. The initial weights can be randomly

set, but normalised, and the input patterns can be iteratively used with several repetitions until convergence is reached. After training, each output node is associated with a fixed set of weights, that is, $W_j = [w_{1j},\ w_{2j},\ \ldots, w_{nj}]^T$. Each input pattern can then be measured for its distance to all the output nodes. Similar input patterns will show relatively short distances to the same output nodes that are already grouped in the output space. The features of the input patterns are consequently identified. The structure and the learning scheme of the neural network give rise to its ability of self-organising mapping (SOM), Sze *et al.* (2017).

Penman *et al.* (1994) describe the details of the construction and learning process of such networks for CM of induction motors. Figure 14.13 shows the vibration signal feature maps for three machine conditions:

- Normal,
- Unbalanced supply,
- Mechanical looseness of frame mounting.

In each case, the input to the neural network is a large number of vibration components obtained from accelerometer output FFTs. These components are then used to calculate the distances from this input pattern to all of the 20 × 20 output nodes and the results are shown in Figure 14.13. The ground plane of which represents the 20 × 20 output node space and the vertical axis indicates the distance calculated. It can be clearly seen that the three conditions give distinctively different feature maps. Of course, the physical meanings of such maps depend on further knowledge that has not been embedded in the training process.

## 14.6 Deep learning with big data

The concept of deep learning was introduced to capture complex relationships from large amounts of data, which are usually subject to random noise. It would be necessary, in a conventional ANN, to create many hidden layers each with many neurons. It is therefore more appropriate to first extract a relatively small number of features from the big data set, and the features are then used to derive CM information such as the remaining useful life (RUL). Deutsch *et al.* (2018) documented

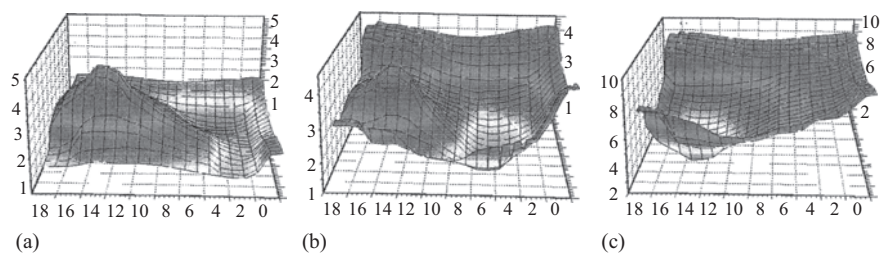


*Figure 14.13 Kohonen feature map of machine conditions: (a) normal; (b) unbalanced supply and (c) mechanical looseness*

the details of such an approach and the following outlines the main aspects and steps.

Deep learning was stimulated by the introduction of a deep belief network (DBN), Hinton *et al.* (2006), which was proposed to permit training of the aforementioned complex network, one layer at a time.

A DBN consists in general of several layers of a restricted-Boltzmann-machine (RBM) which are stacked together, as shown in Figure 14.14 with two RBMs. Each RBM has a visible layer and a hidden layer, while the hidden layer becomes the visible layer of the RBM above it. The visible layer of the bottom RBM is used to input the original data with random errors. The hidden layer of the top-most RBM represents the most distinctive features extracted from the input data. As the data information is passed from the bottom towards the top, the features are gradually extracted.

This is usually unsupervised learning, which is built in the dynamic training of each RBM. As new input data continuously come in during operation, the outcome of the training process, that is, the weights ($w$) and biases ($a$ and $b$) in the RBM are updated. The weights are bidirectional, that is, $w_{ij} = w_{ji}$, where $i$ indexes nodes/neurons in the visible layer and $j$ indexes the nodes/neurons in the hidden layer.

At each time-step, the training is conducted from one RBM to the next above it, with all the RBMs forming the DBN. For any of the RBM, the ability of unsupervised learning is due to the objective function of training, which is to maximise the probability that the RBM assigns to the visible (input) vector $v$:

$$P(v) = \frac{1}{Z}\sum\nolimits_h e^{-E(v,h)} \tag{14.7}$$

where $Z$ is the normalisation constant which is the sum of the possible pairs of visible and hidden vectors:

$$Z = \sum\nolimits_v \sum\nolimits_h e^{-E(v,h)} \tag{14.8}$$

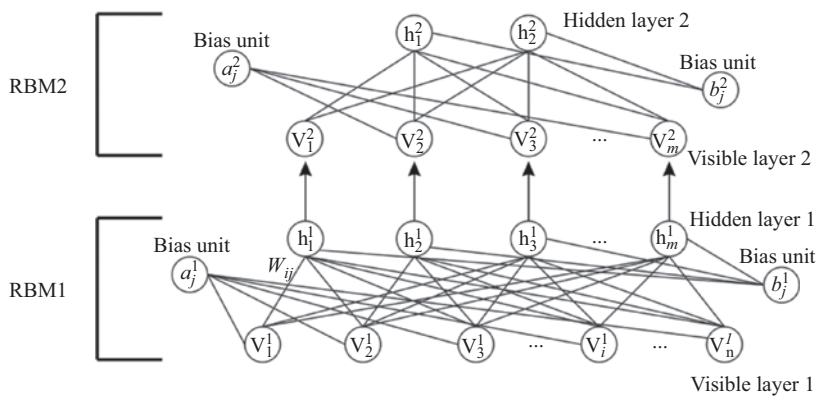


*Figure 14.14 A DBN with two restricted-Boltzmann-machines*

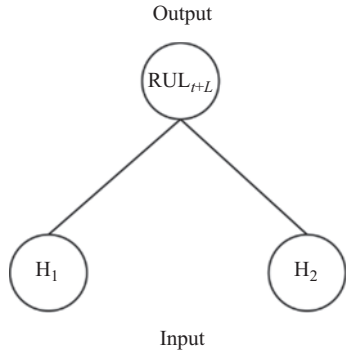


*Figure 14.15 A feed-forward network to predict CM output using the features extracted by the DBN*

and the energy function of the combination $(v, h)$ is:

$$E(v, h) = -a^T v - b^T h - v^T wh \tag{14.9}$$

Finally, the features extracted at the top of the DBN are used to drive a conventional two layer feedforward ANN to indicate the health condition – such as the predicted RUL, as shown in Figure 14.15 which can be trained using back-propagation.

The number of neurons in each RBM layer and the number of RBMs in the DBN are matters of arbitrary selection. But as long as the network is adequately dimensioned, it can handle complicated relationship mined in big data.

Deutsch *et al.* (2018) have shown the use of such networks to predict the remaining useful life of gears and bearings.

## 14.7 An AI example

### *14.7.1 Systems incorporating AI*

The following section has been contributed by Geoff Walker of Faraday Predictive to give an example of how AI is beginning to influence the CM of electrical machines, in particular Model-based voltage and current (MBVI) systems.

MBVI includes devices such as the Bently Nevada AnomAlert, the Artesis motor condition monitor (MCM) and the Faraday Predictive S200, which all incorporate AI techniques. These systems work on the same underlying principles as MCSA, see Chapter 9, relying on the fact that machine current is distorted by a wide range of phenomena affecting the motor and driven equipment system but incorporate AI techniques.

The added dimension brought by MBVI systems is that the analysis is done on the basis only of current waveform distortions, not generated by voltage waveform distortions, and therefore must be caused by phenomena within the motor and/or driven equipment.

In a situation where the supply voltage is perfectly sinusoidal, all distortions in the current waveform must come from phenomena within the motor and driven equipment system, but in most real-world power supplies, the supply voltage is itself distorted to some degree. This is particularly true for inverter driven equipment, where the voltage waveform can be highly distorted. Figure 14.16 below shows two figures demonstrating how far from a sinusoidal shape the voltage waveforms can look in industrial situations. The first, Figure 14.16(a),

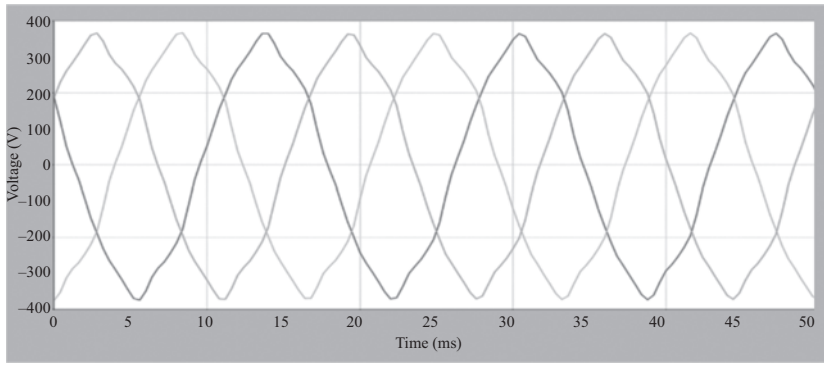


(a)

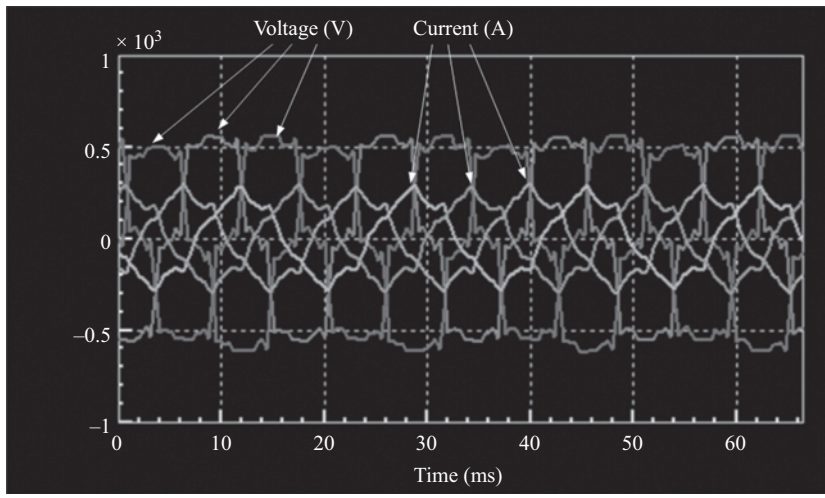


(b)

*Figure 14.16 Practical three phase voltage and current traces from rotating machines: (a) distorted mains voltage waveform from a North Sea oil platform and (b) distorted mains voltage and current waveforms from an inverter-fed motor-driven water pump showing severe distortion*

is the voltage trace from a North Sea oil platform, and shows the voltage profile that would be experienced by all the supplied equipment. It is clearly a long way from a pure sinusoid, and contains a significant level of other harmonic components.

The second trace, Figure 14.16(b), is of the voltage and current measured in the feed from an inverter-fed motor driving water pump, which clearly shows an enormous amount of distortion. Carrying out a straight frequency analysis of this current waveform, as would be done in a conventional MCSA process, will show up huge peaks at many frequencies, and would suggest all sorts of problems with the motor, whereas in reality the distortions to the current waveform have mainly arisen from the distorted voltage and do not indicate any faults in the rotating equipment.

### *14.7.2 How an MBVI system works*

Separating the effects of voltage distortions is done by creating a mathematical model of the relationship between voltage and current, and then using this to predict the expected current for the given shape of voltage waveform, as shown in Figure 14.17. The difference between measured and predicted current, the residual current, is then analysed for frequency components in a manner analogous to vibration analysis. The resulting spectrum can then be analysed to match observed frequencies against characteristic equipment frequencies.

MBVI systems can either be portable, for periodic testing, such as the Faraday Predictive P100, Figure 14.18(a), or be permanently installed CM systems such as the Faraday Predictive S200, Figure 14.18(b).

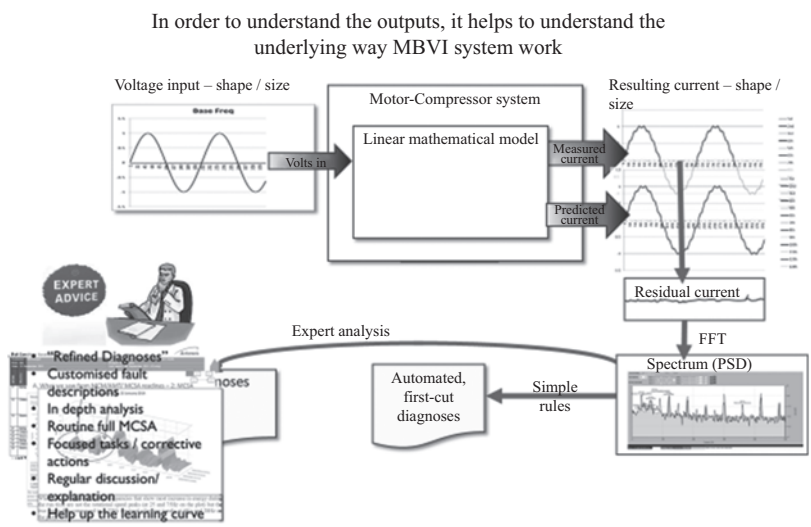


*Figure 14.17 Process for removing voltage distortion and analysing residual current spectral features*

*Figure 14.18 Examples of MBVI systems: (a) a complete portable system and (b) a permanently installed system*

Either system generally measures both voltage and current on all three phases. The installation of the equipment is generally done at the machine switch-gear, typically in a clean, dry, accessible switch-room. As a result, the system is invulnerable to dirt, flammable atmospheres or risk of damage during maintenance work. Permanently installed systems monitor the condition of the equipment around the clock and communicate continuously with software. They display the current state of the equipment, together with alarms if an unacceptable condition is reached and trend graphs to display the rate of deterioration. Typical systems can give an automated diagnosis at the level of unbalance, misalignment, bearing problems, rotor and stator problems based on the location of spectral peaks. They are also able to give direct electrical outputs such as rms current and voltage, active power, power factor, current balance, voltage balance, total harmonic distortion and the levels of harmonic distortion at individual odd harmonics up to thirteenth. In addition, they typically provide outputs with an overall assessment of the condition of the equipment and the electrical supply.

### *14.7.3 An MBVI system and AI*

Despite only measuring voltage and current drawn by the motor, MBVI systems are able to detect a wide range of mechanical and operational factors in the driven equipment as well as the motor mechanical and electrical behaviour.

The diagnostic process can use a number of steps that can be regarded as AI, including automated mathematical model building, machine learning and rules-based reasoning. Further developments in the use of machine learning using neural networks are expected to give more precise diagnostic capability, and the ability to compare the behaviour of one item of equipment against an individually tailored group of similar equipment.

The diagnosis and trending functionality is comparable to vibration monitoring, and the same rules apply to the frequencies at which faults show up – for example, unbalance will show up at $1\times$ rotational speed, vane passing will show up at the appropriate multiple of $n\times$ rotational speed, where $n$ is the number of vanes, and bearing features will show up at exactly the same characteristic frequencies as would be seen by vibration monitoring, see the Table in Figure 14.19.

The signals detected by MBVI systems are not identical to those detected by vibration systems, since the motor current is sensitive to torsional signals, whereas vibration detects radial signals or axial signals, depending on sensor orientation. This makes MBVI systems less sensitive than vibration to unbalance, but more sensitive to things like internal deterioration in centrifugal pumps, affecting internal flow patterns. MBVI systems also seem to be more sensitive than accelerometers to journal bearing features and rubbing behaviour. They are particularly good at picking up belt drive signals.

Because torsional signals are un-attenuated along a rotating shaft, MBVI systems can detect phenomena at the far end of long shafts. So, for example, in the case of a vertical axis centrifugal pump with a long shaft, where the pump is mounted at the bottom of a liquid reservoir and motor mounted at the top in a dry location, many meters above, MBVI can still clearly detect phenomena all the way along the shaft from within the pump. This makes them particularly suitable for

| Feature | Accelerometer sensitivity | Motor sensitivity | Comments |
|---|---|---|---|
| Unbalance | ● | ◐ | |
| Misalignment | ● | ● | |
| Looseness | ◐ | ◕ | |
| Rubbing | ◐ | ● | Integer sub-harmonics |
| Rolling element bearings | ● | ● | |
| Journal bearings | ◐ | ◕ | |
| Flow turbulence | ◔ | ◕ | |
| Cavitation | ◕ | ◐ | |
| Internal corrosion | ○ | ◐ | |
| Belt drives | ◔ | ● | |

The motor outputs are generally MORE sensitive to torsional signals and LESS sensitive to radial signals than conventional accelerometers.

They are surprisingly sensitive to both journal bearing phenomena and REB phenomena.

***And of course also provide info on electrical phenomena***

*Figure 14.19 MBVI systems identify similar phenomena to accelerometers*

submerged or bore-hole pumps, where accelerometer mounting can be difficult and expensive.

Virtually all of these systems also have the capability to provide full MCSA analysis, producing the outputs of similar format, with the same guidelines on acceptability, in terms of decibels difference between fundamental and pole-pass frequency.

## 14.8 Conclusions

The techniques of AI have been potentially valuable for the CM of electrical machines, because the underlying physics of machine operation and dynamics is so rich in fundamental rules, see Chapters 8 and 9, and these can be exploited by an expert system.

This chapter has shown that these techniques could be used to improve the signal-to-noise ratio in a fault situation, particularly in the complex area of monitoring terminal 'performance' conditions and the difficult sub-set of that, the detection and measurement of PD activity.

An abiding lesson from this chapter is to understand the importance in CM of relating various monitoring signals with one another, what was described in the first edition of this text as multi-parameter monitoring. It is clear, however, that the future of machine CM will be heavily affected by multi-parameter monitoring and by the application of AI to that process.

The chapter has outlined three AI techniques, which could improve the electrical machines CM:

- Expert systems,
- Fuzzy logic,
- ANNs also extended to include deep learning from big data to un-mine the information in complex relationships.

An example of the use of AI in electrical machine CM is set out in this chapter using model-based voltage and current (MBVI) systems.

These AI techniques must be the future trend for CM electrical machines, especially in environments where machines are being incorporated into VSD systems, rich in data, and being applied to integrated engineering systems, in high integrity environments, such as electric vehicles, rail traction and ship propulsion.

Perhaps the best outcome for AI would be if it could use data to close the loop between monitoring a machine and deriving its reliability, relating measurements directly to failure rate, availability and asset management. Some of the largest installations with the potential to make that like are our distributed and expanding renewable energy generation assets, such as wind and tidal power farms.

*This page intentionally left blank*

*Chapter 15*

# Safety, training and qualification

## 15.1 Introduction

This book is mainly concerned the science and technology of electrical machine CM. However, since our first edition, this has now become a significant industry in support of our use of electrical machinery for generation and general plant.

As the appendices show there are now international standards applicable to CM of electrical machinery, although these are still in early stages of development. Consequently, industry is demanding a level of expertise from its CM operatives commensurate with the importance of the task in hand. Therefore, this final chapter briefly summarises the safety, training and qualifications that should be expected of staff undertaking CM.

They may not need to be experts in electrical machinery but must be safe and competent in the operation of monitoring equipment and in the recording and accurate presentation of the information that arises from it, if their work is to make a sound contribution to condition-based maintenance and asset management.

## 15.2 Safety

When planning and undertaking CM activities on electrical machines regardless of whether these activities are intrusive or non-intrusive, there are three key human areas that should be considered, summarised in Figure 15.1, and there are three overarching risks:

- Risk of injury and or long-term illness to person(s) undertaking the CM activity,
- Risk of damage to the plant or equipment subject to the CM activity,
- Risk of damage to the CM equipment being used.

Failure to address the hazards and associated risks of a specific CM activity could potentially result in harm to people, damage to plant or equipment, business interruption, organisational reputational damage and damage to CM equipment and the subsequent costs for repair or replacement.

The hazards presented to persons undertaking CM activities fall into two categories:

- General safety hazards, associated with the working area and environment, e.g. slips, trips and falls, vehicle movements, working at height, working outside and lone working,

*Figure 15.1 The main safety risks in carrying out electrical machine CM*

- System derived hazards, associated with the process, e.g. electricity, steam, gas, water, chemicals and stored energy. Most organisations use safe systems of work and working practices to manage risks to persons from both general safety and system derived hazards. Safe systems of work can encompass training and competence requirements, requirements for risk assessments and method statements prior to work, setting to work procedures, application of safety rules for isolation and subsequent work or testing of plant items and returning equipment to service procedures. It is recommended that electrical CM tasks are planned and undertaken in accordance with a suitable safe system of work.

Through inappropriate application or incorrect set-up of electrical CM equipment, it is possible to damage plant or equipment subject to the activity.

This risk exists predominantly when the tool or technique applied is intrusive, for example the injection of excessive current or voltage into a piece of electrical equipment can lead to component, conductor or electrical insulation system damage.

Similarly, it may also be possible to damage the CM equipment through incorrect application or set-up, for example undertaking a voltage measurement with equipment that is not rated for that voltage.

It is therefore essential that prior to undertaking a CM activity, the specific application is assessed and deemed appropriate. Plant or equipment under test and the test equipment must be suitably rated for the activity. When setting up the monitoring equipment, test connections and test settings, for example, injection voltages in insulation resistance tests should be checked and confirmed as correct. The function of any in-built protection measures, such as overloads, should also be confirmed operational prior to commencing. For more complex CM activities the preparation of a step-by-step procedure, detailing the specific equipment connections, settings and test durations may be appropriate.

## 15.3 Training and qualification

There are as yet no standards for training and qualification of operatives for CM of electrical machines and drives, however there are well-developed standards for vibration and MCSA monitoring, see the list at the end of the book.

A categorisation, from ISO 18436 Part 2, of the training and qualifications required for vibration monitoring, would be instructive for any prospective standard on CM of electrical machines and drives training and qualification, as follows.

### *15.3.1 Training and qualification categories*

Individuals recognised or certified for vibration monitoring should be classified in one of four categories depending upon their qualifications. They shall have demonstrated competence in the concepts of machinery vibration CM and diagnostics of machines for their classification as described in the following sections of ascending competence.

### *15.3.2 Category I – data collector*

Individuals meeting the requirements for Category I are recognised as being qualified to perform a range of simple single-channel machinery vibration CM and diagnostics of machines activities in accordance with ISO 17359 and ISO 13373-1. They should neither be responsible, for example, for the choice of sensor or for any analysis to be conducted, nor for the assessment of test results, except for identifying alert conditions against a pre-established alert setting or settings. They shall be qualified to:

- Operate portable instrumentation on pre-assigned or pre-programmed routes,
- Acquire readings from permanently installed instrumentation,
- Input results into a database and download monitoring routes from a computer,
- Conduct testing under steady-state operating conditions following predefined procedures,
- Be able to recognise that no signal is present,
- Be able to compare overall or single value vibration measurements against pre-established alert settings.

### *15.3.3 Category II – specialist*

Individuals certified to Category II are qualified personnel who are certified to perform industrial machinery vibration measurements and basic vibration analysis using single-channel measurements, with or without phase trigger signals, according to established and recognised procedures. Personnel certified to Category II require all the knowledge and skills expected of Category I and shall also be qualified to:

- Select the appropriate machinery vibration measurement technique,
- Set up instruments for basic resolution of amplitude, frequency and time,
- Perform basic vibration analysis of machinery and components, such as shafts, bearings, gears, fans, pumps and motors, using the spectrum analysis,
- Maintain a database of results and trends,
- Perform basic (single-channel) impact tests to determine the natural frequencies,
- Classify, interpret and evaluate the test results (including acceptance tests) in accordance with applicable specifications and standards,

- Recommend minor corrective actions,
- Understand basic single-plane field balancing concepts,
- Be aware of some of the causes and effects of bad measurement data.

### *15.3.4 Category III – analyst*

Individuals certified to Category III are qualified to perform and/or direct and/or establish programmes for vibration CM and diagnostics of machines in accordance with ISO 17359 and ISO 13373-1. Personnel classified to Category III require all the knowledge and skills expected of personnel classified to Category I and Category II and shall also be qualified to:

- Select the appropriate machinery vibration analysis technique,
- Specify the appropriate vibration instrumentation hardware and software for both portable and permanently installed systems,
- Measure and perform diagnosis of single-channel frequency spectra, as well as time domain plots such as waveforms and orbits, under both steady-state and unsteady-state operating conditions, with or without a phase trigger,
- Establish vibration monitoring programmes, including determination of machines for periodic/continuous monitoring, frequency of testing, route plans,
- Establish programmes for the specification of vibration levels and acceptance criteria for new machinery,
- Measure and analyse the basic operating deflection shapes,
- Understand and be able to direct the use of alternative CM technologies, such as acoustic emission, thermography, motor current and oil analysis,
- Recommend field corrective actions, such as balancing, alignment and replacement of machine parts,
- Be able to use acceleration enveloping or demodulation,
- Perform basic single-plane field balancing,
- Report to management regarding programme objectives, budgets, cost justification and personnel development,
- Prepare reports for appropriate personnel on machine condition, recommend the corrective action and report on the effectiveness of repairs,
- Provide instructions and technical direction to vibration trainees.

### *15.3.5 Category IV – expert*

Individuals certified to Category IV are qualified to perform and/or direct vibration CM and diagnostics of machines in accordance with ISO 17359 and ISO 13373-1 and all types of machinery vibration measurements and analysis. Personnel certified to Category IV require all the knowledge and skills expected of personnel certified to Categories I, II, III and shall also be qualified to:

- Apply vibration theory and techniques, including measurement and interpretation of multi-channel spectral results such as frequency response functions, phase and coherence,

- Understand and perform signal analysis, including understanding of frequency and time domain processing, including orbits and their limitations,
- Determine the natural frequencies, mode shapes and damping of systems, components and assemblies,
- Determine the operating deflection shapes of machines and connected structures and recommend means for correction,
- Use generally recognised advanced techniques for vibration analysis, parameter identification and fault diagnosis,
- Apply the basic principles of rotor-bearing dynamics to vibration diagnosis,
- Conduct basic two-plane field balancing,
- Recommend advanced two-plane influence coefficient or static/couple balancing,
- Recommend corrective actions and/or design modifications, including component change or repair, isolation, damping, change of stiffness and change of mass,
- Provide technical guidance to vibration trainees,
- Interpret and evaluate published ISO codes of practice, International Standards and specifications,
- Recognise vibration caused by gas pulsation in machines such as reciprocating machines and screw compressors, and to measure the necessary parameters and recommend means for correction,
- Recommend corrective actions for resilient mounting and other holding-down and foundation problems.

## 15.4 Conclusions

As the CM industry has developed there has been an increasing interest in standardising the techniques used, see Chapter 14. There has also been interest in developing a standard approach to safety, training and qualification and this is exemplified by the development of guides to carrying out CM tasks, pioneered by the British Institute of Non-Destructive Testing (BINDT), a first draft example of which is shown in Appendix B.

*This page intentionally left blank*

*Chapter 16*

# Overall conclusions

## 16.1 CM techniques

Chapters 1–4 have explained how the interpretation of electrical machine condition must be informed by causality and our view is that an important change in CM over the last 40 years is ensuring that it is firmly directed towards detecting and prognosing real machine failure root causes. In so doing, successful CM directly addresses, at the earliest practicable stage, machine unreliability and, more importantly, gives the operator a prognosis, which can be used to improve availability.

Chapters 2–4 introduced the physics of electrical machines their failure modes and reliability, Chapter 5 dealt with signal processing and instrumentation, Chapters 6–10 dealt with a range of online techniques, Chapter 11 dealt with monitoring variable speed machines whilst Chapter 12 deals with offline techniques.

This book has described the following major monitoring techniques for electrical machines, in the following ascending order of usefulness:

- Shaft voltage or current has been suggested as universal panaceas for comprehensive electrical machine monitoring but have not been proven as reliable CM techniques.
- Shaft flux, current and power signals are capable of detecting faults in both the electrical and mechanical parts of a drive train.
- Shaft flux monitoring is non-invasive, broad bandwidth (5 Hz–20 kHz) and uses a single flux coil sensor, but it is complex to analyse and untested in the field. Little further work has been done on this technology since its inception in the 1980s, therefore it cannot be recommended to operators. However, some new industrial applications, such as traction, electric cars or aerospace, could make it exceptionally appealing because of its ease of fitting and universality.
- Motor speed has been analysed to detect rotor electrical faults, IAS, it is simple and requires a low bandwidth signal (<1 kHz) but has not been widely used by operators.
- Vibration and shock pulse monitoring and analysis are non-invasive but use widely available sensors and broad bandwidth with complex analysis (5 Hz–50 kHz). The precise selection and location of these sensors is very important as they are generally distant from the seat of any defect action and signals maybe attenuated by machine and bearing enclosure responses.

However, because of its wide application on rotating machines in the engineering industry, with a comprehensive set of standards and training procedures, vibration analysis and shock pulse analysis for rolling element bearings have established themselves as reliable and widely accepted techniques for electrical machine operators.

- Chemical and wear analysis have been demonstrated to be effective global monitoring techniques for electrical machines producing narrow bandwidth signals (<1 Hz), but the high cost of the equipment needed and large quantities of data generated by chemical analysis currently confine their application to only the largest electrical machines where such analyses can be processed.
- Electrical discharge activity requires wide bandwidth (up to 10 MHz). PD measurement has shown itself to be the most problematic electrical method of machine insulation CM. It requires special sensors and complex analysis for fault detection. However, it addresses one of the most vital parts of the electrical machine, it can detect global effects, including possibly remanent life of machine insulation, and it does give a long warning before failure. Yet analysis shows that with modern materials the proportion of machine failures due to insulation faults is now less than a third. Furthermore, the detection methods rely on the most advanced signal processing to extract useful indications, which are then open to wide interpretation by PD experts. When applied to the distributed, multi-path, multi-connection, variably stressed insulation system of an electrical machine winding it has a difficult task. Work still continues to develop this method, including AI, particularly to the largest electrical machines, turbo-generators and hydro-generators, to determine overall winding insulation deterioration but that objective has not yet been reached reliably.
- Current monitoring is also non-invasive, but uses existing sensors, requires significant bandwidth (5 Hz–20 kHz) and has established itself, as MCSA, as a reliable and widely-accepted machine monitoring technique for operators. Power monitoring is also non-invasive, uses existing sensors but requires less bandwidth (<10 kHz) and less complex spectral interpretation to detect faults than MCSA, but it is still not widely accepted by operators and thus deserves investigation for future development by operators.
- Temperature detection (°C), a low bandwidth (<0.1 kHz) simple measurement, has repeatedly been shown to be an effective global monitoring technique for electrical machines and is widely used by operators, because temperature limits the withstand capabilities of magnetic and insulation materials, at the heart of electrical machines.

  Temperature rise (ΔK) is particularly valuable because it is directly related to power loss, an important indicator of core and winding fault development.

  Therefore, temperature measurement, both °C and ΔK, should be employed more widely by operators making use of temperature imaging and modern sensor technology such as fibre optics. Experience shows that by tying such measurements to learnt thermal models could make such monitoring much more effective at predicting deterioration and can be linked to CBM.

- Comprehensive monitoring of an electrical machine can be achieved by measuring current, power, vibration, chemical, wear, temperature and PD activity. Together these signals contain inter-related information. We have seen how closely electrical and vibration signals follow one another, although the vibration is attenuated by machine and bearing enclosure responses. The availability of high-quality, digitally sampled, mechanical vibration and electrical terminal 'performance' data from electrical machines opens the way to comprehensive machine and prime mover monitoring. However, these signals require a high data rate and broad bandwidth (up to 50 kHz) for adequate machine analysis, but in VSDs these signals may already be available from the VSD controller.

  Information from these wide bandwidth signals requires complex analysis, which must take account of the inter-relationship between electrical and mechanical signals to accurately detect faults, provide fault prognosis and contribute to CB. This process is still in its infancy, but it is notable that electrical and mechanical signals give more immediate indication of machine damage, whereas chemical, wear and temperature signals integrate damage progression, have a lower bandwidth and are probably closer to the relationship between root cause and failure Mode. This could also benefit from wider bandwidth but fundamental information available from PD.
- Future CM of electrical machines must be oriented more closely towards the detection of known, identified machine failure root causes, including bearing faults. Future research on CM of electrical machines should reflect the above and concentrate more on proving the effectiveness of new techniques on operating plant.

## 16.2 AI and ML

Chapters 13 and 14 have shown that AI and ML are likely to play an increasingly important role in the CM of electrical machines, especially as an increasing number of them are being supplied from VSDs, which already have a rich store of signals being monitored by VSD controllers. This is emphasised by the increasing importance of AI provided data for asset management of capital plant that incorporates large numbers of electrical machines, particularly in the oil and gas, conventional and renewable power generation, metropolitan and high-speed rail, aerospace and ship propulsion industries. However, this book has shown that there are a few important lessons to be learned from experience to date, as follows:

- Application of simple well-understood CM methods, such as MCSA and MBVI, will be employed by many traditional operators and continue to be of importance,
- The availability of a wealth of application of diverse signal analysis, e.g. vibration, IAS, MCSA and MBVI expressions in this book facilitate progress in the direction of multi-parameter monitoring. This has proved very successful in bridging the knowledge gap between operating engineers and managers

to improve the response to monitoring signals and should continue to pave the way to more complex AI,

- Simplistic 'Rule-based' AI methods are more likely to gain application in the initial stages of AI because they are easier for practical engineers and managers to understand,
- Complex 'Neural network' AI methods, while potentially more powerful, maybe difficult to apply because of resistance by practical engineers and managers, in spite of having the potential to deliver more comprehensive results with clearer and longer prognoses,
- Improving management confidence in more complex AI methods to facilitate CBM, LCC and Asset Management techniques applied to electrical machine drives will be of key importance in the future. This will be influenced by the capital value of complex plant and the large potential savings such techniques could deliver. There will be an important need in the future to provide much clearer evidence of the cost and prognosis benefits of these methods,
- The areas where the above techniques, CM, AI and CBM, are likely to be applicable in the emerging technologies of electrical drives in the oil and gas, conventional and renewable power generation, metropolitan and high-speed rail, aerospace and ship propulsion industries, where Asset Management is very important.

## 16.3 Standards, training, safety and qualification

Standards have now been developed for the industry, see Appendix Standards, but training, safety and qualification knowledge in electrical machines CM is, as yet embryonic. Our Chapters 15 and Appendix B aim to improve the knowledge in these areas, which will be essential as we transition to AI methods for CBM and asset management of complex VSD and electrical machine installations in oil and gas, conventional or renewable power generation, metropolitan or high-speed rail, aerospace and ship propulsion industries.

## 16.4 The future importance

AI and ML techniques applied to electrical machine drives will be successful in the future if they exploit the comprehensive signals and fundamental physical rules included in this book in a safe, repeatable and trainable way.

AI and ML techniques should also use multi-parameter monitoring to raise signal-to-noise ratio and increase operator confidence in CM interpretation and will provide powerful interpretive information for machine-drive systems in the future.

PD monitoring has started to use these techniques and MBVI has shown that these methods can be valuable.

At the moment the industry is still in a learning phase but there is a lot that could be done in machine CM, especially in future support of CBM and asset management of plant in high capital value industries.

# References


Hopkinson, J. (1886) Dynamo-Electric Machinery, Philosophical Transactions of the Royal Society, London, UK.

Ward Leonard, H. (1896) Volts vs Ohms, speed regulation of electric motors, Proc AIEE, USA.

Concordia, C. (1908) Synchronous Machines, Theory and Performance, J. Wiley, New York, USA.

de Pistoye, H. (1927) Les pertes parasites aux extrémités du stator des machines à grand pas polaire, et les moyens de les reduire, Revue Générale de l'Eléctricité, France.

Walker, M. (1929) The Diagnosing of Trouble in Electrical Machines, The Library Press, 1st Ed. 1921, reprinted by Longmans, Green & Co, 2nd Ed, London, UK.

Langlois-Berthelot, R. (1949) Étude Électromagnétique Générale des Machines Électriques, Eyolles, Paris, France.

Jordan, H. (1950) Geräuscharme Elektromotoren, Springer Verlag Essen, Germany.

Lim, C. Y. (1951) Characteristics of reluctance motors. Trans IEEE on Power Apparatus & Systems PAS-70(Pt. II): 1971–1978.

Moullin, E. B. (1955) Electro-magnetic Principles of the Dynamo, Oxford, Clarendon Press, UK.

Erdelyi, E., Horvay, G. (1956) Vibration modes of states of induction motors. Trans ASME, Paper A-28: 39–45.

Sen, S. K., Adkins, B. (1956) The application of the frequency-response method to electrical machines, Proc IEE Monograph No. 178.

Hammond, P. (1958) Electromagnetic energy transfer, Proc IEE – Part C: Monographs, 105(8): 352–358.

Carpenter, C. J. (1959) Surface integral methods of calculating force on magnetized iron parts, Proc IEE Monograph No. 342.

Hammond, P. (1959) The calculation of the magnetic field of rotating machines-Part 1: The field of a tubular current, Proc IEE Monograph No. 333.

Ashworth, D. S., Hammond P. (1961) The calculation of the magnetic field of rotating machines-Part 2: The field of turbo-generator end-windings, Proc IEE Paper 3489S: 527–538.

Dimentberg, F. M. (1961) Flexural Vibrations of Rotating Shafts. Butterworths, London, UK.

Khudabashev, K. A. (1961) Effect of turn short-circuits in a turbo generator rotor on its state of vibration, Elekt Stantsii USSR (7): 40–45.

Hammond P. (1962) The calculation of the magnetic field of rotating machines-Part 3: Eddy currents induced in a solid slab by a circular current loop, Proc IEE Monograph No. 514S: 508–515.

Hague, B. (1962) Principles of Electromagnetism Applied to Electrical Machines. Dover, New York, USA.

Swann, S. A. (1963) Effect of rotor eccentricity on the magnetic field of a non-salient pole machine. IEE Proc. 110: 903–915.

Jordan, H., (1964) Wellenflusse infolge con schwankungen des Luftapalteitwertes. Electrotechnik und Zeitschrift, 85: 865–867.

Alger, P. L. (1965) The Nature of Induction Machines. Gordon and Beach. NY, USA.

Jordan, H., Kovacs, K., Order, P. (1965) Messungen des schlupfes von asynchronmaschinen mit einer spule. Elektrotechnik und Zeitschrift 86: 294–296.

Stoll, R. L., Hammond P. (1965) The calculation of the magnetic field of rotating machines-Part 4: Approximate determination of the field and the losses associated with eddy currents in conducting surfaces, Proc IEE, 112(11): 2083–2094.

Skala, G. F. (1966) The ion chamber detector as a monitor of thermally produced particulates. 6th International Conference on Condensation Nuclei, Albany, NY, USA.

Stoll, R. L., Hammond P. (1966) The calculation of the magnetic field of rotating machines-Part 5: Field in the end region of turbo-generators and the eddy-current loss in the end plates of stator cores, Proc IEE, 113(11): 1793–1804.

Jones, C. V. (1967) The Unified Theory of Electrical Machines, Butterworths, London, UK.

Stafl, M. (1967) Electrodynamics of Electrical Machines. Academia, Prague, Czechoslovakia.

Binns, K. J. (1968) Cogging torques in induction machines. IEE Proc. 115: 1783–1790.

Albright, D. R. (1971) Inter-turn short circuit detector for turbine generator rotor windings. IEEE Trans Power Applications & Systems, PAS-50: 478–483.

Erlicki, M. S., Porat, Y., Alexandrovic, A. (1971) Leakage field changes of an induction motor as indication of non-symmetric supply. IEEE Trans on General Applications GA-7(6): 713–717.

Kryukhin, S. S. (1972) A new principle for synchronous machine protection from rotor winding inter-turn and double earth faults. Elect. Technol. USSR (2): 47–59.

Binns, K. J., Dye, M. (1973) Identification of principal factors affecting unbalanced magnetic pull in cage induction motors. IEE Proc, Part B, 120(March): 349–354.

Carson, C. C., Barton, S. C., Echeverria, F. S. (1973) Immediate warning of local over-heating in electrical machines by the detection of pyrolysis products. Trans IEEE on Power Applications & Systems, PAS-92(January/June): 533–542.

Neale, M. J., (1973) Tribology Handbook, Butterworths, London, UK.

Dickinson, W. H. (1974) IEEE Reliability Working Group, Report on reliability of electric plant, Part I, II & III. IEEE Trans on Industrial Applications IA-10 (Mar/Apr): 201–252

Kamerbeek, E. M. H. (1974) Torque measurements on induction motors using Hall generators or measuring windings. Philips Technical Review, 34(7): 152–162.

Rai, R. B. (1974) Air-gap eccentricity in induction motors, ERA Report: 1174–1188.

Timoshenko, S. (1974) Vibration Problems in Engineering. John Wiley & Sons, Van Nostrand, New York, USA.

Walker, D. N., Bowler, C. E. J., Jackson, R. L, Hodges, D. (1975) Results of sub-synchronous resonance test at Mohave. IEEE Trans on Power Apparatus and Systems, PAS-94(5): 1878–1889.

Bowen, R., Scott, D., Seifert, W., Westcott, W. C. (1976) Ferrography, Tribology International, 9(3, June): 109–115.

Kelley, J. K., Auld. J. W., Herter, V. J., Hutchinson, K. A., Rugenstein, W. A. (1976) Early detection and diagnosis of over-heating problems in turbine generators by instrumental chemical analysis. Trans IEEE on Power Applications & Systems, PAS-95(3): 879–886.

Dear, D. J. A., Dillon, A. F., Freedman, A. N. (1977) Determination of organic compounds in the hydrogen used for cooling large electricity generators. Journal of Chromatography, 137: 315–322.

Carson, C. C., Barton, S. C., Gill, R. S. (1978) The occurrence and control of interference from oil-mist in the detection of over-heating in a generator. Trans IEEE on Power Applications & Systems, PAS-57(5): 1590–1514.

Evans, C., (1978) Wear debris analysis and condition monitoring. NDT International, 11(3): 132–134.

Jufer, M., Abdulaziz, M. (1978) Influence d'une rupture de barre ou d'un anneau sur les characteristiques externes d'un moteur asynchrone a cage. Bulletin SEV/VSE, Switzerland, 69(17).

Rogers, R. (1978) Concepts used in the development of the IEEE and IEC codes for the interpretation of incipient faults in power transformers by dissolved gas in oil analysis. IEEE Trans On Electrical Insulation, EI-13(5): 349–354.

Collacott, R. A. (1979) Vibration Monitoring and Diagnostics. London, UK.

Harrold, R. T., Emery, F. T., Murphy, F. J., Drinkut, S. A. (1979) Radio frequency sensing of incipient arcing faults within large turbine generators. IEEE Trans on Power Applications & Systems, PAS-98(4): 1167–1173.

Kurtz, M., Stone, G. C. (1979), In-service partial discharge testing of generator insulation. IEEE Trans of Electrical Insulation, EI-14(2): 94–100.

Neale, N. and Associates (1979) A guide to the condition monitoring of machinery, HMSO, London, UK.

Ryder, D. M., Wood, J. W., Gallagher, P. L. (1979) The detection and identification of overheated insulation in turbo-generators. Trans IEEE on Power Applications and Systems, PAS-98(7): 333–336.

Brandl, P. (1980) Forces on the end windings of AC machines. Brown Boveri Review, 2: 128–134.

Joyce, J. S., Lambrecht, D. (1980) Status of evaluating fatigue of large steam turbine generation caused by electrical disturbances. IEEE Trans, Power Apparatus and Systems, PAS-99:111–119.

Kurtz, M., Stone, G. C., Freeman, D., Mulhall, V. R., Lonseth, P. (1980) Diagnostic testing of generator insulation without service interruption. CIGRE.

Lawrenson, P. J., Stephenson, J. M., Blenkinsop, P. T., Corda, J., Fulton, N. N. (1980) Variable-speed switched reluctance motors. IEE Proc. Part B, 127(4): 253–265.

Ohtaguro, M., Yagiuchi, K., Yamaguchi, H. (1980) Mechanical behaviour of stator end-windings. Trans IEEE on Power Applications & Systems, PAS-99(3): 1181–1185.

Penman, J., Hadwick, J. G., Stronach, A. F. (1980) Protection strategy against the occurrence of fault in electrical machines IEE Conf. Publ. 185, 54–58.

Sutton, J. (1980) EL CID: an easier way to test stator cores, UK, Electrical Review, 207, July.

Emery, F. T., Lenderking, B. N., Couch, R. D. (1981) Turbine- generator on-line diagnostics using RF monitoring. IEEE Trans on Power Applications & Systems, PAS-100(12): 4974–4982.

Evans, D. L. (1981) IEEE Reliability Working Group, Report on problems with hydro-generator thermoset stator windings, Part I, II & III. IEEE Trans on Power Applications & Systems, PAS-100: 3284–3303.

Lloyd, O., Cox, A. F. (1981) Monitoring debris in turbine generator oil. Wear, 71: 79–91.

Schlake, R. L, Buckley, G. W, McPherson, G. (1981) Performance of third harmonic ground fault protection schemes for generator stator windings. IEEE Trans PAS, PAS-100(7): 3195–3202.

Verma, S. P., Girgis, R. S. (1981) Shaft potentials and currents in large turbo-generators, Report for the Canadian Electrical Association, Canada.

Walker, D. N., Adams, S. L., Placek, R. J. (1981) Torsional vibration and fatigue of turbine-generator shafts. Trans IEEE on Power Apparatus & Systems, PAS-100(11): 4373–4380.

Yang, S. (1981) Low Noise Electric Motors. Oxford, Clarendon Press, UK.

Barker, B. Hodge, J. M. (1982) A decade of experience with generator and large motor reliability. CIGRE, Paris, France.

Brandt, G. B., Gottlieb, M. (1982) Fiber-optic temperature sensors using optical fibers. Abstracts of Papers of the American Chemical Society, 184(SEP): 64-.ANYL

Hargis, C., Gaydon, B. G., Kamash, K. (1982) The detection of rotor defects in induction motors. 375 IEE Conf. Publ. 213, pp. 216–220.

Hunter, D. J., Tavner, P. J., Ward, D. M., Benaragama, D. (1982) Measurements of the harmonic components of instantaneous electrical power delivered at the terminals of a 500 MW turbogenerator. 3rd International Conference on Sources and Effects of Power System Disturbances, London.

Jackson, R. J., Wilson, A. (1982) Slot-discharge activity in air-cooled motors and generators. IEE Proc.-B, Electric Power Applications, 129(3): 159–167.

Rogers, A. J., (1982) Optical temperature sensor for high voltage applications. Applied Optics, 21(5): 882–885.

Williamson, S., Smith, A. C. (1980) Field analysis for rotating induction machines and its relationship to the equivalent circuit method. IEE Proc, Part B, 127(2): 83–90.

Wilson, A., Nye, A. E. T., Hopgood, D. J. (1982) On-line detection of partial discharges in HV plant. 4th BEAMA International Electrical Insulation Conference, BEAMA, Brighton, UK.

Hargis, C. (1983) Steady-state analysis of 3-phase cage motors with rotor-bar and end-ring faults. IEE Proc, Part B, Electric Power Applications, 130(3): 225–225.

Michiguchi, Y., Tanisaka, S., Izumi, S., Watanabe, T., Miyashita, I. (1983) Development of a collector ring monitor for sparking detection on generators. IEEE Trans of Power Applications & Systems PAS-102(4): 928–933.

Rickson, C. D. (1983) Protecting motors from over-load due to asymmetrical fault conditions. Electrical Review: 778–780.

Timperley, J. E. (1983) Incipient fault detection through neutral RF monitoring of large rotating machines. IEEE Trans on Power Applications & Systems, PAS-102(3): 693–698.

Campbell, J. J., Clark, P. E., McShane, I. E., Wakeley, K. (1984) Strains on motor end-windings. Trans IEEE on Industrial Applications, IA-20(1): 37–44.

Cudworth, C. J., Smith, J. R. (1984) Mechanical damping of torsional vibrations in turbo-generators due to network disturbances. Journal Institution of Mechanical Engineers: 139–145.

Ehrich, F., Childs, D. (1984) Self-excited vibration in high-performance turbo-machinery. Mechanical Engineering, 106(5): 66–79.

O'Donnell, P. (1985) IEEE Reliability Working Group, Report of large motor reliability survey of industrial and commercial installations, Part I, II & III. IEEE Trans on Industrial Applications, IA-21 (Jul/Aug): 853–872.

Albrecht, P. F., Appiarius, J. C., McCoy, R. M., Owen, E. L., Sharma, D. K. (1986) Assessment of the reliability of motors in utility applications-updated. IEEE Trans on Energy Conversion, EC-1: 39–46.

Birmingham W., Joobbani R., Kim J. (1986) Knowledge-based expert systems and their applications, ACM/IEEE 23rd Conference on Design Automation, Las Vegas, USA: 531–539.

Harrold, R. T., Emery, F. T. (1986) Radio frequency diagnostic monitoring of electrical machines. Electrical Insulation Magazine, IEEE 2(2): 18–24.

Herbert, R. G. (1986) Computer techniques applied to the routine analysis of run-down vibration data for condition monitoring of turbine-alternators. British Journal of Non-Destructive Testing, 28(6): 371–375.

Rogers, A. J. (1986) Distributed optical-fibre sensors. Journal of Physics D: Applied Physics, 19(12): 2237–2266.

Seinsch, H. O. (1986) Detection and diagnosis of abnormal operating conditions and/or faults in rotating electrical machines. Schorch Berichte.

Tavner, P. J., Gaydon B. G., Ward D. M. (1986) Monitoring generators and large motors. IEE Proc, Part B, Electric Power Applications, 133(3): 169–180.

Tavner, P. J., Penman, J. (1987) Condition Monitoring of Electrical Machines. Research Studies Press and John Wiley & Sons, Letchworth, UK.

Chalmers, B. J. Ed (1988) Electrical Motor Handbook. Butterworths, London, UK.

Stone, G. C., Sedding, H. G., Lloyd, B. A., Gupta, B. K. (1988) The ability of diagnostic tests to estimate the remaining life of stator insulation. IEEE Trans on Energy Conversion, EC-3(4): 833–841.

Tavner, P. J., Jackson, R. J. (1988) Coupling of discharge currents between conductors of electrical machines owing to laminated steel core. IEE Proc. Part B, Electric Power Applications, 135(6): 295–307.

Williamson, S., Ellis, M. R. E. (1988) Influence of Rotor Currents on End-Winding Forces in Cage Motor. IEE Proc, Part B, Electric Power Applications, 135(6): 371–379.

Sedding, H. G., Stone, G. C. (1989) A discharge locating probe for rotating machines. IEEE Electrical Insulation Magazine, 5(5): 14–17.

Braun, J. M., Brown, G. (1990) Operational performance of generator condition monitors: comparison of heated and unheated ion chambers. IEEE Trans on Energy Conversion, EC-5(2): 344–349.

Geary, R., Kemp, I. J., Wood, J. W. (1990) Towards improved calibration in the measurement of partial discharges in rotating machinery. International Conference on Electrical Insulation, IEEE, Toronto, Canada.

Zocholl, S. E. (1990) Motor analysis and thermal protection. IEEE Trans on Power Delivery, PD-5(3): 1275–1280.

Mellor, P. H., Roberts, D., Turner, D. R. (1991) Lumped parameter thermal model for electrical machines of TEFC design. Electric Power Applications, IEE Proc. Part B, Electric Power Applications, 138(5): 205–218.

Pedersen, A., Crichton, G. C., McAllister, I. W. (1991) The theory and measurement of partial discharge transients. IEEE Trans on Electrical Insulation, 26(3): 487–497.

Sedding, H. G., Campbell, S. R., Stone, G. C., Klempner, G. S. (1991) A new sensor for detecting partial discharges in operating turbine generators. IEEE Trans on Energy Conversion, EC-6(4): 700–706.

Wilson, A. (1991) Slot discharge damage in air cooled stator windings. IEE Proc.-B, Science Measurement and Technology, 138(3): 153–160.

Billinton, R., Allan, R. N. (1992) Reliability evaluation of engineering systems – Concepts and systems. 2nd Ed, Plenum, New York, USA.

Bonnett, A. H., Soukup, G. C. (1992) Cause and analysis of stator and rotor failures in three-phase squirrel-cage induction motors. IEEE Trans on Industry Applications, IA-28(4): 921–937.

Tandon, N., Nakra, B. C. (1992) Comparison of vibration and acoustic measurement techniques for the condition monitoring of rolling element bearings. Tribology International, 25(3): 205–212.

Stone, G. C., Sedding, H. G., Fujimoto, N., Braun, J. M. (1992) Practical implementation of ultrawideband partial discharge detectors. IEEE Trans on Electrical Insulation, EI-27(1): 70–81.

Whittington, H. W., Flynn, B. W., Mills, G. H. (1992) An on-line wear debris monitor. Measurement Science Technology: 656–661.

Lyles, J. F., Goodeve, T. E. (1993) Using diagnostic technology for identifying generator winding needs, Hydro Review: June 1993: 58–67.

Onadera S., Yamasawa K., (1993) Electro-magnetic vibration analysis of a squirrel-cage induction motor, IEEE Trans on Magnetism, M-29(6), 2410–2412.

Siyambalapitiya, D. J. T., McLaren, P. G., Tavner, P. J. (1988) Transient thermal characteristics of induction machine rotor cage. IEEE Trans on Energy Conversion, EC-3(4): 849–854.

Vas, P. (1993) Parameter Estimation, Condition Monitoring and Diagnosis of Electrical Machines, 1st Ed, Oxford University Press, Oxford, UK.

Ward, D. A., Exon, J. L. T. (1993) Using Rogowski coils for transient current measurements. Engineering Science and Education Journal, 2(3): 105–113.

Wood, J. W., Sedding, H. G., Hogg, W. K., Kemp, I. J., Zhu, H. (1993) Partial discharges in HV machines; initial considerations for a PD specification. IEE Proc, Part A, Science, Measurement and Technology, 140(5): 409–416.

Campbell, S. R., Stone, G. C., Sedding, H. G., Klempner, G. S., McDermid, W., Bussey, R. G. (1994) Practical on-line partial discharge tests for turbine generators and motors. IEEE Trans on Energy Conversion, EC-9(2): 281–287.

Chen, S., Zhong, E., Lipo, T. A. (1994) A new approach to motor condition monitoring in induction motor drives. IEEE Trans on Industry Applications, IA-30(4): 905–911.

Finley, W. R., Burke, R. R. (1994) Troubleshooting motor problems. IEEE Trans on Industry Applications, IA-30(5): 1383–1397.

Lyles, J. F., Goodeve, T. E., Sedding, H. (1994) Parameters required to maximize a thermoset hydro-generator stator winding life. Part II-monitoring, maintenance. IEEE Trans on Energy Conversion, EC-9(3): 628–635.

Mayes, I. W. (1994) Use of neutral networks for online vibration monitoring. Proc. of the Institution of Mechanical Engineers Part A, Journal of Power and Energy, 208(A4): 267–274.

Penman, J., Sedding, H. G., Lloyd, B. A., Fink, W. T. (1994) Detection and location of inter-turn short circuits in the stator windings of operating motors. IEEE Trans on Energy Conversion EC-9(4): 652–658.

Penman J., Yin C. M. (1994), Feasibility of using unsupervised learning, artificial neural networks for the condition monitoring of electrical machines, IEE Proc. Part B, Electric Power Applications, 141(6): 317–322.

Boiarski, A. Pilate, G., Fink, T., Nilsson, N. (1995) Temperature measurements in power plant equipment using distributed fiber-optic sensing. IEEE Trans on Power Delivery, PD-10(4): 1771–1778.

Filippetti F., Franceschini G., Tassoni C. (1995) Neural networks aided on-line diagnostics of induction motor rotor faults, IEEE Trans. on Industry Applications, 31(4): 892–899.

Stone, G. C., Sedding, H. G. (1995) In-service evaluation of motor and generator stator windings using partial discharge tests. IEEE Trans on Industry Applications, IA-31(2): 299–303.

Thorsen, O. V., Dalva, M. (1995) A survey of faults on induction motors in offshore oil industry, petrochemical industry, gas terminals, and oil refineries. IEEE Trans on Industry Applications, IA-31(5): 1186–1196.

Barron, R. (1996) Engineering Condition Monitoring: Practice, Methods and Applications. Longman, Harlow, UK.

Erdman J., Kerkman R., Schlegel D. (1996) Effect of PWM inverters on ac motor bearing currents and shaft voltages, IEEE Trans. Industry Applications, 32(2): 250–259.

Hodges, N. (1996) The Economic Management Of Physical Assets. Mechanical Engineering Publications, London, UK.

Kemp, I. J., Zhu, H., Sedding, H. G., Wood, J. W., Hogg, W. K. (1996) Towards a new partial discharge calibration strategy based on the transfer function of machine stator windings. IEE Proc, Part A, Science, Measurement and Technology, 143(1): 57–62.

Milanfar, P., Lang, J. H. (1996) Monitoring the thermal condition of permanent-magnet synchronous motors. IEEE Trans on Aerospace and Electronic Systems, AES-32(4): 1421–1429.

Ogasawara S., Akagi H. (1996) Modeling and damping of high-frequency leakage currents in PWM inverter-fed AC motor drive systems, IEEE Trans. on Industry Applications, 32(5): 1105–1114.

Penman, J., Stavrou, A. (1996) Broken rotor bars: their effect on the transient performance of induction machines. IEE Proc, Part B, Electric Power Applications, 143(6): 449–457.

Ran, L., Yacamini, R., Smith K. S. (1996) Torsional vibrations in electrical induction motor drives during start up. Trans of the ASME-Journal of Vibration and Acoustics, 118(2): 242–251.

Rao, B. K. N. (1996) Handbook of Condition Monitoring. Elsevier, Oxford, UK.

Stone, G. C., Sedding, H. G., Costello, M. J. (1996) Application of partial discharge testing to motor and generator stator winding maintenance. IEEE Trans on Industry Applications, IA-32(2): 459–464.

Streifel, R. J., Marks, R., El-Sharkawi, M. A., Kerszenbaum, I. (1996) Detection of shorted-turns in the field winding of turbine-generator rotors using novelty detectors-development and field test. IEEE Trans on Energy Conversion, EC-11(2): 312–317.

Beehler, M. E. (1997) Reliability centered maintenance for transmission systems. IEEE Trans on Power Delivery, PD-12(2): 1023–1028.

Caldara S., Nuccio S., Ricco Galluzzo G., Trapanese M. (1997) A fuzzy diagnostic system: application to linear induction motor drives, IEEE Instrumentation and Measurement Technology Conference, Ottawa, Canada, 1: 257–262.

Cawsey A. (1997) Essence of Artificial Intelligence, Prentice-Hall, UK & USA.

Dorrell, D. G., Thomson, W. T., Roach, S. (1997) Analysis of air-gap flux, current, and vibration signals as a function of the combination of static and dynamic air-gap eccentricity in 3-phase induction motors. IEEE Trans on Industry Applications, IA-33(1): 24–34.

Dutton K., Thompson S., Barraclough B. (1997) The Art of Control Engineering, Prentice Hall, Essex, UK, pp. 438–495.

Halpin S. M., Burch R. F. (1997) Applicability of neural networks to industrial and commercial power systems: a tutorial overview, IEEE Trans. on Industry Applications, 33(5): 1355–1361.

IEEE Gold Book (1997) Recommended Practice for Design of Reliable Industrial & Commercial Power Systems, IEEE Std 493-1997, Piscataway, NJ, USA.

Murray A., Penman J. (1997) Extracting useful higher order features for condition monitoring using artificial neural networks, IEEE Trans on Signal Processing, SP 45(11): 2821–2828.

Stone G. C., Kapler J. (1997) Condition-based maintenance for the electrical windings of large motor and generators, IEEE Pulp and Paper Industry Conference, Cincinnati, USA: 57–63.

Chen S., Lipo T. A. (1998) Circulating type motor bearing current in inverter drives, IEEE Industry Applications Magazine, 4(1): 32–38.

Flankin G. F., Powell J. D., Workman M. (1998) Digital Control of Dynamic Systems: 160–166, Addison-Wesley Longman, Menlo Park, CA, USA.

Madisetti V. K., Williams D. B. (eds) (1998) The Digital Signal Processing Handbook, 1–21 to 1–23, CRC Press, Boca Raton, FL, USA.

Ran L., Gokani S., Clare J. C., Bradley K. J., Christopoulos C. (1998) Conducted Electromagnetic Emissions in Induction Motor Drive Systems, Part 2: Frequency Domain Models, IEEE Trans. on Power Electronics, 13(4) (July): 768–776.

Thomson, W. T., Barbour, A. (1998) On-line current monitoring and application of a finite element method to predict the level of static air-gap eccentricity in three-phase induction motors. IEEE Trans on Energy Conversion, EC-13(4): 347–357.

Yacamini R., Smith K. S., Ran L. (1998) Monitoring torsional vibrations of electromechanical systems using stator currents. Journal of Vibration and Acoustics, Trans of ASME, 120 (January): 72–79.

Beihoff, B. (1999) A survey of torque transduction methodologies for industrial applications. Pulp and Paper Industry Technical Conference, IEEE, Birmingham, AL, USA.

Benbouzid, M. E. H. (1999) Bibliography on induction motors faults detection and diagnosis. IEEE Trans Energy Conversion, 14(4) (December): 1065–1074.

Flordin P. (1999) Time-Frequency Time-scale Analysis, Academic Press, Elsevier, Cambridge, Ma, USA.

Gao, G., Steinhauser, M., Kavanaugh, R., Chen, W. (1999) Using fiber-optic sensors to measure strain in motor stator end windings during operation. Electrical Insulation Conference and Electrical Manufacturing & Coil Winding Conference, Cincinnati, OH, USA.

Kohler, J. L., Sottile, J., Trutt, F. C. (1999) Condition-based maintenance of electrical machines. Proc. of IEEE Industry Applications Conference, 34th IAS Annual Meeting, Phoenix. Piscataway: IEEE. pp. 205–211.

Morton, K. (1999) Asset management in the electricity supply industry. Power Engineering Journal, 13(5): 233–240.

Rogers, A. J. (1999) Distributed optical-fibre sensing. Measurement Science & Technology, 10(8): R75–R99.

Tavner, P. J., Hasson, J. P. (1999) Predicting the design life of high integrity rotating electrical machines. 9th IEE International Conference on Electrical Machines and Drives (EMD), IEE, Canterbury, UK.

Tetrault, S. M., Stone, G. C., Sedding, H. G. (1999) Monitoring partial discharges on 4-kV motor windings. IEEE Trans on Industry Applications, IA-35(3): 682–688.

Thomson, W. T., Rankin, D., Dorrell, D. G. (1999) On-line current monitoring to diagnose air-gap eccentricity in large three-phase induction motors-industrial case histories verify the predictions. IEEE Trans on Energy Conversion, EC-14 (4): 1372–1378.

Thorsen, O. V., Dalva, M. (1999) Failure identification and analysis for high-voltage induction motors in the petrochemical industry. IEEE Trans on Industry Applications, IA-35(4): 810–818.

Trzynadlowski, A. M., Ghassemzadeh, M., Legowski, S. F. (1999) Diagnostics of mechanical abnormalities in induction motors using instantaneous electric power. IEEE Trans on Energy Conversion, EC-14(4): 1417–1423.

Arthur, N., Penman, J., (2000) Induction machine condition monitoring with higher order spectra. IEEE Trans on Industrial Electronics, IE-47(5): 1031–1041.

Benbouzid, M. H. (2000) A review of induction motors signature analysis as a medium for faults detection. IEEE Transactions on Industrial Electronics, 47(5): 984–993.

Bellini, A., Filippetti, F., Franceschini, G., Tassoni, C. (2000) Closed-loop control impact on the diagnosis of induction motors faults. IEEE Trans on Industry Applications IA, 36(5): 1318–1329.

Filippetti F., Franceschini G., Tassoni C. and Vas P. (2000) Recent developments of induction motor drives fault diagnosis using AI techniques. IEEE Trans on Industrial Electronics, IE 47(5): 994–1004.

Iwaki, H., Yamakawa, H., Mita, A. (2000) FBG-based displacement and strain sensors for health monitoring of smart structures. 5th International Conference on Motion and Vibration Control, Sydney, Australia.

Joksimovic, G. M., Penman, J. (2000) The detection of inter-turn short circuits in the stator windings of operating motors. IEEE Trans on Industrial Electronics, IA-47(5): 1078–1084.

Smart, M. G., Friswell, M. I., Lees, A. W. (2000) Estimating turbo-generator foundation parameters: model selection and regularization. Proc. of the Royal Society A: Mathematical, Physical and Engineering Sciences, 456(1999): 1583–1607.

Sorita, T, Emmanji, K, Takashima, M, Nakamura, K (2000) A novel on-line method and equipment to detect local problems in turbine generators, Proc Annual IEEE Conference on Electrical Insulation & Dielectric Phenomena, Victoria, Canada: 552–555.

Bellini, A., Filippetti, F., Franceschini, G., Tassoni, C., Kliman, G. B. (2001) Quantitative evaluation of induction motor broken bars by means of electrical signature analysis. IEEE Trans on Industry Applications, IA-37(5): 1248–1255.

Benbouzid M. E. H., Nejjari H. (2001) A simple fuzzy logic approach for induction motors stator condition monitoring. IEEE Electric Machines and Drives Conference: 634–639, MA, USA.

Kang, P., Birtwhistle, D., (2001) Condition monitoring of power transformer on-load tap-changers, Part 1: automatic condition diagnostics. Proc IEE, Generation Transmission Distribution, 148:301–306.

Morris, A. S. (2001) Measurement & Instrumentation Principles. Oxford, UK, Butterworth-Heinemann.

Ramirez-Nino, J., Pascacio, A. (2001) Detecting inter-turn short circuits in rotor windings. IEEE Trans on Computer Applications in Power, CAP-14(4): 39–42.

Stavrou, A., Sedding, H. G., Penman, J. (2001) Current monitoring for detecting inter-turn short circuits in induction motors. IEEE Trans on Energy Conversion, EC-16(1): 32–37.

Thomson, W. T., Fenger, M. (2001) Current signature analysis to detect induction motor faults. IEEE Industry Applications Magazine, 7(4): 26–34

Trutt, F. C., Sottile, J., Kohler, J. L. (2001) Detection of AC machine winding deterioration using electrically excited vibrations. IEEE Trans on Industry Applications, IA-37(1): 10–14.

Bateman A., Paterson-Stephens I. (2002) The DSP Handbook, Prentice-Hall, Essex, UK, pp. 419–435.

Bellini, A., Filippetti, F., Franceschini, G., Tassoni, C., Passaglia, R., Saottini, M., Tontini, G., Giovannini, M., Rossi, A. (2002) On-field experience with online diagnosis of large induction motors cage failures using MCSA. IEEE Trans on Industry Applications, IA-38(4): 1045–1053.

Jintakosonwit P., Fijita H., Akagi H., (2002) Control and performance of a fully-digital-controlled shunt active filter for installation on a power distribution system. IEEE Trans on Power Electronics, PE-17(1): 132–140.

Judd, M. D., McArthur, S. D. J., McDonald, J. R., Farish, O. (2002) Intelligent condition monitoring and asset management. Partial discharge monitoring for power transformers. Power Engineering Journal, IEE 16(6): 297–304.

Kohler, J. L., Sottile, J., Trutt, F. C. (2002) Condition monitoring of stator windings in induction motors. I. Experimental investigation of the effective negative-sequence impedance detector. IEEE Trans on Industry Applications, IA-38(5): 1447–1453.

Lewis, C. (2002) The advanced induction motor, IEEE Conf.

Nandi, S., Bharadwaj, R. M., Toliyat, H. A. (2002) Performance analysis of a three-phase induction motor under mixed eccentricity condition. IEEE Trans on Energy Conversion, EC-17(3): 392–399.

Sottile, J., Trutt, F. C., Kohler, J. L. (2002) Condition monitoring of stator windings in induction motors. II. Experimental investigation of voltage mismatch detectors. IEEE Trans on Industry Applications, IA-38(5): 1454–1459.

Trutt, F. C., Sottile, J., Kohler, J. L. (2002) Online condition monitoring of induction motors. IEEE Trans on Industry Applications, IA-38(6): 1627–1632.

Cavallini A., Montanari G. C., Contin A., Puletti F. (2003) A new approach to the diagnosis of solid insulation systems based on PD signal processing. IEEE Electrical Insulation Magazine, 19(2): 23–30.

Han, Y., Song, Y. H. (2003) Condition monitoring techniques for electrical equipment – A literature survey. IEEE Trans on Power Delivery, PD-18(1): 4–13.

Henao, H., Demian C., Capolino G. A. (2003) A frequency-domain detection of stator winding faults in induction machines using an external flux sensor. IEEE Trans on Industry Applications, IA-39(5): 1272–1279.

Lin J., Zuo M. J. (2003) Gearbox fault diagnosis using adaptive wavelet filter. Mechanical Systems and Signal Processing, 17(6): 1259–1269.

Miyazaki, A., Takinami, N., Kobayashi, S. *et al*. (2003) Long-distance 275 kV GIL monitoring system using fiber-optic technology. IEEE Trans on Power Delivery, PD-18(4): 1545–1553.

Mohan N., Undeland T. M., Robbins W. P., (2003) Power Electronics-Converters, Applications and Design, John Wiley & Sons, New York, 225–230.

Poyhonen, S., Negrea, M., Jover, P., Arkkio, A., Hyotyniemi, H. (2003) Numerical magnetic field analysis and signal processing for fault diagnostics of electrical machines. COMPEL: The International Journal for Computation and Mathematics in Electrical and Electronic Engineering, 22 (4): 969–981.

Singh, G. K., Al Kazzaz, S. A. S. (2003) Induction machine drive condition monitoring and diagnostic research – a survey. Electric Power Systems Research, 64(2): 145–158.

Stephan C. E., Laird T. (2003) Condition-based maintenance of turbine generators: what makes it real? IEEE Electric Machines and Drive Conference, USA, vol. 2: 895–899, Madison, WI, USA.

Xiao, C., Zhao, L., Asada, T., Odendaal, W. G., van Wyk, J. D. (2003) An overview of integratable current sensor technologies. 38th IEEE IAS Annual Meeting, Vol. 2, Salt Lake City, UT, USA.

Zhang Z., Ren Z., Huang W. (2003) A novel detection method of motor broken rotor bars based on wavelet ridge. IEEE Trans on Energy Conversion, EC-18 (3): 417–423.

Ben Sasi, A. Y., Gu, F., Payne, B. S., Ball, A. D. (2004) Instantaneous angular speed monitoring of electric motors. Journal of Quality in Maintenance Engineering, 10(2): 123–135.

Douglas, H., Pillay P., Ziarani A. K., (2004) A new algorithm for transient motor current signature analysis using wavelets. IEEE Trans on Industry Applications, IA-40(5): 1361–1368.

Durocher, D. B., Feldmeier, G. R. (2004) Predictive versus preventive maintenance. IEEE Industry Applications Magazine (September/October): 12–21.

Fangxing, L., Brown, R. E. (2004) A cost-effective approach of prioritizing distribution maintenance based on system reliability. IEEE Trans on Power Delivery, 19(1): 439–441.

Kheirmand, A., Leijon, M., Gubanski, S. M (2004) Advances in online monitoring and localization of partial discharges in large rotating machines. IEEE Trans on Energy Conversion, EC-19(1): 53–59.

Kher, S., Gurram, S., Saxena, M. K., Nathan, T. P. S. (2004) Development of distributed fibre optic sensor with sub-metre resolution. Current Science, 86(9): 1202–1204.

Menacer, A., Nat-Said, M. S., Benachka, A. H., Drid, S. (2004) Stator current analysis of incipient fault into induction machine rotor bars. Journal of Electrical Engineering, 4(2): 122–130.

Nippes, P. I. (2004) Early warning of developing problems in rotating machinery as provided by monitoring shaft voltages and grounding currents. IEEE Trans on Energy Conversion, EC-19(2): 340–345.

Sonderegger, R. C., Henderson, D., Bubb, S., Steury, J. (2004) Distributed asset insight. Power and Energy Magazine, IEEE, 2(3): 32–39.

Stack, J. R., Habetler, T. G., Harley, R. G. (2004) Fault classification and fault signature production for rolling element bearings in electric machines. IEEE Trans on Industry Applications, IA-40(3): 735–739.

Stack, J. R., Habetler, T. G., Harley, R. G., (2004) Bearing fault detection via auto-regressive stator current modeling. IEEE Trans on Industry Applications, IA-40(3), 740–747.

Stone, G. C., Boulter E. A., Culbert, I., Dhirani, H. (2004) Electrical Insulation for Rotating Machines, Design, Evaluation, Aging, Testing, and Repair.Wiley-IEEE Press, New York, USA.

Wu, S., Chow, T. W. S. (2004) Induction machine fault detection using SOM-based RBF neural networks. IEEE Trans on Industrial Electronics, 51(1): 183–194.

Yazici, B. (2004) Statistical pattern analysis of partial discharge measurements for quality assessment of insulation systems in high-voltage electrical machinery. IEEE Trans on Industry Applications, IA-40(6): 1579–1594.

Brown, R. E. Humphrey, B. G. (2005) Asset management for transmission and distribution. Power and Energy Magazine, IEEE, 3(3): 39–45.

Henao, H., Razik, H., Capolino, G. A. (2005) Analytical approach of the stator current frequency harmonics computation for detection of induction machine rotor faults. IEEE Trans on Industry Applications, IA-41(3): 801–807.

Lee, S. B., Younsi, K., Kliman, G. B. (2005) An online technique for monitoring the insulation condition of AC machine stator windings. IEEE Trans on Energy Conversion, EC-20(4): 737–745.

Nandi, S., Toliyat, H. A., Xiaodong, L. (2005) Condition monitoring and fault diagnosis of electrical motors: a review. IEEE Trans on Energy Conversion, EC-20(4): 719–729.

Sihler, C., Miri, A. M. (2005) A stabilizer for oscillating torques in synchronous machines. IEEE Trans on Industry Applications, 41(3): 748–755.

Tavner, P. J., Anderson, A. F. (2005) Core faults in large generators. IEE Proc, Electric Power Applications, 152(6): 1427–1439.

Andrawus, J., Watson, J., Kishk, M., Adam, A. (2006) The selection of a suitable maintenance strategy for wind turbines. Wind Energy, 30(6): 471–486.

Ben Sasi, A. Y., Gu, F., Li, Y., Ball, A. D. (2006) A validated model for the prediction of rotor bar failure in squirrel-cage motors using instantaneous angular speed. Journal of Mechanical Systems and Signal Processing, 20(7): 1572–1589.

Dominelli, N., Rao, A., Kundur, P. (2006) Life extension and condition assessment: techniques for an aging utility infrastructure. Power and Energy Magazine, IEEE, 4(3): 24–35.

Hinton, G. E., Osindero, S., Teh, Y. W. (2006) A fast learning algorithm for deep belief nets. Neural Computing, 18(7): 1527–1554.

Jayasinghe, J. A. S. B., Wang, Z. D., Jarman, P. N., Darwin, A. W. (2006) Winding movement in power transformers. A comparison of FRA measurement connection methods. IEEE Trans Dielectrics & Insulation, 16(6): 1342–1349.

Li, W. D., Mechefske, C. K. (2006) Detection of induction motor faults: a comparison of stator current, vibration and acoustic methods. Journal of Vibration and Control, 12(2): 165–188.

Sottile, J., Trutt, F. C., Leedy, A. W. (2006) Condition monitoring of brushless three-phase synchronous generators with stator winding or rotor circuit deterioration. IEEE Trans Industry Applications, IA-42(5): 1209–1215.

Spinato, F., Tavner, P. J., van Bussel, G. J. W., Koutoulakos, E. (2006) Reliability of wind turbine sub-assemblies. IET Renew. Power Gener., 2009, 3(4): 387–401.

Levi, E., Bojoi, R., Profumo, F., Toliyat, H. A., Williamson, S. (2007) Multiphase induction motor drives – a technology status review. Proc IET, Electr. Power Appl, 2(4): pp. 489–516.

Ridley, G. K. (2007) El CID-Application and Analysis, 3rd Ed, Adwel International Ltd/IRIS Power LP, Watford, UK.

Su, H., Chong, K. T. (2007) Induction machine condition monitoring using neural network modeling. IEEE Trans Industrial Electronics, 54(1) (February): 241–249.

Tandon, N., Yadava, G. S., Ramakrishna, K. M. (2007) A comparison of some condition monitoring techniques for the detection of defect in induction motor ball bearings. Mechanical Systems and Signal Processing, 21(1): 244–256.

Andrawus, J. (2008) Maintenance optimisation for wind turbines. PhD. Robert Gordon University, Aberdeen, UK.

McMillan, D., Ault, G. (2008) Condition monitoring benefit for onshore wind turbines: Sensitivity to operational parameters. IET Renewable Power Generation, 2(1): 60–72.

Tavner, P. J., Ran, L., Penman, J., Sedding, H. (2008) Condition Monitoring of Rotating Machines, 2nd Edition, Power and Energy Series, No. 59, IET, Stevenage, UK.

Tavner, P. J. (2008) Review of condition monitoring of rotating electrical machines. Proc IET Electr. Power Appl, 2(4): 215–247.

Drury, W. (2009) The Control Techniques Drives and Control Handbook, IET Power & Energy Series, 3rd Ed, Stevenage, UK.

Clerici, D., Della Torre, F., Paolo Morando, A. (2010) A form-wound induction machine model for the study of three-phase surge propagation. IEEE Trans. on Energy Conversion, 25(1): 199–206.

Lee, K., Hong, J., Lee, K. W., Lee, S. B., Wiedenbrug, E. J. (2010) A stator-core quality-assessment technique for inverter-fed induction machines, 46(1): 213–221.

Martinez-Roman, J. (2010) Harmonic order tracking analysis: a novel method for fault diagnosis in induction machines. IEEE Trans Energy Conversion, 30(3): 833–841.

Mills, S. R. W. (2010) Vibration Monitoring & Analysis Handbook, British Institute of Non-Destructive Testing, Northampton, UK.

Sapena-Bano, A., Pineda-Sanchez, M., Puche-Panadero, R. *et al.* (2010) Analysis of thermal stresses in medium voltage motor coils under repetitive fast and high frequency pulses. IEEE Trans on Dielectrics and Electrical Insulation, 17(5): 1378–1384.

Tozzi, M., Cavallini, A., Montanari, G. C. (2010) Monitoring off-line and on-line PD under impulsive voltage on induction motors, part 1: standard procedure. IEEE Electrical Insulation Magazine, 26(4): pp. 16–26.

Watson, S. J., Xiang, B. J., Yang, W., Tavner, P. J., Crabtree, C. J. (2010) Condition monitoring of the power output of wind turbine generators using wavelets. IEEE Trans Energy Conversion, 25(3) (September): 715–721.

Wittek, E., Kreise, M., Tischmacher, H., Gattermann, S., Ponick, B., Poll, G. (2010) Capacitances and lubricant film thickness of motor bearings under different operating conditions. Proceedings of ICEM, Rome, Italy.

Yang, S., Xiang, D., Bryant, A., Mawby, P., Ran, L., Tavner, P. J. (2010) Condition monitoring for device reliability in power electronic converters: a review. IEEE Trans Power Electronics, 25(11): 2734–2752.

Arellano-Padilla, J., Sumner, M., Gerada, C. (2011) Winding condition monitoring scheme for a permanent magnet machine using high-frequency injection. IET Electr. Power Appl., 2011, 5(1): pp. 89–99.

Contin, A., Zhu, H. (2011) Partial discharge influence on dissipation factor values during stator-bar testing. IEEE Electrical Insulation Magazine, 8–14.

Dorrell, D. G. (2011) Sources and characteristics of unbalanced magnetic pull in three-phase cage induction motors with axial-varying rotor eccentricity. IEEE Trans. on Industry Applications, 47(1): 12–24.

Hyun, D., Hong, J., Lee, S. B. *et al.* (2011) Automated monitoring of air-gap eccentricity for inverter-fed induction motors under standstill conditions. IEEE Trans Industry Applications, 47(3) (May/June): 1257–1266.

Lee, S. B., Yang, J., Hong, J. *et al.* (2011) A new strategy for condition monitoring of adjustable speed induction machine drive systems. IEEE Trans Power Electronics, 26(2) (February): 389–398.

Muetze, A., Tamminen, J., Ahola, J. (2011) Influence of motor operating parameters on discharge bearing current activity. IEEE Trans on Industry Applications, 47(4): 1767–1777.

Zhang, P., Du, Y., Habetler, T. G., Lu, B. (2011) A survey of condition monitoring and protection methods for medium-voltage induction motors. IEEE Trans Industry Applications, 47(1) (January/February): 34–46.

Xiang, D., Ran, L., Tavner, P. J., Bryant, A., Yang, S., Mawby, P. A. (2011) Monitoring solder fatigue in a power module using case-above-ambient temperature rise. IEEE Trans on Industry Applications, 47(6): 2578–2591.

Antonino-Daviu, J. A., Riera-Guasp, M., Pons-Llinares, J., Roger-Folch, J., P´erez, R. B., Charlton-P´erez, C. (2012) Toward condition monitoring of damper windings in synchronous motors via EMD analysis. IEEE Trans Energy Conversion, 27(2) (June): 432–439.

Feng, Y., Qiu, Y., Crabtree, C. J., Long, H., Tavner, P. J. (2012) Monitoring wind turbine gearboxes. Wind Energy, 17(5): 673–693.

Hou, L., Bergmann, N. W. (2012) Novel industrial wireless sensor networks for machine condition monitoring and fault diagnosis. IEEE Trans Instrumentation and Measurement, 61(10) (October): 2787–2798.

Stone, G. C. (2012) A perspective on online partial discharge monitoring for assessment of the condition of rotating machine stator winding insulation. IEEE Electrical Insulation Magazine, 28(5): 8–13.

Yang, J., Kang, T. J., Kim, B., *et al*. (2012) Experimental evaluation of using the surge PD test as a predictive maintenance tool for monitoring turn insulation quality in random wound AC motor stator windings. IEEE Trans on Dielectric and Electrical Insulation, 19(1): 53–60.

Guideline for Certification of Condition Monitoring Systems for Wind Turbines. (2013) GL Renewables Certification, Hamburg.

Krause, P., Wasynczuk, O., Sudhoff, S., Pekarek, S. (2013) Analysis of Electric Machinery and Drive Systems. IEEE Press Power Engineering Series, 4th Ed, Piscataway, NJ, USA.

Lee, S., Hong, J., Lee, S. B., Wiedenbrug, E. J., Teska, M., Kim, H. (2013) Evaluation of the influence of rotor axial air ducts on condition monitoring of induction motors. IEEE Trans Industry Applications, 49(5) (September/October): 2024–2033.

Stone, G. C. (2013) Condition monitoring and diagnostics of motor and stator windings: a review. IEEE Trans Dielectrics & Electrical Insulation, 20(6) (December): 2073–2080.

Bertenshaw, D. R. (2014) Stator core interlamination faults and their detection by electro-magnetic means, PhD Thesis, School of Electrical and Electronic Engineering, University of Manchester, UK.

Chen, B., Zappala, D., Crabtree, C. Tavner, P. J. (2014) Survey of commercially available SCADA data analysis tools for wind turbine health monitoring. Technical report, Durham University School of Engineering and Computing Sciences. Available at http://dro.dur.ac.uk/12563/ [Accessed 10 Jan. 2019].

Crabtree, C., Zappala, D., Tavner, P. J. (2014) Survey of commercially available condition monitoring systems for wind turbines. Technical report, Durham University School of Engineering and Computing Sciences. Available at http://dro.dur.ac.uk/12497/ [Accessed 10 Jan. 2019].

Neuzil, J., Kreibich, O., Smid, R. (2014) A distributed fault detection system based on IWSN for machine condition monitoring. IEEE Trans Industrial Informatics, 10(2) (May): 1118–1123.

Niskanen, V., Muetze, A., Ahola, J. (2014) Study on bearing impedance properties at several hundred kilohertz for different electric machine operating parameters. IEEE Trans on Industry Applications, 50(5): 3438–3447.

Renforth, L. A., Armstrong, R., Clark, D., Goodfellow, S., Hamer, P. S. (2014) High voltage rotating machines – A new technique for remote partial discharge monitoring of the stator insulation condition. IEEE Industry Applications Magazine, Nov/Dec, 79–89.

Seshadrinath, J., Singh, B., Panigrahi, B. K. (2014) Incipient turn fault detection and condition monitoring of induction machine using analytical wavelet transform. IEEE Transactions on Industry Applications, 50(3) (May/June): 2235–2242.

Stone, G. C., Culbert, I., Boulter, E. A., Dhirani, H. (2014) Electrical Insulation for Rotating Machines: Design, Evaluation, Aging, Testing, and Repair, IEEE

Press Power Engineering Series, 2nd Ed, Piscataway, NJ, USA, particularly pp. 27–29 and 70–71.

Zaggout, M., Tavner, P. J., Crabtree, C., Ran, L. (2014) Detection of rotor electrical asymmetry in wind turbine doubly-fed induction generators. IET Renew. Power Gener, 8(8): 1–9.

Zhang, D., Li, W., Xiong, X. (2014) Overhead line preventive maintenance strategy based on condition monitoring and system reliability assessment. IEEE Trans on Power Systems, 29(4): 1839–1846.

Chelvan, I. T., Nandi, S., Subramanian, J. (2015) A disassembly-free off-line detection and condition monitoring technique for eccentricity faults in salient-pole synchronous machines. IEEE Trans Industry Applications, 51(2) (March/April): 1505–1515.

Choi, S., Pazouki, E., Baek, J., Bahrami, H. R. (2015) Iterative condition monitoring and fault diagnosis scheme of electric motor for harsh industrial application. IEEE Transactions on Industrial Electronics, 62(3) (March): 1760–1769.

Crabtree, C., Zappala, D., Hogg, S. (2015) Wind energy: UK experiences and offshore operational challenges. Proc. IMechE Part A: Journal of Power and Energy, 229(7): 727–746.

Duan, F., Živanović, R. (2015) Condition monitoring of an induction motor stator windings via global optimization based on the hyperbolic cross points. IEEE Trans Industrial Electronics, 62(3) (March): 1826–1834.

Kerres, B., Fischer, K., Madlener, R. (2015) Economic evaluation of maintenance strategies for wind turbines: a stochastic analysis. IET Renewable Power Generation, 9(7): 766–774.

Li, D. Z., Wang, W., Ismail, F. (2015) An enhanced bispectrum technique with auxiliary frequency injection for induction motor health condition monitoring. IEEE Trans Instrumentation & Measurement, 64(10) (October): 2679–2687.

Li, D. Z., Wang, W., Ismail, F. (2015) A spectrum synch technique for induction motor health condition monitoring. IEEE Trans Energy Conversion, 30(4) (December): 1348–1355.

Ma, H., Saha, T. K., Ekanayake, C., Martin, D. (2015) Smart transformer for smart grid – intelligent framework and techniques for power transformer asset management. IEEE Trans. on Smart Grid, 6(2): 1026–1034.

May, A., McMillan, D., Thöns, S. (2015) Economic analysis of condition monitoring systems for offshore wind turbine sub-systems. IET Renewable Power Generation, 9(8): 900–907.

Qiu, J., Wang, H. F., Lin, D. Y., He, B. T., Zhao, W. F., Xu, W. (2015) Nonparametric regression-based failure rate model for electric power equipment using lifecycle data. IEEE Trans. On Smart Grid, 6(2): 955–964.

Riera-Guasp, M., Antonino-Daviu, J. A., Capolino, G-A. (2015) Advances in electrical machine, power electronic, and drive condition monitoring and fault detection: state of the art. IEEE Trans Industrial Electronics, 62(3) (March): 1746–1759.

Shin, S., Kim, J., Lee, S. B., Lim, C., Wiedenbrug, E. J. (2015) Evaluation of the influence of rotor magnetic anisotropy on condition monitoring of two-pole induction motors. IEEE Trans Industry Applications, 51(4) (July/August): 2896–2904.

Zhang, P., Younsi, K., Neti, P. (2015) A novel online stator ground-wall insulation monitoring scheme for inverter-fed AC motors. IEEE Trans. on Industry Applications, 51(3): 2201–2207.

Arellano-Padilla, J., Sumner, M., Gerada, C. (2016) Condition monitoring approach for permanent magnet synchronous motor drives based on the INFORM method. IET Electr. Power Appl, 10(1): 54–62.

Chung, H. S., Wang, H., Blaabjerg, F., Pecht, M. (2016) Reliability of Power Electronic Converter Systems, IET Power & Energy Series, Stevenage, UK.

Dalvand, F., Kalantar, A., Safizadeh, M. S. (2016) A novel bearing condition monitoring method in induction motors based on instantaneous frequency of motor voltage. IEEE Trans, Industrial Electronics, 63(1) (January): 364–376.

Han, S., Jung, J., Lee, K. W., Lee, S. B., Nandi, S., Kim, B., Kang, B. (2016) In-service monitoring of stator-slot magnetic wedge condition for induction motors. IEEE Trans Industry Applications, 52(4) (July/August): 2900–2910.

Lai, W., Chen, M., Ran, L. Xu S., Qin H., Alatise O., Mawby P. A. (2016) A Study on the Lifetime Characteristics of Power Modules under Power Cycling Conditions. IET Power Electronics, 1045(5): 1045–1052.

Barater, D., Arellano-Padilla, J., Gerada, C. (2017) Incipient fault diagnosis in ultrareliable electric machines. IEEE Trans. on Industry Applications, 53(3): 2906–2914.

Costello, J. J. A., West, G. M., McArthur, S. D. J. (2017) Machine learning model for event-based prognostics in gas circulator condition monitoring. IEEE Trans, Reliability, 66(4) (December): 1048–1057.

Garcia-Escudero, L. A., Duque-Perez, O., Fernandez-Temprano, M., Morinigo-Sotelo, D. (2017) Robust detection of incipient faults in VSI-fed induction motors using quality control charts. IEEE Trans. on Industry Applications, 53(3): 3076–3085.

Gerstenkorn, R., Somes, T. (2017) Impacts of reduced motor cooling on reliability. IEEE Trans. on Industry Applications, 53(1): 739–744.

Mohammed, A., Djurović, S. (2017) FBG thermal sensing features for hot spot monitoring in random wound electric machine coils. IEEE Sensors Journal, 17(10) (May): 3058–3067.

Montanari, G. C. (2017) Time behaviour of partial discharges and life of type II turn insulation specimens under repetitive impulse and sinusoidal waveforms. IEEE Electrical Insulation Magazine, 33(6): 17–26.

Queiroz, A., Senger, E., Queiroz, L., Rangel, E., de Paula, V. (2017) Maintenance strategy for electrical equipment based on integrated operations. IEEE Trans on Industry Applications, 53(3): 3189–3197.

Ridley, G. K. (2017) Application of EL CID to salient-pole electrical machines, PhD Thesis, School of Engineering, University of Warwick, UK.

Sabin, D., MacLeod, G., Wojdan, M. (2017) Using smart grid sensors and advanced software applications as an asset management tool at Hydro Ottawa. IET Open Access Journal, CIRED, 2017(1): 490–494.

Sarantakos, I., Lyons, P., Blake, S., Taylor, P. (2017) Incorporating asset management into power system operations. IET CIRED Open Access Proc, 2017(1): 1227–1231.

Schantz, C. J., Leeb, S. B. (2017) Self-sensing induction motors for condition monitoring. IEEE Sensors Journal, 17(12) (June): 3735–3743.

Sze, V., Chen, Y. H., Yang, T. Y., Emer, J. S. (2017) Efficient processing of deep neural networks: a tutorial and survey. Proceedings of the IEEE, 105(12): 2295–2329.

Tsypkin, M. (2017) The origin of the electromagnetic vibration of induction motors operating in modern industry: practical experience – analysis and diagnosis. IEEE Trans. on Industry Applications, 53(2): 1669–1676.

Zoeller, C., Vogelsberger, M. A., Fasching, R., Grubelnik, W., Wolbank, T. M. (2017) Evaluation and current-based identification of insulation degradation for high utilization electrical machines in railway application. IEEE Trans. on Industry Applications, 53(3): 2679–2689.

Abu-Siada, A. (Ed) (2018) Power Transformer Condition Monitoring and Diagnosis, Energy Series No. 78, IET, Stevenage, UK.

Deutsch, J., He, D. (2018) Using deep learning-based approach to predict remaining useful life of rotating components. IEEE Trans. on Systems, Man and Cybernetics: systems, 48(1): 11–20.

Electric Machines Roadmap (2018) Advanced Propulsion Centre UK in collaboration with and on behalf of the Automotive Council, UK.

Feng, G., Lai, C., Tjong, Jimi, N., Kar, N. C. (2018) Non-invasive Kalman filter based permanent magnet temperature estimation for permanent magnet synchronous machines. IEEE Trans Power Electronics, 33(12) (Nov): 10673–10682.

Ibrahim, R. K., Watson, S. J., Djurović, S., Crabtree, C. J. (2018) An effective approach for rotor electrical asymmetry detection in wind turbine DFIGs. IEEE Trans Industrial Electronics, 65(11) (Nov): 8872–8881.

Krummenacher, G., Ong, C. S., Koller, S., Kobayashi, S., Buhmann, J. M. (2018) Wheel defect detection with machine learning. IEEE Trans. On Intelligent Transportation Systems, 19(4): 1176–1187.

Lee, K. F. (2018) AI Superpowers, China, Silicon Valley, New World Order, Houghton, Mifflin, Harcourt, Boston, USA,

Kumar, P. S., Xie, L., Soong, B., Lee, M. Y. (2018) Feasibility for utilizing IEEE 802.15.4 compliant radios inside rotating electrical machines for wireless condition monitoring applications. IEEE Sensors Journal, 18(10) (May): 4293–4302.

Mohammed, A., Djurović, S. (2018) Stator winding internal thermal stress monitoring and analysis using in-situ FBG sensing technology. IEEE Trans Energy Conversion, 3(33) (September): 1508–1518.

Shahriar, M. R., Borghesani, P., Tan, A. C. C. (2018) Electrical signature analysis-based detection of external bearing fault in electro-mechanical drive trains. IEEE Trans Industrial Electronics, 65(7): 5941–5950.

Xin, Y., Kong, L. S., Liu, Z., *et al*. (2018) Machine learning and deep learning methods for cybersecurity. IEEE Access, 6: 35365–35381.

Zappalá, D., Sarma, N. , Djurović, S., Crabtree, C. J., Mohammad, A., Tavner, P. J. (2019) Electrical & mechanical diagnostic indicators of wind turbine induction generator rotor faults. Renewable Energy, 131(February): 14–24.

Moses, A., Anderson, P., Jenkins, K., Stanbury, H. (2019) Electrical Steels, Vol 1 Fundamentals & Basic Concepts, Power and Energy Series, No. 157, IET, Stevenage, UK.

Moses, A., Anderson, P., Jenkins, K., Stanbury, H. (2019) Electrical Steels, Vol 2 Performance & Applications, Power and Energy Series, No. 157, IET, Stevenage, UK.

# Standards


BS EN IEC 60034-1:2010 Rotating electrical machines. Rating and performance.

BS EN IEC 60034-2-1:2014 Rotating electrical machines. Standard methods for determining losses and efficiency from tests, excluding machines for traction vehicles.

BS EN IEC 60034-2-2:2010 Rotating electrical machines. Specific methods for determining separate losses of large machines from tests. Supplement to BS EN 60034-2-1:2014.

BS EN IEC 60034-14:2004 Rotating electrical machines. Mechanical vibration of certain machines with shaft heights 56 mm and higher. Measurement, evaluation and limits of vibration severity.

BS EN IEC 60034-18-42:2017 Rotating electrical machines. Partial discharge resistant electrical insulation systems (Type II) used in rotating electrical machines fed from voltage converters – Qualification tests.

BS EN IEC 60034-27-1:2018 Rotating electrical machines. Off-line partial discharge measurements on the winding insulation.

BS EN 60034-27-3:2016 Rotating electrical machines. Dielectric dissipation factor measurement on stator winding insulation of rotating electrical machines.

BS EN IEC 60034-27-4:2018 Rotating electrical machines. Measurement of insulation resistance and polarization index on winding insulation of rotating electrical machines.

BS EN IEC 60085:2007 Electrical insulation – Thermal evaluation and designation.

BS EN IEC 60300-3-3:2017 Dependability management – Application guide – Life cycle costing

BS EN IEC 60812:2018 Failure modes and effects analysis (FMEA and FMECA).

BS EN IEC 61400-25-6:2016 Communications for monitoring and control of wind power plants – Logical node classes and data classes for condition monitoring.

CDA/MS/NVSH107 Canadian Government Vibration Specification, no longer issued.

GL Renewables Certification 2013. Guideline for the certification of condition monitoring systems for wind turbines, Hamburg, Germany.

IEEE Std 43:2013 Recommended Practice for Testing Insulation Resistance of Electric Machinery.
IEEE 56:2016 Guide for Insulation Maintenance of Electric Machines.
IEEE Std 95:2002 Recommended Practice for Insulation Testing of AC Electric Machinery (2300 V and Above) With High Direct Voltage.
IEEE Std 117:2015 Standard Test Procedure for Thermal Evaluation of Systems of Insulating Materials for Random-Wound AC Electric Machinery.
IEEE Std 286:2000 Recommended Practice for Measurement of Power Factor Tip-Up of Electric Machinery Stator Coil Insulation.
IEEE Std 433:2009 Recommended Practice for Insulation Testing of AC Electric Machinery with High Voltage at Very Low Frequency.
IEEE Std 434:2006 Guide for Functional Evaluation of Insulation Systems for AC Electric Machines Rated 2300 V and Above.
IEEE Std 493:1997 Gold Book – Recommended Practice for Design of Reliable Industrial & Commercial Power.
IEEE Std 522:2004 Guide for Testing Turn Insulation of Form-Wound Stator Coils for Alternating-Current Electric Machines.
IEEE Std 1434:2014 Guide for the Measurement of Partial Discharges in AC Electric Machinery.
ISO 1940-1:2003 Mechanical vibration – Balance quality requirements for rotors in a constant (rigid) state Part 1: Specification and verification of balance tolerances.
ISO 10816-1:1995 Mechanical vibration – Evaluation of machine vibration by measurements on non-rotating parts – Part 1: General guidelines.
ISO 10816-3:2009 Mechanical vibration – Evaluation of machine vibration by measurements on non-rotating parts – Part 3: Industrial machines with nominal power above 15 kW and nominal speeds between 120 and 15 000 rev/min when measured in situ.
ISO 18436 Condition monitoring and diagnostics of machines – Requirements for training and certification of personnel – Part 2: Vibration condition monitoring and diagnostics.
ISO 13372:2012 Condition monitoring and diagnostics of machines – Vocabulary.
ISO 13373-1:2002 Condition monitoring and diagnostics of machines – Vibration condition monitoring – Part 1: General procedures.
ISO 13374-1:2003 Condition monitoring and diagnostics of machines – Data processing, communication and presentation – Part 1: General guidelines.
ISO 13374-3:2012 Condition monitoring and diagnostics of machines – Data processing, communication and presentation – Part 3: Communication.
ISO 13374-4:2015 Condition monitoring and diagnostics of machine systems – Data processing, communication and presentation – Part 4: Presentation.
ISO 13379-1:2012 Condition monitoring and diagnostics of machines – Data interpretation and diagnostics techniques – Part 1: General guidelines.

ISO 13379-2:2015 Condition monitoring and diagnostics of machines – Data interpretation and diagnostics techniques – Part 2: Data-driven applications.
ISO 13381-1:2015 Condition monitoring and diagnostics of machines – Prognostics Part 1: General guidelines.
ISO 17359:2018 Condition monitoring and diagnostics of machines – General guidelines.
ISO 18129:2015 Condition monitoring and diagnostics of machines – Approaches for performance diagnosis.
ISO 18434-1:2008 Condition monitoring and diagnostics of machines – Thermography-Part 1: General procedures.
ISO 18436-1:2012 Condition monitoring and diagnostics of machines – Requirements for qualification and assessment of personnel – Part 1: Requirements for assessment bodies and the assessment process.
ISO 18436-2:2014 Condition monitoring and diagnostics of machines – Requirements for qualification and assessment of personnel – Part 2: Vibration condition monitoring and diagnostics.
ISO 18436-3:2012 Condition monitoring and diagnostics of machines – Requirements for qualification and assessment of personnel – Part 3: Requirements for training bodies and the training process.
ISO 20958:2013 Condition monitoring and diagnostics of machine systems – Electrical signature analysis of three-phase induction motors.
ISO 22096:2007 Condition monitoring and diagnostics of machines – Acoustic emission.
ISO 29821:2018 Condition monitoring and diagnostics of machines – Ultrasound – General guidelines, procedures and validation.
MIL-HNDBK 217:1991 Military Handbook: Reliability Prediction Of Electronic Equipment, no longer issued.
NEMA MG-1:2016 Motor Generator Standard.
VDI 2056:1997 Assessment standards for mechanical vibrations of machines, no longer issued.

*This page intentionally left blank*

*Appendix A*

# Failure modes and root causes in the rotating electrical machines

Based on the machine structure shown in Figure 4.8.

| Sub-assembly | Component | Failure mode | Root cause | Early indicators of the fault |
|---|---|---|---|---|
| Enclosure | Heat exchanger | Failure of heat exchanger pipework | Defective material | Higher winding temperature |
| | | | Defective installation | Higher coolant temperature |
| | | | Corrosion | Moisture and lowered insulation resistance |
| | | | Vibration | Increased winding discharge activity |
| | | | Shock | Vibration |
| | | Failure of heat exchanger tubes | Defective material | |
| | | | Defective installation | |
| | | | Corrosion | |
| | | | Vibration | |
| | | | Shock | |
| | Electrical connections | Insulation failure of the connector | Defective material | Increased connector discharge activity |
| | | | Defective installation | |
| | | | Excessive dielectric stress | |
| | | | Excessive temperature | |
| | | Mechanical failure of connector | Defective material | Higher winding temperature |
| | | | Defective installation | Vibration |
| | | | Vibration | Altered machine performance |
| | | | Shock | |
| | Bushings | Insulation failure of bushing | Defective material | Increased bushing discharge activity |
| | | | Defective installation | |
| | | | Excessive dielectric stress | |
| | | | Excessive temperature | |
| | | | Vibration | |
| | | | Shock | |

*(Continues)*

(*Continued*)

| Sub-assembly | Component | Failure mode | Root cause | Early indicators of the fault |
|---|---|---|---|---|
| | | Mechanical failure of bushing | Defective material<br>Defective installation<br>Vibration<br>Shock | |
| | Bearings and seals | Loss of lubrication, grease or oil | Lubrication system failure<br>Lack of maintenance<br>Failure of seals | Higher bearing temperature<br>Bearing vibration<br>Bearing noise |
| | | Mechanical failure of the bearing element | Loss of lubrication<br>Vibration<br>Shock<br>Overload | |
| | | Excessive wear | Loss of lubrication<br>Vibration<br>Shock<br>Overload | |
| | | Electrically provoked failure of the bearing element | Shaft voltage<br>Vibration<br>Shock<br>Electrical fault | Higher bearing temperature<br>Bearing vibration-Bearing noise<br>Shaft current |
| Stator core | Frame | Vibration | Defective design<br>Defective installation<br>Vibration in the driven load or prime mover | Vibration |
| | | Circulating current | Defective design | Higher frame temperature |
| | Core | Core hot spot | Defective design<br>Defective manufacture<br>Contamination or debris<br>Excessive vibration<br>Circulating current<br>Excessive temperature | Higher core temperature |
| | | Core slackening | Defective design<br>Defective manufacture, faulty assembly<br>Excessive vibration<br>Component failure | Vibration |
| | Core clamp | Clamp hot spot | Defective design<br>Defective manufacture<br>Circulating current<br>Excessive temperature | Higher clamp temperature |
| | | Core clamp failure | Defective manufacture<br>Excessive vibration<br>Excessive temperature | Vibration<br>Higher clamp temperature |
| Stator winding | Conductors | Failure of conductor cooling hoses | Defective design<br>Defective manufacture<br>Excessive vibration<br>Excessive temperature | Vibration |

(*Continued*)

| Sub-assembly | Component | Failure mode | Root cause | Early indicators of the fault |
|---|---|---|---|---|
| | | Failure of sub-conductors | Excessive vibration | Vibration |
| | | | Shock | Increased winding discharge activity |
| | | | Component failure | Increased winding arcing activity |
| | | Failure of the conductor bar | Excessive vibration | Vibration |
| | | | Shock | Increased winding discharge activity |
| | | | Component failure | |
| | Insulation | Insulation failure of the main wall insulation | Defective design | Increased winding discharge activity |
| | | | Defective manufacture | |
| | | | Overtemperature | |
| | | | Excessive dielectric stress due to overvoltage | |
| | | | Excessive vibration | |
| | | | Excessive temperature | |
| | | Insulation failure of the sub-conductor insulation | Defective design | |
| | | | Defective manufacture | |
| | | | Overtemperature | |
| | | | Excessive dielectric stress, due to high $dV/dt$ | |
| | | | Excessive vibration | |
| | | | Excessive temperature | |
| | End winding | End winding insulation failure | Defective design | Vibration |
| | | | Defective manufacture | Increased winding discharge activity |
| | | | Excessive temperature | |
| | | | Excessive dielectric stress due to overvoltage | |
| | | | Excessive dielectric stress, due to high $dV/dt$ | |
| | | | Excessive vibration | |
| | | | Contamination or debris | |
| | | End winding movement or fretting | Defective design | |
| | | | Defective manufacture | |
| | | | Excessive vibration | |
| | | | Contamination or debris | |
| | | End winding contamination | Oil in enclosure | |
| | | | Moisture in the enclosure | |
| | | | Contamination or debris | |
| Rotor winding | Conductors | Failure of sub-conductors | Excessive vibration | Vibration |
| | | | Shock | Increased winding discharge activity |
| | | | Component failure | Increased winding arcing activity |
| | | | Excessive temperature | |
| | | Failure of conductor bar | Excessive vibration | Vibration |
| | | | Shock | Increased winding discharge activity |
| | | | Component failure | |
| | | | Excessive temperature | |

*(Continues)*

(*Continued*)

| Sub-assembly | Component | Failure mode | Root cause | Early indicators of the fault |
|---|---|---|---|---|
| | Insulation | Insulation failure of main wall insulation | Defective design | Increased winding discharge activity |
| | | | Defective manufacture | |
| | | | Overtemperature | |
| | | | Excessive dielectric stress due to overvoltage | |
| | | | Excessive vibration | |
| | | | Excessive temperature | |
| | | Insulation failure of sub-conductor insulation | Defective design | |
| | | | Defective manufacture | |
| | | | Overtemperature | |
| | | | Excessive dielectric stress, due to high $dV/dt$ | |
| | | | Excessive vibration | |
| | | | Excessive temperature | |
| | End winding | End winding insulation failure | Defective design | Vibration |
| | | | Defective manufacture | Increased winding discharge activity |
| | | | Overtemperature | |
| | | | Excessive dielectric stress due to overvoltage | |
| | | | Excessive dielectric stress, due to high $dV/dt$ | |
| | | | Excessive vibration | |
| | | | Excessive temperature-Contamination or debris | |
| | | End winding movement or fretting | Defective design | |
| | | | Defective manufacture | |
| | | | Excessive vibration | |
| | | | Contamination or debris | |
| | | End winding banding failure | Defective design | |
| | | | Defective manufacture | |
| | | | Overspeed | |
| | | | Overload | |
| | | | Excessive vibration | |
| | | | Excessive temperature | |
| | | | Contamination or debris | |
| Rotor body | Shaft | Shaft failure | Torsional vibration | Cracks located by NDT or run Down tests |
| | | | Shock loading | Vibration |
| | | | Overload | |
| | Rotor core and body | Core hot spot | Defective design | Higher core temperature |
| | | | Defective manufacture | |
| | | | Debris in core | |
| | | | Excessive vibration | |
| | | | Circulating current | |
| | | | Excessive temperature | |

(*Continued*)

| Sub-assembly | Component | Failure mode | Root cause | Early indicators of the fault |
|---|---|---|---|---|
| | | Core slackening | Defective design<br>Defective manufacture, faulty assembly<br>Excessive vibration<br>Core clamp failure | Vibration |
| | | Integrity failure of body or wedges | Defective design<br>Defective manufacture<br>Excessive vibration | Cracks located by NDT or run Down tests<br>Vibration |
| | Slip rings | Sparking | Defective maintenance | Increased brush-gear arcing activity |
| | | Overheating | Defective brushes | Increased brush wear |
| | | Damaged slip rings | Excessive temperature | Increased brush-gear temperature |
| | Commutator | Sparking | Defective maintenance | |
| | | Overheating | Defective brushes | |
| | | Damaged commutator | Excessive temperature | |
| | Brush-gear | Overheating | Defective maintenance | |
| | | Damaged brush-gear | Defective brushes<br>Excessive temperature | |

*This page intentionally left blank*

*Appendix B*

# Draft CM good practice guide, MCSA

## B.1 Introduction

### *B.1.1 What this series of guides is about*

- This is proposed to be the first of a series of the British Institute of Non-Destructive Testing (BINDT) Good Practice Guides that seeks to set out a standard to be followed by the users, practitioners and vendors of this technology for monitoring the condition of electrical machines using condition-monitoring techniques,
- This guide is currently in draft, under discussion and has not yet been issued,
- The objective is to help the users adopt the most appropriate technique for their requirement, and to apply it in a safe and an effective manner,
- It also aims to provide a framework for informed discussions between technology providers, practitioners, asset owners and operators, which informs condition-monitoring output end-users. This is so that the monitoring expectations of all parties can realistically be achieved, and the nature, reliability and specificity of results obtained, are aligned before commercial contracts for the work are agreed,
- This guide suggests that MCSA readings, taken regularly at perhaps 1 year intervals, can be used to monitor the integrity of a large electrical machine assets as proposed by ISO 17359 (2018) in the manner set out by ISO 20958 (2013),
- These good practice guides are intended as guides rather than a detailed technical manual.

### *B.1.2 What this particular guide is about*

This guide covers motor current signature analysis (MCSA) applied to electrical motors and generators.

## B.2 Overall description

Motor current signature analysis (MCSA) is an electrical condition-monitoring technique for detecting electrical and mechanical defects in rotating machines by making accurate measurements of the stator current and identifying and analysing the frequency components within this current.

The air-gap of an electrical machine is the clearance between a rotating rotor and the fixed stator core. The magnetic field of the machine crosses this air-gap and modulates the stator current, whether it is a motor or generator.

Any defect in the machine, which affects that air-gap magnetic field, will modulate the machine current signature and can be detected by measurement of those modulations. This is MCSA, which is performed using equipment such as shown in Figure B.1.

Various types of defects can be detected by MCSA for various types of machines, see Table B.1, including:

- Faulty air-gap eccentricity due to worn bearings of the machine or inaccurate manufacture,
- Unbalanced phase current caused by machine stator winding defects,
- Altered phase currents caused by the machine rotor winding damage, whether it is squirrel cage broken bars, such as Figure B.2, or defects in a traditional winding.

(a)

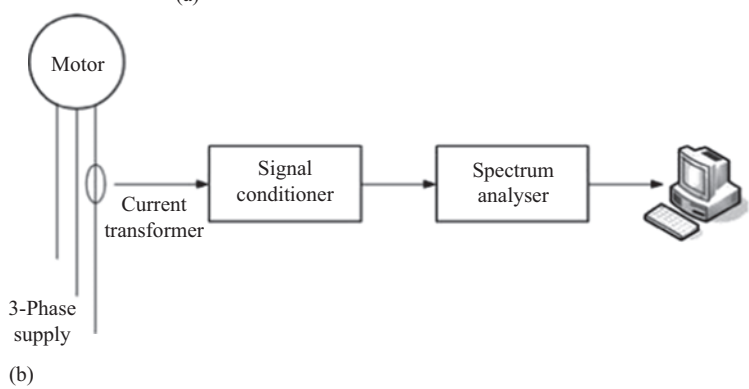


(b)

*Figure B.1 Typical MCSA set-up in the field: (a) measurements in the field and (b) MCSA data collection system*

*Table B.1 Typical air gap values for a range of machine types and MCSA applicability*

| **Machine type** | **Rating, MW** | **Air-gap size, mm** | **Applicability** |
|---|---|---|---|
| AC induction motors or generators | <0.1<br>0.1–3<br>>3 | 1–2<br>2–3<br>>4 | Applicable |
| AC synchronous machines | 0.1–3<br>3–50<br>>50 | 7–10<br>10–30<br>>30 | Applicable requiring careful analysis<br>Applicable but more care required<br>At the limit of MCSA applicability |
| DC machines | Various sizes and ratings | | Not yet considered for MCSA but could be applicable |

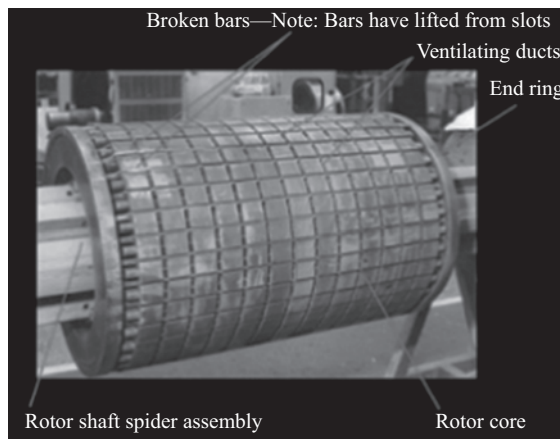


*Figure B.2 Type of fault that could be detected by MCSA ©IEEE*

The seriousness and growth rate of these defects can also be detected and measured against time by means of MCSA.

Information on the motor size/rating, voltage, current and whether it is single phase or three phase, is typically found on the motor plate that is fixed to the motor by the supplier. However, air-gap is rarely shown on such motor plates.

The method involves:

- Record details of the electrical machine being monitored,
- Take measurements on a section of cable supplying the machine, using current sensors around the cable, where the phases are separated and not encased in armouring,
- Obtain readings of frequency side-bands present in the current signal,
- Record those readings and compare with historical results.

## B.3 Scope

MCSA is applicable to all rotating electrical machines, although it is most often used on AC machines.

DC machines pose greater MCSA measurement and signal interpretation issues and at present this is confined to university use.

The ability of MCSA to detect defects is dependent on the variations in the magnetic field in the machine air-gap.

For any given magnitude of disturbance to the magnetic field, the shorter the air-gap the more intense the change in the magnetic field intensity associated with this disturbance, and hence greater the amplitude and the broader the bandwidth of the modulations.

Therefore, the usefulness of MCSA to different machines can be classified as follows:

- MCSA has been most effective and most widely applied to machines with short air-gaps, 1–4 mm, such as squirrel cage induction machines,
- Machines with larger air-gaps, 4–7 mm, such as wound rotor induction machines or 4 and multi-pole synchronous generators also display some modulation of the stator current in the presence of defects. The MCSA effects are smaller but can still be detected,
- MCSA has not been as effective for synchronous machines with larger air-gaps $> 7$ mm, such as large 2- and 4-pole turbo-generators, where the modulation of stator current by defects is more difficult to extract,
- Motors driven by converters display a much broader bandwidth of signals, which may still reveal defects but more sensitive measurement equipment may be required, and interpretation of the results requires a greater depth of expertise in the analyst,
- MCSA could also be used on DC motors but more sensitive measurement equipment may be required, and interpretation of the results requires a greater depth of expertise in the analyst. The use of MCSA on DC motors is not generally a commercially available service yet,
- MCSA is applicable to single phase, 3-phase or multiphase machines.

## B.4 Expected outputs

MCSA is a simple survey technique using equipment such as shown in Figure B.1 to look for the machine defects by the stator current spectral analysis. The measurement of stator current is not made directly but in the secondary of a current transformer (CT) or Rogowski coil.

The data presented is a stator current spectrum like Figure B.3. This shows the energy present in the stator current at each frequency. Faults or defects show up as peaks on this spectrum, which are located either side of the peak that corresponds to the main supply frequency. These peaks each side, which are referred to as ‘side-bands’, are separated from the supply frequency peak by the fault frequency. So, for example, in a

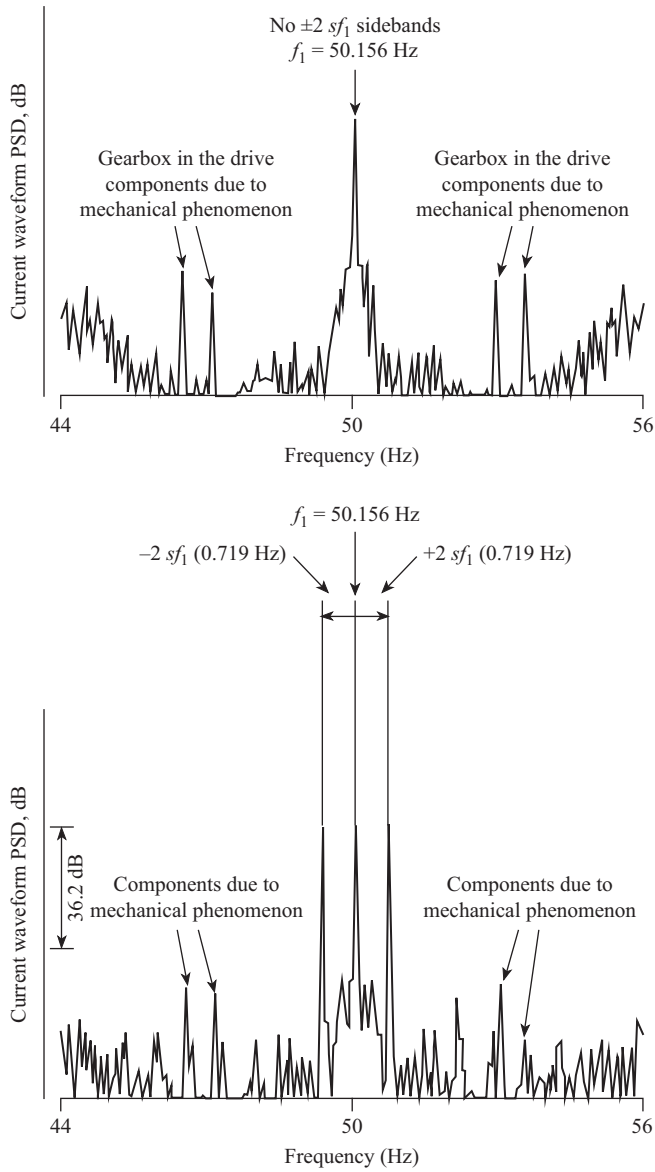


*Figure B.3 Typical MCSA spectra for a defective induction motor. Taken from Thomson et al. (2001)*

system fed by a 50 Hz supply frequency, a fault with a characteristic frequency of 1 Hz will show up as a pair of side-bands at 50 ± 1 Hz, i.e. at 49 and 51 Hz. Figure B.3 above shows a main peak at 60 Hz with side-bands at 58.5 and 61.5 Hz, i.e. indicating the presence of a phenomenon with a fault frequency of 1.5 Hz.

An appropriately trained and experienced operator can distinguish between different types of machine defects by spectral analysis of the machine stator current, matching the frequencies detected against the characteristic frequencies of known defects, indicating the likely sources of these effects.

If MCSA spectral analysis detects particular stator current frequency components, seen as peaks on the spectrum, an estimation of the defect magnitude can be made by comparing the height of the peaks at the fault frequency with the height of the peak corresponding to the fundamental supply frequency.

The energy associated with faults is generally very small in comparison with the fundamental frequency, perhaps of the order of one thousandth of the magnitude. A linear plot of the spectrum would make the peaks corresponding to the fault frequencies so small as to be virtually undetectable. By using a logarithmic scale, the smaller features are effectively magnified in comparison with the larger peaks, making it much easier to identify them. The logarithmic scale is also useful as a more convenient measure for comparing the relative heights of the fault peaks to the fundamental supply frequency, with the difference being expressed in decibels (dB). For example, in Figure B.3 above, the fault peak at 58.5 Hz has a value of about −35 dB compared to the height of the fundamental frequency which is positioned by definition at 0 dB. The peak at 61.5 Hz is about −45 dB. Note that the use of this scale means that a taller peak (which indicates more energy at that frequency, and therefore a bigger phenomenon, i.e. typically a worse fault), has a smaller dB rating.

The magnitude of this dB figure can be used to detect and assess the severity of particular faults. For example, Table B.2 below shows rules of thumb for assessing the severity of rotor bar problems. Notice how a larger dB figure corresponds to a BETTER condition of the motor.

When a problem situation is identified, further scheduled MCSA testing may reveal the rate of further deterioration and guide when shut-down and repair is needed.

*Table B.2 Typical MCSA signal values*

| Category | $I_{line}/I_{polepass}$ | Assessment | Action |
|---|---|---|---|
| 1 | 60 dB or more | Excellent | None |
| 2 | 54–60 dB | Good | None |
| 3 | 48–54 dB | Moderate | Continue surveys, trend |
| 4 | 42–48 dB | Rotor bar crack developing or high resistance joint(s) | Reduce survey interval, trend closely |
| 5 | 36–42 dB | Two bars likely cracked/broken or high resistance joint likely | Perform vibration tests to confirm the problem source |
| 6 | 30–36 dB | Multiple cracked/broken rotor bars or end rings indicated | Overhaul asap |
| 7 | Less than 30 dB | Multiple cracked/broken rotor bars or end rings very likely; severe problems throughout | Overhaul or replace as soon as possible |

## B.5 Controls and capabilities

Surveying equipment should typically be able to:

- Measure machine stator currents indirectly using a CT or Rogowski coil of 0.1 mA to 5 A,
- Analyse the current signature in the frequency range 1–1 000 Hz,
- Provide appropriately fine spectral resolution (spacing between adjacent spectral lines). A spacing of 0.1 Hz or less is generally required in order to detect problems such as damaged rotor bars.
- Present and display frequency spectra of this range on a screen,
- Be able to download such spectra to a computer, printer and storage system for long-term trending,
- Optionally the equipment should be capable of carrying and implementing the analysis software to implement present and upcoming defect detection algorithms, based on the amplitude of specific current spectra peaks.

## B.6 Issues

The following issues should be considered:

There are a large number of sources of electrical machine stator current modulation, which may be due to acceptable machine construction irregularities or the nature of the driven load. Therefore, machine defect investigation should always be preceded by clear understanding of the current spectrum from a healthy motor, preferably of the same rating, voltage, number of poles and load;

Electrical machines can be supplied from LV and MV bus-bars, so measurements made on one motor can be affected by conducted interference from other machines connected to the same bus-bar, resulting in distortions on the voltage waveform. However, this is not a major problem.

Electrical machines fed by variable-speed drives will contain many high frequency harmonics in their stator current, as a result of drive switching. The MCSA method could still be used in these cases but great care needs to be taken. At this time it is generally best to avoid conventional MCSA on inverter driven equipment; techniques such as mode-based voltage and current (MBVI) systems which automatically compensate for distorted voltage waveforms are more appropriate in these situations.

## B.7 How to apply MCSA

Typically, MCSA is applied to higher criticality equipment. Portable/hand-held systems are typically used, such as shown in Figure B.1:

- On a regular periodic frequency, typically annually on equipment that is not known to be encountering particular problems,

  - As a one-off, to detect whether problems have been created after a significant event, for example:
  - Exceptional load changes in service due to unusual operational conditions, e.g. unusual starts or stops under load,

- On a tighter periodicity after a known weakness has been observed, for example:
  - Because of failure in a similar machine,
  - Because of known machine load variation problems due to operational need,
  - Survey with increasing frequency if increasing fault signals are detected,
- The person doing the test needs to be familiar with how the equipment should be used and possible sources of imbalance signals,
- Datasets should be trended by maintaining a library of results.

## B.8 Data communication

There is as yet no standard data format but typical graphs showing frequency-domain current graphs from individual machine phases in the form shown in Figure B.3 are widely used and displayed in the References.

Tabular output of overall assessments of each machine, typically showing the dB drop between fundamental frequency peak and the peaks corresponding to the phenomenon of interest, which is most commonly the pole pass frequency, indicating rotor asymmetry that is associated with rotor problems.

Where an external consultant has carried out the MCSA testing, a written report including the data, graphs, interpretation of the results and recommended action may be expected.

Underlying data may be presented in a machine readable form such as CSV files or in a proprietary format allowing comparison over time.

## B.9 Data interpretation

The main indications of machine damage are the current spectra side-bands and the magnitudes of these side-bands, which are of predictable frequency, indicate the degree of damage. Some publications have provided very detailed descriptions of the expected side-band frequencies, see Table 9.2.

## B.10 Safety

Surveys will be carried out on operating machines in an industrial, power station or factory environment and therefore there is the potential for risk of electric shock or arc-flash if working in or near to open electrical cabinets.

Connection to the motor is made via low-voltage CTs or Rogowski coils wrapped around the machine stator winding phase connection cables. So, there should be no direct exposure to high voltage or current here. However, care must be taken so that:

- If connection is being made using the secondary windings of plant instrument current transformers, as connections could interfere with the machine protection system,
- In the case of large MV machines > 1 MW, prolonged human exposure to local EMC due to electromagnetic fields locally associated with the machine supply conductors and cables may be a risk,
- Therefore, local safety rules must be obeyed at all times,
- Always maintain safety distances from the energised conductors.

## B.11 Skills, competence and training

Three distinct roles can be identified in the MCSA process – those of operator, interpreter and analyst.

- Operator – the objective is to take a correctly representative reading.
  - Operators should be able to perform a range of pre-defined generally simple measurement or monitoring activities in accordance with established procedures.
  - When making measurements on operating machines in an industrial, power station or factory environment, it is recommended that some competency training in that environment be undertaken with the provision of a safety passport or similar,
- Interpreter – the objective is to provide useful advice when the situation is simple and clear cut (some of these aspects may be done automatically by the test device or other software). The interpreter should:
  - Be able to interpret and identify predefined defects and associated signatures.
  - Be able to interpret and evaluate the test results from the routine analysis in accordance with pre-defined guidelines.
  - Have a basic level of ability to interpret data and identify good and bad measurements.
  - Be familiar with the type of test equipment being used
- Analyst – objective is to provide the most useful information from the available data. The analyst should have:
  - The ability to acquire and understand new information, both regarding the data captured and the nature of the asset being tested,
  - The ability to summarise the information in the form of an assessment of the risk associated with the equipment under test, and a recommendation for appropriate action.

- A broad understanding of the underlying principles of the MCSA concept and the specific MCSA equipment. In addition, the analyst should be capable of digesting information about the rotating machinery, and understanding likely failure modes or fault types. If in-depth interpretation of data is required, the analyst should be thoroughly familiar with the material covered by the publications below.

## B.12 Taking readings

When planning and undertaking electrical condition monitoring activities regardless of whether these activities are intrusive or non-intrusive there are three key risk areas that should be addressed:

- Risk of injury and or long-term illness to person(s) undertaking the condition monitoring activity,
- Risk of damage to the plant or equipment subject to the condition-monitoring activity,
- Risk of damage to the condition monitoring equipment being used.

Failure to address the hazards and associated risks of a specific condition monitoring activity could potentially result in harm to people, damage to plant or equipment, business interruption, organisational reputational damage, damage to condition monitoring equipment and the subsequent costs for repair or replacement. The hazards presented to person(s) when undertaking condition monitoring activities are classified into two categories:

- General safety hazards, associated with the working area and environment, e.g. slips, trips and falls, vehicle movements, working at height, working outside and lone working,
- System-derived hazards, associated with the process, e.g. electricity, steam, gas, water, chemicals and stored energy. Most organisations use safe systems of work and working practices to manage risks to person(s) from both general safety and system derived hazards. Safe systems of work can encompass training and competence requirements, requirements for risk assessments and method statements prior to work, setting to work procedures, application of safety rules for isolation and subsequent work or testing of plant items and returning equipment to service procedures. It is recommended that electrical condition-monitoring tasks are planned and undertaken in accordance with a suitable safe system of work.

Through inappropriate application or incorrect set-up of electrical condition monitoring equipment, it is possible to damage plant or equipment subject to the activity.

This risk exists predominantly when the tool or technique applied is intrusive, for example, the injection of excessive current or voltage into a piece of electrical equipment can lead to component, conductor or electrical insulation system damage.

Similarly, it may also be possible to damage the condition monitoring equipment through incorrect application or set-up, for example, undertaking a voltage measurement with equipment that is not rated for that voltage.

It is therefore essential that prior to undertaking a condition monitoring activity, the specific application is assessed and deemed appropriate. Plant or equipment under test and the test equipment must be suitably rated for the activity. When setting up the monitoring equipment, test connections and test settings, for example, injection voltages in insulation resistance tests, should be checked and confirmed as correct. The function of any in-built protection measures, such as overloads, should also be confirmed operational prior to commencing. For more complex condition monitoring activities, the preparation of a step-by-step procedure, detailing the specific equipment connections, settings and test durations may be appropriate.

*This page intentionally left blank*

*Appendix C*

# Electrical machines, drives and condition monitoring timeline

**Key Discoveries**

*Seminal books*

Significant papers

Refer to Drury (2009), Mills (2010) and Chung *et al.* (2016)

| Year | Originator | Discovery | Ref |
|---|---|---|---|
| 1820 | **Oersted** | **Compass needle detects magnetic field around conductor carrying current.** | |
| 1821 | **Faraday** | **Described electro-magnetic field and built two devices to produce the rotation** | |
| 1824 | **Arago** | **Rotation of magnet induces copper disc rotation** | |
| | **Babbage and Herschel** | **Rotation of conducting disc induces magnet rotation, inverse of Arago and simple precursor of the induction motor** | |
| 1831 | **Faraday** | **Using induction ring discovers electromagnetic induction** | |
| 1832 | **Pixii** | **First magneto-electric machine** | |
| 1838 | **Lenz** | **Discovered that a DC generator could also behave as a motor** | |
| 1845 | **Wheatstone and Cooke** | **Patented use of electromagnets instead of permanent magnets** | |
| 1870 and 1873 | **Gramme** | **Developed the ring armature for a DC generator then demonstrated it developing power and transmitting it over 1 km to a DC motor** | |
| 1879 | **Bailey** | **Developed a motor which replaced Babbage and Herschel rotating magnets by a rotating magnetic field produced by switching DC electro-magnets, precursor of the induction motor** | |
| 1885 | **Ferraris** | **Demonstrated a rotating magnetic field by phase-separated single-phase AC flowing into space-quadrature windings, precursor of the induction motor** | |
| 1886 | **Tesla** | **Developed first polyphase AC induction motor** | |
| | Hopkinson | Paper: 'Dynamo-electric machinery'<br>First analysis of electrical machine design for a DC machine | Proc. Royal Society, London, UK |

*(Continues)*

(*Continued*)

| Year | Originator | Discovery | Ref |
|---|---|---|---|
| 1889 and 1890 | **Ferranti** | **World's first AC central electric power station at Deptford, London, using slow-speed reciprocating steam engines to drive LV AC synchronous generators, supplying single-phase transformers connected by 10 kV AC HV cables to central London** | |
| | **Dobrowlsky** | **Developed first 3-phase AC induction motor working independently from Tesla.**<br>**Then, developed a 3-phase AC induction motor with a polyphase slip-ring rotor connection to resistors for starting control** | |
| 1896 | **Ward Leonard** | **Coupled 2 DC machines though a DC Link to produce a variable speed system** | |
| | | Paper: 'Volts vs Ohms, Speed regulation of electric motors'<br>First proposal for varying the speed of electric motors | Proc. AIEE |
| 1904 | **Kramer** | **Developed 2 back-to-back AC/DC motor sets to vary the system frequency, similar to Ward Leonard**<br>**Forerunner of modern current and voltage source converters** | |
| 1909 | **Various industrial companies** | **Mercury arc rectifier, vacuum-tube rectifier and thyratron** | |
| 1911 | **Schrage** | **Developed a system based on an induction motor with a rotating commutator to adjust the rotor winding frequency and vary motor speed.**<br>**Used in locomotives, steel-mills, cement-mills and power stations** | |
| 1921 | *Walker* | *Book: The Diagnosing of Trouble in Electrical Machines* | Library Press, UK |
| 1923 | **Number of inventors** | **Developed ignitron, leading to mercury arc rectifier and thyratron, enabling controlled rectification of AC to DC**<br>**Used to control DC machine voltage, enabling the Ward Leonard philosophy without additional rotating machines** | |
| 1927 | de Pistoye | Paper: 'Les pertes parasites aux extrémités du stator des machines à grand pas polaire, et les moyens de les reduire<br>(Parasitic losses at stator ends of large pole-pitch machines and their means of reduction) | Revue Générale de l'Élec-tricité, France |
| 1930 | **Number of inventors** | **Established inversion between AC/DC systems, by means of switched capacitors, using mercury arc rectifiers and thyratrons, initially switched once or twice per cycle, effectively forced commutation by static commutators** | |
| 1931 | **Number of inventors** | **Direct AC/AC conversion by the cycloconverter using static commutation with mercury arc rectifiers or thyratron switches** | |

*(Continues)*

(*Continued*)

| Year | Originator | Discovery | Ref |
|---|---|---|---|
| 1932 | **Nyquist** | **Nyquist stability control criterion developed** | |
| 1935 | **Schwarz** | **Patented variable-speed AC machine, based on a Schrage motor with rotating commutator controlled by a parallel, shunt-connected or Nebenschluss (NS) transformer and limited-angular-range induction regulator.**<br>**Produced at Schorch, Germany, then Laurence, Scott & Electromotors, UK as an NS variable-speed motor.**<br>**Widely used on steel-mills, water pumps and power station auxiliaries** | |
| 1938 | **Bode** | **Bode stability control criterion developed** | |
| 1949 | *Langlois-Berthelot* | *Book: Étude électromagnétique générale des machines électriques (Electro-magnetic Machines)* | Eyrolles, France |
| 1950 | **Number of inventors** | **Introduction of the silicon-controlled rectifier (SCR) power switch, replacing bulky, inefficient mercury arc rectifiers by thyristors, initially switching once or twice per cycle but with the prospect of increased switching speeds. Thus a static commutator.**<br>**Used in steel-mills, cement-mills and power stations** | |
| 1950 | *Jordan* | *Book: Geräuscharme Elektromotoren*<br>*(The Low Noise Electric Motor)* | Springer Verlag, Germany |
| 1951 | *Concordia* | *Book: Synchronous Machines Theory and Performance* | J Wiley, USA |
| 1955 | *Moullin* | *Book: Electro-magnetic Principles of the Dynamo* | Oxford, Clarendon Press, UK |
| 1956 | Erdelyi *et al.* | Paper: 'Vibration modes of induction motors'<br>First thorough analysis of electrical machine vibration modes | Trans ASME, USA |
| 1957 | **Shockley–Moll** | **Invention of power drive thyristor and firing circuits** | |
| | **Number of inventors** | **Back-to-back reversing of a DC drive using a thyristor bridge with forced static commutation, switched twice per cycle.**<br>**Static commutator will eventually render rotating commutators obsolete**<br>**Used in locomotives** | |
| 1959 | Carpenter | Paper: 'Surface integral methods of calculating force on magnetized iron parts' | Proc. IEE, UK |
| | Hammond *et al.* | Papers: 'The calculation of the magnetic field of rotating machines:<br>Part 1: The field of a tubular current,<br>Part 2: The field of turbo-generator end-windings,<br>Part 3: Eddy currents induced in a solid slab by a circular current loop,<br>Part 4: Approximate determination of field and losses associated with eddy currents in conducting surfaces,<br>Part 5: Field in end region of turbo-generators and eddy-current loss in the end plates of stator cores' | |

*(Continues)*

(*Continued*)

| Year | Originator | Discovery | Ref |
|---|---|---|---|
| 1962 | *Hague* | *Book: Principles of Electromagnetism Applied to Electrical Machines* | Dover, USA |
| 1963 | **Standard** | Establishment of the first vibration standards Technical Committee | ISO TC108 |
| 1964 | Jordan *et al.* | Papers:<br>'Messungen des Schlupfes von Asynchronmaschinen mit einer Spule<br>(Measurements of the slip of induction machines using a coil)'<br>'Wellenflusse infolge con schwankungen des Luftapalteitwertes (Harmonic fluxes consequent on air-gap fluctuations)'<br>First application of current and flux measurements to induction machine condition monitoring | Electrotechnik und Zeitschrift, Germany |
| 1965 | *Alger* | *Book: The Nature of Induction Machines* | Gordon and Breach, USA |
| 1967 | *Stafl* | *Book: Electrodynamics of Electrical Machines* | Academia, Czechoslovakia |
| | *Jones* | *Book: The Unified Theory of Electrical Machines* | Butterworth, UK |
| 1968 | Binns | Paper: 'Cogging torques in induction machines' | Proc. IEE, UK |
| 1971 | Albright | Paper: 'Inter-turn short circuit detector for turbine generator rotor windings'<br>First application of electrical measurement to turbo-generator condition monitoring | IEEE Trans, USA |
| 1973 | Carson *et al.* | Paper: 'Immediate warning of local over-heating in electrical machines by the detection of pyrolysis products'<br>First application of chemical measurement to turbo-generator condition monitoring | IEEE Trans, USA |
| 1974 | Dickinson | Paper: 'IEEE Reliability Working Group, Report on reliability of electric plant'<br>First thorough analysis of electrical machine reliability from measured steady-state failure rate, $\lambda = 1/MTBF$ | IEEE Trans, USA |
| | Kamerbeek | Paper: 'Torque measurements on induction motors using Hall generators or measuring windings'<br>First application of torque measurement to induction machine condition monitoring | Phillips Technical Review, Netherlands |
| 1975 | **General Electric** | **Invention of new fast-acting semiconductor devices** | |
| 1978 | Jufer *et al.* | Paper: 'Influence d'une rupture de barre ou d'un anneau sur les characteristiques externes d'un moteur asynchrone à cage<br>(Influence of a cage bar or ring break on the external characteristics of a cage induction motor)'<br>First application of current measurement to induction machine condition monitoring, the forerunner of MCSA | SEV/VSE Bulletin, Switzerland |

*(Continues)*

(*Continued*)

| Year | Originator | Discovery | Ref |
|---|---|---|---|
| 1979 | Kurtz *et al.* | Paper: 'In-service partial discharge testing of generator insulation'<br>First application of partial discharge measurement to turbo-generator condition monitoring | IEEE Trans, USA |
| 1980 | **Scharf and Plummer** | **Invention of the inverse gate bipolar transistor (IGBT) power switch** | |
| | **Inventors and Commercial Companies** | **Replacement of thyristors in drive bridges by faster, cheaper, silicon switches including the insulated gate bipolar transistors (IGBT), offering greatly increased switching speeds, way above once or twice per cycle**<br>**Development of PWM IGBT voltage source converters (VSC) drives and early controllers, static commutators enabling simple 1-, 2- and 4-quadrant control of electrical machines, rendering earlier rotating commutators obsolete** | |
| | Brandl | Paper: 'Forces on the end windings of AC machines'<br>First consideration of end winding problems | Brown-Boveri Review, Switzerland |
| | Joyce *et al.* | Paper: 'Status of evaluating the fatigue of large steam turbine generation caused by electrical disturbances'<br>First identification of torsional vibration as a turbo-generator failure mode | IEEE Trans, USA |
| | Penman *et al.* | Paper: 'Protection strategy against faults in electrical machines'<br>First application of flux measurement for induction machine condition monitoring | Proc. IEE, UK |
| | Lawrenson *et al.* | Paper: 'Variable-speed switched reluctance motors'<br>First introduction of the switched reluctance machine | |
| | Williamson *et al.* | Paper: 'Field analysis for rotating induction machines and its relationship to the equivalent circuit method' | |
| 1981 | **Inventors and commercial companies** | **Widespread introduction of PWM IGBT VSC drives to feed both kW and MW range motors to control machine speed in industrial processes** | |
| | *Hammond*<br>*Yang* | *Book: Energy Methods in Electromagnetism*<br>*Book: Low Noise Electric Motors* | Oxford Clarendon Press, UK |
| | Lloyd *et al.* | Paper: 'Monitoring debris in turbine generator oil'<br>First application of oil debris measurement to turbo-generator condition monitoring | Wear, UK |
| 1982 | Barker *et al.* | Paper: 'A decade of experience with generator and large motor reliability'<br>Retrospective of large machine reliability experience from 1970–82 | CIGRE |
| | Rogers | Paper: 'Optical temperature sensor for high voltage applications'<br>First application of fibre optics to electrical condition monitoring | Applied Optics, UK |

*(Continues)*

(*Continued*)

| Year | Originator | Discovery | Ref |
|---|---|---|---|
| 1983 | Hargis *et al.* | Paper: 'The detection of rotor defects in induction motors'<br>First to show induction machine faults can be detected by measuring current, speed or vibration | Proc IEE, UK |
| 1986 | **Many inventors and commercial companies** | **Development of digital controllers for PWM IGBT VSC drives supplying electrical machines, including direct torque control and flux control**<br>**Sophisticated static commutator controllers enabling full 4-quadrant control of electrical machines. Widely used on locomotives, trams, electrical multiple units, paper-mills, steel-mills, water pumps, cement mills and power stations** | |
| | Seinsch | Paper: 'Erkennung und Diagnose von anomalen Betriebsbedingungen und/oder Fehlern in rotierenden elektrischen Maschinen<br>(Detection and diagnosis of abnormal operating conditions and/or faults in rotating electrical machines)' | Schorch Berichte, Germany |
| 1987 | *Tavner et al.* | *Book: Condition Monitoring of Rotating Electrical Machines*<br>*Based on the work of Jordan, Jufer, Brandl, Joyce, Dickinson, Penman, Lloyd, Barker, Hargis, Rogers, Ran and Seinsch above* | RSP, UK, Ed 1, 1987<br>IET, UK, Ed 2 2008, IET, UK, Ed 3, 2019 |
| 1989 | *Stone et al.* | *Book: Electrical Insulation for Rotating Machines: Design, Evaluation, Aging, Testing, and Repair*<br>*Developing work of Albright, Carson, Kurtz and Stone above* | EPRI, USA, Ed 1, 1989<br>IEEE, USA, Ed 2, 2014 |
| 1990 | **Many commercial companies** | **Digital-controlled PWM IGBT VSC drives supplying electrical machines are deployed in all energy, process, manufacturing and transport industries using advanced controllers adapted for specific applications** | |
| | Geary *et al.* | Paper: 'Towards improved calibration in the measurement of partial discharges in rotating machinery'<br>First attempt to calibrate partial discharge measurements to indicate insulation faults | IEEE Trans, USA |
| 1991 | MIL-HNDBK 217 | *Military Handbook: Reliability Prediction Of Electronic Equipment* | Department of Defense, USA |
| | Mellor *et al.* | Paper: 'Lumped parameter thermal model for electrical machines of TEFC design'<br>First application of thermal modelling and temperature measurement to induction machine condition monitoring | Proc IEE, UK |
| 1992 | Tandon *et al.* | Paper: 'Comparison of vibration and acoustic measurement techniques for the condition monitoring of rolling element bearings'<br>First application of vibration and acoustic measurement to rolling element bearings | Tribology Int, USA |

*(Continues)*

(*Continued*)

| Year | Originator | Discovery | Ref |
|---|---|---|---|
| 1993 | *Vas* | *Book:, Parameter Estimation, Condition Monitoring and Diagnosis of Electrical Machines*<br>*Based on the work of Jordan, Jufer, Stafl, Jones, Penman, Hargis, Seinsch above and the development of digital controlled VSCs* | Oxford University Press, UK |
| 1994 | Mayes | Paper: 'Use of neural networks for online vibration monitoring'<br>First application of neural networks to turbo-generator vibration condition monitoring | Proc IMechE, UK |
| 1995 | Filippetti *et al.* | Paper: 'Neural networks aided on-line diagnostics of induction motor rotor faults'<br>First application of neural networks to induction machine electrical condition monitoring | IEEE Trans, USA |
| | Thorsen *et al.* | Paper: 'A survey of faults on induction motors in offshore oil industry, petrochemical industry, gas terminals, and oil refineries'<br>Comprehensive survey of reliability of electrical machines across an industry | IEEE Trans, USA |
| 2000 | **Number of commercial companies** | **First Schottky SiC diode to the market** | |
| 2001 | Benbouzid *et al.* | Paper: 'A simple fuzzy logic approach for induction motors stator condition monitoring'<br>First application of fuzzy logic to induction machine condition monitoring | IEEE Trans, USA |
| | Thomson *et al.* | Paper: 'Current signature analysis to detect induction motor faults'<br>First full exposition of motor current signature analysis (MCSA) for induction machine condition monitoring,<br>Based on the work of Jordan, Jufer, Penman and Hargis above | IEEE Industry Appl Mag, USA |
| | Trutt *et al.* | Paper: 'Detection of AC machine winding deterioration using electrically excited vibrations'<br>First exposition of vibration measurement for induction machine winding condition monitoring,<br>Based on the work of Jordan, Erdeleyi, Binns, Williamson and Brandl above | IEEE Trans, USA |
| 2005 | Nandi *et al.* | Paper: 'Condition monitoring and fault diagnosis of electrical motors – a review'<br>Retrospective of machine condition monitoring experience from 1979 to 2005 | IEEE Trans, USA |
| 2007 | Levi *et al.* | Paper: 'Multiphase induction motor drives – a technology status review'<br>First full review of the design and application of multi-phase induction machines. | Proc IET, UK |
| 2009 | *Drury* | *Book: The Control Techniques Drives and Control Handbook* | IET, UK |
| 2010 | **Number of commercial companies** | **Application of SiC, MOSFETs, JFETs, BJTs and GaN power devices to VSDs** | |
| | Yang and Ran *et al.* | Paper: 'Condition monitoring for device reliability in power electronic converters: a review'<br>First retrospective of power electronics condition monitoring | IEEE Trans, USA |

*(Continues)*

(*Continued*)

| Year | Originator | Discovery | Ref |
|---|---|---|---|
| 2013 | Krause *et al.* | *Book: Analysis of Electric Machinery and Drive Systems*<br>*Based on the work of Jordan, Hague, Alger, Stafl, Jones, Jufer, Seinsch and Williamson above* | IEEE Power Engineering Series, 4th Ed. USA |
| 2015 | **Number of commercial companies** | **Cost reduction of wide band-gap power devices**<br>**Improved performance of SiC power devices**<br>**Intelligent power stacks** | |
| 2016 | Chung *et al.* | *Book: Reliability of Power Electronic Converter Systems* | IET, UK |
| 2019 | Moses *et al.* | *Book: 'Electrical Steels – Vols 1 and 2'* | IET, UK |

# Index


accelerometers 124, 128–9, 184, 191–2
AC machines
  asynchronous/induction 28–33
  synchronous 26–8
ageing of insulation 50
  electrical ageing 52
    general 52
    partial discharges 52
    surface tracking and moisture absorption 52–3
    transient voltages 53–4
  environmental ageing 54–5
  mechanical ageing 54
  synergism between ageing stresses 55
  thermal ageing 51–2
aggregate failure rate 85–6
air-gap search coils 212–16, 220
aliasing 101–2
analogue-to-digital conversion (ADC) 139
analyst 334
ANNs (artificial neural networks)
  supervised learning through 317–20
artificial intelligence (AI) techniques 10, 303
  deep learning with big data 322–4
  expert systems 309–12
  fuzzy logic 312–15
  machine learning using ANNs
    supervised learning through ANN 317–20
    unsupervised learning 320–2
  MBVI system 326–7
    and AI 327–9
  and ML 339–40
  multi-parameter monitoring 305–9
  systems incorporating AI 324–6
assembly structure 87, 93
  distribution of failures 91–3
asset management 297–301
asynchronous machine 31
auto-correlation function 105
availability, definition 79
axial flux monitoring technique 229
axial leakage flux: *see* shaft flux

back-propagation (BP) algorithm 317, 319
bearings
  current discharges 258–61
    detection 261–3
  damage caused by shaft voltages 75
  failure rates 91–2
  faults 73–5
  lubrication oil analysis 169–73
  response 190
    rolling element bearings 190–2
    sleeve bearings 192–3
  selection criteria 73–5
  types 43–7
big data, deep learning with 322–4
bitumen-based insulation 56
Boolean logic 313
breakdown maintenance 7
British Institute of Non-Destructive Testing (BINDT) 335
brush-gear 47
  fault detection 210
  materials 48
brushless doubly-fed machine (BDFIM) 36–7

bulk measurement 149–51
bus-bars 47
bushings, insulation failures 72–3

capacitance and dissipation factor measurement 266–7
capacitive coupling method 245–6
carbon brushes 290
cause-and-effect diagram 81, 87
cepstrum analysis 108
Chattock potentiometer 276–7
chemical and wear analysis 338
circulating current measurement 216–20
commutators 47
comprehensive monitoring 339
condition-based maintenance (CBM) 285, 288
  advantage of 287
  cost–benefit analysis of condition monitoring for 296–7
  signals and data for 288–90
  targeted monitoring 290–2
condition monitoring
  definition of terms 78–80
connection faults 72
connections: *see* electrical connections
construction of electrical machines 43–50
  connections and heat exchangers 47
  enclosures 46
  materials used 48
  rotors and windings 45–6
  stator core and frame 44
  stator windings 44–5
contamination 54
  insulation 60–1
control in-loop machine fault detection 269–72
convolutional neural network (CNN) 320
coolant systems 156, 158, 164–6
  blocking 67, 73
  heat exchangers 47
  leaks 63–5, 73
core monitors 158–62
correlation analysis 105–7
cost-effectiveness 9
cross correlation function 105–7
current monitoring 338

data acquisition 139–41
data collector 333
data sampling
  aliasing 101–3
  discrete Fourier transform (DFT) 100
  time averaging 110–11
data storage 98
DC machines 25–6
DC motors 45
  construction 43
  rotor winding faults 71
debris measurement
  lubrication oil analysis 169–73
debris sensitive detector 136
declarative knowledge 310
deep belief network (DBN) 323–4
deep learning with big data 322–4
definition of terms 78–80
delamination of insulation 56–7
digital processors 2
digital relays 3
digital signal processors (DSP) 10, 149
discharge-bearing current, detection of 261–2
discharge detection, background to 239–41
discharge locator (DL) 249
discharge pulses 245
discrete Fourier transform (DFT) 100, 111
displacement transducers 124–7
doubly fed and variable-speed drive machines 35–7
doubly-fed induction machine (DFIM) 36–7
duration of the failure sequence 79, 81

early discharge detection methods
  capacitive coupling method 245–6
  earth loop transient method 244–5

insulation remanent life 248
RF coupling method 241–4
wide-band RF method 246–8
earth leakage faults on-line 211–12
earth loop transient method 244–5
EHV isolation 149
El CID 275–7
electrical ageing, insulation 52
electrical connections 47
faults 72–3
electrical discharge activity 388
electrical insulation
contamination 60–1
degradation 153–4
ageing mechanisms 50–5
detectability 154–8
detection methods 158–69
failure modes 55–71
bushings 72–3
rotor windings 71–5
stator windings 56–67
root causes of faults 61–7
rotor windings 45–6
stator windings 44–5
thermal properties 39–40
electrical machine protection systems 3
electrical machine reliability 77
electrical machines 1–2, 5, 17
drives and condition monitoring timeline 383–90
power-to-weight ratio of 2
sources of vibration in 175
structures and types 18–25
electrical protective relay, function of 2
electricity 1
electric motors 1
electromagnetic instrumentation 132–6
electromagnetic interference (EMI) detection methods 246
electromechanical action 2
embedded temperature detectors (ETDs) 143–4, 146
enclosures 46–7
materials 48
end windings 44–5
bracing 46
failure modes and root causes 71
insulation 60–1
materials 48
stress grading 61
environmental ageing 54–5
environmental conditions 49, 51
insulation contamination 54–5, 61
equivalent capacitance 267
Euler–Lagrange equation 178
expert 334–5
expert knowledge 311
expert systems 309–12

failure, definition 79
failure intensity
definition 79–80
failure mechanism, definition 79
failure mode and effects analysis (FMEA) 80
failure modes
bearing faults 73–5
connection faults 72–3
definition 79
electrical insulation 55–71
and machine specification 48–50
probability density function 83
and root causes 365–9
rotor windings 71–5
shaft voltages 75
stator core faults 71–2
stator winding faults 61–7
stator winding insulation 56–67
types 82–3
water coolant faults 73
failure rate 84–7
aggregate 85–6
life-cycle variation 85–6
typical 89–93
failure sequence 81–2
Faraday Predictive S200 326
fast Fourier transform (FFT) 100

faults detectable from the stator force wave 199–200
ferrite-cored RF current transformer (RFCT) 243
ferromagnetic debris 137
ferromagnetic techniques, lubrication oil analysis 170–2
fibre Bragg grating (FBG) 123, 147
fibre-optic proximetry 126
fibre-optic temperature sensing 123
  principle of 147
field-programmable gate arrays (FPGA) 10
flame ionisation detector (FID) 165, 167
flexible rotors 186–8
flux waveform 216
force and torque instrumentation 129–32
frame-based systems 309
frequency response analysis (FRA) 278
frequency spectrum monitoring 196–9
future CM of electrical machines 339
fuzzification 313
fuzzy logic 312–15
'AND' operation 314
'NOT' operation 314
'OR' operation 314

gas analysis 164–9
gas chromatography 162–4
  off-line analysis 165
  oil degradation detection 170
gearboxes, vibration analysis 108
general safety hazards 332
generator and motor comprehensive methods 225
  mechanical and electrical interaction 236
  power spectrum 231–5
  shaft flux 226–30
  shaft voltage or current 235–6
  stator and rotor currents 230–1
generator and motor stator faults
  brush-gear fault detection 210
  generator stator winding insulation detection 209
  rotor-mounted search coils 210
  stator current monitoring for stator faults 209–10
generator rotor faults 210
  earth leakage faults on-line 211–12
  turn-to-turn faults on-line
    air-gap search coils 212–16
    circulating current measurement 216–20
generator stator winding insulation detection 209
Germanischer Lloyd 300
German Vibration Standard VDl 2056 194, 197

Hall-effect principle 134
harmonics, converter 105
hazard function 79
heat exchangers 47
heat-sensitive semi-conducting material 151
Hewlett–Packard Journal 6
high flux test (HFT) 275
high-order spectral analysis 104–5
hot-spot measurement and thermal images 149
HV motors and generators 72–3
hydro-generators 59, 62, 71–2, 277–8

ignitron 17
imperative knowledge 310
induction machine, vector control for 269
induction motors 68
  construction 45–6, 68
  failure rates 90–2
  root causes of faults 68
  rotor faults 68
inductive debris detectors 136, 171
infrared gas analyser 169
instrumentation amplifier 138
insulated gate bipolar transistors (IGBTs) 17

insulation: *see* electrical insulation
insulation remanent life 248
ionising radiation, insulation ageing 54

Jaguar E-Pace car 1

Kalman filter 114–16
key phasors 125
Kohonen's algorithm 320

leakage flux monitoring 120
levelised cost of energy (LCOE) 295
life-cycle costing 294–5
life-cycle variation in failure rates 85–6
local temperature measurement 143–8
low-voltage (LV) stator core test 275–7
lubrication oil analysis 169–73

machine faults 201
machine learning using ANNs
  supervised learning through ANN 317–20
  unsupervised learning 320–2
machine-related electronic systems 291
machine specification and failure modes 48–50
machine stator winding, complex structure of 241
magnetic drain plugs 172
maintenance regimes 93–4
maintenance strategies, economics of 292
  asset management 297–300
  basic economic justification 292–4
  cost–benefit analysis of condition monitoring for CBM 296–7
  life-cycle costing 294–5
Markov modelling 296
material properties 39–43
  electrical steel 44
  stator core and frame 44
materials, types for various components 48
Maxwell stresses 183
mean time between failure (MTBF) 80, 89–93
mean time to failure (MTTF) 80
mean time to repair (MTTR) 80
mechanical ageing, insulation 54
mechanical properties 40
mercury arc rectifier (MAR) 17
metal foil-type strain gauge 130
model-based information extraction 113
  Kalman filter 114–16
  observer 116
model-based voltage and current (MBVI) system 324, 326–7
  and artificial intelligence 327–9
modern discharge detection methods 250–3
modular expert system 311–12
moisture absorption by insulation 52–3
monitoring techniques 193–4
  faults detectable from the stator force wave 199–200
  frequency spectrum monitoring 196–9
  need for 4–7
  overall level monitoring 194–6
  shock pulse monitoring 204–6
  torsional oscillation monitoring 200–4
  what and when to monitor 8–10
motor condition monitor (MCM) 324
motor current signature analysis (MCSA)
  application of 377–8
  controls and capabilities 377
  data communication 378
  data interpretation 378
  draft CM good practice guide 371–81
  expected outputs 374–6
  issues 377
  safety 378–9
  scope 374

skills, competence and training 379–80
taking readings 380–1
motor rotor faults 220
air-gap search coils 220
rotor current monitoring 223–5
stator current monitoring for rotor faults (MCSA) 220–3
motor speed 337
multi-channel neural network system 319
multi-layered perceptron (MLP) 317
multi-parameter monitoring 305–9
multi-phase machines 33–5

'neural network' AI methods 305, 340

observer 116
offline monitoring 273
rotor windings 278
offline tests 280
synchronous rotor surge tests 281–4
stator core 273
hydro-generators 277–8
turbo-generators 277
stator windings
frequency response analysis (FRA) 278
offline tests 279
offline rotor winding tests 280
offline stator winding tests 279
online chemical monitoring 153–74
detectability 154–8
gas analysis 164–9
insulation degradation
detection 158–69
mechanisms 153–4
lubrication oil analysis 169–73
particulate detection
chemical analysis 162–4
core monitors 158–62
online current, flux and power monitoring 209
generator and motor comprehensive methods 225
mechanical and electrical interaction 236
power spectrum 231–5
shaft flux 226–30
shaft voltage or current 235–6
stator and rotor currents 230–1
generator and motor stator faults
brush-gear fault detection 210
generator stator winding insulation detection 209
rotor-mounted search coils 210
stator current monitoring for stator faults 209–10
generator rotor faults 210
earth leakage faults on-line 211–12
turn-to-turn faults on-line 212–20
motor rotor faults 220
air-gap search coils 220
rotor current monitoring 223–5
stator current monitoring for rotor faults (MCSA) 220–3
online partial discharge (PD) electrical monitoring 239
detection problems 248–50
discharge detection, background to 239–41
early discharge detection methods
capacitive coupling method 245–6
earth loop transient method 244–5
insulation remanent life 248
RF coupling method 241–4
wide-band RF method 246–8
modern discharge detection methods 250–3
online temperature monitoring 143
bulk measurement 149–51
hot-spot measurement and thermal images 149
local temperature measurement 143–8
online vibration monitoring 175
bearing response 190
rolling element bearings 190–2

sleeve bearings 192–3
monitoring techniques 193–4
faults detectable from the stator force wave 199–200
frequency spectrum monitoring 196–9
overall level monitoring 194–6
shock pulse monitoring 204–6
torsional oscillation monitoring 200–4
rotor response 185
torsional response 188–90
transverse response 185–8
stator core response 175
natural modes, calculation of 177–80
stator electromagnetic force wave 181–3
stator end winding response 183–4
operational conditions 49
operational expenditure (OPEX) 295
optical debris sensor 137
optical time domain reflectometry (OTDR) 123
organic insulation 263
overall level monitoring 194–6
ozone detection 165–6

partial discharge analyser (PDA) 250
partial discharges (PDs) 52
and analysis 158–64
electrical monitoring: *see* Online partial discharge (PD) electrical monitoring
insulation degradation 154
internal void discharge 52
measurement 263–5
triggered sampling and analysis scheme 265
monitoring 340
slot discharge 58–60
permanent magnet 33–4
photoionisation detector (PID) 167
'picket fence' effect 101
picocoulombs (pC) 239
piezoelectric accelerometer 128
potentiometer 211
power plants 1
power spectral density 105
power spectrum 108, 231–5
power-to-weight ratio of electrical machines 2, 19
pre-set value 2
preventative maintenance 285–7
probability density function 84–7
prognostics and health management (PHM) 303
proportional-integral-derivative (PID) algorithm 116
protective relaying 2–3
pulsed voltage generator 264
pulse-width-modulation (PWM) 255

radio frequency current transformer (RFCT) 243
radio interference field intensity (RIFI) meter 243–4
Rayleigh–Ritz method 178
recurrent surge oscillography (RSO) 213, 282–3
redundancy 87
reliability
analysis 84–7
definition 79
as a function 79, 84
theory 80
reluctance machines 33–4
remaining useful life (RUL) 322
repetitive partial discharge inception voltage (RPDIV) 264
resistance temperature detection (RTD) 117, 145
restricted-Boltzmann-machine (RBM) 323–4
RF coupling method 241–4
rigid rotors 185–6
Roebel technique 63
Rogowski coil 219, 225, 244, 249, 276
rolling element bearings 190–2
root cause analysis (RCA) 79, 82

root causes
  definition 79
  types 82–3
rotating electrical machines 17
  AC machines
    asynchronous/induction 28–33
    synchronous 26–8
  DC machines 25–6
  doubly fed and variable-speed drive machines 35–7
  electrical machines structures and types 18–25
  multi-phase machines 33–5
  permanent magnet or reluctance machines 33–4
rotor current monitoring 223–5
rotor faults 209
rotor-mounted search coils 210
rotor response 185
  torsional response 188–90
  transverse response 185
    flexible rotors 186–8
    rigid rotors 185–6
rotors
  airgap eccentricity 75, 93
  bearing types 45–6
  cooling 45–6
  materials 48
  mechanical design 45–6
  and windings 45–6
rotor windings 278
  broken rotor bars 68
    detection 105, 111
  failure modes 71–5
  failure rates 91–2
  faults 67–8
    DC machines 71
    turbo-generators 69–70
    winding faults 68–71
  materials 48
  offline tests 280
  root causes of faults 71–5
  synchronous rotor surge tests 281–4
rule-based systems 310
'rule-based' AI methods 305, 340
safety 331–2
self-organising mapping (SOM) 322
semantic networks 310
sequence of failure 81–2
shaft flux 226–30
shaft flux monitoring 123, 337
shaft voltage/current 235–6, 337
shaft voltages 75
  bearing and lubricating oil degradation 75, 169
  damage caused to bearings 75, 169
shock pulse monitoring 204–6
shock pulse value (SPV) 205
signal condition and data acquisition systems (SCADA) 10, 289–90
signal conditioning 137–9
signal processing 95
  correlation analysis 105–7
  spectral analysis 99–104
  time averaging 110–11
  vibration measurement 127
SKF CM system 290
sleeve bearings 192–3
slip-rings 47
  materials 48
slot discharge 58–60
smoke detection 158–62
specialist 333–4
spectral analysis
  aliasing 103
  basic theory 99–104
  correlation analysis 105–7
  high-order analysis 104–5
'picket fence' effect 101
  vibration measurement 127
  wavelet analysis 111–13
  window functions 100
star-connected machine floating 266
statistic methods 310
stator and rotor currents 230–1
stator core 273
  hydro-generators 277–8
  turbo-generators 277
stator core and frame 44–5
  core faults 71–2

materials 48
stator core response 175
natural modes, calculation of 177–80
stator electromagnetic force wave 181–3
stator current monitoring
for rotor faults 220–3
for stator faults 209–10
stator end winding response 183–4
stator slot coupler (SSC) 249
stator winding insulation structure 257
stator windings 44–5, 56–7
coolant systems 63–5
end windings 44–5
bracing 46
faults 71
insulation failure modes 61
stress grading 61
failure rates 91–2
frequency response analysis (FRA) 278
insulation failure modes 56–67
delamination and voids 56
end winding faults 65
end windings 61
inter-turn faults 64–5
repetitive transients 61
slot discharge 58–60
transient voltages 61
winding conductor faults 62–4
winding coolant system faults 65–7
winding faults 61–2
materials 48
offline tests 279
root causes of faults 61
winding conductor faults 61–7
winding coolant system faults 65–7
steel used in cars 1
structural design 87–9
sub-assemblies 87
distribution of failures 92–3
supervised learning through ANN 317–20
surface tracking 52–3, 72–3
surge techniques 281
survivor function 79
switched reluctance motor 33
synchronous machine design 26
synchronous rotor surge tests 281–4
synergism between ageing stresses 55
system derived hazards 332

targeted monitoring 290–2
TEAM 256–7
technological timelines 10–13
temperature detection 338
temperature instrumentation 117–23
temperature monitoring, approaches to 143
temperature rise 338
Tennessee Valley Authority (TVA) 249
thermal ageing, electrical insulation 51–2, 153–4
thermal properties 39–43
thermal stress 52, 66
thermistors 117, 122
thermocouples 117, 145
time averaging 110–11
time between failure (TBF) 80
time to failure (TTF) 80
time to repair (TTR) 80
torsional oscillation monitoring 200–4
torsional response 188–90
totally enclosed fan-cooled (TEFC) machines 147, 149
training and qualification 332
Category I – data collector 333
Category II – specialist 333–4
Category III – analyst 334
Category IV – expert 334–5
transducer, signal provided by 2
transient voltages 52–4, 61
transmission assets 299
transverse response 185
flexible rotors 186–8
rigid rotors 185–6
trend analysis 110–11

turbine generators
  construction 43–7
  failure rates 90
  rotor winding faults 67–70
turbo-generator analyser (TGA) 250
turbo-generators 71–2, 277
turn-to-turn faults on-line
  air-gap search coils 212–16
  circulating current measurement 216–20
2-pole AC synchronous machine 29
2-pole DC machine 27
Tyndall effect 137
Type I machines 263–4
Type II machines 264
types of rotating electrical machines 20–3
typical sizes and loadings, of rotating electrical machine 24

ultra-violet techniques, chemical analysis 163
unbalanced magnetic pull (UMP) 69–70, 181
unsupervised learning 320–2

variable speed drive (VSD) machine monitoring 255
  bearing current discharge detection 261–3
  control in-loop machine fault detection 269–72
  insulation degradation detection 263
    built-in winding insulation degradation detector 267–9
    capacitance and dissipation factor measurement 266–7
    PD measurement 263–5
  operation and fault mechanisms 256
    bearing current discharges 258–61
    insulation degradation mechanisms 256–8
variable-speed drives (VSDs) 17, 35
velocity transducers 127–8
vibration and shock pulse monitoring and analysis 337
vibration instrumentation 123
  accelerometers 128–9
  displacement transducers 124–7
  velocity transducers 127–8
vibration measurement
  signal processing 107–11
vibration-monitoring techniques 130
voids, insulation 56–7, 62

Ward Leonard's principles 17
water and waste systems 2
water coolant faults 73
wavelet analysis 111–13
wear and debris instrumentation 136–7
wear measurement
  lubrication oil analysis 169–73
Wheatstone bridge 131
whole-life costing: *see* life-cycle costing
wide-band RF method 246–8
windings 45–6
  materials 48
  *see also* rotor windings; stator windings
window functions 100
wind turbine generators
  cause-and-effect diagram 87
  failure rates 90

x-ray fluorescence (XRF) detection 173

# Condition Monitoring of Rotating Electrical Machines
3rd Edition

Condition monitoring of engineering plants has increased in importance as engineering processes have become increasingly automated. However, electrical machinery usually receives attention only at infrequent intervals when the plant or the electricity generator is shut down. The economics of industry have been changing, placing ever more emphasis on the importance of reliable operation of the plants. Electronics and software in instrumentation, computers, and digital signal processors have improved our ability to analyse machinery online. Condition monitoring is now being applied to a range of systems from fault-tolerant drives of a few hundred watts to machinery of a few hundred MW in major plants.

This book covers a large range of machines and their condition monitoring. This 3rd edition builds on the 2nd edition through a major revision, update of chapters and a comprehensive list of references & standards. Permanent magnet, switched reluctance and other types of machines are now covered, as well as variable speed drive machines and off-line techniques.

Contents cover an introduction to condition monitoring; rotating electrical machines; electrical machine construction, operation and failure modes; reliability of machines and typical failure rates; signal processing and instrumentation requirements; on-line temperature monitoring; on-line chemical monitoring; on-line vibration monitoring; on-line current, flux and power monitoring; on-line partial discharge (PD) electrical monitoring; on-line variable speed drive machine monitoring; off-line monitoring; condition-based maintenance and asset management; application of artificial intelligence techniques to CM; and safety, training and qualification.

## About the Authors

**Peter Tavner** is an emeritus professor at Durham University, UK.

**Li Ran** is the SMIEEE chair in power electronics-systems at the School of Engineering, University of Warwick, UK

**Christopher Crabtree** is an assistant professor in the Department of Engineering at Durham University, UK

ISBN 978-1-78561-865-9

9 781785 618659 >

**The Institution of Engineering and Technology**
theiet.org
978-1-78561-865-9